ZooKeys 1219: 1–60 (2024)
DOI: 10.3897/zookeys.1219.133002

Research Article

A comparative morphology of trichobothrial bases in araneoid spiders and its significance for the phylogeny and system of the superfamily Araneoidea (Arachnida, Araneae)

Kirill Y. Eskov[1], Yuri M. Marusik[2,3,4]

1 Borissiak Paleontological Institute, Russian Academy of Sciences, Profsoyuznaya Str., 123, Moscow 117647, Russia
2 Institute of Biological Problems of the North, Far Eastern Branch, Russian Academy of Sciences, Portovaya Str., 18, Magadan 68500, Russia
3 Department of Zoology and Entomology, University of the Free State, Bloemfontein 9300, South Africa
4 Altai State University, 61 Lenina Pr., Barnaul, RF-656049, Russia
Corresponding author: Yuri M. Marusik (yurmar@mail.ru)

Abstract

Bothrial morphology was studied by SEM in 137 araneoid genera representing all 22 currently recognized extant families and all 42 conventional subfamilies of the Araneoidea. The ancestral type in the superfamily Araneoidea is a 'hooded' bothrium with a single well-developed transverse ridge, dividing its proximal and distal plates ('*Erigone*-type'); the advanced type is a solid dome-like bothrium without vestiges of the ridge ('*Theridion*-type'); there are several intermediate types reflecting various pathways and stages of the ridge reduction (united here as '*Argiope*-type'). The parallel trends in bothrial evolution, recognized as continuous series from the ancestral type up to the advanced one through some intermediate stages, are distinguished in each of the seven main phylogenetic lineages of the superfamily: 'tetragnathoids', 'araneoids', 'cyatholipoids', and 'theridioids' possess a complete set of the three types, while 'malkariods', 'symphytognathoids'. and 'linyphioids' lack the advanced, dome-like type ('*Theridion*-type'). Only three taxa have been proposed earlier as the sister group of the superfamily Araneoidea: Nicodamoidea, Deinopoidea, and Leptonetoidea; morphology of bothria, as well as other cuticular microstructures, clearly supports the araneoid-nicodamoid relationship hypothesis, purely 'molecular' to date. Bothrial morphology provides the additional arguments for several taxonomic acts, e.g., for the reranking the Agnarsson's (2004) 'clade 35' (*Theonoe*, *Carniella*, *Robertus*, and *Pholcomma*) up to the Theonoeinae Simon, 1894, **stat. nov.**, and for the revalidation the micropholcommatid *Plectochetos* Butler, 1932, **gen. revalid.** and zygiellid *Parazygiella* Wunderlich, 2004, **gen. revalid.**

Key words: Aranei, Araneomorphae, bothrial morphology, bothrial evolution

OPEN ACCESS

Academic editor: Sergei Zonstein
Received: 24 July 2024
Accepted: 6 September 2024
Published: 26 November 2024

ZooBank: https://zoobank.org/060C0C51-C95E-49C0-B828-B64D821037CF

Citation: Eskov KY, Marusik YM (2024) A comparative morphology of trichobothrial bases in araneoid spiders and its significance for the phylogeny and system of the superfamily Araneoidea (Arachnida, Araneae). ZooKeys 1219: 1–60. https://doi.org/10.3897/zookeys.1219.133002

Introduction

Trichobothria are a conspicuous type of mechanoreceptive sensilla in terrestrial arthropods. They are represented by erect, very elongated setae that are set in a deep cup-like socket, the bothrium. The morphology of trichobothrial bases is very diverse in spiders and has become a popular subject of investigation since the very beginning of regular usage of scanning electron microscopy in taxonomy and phylogeny of the order. For instance, trichobothrial characters were successfully used in the diagnostics of suprageneric taxa and reconstruction of evolutionary trends in mygalomorphs by Raven (1985) and Eskov et al. (2024), in 'hypochiloids' by Forster et al. (1987), and particularly in dionychans by Ramírez (2014).

However, the largest superfamily of the order, Araneoidea, which comprises 22 extant families and more than a quarter of the described species, was almost ignored by arachnologists in this respect: araneoid trichobothria are highly uniform and therefore seem useless for high-level (suprageneric) systematics and phylogeny. It is indicative that the fundamental 'Atlas of phylogenetic data for entelegyne spiders' by Griswold et al. (2005) presents SEM images of bothria of 49 species of 23 families, but only one of them (!) represents the araneoids (the mimetid *Mimetus hesperus* Chamberlin, 1923: fig. 149 G); the diagnosis of the superfamily contains only a laconic remark: "...Trichobothrial bases are smooth" (Griswold et al. 2005:14).

The review of Simphytognathoidea by Lopardo and Hormiga (2015) comprises 23 characters concerning, one way or another, the trichobothria, but only one of them touches the morphology of the trichobothrial shaft ("smooth/serrated" or "distinctly plumose": char. 150), and not a single one considering the morphology of the bothria. Álvarez-Padilla and Hormiga (2011: 713) declared a special attention to the trichobothria in their review of tetragnathid morphology: "We study the evolution of six morphological character systems within Tetragnathidae: spinneret spigots, respiratory structures, trichobothria, chelicerae, and male and female genitalia"; however, they presented numerous SEM images trichobothrial pattern of the legs, but not a single enlarged image of the bothria permitting to discern its structure.

Even in cases where arachnologists have paid attention to this structure and described the bothria of the studied araneoid taxa in detail, e.g., Forster et al. (1990) in Synotaxidae s. l., Rix and Harvey (2010) in Micropholcommatidae, they have not attempted any generalization. So, an evolutionary 'big picture' of the development of these structures in Araneoidea, comparable with abovementioned conclusions by Ramírez (2014) for Dionycha, is completely absent.

The only case of an interfamilial comparison of bothrial morphology in araneoids was provided by Miller (2007), in a study of synaphrid relationships; only two bothrial types were distinguished by him, 'hooded' and those that are 'evenly rounded and lack a hood': "The typical bothrium form in Synaphridae is hooded, a characteristic shared at least with Anapidae (Platnick and Forster 1989: fig. 15), Micropholcommatidae (Forster and Platnick 1984: figs 374, 375), Mysmenidae (Griswold 1985: fig. 8), Theridiosomatidae (unpublished data), Malkaridae (Platnick and Forster 1987: fig. 18), Linyphiidae (Hormiga 2002: fig. 46G), Synotaxidae (Forster et al. 1990: figs 144, 260), and many non-araneoid spider families (Forster and Platnick 1984; Griswold et al. 2005); bothria in other araneoid families including araneids (Griswold et al. 1998: fig. 22E), theridiids (Agnarsson 2004: figs 31G, 69E, 74D), cyatholipids (Griswold 2001: fig. 6B), and mimetids (Griswold et al. 2005: fig. 149G) are evenly rounded and lack a hood" (Miller 2007: 30).

Distribution of these two bothrial types through the listed araneoid families seems completely chaotic and lacking any phylogenetic sense; Miller (2007) has not formulated such a conclusion directly, but it is quite obvious. And probably due to this deceptive 'obviousness', subsequent investigators lost any interest in this problem and turned away from searching for any regularities in this field.

We, however, suspected that the above 'phylogenetic chaos' was an artifact, caused by the following factors: (1) a too rough typology of bothria (two opposite types only); (2) a too limited number of studied araneoid species/genera; and (3) a too random set of the studied araneoid families/ subfamilies (the latter two because of a deficiency of his own or published data available to Miller (2007) at that time).

Testing this supposition, we have studied the bothrial morphology in 137 araneoid genera representing all 22 currently recognized extant araneoid families and all 42 conventional subfamilies; so, a complete (or close to complete) diversity of these structures through superfamily Araneoidea seems to have been revealed. Araneoid bothria turned out to be much more uniform than, e.g., dionychan (see Ramírez 2014), but the 'fine-tuning' of bothrial typology indicated some bothrial types in addition to the above-mentioned couple 'hooded' (basal) and 'evenly rounded' (terminal).

Forster (1988: 11), in his study of the Cyatholipidae of New Zealand, noted in the family diagnosis: "Bothria with the posterior hood reduced to two small ridges or absent", and then guessed the following: "The reduction of the posterior hood of the bothrium and the small aperture of the domed tarsal organ are all derived characters which have developed apparently in parallel in many of the families" (Forster 1988: 15). And the 'big picture' of bothrial evolution in various Araneoidea lineages revealed in this work convincingly supports this assumption.

Material and methods

SEM images were taken on a Tescan Vega2 and a Tescan Vega3 scanning electron microscopes in Palaeontological Institute (Moscow), operated in a high vacuum mode at the accelerating voltages of 10–20 kV, using SE and BSE detectors. Specimens were gradually dehydrated in 100% ethanol, dried, and sputter-coated with gold-palladium.

The bothria of 142 araneoid and five non-araneoid species are figured; in addition, the original images of three araneoid bothria were obtained from colleagues. For a list of the specimens examined, see Suppl. material 1. Terminology of the bothrial parts follows that in Eskov et al. (2024). All measurements are given in µm. Abbreviations of leg joints: **mt** – metatarsus, **ti** – tibia.

Abbreviations for trichobothria parts: ***al*** alveolus; ***AP*** angle with clear apex of proximal plate; ***dp*** distal plate; ***ff*** frontal fold; ***pp*** proximal plate; ***pp+dp*** fused proximal and distal plates; ***RA*** round apex; **SbA** semicircular arch; **sh** shaft; **tr** transverse ridge of proximal plate.

Results

Preliminary notes on the sister group of the superfamily Araneoidea

Three phylogenetically distant taxa have always been supposed to be the sister group of the superfamily Araneoidea:

1. Nicodamoidea: cribellate Megadictynidae Lehtinen, 1967 and ecribellate Nicodamidae Simon, 1897. "The Nicodamidae is one of the few spider

families for which there is no well supported hypothesis on its position" (Jocqué and Dippenaar-Schoeman 2006: 184: fig. 5).

2. Deinopoidea: Deinopidae C.L. Koch, 1850 and Uloboridae Thorell, 1869. "The entirely cribellate Deinopoidea [...] All spin modified orbs. Some controversy existed in the past over placement of Deinopidae (ogre-faced spiders), but ethological work showed that they shared derived motor patterns unique to orb weavers, despite the derived web architecture" (Coddington and Levi 1991: 585). Deinopoids were coupled with another orb-web builders, ecribellate araneoids, in frame of the concept 'Orbicularia' (Coddington 1986a; Jocqué and Dippenaar-Schoeman 2006: fig. 5).
3. Leptonetoidea (sensu Wunderlich and Müller 2018): cribellate Archoleptonetidae Gertsch,1974, ecribellate Leptonetidae Simon, 1890, and Telemidae Fage, 1913 (all extant), cribellate Protoaraneodidae Wunderlich & Müller, 2018 and ecribellate Praeterleptonetidae Wunderlich, 2008 (both extinct). The sister pair Leptonetidae + Telemidae was traditionally nested within Haplogynae (Platnick et al. 1991; Jocqué and Dippenaar-Schoeman 2006: 150: fig. 4). However, "The distribution of several features of the spinning organs [in recently discovered the cribellate leptonetids], respiratory system, and genitalia suggests that the phylogenetic position of the Leptonetidae needs to be reevaluated and makes their position within the Haplogynae uncertain" (Ledford and Griswold 2010: 2). Finally, the new molecular data (Wheeler et al. 2017) placed leptonetids far outside the robustly supported Synspermiata (all the ecribellate 'haplogynes', including the telemids).

The hypothesis of the araneoid-nicodamid relationship (as well as the incorporation of the cribellate *Megadictyna* Dahl, 1906 in the ecribellate Nicodamidae) was first put forward by Forster (1970). The trichobothrial pattern of the legs was listed as one of the main characters suggests the affinities of the Nicodamidae with the Araneoidea (Forster 1970: 177): single trichobothrium on each of the metatarsi I–III, trichobothria absent on metatarsus IV and absent on tarsus.

However, this hypothesis was not accepted: Harvey (1995) nested Nicodamidae within the 'RTA-clade', close to Titanoecidae, and rejected the araneoid-nicodamid relationship. One of his main objections was the dissimilarity of the spinning organs: "The identification of synapomorphies for the Orbiculariae and Araneoidea by Coddington (1990a, 1990b) conclusively excludes the Nicodamidae from these groups, particularly as nicodamids possess two major ampullate spigots on the anterior lateral spinnerets [Fig. 11], whereas all orbicularians possess only one" (Harvey 1995: 283). Regarding the simplified trichobothrial pattern (the lack of tarsal trichobothria and the presence of only a single metatarsal trichobothrium) in both araneoids and nicodamids, Harvey (1995: 287), following Coddington and Levi (1991), considered it "plesiomorphic within the Araneomorphae" and, consequently, insufficient (see discussion of the polarity of this character below).

The concept of 'Orbicularia' became a step in another direction: "Reconstitution of the orb weavers, or Orbiculariae, also resulted from cladistic analysis of a classical cribellate-ecribellate dichotomy. Classically orb webs were thought to have evolved twice: once among the (paraphyletic) Cribellatae, and once among the (polyphyletic) Ecribellatae. [...] Given the collapse of the Cribellatae and Ecribellatae as valid taxa, the orb web itself constituted initial evidence for monophyly. A series of detailed ethological and morphological investigations has failed to refute this hypothesis, thus corroborating that cribellate orb weavers (Deinopoidea) are the sister group of Araneoidea" (Coddington and Levi 1991: 584–585). This concept was put forward by Coddington (1986a, 1990a, b) and was widely accepted and prevailed for the next two decades (e.g., Griswold et al. 1998, 1999; Jocqué and Dippenaar-Schoeman 2006). It should be noted that almost all morphological characters supporting the 'Orbicularia' as a monophyletic clade seem limited by the fine structure of the spinning organs (see Griswold et al. 2005).

Nowadays, Forster's (1970) earlier assumption on the araneoid-nicodamoid relationship (as well as the unity of cribellate and ecribellate nicodamoids) was resurrected by molecular methods and is accepted in most modern phylogenies (see Kallal et al. 2018: fig. 1B–F). "Our data refute the long-held paradigm of orbicularian monophyly [...] by including the RTA clade in the same lineage that groups the cribellate (Deinopoidea) and ecribellate (Araneoidea) orb-weavers. This latter result, based on DNA sequence data, is by no means new [...], but has been dismissed repeatedly in favour of the orbicularian monophyly hypothesis. [...] The results presented herein suggest that nicodamids are the closest relatives to a clade that includes all ecribellate orb-weavers" (Dimitrov et al. 2017: 231–234).

It is not surprising that this result "has been dismissed repeatedly", because the 'molecular clade' Nicodamoidea + Araneoidea still lacks any sufficient morphological support: "Morphological evidence for this arrangement remains weak [...] The morphological evidence for placing nicodamids near or far from orb-weavers is not robust. It is molecular evidence, albeit from the same genes but with a diverse array of taxon samples, that strongly associates Nicodamoidea with Araneoidea" (Dimitrov et al. 2017: 240).

Wunderlich and Müller (2018) recently proposed their 'Leptonetoidea' (i.e., well-known haplogyne couple Leptonetidae + Telemidae, supplemented with several extinct haplogynes, both ecribellate and cribellate) as the Araneoidea sister group. The 'Leptonetoid-Araneoid branch' was placed by Wunderlich and Müller (2018: fig. 1) near the base of araneomorphs and characterized by the following characters: "large and erect paracymbium; loss of feathery hairs; tendencies to existence of lateral cheliceral files and the loss of the cribellum". All the listed characters of the supposed branch seem ambiguous: several leptonetoids (both extant and extinct) possess the cribellum; the majority of araneoids lack the cheliceral files; the homology of the araneoid paracymbium and the leptonetoid cymbial outgrowth was not proved; and the loss of feathery hairs seems to be rather a homoplasy than a synapomorphy. In addition, Wunderlich and Müller (2018: 41) pay special attention to the leg autotomy, but this character in any case is not a synapomorphy of 'Leptonetoid-Araneoid branch': on the one hand, it was not recorded in the majority of araneoids, and on the other hand it was recorded in the very distantly related Filistatidae and Herseliidae (Scharff and Coddington 1997: char. 36).

Before testing these three hypotheses by the characters of cuticular microstructure (including the bothrial morphology, ignored previously in this respect) let us return to the above-mentioned trichobothrial pattern of the legs. Conclusion on the polarity of this character in the araneomorphs is still based on Lehtinen's early hypothesis: "Type I. The plesiomorphic pattern of trichobothria in spiders consists of a single subdistal metatarsal and two parallel rows of tibial trichobothria, but none on tarsi or femora" (Lehtinen 1980: 493), and "The simplest trichobothrial pattern, with two longitudinal parallel rows dorsally on tibiae and a single row on metatarsi, is shared by most Araneoidea and related groups, most haplogyne groups, some Nicodamidae and Eresidae. The trichobothrial pattern of most theraphosomorph spiders [i.e., Liphistiomorphae and Mygalomorphae] is much more complicated [i.e., with tarsal and several metatarsal trichobothria]. However, I regard the latter as an apomorphic pattern, and probably the simple pattern described above is close to an ancestral pattern" (Lehtinen 1978: 265).

There was no discussion as to why he chose to "regard the latter as an apomorphic pattern". Nevertheless, this viewpoint was supported, without any additional arguments, by Coddington and Levi (1991: 581–582): "The distribution of trichobothria (fine sensory hairs) on the metatarsi and tarsi is another important character [...]. The plesiomorphic araneomorph pattern seems to be [the] absence or near absence on the metatarsi and tarsi (although present on mygalomorph and liphistiomorph tarsi). The derived condition is single or multiple rows of trichobothria", and this hypothesis persists until now (e.g., Miller et al. 2010). It should be emphasized that for the mygalomorh trichobothrial pattern Coddington and Levi (1991: 575) adhered (without any special argument again) to the opposite polarity: "It is interesting that one apomorphy of the atypoids is the great reduction or absence of tarsal trichobothria".

In our opinion, an obvious phylogenetic protocol of comparison of the Araneomorphae with its sister group, Orthognatha (Liphistiomorphae and Mygalomorphae), assumes the opposite polarity of this character: just the 'complex pattern' (with tarsal and several metatarsal trichobothria) is an ancestral condition, directly inherited by the araneomorphs from the orthognathans. This pattern has persisted in some araneomorph lineages (e.g., RTA-clade and Salticidae), or partially reversed in others: e.g., the appearance of the tarsal trichobothria in haplogyne Caponidae (Jocqué and Dippenaar-Schoeman 2006: 88), and of the additional metatarsal trichobothria in some unrelated araneoids, such as the araneid *Melychiopharis* Simon, 1895 (Fig. 12A) and linyphiid *Allomengea* Strand, 1912 (Helsdingen 1974).

A further simplification of the initial 'complex' pattern in various araneomorph lineages (due to parallel reductions) is a more easily explained evolutionary trend than a complication of the initial 'simple' pattern (due to numerous parallel origins). Thus, Scharff and Coddington (1997: char. 37) supposed the abovementioned multiplication of the metatarsal trichobothria in several unrelated araneid genera (cyrtarachnin *Mastophora* Holmberg, 1876, gasteracanthin *Gasteracantha* Sundevall, 1833, aranein *Cyclosa* Menge, 1866, etc.) were autapomorphies, but reversions to the common plesiomorphic/ancestral condition seem more convincing. So, the single 'simplified' type of trichobothrial pattern in both nicodamoids and araneoids was correctly considered by Forster (1970) as evidence of their relatedness.

Regarding the morphology of trichobothrial bases (as well as the remaining cuticular microstructures) Lehtinen (1996: 407) concluded: "The leg skin structure of Amaurobiomorpha and the primitive outgroups (Hypochilidae, Gradungulidae and Austrochilidae) as well as all true labidognath Haplogyne groups (Dysderoidea, Scytodoidea and Caponiidae) is either ridged or secondarily smooth, while the longitudinally ridged bothrial base is dominant throughout these lines of evolution, strongly suggesting the plesiomorphic state of the ridged skin and longitudinally ridged bothrial base in labidognath spiders". The same polarity of this cuticular character, i.e., from the fingerprint (ridged) leg cuticle to the scaly via the smooth ones, was stated by Ramírez (2014: char. 100), and we also agree with this conclusion.

The ridged cuticle is absent in all of the most archaic spider taxa (Liphistiomorphae, Mygalomorphae, and Filistatidae) and seems a synapomorphy of the 'non-filistatid araneomorphs'; the 'longitudinally ridged bothria', in an obvious way, arise from the surrounding ridged cuticle. This cuticular/bothrial type is really plesiomorphic for the suborder, being present in all basal 'non-filistatid araneomorphs', as all 'hypochiloid' lineages (e.g., Hypochilidae: Fig. 2F) and Synspermiata (e.g., Ochyroceratidae: Brescovit et al. 2018: fig. 6A). The cuticle/bothria in Leptonetoidea (Fig. 2E) and Deinopoidea (Fig. 2C) belong to this plesiomorphic type. In addition, "Ridged skin is correlated with the presence of several [non-serrate] types of hairs" (Lehtinen 1996: 399), which also appears plesiomorphic (e.g., Uloboridae: Fig. 2D).

In advanced Araneomorph lineages, the ridged cuticle is replaced by a scaly (or secondarily smooth) one; plumose and pseudoserrate (plumose-laminar) setae are replaced by serrate ones; and longitudinally ridged bothria are replaced by transversally ridged (or smooth dome-like) ones. Scaly cuticles and serrate setae are conventionally listed as synapomorphies of Araneoidea (e.g., Griswold et al. 1998; Ramírez 2014), and these characters are shared with Nicodamidae (Fig. 2B). The bothria of Nicodamoidea, both Nicodamidae (Fig. 2A) and Megadictynidae (Griswold et al. 2005: fig. 154F), are non-longitudinally ridged, as well as of all the araneoid ones (Figs 3A–F, 4A–F).

To sum up: in addition to (1) the 'simplified' trichobothrial pattern (no tarsal, a single metatarsal), both Araneoidea and Nicodamidae share the following characters: (2) serrate (not plumose) setae; (3) scaly (not ridged) leg cuticle; and (4) trichobothrial bases not longitudinally ridged; all of these are derived characters. These characters stated here in the set of morphological synapomorphies, support the 'purely molecular', until now, clade Nicodamoidea + Araneoidea. It should be noted that Lehtinen (1996: 399) doubted a close relationship of nicodamids with their scaly skin and serrate setae and megadictynids with their smooth skin and plumose-laminar setae (see Lehtinen 1996: fig. 46; Griswold et al. 2005: fig. 137A, B); however, the cribellate *Megadictyna* may be supposed a basal sister group of all the remaining, ecribellate, members of the above clade.

It should be noted that there are two directions of the initial transformation of the 'bothrial hood', leading to the two opposite derived bothrial types: the 'dome-like' (see details below) and the other, here termed 'multiridged': "Trichobothria proximal plate transverse ridges: 0. Smooth. The hood is smooth, without definite transverse ridges; it may have similar sculpture as the surrounding cuticle [...]. 1. With transverse ridges. The hood has well-defined transverse ridges [...]. These ridges are much larger than the sculpture of the surrounding cuticle" (Ramírez 2014: char. 178).

The multiridged bothria are absent in all the basal Araneomorphae ('hypochiloids', Filistatidae and Synspermiata), and present in all the advanced araneomorph clades (Wheeler et al. 2017: figs 3–8): Palpimanoidea (e.g., Huttoniidae), 'RTA-clade' (e.g., Amaurobiidae), 'Oval calamistrum clade' (e.g., Zoropsidae), Dionycha (e.g., Trachelidae) (see Ramírez 2014: figs 94E, F, K, 96C, respectively). The only advanced araneomorph clade completely lacking this advanced bothrial type is Araneoidea + Nicodamidae; at the same time, Megadictynidae possesses the multiridged bothria (Griswold et al. 2005: fig. 154F), and it seems an apomorphy of the basal cribellate lineage of this clade.

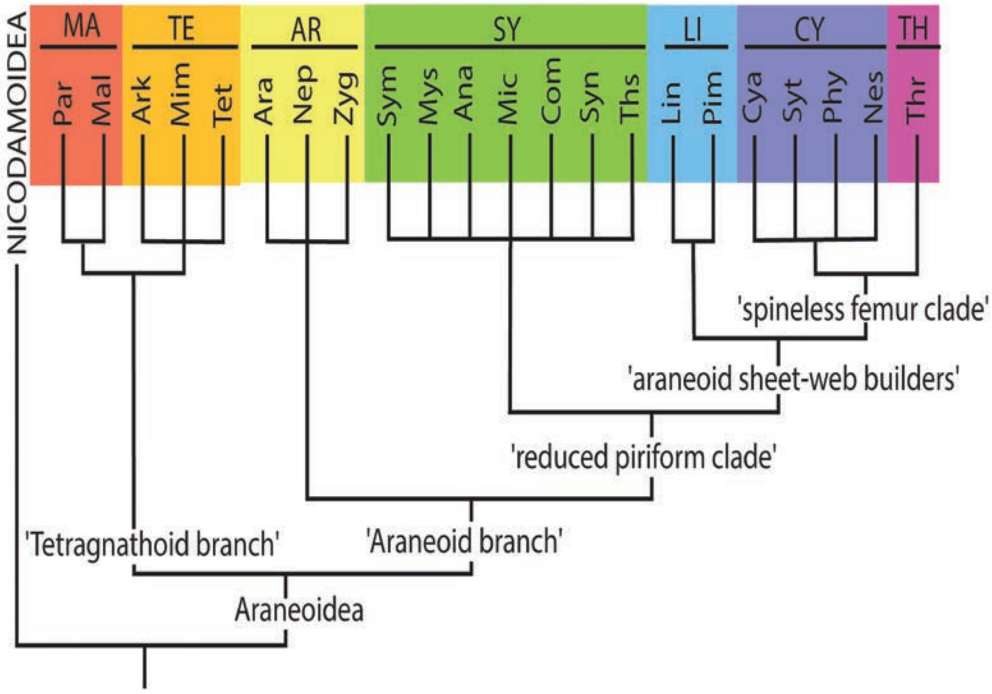

Figure 1. Accepted system of the superfamily Araneoidea, down to families (by Eskov and Marusik 2023). Abbreviations: AR – Araneoid lineage (Ara – Araneidae, Nep – Nephilidae, Zyg – Zygiellidae); CY – Cyatholipoid lineage (Cya – Cyatholipidae, Nes – Nesticidae, Phy – Physoglenidae, Syt – Synotaxidae); LI – Linyphioid lineage (Lin – Linyhiidae, Pim – Pimoidae); MA – Malkaroid lineage (Mal – Malkaridae, Par – Pararchaeidae); SY – Symphytognathoid lineage (Ana – Anapidae, Com – Comaromidae, Mic – Micropholcommatidae, Mys – Mysmenidae, Sym – Symphylognathidae, Syn – Synaphridae, Ths – Theridiosomatidae); TE – Tetragnathoid lineage (Ark – Arkyidae, Mim – Mimetidae, Tet – Tetragnathidae); TH – Theridioid lineage (Thr – Theridiidae).

In other words, bothrial morphology, as well as the morphology of the remaining cuticle microstructures, clearly support the nicodamoid-araneoid relationship hypothesis, and rejects the two competing ones (i.e., deinopoid-araneoid and leptonetoid-araneoid relationship).

Preliminary notes on the typology of the trichobothrial bases in Araneoidea

The structure of spider trichobothria and the names of their parts is given following Ramírez (2014: 122–125): “The trichobothria […] are sensory setae on the dorsal surfaces of legs and palps, specialized in detecting air movement. The *setal shaft* is slender, perpendicular to the cuticle surface [...]. The socket forms a cup or *bothrium*, with an ample central cavity. The opening of the cup (*alveolus*) restricts the movement of the *setal shaft*. The *bothrium* is usually divided in *proximal* and *distal plates*; the *proximal plate* is often called *trichobothrial ‘hood’*.” The bothria of nicodamids, confirmed herein as a sister group of araneoids, is ‘hooded’ (Fig. 2A, B; Harvey 1995: fig. 6; Lehtinen 1996: fig. 45): its proximal plate, the ‘trichobothrial hood’, is clearly differentiated from the distal plate (see Ramírez 2014: fig. 84D). So, the ‘hooded’ bothria should be recognized as the ancestral type in the superfamily Araneoidea.

An ancestral (‘hooded’) araneomorph bothrium consists of the following structures: a more or less flattened distal plate (dp) with a rounded opening for a

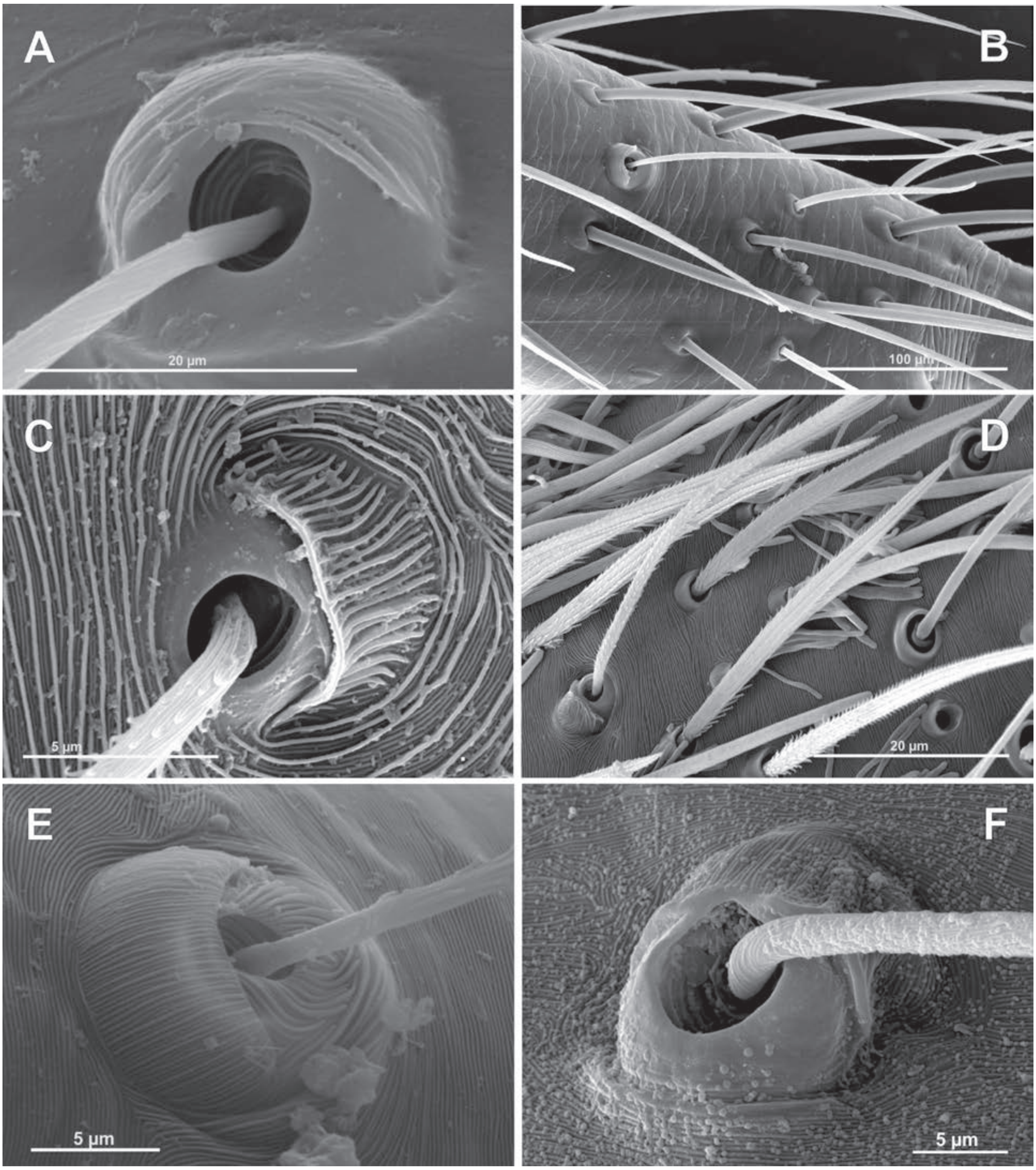

Figure 2. Bothria of the supposed sister groups of Araneoidea (**A, B** Nicodamoidea: Nicodamidae **C, D** Deinopoidea: Uloboridae **E** Leptonetoidea: Leptonetidae) and of the basal Araneomorphae (**F** 'Hypochloidea': Hypochilidae) **A** *Litodamus hickmani*, ti 3 **B** *Litodamus hickmani*, mt 3 **C** *Myagrammopis* sp. ti 2 **D** *Zozis* sp., ti 3 **E** *Leptonetela caucasica*, mt 1 **F** *Hypochilus pococki*, ti 3.

setal shaft (alveolus: al); a more or less swollen proximal pate ('hood': pp) with its distal margin forming a clear transverse ridge (tr); and a cuticular fold that delimits the bothrium from the front, termed here the 'frontal fold' (ff) (see Fig. 3A–D).

A single high-rank spider clade where the bothrial transformations have been studied in detail and on a large scale is Dionycha: "Trichobothria proximal and distal plate limit: 0. Well differentiated. The distal margin of the trichobothrial hood is well defined, often overhanging the distal plate and the opening of the

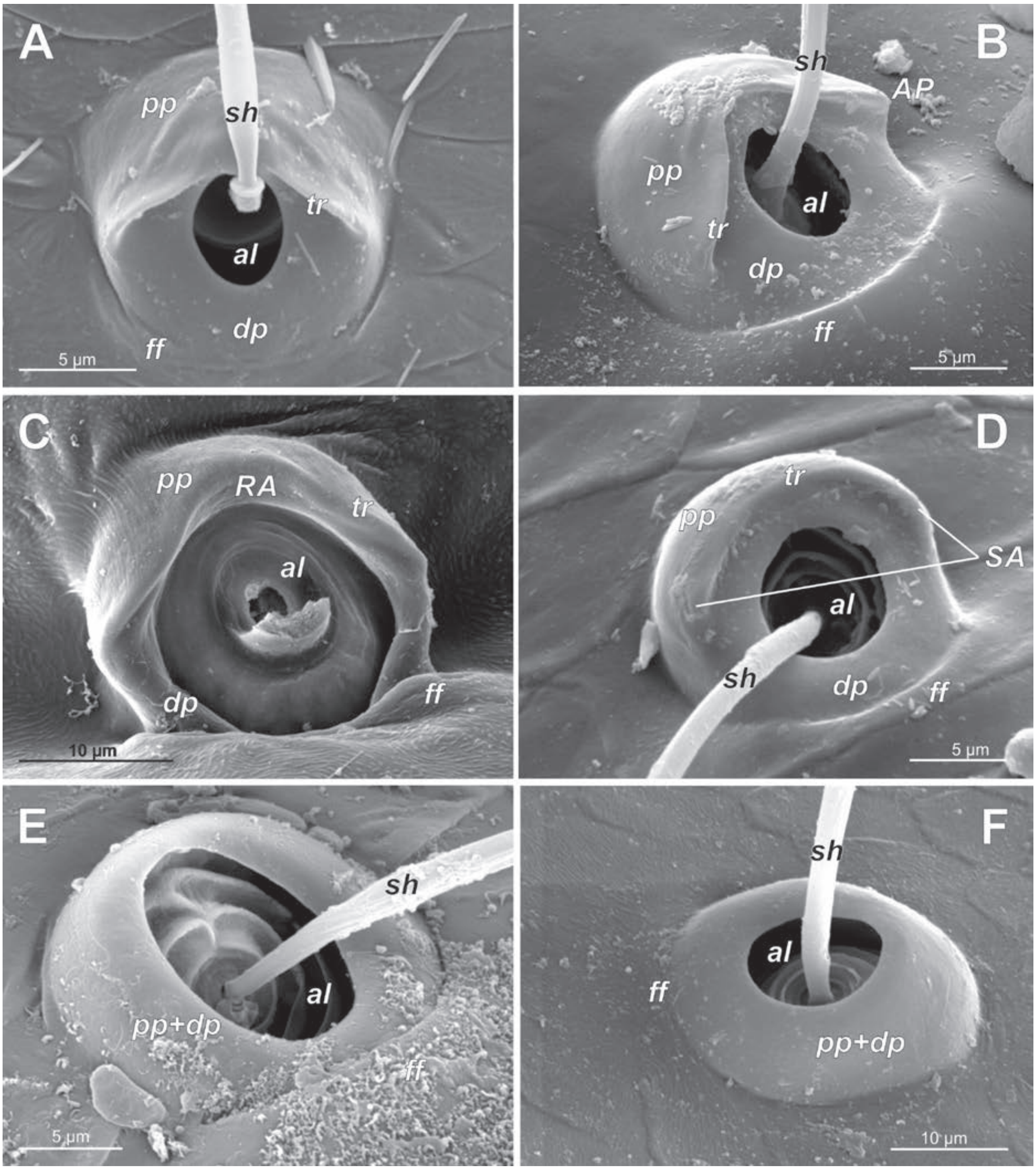

Figure 3. Typology of araneoid bothria (I). **A–D** 'E-type, *Erigone* type' (ancestral) **E, F** 'T-type, *Theridion* type' (advanced) **A** *Erigone dentipalpis*, (E-type) **B** *Chilenodes australis* (E-type) **C** *Chrysometa alajuela* (E-type) **D** *Melychiopharis* sp. (E-type) **E** *Theridion tinctum* (T-type) **F** *Nephila* sp. (T-type). Abbreviations: *al* alveolus; *AP* angle with clear apex of proximal plate; *dp* distal plate; *ff* frontal fold; *pp* proximal plate; *pp+dp* fused proximal and distal plates; *RA* round apex; *SA* semicircular arch; *sh* shaft; *tr* transverse ridge of proximal plate.

socket [...]. In some cases, the margin is well marked, although not overhanging [...]. 1. Not well differentiated. The distal margin of the hood is tenuous, superficial, not well marked [...]. 2. Homogeneous. The bothrium is smooth, without distinction into proximal and distal plates [...]. States are ordered, as state 1 is intermediate between states 0 and 2" (Ramírez 2014: char. 176).

The trend in the araneoid bothria transformation seems exactly like this. The ancestral type in the superfamily Araneoidea is a 'hooded' bothria with a single well-developed transverse ridge, dividing its proximal and distal plates, named herein ‘*Erigone*-type’ (Fig. 3A–D); the advanced type is a solid dome-like (“homogeneous”, “evenly rounded and lack a hood”) bothria without vestiges of the ridge: ‘*Theridion*-type’ (Fig. 3E, F); and there are several intermediate cases reflecting various pathways and stages of the ridge reduction, all united herein as the ‘*Argiope*-type’ (Fig. 4A–F).

Several subtypes in each of the three above types may be recognized. However, in, e.g., the ‘*Erigone*-type’ we face a continuous series of a bothria ridge configuration, from an angle with a clear apex (*AP*, Fig. 3B) to a semicircular arch (*SA*, Fig. 3D), via an angle with a rounded apex (*RA*, Fig. 3C). The regularities of a gradual ridge reduction in the ‘*Argiope*-type’ strictly correspond to those described in dionychans: “Trichobothria proximal and distal plates medial differentiation: 0. Hood entire, differentiated [...]. 1. Hood not differentiated medially. The distal margin of the hood is only marked at the sides [...]” (Ramírez 2014: char. 177). The disappearance of a ridge, if it occurs, always begins from its medial portion (Fig. 4C, D), and at the edges of this gradient, bothria hard to classify may be found; is it (Fig. 4B) already the ‘*Argiope*’ or yet the ‘*Erigone*’ type? Is it (Fig. 4E, F) yet the ‘*Argiope*’ or already the ‘*Theridion*’ type? Ramírez (2014: char. 178) has faced such a problem too: “Some terminals had intermediate or ambiguous conditions”, and it is an objective irremovable difficulty of any typological procedure.

However, let us try to formalize the ‘dividing lines’ between the recognized here three main bothrial types: the ancestral ‘*Erigone*-type’, the advanced ‘*Theridion*-type’, and the intermediate ‘*Argiope*-type’. We count a bothrium among the ancestral ‘*Erigone*-type’ if its transverse ridge, angled or rounded, persists an unbroken (vs a ridge distinctly erased in at least its medial portion, as in, e.g., Fig. 4B). And we count a bothrium among the advanced ‘*Theridion*-type’ type if it is a correct dome without any vestiges of a ridge and with an alveolus is present strictly at the dome top (vs an alveolus persists at the more or less fattened frontal portion of a dome corresponding to a distal plate, as in e.g., Fig. 4F).

Thus, a simplification seems a general trend in bothrial evolution in araneoids, as well in dionychans (Ramírez 2014) and in mygalomorphs (Eskov et al. 2024); its final point is the bothria with the initial structures fused in one dome.

Distribution of various bothrial types in various lineages of Araneoidea

The system of Araneoidea adopted in this study was proposed by Eskov and Marusik (2023) as a reconciliation of the ‘morphological’ and ‘molecular’ cladograms of the superfamily by Griswold et al. (1998) and by Dimitrov et al. (2017). The higher-rank Araneoidea subtaxa (‘branches’ and ‘lineages’) are listed below in the systematic order corresponding to the superfamily cladogram (Fig. 1), whereas the lower-rank subtaxa (the families in a ‘lineage’ and subfamilies/tribes in a family) are listed in alphabetical order. The names and abbreviation of the suprageneric taxa are listed according to their ranks, in the text below, in the list of specimens examined (Suppl. material 1), as well as in the cladograms, are as follows: ‘branches’ (four capital letters), ‘lineages’ (two capital letters), families (three lowercase letters, in round brackets) and subfamilies/tribes (five lowercase letters, in brackets). If the conventional division of a family to subfamilies/tribes is not established, we conditionally list all its members as a ‘nominative subfamily’ (marking it by the usual five lowercase letters in brackets).

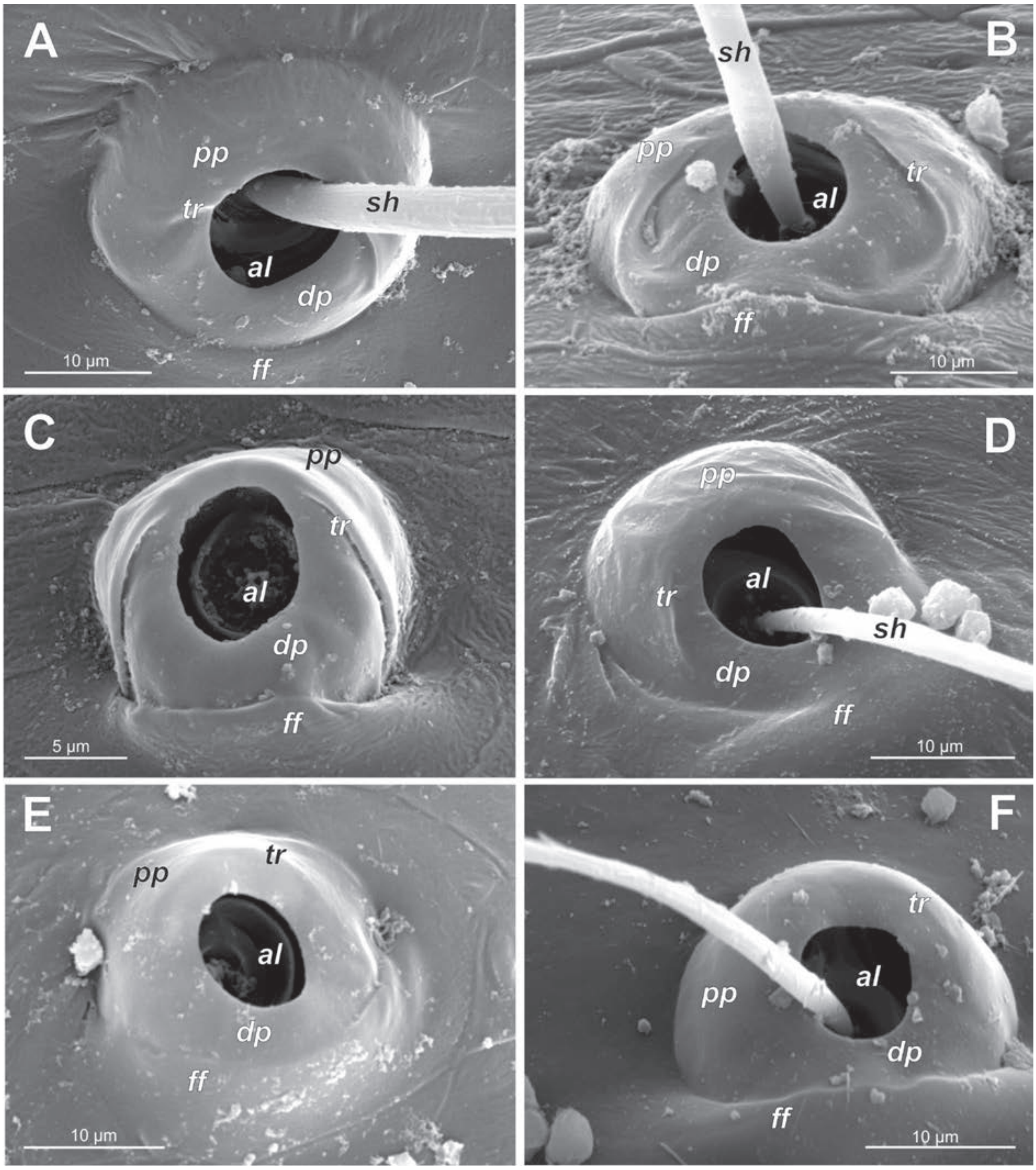

Figure 4. Typology of araneoid bothria of the *Argiope* type (intermediate) (II) **A** *Argiope bruennichi* **B** *Nanometa* sp. **C** *Synotaxus* sp. **D** *Stemonyphantes lineatus* **E** *Ero furcata*, leg 2 tibia **F** *Eidmannella pallida*. Abbreviations: *al* alveolus; *dp* distal plate; *ff* frontal fold; *pp* proximal plate; *pp+dp* fused proximal and distal plates; *sh* shaft; *tr* transverse ridge of proximal plate.

'Tetragnathoid branch', TETR

1. 'Malkariod lineage', MA
1.1. Malkaridae Davies, 1980 (Mal).
1.1.1. Malkarinae Davies, 1980 [Malka].
1.1.2. Sternoidinae Moran, 1986 [Stern].
1.1.3. Tingotinginae Hormiga & Scharff, 2020 [Tingo].
1.2. Pararchaeidae Forster & Platnick, 1984 (Par). Conventional subfamilies/tribes are not established [Parar].

Malkaroids were listed in former times in various, very distant, spider superfamilies: Palpimanidae, Zodariidae, Archaeidae, Mecysmaucheniidae, Mimetidae, and Araneidae (see review in Hormiga and Scharff 2020). Finally, Dimitrov et al. (2017) based on molecular data, united pararchaeids with malkarids in a common lineage and nested it into the superfamily Araneoidea as the sister group of 'tetragnatoids'; the family Pararchaeidae was ranked by them as a subfamily of Malkaridae.

However, pararchaeids are distinguished from all other malkarids by a number of important apomorphies (i.e., the elevated chelicerae arising from a distinct, fully sclerotized foramen in the prosoma; pars cephalica steeply elevated from pars thoracica above the level of coxae III or IV; the presence of cheliceral peg teeth and the absence of a tarsal claw on the female pedipalp). Due to the fact that both taxa "turned out to be reciprocally monophyletic" (Hormiga and Scharff 2020: 348), Eskov and Marusik (2023) conserved for them ranks of independent sister families. No suprageneric taxa were distinguished in Pararchaeidae by Rix (2006); malkarids were divided by Hormiga and Scharff (2020) to Sternoidinae, Tingotinginae, and Malkarinae.

1.1. Malkaridae (Mal).

The bothria of three genera representing all three malkarid subfamilies are studied here:

Malkarinae: *Malkara* Davies, 1980 (Fig. 5B);
Sternoidinae: *Chilenodes* Platnick & Forster, 1987 (Fig. 5A);
Tingotinginae: *Tingotingo* Hormiga & Scharff, 2020 (Fig. 5C, D).

In addition, the bothria of the three malkarid genera have been illustrated earlier: the sternoidin *Perissopmeros* Butler, 1932 (Moran 1986: fig. 17, as *Sternodes* Butler, 1932), *Malkara* (Davies 1980: fig. 9), and *Chilenodes* (Platnick and Forster 1987: fig. 18). The bothria of all three malkarid subfamilies belong to the '*Erigone*-type' but differ in shape. A transverse ridge dividing the proximal bothrial plate (the 'hood') and the distal one is angled in sternodines (*ap*, Figs 3B, 5A; Moran 1986: fig. 17) and widely rounded in tingotingines (Fig. 5C, D); in the malkarines the ridge is angled, while the 'hood' itself is strongly swollen (Fig. 5B; Davies 1980: fig. 9), and its shape seems to be unique among araneoids. The setal shaft of *Tingotingo* (Fig. 5C) is very long and distinctly plumose.

1.2. Pararchaeidae (Par).

The bothria of two pararchaeid genera are studied here: *Anarchaea* Rix, 2006 and *Flavarchaea* Rix, 2006 (Fig. 5E, F). In addition, the bothrium of *Forstrarchaea* Rix, 2006 has been illustrated earlier by Forster and Platnick (1984: fig. 224, as *Pararchaea* Forster, 1955). The bothria of pararchaeids appear very uniform: the 'hooded' bothria of the '*Erigone*-type', with a distinct angled transverse ridge. The diversity of the bothrial types in the 'malkaroid lineage' is summed in Fig. 28.

2. 'Tetragnathoid lineage', TE.
2.1. Arkyidae L.Koch, 1872 (Ark). Conventional subfamilies/tribes are not established [Arkyi].
2.2. Mimetidae Simon, 1881 (Mim).
2.2.1. Gelanorinae Mello-Leitão, 1935 [Gelan].

2.2.2. Mimetinae Simon, 1881 [Mimet].
2.2.3. Oarcinae Simon, 1890 [Oarci].
2.3. Tetragnathidae Menge, 1866 (Tet).
2.3.1. Diphyainae Simon, 1894 [Diphy].
2.3.2. Leucauginae Caporiacco, 1955 [Leuca].
2.3.3. Metainae Simon, 1894 [Metai].
2.3.4. Nanometinae Forster, 1999 [Nanom].
2.3.5. Tetragnathinae Menge, 1866 [Tetra].

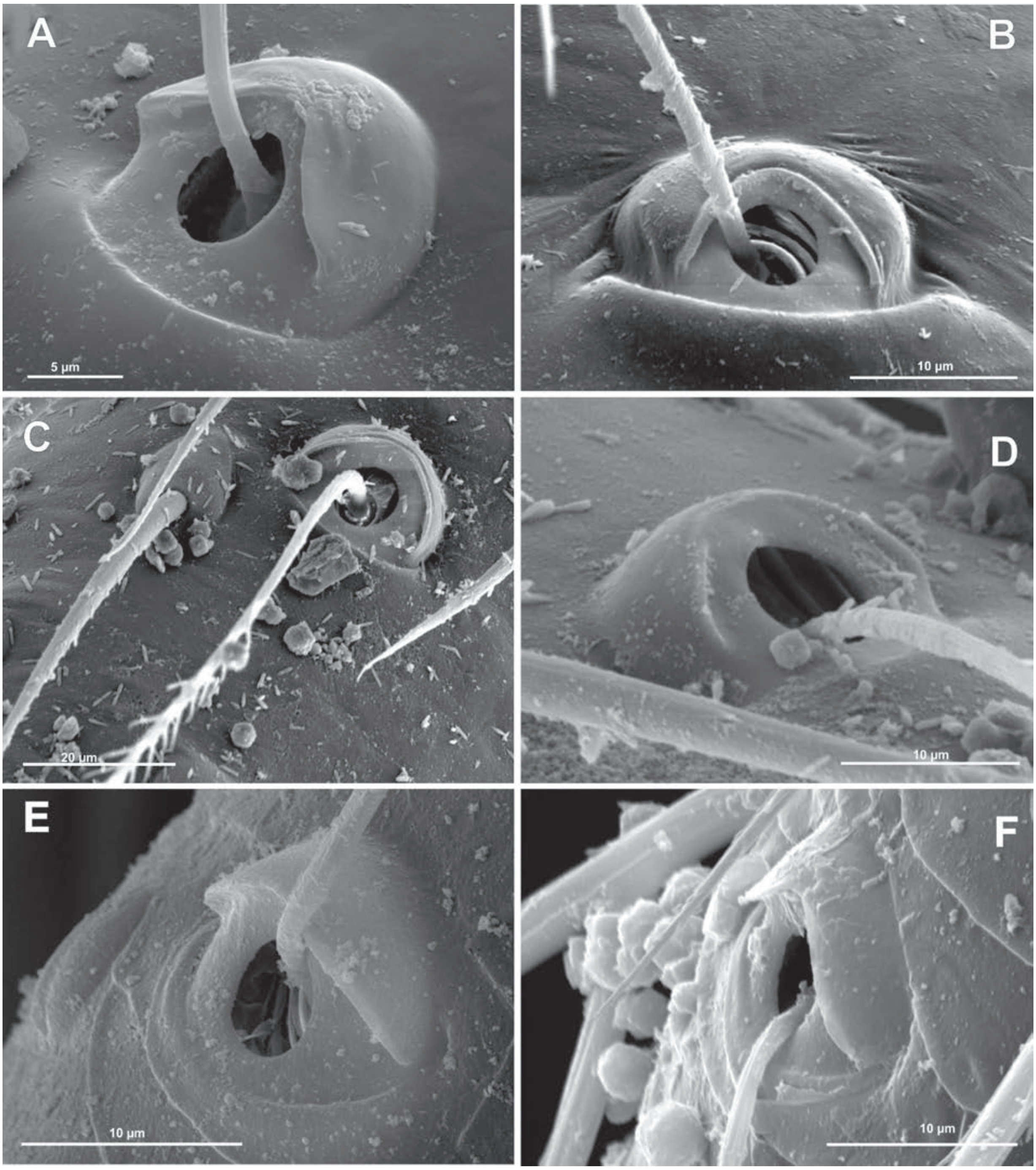

Figure 5. Bothria of 'Malkaroid lineage' of the *Erigone* type: Malkaridae (Malkarinae, Sternoidinae, Tingotinginae), Pararchaeidae **A** *Chilenodes australis*, ti 3 (E-type) **B** *Malkara* sp., ti 2 (E-type) **C** *Tingotingo* sp., ti 4 (E-type) **D** the same **E** *Flavarchaea lulu*, ti 1 (E-type) **F** *Anarchaea corticola*, mt 3 (E-type).

‘Enlarged tetragnathoids’ were established by Dimitrov and Hormiga (2011) and Dimitrov et al. (2017) based on the molecular data; this lineage unites Tetragnathidae, Arkyidae, and Mimetidae, and is the sister group of ‘malkaroids’ (Hormiga and Scharff 2020: fig. 2). Arkyids were formerly considered an araneid subfamily, comprising two endemic Australian genera, *Arkys* Walckenaer, 1837 and *Demadiana* Strand, 1929 (Scharff and Coddington 1997; Framenau et al. 2010). Later they were re-ranked and relocated: “The arkyines (which we rank at the family level in our revised classification), represented here by nine terminals, are monophyletic and well supported but do not fall within Araneidae (where they are currently classified); instead, the arkyine clade is sister group to Tetragnathidae and this lineage is sister to Mimetidae” (Dimitrov et al. 2017: 229).

Mimetids (‘pirate spiders’ or ‘werewolf spiders’) are webless specialized araneophages, using the so-called ‘aggressive mimicry’. Currently, three subfamilies are recognized in mimetids: the globally distributed Mimetinae, the Neotropical Gelanorinae, and the endemic (southernmost South America) Oarcinae (Platnick and Shadab 1993). Recently, Benavides and Hormiga (2020), based on the molecular data and following Dimitrov et al. (2012), nested oarcins in araneids, but Eskov and Marusik (2023) refuted this relocation. In addition to the webless lifestyle and leg spination with the typically mimetid ‘capture basket’ (Platnick and Shadab 1993: figs 10, 11), the chelicerae of both oarcin genera, *Oarces* Simon, 1879 and *Gnolus* Simon, 1879, possess pore-bearing gland mounds and promarginal peg teeth replacing true teeth (Platnick and Shadab 1993: figs 16–18, 21–23), i.e., the key synapomorphies of Mimetidae never reported in Araneidae.

The orb-weaving tetragnathids were divided by Dimitrov and Hormiga (2011) into five subfamilies: Tetragnathinae, Leucauginae, Metainae, Diphyainae, and Nanometinae. Four tetragnathid genera of unclear subfamilial position (according to Álvarez-Padilla et al. 2009) are nested in this study according the cladogram given by Álvarez-Padilla and Hormiga (2011: fig. 144): *Allende* Álvarez-Padilla, 2007 and *Mollemeta* Álvarez-Padilla, 2007 in Tetragnathinae, *Chrysometa* Simon, 1894 in Diphyainae; as regards *Azilia* Keyserling, 1881, it is “either sister to Leucauginae with the morphology and behaviour data, or sister to all other tetragnathids with all data [mainly molecular] combined” (Álvarez-Padilla and Hormiga 2011: 728), and is listed here as ‘Tetragnathidae incertae sedis’. The East Asian genus *Guizygiella* Zhu, Kim & Song, 1997, placed in the monotypic subfamily Guizygiellinae by Zhu et al. (2003), was recently transferred by Kallal and Hormiga (2022) from Tetragnathidae to Araneidae.

2.1. Arkyidae (Ark).

The bothria of the single arkyid genus (of the couple comprising this family), *Arkys* Walckenaer, 1837, is studied here (Fig. 6F). It has the ‘hooded’ bothria of the ‘*Erigone*-type’ with an angled transverse ridge.

2.2. Mimetidae (Mim)

The bothria of four genera representing all three mimetid subfamilies are studied here:

Oarcinae: *Oarces* Simon, 1879 (Fig. 6A); Gelanorinae: *Gelanor* Thorell, 1869 (Fig. 6B); Mimetinae: *Ero* C. L. Koch, 1836 and *Australomimetus* Heimer, 1986

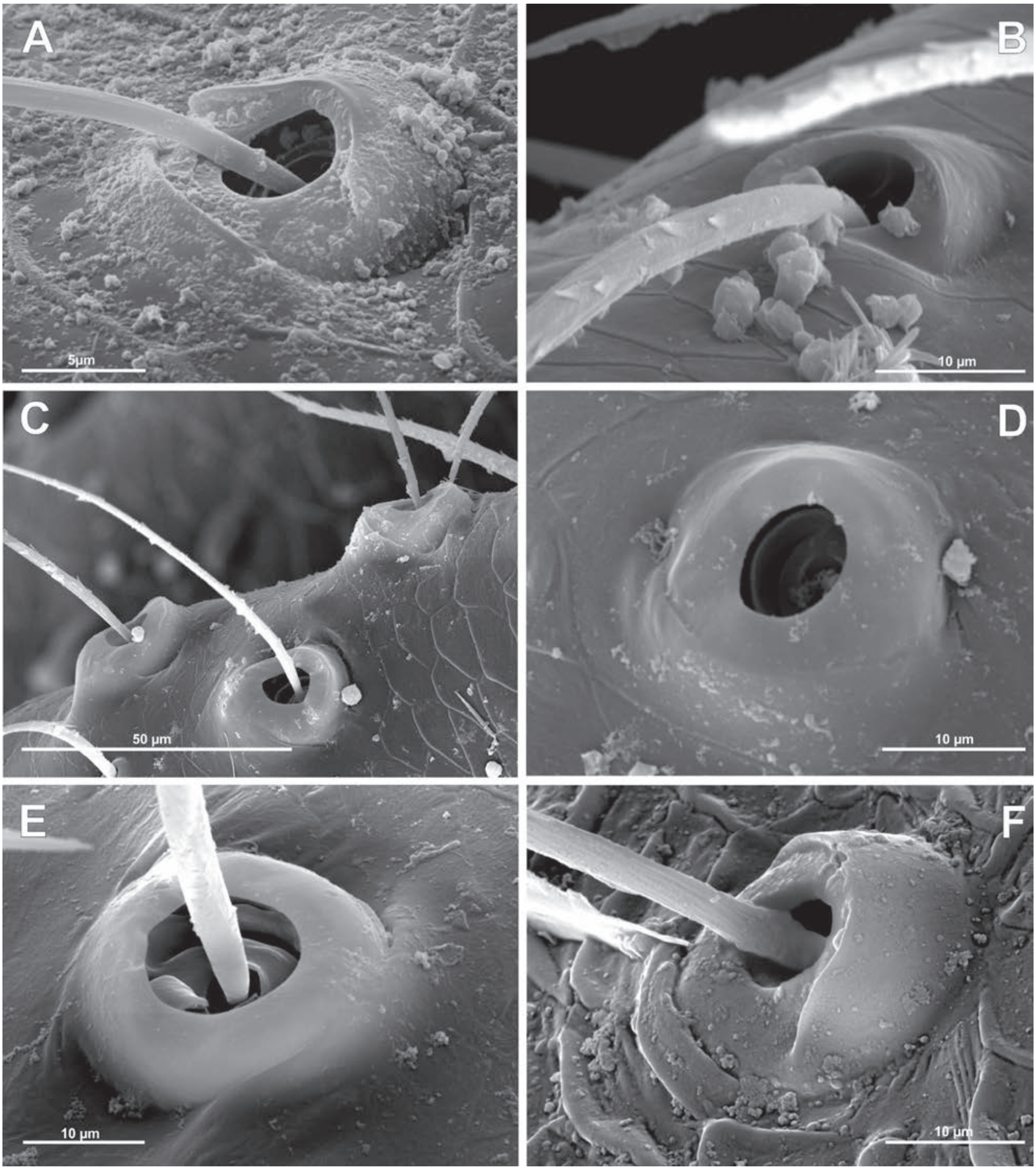

Figure 6. Bothria of 'Tetragnathoid lineage': Mimetidae (Oarcinae, Gelanorinae, Mimetinae), Arkyidae **A** *Oarces reticulatus*, ti 3 (E-type) **B** *Gelanor* sp., ti 3 (E-type) **C** *Ero furcata*, male palpal tibia (E-type) **D** *Ero furcata*, ti 2, (A-type) **E** *Australomimetus tasmanensis*, ti 3 (T-type) **F** *Arkys alticephala*, ti 2 (E-type).

(Figs 4E, 6C–E). In addition, the bothria of the two mimetin genera have been illustrated earlier: *Mimetus* Hentz, 1832 (Griswold et al. 2005: fig. 149G) and *Australomimetus* (Forster and Platnick 1984: fig. 385). Platnick and Shadab (1993: fig. 13) have figured the bothrium of *Oarces*, and even mentioned its shape in the diagnosis of the subfamily: "[Oarcines] resemble mimetines in cheliceral gland mound and peg tooth morphology, as well as in having relatively smooth trichobothrial bases" (Platnick and Shadab 1993: 13); but this is clearly a misidentification: they dealt, in fact, with a setal socket instead of a bothrium. All three main bothrial types are present in Mimetidae. The bothria of Oarcinae and Gelanorinae both belong to the '*Erigone*-type', although the bothrial transverse ridge is angled in oarcines (Fig. 6A) but rounded in the gelanorines (Fig. 6B). By contrast, the mimetin genera *Australomimetus* (Fig. 6E; Forster and Platnick 1984: fig. 385) and *Mimetus* (Griswold et al. 2005: fig. 149G) both possess dome-like bothria that belong to the '*Theridion*-type'. However, in the other mimetin genus, *Ero*, the composition of bothrial types seems to be unique. The bothria of its leg joints have a ridge smoothed over the entire length (Fig. 6D) and belong to the intermediate '*Argiope*-type'. By contrast, the bothria of a male papal tibia possess a clear rounded ridge (Fig. 6E), and thus should be attributed to the '*Erigone*-type'. The bothria of the male papal tibia sometimes differ from those of the leg joints (e.g., in physoglenid *Pahora* Forster, 1990: fig. 23A, B), but they never belong to two different types.

2.3. Tetragnathidae (Tet).

The bothria of 16 genera representing all five tetragnathid subfamilies are studied here:

Diphyainae: *Chrysometa* Simon, 1894, *Diphya* Nicolet, 1849, and Diphyainae gen. sp. 1 (Fig. 7A–C); Leucauginae: *Leucauge* White, 1841 and *Metleucauge* Levi, 1980 (Fig. 8A, B); Metainae: *Meta* C.L. Koch, 1835 and *Metellina* Chamberlin & Ivie, 1941 (Fig. 8C, D); Nanometinae: *Nanometa* Simon, 1908, *Orsinome* Thorell, 1890 and *Pinkfloydia* Dimitrov & Hormiga, 2011 (Fig. 7D–F); Tetragnathinae: *Allende* Álvarez-Padilla, 2007, *Cyrtognatha* Keyserling, 1881, *Mollemeta* Álvarez-Padilla, 2007, *Pachygnatha* Sundevall, 1823 and *Tetragnatha* Latreille, 1804 (Fig. 9A–E); Tetragnathidae incertae sedis: *Azilia* Keyserling, 1881 (Fig. 9F).

No tetragnathid bothria have been illustrated in detail previously; numerous SEM images by Álvarez-Padilla and Hormiga (2011) reflect only the trichobothrial pattern of the legs, but not the bothrial morphology. All three bothrial types are represented in Tetragnathidae, and there are at least two types in every subfamily. Both the '*Erigone*-type' and the more advanced '*Argiope*-type' are combined in the three subfamilies: the Diphyainae (*Chrysometa*: Fig. 7A and Diphyainae gen. sp.1: Fig. 7B vs *Diphya*: Fig. 7C, respectively); in Nanometinae (*Pinkfloydia*: Fig. 7D vs *Nanometa*: Fig. 7E and *Orsinome*: Fig. 7F, respectively); and in Leucauginae (*Leucauge*: Fig. 8A vs *Metleucauge*: Fig. 8B, respectively). Both the intermediate '*Argiope*-type' and the advanced '*Theridion*-type' are combined in the subfamily Metainae (*Meta*: Fig. 8C vs *Metellina*: Fig. 8D, respectively). Finally, all three bothrial types are represented in Tetragnathinae: '*Erigone*-type' in *Cyrtognatha* and *Allende* (Fig. 9A and Fig. 9B, respectively); '*Argiope*-type' in *Mollemeta* (Fig. 9C); and '*Theridion*-type' in *Pachygnatha* and *Tetragnatha* (Fig. 9D and Fig. 9E, respectively). The diversity of the bothrial types in the 'Tetragnatoid lineage' is summarized in Fig. 28.

'Araneoid branch', ARAN

3. 'Araneoid lineage', AR
3.1. Araneidae Clerck, 1757 (Ara).
3.1.1. Araneinae Clerck, 1757 [Arane].

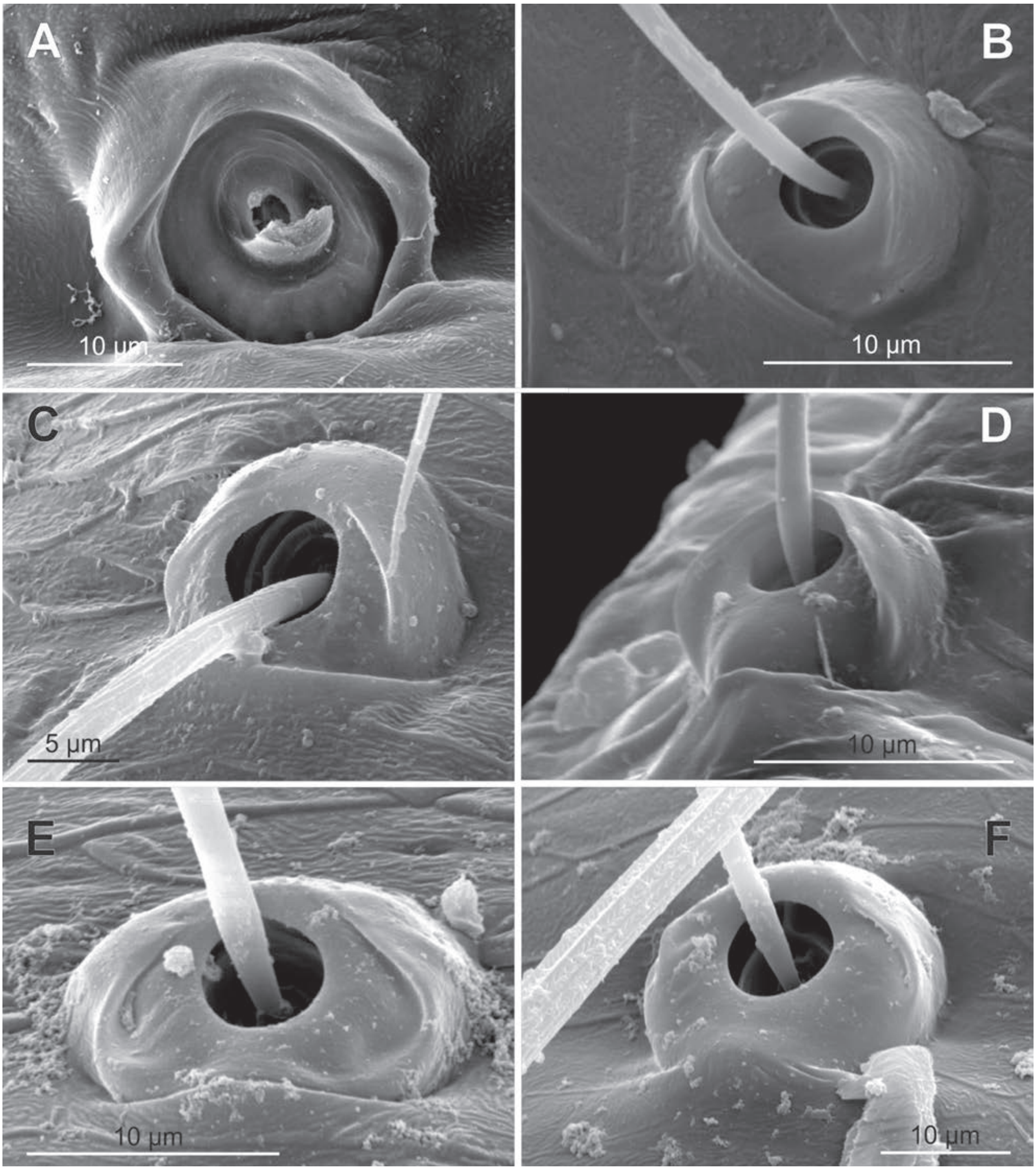

Figure 7. Bothria of 'Tetragnathoid lineage': Tetragnathidae (Diphyainae, Nanometinae) **A** *Chrysometa alajuela*, ti 3 (E-type) **B** Diphyainae gen. sp., ti 4 (E-type) **C** *Diphya wulingensis*, ti 3 (A-type) **D** *Pinkfloydia* sp., ti 3 (E-type) **E** *Nanometa* sp., ti 3 (A-type) **F** *Orsinome sarasini*, ti 3 (A-type).

3.1.2. Argiopinae Simon, 1890 [Argio].
3.1.3. Cyrtarachninae Simon, 1895 [Cyara].
3.1.4. Cyrtophorinae Simon, 1895 [Cypho].
3.1.5. Gasteracanthinae O. Pickard-Cambridge, 1871 [Gaste].
3.1.6. Micratheninae Simon, 1895 [Mithe].
3.1.7. Guizygiellinae Zhu, Song & Zhang, 2003 [Guizy].
3.1.8. Caerostrini Simon, 1895 [Caero].

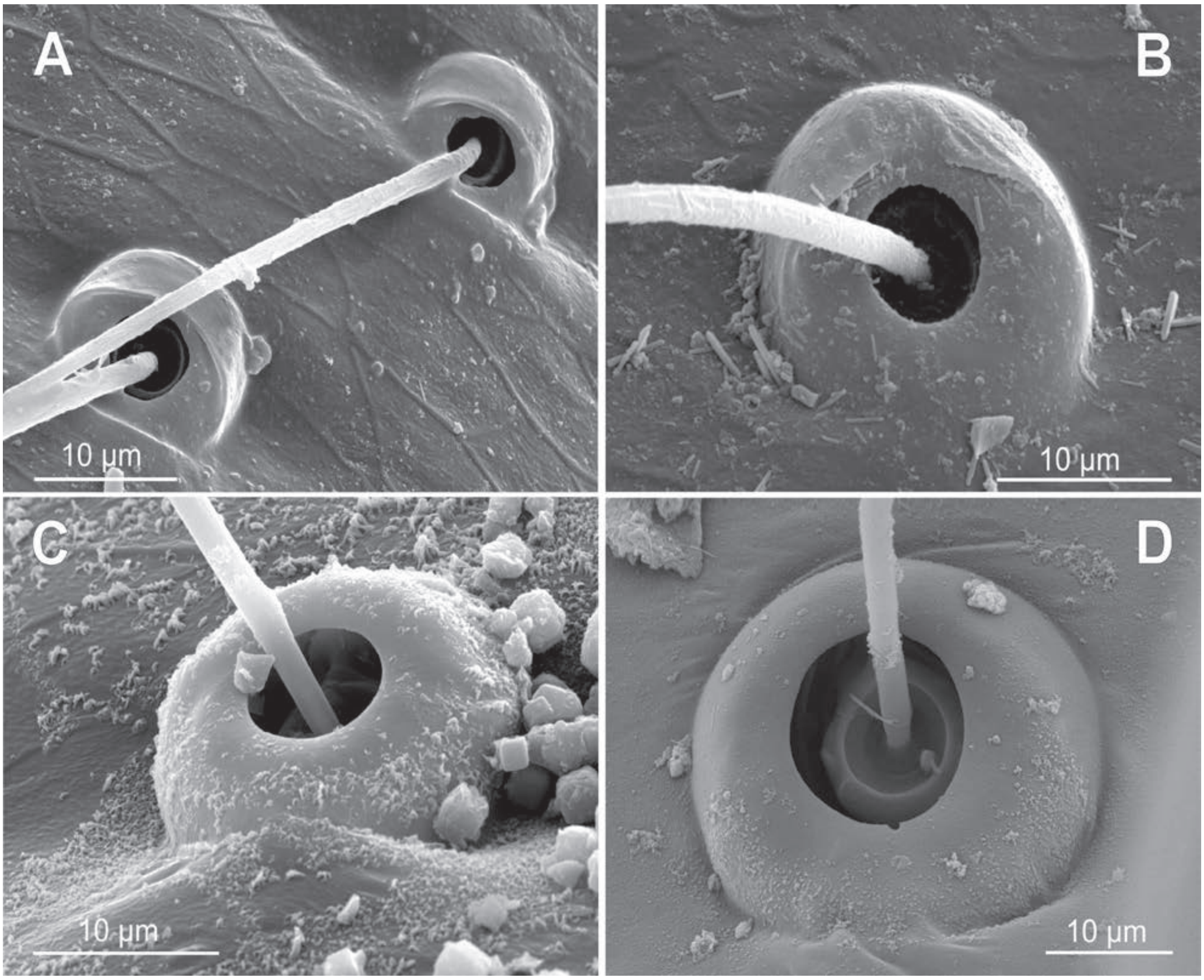

Figure 8. Bothria of 'Tetragnathoid lineage', Tetragnathidae (Leucauginae, Metainae) **A** *Leucauge granulata*, ti 3 (E-type) **B** *Metleucauge dentipalpis*, ti 3 (A-type) **C** *Metellina mengei*, ti1 (A-type) **D** *Meta menardi*, ti 3 (T-type).

3.1.9. Hypognathini Simon, 1895 [Hypog].
3.1.10. Poltyini Simon, 1895 [Polty].
3. 1. 11. Testudinarini Simon, 1895 [Testu].
3.2. Nephilidae Simon, 1894 (Nep). Conventional subfamilies/tribes are not established [Nephi].
3.3. Zygiellidae Simon, 1929 (Zyg). Conventional subfamilies/tribes are not established [Zygie].

Araneidae formerly were usually considered (i.e., before the recognition of 'enlarged Tetragnathoids' by Dimitrov et al. [2017]) as a sister group of the other Araneoidea (e.g., Scharff and Coddington 1997; Griswold et al. 1998). In the classification of araneids accepted in this paper, we follow Scharff and Coddington (1997), who recognized six subfamilies(Araneinae, Argiopinae, Cyrtarachninae, Cyrtophorinae, Gasteracanthinae, and Micratheninae), mainly corresponding to the araneid subfamilies recognized by Simon (1895); in addition, the cyrtarachnin tribe Mastophorini Mello-Leitão, 1931 (the 'bolas spiders,' possessing a unique foraging behavior) is sometimes elevated to the subfamilial rank (see Scharff and Hormiga 2012). Subfamilial assignment of several

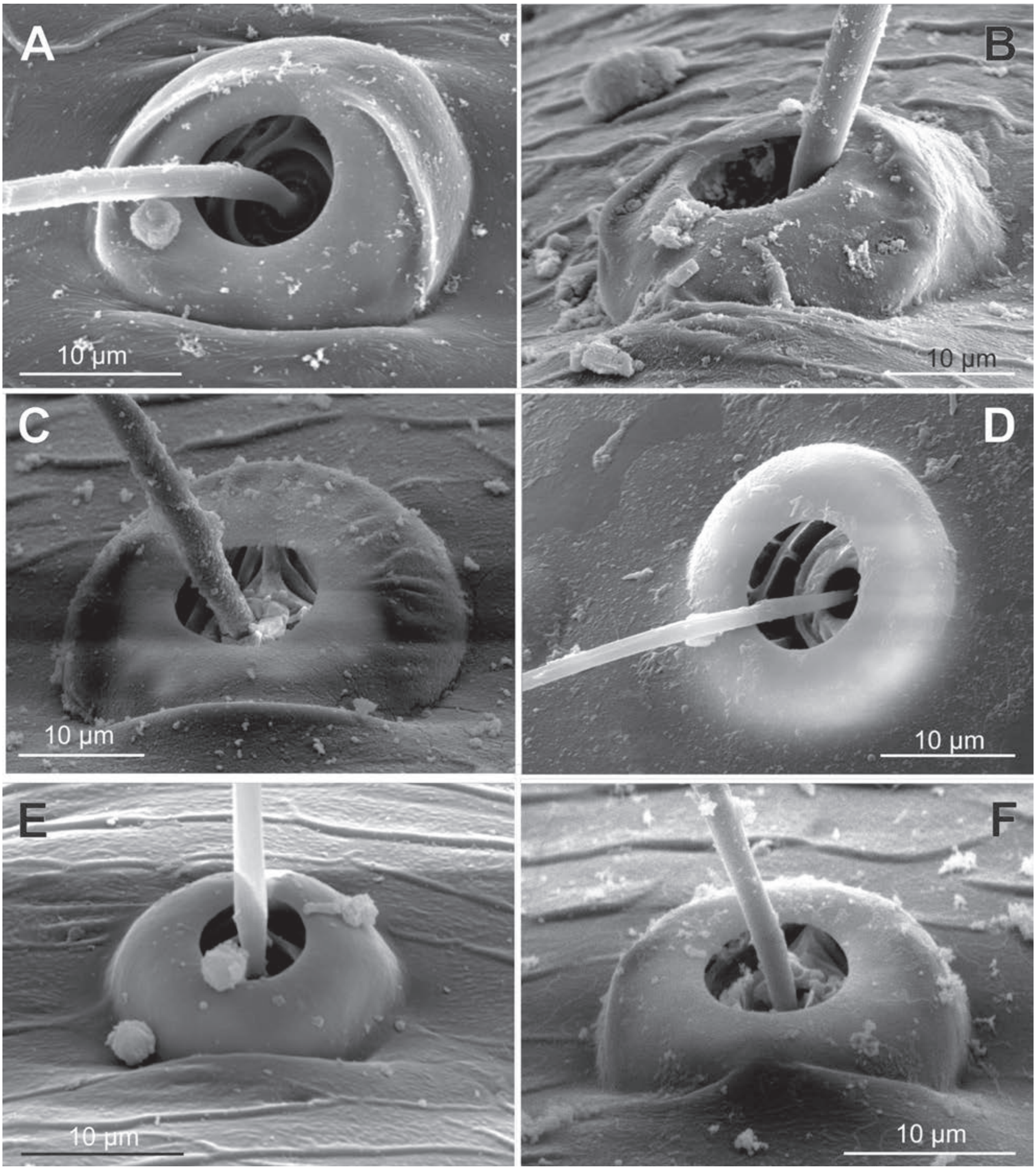

Figure 9. Bothria of 'Tetragnathoid lineage': Tetragnathidae (Tetragnathinae, Tetragnathidae incertae sedis) **A** *Cyrtognatha pachygnathoides*, ti 3 (E-type) **B** *Allende* sp., ti 3 (A-type) **C** *Mollemeta edwardsi*, ti 3 (A-type) **D** *Pachygnatha listeri*, ti 2 (T-type) **E** *Tetragnatha extensa*, ti 4 (T-type) **F** *Azilia* sp., ti 2 (A-type).

araneid genera (*Caerostris* Thorell, 1868, *Hypognatha* Guérin, 1839, *Poltys* C.L. Koch, 1843, and *Melychiopharis* Simon, 1895) is still uncertain, and herein they are listed, conditionally, in the 'old' Simon`s (1895) tribes (Caerostrini, Hypognathini, Poltyini, and Testudinarini, respectively). Kallal and Hormiga (2022) transferred the genus *Guizygiella* from Tetragnathidae to Araneidae, but did not indicate its subfamilial status; so, we are listing this genus here in the subfamily Guizygiellinae, which was not discussed by Kallal and Hormiga (2022).

Additionally, several new suprageneric clades were recently distinguished in the family cladogram by molecular methods, but the authors frankly pointed out that "few of these groups are currently corroborated by morphology, behaviour, natural history or biogeography" (Scharff et al. 2020: 1) so we have also refrained from recognizing these 'virtual clades'. Kuntner et al. (2023) established the new family Paraplectanoididae Kuntner, Coddington, Agnarsson & Bond, 2023 for the monotypic araneid genus *Paraplectanoides* Keyserling, 1886; however, Hormiga et al. (2023) returned it to Araneidae. Nephilids ('golden orbweavers') were for a long time considered a sister group of Tetragnathidae or even included in tetragnathids as a subfamily (e.g., Levi and Eickstedt 1989; Zhu et al. 2003), but recently they were clearly nested into the 'Areneoid lineage' (Álvarez-Padilla et al. 2009; Dimitrov et al. 2017; Kuntner et al. 2019). Zygiellids have been frequently relocated from araneids to tetragnathids and vice versa (see review in Gregorič et al. 2015), and finally were also nested in the 'Araneoid lineage'. Kuntner et al. (2019) transferred the Australian genus *Phonognatha* Simon, 1894 to Zygiellidae (based on molecular data) and resurrected the old name Phonognatheae Simon, 1894 (as Phonognathidae) for this newly established clade. This name was not accepted by Scharff et al. (2020) and Eskov and Marusik (2023) but confirmed by Kallal et al. (2020) and Kuntner et al. (2023).

However, the diagnosis of Phonognathidae provided by Kuntner et al. (2023: 969) contains a single morphological character: "…Distal grouping of setae on palpal tibia and elongated male palpal femur", and this character does not seem convincing. So, Phonognathidae sensu Kuntner et al. (2019) remains a purely molecular clade. Until the assignment of both type genera, *Phonognatha* and *Zygiella* F. O. Pickard-Cambridge, 1902, to a united clade is supported by morphological synapomorphies, we prefer to use the established name Zygiellidae for this taxon. Kuntner et al. (2019: 557, 563) listed the genera attributed by them to Nephilidae and Phonognathidae but have not divided these taxa to subfamilies or tribes. Hormiga et al. (2023) reranked these families as subfamilies of Araneidae but also did not assign them to the subtaxa.

3.1. Araneidae (Ara).

The bothria of 17 genera representing all six conventional araneid subfamilies and the four tribes of uncertain position are studied here: Araneinae: *Araneus* Clerck, 1757, *Cyclosa* Menge, 1866, *Hypsosinga* Ausserer, 1871, *Larinia* Simon, 1874, *Mangora* O. Pickard-Cambridge, 1889, and *Singa* C.L. Koch, 1836 (Fig. 11A–F); Argiopinae: *Argiope* Audouin, 1826 (Fig. 10C); Cyrtarachninae: *Chorizopes* O. Pickard-Cambridge, 1871 and *Cyrtarachne* Thorell, 1868 (Fig. 10A, B); Cyrtophorinae: *Cyrtophora* Simon, 1864 (Fig. 10D); Gasteracanthinae: *Gasteracantha* Sundevall, 1833 (Fig. 10F); Micratheninae: *Micrathena* Sundevall, 1833 (Fig. 10E); Caerostrini: *Caerostris* Thorell, 1868 (Fig. 12D); Hypognathini: *Hypognatha* Guérin, 1839 (Fig. 12F); Poltyini: *Poltys* C.L. Koch, 1843 (Fig. 12E); Testudinarini: *Melychiopharis* Simon, 1895 (Fig. 12A, B); Araneidae incertae sedis: Guizygiellinae: *Guizygiella* Zhu, Kim & Song, 1997 (Fig. 12C).

The bothria of only two araneid genera have been illustrated earlier: *Metepeira* F.O. Pickard-Cambridge, 1903 (Griswold et al. 1998: fig. 22E) and *Novaranea* Court & Forster, 1988 (Court and Forster 1988: fig. 552). Despite the scarcity

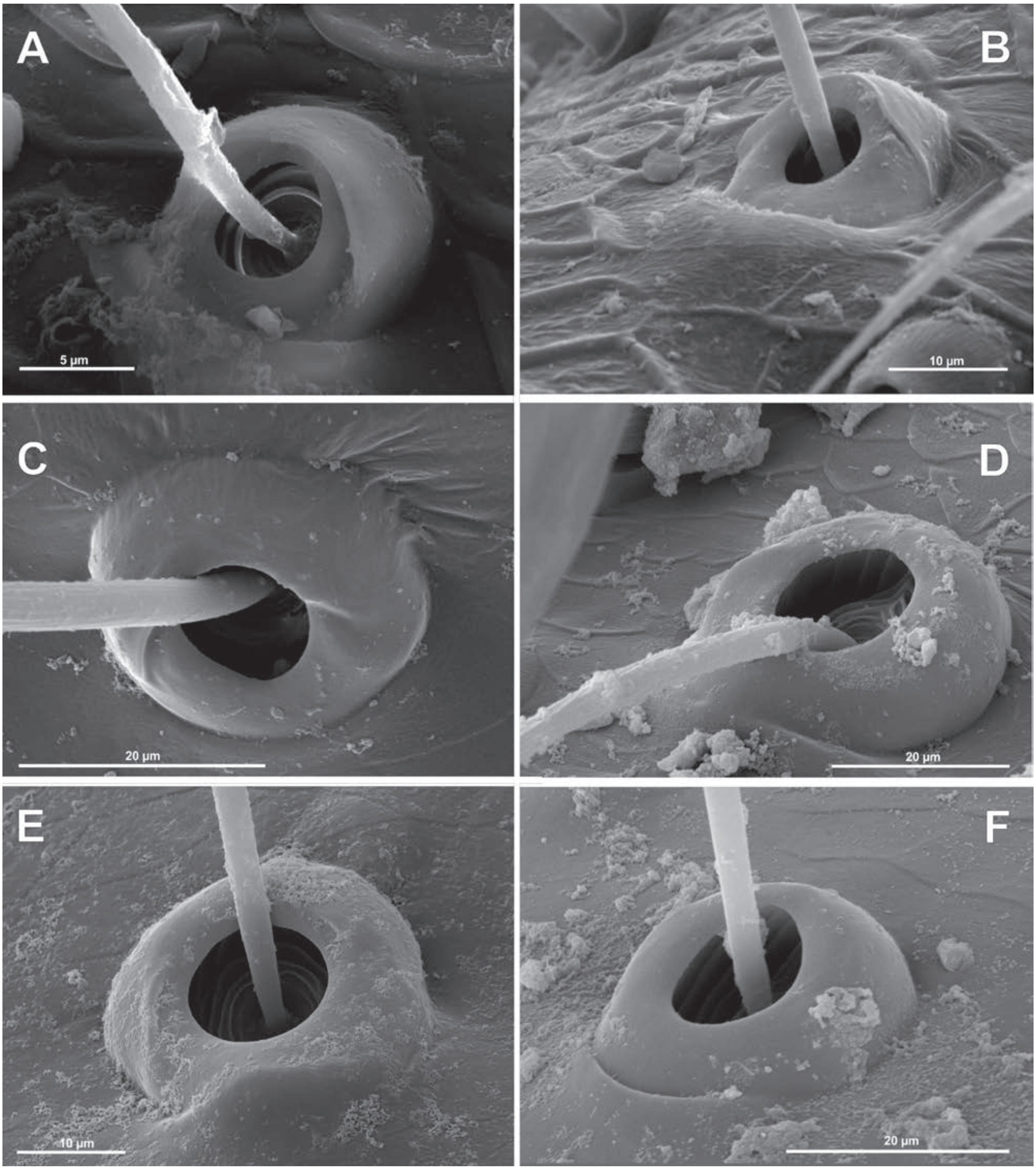

Figure 10. Bothria of 'Araneoid lineage': Araneidae (Cyrtarachninae, Argiopinae, Cyrtophorinae, Micratheninae, Gasteracanthinae) **A** *Cyrtarachne ixoides*, ti 3 (E-type) **B** *Chorizopes* sp., ti 3 (E-type) **C** *Argiope bruennichi*, ti 3 (A-type) **D** *Cyrtophora moluccensis*, ti 3 (A-type) **E** *Micrathena* sp., ti 3 (A-type) **F** *Gasteracantha diadesmia*, ti 3 (T-type).

of the available data, Court and Forster (1988: 70) provided a generalization: "The bothria arc [in araneids] smooth with the posterior hood reduced so that only lateral ridges are visible", which seems like an adequate description of the '*Argiope*-type' of bothria. In fact, however, the intermediate '*Argiope*-type' of the bothria is widespread among the araneid subtaxa, but the other bothrial types, both the ancestral '*Erigone*-type' and the advanced '*Theridion*-type', are also well represented in this family.

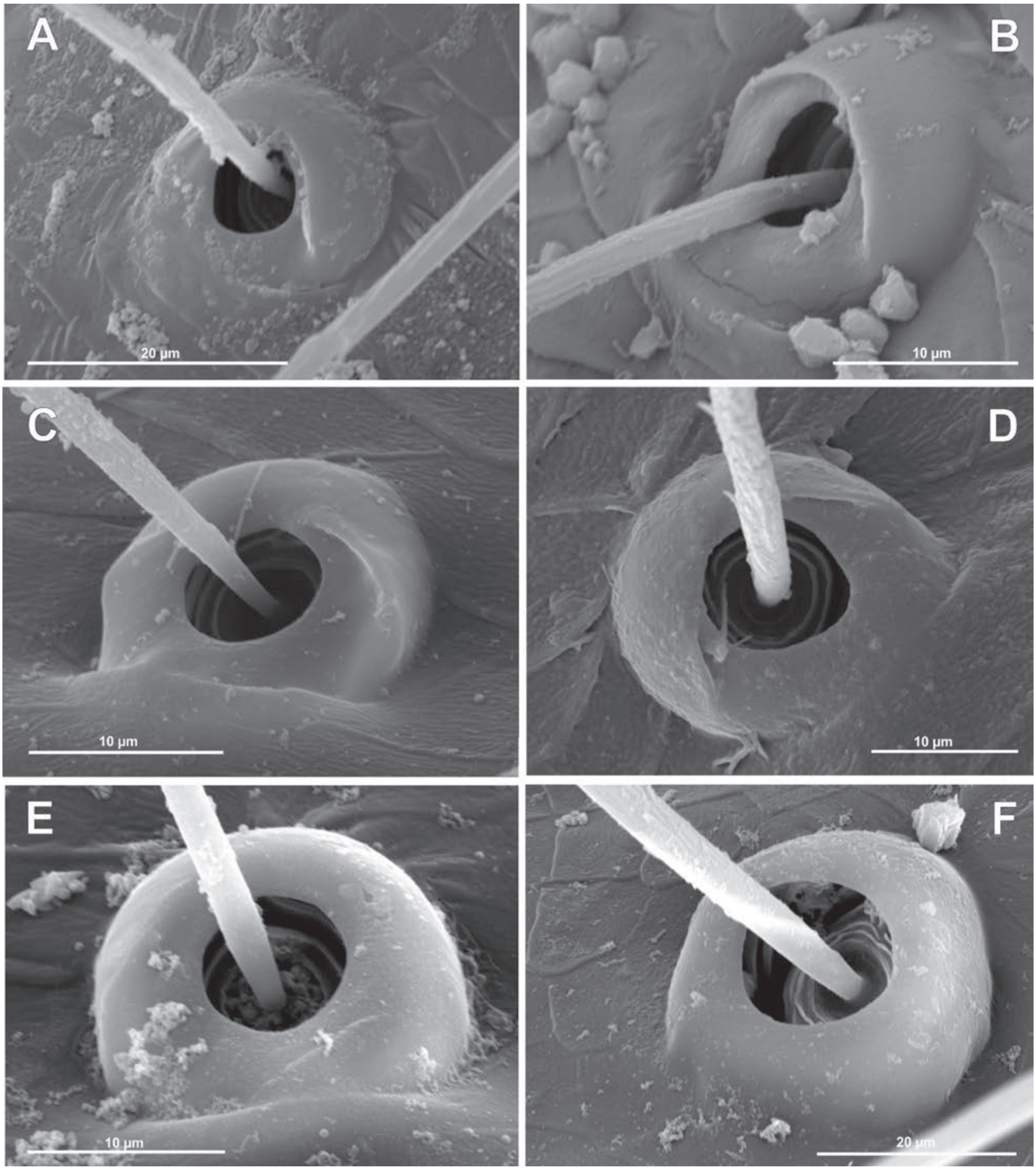

Figure 11. Bothria of 'Araneoid lineage', Araneidae (Araneinae) **A** *Singa hamata*, ti 3 (E-type) **B** *Hypsosinga pygmaea*, ti 3 (E-type) **C** *Larinia bonneti*, ti 3 (A-type) **D** *Mangora acalypha*, ti 3 (A-type) **E** *Cyclosa conica*, ti 3 (T-type) **F** *Araneus diadematus*, ti 3 (T-type).

The '*Argiope*-type' is the character of Argiopinae, Cyrtophorinae, Micratheninae, and Caerostrini (Fig. 10C–E and Fig. 12D, respectively). The '*Erigone*-type' is a character of Cyrtarachninae and Testudinarini (Fig. 10A, B and Fig. 12A, B, respectively), whereas the '*Theridion*-type' is a character of Gasteracanthinae, the Hypognathini, and the Poltyini (Figs 10F, 12F, E, respectively).

Finally, all three bothrial types are represented in Araneinae: the '*Erigone*-type' in *Singa* and *Hypsosinga* (Fig. 11A, B, respectively); the '*Argiope*-type' in *Larinia*

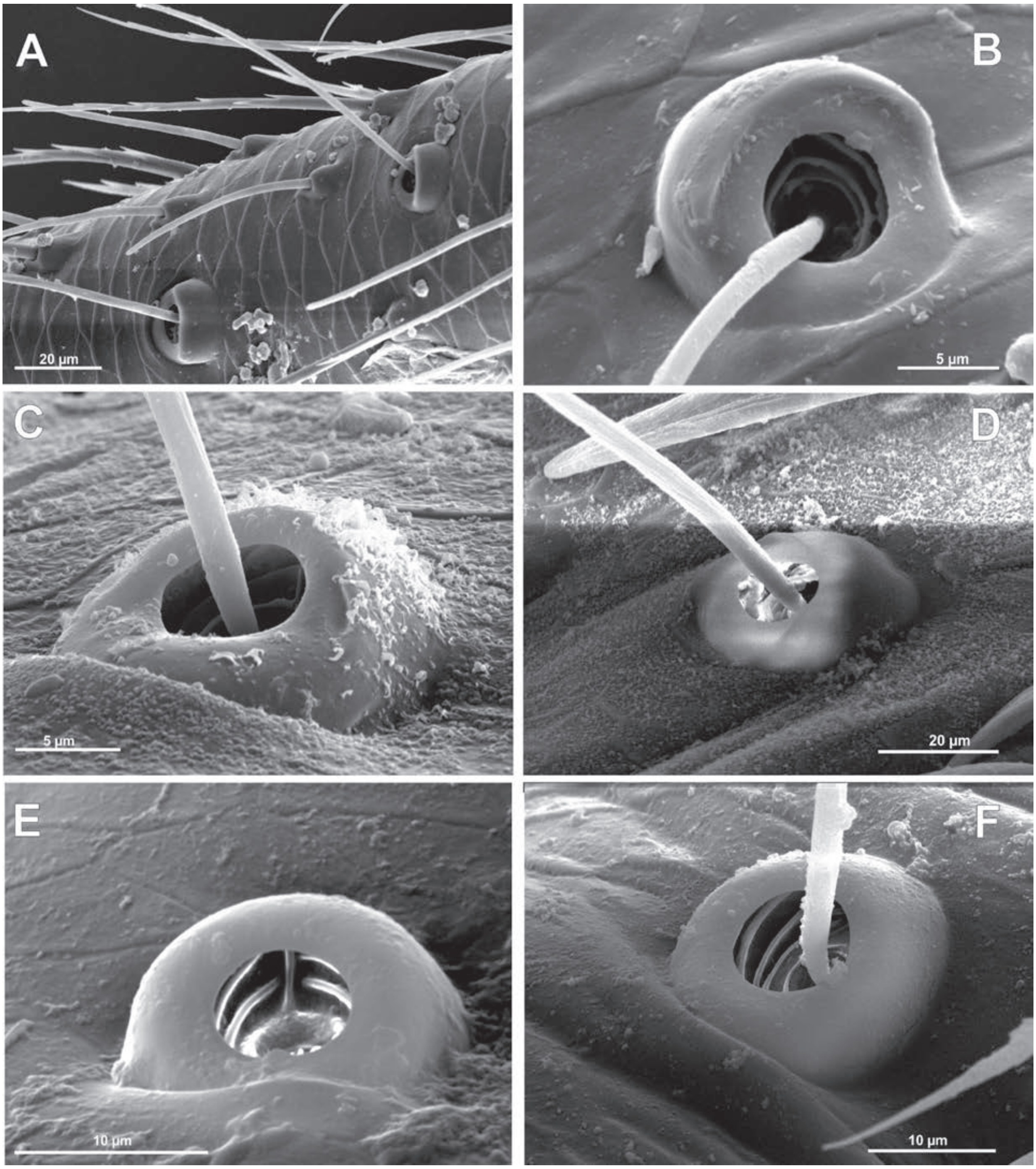

Figure 12. Bothria of 'Araneoid lineage': Araneidae (Testudinareae, Guizygiellinae, Caerostreae, Poltyeae, Hypognatheae) **A** *Melychiopharis* sp., mt 3 (E-type) **B** *Melychiopharis* sp., ti 3 (E-type) **C** *Guizygiella* sp., ti 1 (A-type) **D** *Caerostris sumatrana*, mt 4 (A-type) **E** *Poltys* sp., ti 2 (T-type) **F** *Hypognatha* sp., ti 3 (T-type).

and *Mangora* (Fig. 11C, D, respectively); and the '*Theridion*-type' in *Cyclosa* and *Araneus* (Fig. 11E, F, respectively).

It should be mentioned that the transverse ridge of the '*Erigone*-type' bothria in araneids can be either angled or rounded; however, no regularities are traceable in this respect. In cyrtarachnines the ridge is rounded in *Cyrtarachne* and angled in *Chorizopes* (Fig. 10A, B, respectively); in the araneines the ridge is angled in *Singa* and rounded in *Hypsosinga* (Fig. 11A, B, respectively); in testudinarine *Melychiopharis* the ridge is rounded (Fig. 12B).

3.2. Nephilidae (Nep).

The bothria of two nephilid genera are studied here: *Nephila* Leach, 1815 and *Nephilengys* L. Koch, 1872 (Fig. 13E, F). The bothria of both genera are the uniformly dome-like bothria and belong to the '*Theridion*-type'. It should be noted that the bothria of *Nephila* strongly vary in size (Fig. 13F).

3.3. Zygiellidae (Zyg).

The bothria of three zygiellid genera are studied here: *Leviellus* Wunderlich, 2004, *Zygiella* F. O. Pickard-Cambridge, 1902, and *Parazygiella* Wunderlich, 2004. The bothria of the '*Argiope*-type' and the '*Theridion*-type' are represented in Zygiellidae (*Leviellus*: Fig. 13B vs *Parazygiella*: Fig. 13C). Moreover, both types are recorded in the single genus *Zygiella*: the '*Argiope*-type' in *Z. x-notata* (Clerck, 1757) (Fig. 13A) vs the '*Theridion*-type' in *Z. atrica* (C.L. Koch, 1845) (Fig. 13D). The latter case could be stated as unique, but there is serious surmise that the above two *Zygiella* species are not congeneric (see below, in Discussion). The diversity of the bothrial types in the 'Araneoid lineage' is summarized in Fig. 29.

4. 'Symphytognathoid lineage', SY
4.1. Anapidae Simon, 1895 (Ana).
4.1.1. Anapinae Simon, 1895 [Anapi].
4.1.2. Gigiellinae Rix & Harvey, 2010 [Gigie].
4.1.3. Holarchaeinae Forster & Platnick, 1984 [Holar].
4.1.4. Taphiassinae Rix & Harvey, 2010 [Taphi].
4.1.5. Teutoniellinae Rix & Harvey, 2010 (stat. nov.) [Teuto].
4.2. Comaromidae Wunderlich, 2004 (Com). Conventional subfamilies/tribes are not established [Comar].
4.3. Micropholcommatidae Hickman, 1944 (Mic).
4.3.1. Micropholcommatinae Hickman, 1944 [Micph].
4.3.2. Textricellinae Hickman, 1945 [Textr].
4.4. Mysmenidae Petrunkevitch, 1928 (Mys).
4.4.1. Mysmeninae Petrunkevitch, 1928 [Mysme].
4.4.2. Mysmenopsinae Lopardo & Hormiga, 2015 [Mysps].
4.5. Symphytognathidae Hickman,1931 (Sym). Conventional subfamilies/tribes are not established [Symph].
4.6. Synaphridae Wunderlich, 1986 (Syn). Conventional subfamilies/tribes are not established [Synap].
4.7. Theridiosomatidae Simon, 1881 (Ths).
4.7.1. Epeirotypinae Archer, 1953 [Eptyp].
4.7.2. Ogulninae Coddington, 1986 [Oguln].
4.7.3. Platoninae Coddington, 1986 [Plato].
4.7.4. Theridiosomatinae Simon, 1881 [Thsom].

Forster (1959) united the minute, mainly apneumonic spiders of the families Symphytognathidae, Anapidae, Textricellidae, Micropholcommatidae, and Mysmenidae in his Symphytognathidae s. l. Later Forster and Platnick (1984) attempted to relocate micropholcommatids with textricellids from Araneoidea to their 'enlarged Palpimanoidea', but this hypothesis was refuted by Schütt (2000,

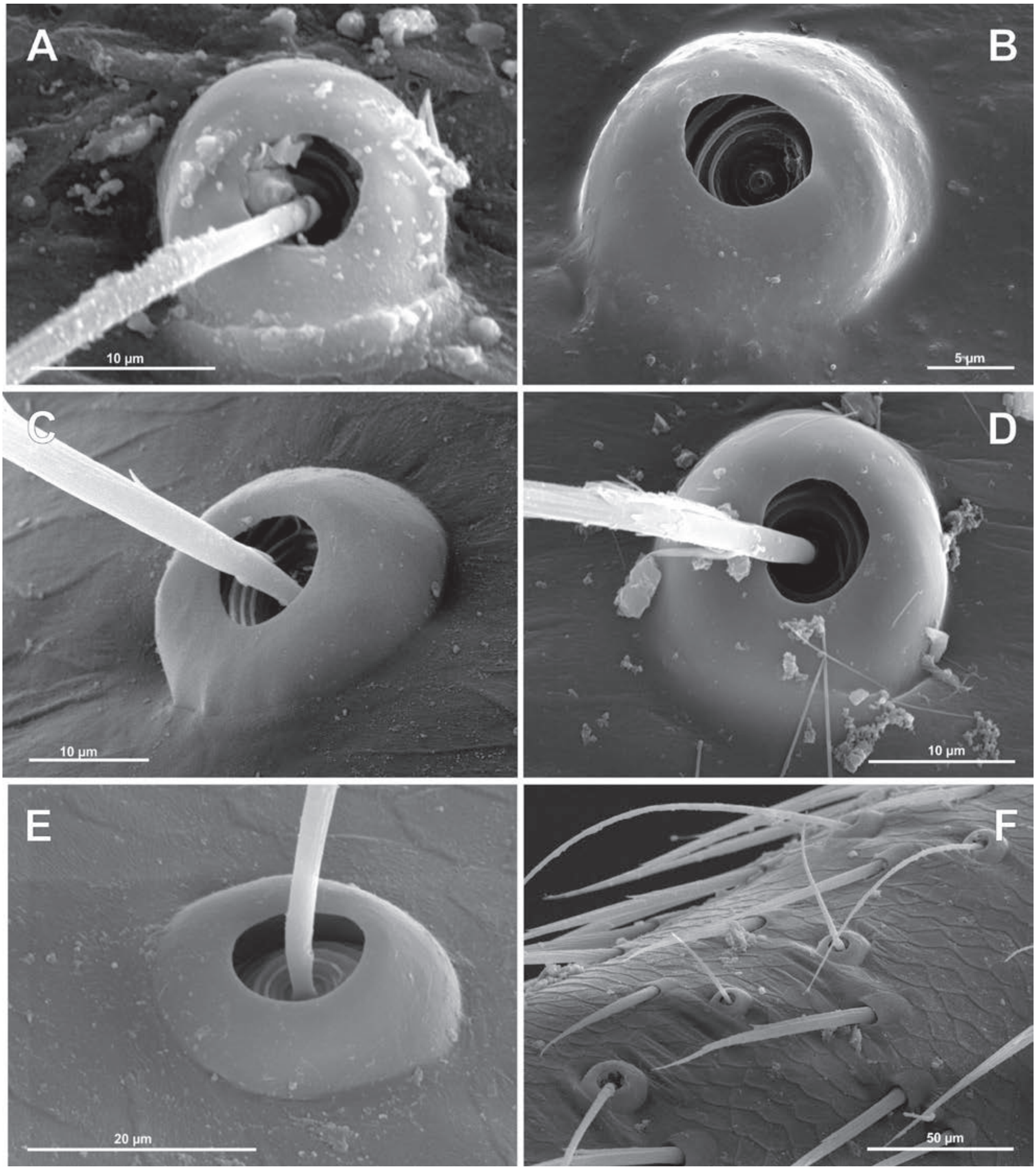

Figure 13. Bothria of 'Araneoid lineage': Zygiellidae, Nephilidae **A** *Zygiella x-notata*, ti 3 (A-type) **B** *Leviellus caspicus*, ti 3 (A-type) **C** *Parazygiella dispar*, ti 3 (T-type) **D** '*Zygiella*' *atrica*, ti 3 (T-type) **E** *Nephila* sp., ti 3 (T-type) **F** *Nephilengys malabarensis*, ti 3 (T-type).

2003) and subsequent authors. Coddington (1986a, b) suggested that Anapidae, Mysmenidae, and Symphytognathidae form a monophyletic taxon and comprise the sister group of Theridiosomatidae. A cladogram of Symphytognathoidea was presented by Lopardo et al. (2011) as Theridiosomatidae (Mysmenidae (Synaphridae (Symphytognathidae (Anapidae s. l. (Anapinae + Micropholcommatinae))))).

However, recently Dimitrov et al. (2017: fig. 2), declared the polyphyly of Symphytognathoidea based on molecular data and distributed symphytognathoid families over various, very distant, araneoid clades: mysmenids appeared coupled with tetragnathoids, theridiosomatids with synotaxids, anapids were divided into 'Anapidae I' and 'Anapidae II' (sic!) and coupled with theridiids and cyatholipids, respectively. However, these 'new molecular clades' are lacking not only morphological, but also a sufficient molecular support: "The symphytognathoid families constitute a polyphyletic group, although all nodes involving these interfamilial relationships receive low support values" (Dimitrov et al. 2017: 228). For these reasons, Eskov and Marusik (2023) restored Symphytognathoidea back to its traditional status as a monophyletic taxon.

The 'Gondwanan' micropholcommatids are regarded in this study, following Rix and Harvey (2010), as a sister group to anapids, but in a separate family, comprising the subfamilies Micropholcommatinae and Textricellinae (Eskov and Marusik 2023). Anapidae s. str. comprises subfamilies Taphiassinae and Gigiellinae (both transferred from micropholcommatids), Holarchaeinae and Anapinae (the rest of the anapid genera, including the basal monotypic *Acrobleps* Hickman, 1979) (Eskov and Marusik 2023). For the 'teutoniellid taxa clade' or 'teutoniellids', designated by Rix and Harvey (2010) and considered a sister group of their micropholcommatids (Rix and Harvey 2010: figs 3, 4), it turned out that it possesses a complete set of the diagnostic characters of Anapidae s. str., including the supramaxillar pore-bearing depressions, and should be treated as Anapidae: Teutoniellinae (stat. nov.).

The key diagnostic characters (i.e., unambiguous synapomorphies found in all clade members without exception and never outside it) of the Anapidae s. l. (Anapidae s. str. + Micropholcommatidae) main taxa are: (1) the cheliceral gland mound fussed with a proximal promarginal tooth, and a particular 'key-lock' mode of fixation of the bulb in a naturally expanded condition (Anapidae s. l.); (2) the cheliceral promargin with peg teeth replacing true teeth, and a pair of fused setal sockets adjacent to the fang base (Micropholcommatidae); and (3) a pair of pore-bearing carapace depressions strictly above the maxilla (Anapidae s. str.) (pers. obs.).

The family Holarchaeidae was established by Forster and Platnick (1984) to accommodate a single genus *Holarchaea* Forster, 1955 from New Zealand and Tasmania. Its taxonomic position was still enigmatic until Dimitrov et al. (2017) found that *Holarchaea* is close to, according to molecular data, the anapid genus *Acrobleps*, and on this ground synonymized Holarchaeidae with Anapidae. The study of *Holarchaea* microstructures (pers. obs.) confirms that it is indeed nothing more than an aberrant anapid: it possesses the complete set of anapid diagnostic characters, including vestiges of the pore-bearing carapace supramaxillary depression, and was treated as the anapid subfamily Holarchaeinae (Eskov and Marusik 2023).

The family Comaromidae was established by Wunderlich (2004b) as the anapid subfamily Comarominae to comprise the controversial genus *Comaroma* Bertkau, 1889, nested in Anapidae by Kropf (1990), and later elevated to family rank (Wunderlich 2011). The status of Comaromidae Wunderlich, 2004 as a separate symphytognathoid family was seconded recently by Eskov and Marusik (2022, 2023). *Comaroma* appeared to lack both unique synapomorphies of Anapidae, i.e., the cheliceral gland-mound fused with the proximal promarginal tooth and the pore-bearing depressions at the edge of the carapace, while retaining the lateral paracymbium, the male epiandrous spigots, and the suprapedicellar setae, lost in all members of symphytognathoidan 'EbCY clade' (Anapidae + Symphytognathidae).

The position of Synaphridae in araneoids was controversial and ping-ponged from family to family. This taxon was established by Wunderlich (1986) as a subfamily of anapids, then elevated to family rank and restricted to two genera, *Synaphris* Simon, 1894 and *Cepheia* Simon, 1894, by Marusik and Lehtinen (2003). It was nested in Symphytognathoidea (Schütt 2003), rejected from this clade by Marusik and Lehtinen (2003) and Lopardo et al. (2007) (who placed it together with Theridiidae and Cyatholipidae, respectively), and finally returned to symphytognathoids (Lopardo et al. 2011; Lopardo and Hormiga 2015).

Regarding the remaining symphytognathoid families, they are accepted herein within traditional scopes and limits. Coddington (1986b) has divided theridiosomatids into four subfamilies (Platoninae, Epeirotypinae, Ogulninae, and Theridiosomatinae); Lopardo and Hormiga (2015) distinguished two subfamilies in mysmenids (Mysmeninae and Mysmenopsinae), leaving several genera unclassified; Symphytognathidae (as well as the above Synaphridae), are still undivided to conventional subfamilies or tribes.

4.1. Anapidae (Ana).

The bothria of 14 genera representing all five anapid subfamilies are studied here:

Anapinae: *Acrobleps* Hickman, 1979; *Minanapis* Platnick & Forster, 1989; *Montanapis* Platnick & Forster, 1989; and *Pseudanapis* Simon, 1905 (Fig. 14A–D); as well as *Crassanapis* Platnick & Forster, 1989; *Elanapis* Platnick & Forster, 1989; *Hickmanapis* Platnick & Forster, 1989; *Sofanapis* Platnick & Forster, 1989; *Zangherella* Caporiacco, 1949; and *Zealanapis* Platnick & Forster, 1989 (images are not presented herein); Gigiellinae: *Gigiella* Rix & Harvey, 2010 (Fig. 15C); Holarchaeinae: *Holarchaea* Forster, 1955 (Fig. 15A); Taphiassinae: *Taphiassa* Simon, 1880 (Fig. 15D); Teutoniellinae: *Teutoniella* Brignoli, 1981 (Fig. 15B).

In addition, the bothria of seven anapid genera have been figured earlier: *Crassanapis*, *Minanapis* and *Risdonius* Hickman, 1939 (by Platnick and Forster 1989: figs 15, 81, and 225, respectively); *Holarchaea* (Forster and Platnick 1984: fig. 247); *Taphiassa* (Rix and Harvey 2010: figs 160C, D, 173C); *Olgania* Hickman, 1979 (Rix and Harvey 2010: fig. 191); and *Gigiella* (Rix and Harvey 2010: figs 200C, D, 207C, D). The ancestral '*Erigone*-type' of bothria dominates in Anapidae; the bothria of the intermediate '*Argiope*-type' are rare, and the advanced '*Theridion*-type' is completely absent. Only the '*Erigone*-type' present in the monogeneric subfamilies Gigiellinae (Fig. 15C; Rix and Harvey 2010: figs 200C, D, 207C, D), Holarchaeinae (Fig. 15A; Forster and Platnick 1984: fig. 247), and Teutoniellinae (Fig. 15B).

An unusual case is observed in the subfamily Anapinae. Among its 15 studied members, 14 have bothria of the '*Erigone*-type' with the angled ridge (e.g., *Acrobleps*, *Minanapis*, and *Montanapis*: Fig. 14A–C, respectively). However, a single exception was recorded: the otherwise unremarkable advanced genus *Pseudanapis* has the '*Argiope*-type' of bothria (Fig. 14D). Coexistence of the two bothrial types in a single taxon is not unusual, e.g., Mimetinae (see above), Taphiassinae, and Micropholcommatinae (see below), but the Anapinae would have been considered 'uniform' with respect to bothrial type, if not for the case of *Pseudanapis*, which is the "pebble in a shoe". The second case of '*Argiope*-type' bothria in anapids is in the subfamily Taphiassinae (Fig. 15D). This bothrial type was recorded in both studied *Taphiassa* species, *T. robertsi* Rix & Harvey, 2010

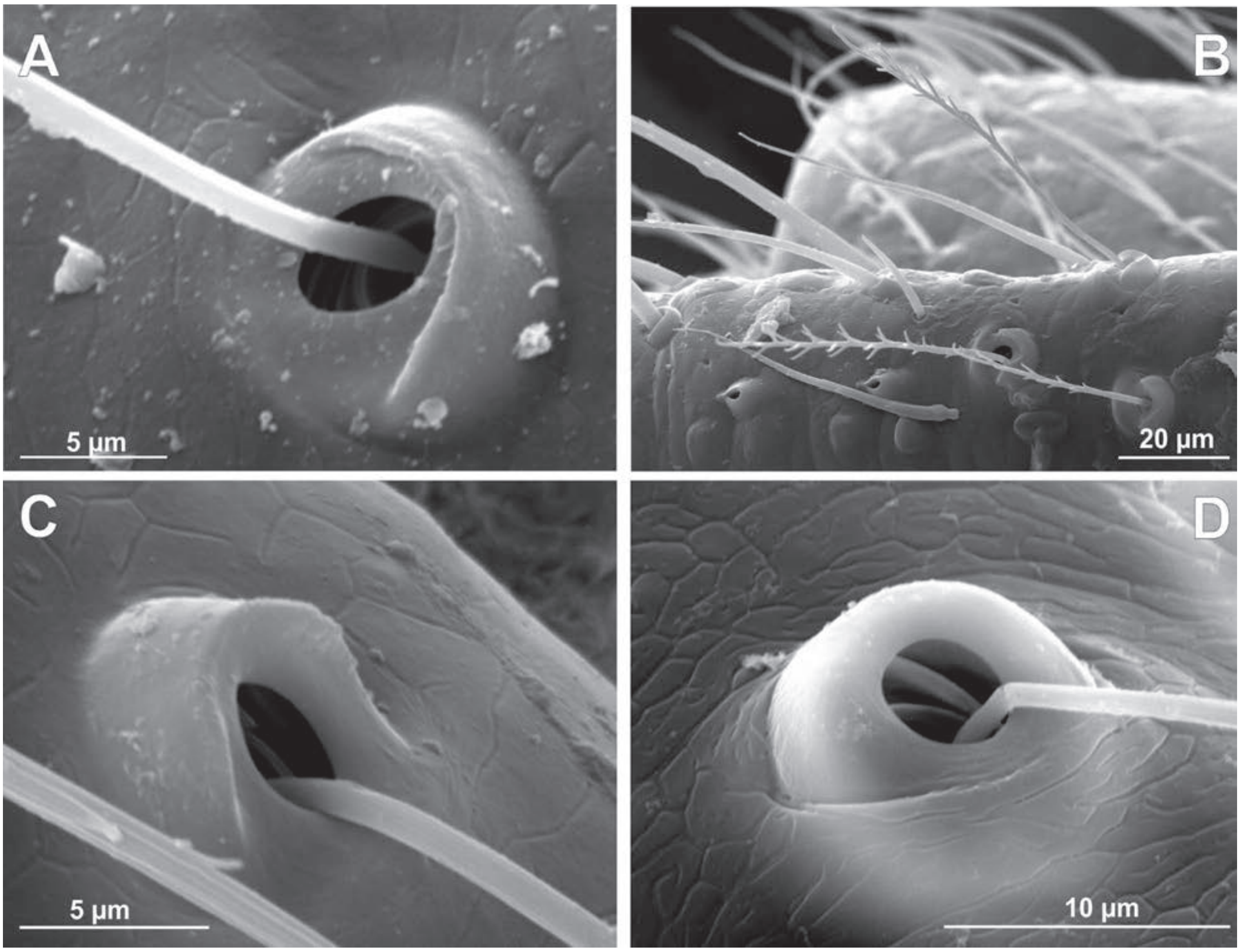

Figure 14. Bothria of 'Symphytognathoid lineage': Anapidae (Anapinae) **A** *Acrobleps hygrophilus*, ti 3 (E-type) **B** *Minanapis* sp., ti 2 (E-type) **C** *Montanapis* sp., ti 3 (E-type) **D** *Pseudanapis* sp., ti 2 (A-type).

and *T. castanea* Rix & Harvey, 2010 (Rix and Harvey 2010: fig. 160C, D and fig. 173C, respectively). However, the second taphiassin genus, *Olgania*, has the usual anapid bothria of the '*Erigone*-type' (Rix and Harvey 2010: fig. 191C).

4.2. Comaromidae (Com).

The bothria of *Comaroma* Bertkau, 1889 are studied here (Fig. 18B). In addition, the bothrium of *Comaroma* has been illustrated earlier (Lopardo and Hormiga 2015: fig. 80C). The bothria belong to the '*Erigone*-type' with a sharp, orthogonally angled ridge.

4.3. Micropholcommatidae (Mic).

The bothria of ten genera representing both micropholcommatid subfamilies distinguished herein have been examined: Micropholcommatinae: *Austropholcomma* Rix & Harvey, 2010; *Micropholcomma* Crosby & Bishop, 1927; *Plectochetos* Butler, 1932; *Tricellina* Forster & Platnick, 1989 (Fig. 16A–E); Textricellinae: *Rayforstia* Rix & Harvey, 2010 (Fig. 16F); *Eperiella* Rix & Harvey, 2010; *Epigastrina* Rix & Harvey, 2010; *Eterosonycha* Butler, 1932; *Normplatnicka* Rix & Harvey, 2010; *Raveniella* Rix & Harvey, 2010 (images are not presented herein). In addition, the bo-

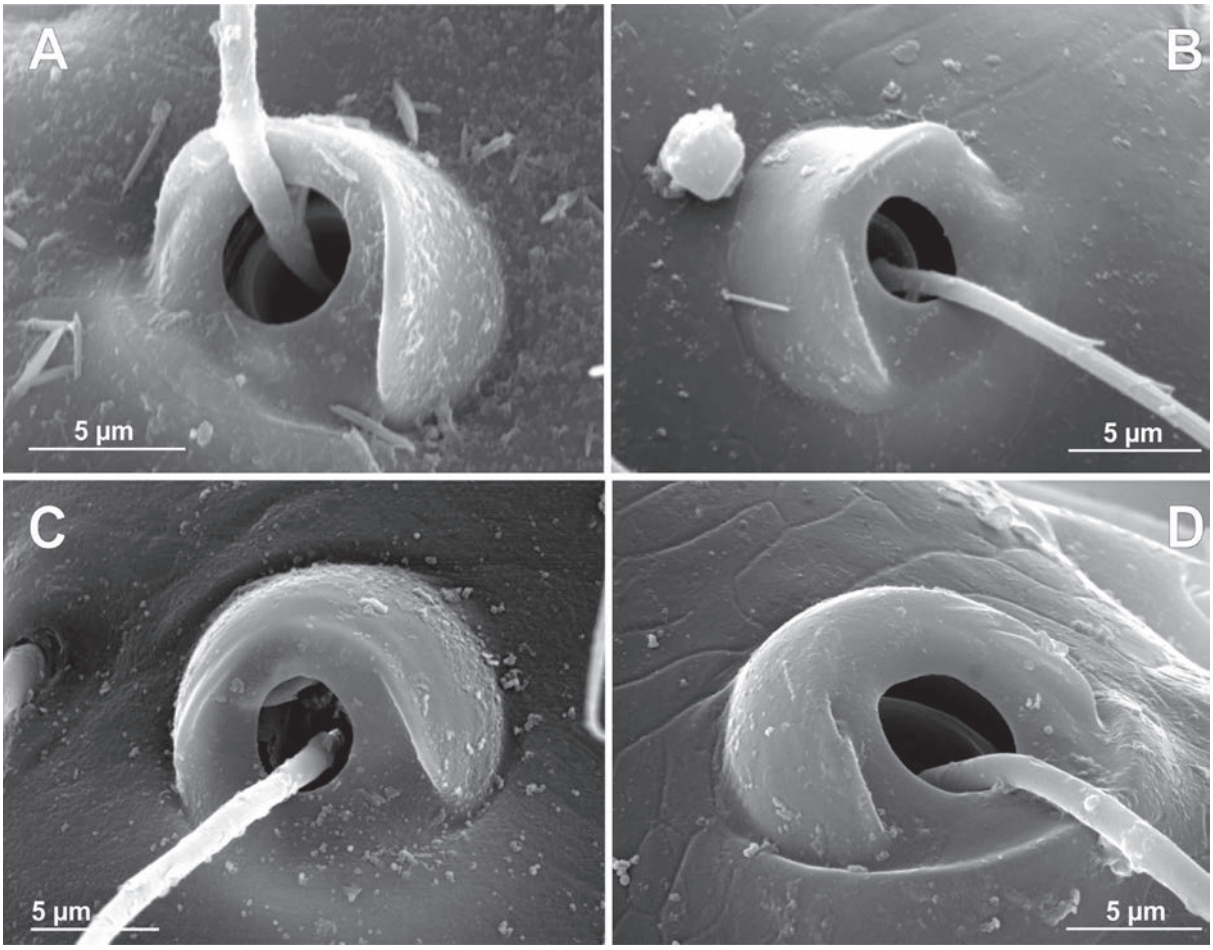

Figure 15. Bothria of 'Symphytognathoid lineage': Anapidae (Holarchaeinae, Teutoniellinae, Gigiellinae, Taphiassinae) **A** *Holarchaea novaeseelandiae*, ti 3 (E-type) **B** *Teutoniella cekalovici*, ti 4 (E-type) **C** *Gigiella millidgei*, mt 2 (E-type) **D** *Taphiassa castanea*, ti 2 (A-type).

thria of the nine micropholcommatid genera were figured earlier: Micropholcommatinae: *Plectochetos* (Forster and Platnick 1984: fig. 375, as *Micropholcomma*); *Micropholcomma*; *Pua* Forster, 1959; *Austropholcomma*; *Tricellina*; and *Patelliella* Rix & Harvey, 2010 (Rix and Harvey 2010: figs 20C, 28C, 38C, 44C, and 149C, respectively); Textricellinae: *Rayforstia* (Forster and Platnick 1984: fig. 374, as *Textricella*); *Algidiella* Rix & Harvey, 2010; *Taliniella* Rix & Harvey, 2010; and *Tinytrella* Rix & Harvey, 2010 (Rix and Harvey 2010: figs 124C, 133C, and 141C, respectively).

All the genera of Textricellinae have a highly uniform bothria of the '*Erigone*-type' with an angled ridge (e.g., Fig. 16F; Rix and Harvey 2010: figs 124C, 133C, 141C). In contrast, both the ancestral '*Erigone*-type' and the more advanced '*Argiope*-type' are present in the Micropholcommatinae, and, in addition, the transverse ridge is rounded rather than angled. The genera with the clear '*Erigone*-type' bothria are *Tricellina* (Fig. 16C; Rix and Harvey 2010: fig. 44C) and *Pua* (Rix and Harvey 2010: fig. 28C). The genera with the clear '*Argiope*-type' bothria are *Austropholcomma* (Fig. 16E; Rix and Harvey 2010: fig. 38C), *Plectochetos* (Fig. 16D; Forster and Platnick 1984: fig. 375), and *Patelliella* (Rix and Harvey 2010: fig. 149C). Finally, in the species of *Micropholcomma* the bothria seem to be of an intermediate between the '*Erigone*-type' and the '*Argiope*-type'; moreover, even within this genus *M. bryophilum* (Butler, 1932) (Fig. 16B; Rix and Harvey 2010: fig. 20C) seems to be closer to the '*Argiope*-type' than *M. parmatum* Hickman, 1944 (Fig. 16A).

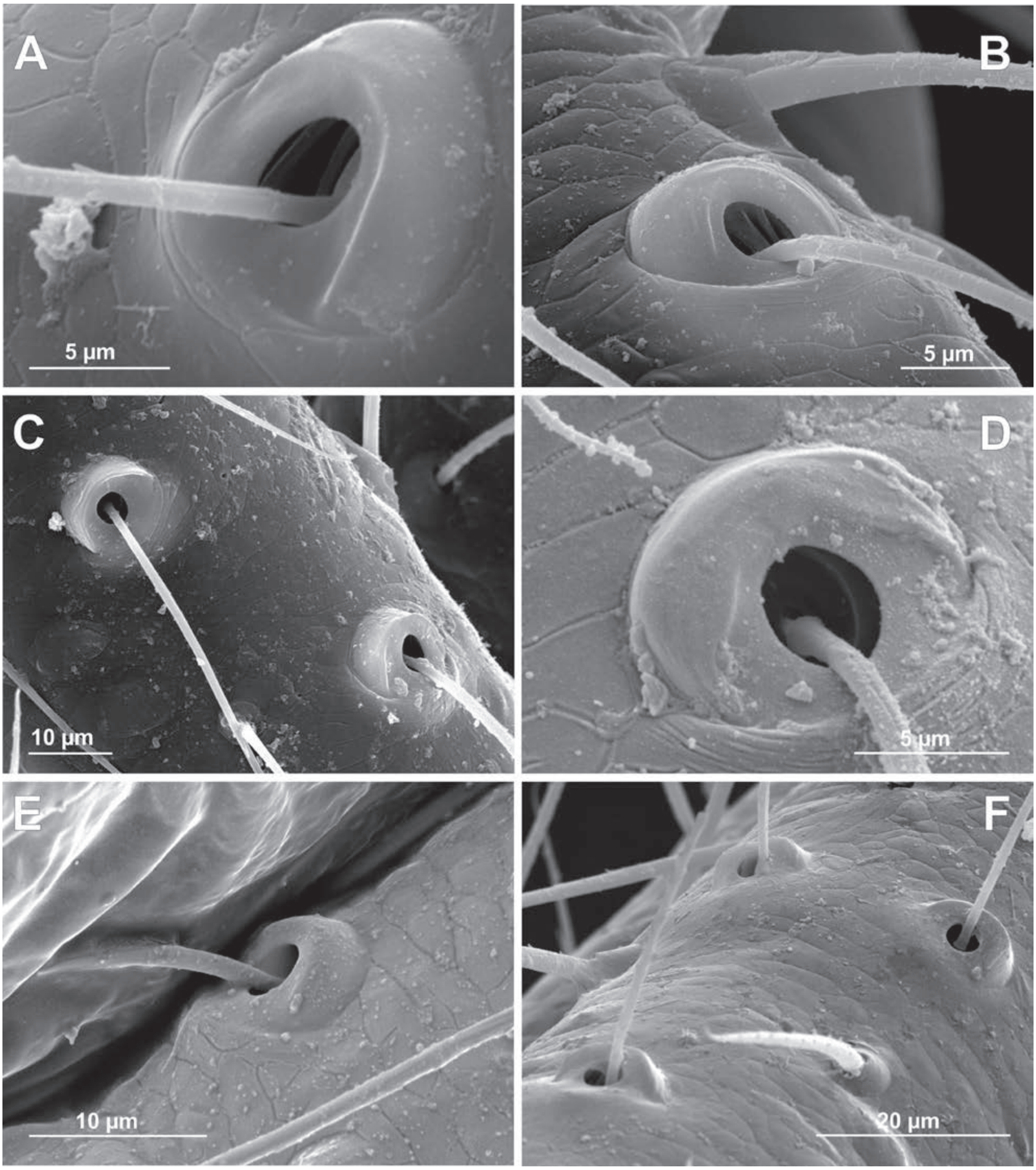

Figure 16. Bothria of 'Symphytognathoid lineage': Micropholcommatidae (Micropholcommatinae, Textricellinae) **A** *Micropholcomma parmata*, ti 4 (E-type) **B** *Micropholcomma bryophilum*, ti 3 (E-type) **C** *Tricellina gertschi*, ti 2 (E-type) **D** *Plectochetos longissimus*, ti 4 (A-type) **E** *Austropholcomma* sp., ti 3 (A-type) **F** *Rayforstia vulgaris*, ti 1 (E-type).

4.4. Mysmenidae (Mys).

The bothria of four genera representing both conventional mysmenid subfamilies are studied here: Mysmeninae: *Mysmena* Simon, 1894 and *Microdipoena* Banks, 1895 (Fig. 17A, B); Mysmenopsinae: *Mysmenopsis* Simon, 1898 and *Isela* Griswold, 1985 (Fig. 17C, D). In addition, the bothria of the three mysmenid genera were figured previously: *Microdipoena* and *Mysmena* (Lopardo and Hor-

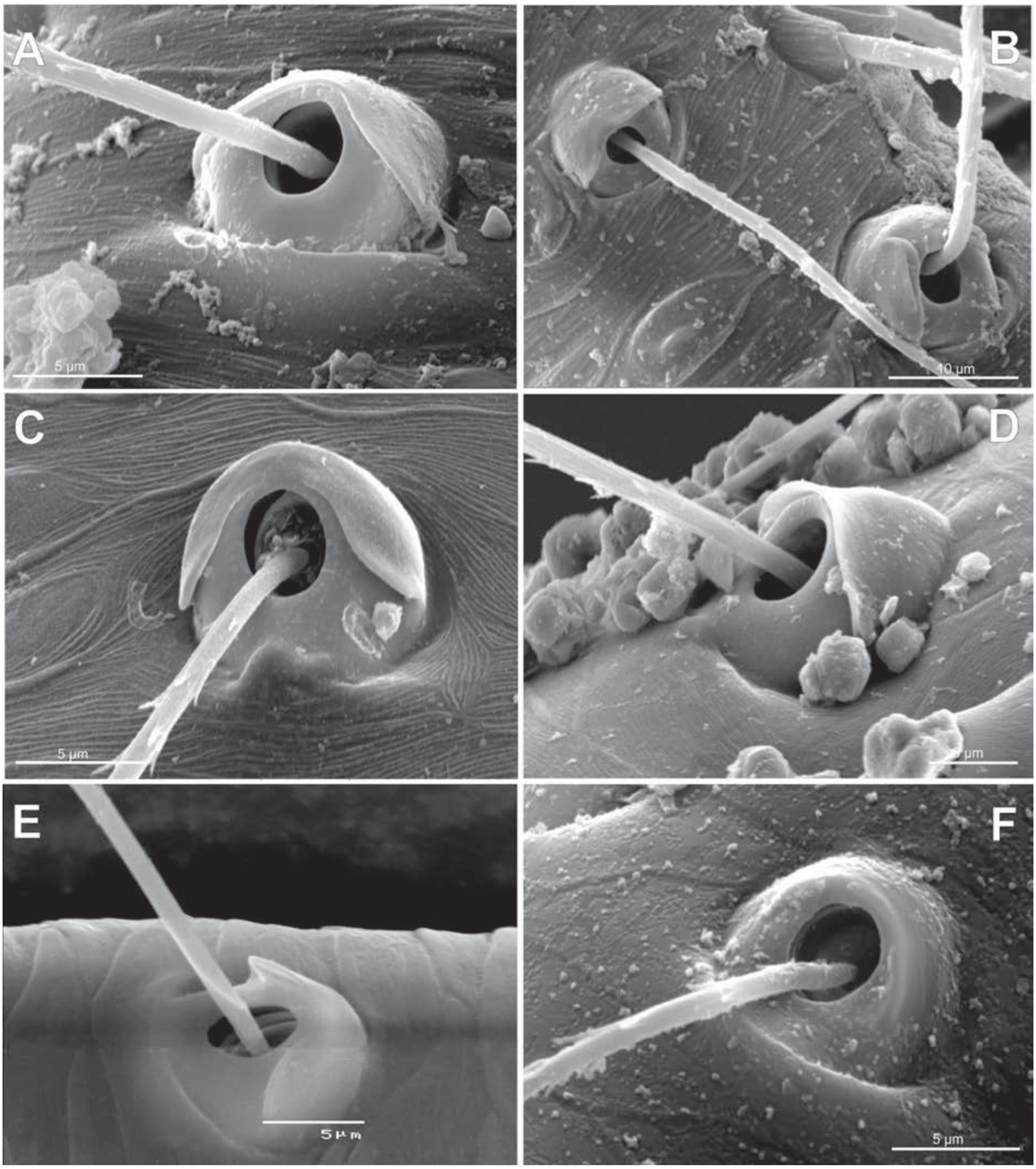

Figure 17. Bothria of 'Symphytognathoid lineage': Mysmenidae (Mysmeninae, Mysmenopsinae), Synaphridae **A** *Mysmena leucoplagiata*, ti 3 (E-type) **B** *Microdipoena* sp., ti 1 (E-type) **C** *Mysmenopsis tengellacompa*, ti 2 (E-type) **D** *Isela inquilina*, ti 2 (E-type) **E** *Synaphris lehtineni*, ti 2 (E-type) **F** *Cepheia longiseta*, ti 2 (A-type).

miga 2015: fig. 21I and fig. 34B, respectively), and *Isela* (Griswold 1985: fig. 8). The bothria of all mysmenids are highly uniform and belong to the '*Erigone*-type' with an angled ridge.

4.5. Symphytognathidae (Sym).

The bothria of two symphytognathid genera have been examined here: *Symphytognatha* Hickman, 1931 (Fig. 18A) and *Anapistula* Gertsch, 1941 (image is not presented herein). In addition, the bothrium of Symphytognathidae gen. sp. has

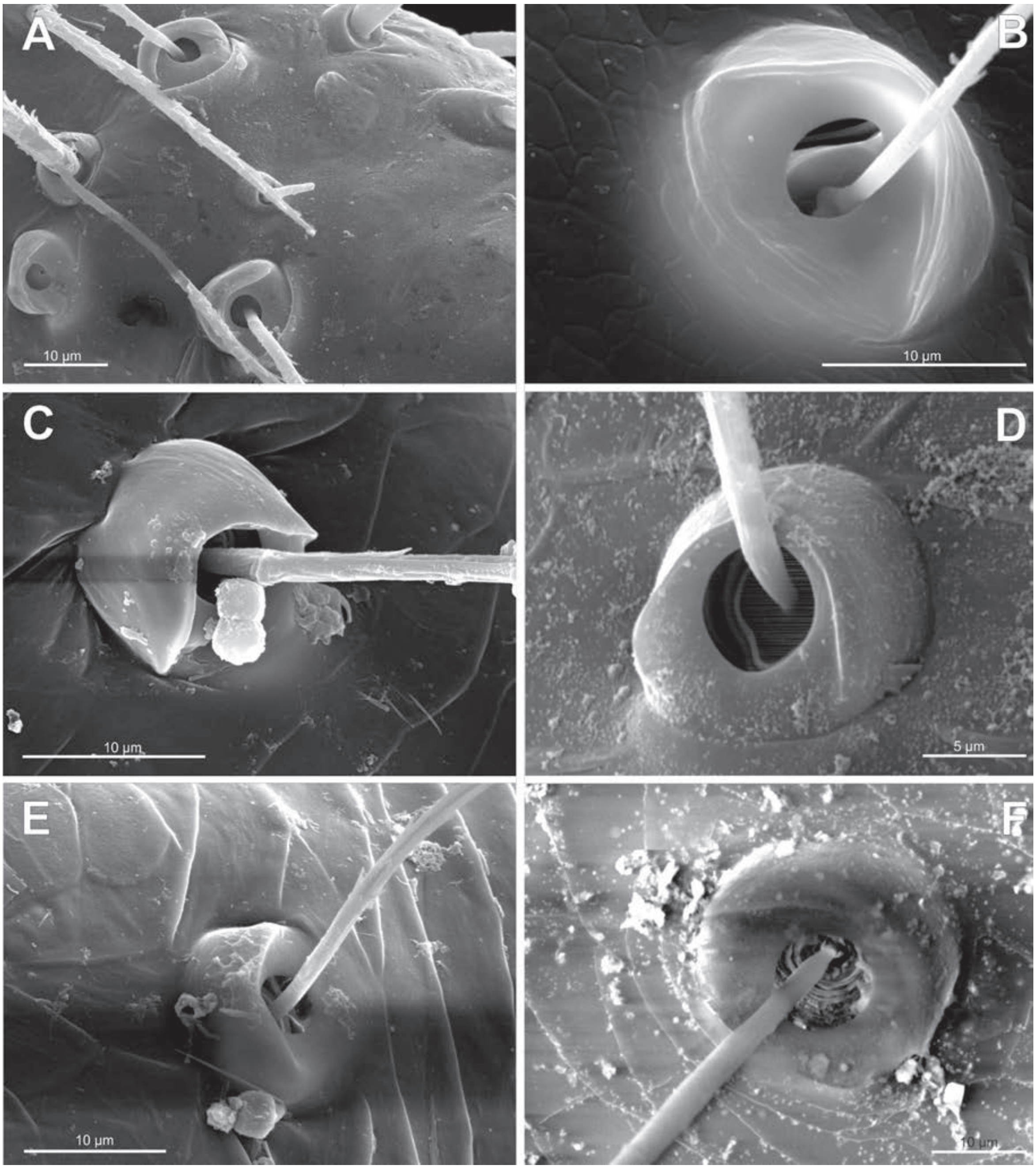

Figure 18. Bothria of 'Symphytognathoid lineage': Symphytognathidae, Comaromidae, Theridiosomatidae (Theridiosomatinae, Epeirotypinae, Ogulninae, Platoninae) **A** *Symphytognatha globosa*, ti 1 (E-type) **B** *Comaroma simoni*, mt 1 (E-type) **C** *Theridiosoma radiosum*, mt 1 (E-type) **D** *Naatlo* sp., ti 1, (E-type) **E** *Ogulnius* sp., mt 3 (E-type) **F** *Plato troglodita*, ti 3 (A-type) (courtesy N. Dupérré).

been previously illustrated (Lopardo and Hormiga 2015: fig. 119F, as SYMP-006-AUST). The bothria of the all symphytognathids seem to be highly uniform and belong to the '*Erigone*-type' with an angled ridge.

4.6. Synaphridae (Syn).

The bothria of two synaphrid genera are studied here: *Synaphris* Simon, 1894 and *Cepheia* Simon, 1894 (Fig. 17E, F). In addition, the bothria of the three synaphrid genera have been figured previously: *Africepheia* Miller, 2007 (Miller

2007: figs 14, 15) and *Cepheia* (Lopardo and Hormiga 2007: fig. 25); in the genus *Synaphris* the bothria of the five species have been illustrated (Marusik and Lehtinen 2003: figs 22, 23; Marusik et al. 2005: fig. 30; Miller 2007: figs 50, 51, 59, 74; Lopardo et al. 2007: figs 15, 21, 22, 56). The bothria of the all *Synaphris* species studied belong to the '*Erigone*-type' with a distinct angled ridge (Fig. 17E), whereas the bothria of both *Cepheia* (Fig. 17F) and *Africepheia* belong to the '*Argiope*-type'. Thus, the resemblance of bothrial shape confirms the close relationship between *Africepheia* and *Cepheia*, as suggested by Miller (2007).

4.7. Theridiosomatidae (Ths).

The bothria of five genera representing all four conventional theridiosomatid subfamilies have been examined: Theridiosomatinae: *Theridiosoma* O. Pickard-Cambridge, 1879 (Fig. 18C) and *Epilineutes* Coddington, 1986 (images are not presented herein); Epeirotypinae: *Naatlo* Coddington, 1986 (Fig. 18D); Ogulninae: *Ogulnius* O. Pickard-Cambridge, 1882 (Fig. 18E); Platoninae: *Plato* Coddington, 1986 (Fig. 18F). In addition, the bothria of the single theridiosomatid genus have been figured previously: *Cuacuba* Prete, Cizauskas & Brescovit, 2018 (Prete et al. 2018: fig. 7D). The bothria of the three theridiosomatid subfamilies, Theridiosomatinae, Epeirotypinae, and Ogulninae, seem to be highly uniform and belong to the '*Erigone*-type' with an angled ridge (Fig. 18C–E). However, the bothria of the Platoninae, at least in the single genus examined, *Plato*, belong to the more advanced '*Argiope*-type' (Fig. 18F). It should be noted that the bothria of *Cuacuba* also belong to the '*Argiope*-type' (see Prete et al. 2018: fig. 7D). The authors have described this genus together with several new species of *Plato* but failed to indicate its subfamilial placement (Prete et al. 2018: 143). The diversity of the bothrial types in the 'Symphytognathoid lineage' is summarized in Fig. 30.

5. 'Linyphioid lineage', Ll
5.1. Linyphiidae Blackwall, 1859 (Lin).
5.1.1. Erigoninae Emerton, 1882 [Erigo].
5.1.2. Linyphiinae Blackwall, 1859 [Linyp].
5.1.3. Micronetinae Hull, 1920 [Minet].
5.1.4. Mynogleninae Lehtinen, 1967 [Myngl].
5.1.5. Stemonyphantinae Wunderlich, 1986 [Stemo].
5.2. Pimoidae Wunderlich, 1986 (Pim). Conventional subfamilies/tribes are not established [Pimoi].

The 'linyphioid lineage,' forming, together with the 'cyatholipoids' and 'theridioids,' a distal branch of the superfamily Araneoidea (i.e., 'clade 12', or 'araneoid sheet web weavers,' according to Griswold et al. 1998: 16) represents the sister group of the latter pair (Griswold et al. 1998: fig. 7). Linyphiidae, the second most speciose family in the order, comprises five conventional subfamilies: the Holarctic Stemonyphantinae, the cosmopolitan Erigoninae, Linyphiinae, and Micronetinae, and the southern hemisphere Mynogleninae (Arnedo et al. 2009; Frick and Scharff 2014); the status of such linyphiid subfamilies as Dubiaraneinae Millidge, 1993, Ipainae Saaristo, 2007, and Sinopimoinae Li & Wunderlich, 2008, treated as distinct families by Eskov and Marusik (2023), requires further clarification. Pimoinae was established as a linyphiid subfamily to comprise the controversial genus *Pimoa* Chamberlin & Ivie, 1943 with a relict disjunct distribution (mountains of southern Europe, Himalaya, and western North America), previously transferred by Wunderlich (1979) to Linyphiidae from Metidae (= Tetragnathidae). Hormiga (1993) elevated it to a family, the sister group to Linyphiidae. Currently, only two geners are contained in the family Pimoidae, one of which is the enigmatic monotypic genus *Nanoa* Hormiga, Buckle & Scharff, 2005 from California and Oregon (Hormiga et al. 2005). Wunderlich (2008: 127) attributed *Nanoa* to the extinct family Pumiliopimoidae Wunderlich, 2008; it probably deserves the status of an independent linyphioid family or subfamily. Incidentally, the trichobothrial bases of the pimoid genera *Pimoa* and *Nanoa* differ dramatically from each other (see below).

5.1. Linyphiidae (Lin).

Bothria of 16 genera representing all five conventional linyphiid subfamilies are studied here: Erigoninae: *Erigone* Audouin, 1826; *Lophomma* Menge, 1868; *Pelecopsis* Simon, 1864; and *Scutpelecopsis* Marusik & Gnelitsa, 2009 (Fig. 19A–D) and *Minyriolus* Simon, 1884 (its images are not presented herein); Linyphiinae: *Allomengea* Strand, 1912; *Linyphia* Latreille, 1804; and *Porrhomma* Simon, 1884 (Fig. 20D–F) and *Lepthyphantes* Menge, 1866 (its images are not presented herein); Micronetinae: *Agyneta* Hull, 1911; *Maro* O. Pickard-Cambridge, 1907 and *Microneta* Menge, 1869 (Fig. 20A–C); Mynogleninae: *Haplinis* Simon, 1894 and *Parafroneta* Blest, 1979 (Fig. 21C, D); Stemonyphantinae: *Stemonyphantes* Menge, 1866 and *Weintrauboa* Hormiga, 2003 (Fig. 21A, B). In addition, the bothria of the two linyphiid genera have been figured earlier: *Maso sundevalli* (Westring, 1851) (Lehtinen 1975: fig. 18), and *Orsonwelles* Hormiga, 2002, a giant Linyphiinae from the Hawaiian Islands (Hormiga 2002: fig. 46G).

The bothria of all the studied Erigoninae, as well as *Maso*, are highly uniform and belong to the '*Erigone*-type' with the clearly angled ridge (Fig. 19A–D; Lehtinen 1975: fig. 18). In both subfamilies Linyphiinae and Micronetinae (it should be noted that they are often considered as tribes of the single subfamily Linyphiinae s. l.) the bothria of both the '*Erigone*-type' and the '*Argiope*-type' are combined, and the transverse ridges seem more rounded than angled. The '*Erigone*-type' include *Maro*, *Agyneta*, and *Porrhomma* (Fig. 20A, B, and Fig. 20D, respectively); the '*Argiope*-type' include *Microneta*, *Linyphia*, *Allomengea* (Fig. 20C, E, and Fig. 20F, respectively), *Lepthyphantes*; and *Orsonwelles* (Hormiga, 2002: fig. 46G). Finally, only the intermediate '*Argiope*-type' bothria are found in the subfamilies Mynogleninae (Fig. 21C, D) and Stemonyphantinae (Fig. 21A, B).

5.2. Pimoidae (Pim).

The bothria of both pimoid genera *Nanoa* Hormiga, Buckle & Scharff, 2005 (Fig. 21E) and *Pimoa* Chamberlin & Ivie, 1943 (Fig. 21F) are studied here. They have dramatically different bothria: the '*Erigone*-type' with the clearly angled ridge in *Nanoa* and the '*Argiope*-type' in *Pimoa*. The diversity of the bothrial types in the 'Linyphioid lineage' is summarized in Fig. 31.

6 'Cyatholipoid lineage', CY
6.1. Synotaxidae Simon, 1894 (Syt). Conventional subfamilies/tribes are not established [Sytax].

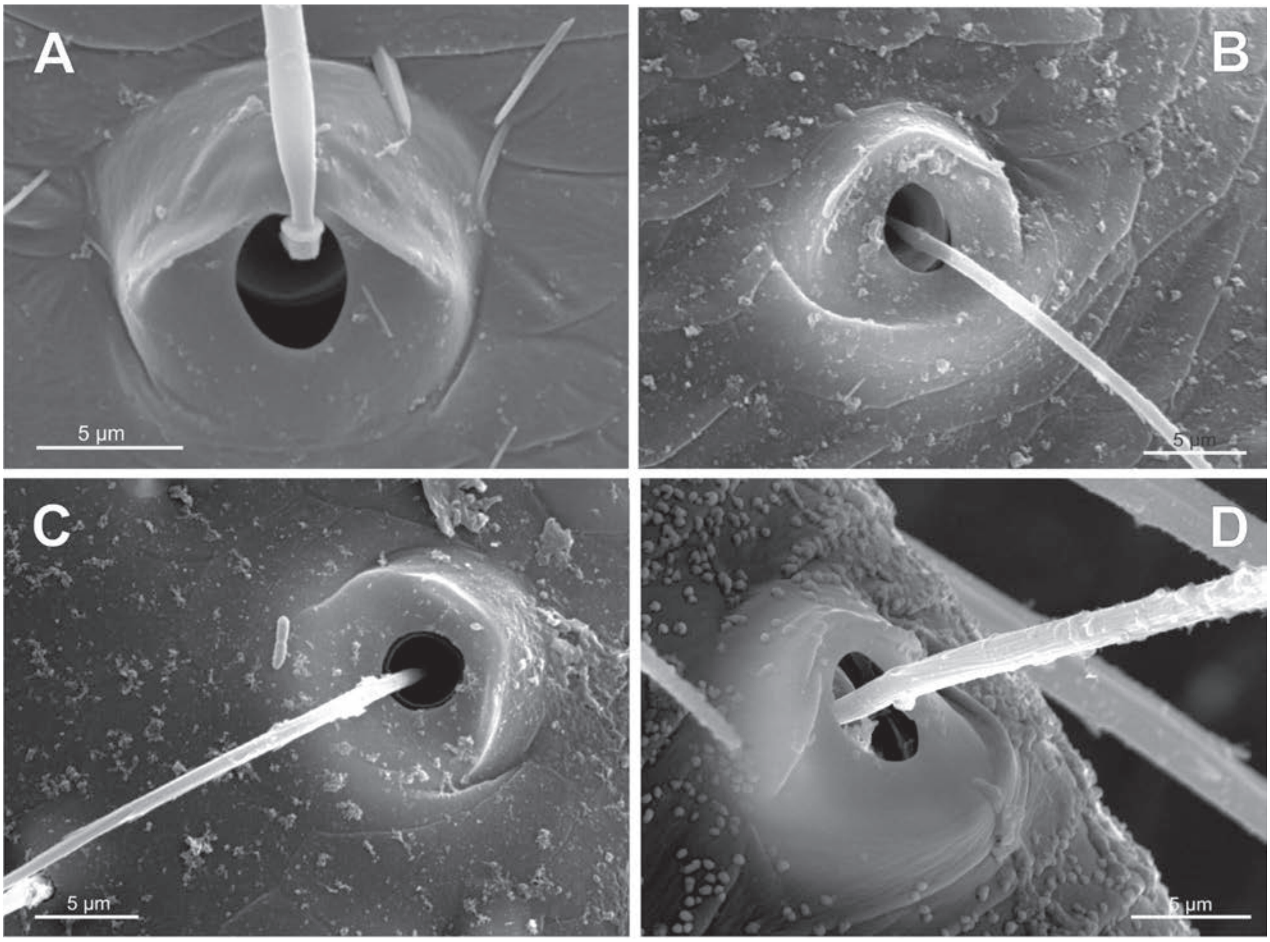

Figure 19. Bothria of 'Linyphioid lineage': Linyphiidae (Erigoninae) **A** *Erigone dentipalpis*, mt 1 (E-type) **B** *Pelecopsis mengei*, ti 3 (E-type) **C** *Scutpelecopsis wunderlichi*, ti 3 (E-type) **D** *Minyriolus pusilus*, mt 1 (E-type).

6.2. Physoglenidae Petrunkevitch, 1928 (Phy).
6.2.1. Pahorinae Forster, 1990 [Pahor].
6.2.2. Physogleninae Petrunkevitch, 1928 [Physo].
6.3. Cyatholipidae Simon, 1894 (Cya). Conventional subfamilies/tribes are not established [Cyath].
6.4. Nesticidae Simon, 1894 (Nes).
6.4.1. '*Eidmannella* clade' [Eidma].
6.4.2. Nesticellini Lehtinen & Saaristo, 1980 [Necel].
6.4.3. Nesticini Simon, 1894 [Nesti].

The 'cyatholipoid lineage' (Cyatholipidae + Synotaxidae sensu Forster et al.1990) and the 'theridioid lineage' (Theridiidae + Nesticidae) were treated by Griswold et al. (1998: fig. 7) as sister groups forming the terminal clade of the araneoid cladogram: the 'spineless femur clade', clade 10. Ramírez et al. (2022: fig. 1) replaced nesticids from 'theridioids' to 'cyatholipoids' based on both morphological and molecular data. Kulkarni et al. (2021) nested cyatholipids together with Linyphiidae + Pimoidae based solely on molecular data, but this nesting lacks morphological support.

Forster et al. (1990) united the monotypic tribe Synotaxini (from theridiids), subfamily Physogleninae (from pholcids), and numerous newly described southern temperate taxa (New Zealand, Australia, and southern South America)

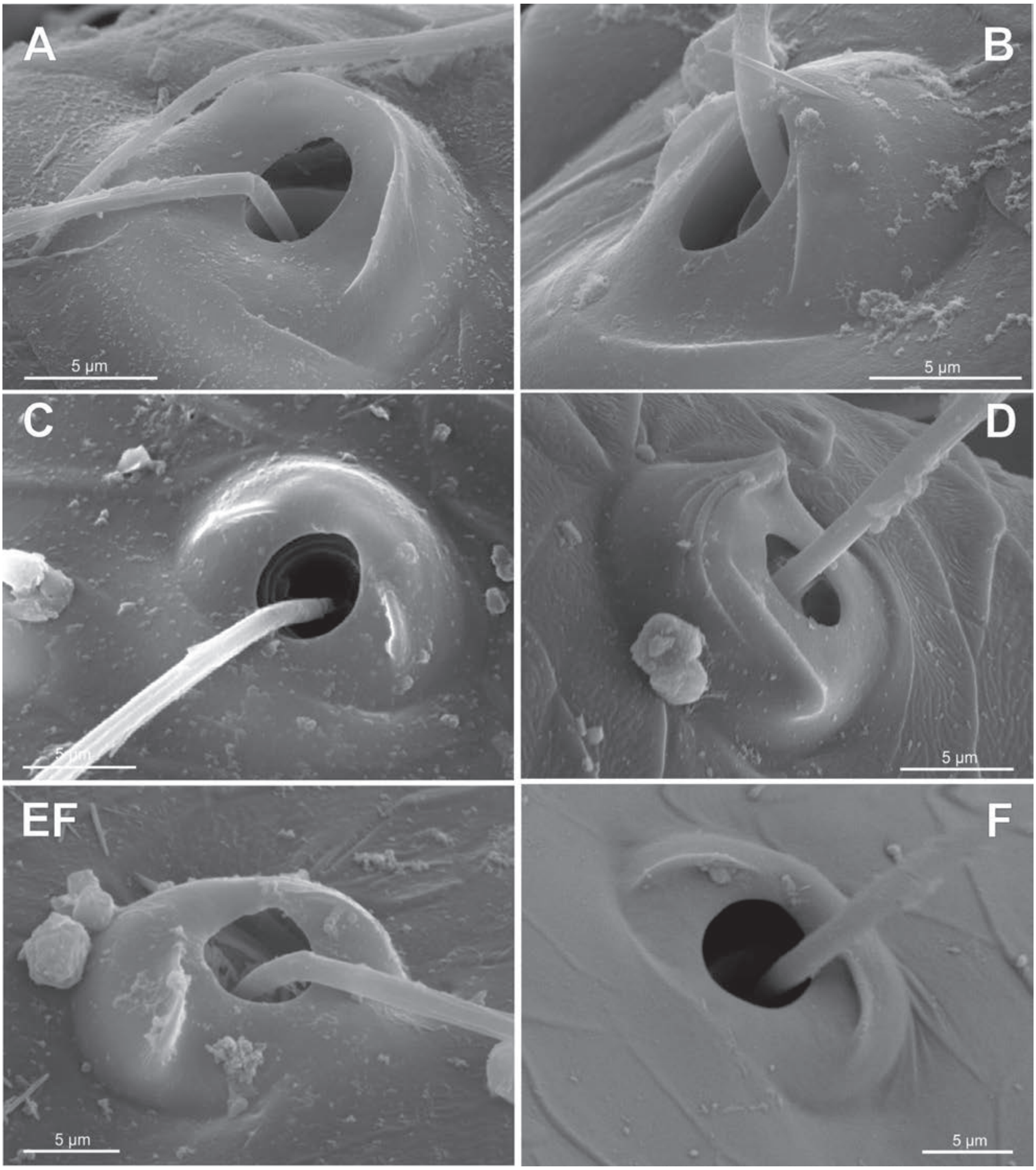

Figure 20. Bothria of 'Linyphioid lineage': Linyphiidae (Micronetinae, Linyphiinae). **A** *Maro pansibiricus*, ti 3 (E-type) **B** *Agyneta cauta*, ti 3 (E-type) **C** *Microneta viaria*, ti 1 (A-type) **D** *Porrhomma pygmaeum*, mt 2 (E-type) **E** *Linyphia triangularis*, ti 2 (A-type) **F** *Allomengea scopigera*, mt 2 (A-type).

in the 'enlarged Synotaxidae' with three subfamilies (Synotaxinae, Physogleninae, and Pahorinae), and recognized the Cyatholipidae as its sister group. However, Dimitrov et al. (2017) redelimited Synotaxidae to a single Neotropic genus, *Synotaxus* Simon, 1895, and united all the other synotaxids (sensu Forster et al. 1990) in the Physogleninae, which was then elevated to family and divided into the subfamilies Physogleninae and Pahorinae. Synotaxidae s. str. and Physoglenidae were nested in distant araneoid branches, as the sister

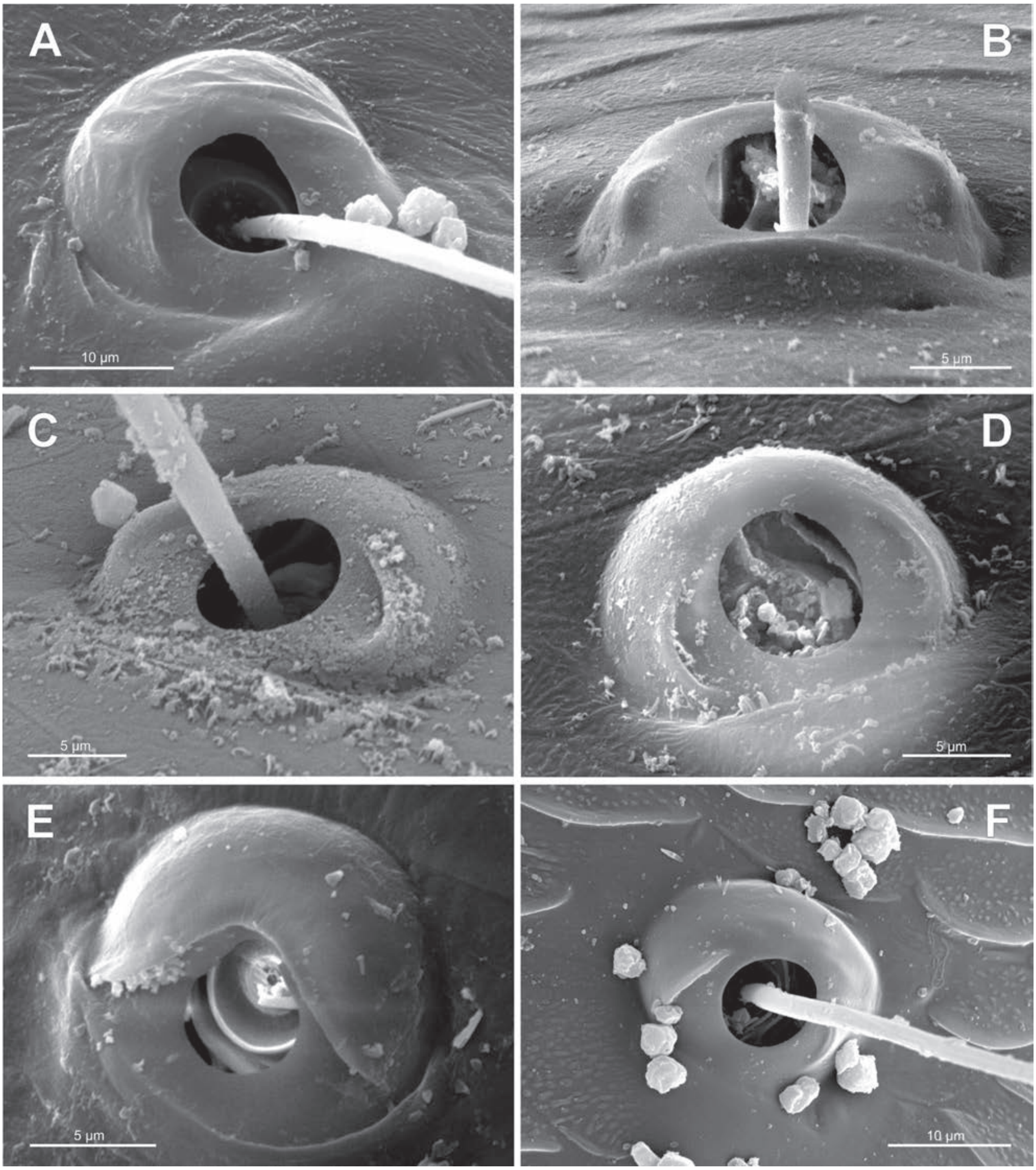

Figure 21. Bothria of 'Linyphioid lineage': Linyphiidae (Stemonyphantinae, Mynogleninae), Pimoidae **A** *Stemonyphantes lineatus*, male palpal tibia (A-type) **B** *Weintrauboa insularis*, ti 2 (A-type) **C** *Haplinis mundenia*, ti 3 (A-type) **D** *Parafroneta confusa*, ti 3 (A-type) **E** *Nanoa enana*, ti3 (E-type) **F** *Pimoa rupicola*, ti 3 (A-type).

groups of theridiosomatids and linyphioids, respectively (Dimitrov et al. 2017: fig. 2). Finally, Ramírez et al. (2022) transferred the controversial theridiid genus *Tekellina* Levi, 1957 and three nesticid genera, *Gaucelmus* Keyserling, 1884, *Hamus* Ballarin & Li, 2015, and *Nescina* Ballarin & Li, 2015, to the Synotaxidae s. str. based on both morphological and molecular data. In addition, Physoglenidae and the 'newly enlarged Synotaxidae' were recognized as independent but sister families (Ramírez et al. 2022: fig. 1). Based on the same morphological and molecular data, Nesticidae can be treated as the sister group of the pair Synotaxidae + Physoglenidae, but not of Theridiidae (Ramírez et al. 2022: fig. 1). Lehtinen and Saaristo (1980) established two tribes (instead of subfamilies) in Nesticidae, Nesticini and Nesticellini, but left the well-known Nearctic genera *Gaucelmus* and *Eidmannella* unclassified. *Gaucelmus*, as well as the recently described nesticid genera *Nescina* and *Hamus*, have already been transferred to Synotaxidae (see above); *Eidmannella* clearly differs from all 'typical nesticids' (Ballarin, pers. com. 18.08.2022) and is listed herein as an '*Eidmannella* clade'. The southern hemisphere Cyatholipidae (South Africa, Australia, and New Zealand) remains undivided into conventional subfamilies or tribes (Griswold 2001).

6.1. Synotaxidae (Syt).

Bothria of all six synotaxid genera are studied here: *Gaucelmus* Keyserling, 1884; *Hamus* Ballarin & Li, 2015; *Nescina* Lin, Ballarin & Li, 2016; *Synotaxus* Simon, 1895; *Tekellina* Levi, 1957; and '*Tekellina*' *araucana* Marusik, Eskov & Ramírez, 2022, probably representing an undescribed genus (Fig. 22A–F). In addition, the bothria of '*Tekellina*' *araucana* have been figured (Ramírez et al. 2022: fig. 5C). Bothria of the two types are presented in Synotaxidae: the '*Erigone*-type' in *Tekellina*, '*Tekellina*' *araucana*, *Nescina*, and *Hamus* (Fig. 22A, B, C, and Fig. 22D, respectively), and the '*Argiope*-type' in *Gaucelmus* and *Synotaxus* (Fig. 22E and Fig. 22F, respectively).

6.2. Physoglenidae (Phy).

The bothria of three genera representing both physoglenid subfamilies are studied here: Pahorinae: *Pahora* Forster, 1990 (Fig. 23A, B); Physogleninae: *Tupua* Platnick, 1990 and *Physoglenes* Simon, 1904 (Fig. 23C, D). In addition, the bothria of the three physoglenid genera have been figured earlier: *Pahora*, three species (Forster et al. 1990: figs 144, 163, 178) and the *Mangua* Forster, 1990, three species (Forster et al. 1990: figs 260, 276, 299) from the Pahorinae, and the *Meringa* Forster, 1990, four species (Forster et al. 1990: figs 34, 53, 65, 78) from the Physogleninae. Each of the two physoglenid subfamilies has its own bothrial type. Both studied genera of Pahorinae, *Pahora* (Fig. 23A, B; Forster et al. 1990: fig. 163) and *Mangua* (Forster et al. 1990: fig. 299), possess the '*Erigone*-type' of bothria. All studied genera of the Physogleninae, *Tupua* (Fig. 23C), *Physoglenes* (Fig. 23D), and *Meringa* (Forster et al. 1990: figs 53, 54) possess the '*Argiope*-type' of bothria; this character was included in the subfamily diagnosis by Forster et al. (1990: 5): "Trichobothria present at least on tibiae, bases with only traces of posterior hood". It should be noted that in the genus *Pahora* the "modified trichobothria sometimes present on male palpal tibia" (Forster et al. 1990: 38), and the male palpal tibia is provided with a particular structure, named the 'trichobothrium-bearing spur' (Forster et al. 1990: 41). The transverse ridge of the '*Erigone*-type' bothria on leg joints is rounded (Fig. 23A), whereas a ridge of the bothria on 'trichobothrium-bearing spur' is clearly angled (Fig. 23B; Forster et al. 1990: 144, 163). This case resembles to the mimetine genus *Ero* (see above), where the bothria on the leg joints and the male palp tibia belong to the different bothrial types (Fig. 6C and Fig. 6D, respectively).

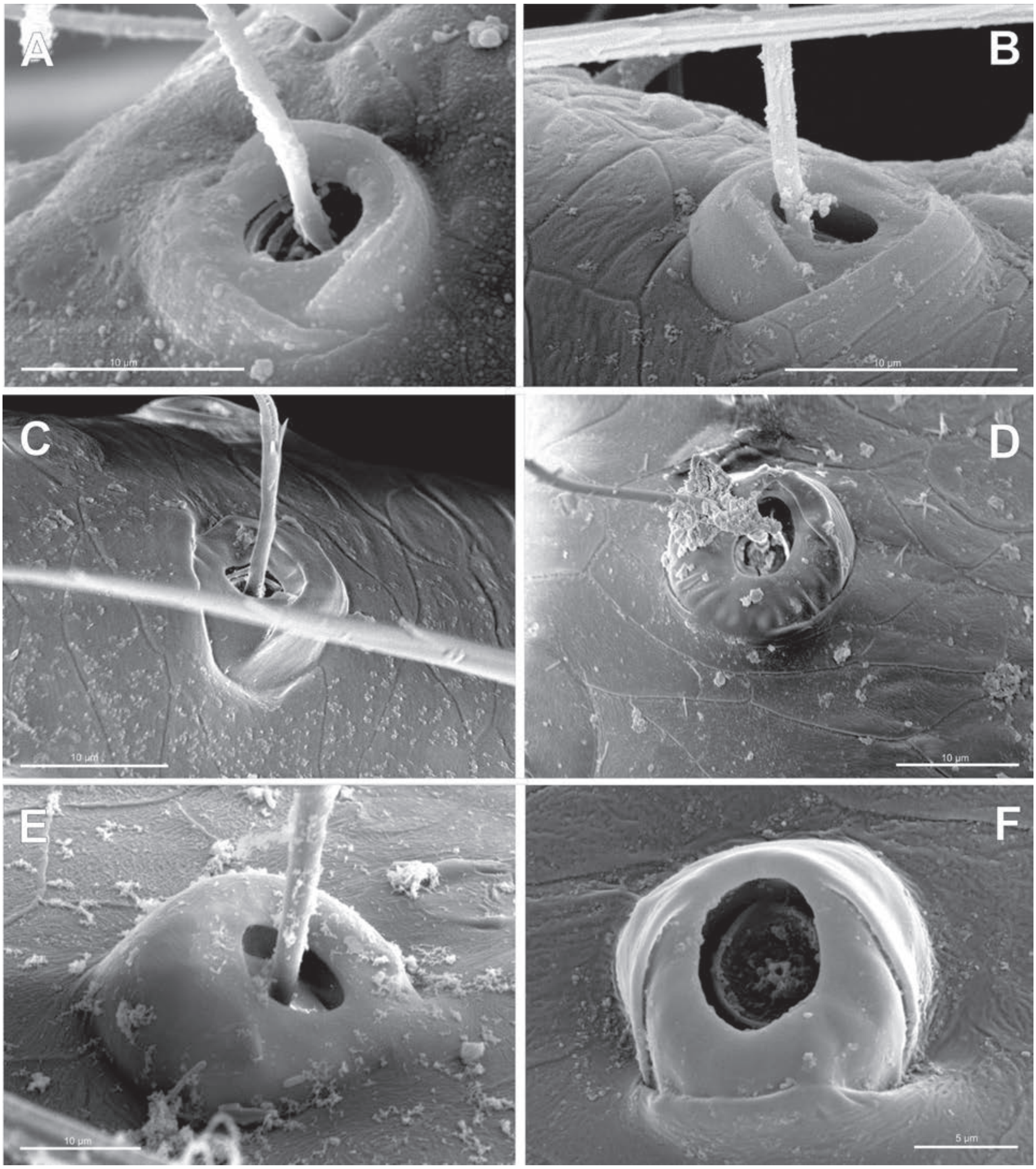

Figure 22. Bothria of 'Cyatholipoid lineage': Synotaxidae **A** *Tekellina sadamotoi*, mt 1 (E-type) **B** '*Tekellina*' *araucana*, ti 3 (E-type) **C** *Nescina* sp., ti 3 (E-type) **D** *Hamus cornutus*, ti 2 (E-type) (courtesy F. Ballarin) **E** *Gaucelmus* sp., ti 3 (A-type) **F** *Synotaxus* sp., ti 1 (A-type).

6.3. Cyatholipidae (Cya).

The bothria of four cyatholipid genera are studied here: *Matilda* Forster, 1988; *Tekella* Urquhart, 1894; *Teemenaarus* Davies, 1978; and *Ilisoa* Griswold, 1987 (Fig. 24A–F). In addition, the bothria of the 5 cyatholipid genera have been figured previously: *Tekella*, *Teemenaarus*, *Cyatholipus* Simon, 1894 and *Matilda* (Forster 1988: figs 26, 30, 31, and 140, respectively), and *Pembatatu* Griswold, 2001 (Griswold 2001: fig. 6B). Forster (1988: 11) has included the '*Argiope*-type'

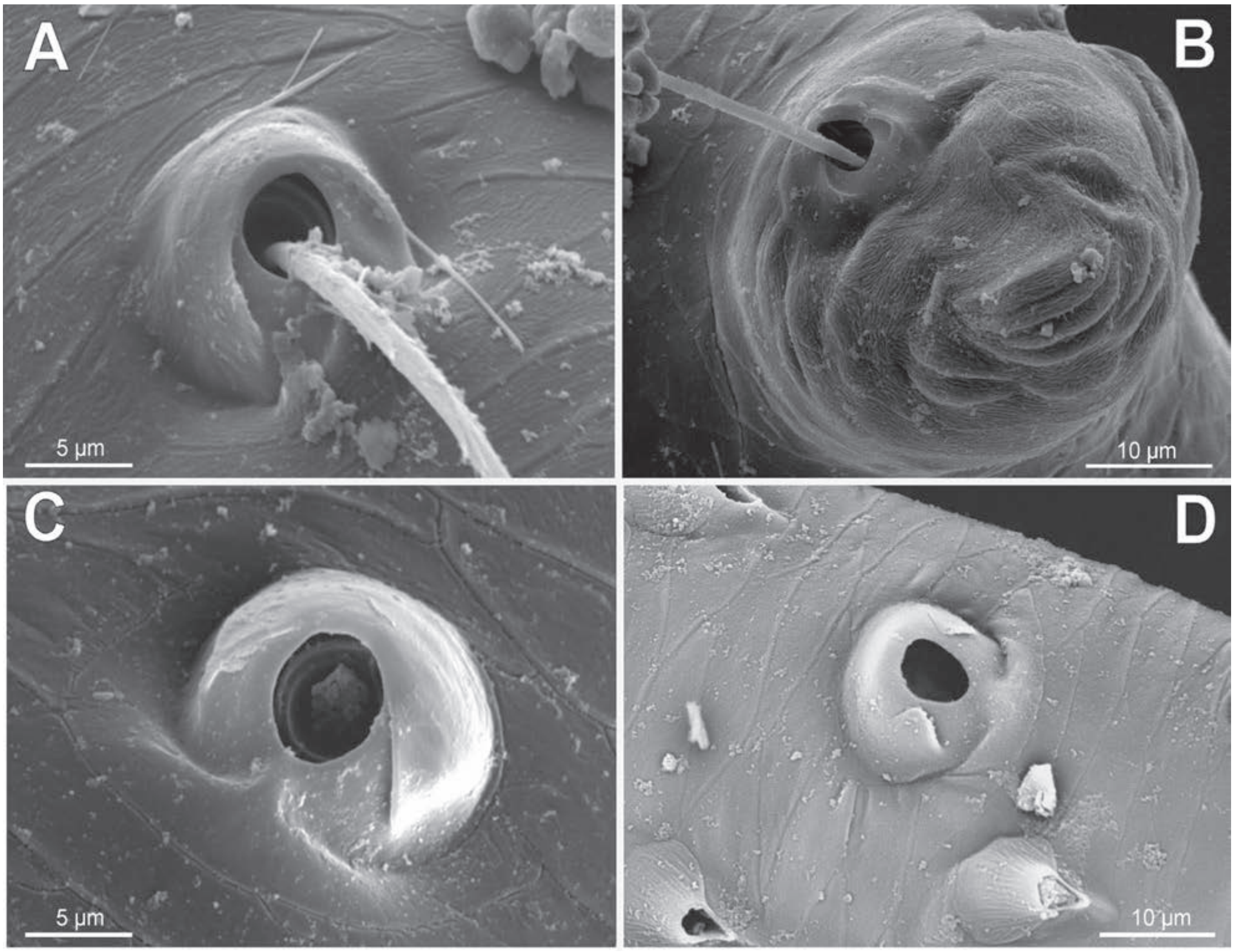

Figure 23. Bothria of 'Cyatholipoid lineage': Physoglenidae (Pahorinae, Physogleninae) **A** *Pahora murihiku*, ti 2 (E-type) **B** *Pahora murihiku*, trichobothrium-bearing spur on male palpal tibia (E-type) **C** *Tupua bisetosa*, ti 2 (A-type) **D** *Physoglenes puyehue*, mt 3 (A-type).

of bothria, described as "Bothria with the posterior hood reduced to two small ridges or absent", in the diagnosis of the family. The intermediate '*Argiope*-type' of bothria indeed seems most usual in the cyatholipids: *Tekella* (Fig. 24B; Forster 1988: fig. 26), *Teemenaarus* (Fig. 24C–E; Forster 1988: fig. 30), and *Cyatholipus* (Forster 1988: fig. 31). However, the ancestral '*Erigone*-type' of bothria is recorded in *Matilda* (Fig. 24A; Forster 1988: fig. 140), as well as the advanced '*Theridion*-type' in *Ilisoa* (Fig. 24F) and *Pembatatu* (Griswold 2001: fig. 6B). So, the complete set of the three bothrial types is presented in the Cyatholipidae. It should be noted that bothrium shape varies unusually in some cyatholipid genera, e.g., in *Matilda* (cf. *Matilda* sp. 1: Fig. 24A, and *Matilda australia*: Forster 1988: fig. 140). Moreover, sometimes the bothrium shape varies even in the same cyatholipid specimen (see *Teemenaarus silvestris*: Fig. 24C–E).

6.4. Nesticidae (Nes).

The bothria of four genera representing all three nesticid subtaxa, distinguished now, are studied here: Nesticini: *Aituaria* Esyunin & Efimik, 1998 and *Daginesticus* Fomichev, Ballarin & Marusik, 2022 (Fig. 25A, B); Nesticellini: *Nesticella* Lehtinen & Saaristo, 1980 (Fig. 25C); '*Eidmannella* clade': *Eidmannella* Roewer,

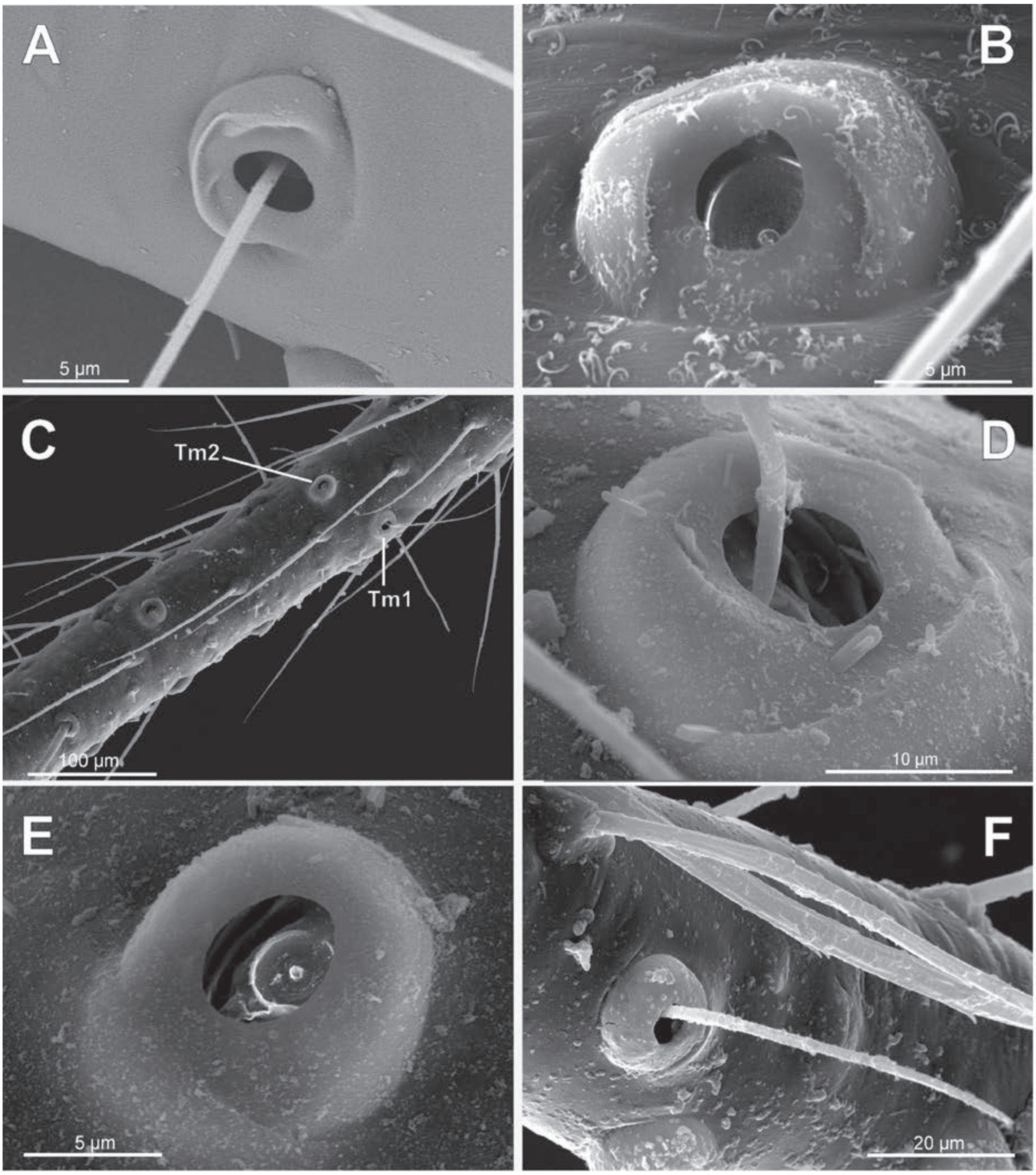

Figure 24. Bothria of 'Cyatholipoid lineage': Cyatholipidae **A** *Matilda* sp.1, ti 2 (E-type) (courtesy R. Raven) **B** *Tekella absidata*, ti 2 (A-type) **C** *Teemenaarus silvestris*, ti 3 (Tm1 and Tm2, arrows – two bothria of A-type, but differs in form) **D** the same, Tm1 (A-type) **E** the same, Tm2 (A-type) **F** *Ilisoa* sp., ti 2 (T-type).

1935 (Fig. 25D). The bothria of both Nesticini and Nesticellini are highly uniform and belong to the '*Theridion*-type'. However, bothria of '*Eidmannella* clade' belong to the '*Argiope*-type'. The diversity of the bothrial types in the 'Cyatholipoid lineage' is summarized in Fig. 32.

7. 'Theridioid lineage', TH:
7.1. Theridiidae Sundevall, 1833 (Thr).
7.1.1. Argyrodinae Simon, 1881 [Argyr].
7.1.2. Hadrotarsinae Thorell, 1881 [Hadro].

7.1.3. Latrodectinae Petrunkevitch, 1928 [Latro].
7.1.4. Pholcommatinae Simon, 1894 [Pholc].
7.1.5. Spintharinae Simon, 1894 [Spint].
7.1.6. Theridiinae Sundevall, 1833 [Thrid].
7.1.7. Phoroncidini O. Pickard-Cambridge, 1874 [Phorn].

After the relocation of Nesticidae by Ramírez et al. (2022) to 'Cyatholipoids', the sister lineage of the 'spineless femur clade,' Theridiidae remained the only member of the 'theridioid line' (Griswold et al. 1998: fig. 7). Agnarsson (2004: fig. 105) recognized six theridiid subfamilies: Hadrotarsinae, Latrodectinae, Spintharinae, Pholcommatinae, Argyrodinae, and Theridiinae. However, the subfamily affiliation of some theridiid genera remained uncertain; and we preferred to listing herein, e.g., *Phoroncidia* Westwood, 1835 in old Simon's (1894) tribe Phoroncidini. Hadrotarsines were formerly described as an independent family and listed in Haplogynae (see discussions in Forster et al. 1990 and Agnarsson 2004), but today they are recognized as a theridiid subfamily.

7.1. Theridiidae (Thr).

The bothria of 13 genera representing all six conventional theridiid subfamilies and the one tribe of uncertain position are studied here: Hadrotarsinae: *Euryopis* Menge, 1868 and *Phycosoma* O. Pickard-Cambridge, 1880 (Fig. 26A, B); Latrodectinae: *Latrodectus* Walckenaer, 1805 (Fig. 26D) and *Crustulina*

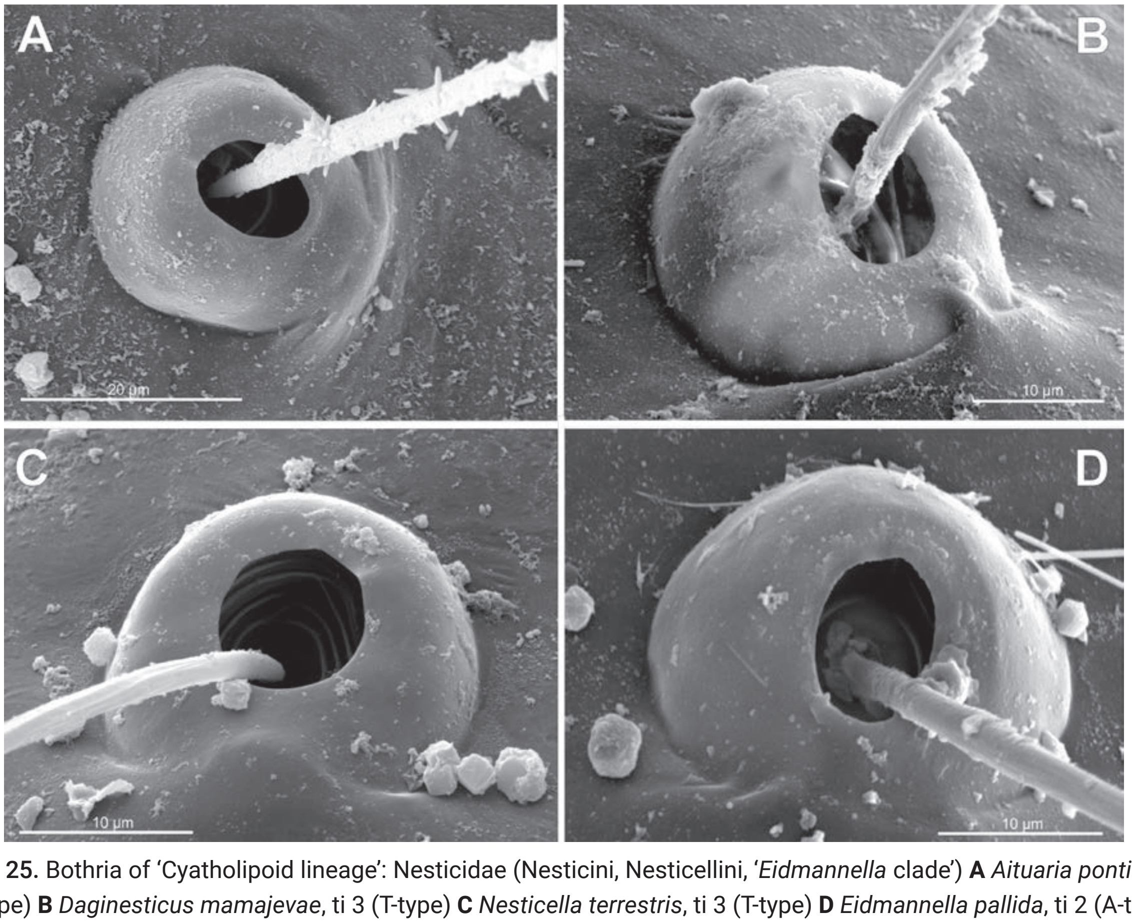

Figure 25. Bothria of 'Cyatholipoid lineage': Nesticidae (Nesticini, Nesticellini, '*Eidmannella* clade') **A** *Aituaria pontica*, mt 1 (T-type) **B** *Daginesticus mamajevae*, ti 3 (T-type) **C** *Nesticella terrestris*, ti 3 (T-type) **D** *Eidmannella pallida*, ti 2 (A-type).

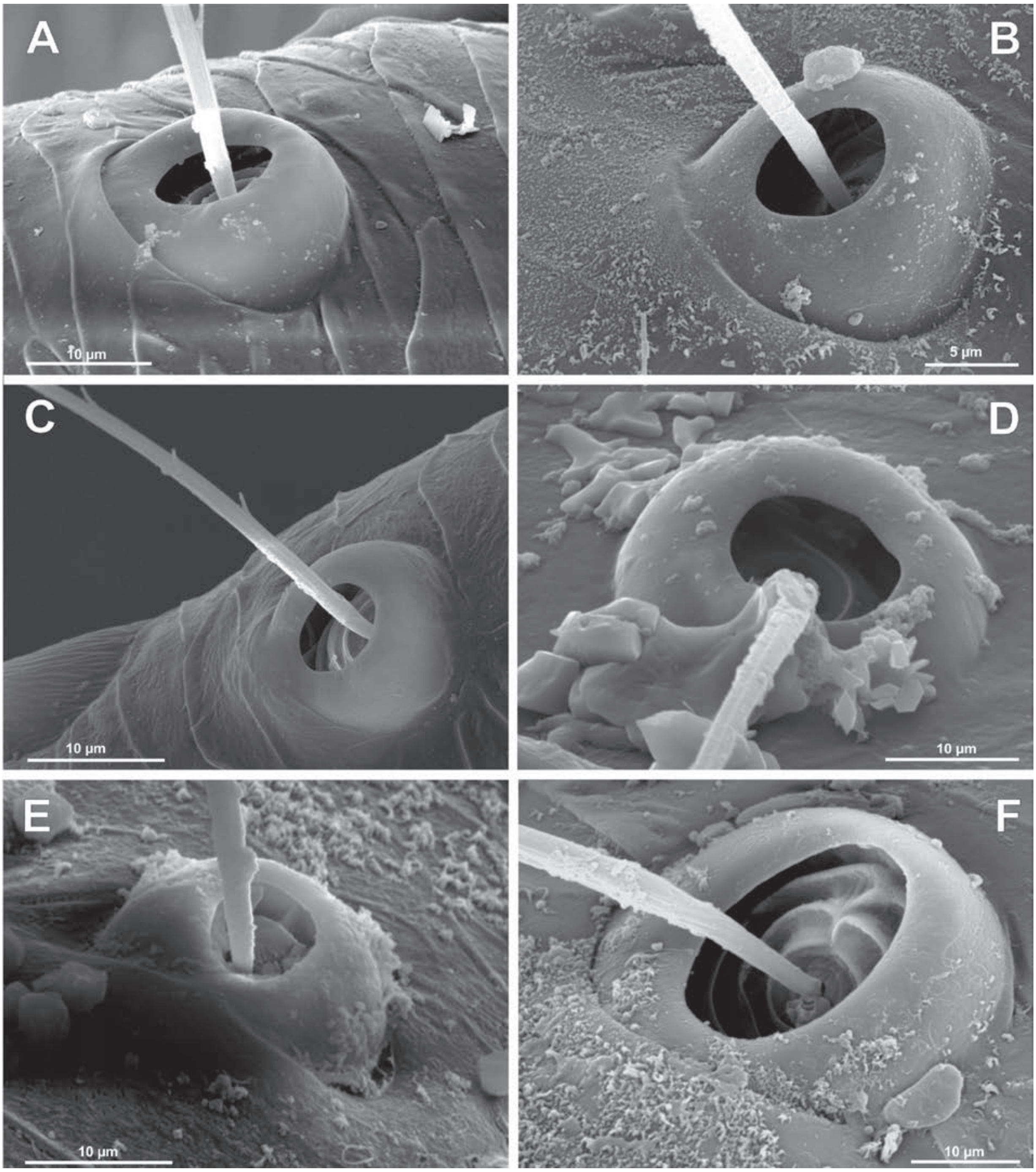

Figure 26. Bothria of 'Theridioid lineage': Theridiidae (Hadrotarsinae, Argyrodinae, Latrodectinae, Spintharinae, Theridiinae) **A** *Euryopis flavomaculata*, mt 2 **B** *Phycosoma* sp., ti 3 **C** *Argyrodes* sp., ti 3 **D** *Latrodectus tredecimguttatus*, ti 3 **E** *Episinus angulatus*, ti 3 **F** *Theridion tinctum*, ti 3.

Menge, 1868 (which images are not presented herein); Spintharinae: *Episinus* Walckenaer, 1809 (Fig. 26E); Pholcommatinae: *Carniella* Thaler & Steinberger, 1988; *Theonoe* Simon, 1881; *Robertus* O. Pickard-Cambridge, 1879; *Pholcomma* Thorell, 1869; and *Glebych* Eskov & Marusik, 2021 (Fig. 27A–E); Argyrodinae: *Argyrodes* Simon, 1864 (Fig. 26C); Theridiinae: *Theridion* Walckenaer, 1805 (Fig. 26F); and Phoroncidini: *Phoroncidia* Westwood, 1835 (Fig. 27F). In addition, the bothria of the five theridiid genera have been figured earlier: *Anelosimus* Simon, 1891, *Argyrodes*, *Spintharus* Hentz, 1850, and *Stemmops*

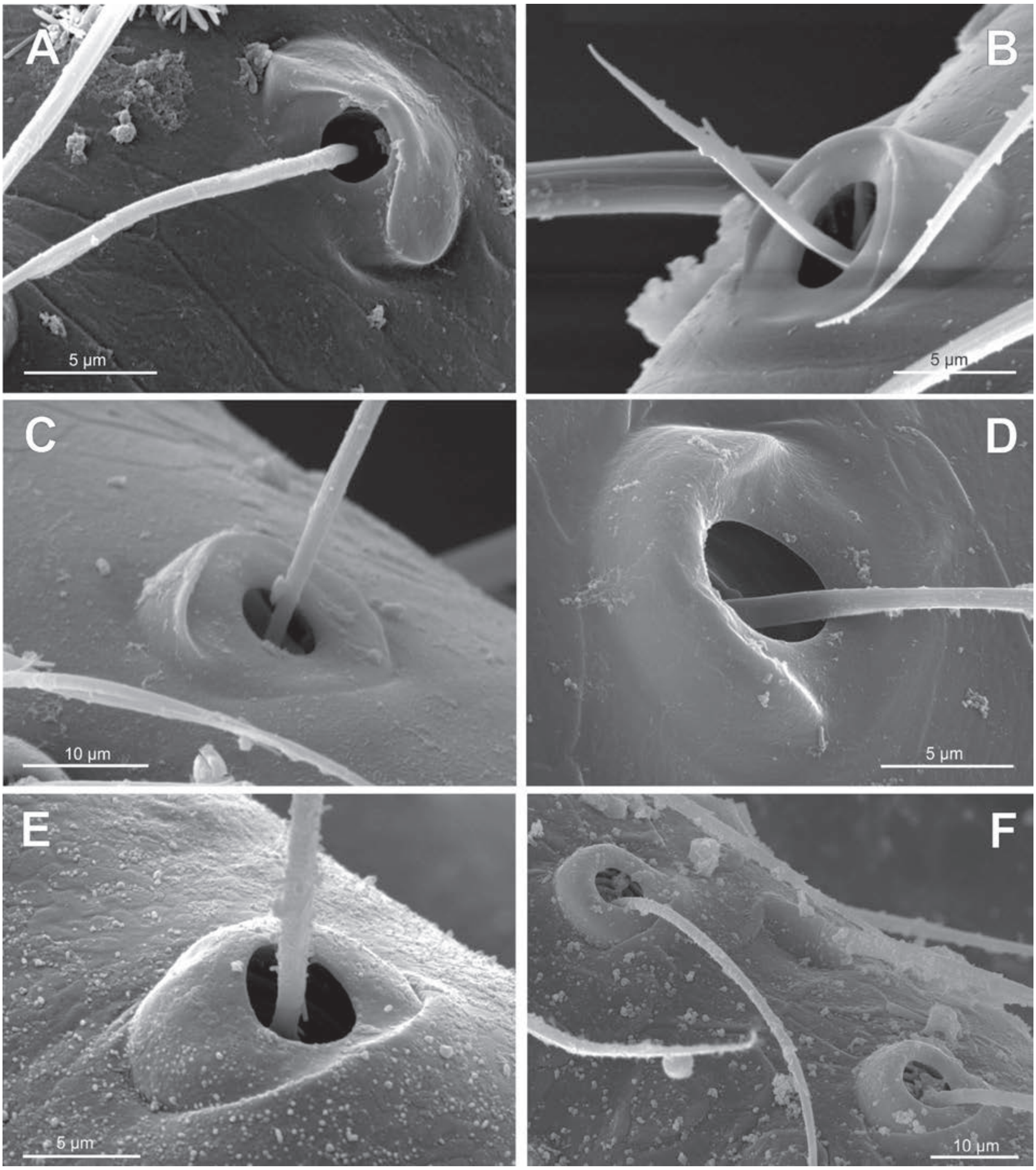

Figure 27. Bothria of 'Theridioid lineage': Theridiidae (Pholcommatinae, Phoroncidini) **A** *Carniella nepalensis*, ti 3 (E-type) **B** *Theonoe minutissima*, ti 1 (E-type) **C** *Robertus lividus*, ti 3 (E-type) **D** *Pholcomma gibbum*, ti 3 (A-type) **E** *Glebych minutissimus*, ti 1 (T-type) **F** *Phoroncidia* sp., ti 1 (T-type).

O. Pickard-Cambridge, 1894 (Agnarsson 2004: figs 24C, 31G, 69E, and 74D, respectively), and *Knoflachia* Marusik & Eskov, 2024 (Marusik and Eskov 2024: fig. 5F). The bothria of the almost all theridiid subfamilies and tribes (Hadrotarsinae, Latrodectinae, Spintharinae, Argyrodinae, Theridiinae, and Phoroncidini) are highly uniform and belong to the advanced '*Theridion*-type' (Figs 26A–F, 27F). The single remarkable exception is the subfamily Pholcommatinae, having the complete set of the all three bothrial types: the ancestral '*Erigone*-type' in *Carniella*, *Theonoe* and *Robertus* (Fig. 27A, B, and Fig. 27C, respectively); the intermediate ‘*Argiope*-type’ in *Pholcomma* (Fig. 27D); and the advanced ‘*Theridion*-type’ in *Glebych* (Fig. 27F). The diversity of the bothrial types in the ‘Theridioid lineage’ is summarized in Fig. 32.

Discussion

Distribution, at the subfamily/tribe level, of the three main bothrial types (the ancestral ‘*Erigone*-type’, the advanced ‘*Theridion*-type’, and the intermediate ‘*Argiope*-type’) in the seven main lineages of Araneoidea (‘malkariods’, ‘tetragnathoids’, ‘araneoids’, ‘symphytognathoids’, ‘linyphioids’, ‘cyatholipoids’ and ‘theridioids’) is summarized in Figs 28–32. It should be emphasized that these are not cladograms in the strict sense: the families/subfamilies within of the seven main lineages (Fig. 1) are not subordinated. They are arranged in one row so that taxa with the ancestral type of bothria are on the left side of the row, and those with an advanced type are on the right.

A subfamily or tribe can have a single bothrial type or a sequence of several types. The sequence can be complete, comprising all three types (from the ancestral, most complicated ‘*Erigone*-type’ to the advanced, simplest ‘*Theridion*-type’, via the intermediate ‘*Argiope*-type’), or shortened to two types: the basal (from the ancestral ‘*Erigone*-type’ to the intermediate ‘*Argiope*-type’) or the terminal (from the intermediate ‘*Argiope*-type’ to the advanced ‘*Theridion*-type’). We will name them further ‘the complete E-A-T sequence’, ‘the shortened basal E-A sequence’ and ‘the shortened terminal A-T sequence’, respectively.

It should be emphasized that not a single combination of the ancestral ‘*Erigone*-type’ and the advanced ‘*Theridion*-type’, without the intermediate ‘*Argiope*-type’, was found in the any of the 61 studied subfamilies/tribes (Figs 28–32). It confirms, in our opinion, that we are dealing exactly with sequences, not with ‘mechanical sets’ of bothrial types.

In the ‘Malkaroid lineage’ (Fig. 28), there are no bothrial sequences, and all its members (the malkarids Malkarinae, Sternoidinae and Tingotinginae, and Pararchaeidae) have a single bothrial type: the ancestral ‘*Erigone*-type’.

In the ‘Tetragnathoid lineage’ (Fig. 28), there are two complete E-A-T sequences: in the mimetids Mimetinae and the tetragnathids Tetragnathinae. The remaining mimetids, Oarcinae and Gelanorinae, as well as the Arkyidae, have the ancestral ‘*Erigone*-type’ only. By contrast, the remaining tetragnathids do not have a single bothrial type, but bothrial sequences: the shortened basal E-A sequences (in Diphyainae, Nanometinae and Leucauginae) and the shortened terminal A-T sequence in Metainae.

In the ‘Araneoid lineage’ (Fig. 29), only two sequences are present: the complete E-A-T sequence in the araneids Araneinae, and the shortened terminal A-T sequence in Zygiellidae. All the remaining taxa have a single bothrial type: two have the ‘*Erigone*-type’ (the araneids Cyrtarachninae and Testudinarini), four have the ‘*Argiope*-type’ (the araneids Argiopinae, Cyrtophorinae, Micratheninae, and Caerostrini), and four have the ‘*Theridion*-type’ (the araneids Gasteracanthinae, Hypognathini and Poltyini, and in Nephilidae).

In the ‘Symphytognathoid lineage’ (Fig. 30), the complete E-A-T sequences are absent, and a single type of the bothrial sequence, the shortened basal E-A sequence, is present in four taxa (in the anapids Anapinae and Taphiassinae, the micropholcommatids Micropholcommatinae, and in Synaphridae).

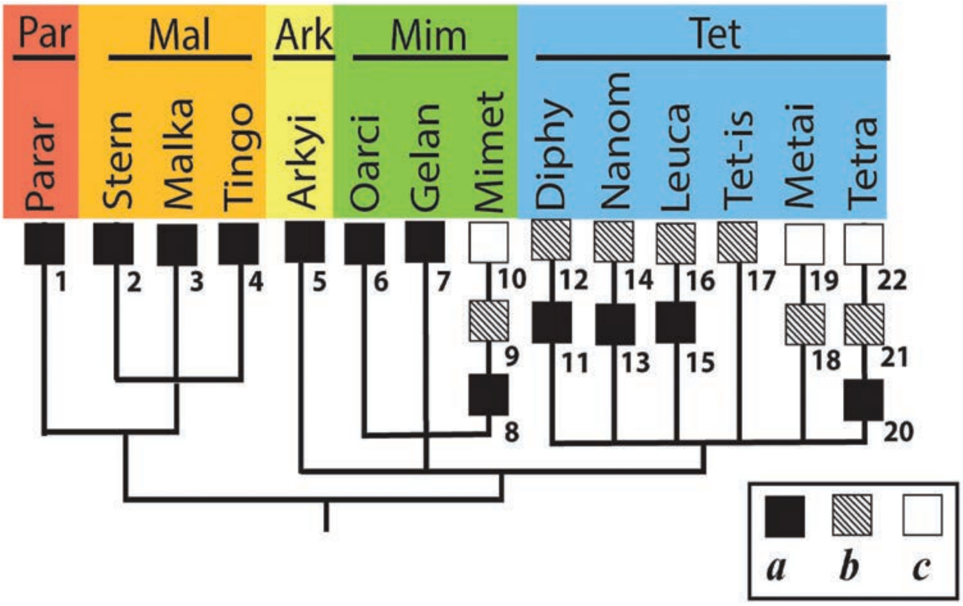

Figure 28. Distribution of the three main bothrial types in the subfamilies/tribes of the 'Tetragnathoid branch' (the 'Malkariod' and the 'Tetragnathoid' lineages). Abbreviations: a – the ancestral '*Erigone*-type', b – the intermediate '*Argiope*-type', c – the advanced '*Theridion*-type'; Ark – Arkyidae (Arkyi – 'Arkyinae'); Mal – Malkaridae (Malka – Malkarinae, Stern – Sternoidinae, Tingo – Tingotinginae); Mim – Mimetidae (Gelan – Gelanorinae, Mimet – Mimetinae, Oarci – Oarcinae); Par – Pararchaeidae (Parar – 'Pararchaeinae'); Tet – Tetragnathidae (Diphy – Diphyainae, Leuca – Leucauginae, Metai – Metainae, Nanom – Nanometinae, Tetra – Tetragnathinae). The numbers refer to the studied genera: 1 *Anarchaea*, *Flavarchaea*; 2 *Chilenodes*; 3 *Malkara*; 4 *Tingotingo*; 5 *Arkys*; 6 *Oarces*; 7 *Gelanor*; 8 *Ero* (male palp tibia); 9 *Ero* (leg joints); 10 *Australomimetus*; 11 *Chrysometa*, Diphyainae gen. sp.; 12 *Diphya*; 13 *Pinkfloydia*; 14 *Nanometa*, *Orsinome*; 15 *Leucauge*; 16 *Metleucauge*; 17 *Azilia*; 18 *Metellina*; 19 *Meta*; 20 *Cyrtognatha*; 21 *Allende*, *Mollemeta*; 22 *Pachygnatha*, *Tetragnatha*.

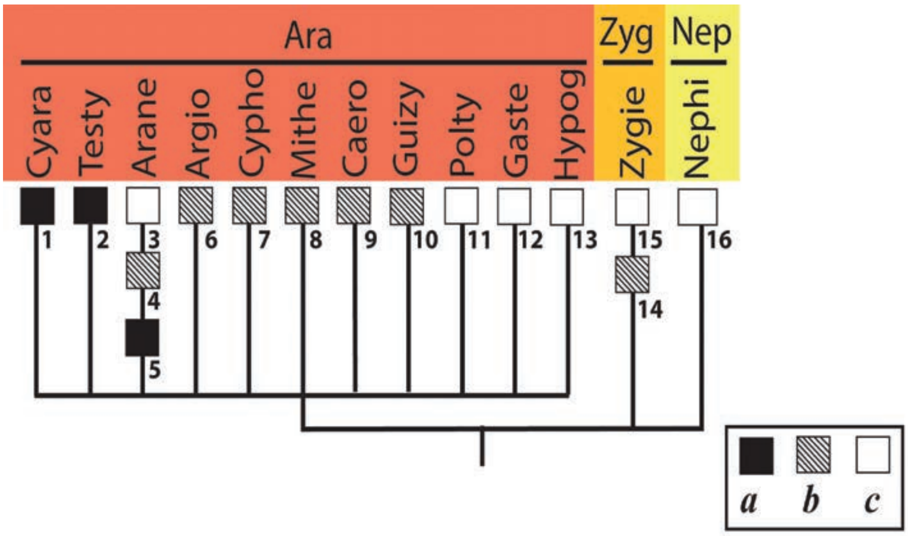

Figure 29. Distribution of the three main bothrial types in the subfamilies/tribes of the 'Araneoid lineage'. Abbreviations: a – the ancestral '*Erigone*-type', b – the intermediate '*Argiope*-type', c – the advanced '*Theridion*-type'; Ara – Araneidae (Arane – Araneinae, Argio – Argiopinae, Caero – Caerostrini, Cyara – Cyrtarachninae, Cypho – Cyrtophorinae, Gaste – Gasteracanthinae, Guizy – Guizygiellinae; Hypog – Hypognathini, Mithe – Micratheninae, Polty – Poltyini, Testu – Testudinarini); Nep – Nephilidae (Nephi – 'Nephilinae'); Zyg – Zygiellidae (Zygie – 'Zygiellinae'). The numbers refer to the studied genera:1 *Cyrtarachne*, *Chorizopes*; 2 *Melychiopharis*; 3 *Araneus*; 4 *Larinia*, *Mangora*, *Cyclosa*; 5 *Singa, Hypsosinga*; 6 *Argiope*; 7 *Cyrtophora*; 8 *Micrathena*; 9 *Caerostris*; 10 *Guizygiella*; 11 *Poltys*; 12 *Gasteracantha*; 13 *Hypognatha*;14 *Zygiella x-notata*, *Leviellus*; 15 '*Zygiella*' *atrica*, *Parazygiella*; 16 *Nephila*, *Nephilengys*.

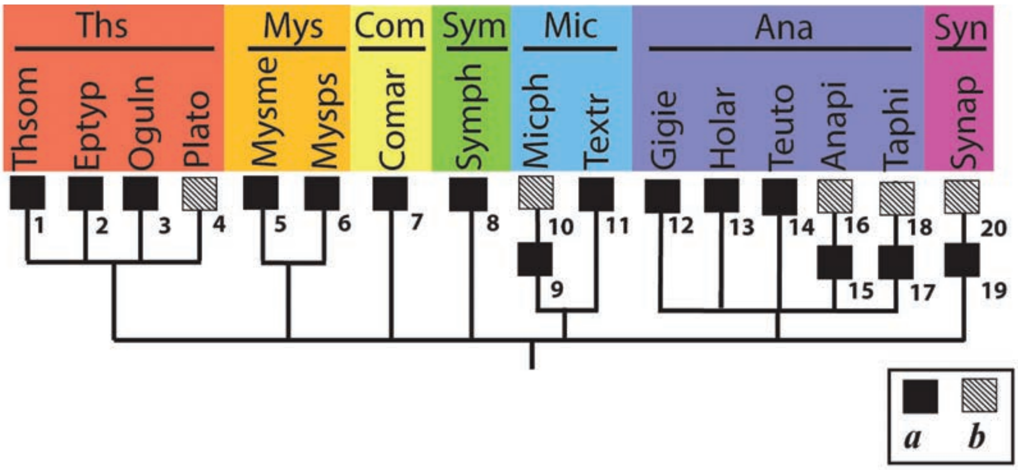

Figure 30. Distribution of the two main bothrial types in the subfamilies/tribes of the 'Symphytognathoid lineage'. Abbreviations: a – the ancestral '*Erigone*-type', b – the intermediate '*Argiope*-type'; Ana – Anapidae (Anapi – Anapinae, Gigie – Gigiellinae, Holar – Holarchaeinae, Taphi – Taphiassinae, Teuto – Teutoniellinae);Com – Comaromidae (Comar – 'Comarominae');Mic – Micropholcommatidae (Micph – Micropholcommatinae, Textr – Textricellinae);Mys – Mysmenidae (Mysme – Mysmeninae, Mysps – Mysmenopsinae);Sym – Symphytognathidae (Symph – 'Symphytognathinae');Syn – Synaphridae (Synap – 'Synaphrinae');Ths – Theridiosomatidae (Eptyp – Epeirotypinae, Oguln – Ogulninae, Plato – Platoninae, Thsom – Theridiosomatinae). The numbers refer to the studied genera (in square brackets a literature data): 1 *Theridiosoma*; 2 *Naatlo*; 3 *Ogulnius*; 4 *Plato*, [*Cuacuba*]; 5 *Mysmena*, *Microdipoena*; 6 *Mysmenopsis*, *Isela*; 7 *Comaroma*, *Balticoroma*; 8 *Symphytognatha*; 9 *Micropholcomma*, *Tricellina*, [*Pua*]; 10 *Plectochetos*, *Austropholcomma*, [*Patelliella*]; 11 *Rayforstia*, *Eterosonycha*, *Epigastrina*, *Raveniella*, *Normplatnicka*, *Eperiella*, [*Algidiella*, *Taliniella*, *Tinytrella*]; 12 *Gigiella*; 13 *Holarchaea*; 14 *Teutoniella*; 15 *Acrobleps*, *Minanapis*, *Montanapis*, *Crassanapis*, *Sheranapis*, *Elanapis*, *Sofanapis*, *Hickmanapis*, *Zealanapis*, *Zangherella*, [*Risdonius*]; 16 *Pseudanapis*; 17 [*Olgania*]; 18 *Taphiassa*; 19 *Synaphris*; 20 *Cepheia*.

The majority of the symphytognathoid taxa have a single bothrial type: ten have the '*Erigone*-type' (the theridiosomatids Theridiosomatinae, Epeirotypinae, and Ogulninae, the mysmenids Mysmeninae and Mysmenopsinae, Symphytognathidae, Comaromidae, the micropholcommatids Textricellinae, and the anapids Holarchaeinae, Teutoniellinae, and Gigiellinae), and one has the '*Argiope*-type' (the theridiosomatids Platoninae).

In the 'Linyphioid lineage' (Fig. 31), the complete E-A-T sequences are also absent. There are three shortened basal E-A sequences (in the linyphiids Micronetinae and Linyphiinae, and in Pimoidae). The remaining taxa have a single bothrial type: the '*Erigone*-type' in the linyphiids Erigoninae, and the '*Argiope*-type' in the linyphiids Stemonyphantinae and Mynogleninae.

In the 'Cyatholipoid lineage' (Fig. 32), a high diversity of bothrial types and their sequences is found: the complete E-A-T sequence in Cyatholipidae; the shortened basal E-A sequence in Synotaxidae; the '*Erigone*-type' in the physoglenids Physogleninae; the '*Argiope*-type' in the physoglenids Pahorinae and nesticids of the '*Eidmannella* clade'; and the '*Theridion*-type' in the nesticids Nesticini and Nesticellini.

In the 'Theridioid lineage' (Fig. 32), the picture seems unique. Almost all the subfamilies/tribes (Hadrotarsinae, Latrodectinae, Spintharinae, Argyrodinae, Theridiinae, and Phoroncidini) have uniform bothria of the '*Theridion*-type'. However, there is a single remarkable exception: the subfamily Pholcommatinae has a complete E-A-T sequence. These data are summarized in Table 1 and Fig. 33.

We can see (Fig. 33) the parallel evolutionary trends of the step-by-step replacing the basal '*Erigone*-type' of bothria by the more advanced '*Argiope*-type'

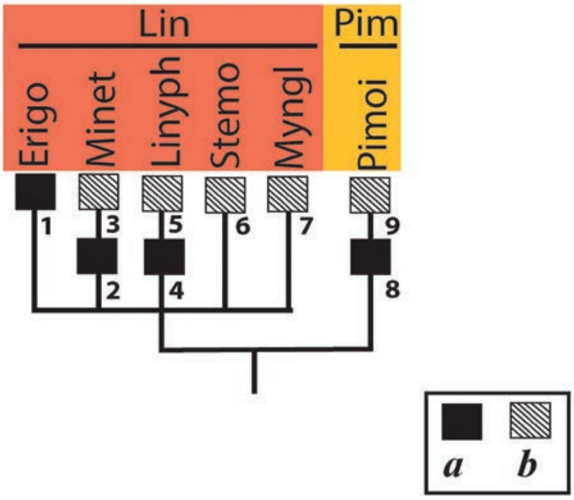

Figure 31. Distribution of the two main bothrial types in the subfamilies/tribes of the 'Linyphioid lineage'. Abbreviations: a – the ancestral '*Erigone*-type', b – the intermediate '*Argiope*-type'; Lin – Linyphiidae (Erigo – Erigoninae, Linyp – Linyphiinae, Minet – Micronetinae, Myngl – Mynogleninae, Stemo – Stemonyphantinae); Pim – Pimoidae (Pimoi – 'Pimoidae'). The numbers refer to the studied genera: 1 *Erigone*, *Pelecopsis*, *Scutpelecopsis*, *Minyriolus*, *Lophomma*; 2 *Maro*, *Agyneta*; 3 *Microneta*; 4 *Porrhomma*; 5 *Linyphia*, *Allomengea*, *Lepthyphantes*; 6 *Stemonyphantes*, *Weintrauboa*; 7 *Haplinis*, *Parafroneta*; 8 *Nanoa*; 9 *Pimoa*.

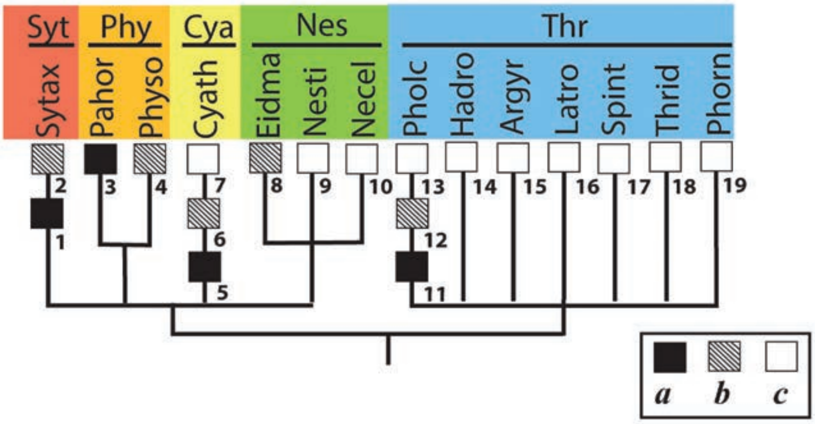

Figure 32. Distribution of the three main bothrial types in the subfamilies/tribes of the 'Spineless femur clade' (the 'Cyatholipoid' and the 'Theridioid' lineages). Abbreviations: a – the ancestral '*Erigone*-type', b – the intermediate '*Argiope*-type', c – the advanced '*Theridion*-type'; Cya – Cyatholipidae (Cyath – 'Cyatholipidae'); Nes – Nesticidae (Eidma – '*Eidmannella* clade', Necel – Nesticellini, Nesti – Nesticini); Phy – Physoglenidae (Pahor – Pahorinae, Physo – Physogleninae); Syt – Synotaxidae (Sytax – 'Synotaxidae'); Thr – Theridiidae (Argyr – Argyrodinae, Hadro – Hadrotarsinae, Latro – Latrodectinae, Pholc – Pholcommatinae, Phorn – Phoroncidini, Spint – Spintharinae, Thrid – Theridiinae).The numbers refer to the studied genera (in square brackets a literature data): 1 *Tekellina*, '*Tekellina*' *araucana*, *Nescina*, *Hamus*; 2 *Gaucelmus*, *Synotaxus*; 3 *Pahora*, [*Mangua*]; 4 *Tupua*, *Physoglenes*, [*Meringa*]; 5 *Matilda*; 6 *Tekella*, *Teemenaarus*; 7 *Ilisoa*; 8 *Eidmannella*; 9 *Aituaria pontica*, *Daginesticus*; 10 *Nesticella*; 11 *Carniella*, *Theonoe*, *Robertus*; 12 *Pholcomma*; 13 *Glebych*; 14 *Euryopis*, *Phycosoma*; 15 *Argyrodes* 16 *Latrodectus*, *Crustulina*; 17 *Episinus*; 18 *Theridion*; 19 *Phoroncidia*.

and, finally, by the terminal '*Theridion*-type' in both main branches of the superfamily, the 'tetragnathoid branch' and the 'araneoid branch' (Fig. 33). Not even one of the seven main araneoid lineages lacks the basal '*Erigone*-type'. It is a single bothrial type present in the 'malkariods'; it is included in the shortened basal E-A sequence in the 'symphytognathoids' and 'linyphioids'; and it is included in the complete E-A-T sequences in the 'tetragnathoids', 'araneoids' 'cyatholipoids' and 'theridioids'. It should be emphasized that the terminal '*Theridion*-type' exists

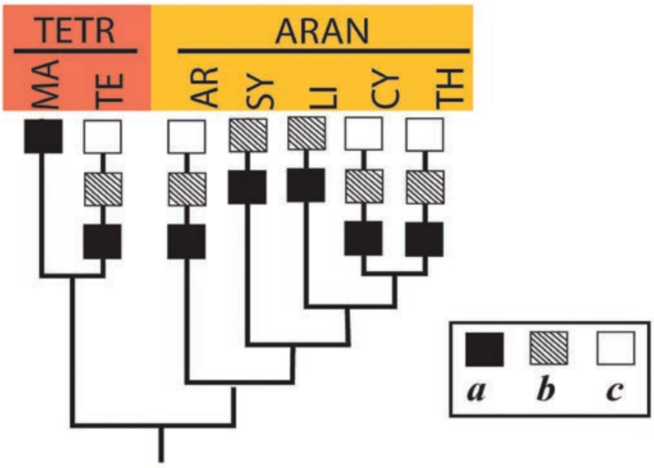

Figure 33. Distribution of the three main bothrial types in the main divisions of the superfamily Araneoidea, 'branches' and 'lineages'. Abbreviations: a – the ancestral '*Erigone*-type'; b – the intermediate '*Argiope*-type'; c – the advanced '*Theridion*-type'. ARAN – Araneoid branch; TETR – Tetragnathoid branch; AR – Araneoid lineage; CY – Cyatolipoid lineage; LI – Linyphioid lineage; MA – Malkaroid lineage; SY – Symphytognathoid lineage; TE – Tetragnathoid lineage; TH – Theridioid lineage.

Table 1. Distribution, at the subfamily/tribe level, of the three main bothrial types and their sequences in the seven main lineages of Araneoidea. AR – 'araneoids', CY – 'cyatholipoids', LI – 'linyphioids', MA – 'malkariods', SY – 'symphytognathoids', TE – 'tetragnathoids', and TH – 'theridioids'.

	MA	TE	AR	SY	LI	CY	TH	Σ
ancestral '*Erigone*-type', E	4	3	2	10	1	1	–	21
shortened basal E-A sequence	–	3	–	4	3	1	–	12
intermediate '*Argiope*-type', A	–	–	4	1	2	2	–	9
complete E-A-T sequence	–	2	1	–	–	1	1	5
shortened terminal A-T sequence	–	1	1	–	–	–	–	2
advanced '*Theridion*-type', T	–	–	4	–	–	2	6	12

only as a portion of the complete E-A-T sequences and seems but a crown of this trend. There are not a single lineage having a solely the advanced '*Theridion*-type' (cf. the 'malkariods'), and even having the shortened terminal A-T sequence (cf. the 'symphytognathoids' and 'linyphioids').

The shortened terminal A-T sequence is very rare even at the subfamily/tribe level: only two cases, in the 'tetragnathoids' and the 'araneoids', vs 12 cases of the shortened basal E-A sequence (Table 1). The subfamilies/tribes having the advanced '*Theridion*-type' are not so rare (12 cases), and even somewhat more numerous than the intermediate '*Argiope*-type' (nine cases), but their number is almost half as large as the number of those having the basal '*Erigone*-type' (21 cases).

In addition, bothrial morphology provides additional morphological arguments in some controversial cases of araneoid taxonomy.

(1) The genera *Gaucelmus*, *Hamus*, and *Nescina* were relocated by Ramírez et al. (2022) from Nesticidae into the 'newly enlarged Synotaxidae', based on copulatory organ characters and molecular data. Bothrial morphology strongly supports this transfer: the relocated genera have bothria of the '*Erigone*-type' or '*Argiope*-type', whereas all the 'typical nesticids' have

bothria of the '*Theridion*-type' (cf. Figs 22C–E, 25A–C). It should be noted that the isolated position of the genus *Eidmannella* in the Nesticidae (termed the '*Eidmannella* clade' in this study), supposed by Lehtinen and Saaristo (1980) and confirmed now by Ballarin (pers. comm. 1.07.2022), is supported by its '*Argiope*-type' bothria (Fig. 25D).

(2) Almost all theridiids, from all the subfamilies, have highly uniform dome-like bothria of the '*Theridion*-type' (Fig. 26A–F). A remarkable exception is the tetrad of the genera listed in the subfamily Pholcommatinae: *Carniella*, *Theonoe*, and *Robertus* have the '*Erigone*-type' of bothria (Fig. 27A–C), and the *Pholcomma* has the '*Argiope*-type' (Fig. 27D). Agnarsson (2004: 462) united *Pholcomma*, *Carniella*, and *Robertus* in 'clade 35', and agreed with Knoflach's (1996) opinion about the close relationship between *Carniella* and *Theonoe*: "The results of this study strongly support such a placement [of *Carniella*] as sister to the clade (*Pholcomma*, *Robertus*) [...]. Knoflach (1996) suggested affinities between *Carniella* and *Theonoe* based on the absence of the male palpal tibial trichobothrium and modification of the cymbial tip [...]. *Theonoe* shares several additional features with the clade containing *Carniella*, *Pholcomma* and *Robertus* and thus Knoflach's argument seems well founded" (Agnarsson 2004: 463). Bothrial morphology clearly confirms the particular position of the well-supported Agnarsson's (2004) 'clade 35' in the family Theridiidae. It should be mentioned that according to some molecular data (Arnedo et al. 2004) *Pholcomma* and *Robertus* were considered as the sister group to the remaining theridiids. Thus, we propose to assign to the Agnarsson's (2004) 'clade 35', comprising the four genera of habitually similar small/minute 'erigonid-like theridiids', i.e., *Theonoe*, *Carniella*, *Robertus*, and *Pholcomma*, the rank of a separate subfamily of Theridiidae. When choosing the name for this taxon, comprising both *Theonoe* and *Pholcomma*, the Theonoeinae Simon, 1894, stat. nov. seems to be the most preferable. Theonoeae and Pholcommateae Simon, 1894 were established in the same study (Simon 1894: 586 and 589, respectively), and it allows us to discard the subfamilial name Pholcommatinae Simon, 1894, because the later taxon is well known as a taxonomic 'trash heap' lacking a conventional diagnosis: "The composition of this subfamily is uncertain" (Agnarsson 2004: 468). It is possible that further investigations, including molecular ones, will confirm the status of Theonoeinae as a sister group to the remaining theridiids. The bothria of theonoeines, the most plesiomorphic subfamily of the family, may be an additional morphological argument here.

(3) The micropholcommatid genus *Plectochetos* Butler, 1932 was synonymized with *Micropholcomma* Crosby & Bishop, 1927 by Forster (1959: 297) with no precise justification of this act: "A close examination of both males and females of *Plectochetos longissimus* Butler and the structure of the respiratory system leads me to conclude that this species is also congenenc with *M*[*icropholcomma*] *caeligenus* Crosby and Bishop" (Forster 1959: 298). Surprisingly, this doubtful synonymy was never discussed further, even in the fundamental revision of Micropholcommatidae by Rix and Harvey (2010). In our opinion, however, these two genera have nothing in common, except for the apneumonic respiratory system, which is but a family character. *Plectochetos* has a large bulb, comparable in the size to the prosoma, and

extremely long spiral embolus (Forster 1959: figs 64, 67, 68; Forster and Platnick 1984: fig. 369), whereas the male palp of *Micropholcomma* is so small that without a microscope may be confused with the female one (personal observations), and with short embolus shaped as an incomplete ring (Rix and Harvey 2010: figs 14A, B, 21A, B). Schütt (2003: 131), dealing in her study with *Micropholcomma* only, erroneously considered a minute male palp as the subfamily character of Micropholcommatinae: "61 *Cymbium and bulbus*: (0) normal size; (1) very small, not reaching beyond Fe I; (2) about as large as the prosoma. In Micropholcommatinae the male pedipalp is so shortened that the bulbus tip does not reach beyond the femur of the first leg, which is a synapomorphy for the subfamily" (Schütt 2003: 147). In addition to the drastically dissimilar male palps and endogynal characters such as the "super-coiled insemination ducts" in *Plectochetos* (cf. Rix and Harvey 2010: fig. 15E and fig. 15A–C), these two genera clearly differ in several somatic character, e.g., the presence of a dorsal abdominal scutum in the females of *Micropholcomma* (Rix and Harvey 2010: fig. 13A, B) and its absence in females of *Plectochetos* (Forster 1959: fig. 65). The '*Erigone*-type' of bothria in *Micropholcomma* (Fig. 16A) and the '*Argiope*-type' of bothria in *Plectochetos*, gen. revalid. (Fig. 16D; Forster and Platnick 1984: fig. 375) complements such list of morphological differences.

(4) Gregorič et al. (2015: 241) synonymized zygiellid genus *Parazygiella* Wunderlich, 2004 with *Zygiella* F.O. Pickard-Cambridge, 1902, based on purely molecular data. However, the detailed morphological diagnosis of *Parazygiella* by Wunderlich (2004a: 936) seems more convincing, and we consider it as a separate genus. The bothrial morphology supports such a separation too: *Zygiella* has bothria of the '*Argiope*-type' (Fig. 13A), whereas the bothria of *Parazygiella*, gen. revalid. belong to the '*Theridion*-type' (Fig. 13C).

(5) The male palps of the zygiellid *Zygiella atrica* (C.L. Koch, 1845) and *Z. keyserlingi* (Ausserer, 1871) are very similar and both drastically differ from that of the type species *Z. x-notata* (Clerck, 1757), as well as from all the other *Zygiella* species (Levi 1974: 272) in the extremely elongated seta-bearing tibia and extremely enlarged hook-like paracymbium (cf. Levi 1974: figs 5, 13, and 29, respectively). Thus, a separate genus can be proposed for *Zygiella atrica* (and *Z. keyserlingi*) based on the palp characters. The different bothria, the '*Argiope*-type' in *Z. x-notata* (Fig. 13A) and the '*Theridion*-type' in '*Zygiella*' *atrica* (Fig. 13D) also support such a separation.

(6) Álvarez-Padilla and Hormiga (2011) could not definitely nest several tetragnathid genera into their cladogram of the family: "Inside Tetragnathinae only *Cyrtognatha* changes placement as either sister to *Tetragnatha* or sister to all other tetragnathines. […] *Azilia* is either sister to Leucauginae with the morphology and behaviour data, or sister to all other tetragnathids with all data [mainly molecular] combined" (Álvarez-Padilla and Hormiga 2011: 728). Bothrial morphology can provide some additional arguments for such a choice. *Cyrtognatha* with its ancestral '*Erigone*-type' of bothria (Fig. 9A) seems a sister group rather to "other tetragnathines" with their complete E-A-T sequence (Fig. 9B–D) than to *Tetragnatha* with its advanced '*Theridion*-type' (Fig. 9E). *Azilia* with '*Argiope*-type' of bothria (Fig. 9F) seems a sister group rather to Leucauginae with their shortened basal E-A sequence (Fig. 8A, B) than to "all other tetragnathids" with their complete E-A-T sequence.

Conclusions

Three superfamilies (i.e., Nicodamoidea, Deinopoidea, and Leptonetoidea) have been proposed previously as the sister group of Araneoidea. Both Araneoidea and Nicodamidae share the following characters: (1) the 'simplified' trichobothrial leg pattern (no tarsal, a single metatarsal trichobothrium); (2) serrate (not plumose) setae; (3) scaled (not ridged) leg cuticle; and (4) trichobothrial bases not longitudinally ridged. These characters stated here in the set of morphological synapomorphies support the 'purely molecular', until now, clade Nicodamoidea + Araneoidea. So, bothrial morphology, as well as the morphology of the rest of cuticle microstructures, clearly support the nicodamoid-araneoid relation hypothesis, in contrast to both the competiting ones (i.e., deinopoid-araneoid and leptonetoid-araneoid relations).

The bothrium of nicodamids, confirmed here as a sister group of araneoids, is 'hooded', which indicates the polarity of this character in the Araneoidea + Nicodamidae clade. Hence, the ancestral type in the superfamily Araneoidea is recognized as a 'hooded' bothrium with a single well-developed transverse ridge, dividing proximal and distal plates ('*Erigone*-type'); the advanced type is a solid dome-like bothrium without vestiges of the ridge ('*Theridion*-type'); there are also several intermediate cases reflecting various pathways and stages of ridge reduction (all united in this study as the '*Argiope*-type'). The same trend in the evolution of bothrial types was described in detail by Ramírez (2014) in Dionycha.

Forster's (1988) old hypothesis ("The reduction of the posterior hood of the bothrium is derived character which have developed apparently in parallel in many of the families") has been confirmed. The parallel continuous sequences from the ancestral bothrial type to the advanced one through some intermediate stages are found in each of the seven main phylogenetic lineages of the superfamily Araneoidea. There is not a single lineage lacking the ancestral '*Erigone*-type'. It is a sole bothrial type in the 'malkariods', and it is the shortened basal '*Erigone*-type' — '*Argiope*-type' sequence in the 'symphytognathoids' and 'linyphioids'. Finally, the 'tetragnathoids', 'araneoids' 'cyatholipoids' and 'theridioids' have the complete '*Erigone*-type' — '*Argiope*-type' — '*Theridion*-type' sequences. It should be emphasised that the terminal '*Theridion*-type' exists only in the complete sequences and seems but a crown of this trend.

Bothrial morphology provides additional arguments for several taxonomic acts:

- the genera *Gaucelmus*, *Hamus* and *Nescina* are relocated from nesticids to synotaxids, and the isolated position of the genus *Eidmannella* in Nesticidae (termed '*Eidmannella* clade' in this study) are confirmed; the reranking of Agnarsson's (2004) 'clade 35' (*Theonoe*, *Carniella*, *Robertus* and *Pholcomma*) to the theridiid subfamily Theonoeinae Simon, 1894, stat. nov., is proposed;
- the generic independence of the micropholcommatid genus *Plectochetos*, gen. revalid. (from synonymy with *Micropholcomma*) and the zygiellid genus *Parazygiella*, gen. revalid. (from synonymy with *Zygiella*) is restored; the congenericy of *Zygiella* species *Z. atrica* and *Z. keyserlingi* with the type species *Z. x-notata* is doubted, a separated genus for the former species can be proposed, and the bothrial structures also support such a separation; the controversial position of the tetragnathid genera *Cyrtognatha* and *Azilia* in the family cladograme by Álvarez-Padilla and Hormiga (2011) is clarified.

Acknowledgements

We are grateful to Roman A. Rakitov (Borissiak Paleontological Institute, Moscow, Russia) for his help during the preparation of SEM images and the illustrations; to the museum curators for the material under their care: Francesco Ballarin (Museo Civico di Storia Naturale of Verona), Sarah C. Crews (CAS, San Francisco, USA), Gustavo Hormiga (The George Washington University, Washington, DC, USA), Rahşen Kaya (Uludağ University, Bursa, Turkey), Seung Tae Kim (Konkuk University, Seoul, South Korea), Seppo Koponen (ZMTU, Turku, Finland), Christian Kropf (Bern University, Bern, Switzerland), Pekka T. Lehtinen (ZMTU, Turku, Finland), Dmitri V. Logunov (MMUE, Manchester, UK), and Kirill G. Mikhailov (ZMMU, Moscow, Russia); to the following colleagues for the donation of some original SEM images: Francesco Ballarin (Museo Civico di Storia Naturale of Verona); Nadine Dupérré, (ZMH, Hamburg, Germany); and Robert Raven (QMB, Brisbane, Australia); and to Pyotr N. Petrov (Moscow, Russia) for improving the English of our manuscript. We also thank the subject editor, Sergei L. Zonstein (Tel-Aviv, Israel) and two anonymous reviewers for their comments and suggestions that allowed us to improve our text.

Additional information

Conflict of interest

The authors have declared that no competing interests exist.

Ethical statement

No ethical statement was reported.

Funding

No funding was reported.

Author contributions

Both authors have contributed equally.

Author ORCIDs

Kirill Y. Eskov https://orcid.org/0000-0002-7953-0746
Yuri M. Marusik https://orcid.org/0000-0002-4499-5148

Data availability

All of the data that support the findings of this study are available in the main text or Supplementary Information.

References

Agnarsson I (2004) Morphological phylogeny of cobweb spiders and their relatives (Araneae, Araneoidea, Theridiidae). Zoological Journal of the Linnean Society 141(4): 447–626. https://doi.org/10.1111/j.1096-3642.2004.00120.x

Álvarez-Padilla F, Hormiga G (2011) Morphological and phylogenetic atlas of the orb-weaving spider family Tetragnathidae (Araneae: Araneoidea). Zoological Journal of the Linnean Society 162(4): 713–879. https://doi.org/https://doi.org/10.1111/j.1096-3642.2011.00692.x

Álvarez-Padilla F, Dimitrov D, Giribet G, Hormiga G (2009) Phylogenetic relationships of the spider family Tetragnathidae (Araneae, Araneoidea) based on morphological and DNA sequence data. Cladistics 25: 109–146. https://doi.org/10.1111/j.1096-0031.2008.00242.x

Arnedo MA, Coddington J, Agnarsson I, Gillespie RG (2004) From a comb to a tree: Phylogenetic relationships of the comb-footed spiders (Araneae, Theridiidae) inferred from nuclear and mitochondrial genes. Molecular Phylogenetics and Evolution 31: 225–245. https://doi.org/10.1016/S1055-7903(03)00261-6

Arnedo MA, Hormiga G, Scharff N (2009) Higher-level phylogenetics of linyphiid spiders (Araneae, Linyphiidae) based on morphological and molecular evidence. Cladistics 25: 231–262. https://doi.org/10.1111/j.1096-0031.2009.00249.x

Benavides LR, Hormiga G (2020) A morphological and combined phylogenetic analysis of pirate spiders (Araneae, Mimetidae): evolutionary relationships, taxonomy, and character evolution. Invertebrate Systematics 34(2): 144–191. https://doi.org/10.1071/IS19032

Brescovit AD, Cizauskas I, Mota LP (2018) Seven new species of the spider genus *Ochyrocera* from caves in Floresta Nacional de Carajás, PA, Brazil (Araneae, Ochyroceratidae). ZooKeys 726: 87–130. https://doi.org/10.3897/zookeys.726.19778

Coddington JA (1986a) The monophyletic origin of the orb web. In: WA Shear (Ed.) Spiders. Webs, Behavior, and Evolution, Stanford: Stanford University Press, 319–363.

Coddington JA (1986b) The genera of the spider family Theridiosomatidae. Smithsonian Contribution to Zoology 422: 1–96. https://doi.org/10.5479/si.00810282.422

Coddington JA (1990a) Ontogeny and homology in the male palpus of orb-weaving spiders and their relatives, with comments on phylogeny (Araneoclada: Araneoidea, Deinopoidea). Smithsonian Contributions to Zoology 496: 1–52. https://doi.org/10.5479/si.00810282.496

Coddington JA (1990b) Cladistics and spider classification: araneomorph phylogeny and the monophyly of orbweavers (Araneae: Araneomorphae; Orbiculariae). Acta Zoologica Fennica 190: 75–87.

Coddington JA, Levi HW (1991) Systematics and evolution of spiders (Araneae). Annual Revue of Ecology and Systematics 22: 565–592. https://doi.org/10.1146/annurev.es.22.110191.003025

Court DJ, Forster RR (1988) The spiders of New Zealand: Part VI. Family Araneidae. Otago Museum Bulletin 6: 68–124.

Davies VT (1980) *Malkara loricata*, a new spider (Araneidae: Malkarinae) from Australia. Proceedings 8. Internationaler Arachnologen-Kongress Wien 1980: 377–382.

Dimitrov D, Hormiga G (2011) An extraordinary new genus of spiders from Western Australia with an expanded hypothesis on the phylogeny of Tetragnathidae (Araneae). Zoological Journal of the Linnean Society 161(4): 735–768. https://doi.org/10.1111/j.1096-3642.2010.00662.x

Dimitrov D, Lopardo L, Giribet G, Arnedo MA, Álvarez-Padilla F, Hormiga G (2012) Tangled in a sparse spider web: single origin of orb weavers and their spinning work unravelled by denser taxonomic sampling. Proceedings of the Royal Society B, Biological Sciences 279: 1341–1350 [& Suppl. 1–5]. https://doi.org/10.1098/rspb.2011.2011

Dimitrov D, Benavides LR, Arnedo MA, Giribet G, Griswold CE, Scharff N, Hormiga G (2017) Rounding up the usual suspects: a standard target-gene approach for resolving the interfamilial phylogenetic relationships of ecribellate orb-weaving spiders with a new family-rank classification (Araneae, Araneoidea). Cladistics 33(3): 221–250 [& Suppl]. https://doi.org/10.1111/cla.12165

Eskov KY, Marusik YM (2022) *Comaroma* is not an anapid spider. Abstracts of 33rd European Congress of Arachnology ECA 2022, 4–9 September, Greifswald, 25.

Eskov KY, Marusik YM (2023) “Morphological” and “molecular” systems of araneoids: an attempt at harmonization with a subsequent testing of the obtained cladogram using web-building characters (Aranei: Araneoidea). Arthropoda Selecta 32(3): 337–356. https://doi.org/10.15298/arthsel.32.3.10

Eskov KY, Zonstein SL, Marusik YM (2024) On the liphistiomorph trichobothria and the significance of their structure for tracking the bothria evolution in the order Araneae. Israel Journal of Entomology 53: 93–112. https://doi.org/10.5281/zenodo.12790018

Forster RR (1959) The spiders of the family Symphytognathidae. Transactions and Proceedings of the Royal Society of New Zealand 86: 269–329.

Forster RR (1970) The spiders of New Zealand, part III: Desidae, Dictynidae, Hahniidae, Amaurobioididae, Nicodamidae. Otago Museum Bulletin 3: 1–184.

Forster RR (1988) The spiders of New Zealand: Part VI. Family Cyatholipidae. Otago Museum Bulletin 6: 7–34.

Forster RR, Platnick NI (1984) A review of the archaeid spiders and their relatives, with notes on the limits of the superfamily Palpimanoidea (Arachnida, Araneae). Bulletin of the American Museum of Natural History 178: 1–106.

Forster RR, Platnick NI, Gray MR (1987) A review of the spider superfamilies Hypochiloidea and Austrochiloidea (Araneae, Araneomorphae). Bulletin of the American Museum of Natural History 185: 1–116.

Forster RR, Platnick NI, Coddington J (1990) A proposal and review of the spider family Synotaxidae (Araneae, Araneoidea), with notes on theridiid interrelationships. Bulletin of the American Museum of Natural History 193: 1–116.

Framenau VW, Scharff N, Harvey MS (2010) Systematics of the Australian orb-weaving spider genus *Demadiana* with comments on the generic classification of the Arkyinae (Araneae: Araneidae). Invertebrate Systematics 24(2): 139–171. https://doi.org/10.1071/IS10005

Frick H, Scharff N (2014) Phantoms of Gondwana? – phylogeny of the spider subfamily Mynogleninae (Araneae: Linyphiidae). Cladistics 30(1): 67–106. https://doi.org/10.1111/cla.12025

Gregorič M, Agnarsson I, Blackledge TA, Kuntner M (2015) Phylogenetic position and composition of Zygiellinae and *Caerostris*, with new insight into orb-web evolution and gigantism. Zoological Journal of the Linnean Society 175(2): 225–243. https://doi.org/10.1111/zoj.12281

Griswold CE (1985) *Isela okuncana*, a new genus and species of kleptoparasitic spider from southern Africa (Araneae: Mysmenidae). Annals of the Natal Museum 27: 207–217.

Griswold CE (2001) A monograph of the living world genera and Afrotropical species of cyatholipid spiders (Araneae, Orbiculariae, Araneoidea, Cyatholipidae). Memoirs of the California Academy of Sciences 26: 1–251.

Griswold CE, Coddington JA, Hormiga G, Scharff N (1998) Phylogeny of the orb-web building spiders (Araneae, Orbiculariae: Deinopoidea, Araneoidea). Zoological Journal of the Linnean Society 123(1): 1–99. https://doi.org/10.1111/j.1096-3642.1998.tb01290.x

Griswold CE, Coddington JA, Platnick NI, Forster RR (1999) Towards a phylogeny of entelegyne spiders (Araneae, Araneomorphae, Entelegynae). Journal of Arachnology 27: 53–63.

Griswold CE, Ramírez MJ, Coddington JA, Platnick NI (2005) Atlas of phylogenetic data for entelegyne spiders (Araneae: Araneomorphae: Entelegynae) with comments on their phylogeny. Proceedings of the California Academy of Sciences 56(Suppl. II): 1–324.

Harvey MS (1995) The systematics of the spider family Nicodamidae (Araneae: Amaurobioidea). Invertebrate Taxonomy 9(2): 279–386. https://doi.org/10.1071/IT9950279

Helsdingen PJ van (1974) The affinities of *Wubana* and *Allomengea* with some notes on the latter genus (Araneae, Linyphiidae). Zoologische Mededelingen 46: 295–321.

Hormiga G (1993) Implications of the phylogeny of Pimoidae for the systematics of linyphiid spiders (Araneae, Araneoidea, Linyphiidae). Memoirs of the Queensland Museum 33: 533–542.

Hormiga G (2002) *Orsonwelles*, a new genus of giant linyphiid spiders (Araneae) from the Hawaiian Islands. Invertebrate Systematics 16(3): 369–448. https://doi.org/10.1071/IT01026

Hormiga G, Scharff N (2020) The malkarid spiders of New Zealand (Araneae: Malkaridae). Invertebrate Systematics 34(4): 345–405. https://doi.org/10.1071/IS19073

Hormiga G, Buckle DJ, Scharff N (2005) *Nanoa*, an enigmatic new genus of pimoid spiders from western North America (Pimoidae, Araneae). Zoological Journal of the Linnean Society 145(2): 249–262. https://doi.org/10.1111/j.1096-3642.2005.00192.x

Hormiga G, Kulkarni S, Arnedo MA, Dimitrov D, Giribet G, Kallal RJ, Scharff N (2023) Genitalic morphology and phylogenomic placement of the Australian spider *Paraplectanoides crassipes* Keyserling, 1886 (Araneae, Araneidae) with a discussion on the classification of the family Araneidae. Invertebrate Systematics 37(12): 797–818. https://doi.org/10.1071/IS23050

Jocqué R, Dippenaar-Schoeman AS (2006) Spider families of the world. Musée Royal de l'Afrique Central, Tervuren, 336 pp.

Kallal RJ, Hormiga G (2022) The family placement of the Asian orb-weaving spider genus *Guizygiella* Zhu, Kim & Song, 1997 (Araneae: Araneoidea). Zootaxa 5175(1): 146–150. https://doi.org/10.11646/zootaxa.5175.1.8

Kallal RJ, Fernández R, Giribet G, Hormiga G (2018) A phylotranscriptomic backbone of the orb-weaving spider family Araneidae (Arachnida, Araneae) supported by multiple methodological approaches. Molecular Phylogenetics and Evolution 126: 129–140. https://doi.org/10.1016/j.ympev.2018.04.007

Kallal RJ, Dimitrov D, Arnedo MA, Giribet G, Hormiga G (2020) Monophyly, taxon sampling, and the nature of ranks in the classification of orb-weaving spiders (Araneae: Araneoidea). Systematic Biology 69(2): 401–411. https://doi.org/10.1093/sysbio/syz043

Knoflach B (1996) Three new species of *Carniella* from Thailand (Araneae, Theridiidae). Revue Suisse de Zoologie 103: 567–579. https://doi.org/10.5962/bhl.part.79960

Kropf C (1990) *Comaroma* is an anapid spider (Arachnida, Araneae, Anapidae). Verhandlungen des Naturwissenschaftlichen Vereins in Hamburg (NF) 31/32: 185–203.

Kulkarni S K, Kallal RJ, Wood H, Dimitrov D, Giribet G, Hormiga G (2021) Interrogating genomic-scale data to resolve recalcitrant nodes in the Spider Tree of Life. Molecular Biology and Evolution 38: 891–903. https://doi.org/10.1093/molbev/msaa251

Kuntner M, Hamilton CA, Cheng RC, Gregorič M, Lupse N, Lokovsek T, Lemmon EM, Lemmon AR, Agnarsson I, Coddington JA, Bond JE (2019) Golden orbweavers ignore biological rules: phylogenomic and comparative analyses unravel a complex evolution of sexual size dimorphism. Systematic Biology 68(4): 555–572. https://doi.org/10.1093/sysbio/syy082

Kuntner M, Čandek K, Gregorič M, Turk E, Hamilton CA, Chamberland L, Starrett J, Cheng R, Coddington JA, Agnarsson I, Bond JE (2023) Increasing information content and diagnosability in family-level classifications. Systematic Biology 72(4): 964–971. https://doi.org/10.1093/sysbio/syad021

Ledford JM, Griswold CE (2010) A study of the subfamily Archoleptonetinae (Araneae, Leptonetidae) with a review of the morphology and relationships for the Leptonetidae. Zootaxa 2391: 1–32. https://doi.org/10.11646/zootaxa.2391.1.1

Lehtinen PT (1975) Notes on the phylogenetic classification of Araneae. Proceedings of the 6th International Arachnological Congress, 1974: 26–29.

Lehtinen PT (1978) Definition and limitation of supraspecific taxa in spiders. Symposia of the Zoological Society of London 42: 255–271.

Lehtinen PT (1980) Trichobothrial patterns in high level taxonomy of spiders. Proceedings 8. Internationaler Arachnologen-Kongress Wien 1980: 493–498.

Lehtinen P (1996) The ultrastructure of leg skin in the phylogeny of spiders. Revue Suisse de Zoologie, hors serrie 2: 399–421.

Lehtinen PT, Saaristo MI (1980) Spiders of the Oriental-Australian region. II. Nesticidae. Annales Zoologici Fennici 17: 47–66.

Levi HW (1974) The orb-weaver genus *Zygiella* (Araneae: Araneidae). Bulletin of the Museum of Comparative Zoology 146(5): 267–290.

Levi HW, Eickstedt VRD (1989) The Nephilinae spiders of the Neotropics (Araneae: Tetragnathidae). Memorias Del Instituto Butantan (Sao Paulo) 51: 43–56.

Lopardo L, Hormiga G (2007) On the synaphrid spider *Cepheia longiseta* (Simon 1881) (Araneae, Synaphridae). American Museum Novitates 3575: 1–18. https://doi.org/10.1206/0003-0082(2007)3575[1:OTSSCL]2.0.CO;2

Lopardo L, Hormiga G (2015) Out of the twilight zone: phylogeny and evolutionary morphology of the orb-weaving spider family Mysmenidae, with a focus on spinneret spigot morphology in symphytognathoids (Araneae, Araneoidea). Zoological Journal of the Linnean Society 173(3): 527–786. https://doi.org/10.1111/zoj.12199

Lopardo L, Hormiga G, Melic A (2007) Spinneret spigot morphology in synaphrid spiders (Araneae, Synaphridae), with comments on the systematics of the family and description of a new species of *Synaphris* Simon 1894 from Spain. American Museum Novitates 3556: 1–16. https://doi.org/10.1206/0003-0082(2007)3556[1:SSMISS]2.0.CO;2

Lopardo L, Giribet, G, Hormiga G (2011) Morphology to the rescue: molecular data and the signal of morphological characters in combined phylogenetic analyses – a case study from mysmenid spiders (Araneae, Mysmenidae), with comments on the evolution of web architecture. Cladistics 27(3): 278–330 [supplementary material]. https://doi.org/10.1111/j.1096-0031.2010.00332.x

Marusik YM, Eskov KY (2024) A new monotypic genus of cobweb spiders from the Russian Far East (Araneae, Theridiidae). ZooKeys 1195: 219–238. https://doi.org/10.3897/zookeys.1195.118632

Marusik YM, Lehtinen PT (2003) Synaphridae Wunderlich, 1986 (Aranei: Araneoidea), a new family status, with a description of a new species from Turkmenistan. Arthropoda Selecta 11(2): 143–152.

Marusik YM, Gnelitsa VA, Kovblyuk MM (2005) A new species of *Synaphris* (Araneae, Synaphridae) from Ukraine. Bulletin of the British Arachnological Society 13: 125–130.

Miller JA (2007) Synaphridae of Madagascar (Araneae: Araneoidea): a new family record for the Afrotropical region. Proceedings of the California Academy of Sciences (4) 58(3): 21–48.

Miller JA, Carmichael A, Ramírez MJ, Spagna JC, Haddad CR, Řezáč M, Johannesen J, Král J, Wang XP, Griswold CE (2010) Phylogeny of entelegyne spiders: affinities of the family Penestomidae (NEW RANK), generic phylogeny of Eresidae, and asymmetric rates of change in spinning organ evolution (Araneae, Araneoidea, Entelegynae). Molecular Phylogenetics and Evolution 55: 786–804. https://doi.org/10.1016/j.ympev.2010.02.021

Moran RJ (1986) The Sternodidae (Araneae: Araneomorpha), a new family of spiders from eastern Australia. Bulletin of the British Arachnological Society 7: 87–96.

Platnick NI (1994) A new spider of the genus *Archoleptoneta* (Araneae, Leptonetidae) from Panama. American Museum Novitates 3101: 1–8.

Platnick NI, Forster RR (1987) On the first American spiders of the subfamily Sternodinae (Araneae, Malkaridae). American Museum Novitates 2894: 1–12.

Platnick NI, Forster RR (1989) A revision of the temperate South American and Australasian spiders of the family Anapidae (Araneae, Araneoidea). Bulletin of the American Museum of Natural History 190: 1–139.

Platnick NI, Shadab MU (1993) A review of the pirate spiders (Araneae, Mimetidae) of Chile. American Museum Novitates 3074: 1–30.

Platnick NI, Coddington JA, Forster RR, Griswold CE (1991) Spinneret morphology and the phylogeny of haplogyne spiders (Araneae, Araneomorphae). American Museum Novitates 3016: 1–73.

Prete PH, Cizauskas I, Brescovit AD (2018) Three new species of the spider genus *Plato* and the new genus *Cuacuba* from caves of the states of Pará and Minas Gerais, Brazil (Araneae, Theridiosomatidae). ZooKeys 753: 107–162. https://doi.org/10.3897/zookeys.753.20805

Ramírez MJ (2014) The morphology and phylogeny of dionychan spiders (Araneae: Araneomorphae). Bulletin of the American Museum of Natural History 390: 1–374. https://doi.org/10.1206/821.1

Ramírez MJ, Magalhaes ILF, Pizarro-Araya J, Ballarin F, Marusik YM, Eskov KY (2022) A new species of the spider genus *Tekellina* Levi, 1957 from Chile, with a broadened definition of the family Synotaxidae (Arachnida, Araneae). Zoologischer Anzeiger 301: 76–90. https://doi.org/10.1016/j.jcz.2022.08.005

Raven RJ (1985) The spider infraorder Mygalomorphae (Araneae): cladistics and systematics. Bulletin of the American Museum of Natural History 182: 1–180.

Rix MG (2006) Systematics of the Australasian spider family Pararchaeidae (Arachnida: Araneae). Invertebrate Systematics 20(2): 203–254. https://doi.org/10.1071/IS05032

Rix MG, Harvey MS (2010) The spider family Micropholcommatidae (Arachnida, Araneae, Araneoidea): a relimitation and revision at the generic level. ZooKeys 36: 1–321. https://doi.org/10.3897/zookeys.36.306

Scharff N, Coddington JA (1997) A phylogenetic analysis of the orb-weaving spider family Araneidae (Arachnida, Araneae). Zoological Journal of the Linnean Society 120(4): 355–434. https://doi.org/10.1111/j.1096-3642.1997.tb01281.x

Scharff N, Hormiga G (2012) First evidence of aggressive chemical mimicry in the Malagasy orb weaving spider *Exechocentrus lancearius* Simon, 1889 (Arachnida: Araneae: Araneidae) and description of a second species in the genus. Arthropod Systematics & Phylogeny 70 (2): 107–118.https://doi.org/10.3897/asp.70.e31757

Scharff N, Coddington JA, Blackledge TA, Agnarsson I, Framenau VW, Szűts T, Hayashi CY, Dimitrov D (2020) Phylogeny of the orb-weaving spider family Araneidae (Araneae: Araneoidea). Cladistics 36(1): 1–21. https://doi.org/10.1111/cla.12382

Schütt K (2000) The limits of the Araneoidea (Arachnida: Araneae). Australian Journal of Zoology 48(2): 135–153. https://doi.org/10.1071/ZO99050

Schütt K (2003) Phylogeny of Symphytognathidae s.l. (Araneae, Araneoidea). Zoologica Scripta 32(2): 129–151. https://doi.org/10.1046/j.1463-6409.2003.00103.x

Simon E (1894) Histoire naturelle des araignées. Deuxième édition, tome premier. Roret, Paris, 489–760. https://doi.org/10.5962/bhl.title.51973

Simon E (1895) Histoire naturelle des araignées. Deuxième édition, tome premier. Roret, Paris, 761–1084. https://doi.org/10.5962/bhl.title.51973

Wheeler WC, Coddington JA, Crowley LM, Dimitrov D, Goloboff PA, Griswold CE, Hormiga G, Prendini L, Ramírez MJ, Sierwald P, Almeida-Silva LM, Álvarez-Padilla F, Arnedo MA, Benavides LR, Benjamin SP, Bond JE, Grismado CJ, Hasan E, Hedin M, Izquierdo MA, Labarque FM, Ledford J, Lopardo L, Maddison WP, Miller JA, Piacentini LN, Platnick NI, Polotow, D, Silva-Dávila D, Scharff N, Szűts T, Ubick D, Vink C, Wood HM, Zhang JX (2017) The spider tree of life: phylogeny of Araneae based on target-gene analyses from an extensive taxon sampling. Cladistics 33(6): 576–616. https://doi.org/10.1111/cla.12182

Wunderlich J (1979) Taxonomie und Synonyme von *Acrometa* Petrunkevitch 1942 (Arachnida: Araneae: Tetragnathidae). Senckenbergiana Biologica 59: 411–416.

Wunderlich J (1986) Spinnenfauna gestern und heute: Fossile Spinnen in Bernstein und ihre heute lebenden Verwandten. Quelle & Meyer, Wiesbaden, 283 pp.

Wunderlich J (2004a) The fossil spiders (Araneae) of the families Tetragnathidae and Zygiellidae n. stat. in Baltic and Dominican amber, with notes on higher extant and fossil taxa. Beiträge zur Araneologie 3: 899–955.

Wunderlich J (2004b) The fossil spiders of the family Anapidae *s.l.* (Aeaneae) [sic] in Baltic, Dominican and Mexican amber and their extant relatives, with the description of the new subfamily Comarominae. Beiträge zur Araneologie 3: 1020–1111.

Wunderlich J (2008) Descriptions of fossil spider (Araneae) taxa mainly in Baltic amber, as well as on certain related extant taxa. Beiträge zur Araneologie 5: 44–139, 803–804, 813–818.

Wunderlich J (2011) Some fossil spiders (Araneae) in Eocene European ambers. Beiträge zur Araneologie 6: 472–538.

Wunderlich J, Müller P (2018) Fossil spiders (Araneae) in Cretaceous Burmese amber. Beiträge zur Araneologie 11: 1–167.

Zhu MS, Song DX, Zhang JX (2003) Fauna Sinica: Invertebrata Vol. 35: Arachnida: Araneae: Tetragnathidae. Science Press, Beijing, 418 pp.

Supplementary material 1

List of the specimens examined

Authors: Kirill Y. Eskov, Yuri M. Marusik

Data type: docx

Link: https://doi.org/10.3897/zookeys.1219.133002.suppl1

ZooKeys 1219: 61–72 (2024)
DOI: 10.3897/zookeys.1219.137354

Research Article

Diversity of spiders in Daba Mountain National Nature Reserve, Chongqing, China (I), three new *Cicurina* species of Cicurinidae (Araneae)

Lu-Yu Wang[1,2], Yan-Nan Mu[1], Ling-Xiang Yang[3], Zhi-Sheng Zhang[1]

1 *Key Laboratory of Eco-environments in Three Gorges Reservoir Region (Ministry of Education), School of Life Sciences, Southwest University, Chongqing 400715, China*
2 *Chongqing Urban Ecosystem Positioning Observation and Research Station, Chongqing 400036, China*
3 *Management Center of Daba Mountain National Nature Reserve, Chongqing 405909, China*
Corresponding author: Zhi-Sheng Zhang (zhangzs327@qq.com)

Abstract

Three new species of the genus *Cicurina* Menge, 1871 are described from Daba Mountain National Nature Reserve, Chongqing, China: *C. chengkou* **sp. nov.** (♂♀), *C. dabashan* **sp. nov.** (♂♀) and *C. longihamata* **sp. nov.** (♂♀). Morphological descriptions, photos and illustrations of copulatory organs are provided.

Key words: Morphology, new species, spider, taxonomy

Introduction

The Daba Mountain National Nature Reserve is located in Chengkou County in the southern Dabashan Mountains, southwestern China. Its eastern and northern sides border Shaanxi Province. It is adjacent to Wuxi County and Kaizhou District of Chongqing Municipality in the south and is connected to Sichuan Province in the west. It is a transitional zone from the Qinling Mountains to southern China, extending from 31°37'27" to 32°12'15"N and 108°27'07" to 109°16'40"E. In the Daba Mountain National Nature Reserve, there are numerous valleys crisscrossing. The heterogeneous habitats create conditions for the independent evolution of species and have given birth to many endemic species such as ferns and flowering plants, including *Botrychium sutchuenense*, *Asplenium humistratum*, *Primula fagosa*, and the beetle *Neobisnius chengkouensis* (Deng 2015).

A comprehensive survey of the biological resource background of Chongqing Daba Mountain National Nature Reserve was performed in 2011. In total, 181 macro fungi, 3572 tracheophyte, 884 insects, 68 mammalian, 233 avian, 24 reptilian, 25 amphibian and 44 fish species were recorded (Deng 2015). However, at present, only 13 species of spiders have been recorded in the Reserve: *Amaurobius spinatus* Zhang, Wang & Zhang, 2018 (Amaurobiidae), *Chrosiothes pengqi* Lin & Li, 2024, *Coscinida hantao* Lin & Li, 2024, *Mallinella zhoushengboi* Lin & Li, 2024, *Onomastus zhuwu* Lin & Li, 2024, *Orchestina xiebao* Lin & Li, 2024,

Academic editor: Alireza Zamani
Received: 18 September 2024
Accepted: 21 October 2024
Published: 26 November 2024

ZooBank: https://zoobank.org/0881899D-11BE-485C-9C37-195CE56328BE

Citation: Wang L-Y, Mu Y-N, Yang L-X, Zhang Z-S (2024) Diversity of spiders in Daba Mountain National Nature Reserve, Chongqing, China (I), three new *Cicurina* species of Cicurinidae (Araneae). ZooKeys 1219: 61–72. https://doi.org/10.3897/zookeys.1219.137354

Otacilia lubrica Mu & Zhang, 2021, *O. pyriformis* Fu, Zhang & Zhang, 2016, *O. wuli* Mu & Zhang, 2021, *Phricotelus yangxiong* Lin & Li, 2024, *Synagelides huangxin* Lin & Li, 2024, *Tekellina haosiwen* Lin & Li, 2024 and *Yaginumena xuanzan* Lin & Li, 2024 (Theridiidae) (Fu et al. 2016; Zhang et al. 2018; Mu and Zhang 2021; Lin et al. 2024). The diversity of spiders is clearly underestimated.

Cicurina is the largest genus in the spider family Cicurinidae, with 144 species currently known worldwide. Most of them (114) are recorded from North America and a few (28) are found in Asia (Lin et al. 2023; WSC 2024). At present, there are 20 *Cicurina* species found in China (Li and Wang 2017; Wang et al. 2019; Liao et al. 2022).

This is the first study detailing the spider diversity of Daba Mountain National Nature Reserve. Three new species assigned to *Cicurina* Menge, 1871 are described: *C. chengkou* sp. nov., *C. dabashan* sp. nov. and *C. longihamata* sp. nov.

Materials and methods

All specimens were preserved in 75% ethanol and were examined, illustrated, photographed and measured using a Leica M205A stereomicroscope equipped with a drawing tube, a Leica DFC450 camera and LAS software (ver. 4.6). Male pedipalps and epigynes were examined and illustrated after they were dissected. Epigynes were cleared immersing them in pancreatin (Álvarez-Padilla and Hormiga 2007). Eye sizes were measured as the maximum dorsal diameter. Leg measurements are shown as: total length (femur, patella and tibia, metatarsus, tarsus). All measurements are in millimetres. Specimens examined here are deposited in the Collection of Spiders, School of Life Sciences, Southwest University, Chongqing, China (SWUC).

Abbreviations used in the text: **ALE**, anterior lateral eye; **AME**, anterior median eye; **MOA**, median ocular area; **PLE**, posterior lateral eye; **PME**, posterior median eye.

Taxonomy

Family Cicurinidae Kishida, 1955
Genus *Cicurina* Menge, 1871

Cicurina chengkou sp. nov.

https://zoobank.org/B8AE2F95-84BB-4A4F-954B-6DF16B89869E
Figs 1, 2, 7
Vernacular name: 城口洞叶蛛

Type material. ***Holotype*** • ♂ (SWUC-T-CI-10-01), **China**, Chongqing City, Chengkou County, Longtian Town, Wuli Village, Daba Mountain National Nature Reserve, 32°03.836'N, 108°40.238'E, elev. 1275 m, 21 March 2013, X.K. Jiang and X.W. Meng leg. ***Paratype*** • 1♀ (SWUC-T-CI-10-02), with same data as for holotype (SWUC).

Etymology. The specific name is derived from the type locality.

Diagnosis. The new species is similar to *C. dabashan* sp. nov. (Figs 3, 4) in having wide and short retrolateral tibial apophysis, long and strong embolus, strong and beak-like conductor, posteriorly located epigynal atrium and ball-shaped spermathecae, but differs from the latter by the long RTA (Figs 1B, 2E)

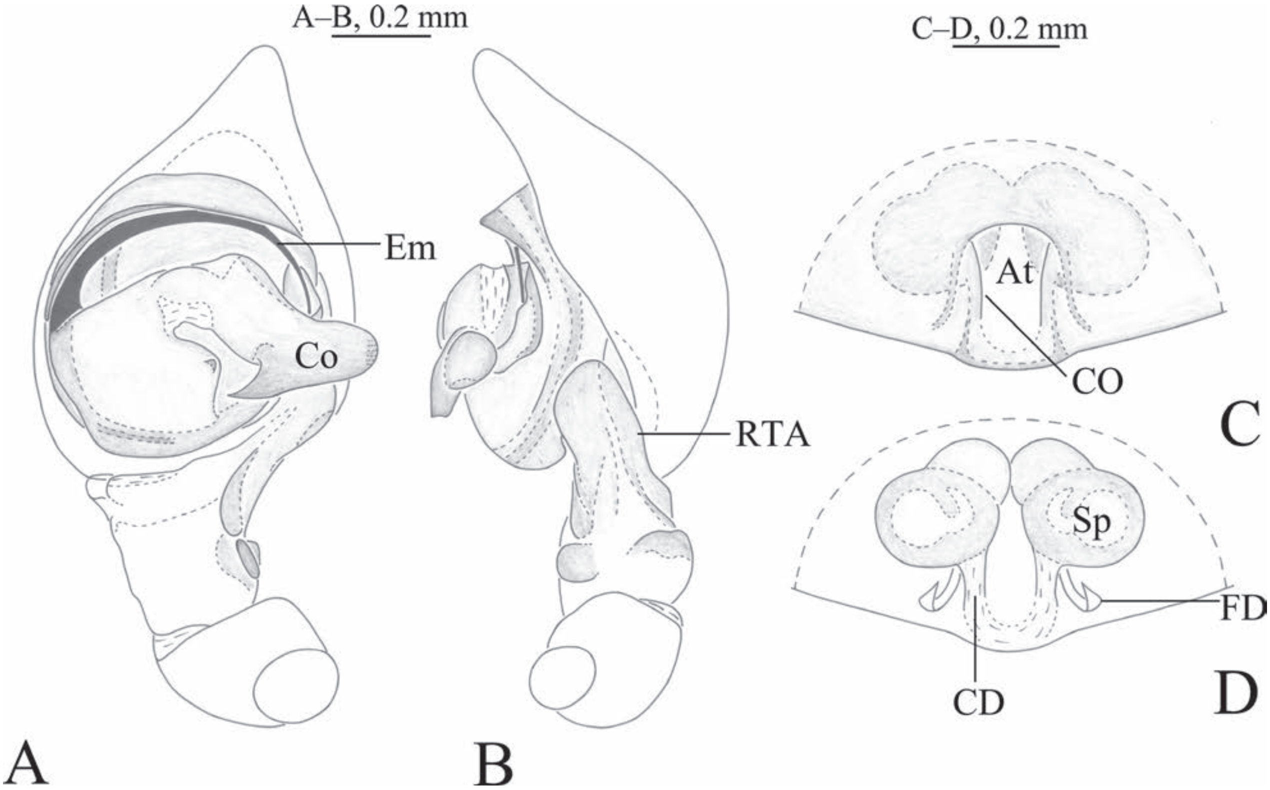

Figure 1. *Cicurina chengkou* sp. nov. holotype male (**A, B**) and paratype female (**C, D**) **A** left male palp, ventral view **B** same, retrolateral view **C** epigyne, ventral view **D** vulva, dorsal view. Abbreviations: At = atrium; CD = copulatory duct; CO = copulatory opening; Co = conductor; Em = embolus; FD = fertilization duct; RTA = retrolateral tibial apophysis; Sp = spermathecae.

(vs. short in *C. dabashan* sp. nov.), the apical part of conductor as long as the width of conductor base (Figs 1A, B, 2C–E) (vs. about half the length of conductor base in *C. dabashan* sp. nov.) and the oblong atrium (Figs 1C, 2F) (vs. somewhat oval in *C. dabashan* sp. nov.), the short copulatory duct (Figs 1D, 2D) (vs. long in *C. dabashan* sp. nov.).

Description. Male holotype (Fig. 2A) total length 4.02. Carapace 2.09 long, 1.75 wide; opisthosoma 1.78 long, 1.35 wide. Eye sizes and interdistances: AME 0.06, ALE 0.12, PME 0.10, PLE, 0.11; AME–AME 0.05, AME–ALE 0.04, PME–PME 0.09, PME–PLE 0.07, ALE–PLE 0.04. MOA 0.23 long, anterior width 0.18, posterior width 0.30. Clypeus height 0.21. Chelicerae with 3 promarginal and 8 retromarginal teeth. Leg measurements: **I** 5.74 (1.63, 1.98, 1.27, 0.86); **II** 5.32 (1.55, 1.80, 1.16, 0.81); **III** 4.78 (1.38, 1.54, 1.13, 0.73); **IV** 6.23 (1.63, 2.06, 1.62, 0.92). Leg formula: 4123.

Palp (Figs 1A, B, 2C–E). Femur long, two times longer than cymbium, without modified. Tibia slightly longer than patella. Retrolateral tibial apophysis wide, with a single fold and rounded apex. Base of retrolateral tibial apophysis with two small apophyses, extending ventrally and dorsally. Bulb circular, tegulum semicircular, with a distinct process at middle part in prolateral and ventral view. Sperm duct obvious. Embolus strong, originating at approximately 9-o'clock position, anterior part resting in the long groove of conductor. Conductor strong, with a sharp end.

Female paratype (Fig. 2B) total length 3.51. Carapace 1.76 long, 1.23 wide; opisthosoma 1.86 long, 1.38 wide. Eye sizes and interdistances: AME 0.05,

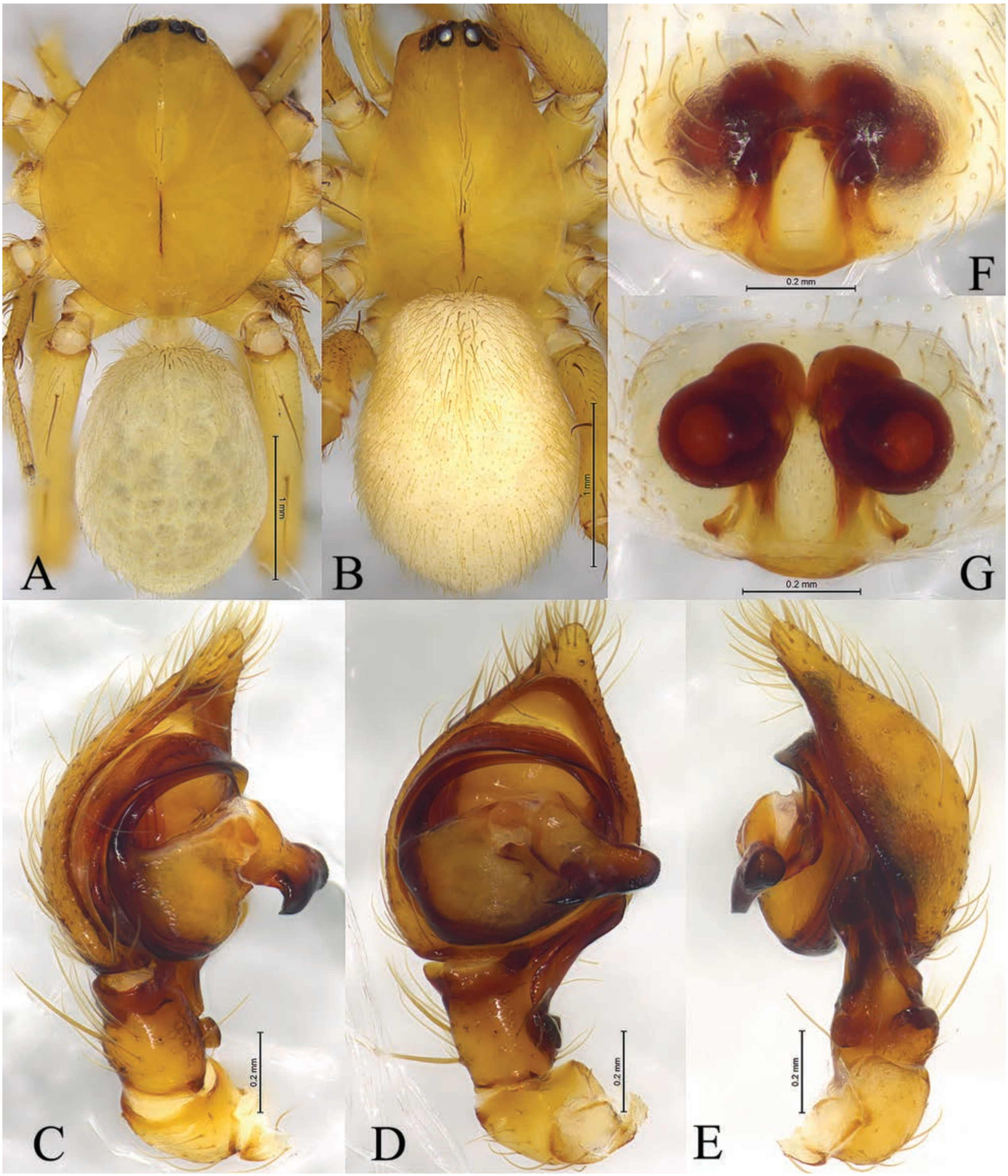

Figure 2. *Cicurina chengkou* sp. nov. holotype male (**A, C–E**) and paratype female (**B, F, G**) **A** male habitus, dorsal view **B** female habitus, dorsal view **C** left male palp, prolateral view **D** same, ventral view **E** same, retrolateral view **F** epigyne, ventral view **G** vulva, dorsal view.

ALE 0.10, PME 0.08, PLE, 0.10; AME–AME 0.05, AME–ALE 0.02, PME–PME 0.08, PME–PLE 0.06, ALE–PLE 0.03. MOA 0.22 long, anterior width 0.15, posterior width 0.27. Clypeus height 0.14. Leg measurements: I 4.67 (1.39, 1.65, 0.95, 0.68); II 4.28 (1.23, 1.44, 0.94, 0.67); III 3.91 (1.15, 1.31, 0.93, 0.52); IV 5.26 (1.48, 1.76, 1.30, 0.72). Leg formula: 4123.

Epigyne (Figs 1C, D, 2F, G). Atrium oval. Copulatory openings located lateral of atrium. Copulatory ducts straight and short, about half length of spermathecae diameter. Spermathecae kidney shaped. Fertilization ducts hook-like.

Distribution. Known only from the type locality (Fig. 7).

Cicurina dabashan sp. nov.

https://zoobank.org/C5223A06-8D90-43EE-A991-385DC9EE7F65
Figs 3, 4, 7
Vernacular name: 大巴山洞叶蛛

Type material. ***Holotype*** • ♂ (SWUC-T-CI-11-01), China, Chongqing City, Chengkou County, Longtian Township, Wuli Village, Daba Mountain National Nature Reserve, 32°03.614'N, 108°40.316'E, elev. 1215 m, 16 September 2012, L.Y. Wang and X.K. Jiang leg. ***Paratypes*** • 1♀ (SWUC-T-CI-11-02), Wuli Village, Daba Mountain National Nature Reserve, 32°04.590'N, 108°39.058'E, elev. 1417 m, 17 September 2012, L.Y. Wang and X.K. Jiang leg. • 1♀ (SWUC-T-CI-11-03), Wuli Village, Daba Mountain National Nature Reserve, 32°04.432'N, 108°39.225'E, elev. 1353 m, 21 March 2013, X.K. Jiang and X.W. Meng leg.

Etymology. The specific name is derived from the type locality (Dabashan = Daba Mountain).

Diagnosis. The new species is similar to *C. lichuanensis* Wang, Zhou & Peng, 2019 (Wang, Zhou and Peng 2019: 354, figs 5A–D, 6A–G) in having similarly

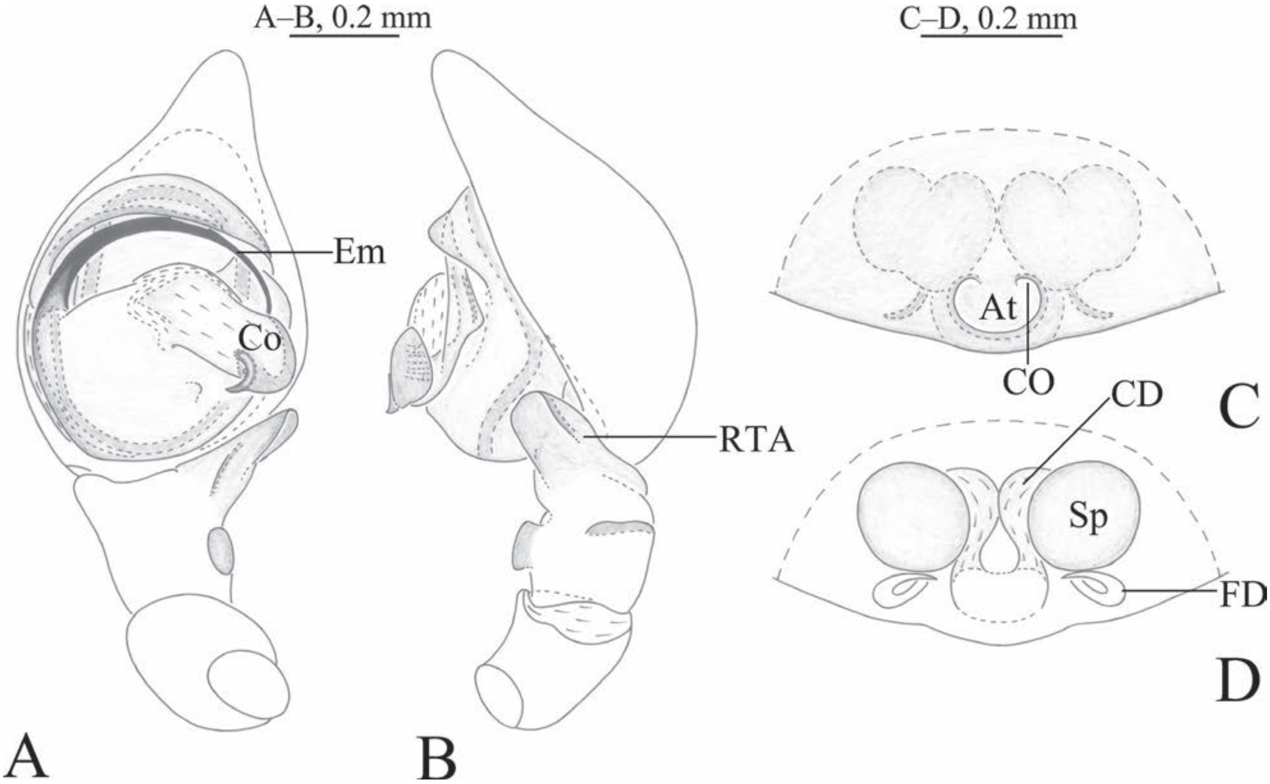

Figure 3. *Cicurina dabashan* sp. nov. holotype male (**A, B**) and paratype female (**C, D**) **A** left male palp, ventral view **B** same, retrolateral view **C** epigyne, ventral view **D** vulva, dorsal view. Abbreviations: At = atrium; CD = copulatory duct; CO = copulatory opening; Co = conductor; Em = embolus; FD = fertilization duct; RTA = retrolateral tibial apophysis; Sp = spermathecae.

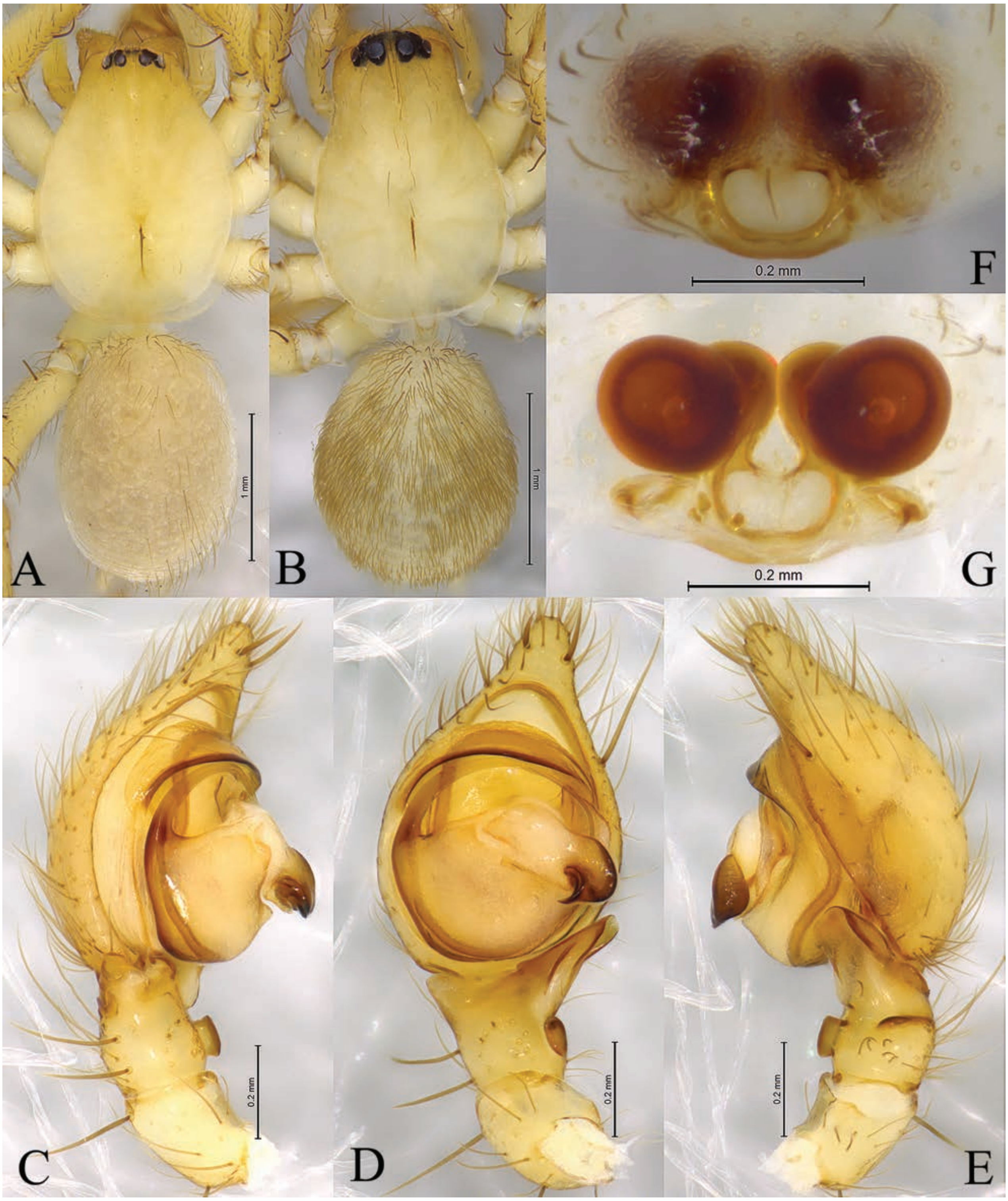

Figure 4. *Cicurina dabashan* sp. nov. holotype male (**A, C–E**) and paratype female (B, F, G) **A** male habitus, dorsal view **B** female habitus, dorsal view **C** left male palp, prolateral view **D** same, ventral view **E** same, retrolateral view **F** epigyne, ventral view **G** vulva, dorsal view.

shaped retrolateral tibial apophysis, long and strong embolus, posteriorly located epigynal atrium and ball-shaped spermathecae, but differs from the latter by the tegulum with a small process (Figs 3A, 4C, D) (vs. without process), the conductor with a short, sclerotic and sharp end (Figs 3A, B, 4C–E) (vs. with a long and blunt end in *C. lichuanensis*) and the anterior edge of atrium unconnected (Figs 3C, 4F) (vs. connect in *C. lichuanensis*).

Description. Male holotype (Fig. 4A) total length 3.66. Carapace 1.91 long, 1.43 wide; opisthosoma 1.72 long, 1.22 wide. Eye sizes and interdistances: AME 0.03, ALE 0.10, PME 0.07, PLE, 0.10; AME–AME 0.04, AME–ALE 0.02, PME–PME 0.10, PME–PLE 0.05, ALE–PLE 0.02. MOA 0.19 long, anterior width 0.10, posterior width 0.25. Clypeus height 0.16. Chelicerae with 3 promarginal and 7 retromarginal teeth. Leg measurements: **I** 4.95 (1.48, 1.73, 0.98, 0.76); **II** 4.45 (1.36, 1.53, 0.92, 0.64); **III** 4.07 (1.20, 1.32, 0.95, 0.60); **IV** 5.49 (1.56, 1.81, 1.34, 0.78). Leg formula: 4123.

Palp (Figs 3A, B, 4C–E). Retrolateral tibial apophysis wide, with a single fold and truncates apex. The base of retrolateral tibial apophysis with two small apophyses, extending ventrally and dorsally. Embolus strong, originating at approximately 9-o'clock position, anterior part resting in the long groove of conductor. Conductor strong, with a beak-like end.

Female paratypes (SWUC-T-CI-11-02, Fig. 4B) total length 3.33–4.95 (*N* = 2). One female total length 3.33. Prosoma 1.70 long, 1.15 wide; opisthosoma 1.48 long, 1.20 wide. Eye sizes and interdistances: AME 0.06, ALE 0.11, PME 0.10, PLE, 0.11; AME–AME 0.05, AME–ALE 0.01, PME–PME 0.08, PME–PLE 0.06, ALE–PLE 0.05. MOA 0.25 long, anterior width 0.16, posterior width 0.28. Clypeus height 0.12. Leg measurements: **I** 4.18 (1.22, 1.542, 0.83, 0.61); **II** 3.65 (1.08, 1.28, 0.75, 0.54); **III** 3.29 (0.95, 1.15, 0.69, 0.50); **IV** 4.44 (1.26, 1.53, 1.05, 0.60). Leg formula: 4123.

Epigyne (Figs 3C, D, 4F, G). Atrium oval. Copulatory openings located anterior of atrium. Copulatory ducts as long as spermathecae diameter, C-shaped. Spermathecae spherical, anteriorly located. Fertilization ducts folded.

Distribution. China (Chongqing) (Fig. 7).

Cicurina longihamata **sp. nov.**

https://zoobank.org/AD3DFE55-EB4B-4BF3-A1B0-85FAF3608780
Figs 5, 6, 7
Vernacular name: 长钩洞叶蛛

Type material. ***Holotype*** • ♂ (SWUC-T-CI-12-01), **China**, Chongqing City, Chengkou County, Longtian Town, Wuli Village, Daba Mountain National Nature Reserve, 32°05.062'N, 108°38.300'E, elev. 1417 m, 17 September 2012, L.Y. Wang and X.K. Jiang leg. (SWUC). ***Paratypes*** • 6♂ 3♀ (SWUC-T-CI-12-02 to 10), with same data as for holotype • 1♂ 1♀ (SWUC-T-CI-12-11 to 12), Wuli Village, Daba Mountain National Nature Reserve, 32°04.443'N, 108°39.278'E, elev. 1264 m, 16 September 2012, L.Y. Wang and X.K. Jiang leg. • 2♀ (SWUC-T-CI-12-13 to 14), Wuli Village, Daba Mountain National Nature Reserve, 32°04.590'N, 108°39.058'E, elev. 1417 m, 17 September 2012, L.Y. Wang and X.K. Jiang leg. • 1♀ (SWUC-T-CI-12-15), Wuli Village, Daba Mountain National Nature Reserve, 32°03.836'N, 108°40.238'E, elev. 1275 m, 21 March 2013, X.K. Jiang and X.W. Meng leg. • 4♀ (SWUC-T-CI-12-16 to 19), Wuli Village, Daba Mountain National Nature Reserve, 32°03.726'N, 108°40.351'E, elev. 1206 m, 16 March 2018, Z.S. Zhang, L.Y. Wang and Z.S. Wu leg. • 5♀ (SWUC-T-CI-12-20 to 24), Wuli Village, Daba Mountain National Nature Reserve, 32°04.269'N, 108°39.914'E, elev. 1286 m, 16 March 2018, Z.S. Zhang, L.Y. Wang and Z.S.

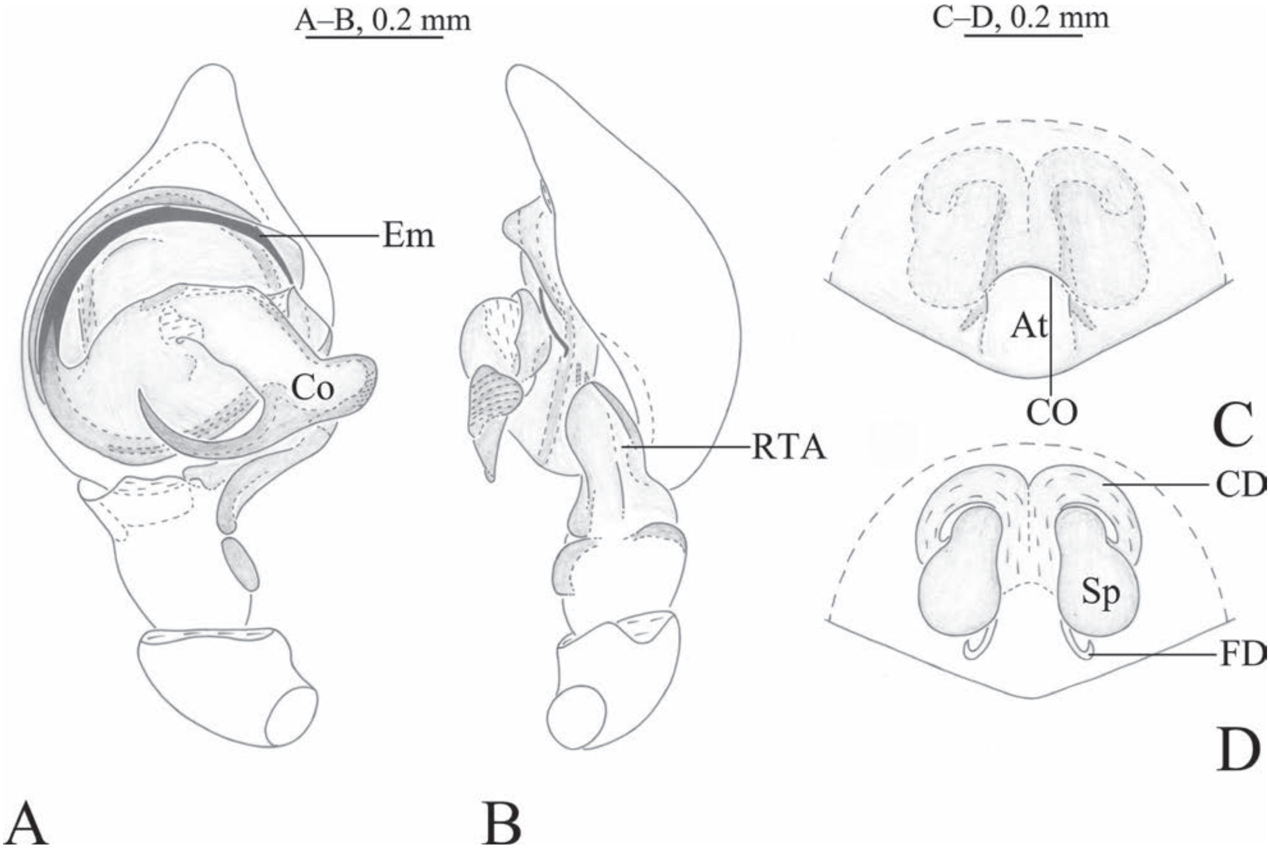

Figure 5. *Cicurina longihamata* sp. nov. holotype male (**A, B**) and paratype female (**C, D**) **A** left male palp, ventral view **B** same, retrolateral view **C** epigyne, ventral view **D** vulva, dorsal view. Abbreviations: At = atrium; CD = copulatory duct; CO = copulatory opening; Co = conductor; Em = embolus; FD = fertilization duct; RTA = retrolateral tibial apophysis; Sp = spermathecae.

Wu leg. • 3♀ (SWUC-T-CI-12-25 to 27), Heyu Town, Xumu Village, Daba Mountain National Nature Reserve, 31°54.484'N, 109°03.556'E, elev. 1670 m, 27 March 2013, X.K. Jiang and X.W. Meng leg. • 1♀ (SWUC-T-CI-12-28), Xumu Village, Daba Mountain National Nature Reserve, 31°55.393'N, 109°01.930'E, elev. 1593 m, 28 March 2013, X.K. Jiang and X.W. Meng leg. • 1♀ (SWUC-T-CI-12-29), Dongan Township, Chaoyang Village, Daba Mountain National Nature Reserve, 31°47.099'N, 109°14.727'E, elev. 1576 m, 29 March 2013, X.K. Jiang and X.W. Meng leg. • 1♀ (SWUC-T-CI-12-30), Dongan Township, Xingtian Village, Daba Mountain National Nature Reserve, 31°43.426'N, 109°08.563'E, 1391 m, 31 March 2013, X.K. Jiang and X.W. Meng leg.

Etymology. The specific name is a combination of '*long*' and '*hamata*', referring to the long and hook-shaped conductor; adjective.

Diagnosis. The new species is similar to *C. eburnata* Wang, 1994 (Wang et al. 2019: 354, figs 9A–D, 10A–G) in having similar shaped retrolateral tibial apophysis, long and strong embolus, strong and hook-like conductor, posteriorly located epigynal atrium, but differs from the latter by the conductor with a long, acicular and C-shaped end (Figs 5A, B, 6C–E) (vs. short and blunt end in *C. eburnata*), the C-shaped copulatory ducts and gourd-shaped spermathecae (Figs 5D, 6G) (vs. rod-shaped and spherical *C. eburnata*).

Description. Male holotype (Fig. 6A) total length 2.93. Prosoma 1.51 long, 1.14 wide; Opisthosoma 1.31 long, 0.86 wide. Eye sizes and interdistances:

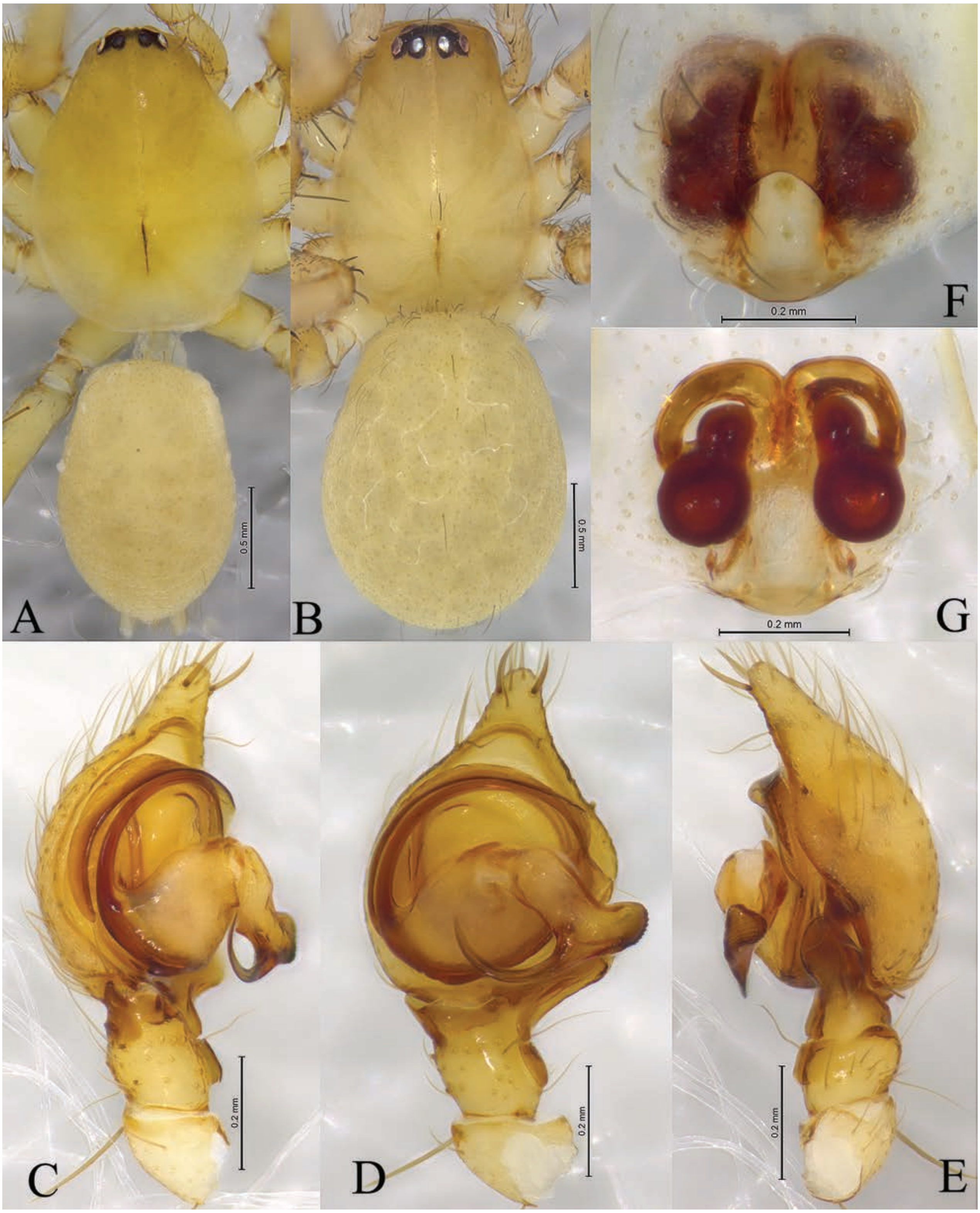

Figure 6. *Cicurina longihamata* sp. nov. holotype male (**A, C–E**) and paratype female (**B, F, G**) **A** male habitus, dorsal view **B** female habitus, dorsal view **C** left male palp, prolateral view **D** same, ventral view **E** same, retrolateral view **F** epigyne, ventral view **G** vulva, dorsal view.

AME 0.03, ALE 0.09, PME 0.07, PLE, 0.08; AME–AME 0.02, AME–ALE 0.02, PME–PME 0.07, PME–PLE 0.04, ALE–PLE 0.02. MOA 0.14 long, anterior width 0.07, posterior width 0.21. Clypeus height 0.14. Chelicerae with 3 promarginal

Figure 7. Distribution records of three *Cicurina* species in Chongqing, China.

and 7 retromarginal teeth. Leg measurements: I 3.66 (1.09, 1.31, 0.70, 0.56); II 3.18 (0.94, 1.08, 0.64, 0.52); III 2.85 (0.83, 0.88, 0.69, 0.45); IV 3.99 (1.10, 1.32, 0.95, 0.62). Leg formula: 4123.

Palp (Figs 5A–B, 6C–E). Retrolateral tibial apophysis wide. The base of retrolateral tibial apophysis with two small apophyses, extending ventrally and dorsally. Embolus strong, originating at approximately 9-o'clock position, anterior part resting in the groove of conductor. Conductor strong, with a long and J-like end.

Female paratype (SWUC-T-CI-12-02, Fig. 6B) total length 2.94. Prosoma 1.46 long, 0.99 wide; opisthosoma 1.57 long, 1.18 wide. Eye sizes and interdistances: AME 0.04, ALE 0.10, PME 0.07, PLE, 0.09; AME–AME 0.02, AME–ALE 0.02, PME–PME 0.07, PME–PLE 0.04, ALE–PLE 0.02. MOA 0.18 long, anterior width 0.08, posterior width 0.22. Clypeus height 0.12. Leg measurements: I 3.56 (1.10, 1.30, 0.65, 0.51); II 3.16 (0.95, 1.11, 0.62, 0.48); III 2.86 (0.87, 0.90, 0.66, 0.43); IV 3.99 (1.18, 1.36, 0.93, 0.52). Leg formula: 4123.

Epigyne (Figs 5C–D, 5F–G). Atrium oval. Copulatory openings located anterior of atrium. Copulatory ducts strongly curved, circular. Spermathecae large and gourd-shaped. Fertilization ducts long and hook-like.

Variation. Males (*N* = 8) total length 2.80–3.15; females (*N* = 22) total length 2.90–3.49.

Distribution. China (Chongqing) (Fig. 7).

Acknowledgements

Many thanks are given Mr Xuan-Kong Jiang, Xiang-Wei Meng and Zhi-Sun Wu (SWUC) for their assistance during the field work and collection. Many thanks to subject editor, Alireza Zamani and two reviewers, Feng Zhang and another anonymous reviewer for their valuable comments that greatly improved the manuscript.

Additional information

Conflict of interest

The authors have declared that no competing interests exist.

Ethical statement

No ethical statement was reported.

Funding

This research was supported by the Scientific investigation project of biological resource background of Chongqing Daba Mountain National Nature Reserve.

Author contributions

All authors have contributed equally.

Author ORCIDs

Lu-Yu Wang https://orcid.org/0000-0002-5250-3473
Yan-Nan Mu https://orcid.org/0000-0002-2504-673X
Zhi-Sheng Zhang https://orcid.org/0000-0002-9304-1789

Data availability

All of the data that support the findings of this study are available in the main text.

References

Álvarez-Padilla F, Hormiga G (2007) A protocol for digesting internal soft tissues and mounting spiders for scanning electron microscopy. Journal of Arachnology 35(3): 538–542. https://doi.org/10.1636/Sh06-55.1

Deng HP (2015) Biodiversity of Chongqing Daba Mountain National Nature Reserve. Science Press, Beijing, 279 pp.

Fu L, Zhang ZS, Zhang F (2016) New *Otacilia* species from Southwest China (Araneae: Phrurolithidae). Zootaxa 4107(2): 197–221. https://doi.org/10.11646/zootaxa.4107.2.4

Li SQ, Wang XX (2017) New cave-dwelling spiders of the family Dictynidae (Arachnida, Araneae) from Guangxi and Guizhou, China. Zoological Systematics 42(2): 125–228. https://doi.org/10.11865/zs.201711

Liao RR, Yin HQ, He AL, Xu X (2022) Description of three new species of the genus *Cicurina* Menge, 1871 from Guangdong, China (Araneae, Hahniidae). Zootaxa 5188(5): 477–488. https://doi.org/10.11646/zootaxa.5188.5.4

Lin YJ, Li SQ, Pham DS (2023) Taxonomic notes on some spider species (Arachnida: Araneae) from China and Vietnam. Zoological Systematics 48(1): 1–99. https://doi.org/10.11865/zs.2023101

Lin YJ, Li SQ, Mo HL, Wang XH (2024) Thirty-eight spider species (Arachnida: Araneae) from China, Indonesia, Japan and Vietnam. Zoological Systematics 49(1): 4–98. https://doi.org/10.11865/zs.2024101

Mu Y, Zhang F (2021) Seven new *Otacilia* Thorell, 1897 species from China (Araneae: Phrurolithidae). Zootaxa 5032(4): 533–548. https://doi.org/10.11646/zootaxa.5032.4.4

Wang LY, Zhou GC, Peng XJ (2019) Four new species of the spider genus *Cicurina* Menge, 1871 from China (Araneae: Dictynidae). Zootaxa 4615(2): 351–364. https://doi.org/10.11646/zootaxa.4615.2.7

WSC (2024) World Spider Catalog. Version 25.5. Natural History Museum Bern. [Accessed on: 2024-10-31] https://doi.org/10.24436/2

Zhang L, Wang LY, Zhang ZS (2018) The first record of *Amaurobius* C.L. Koch, 1837 (Araneae, Amaurobiidae) from China, with description of two new species. Zootaxa 4402(2): 363–372. https://doi.org/10.11646/zootaxa.4402.2.8

ZooKeys 1219: 73–97 (2024)
DOI: 10.3897/zookeys.1219.125754

Research Article

Five new species of the genus *Grouvellinus* Champion, 1923 from Guizhou Province, China (Coleoptera, Elmidae)

Ri-Xin Jiang[1,2,3], Ping-Lan Wu[4], Xiang-Sheng Chen[1,2,3]

1 *Institute of Entomology, Guizhou University, Guiyang 550025, Guizhou, China*
2 *The Provincial Special Key Laboratory for Development and Utilization of Insect Resources of Guizhou, Guizhou University, Guiyang, 550025, Guizhou, China*
3 *The Provincial Key Laboratory for Agricultural Pest Management of Mountainous Region, Guiyang 550025, Guizhou, China*
4 *Agricultural Service Center of Yanlou Town, Huaxi District, Guiyang 550025, Guizhou, China*
Corresponding author: Xiang-Sheng Chen (chenxs3218@163.com)

Abstract

The genus *Grouvellinus* Champion, 1923 comprises 60 described species distributed across the Oriental and Palearctic regions. Species diversity is very high in mainland China, with 28 recorded species. Here, the results of the aquatic beetle survey in Guizhou Province are presented; they began in 2021, when we collected more than 5000 specimens of riffle beetle. All specimens come from small ravine streams where inhabited submerged stones. Using morphological characters of adults such as body form and size, coloration, elytral, pronotal and ventral surface structures, and forms of male and female genitalia, five new species were discovered and are described: *Grouvelinus loong* **sp. nov.**, *G. buyi* **sp. nov.**, *G. wangmoensis* **sp. nov.**, *G. lihaitaoi* **sp. nov.**, *G. muyinlini* **sp. nov.** The species descriptions contain illustrations of diagnostic characters and measurements of metric characters such as body length, pronotal length, pronotal width, elytral length and width, and head length and width. The females are, on average, larger and have only slight differences in external morphology compared to the males. The comparative diagnoses discuss characters of the new and already known species. The results show that the existing species diversity requires more detailed research focusing on larger areas of South China in the future.

Key words: Aquatic beetle, Elminae, riffle beetles, Southwestern China, water environment

Academic editor: Mariano Michat
Received: 19 April 2024
Accepted: 19 October 2024
Published: 27 November 2024

ZooBank: https://zoobank.org/4281D66E-AE5B-4F65-B5C1-92D02B3BFBF6

Citation: Jiang R-X, Wu P-L, Chen X-S (2024) Five new species of the genus *Grouvellinus* Champion, 1923 from Guizhou Province, China (Coleoptera, Elmidae). ZooKeys 1219: 73–97. https://doi.org/10.3897/zookeys.1219.125754

Introduction

The aquatic beetle family Elmidae (also known as riffle beetles) has a worldwide distribution with its highest diversity in the tropics (Kodada et al. 2016). Members of this family are sometimes used as indicators for freshwater quality (Moog and Jäch 2003; Junqueira et al. 2010). Riffle beetles are usually found in undisturbed streams, where they dwell in benthic microhabitats and feed on algae and detritus (Kodada et al. 2016).

The genus *Grouvellinus* Champion, 1923 is widely distributed in the Oriental and Palearctic regions, and has included 60 known species (Jung et al. 2014; Bian and Sun 2016; Jäch et al. 2016; Bian and Jäch 2018, 2019; Freitag et al. 2018, 2020; Bian and Zhang 2023; Jiang et al. 2023). This genus exhibits a high diversity in China, with 28 species recorded from mainland China (Jäch and Kodada 1995; Bian and Zhang 2023; Jiang et al. 2023). The Chinese fauna of this genus was recently reviewed by a series of papers, and many new species were described (Bian and Sun 2016; Bian and Jäch 2018, 2019; Bian and Zhang 2023; Jiang et al. 2023). Previously to this work, there was only one *Grouvellinus* species in Guizhou Province: *Grouvellinus huaxiensis* Jiang, Huang & Chen, 2023, found in an urban river of Guiyang City (Jiang et al. 2023).

Through our aquatic beetle survey in Guizhou Province, which began in 2021, a large number (more than 5000 specimens) of riffle beetles were collected, many of them belonging to the genus *Grouvellinus*. In the present paper, five new species of this genus are described and illustrated. A distribution map (Fig. 13) of the known *Grouvellinus* species from Guizhou Province is also provided.

Materials and methods

The examined material is deposited in the Institute of Entomology, Guizhou University, Guiyang, China (**GUGC**). Label data are quoted verbatim. The Chinese translation of each locality below the provincial level is included in parentheses at its first appearance in the text. Each type specimen bears the following label: ‘HOLOTYPE (red) (or PARATYPE (yellow)), m# (or f#), *Grouvellinus* + specific name sp. nov., Jiang, Wu & Chen, 2024.’

Dissected parts were preserved in Euparal on plastic slides and were placed on the same pin with the specimen. Habitus images were taken using a Canon 5D Mark IV digital camera with MP-E 65 mm f/2.8 1–5× macro lens. A Godox MF12 flash was used as the light source. Images of the morphological structures were taken using a Canon 5D Mark IV digital camera with a Mitutoyo Plan NIR 10 lens and a Godox MF12 flash was used as the light source, or a Nikon SMZ25 stereoscopic microscope with a Nikon DS-Ri2 camera. Genitalia were soaked in 10% NaOH solution for half an hour, and dehydrated in 100% alcohol, then preserved in Euparal on plastic slides. Images of genitalia were taken using a Nikon N1-E microscope with a Nikon DS-Ri2 camera. Zerene Stacker v. 1.04 was used for image stacking. All images were modified and grouped into plates using Adobe Photoshop CS5 Extended. Measurements of metric characters were taken by NIS-Elements AR, and added in Microsoft Excel to compute mean and standard deviations.

Morphological terminology and the format for the descriptions follow those of Bian and Sun (2016). The following abbreviations are used: **HL**—length of head from the anterior clypeal margin to the occipital constriction; **HW**—width of head across eyes; **PL**—length of pronotum along the midline; **PW**—maximum width of pronotum; **EL**—length of elytra along the suture; **EW**—maximum width of elytra; **CL**—length of body, as the sum PL + EL.

Taxonomy

Grouvellinus **Champion, 1923**
(戈溪泥甲属)

Grouvellinus Champion, 1923: 168. Type species: *Macronychus caucasicus* Victor, 1839.

Grouvellinus loong **sp. nov.**

https://zoobank.org/134104C8-B9C1-4B30-BCF1-B009441214C4
Figs 1A, 2, 3, 12A, F
(辰龙戈溪泥甲)

Material examined. (42 exs: 21 ♂♂, 21 ♀♀): ***Holotype***: **China** • ♂, labeled ‘China: Guizhou, Qiannan Buyi and Miao Autonomous Prefecture (黔南布依族苗族自治州), Luodian County (罗甸县), Luokun Town (罗悃镇), Xiangshui Village (响水村), 25°19'43"N, 106°38'28"E, H: 666.10±6.40m, 09.XI.2022, Jiang Ri-Xin leg.’ (GUGC). ***Paratypes***: **China** • 20 ♂♂, 21 ♀♀, with same label data as the holotype (GUGC).

Diagnosis. Body obovate; elytra dark brown, with weak cupreous metallic luster, each elytron with yellowish brown spot at base and near apex. Elytral intervals III, V, VII, and VIII carinated; carinae granulated, those on interval III short,

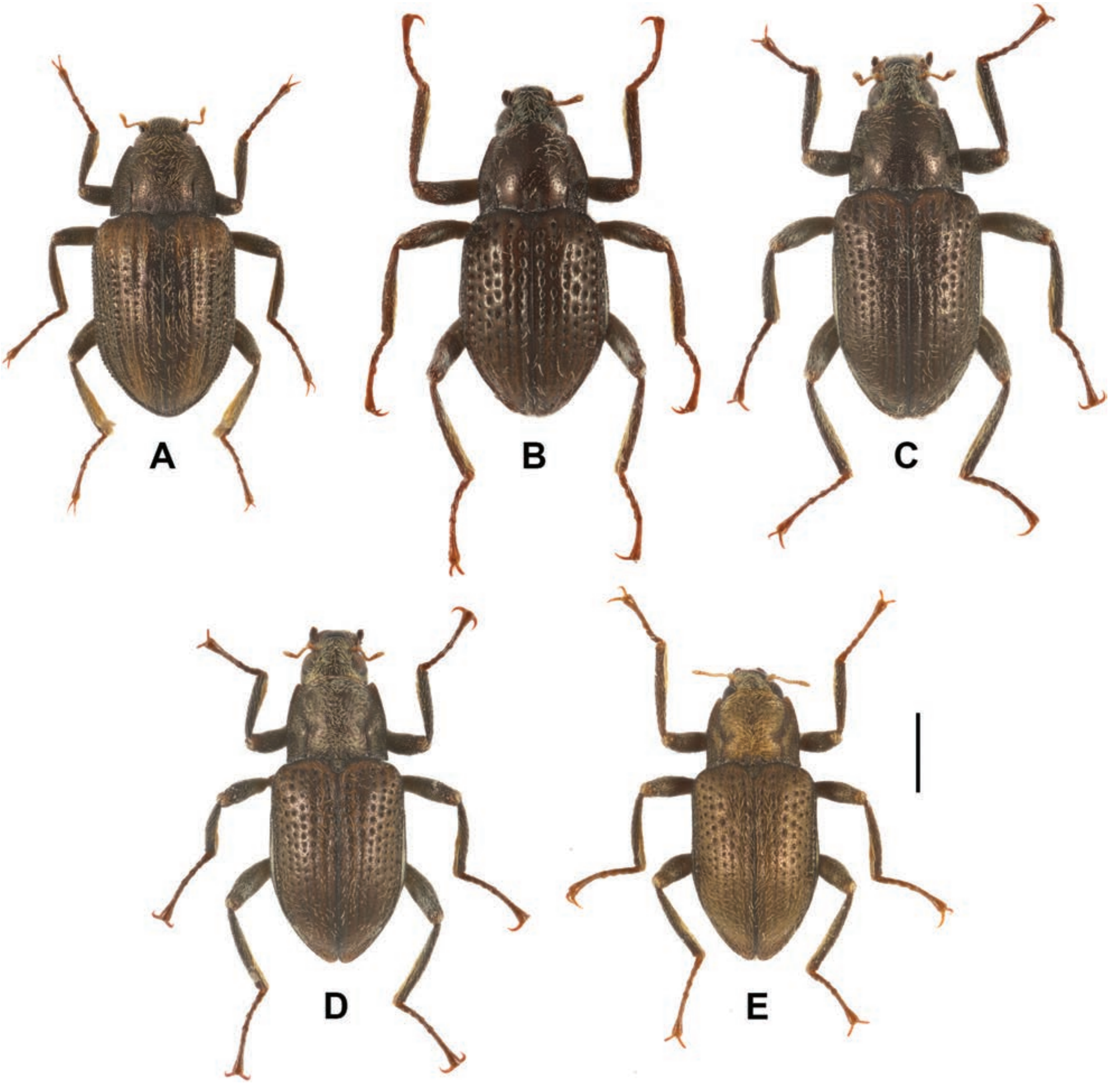

Figure 1. Dorsal habitus of *Grouvellinus* species, holotypes **A** *G. loong* sp. nov. **B** *G. buyi* sp. nov. **C** *G. wangmoensis* sp. nov. **D** *G. lihaitaoi* sp. nov. **E** *G. muyinlini* sp. nov. Scale bar: 0.5 mm.

extending from base to ~ 1/3 of elytral length; other carinae long and extending from base nearly to elytral apex. Lateral margins of elytra granulated. Aedeagus with median lobe constricted near middle and in apical 1/3; apex narrowed, subacute. Parameres nearly as long as median lobes, strongly narrowed at basal 1/3, apex rounded, lateral portion with long setae at apical 1/3.

Description. Male. Body obovate (Fig. 1A); head, pronotum and elytra black or dark brown, with weak cupreous metallic luster; femora and tibiae black; tarsi and antenna reddish brown; elytra with four reddish brown spots. Plastron area confined to head except for frons, vertex, and clypeus, lateral portions of prosternum, ninth elytral interval and epipleura, lateral portions of mesosternum, metaventrite, abdomen, femora, and tibia.

Head (Fig. 2A) wider than long, dorsal surface with dense short setae (except discal part) and large round punctures, longer setae sparsely and finely located at dorsal surface. Clypeus evenly punctate with large round punctures and with sparse long setae. Labrum transverse, slightly narrower than clypeus, surface distinctly microreticulated, apical 1/2 covered with sparse long setae, lateral margins with long bristles, apical margin rounded.

Pronotum (Fig. 2B) wider than long, widest at base, narrowed anteriad. Disc sparsely punctured on admesal portion, punctures with longer adpressed setae, intervals glabrous, shiny; longitudinal mesal portion with dense small punctures along posterior 2/3, impression absent; surface densely granulated. Anterior margin arcuate, anterior angles distinctly produced and acutangular with subacute apex; pronotal margins finely curved. Basal margin trisinuate, posterior angles acutangular, with apex rounded. Sublateral carinae distinct, extending from base to ~ 1/2 length of pronotum; basal 1/2 straight, near parallel; apical 1/2 curved; each side of sublateral carinae with a shallow and indistinct oblique impression, extending from apical end of carina to near anterior angle. Prosternal process (Fig. 2D) with weakly curved apex, surface densely covered with large punctures.

Scutellum (Fig. 2B) subtriangular, wider than long, widest near middle; surface covered with large punctures and each puncture bearing a short seta; lateral margins finely curved, apex obtuse.

Elytra (Fig. 2C) > 1.5 × as long as wide, widest at base, narrowed to apex. Granulate carinae on intervals III, V, VII, and VIII; carina on interval III short, ~ 1/3 length of elytra; other carinae long, extending from base of elytra to near apex. Lateral margins of elytra granulated. Each elytron with two reddish brown spots, one at base and another one near apex.

Metaventrite (Fig. 2D), surface rough with sparse long setae and large round punctures at disc. Median sulcus long but indistinct, extending from posterior margin to anterior 1/4, basal 1/4 wide and deep, apical 3/4 thin and shallow. Lateral sides of disc with series of elliptical shallow impression.

Abdomen. Middle regions of ventrites I–IV and anterior part of ventrite V punctured (Fig. 2D), covered with sparse large round punctures, each puncture bearing a long seta. Other parts of abdomen (Fig. 2D) covered with plastron and mixed with sparse long setae. Apex of ventrite V rounded. Ventrite I with well-developed pair of admedian carinae, straight, extending from base to apex.

Legs simple, surface granulated; femora widened, surface with plastron; inner side of tibiae with cleaning fringes; metatibiae (Fig. 2E) distinctly narrowed near apex; tarsi slightly shorter tibiae; tarsal claws simple.

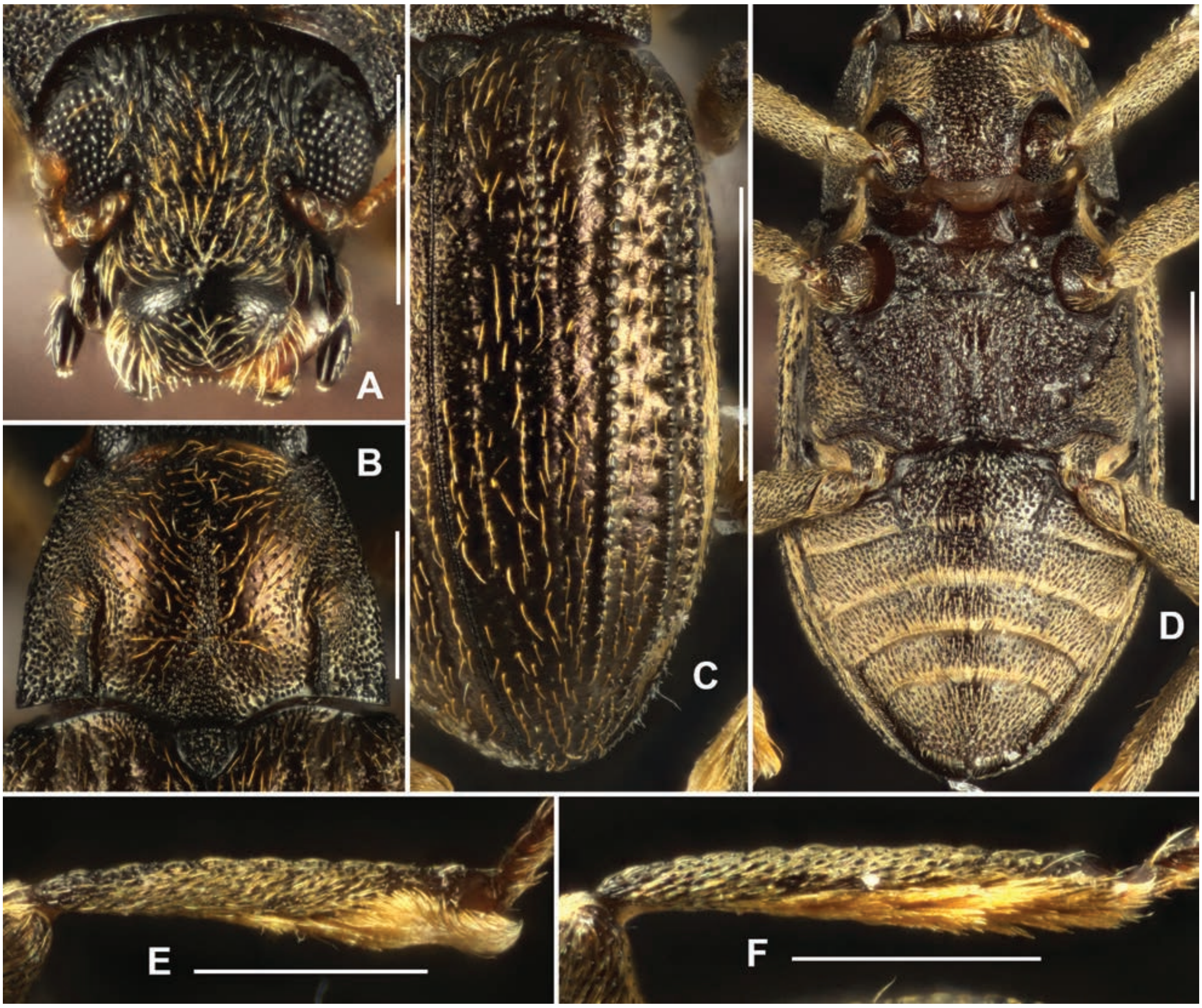

Figure 2. Diagnostic features of *Grouvellinus loong* sp. nov., paratype **A** head, dorsal view **B** pronotum, dorsal view **C** elytra, dorsal view **D** ventral habitus **E** metatibia, male **F** same, female. Scale bars: 0.25 mm (**A, B, E, F**); 0.5 mm (**C, D**).

Genitalia. Aedeagus (Fig. 3A–D), long and wide, symmetrical; median lobe slightly surpasses parameres, narrowed near middle and in apical 1/3, apex narrowed, subacute. Parameres (Fig. 3D) strongly narrowed at basal 1/3, with apical portion narrowed; apical 2/5 covered with long setae.

Female. Externally similar to the male, averagely larger, metatibiae (Fig. 2F) not narrowed near apex. Ovipositor as in Figs 12A, F. Stylus short and narrow, weakly curved, ~ 1/6 as long as distal portion of coxite. Coxite long, with apex distinctly expanded, roundly broadened at outer margin, apex with several short and curved sensilla. Distal portion of coxite nearly straight, surface with sparse, very short and acute setae. Proximal portion of coxite short, longer than 1/3 length of distal portion, surface with sparse, very short and acute setae. Valvifers slightly shorter than coxite, longitudinal baculum curved.

Measurements. Male (*n* = 10): CL: 1.81–1.89 mm (1.85±0.03); PL: 0.51–0.54 mm (0.52±0.01), PW: 0.68–0.74 mm (0.70±0.02); EL: 1.30–1.35 mm (1.33±0.02), EW: 0.90–0.93 mm (0.91±0.01).

Female (*n* = 10): CL: 1.68–2.08 mm (1.90±0.12); PL: 0.49–0.63 mm (0.56±0.05), PW: 0.62–0.80 mm (0.71±0.06); EL: 1.20–1.45 mm (1.35±0.09), EW: 0.86–0.96 mm (0.91±0.04).

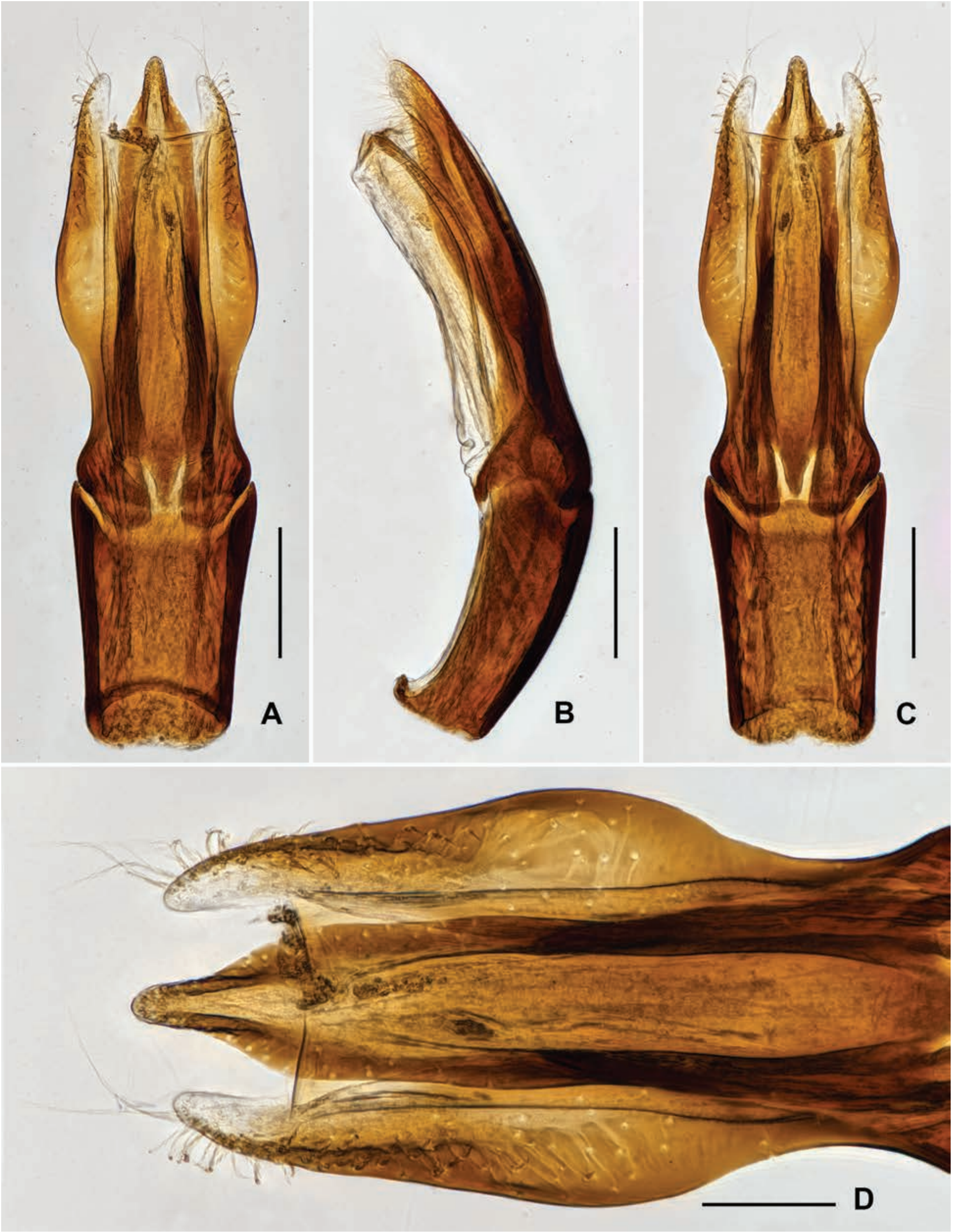

Figure 3. Aedeagus of *Grouvellinus loong* sp. nov., paratype **A** ventral view **B** lateral view **C** dorsal view **D** apex of median lobe and parameres. Scale bars: 0.05 mm (**D**); 0.1 mm (**A–C**).

Distribution. China (Guizhou).

Biology. All adults were collected from submerged stone in small ravine stream (Fig. 14A–C).

Etymology. The specific epithet ‘loong’ is the most famous auspicious beast in Chinese ancient myth, and also is a member of the Chinese Zodiac Signs.

Comparative diagnosis. The new species can be placed in the *Grouvellinus acutus* species group by the following characters: 1) body small; 2) elytra with yellowish brown markings; 3) pronotum without longitudinal impression; 4) surface of elytra with granulate carinae on strial intervals III, V, VII, and VIII; 5) ventrite I with a pair of well-developed admedian carinae. The *G. acutus* species group includes three known species, all of them occurring in China. Members of this group are similar in habitus. *G. loong* sp. nov. can be easily distinguished from other members of this group by the obviously different shape of the aedeagus: strongly narrowed at middle (vs not as above).

Grouvellinus loong sp. nov. is most similar to *G. acutus* Bian & Jäch, 2018 in habitus. These species can be distinguished by the following characters: 1) prosternal process with weakly curved apex, surface not granulated, densely covered with large punctures in *G. loong* sp. nov. (vs prosternal process with broadly rounded apex, surface sparsely granulated in *G. acutus*); 2) metatibia distinctly narrowed near apex, without hooked appendage at apex in *G. loong* sp. nov. (vs apex of metatibia conspicuously broad and sclerotized, usually with hooked appendage in *G. acutus*); 3) parameres of aedeagus strongly narrowed at basal 1/3 in *G. loong* sp. nov. (vs only weakly narrowed near base in *G. acutus*).

Grouvellinus buyi sp. nov.

https://zoobank.org/8C824860-8A11-4910-BA45-830E72C9D67A
Figs 1B, 4, 5, 12B, G
(布依戈溪泥甲)

Material examined. (11 exs: 5 ♂♂, 6 ♀♀): ***Holotype*****:** **China** • ♂, labeled ‘China: Guizhou, Guiyang City (贵阳市), Wudang District (乌当区), Xinbaobuyi Township (新堡布依族乡), Xiangzhigou Scenic Area (香纸沟景区), 26°47'02"N, 106°56'09"E, H: 1187m, 06.XI.2022, Jiang Ri-Xin leg.’ (GUGC). ***Paratypes*****:** **China** • 4 ♂♂, 6 ♀♀, with same label data as the holotype (GUGC).

Diagnosis. Body, long-oval, dark brown, surface shiny with cupreous metallic luster. Pronotum widest at basal 2/5, finely covered with small punctures, anterior and posterior angles densely covered with large punctures. Elytral intervals VII and VIII carinated, carinae granulated. Strial punctures of elytra very large in basal 2/3 and much smaller in apical 1/3. Sides of aedeagus generally subparallel in dorsal and ventral view, with median lobe slightly longer than parameres, distinctly curved in lateral view, apex narrowed and subacute. Parameres with apex rounded, lateral portion with long setae at apical 2/5.

Description. Male. Body long-oval (Fig. 1B), dark brown with tibiae and antenna pale brown, surface shiny with distinct cupreous metallic luster. Plastron area confined to head except for frons, vertex and clypeus, lateral portions of prosternum, ninth elytral interval and epipleura, lateral portions of mesosternum, metaventrite, abdomen, and femora.

Head (Fig. 4A) wider than long, dorsal surface shiny, densely with short setae (except discal part) and with sparse large punctures, each bearing a longer seta. Surface of clypeus shiny, with sparse small punctures and long setae.

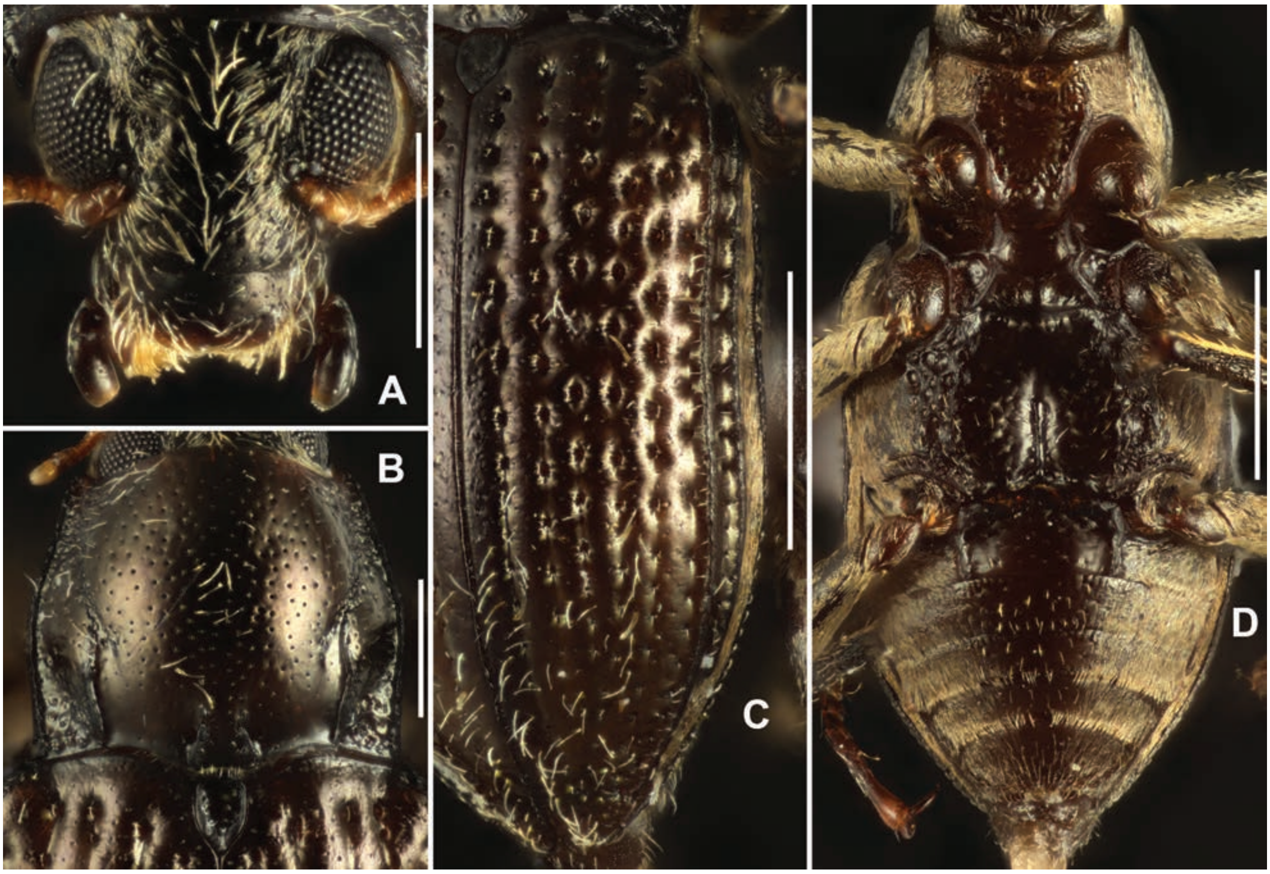

Figure 4. Diagnostic features of *Grouvellinus buyi* sp. nov., paratype **A** head, dorsal view **B** pronotum, dorsal view **C** elytra, dorsal view **D** ventral habitus. Scale bars: 0.25 mm (**A, B**); 0.5 mm (**C, D**).

Labrum transverse, narrower than clypeus, surface shiny, with sparse short setae, lateral margins with long bristles, apical margin rounded.

Pronotum (Fig. 4B), wider than long, widest near middle. Disc finely punctured with sparse small punctures, punctures with longer adpressed setae, intervals glabrous, shiny. Surface of anterior and posterior angles densely with large punctures. Anterior margin arcuate, anterior angles distinctly produced and acutangular, pronotal margins finely curved. Basal margin trisinuate, posterior angles acutangular. Longitudinal impression absent, with several pairs of small granules located in front of angles of scutellum. Sublateral carinae present in basal 1/2 of pronotum, trisinuate, each side of sublateral carinae with a shallow and indistinct oblique impression, extending from apical end of carina to near anterior angle. Prosternal process (Fig. 4D) with straight apex, surface sparsely with large punctures.

Scutellum (Fig. 4B) half fusiform, ~ 1.5 × as long as wide, widest near middle; surface microreticulated, with several small punctures; lateral margins finely curved, apex acutangular.

Elytra (Fig. 4C) ~ 1.5 × as long as wide, widest behind basal 1/2. Surface shiny, with distinct cupreous metallic luster and rows of sparse long setae. Strial punctures larger in basal 1/2, separated by ~ 1.5 × their diameters, much smaller and widely separated in other parts of elytra. Granulated carinae on strial intervals VII and VIII, other intervals flat. Hind wings well developed.

Metaventrite (Fig. 4D), surface rough with sparse long setae and large round punctures at disc. Median sulcus distinct, extending from posterior margin to

Figure 5. Aedeagus of *Grouvellinus buyi* sp. nov., paratype **A** dorsal view **B** lateral view **C** ventral view **D** apex of median lobe and parameres. Scale bars: 0.05 mm (**D**); 0.1 mm (**A–C**).

anterior 1/2. A pair of small round impression located at basal sides of median sulcus. Lateral sides of disc with series of elliptical shallow impression.

***Abdomen*.** Middle regions of ventrites I–IV and anterior part of ventrite V punctured (Fig. 4D), covered with sparse small punctures, each puncture bearing a long seta. Other parts of abdomen (Fig. 4D) covered with plastron and mixed with sparse long setae. Apex of ventrite V weakly concaved. Ventrite I with well-developed pair of admedian carinae, straight, extending from base to apex.

Legs simple, surface granulated; femora widened, surface with plastron; inner side of tibiae with cleaning fringes; tarsi slightly shorter tibiae; tarsal claws simple.

***Genitalia*.** Aedeagus (Fig. 5A–D), long and slender, symmetrical; median lobe slightly longer than parameres, finely get narrowed in basal 3/4, distal 1/4 distinctly sharpened. Parameres (Fig. 5D) curved at apex, with apex rounded; apical 1/2 covered with long setae.

Female. Externally similar to the male, averagely larger. Ovipositor as in Fig. 12B, G. Stylus short and narrow, weakly curved at apex, ~ 1/7 as long as distal portion of coxite. Coxite long, apex weakly expanded, roundly broadened at outer margin, with several short and curved sensilla. Distal portion of coxite nearly straight, surface finely with very short and acute setae. Proximal portion of coxite short, longer than 1/3 length of distal portion, surface finely covered with sparse, very short and acute setae. Valvifers ~ as long as coxite, longitudinal baculum weakly curved.

Measurements. Male (*n* = 5): CL: 1.91–2.09 mm (1.96±0.07); PL: 0.58–0.59 mm (0.58±0.01), PW: 0.71–0.74 mm (0.72±0.01); EL: 1.32–1.50 mm (1.38±0.07), EW: 0.94–1.00 mm (0.97±0.02).

Female: CL (*n* = 6): 2.18–2.23 mm (2.21±0.02); PL: 0.62–0.65 mm (0.63±0.01), PW: 0.72–0.83 mm (0.77±0.04); EL: 1.56–1.58 mm (1.57±0.01), EW: 0.97–1.10 mm (1.01±0.05).

Distribution. China: Guizhou.

Biology. All adults were collected from submerged stone in small ravine stream (Fig. 14D).

Etymology. The specific epithet ‘buyi’ is a nation of Chinese, which is the majority nation of the type locality of this new species: Xinbaobuyi Township (Guiyang City, Guizhou Province, China).

Comparative diagnosis. The new species is similar with *Grouvellinus sinensis* Grouvelle, 1906 and *G. ligulaceus* Bian & Zhang, 2023 in habitus. *Grouvellinus buyi* sp. nov. can be easily distinguished from *G. ligulaceus* by the following characters: 1) strial punctures of elytra very large in basal 1/2 (vs much smaller); 2) prosternal process with straight apex (vs weakly rounded); 3) median lobe of aedeagus slender (vs much broader); 4) parameres of aedeagus distinctly curved at apex (vs not as above).

The new species can be distinguished from *G. sinensis* by having a body with metallic luster and the surface of metaventrite and abdominal ventrites shiny, whereas the body lacks metallic luster and the surface of metaventrite and abdominal ventrites is distinctly rough in *G. sinensis*.

***Grouvellinus wangmoensis* sp. nov.**

https://zoobank.org/08E7A5E2-AD72-4799-B81B-B7283F8FD4BE
Figs 1C, 6, 7, 12C, H
(望谟戈溪泥甲)

Material examined. (31 exs: 11 ♂♂, 20 ♀♀)**: *Holotype*: China** • ♂, labeled ‘China: Guizhou, Qiannan Buyi and Miao Autonomous Prefecture (黔南布依族苗族自治州), Wangmo County (望谟县), Mashan Town (麻山镇), Kafa Village (卡法村), H:

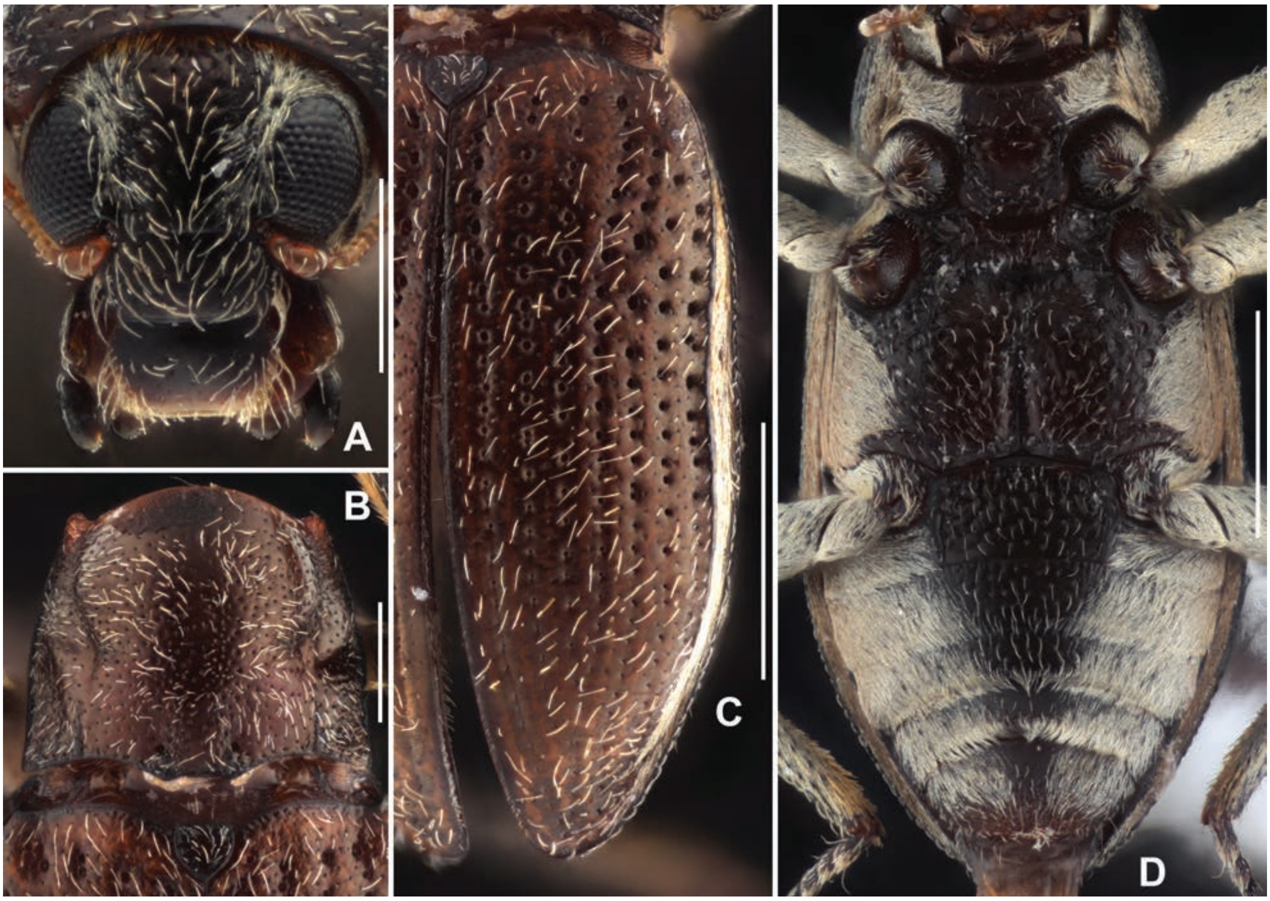

Figure 6. Diagnostic features of *Grouvellinus wangmoensis* sp. nov., paratype **A** head, dorsal view **B** pronotum, dorsal view **C** elytra, dorsal view **D** ventral habitus. Scale bars: 0.25 mm (**A, B**); 0.5 mm (**C, D**).

~ 857 m, 10.VII.2022, Jiang Ri-Xin leg.’ (GUGC). ***Paratypes*: China** • 10 ♂♂, 20 ♀♀, with same label data as the holotype (GUGC).

Diagnosis. Body long-oval, dark brown, with weak cupreous metallic luster. Pronotum widest at base, surface finely covered with small punctures, portions of anterior and posterior angles distinctly wrinkled. Base of pronotum with a pair of round foveae located at middle. Elytron interval VIII carinated. Median sulcus of metaventrite thin but distinct, extending from base to 3/4 length of metaventrite. Aedeagus with median lobe slightly longer than parameres, finely narrowed from basal 1/3 to apex, basal 1/6 distinctly narrowed, apex rounded and weakly expanded. Parameres of aedeagus very thin, weakly curved, apex rounded, lateral portion with long setae at apical 1/3, apex with several much longer setae.

Description. Male. Body elongate-oval (Fig. 1C), dark brown with cupreous metallic luster, tibiae, antennae, and elytra light brown. Plastron area confined to head, except for frons, vertex and clypeus, lateral portions of prosternum, ninth elytral interval and epipleura, lateral portions of mesosternum, metaventrite, abdomen, and surfaces of femora.

Head (Fig. 6A) wider than long, dorsal surface shiny, densely covered with short setae (except discal part) and with sparse large punctures, each bearing a longer seta. Surface of clypeus shiny, with sparse small punctures and each bearing a long seta. Labrum transverse, approximately as long as clypeus, surface shiny, basal 1/2 hairless, apical 1/2 with sparse short setae, lateral margins with long bristles, apical margin rounded.

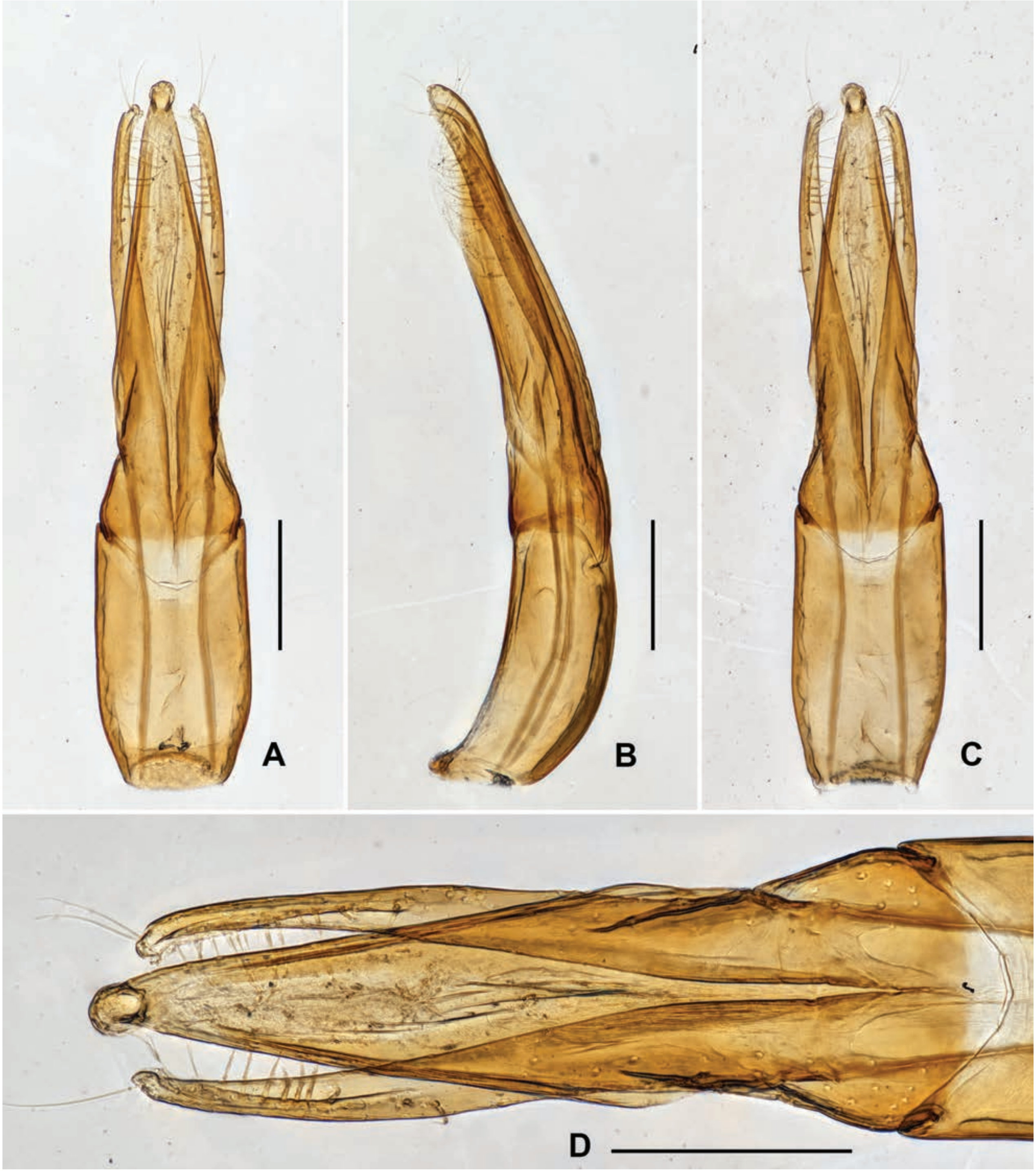

Figure 7. Aedeagus of *Grouvellinus wangmoensis* sp. nov., paratype **A** ventral view **B** lateral view **C** dorsal view **D** apex of median lobe and parameres. Scale bars: 0.05 mm (**D**); 0.1 mm (**A–C**).

Pronotum (Fig. 6B), slightly wider than long, widest at base, narrowed anteriad. Surface shiny, disc finely with sparse small punctures and long setae, surface of anterior and posterior angles distinctly wrinkled. Longitudinal impression absent, with a pair of small round foveae at middle of pronotal base. Anterior margin arcuate, anterior angles distinctly produced and acutangular. Lateral margins finely curved. Basal margin trisinuate, emarginated before scutellum, posterior angles acutangular. Sublateral carinae short, ~ 1/5 length of pronotum, each side of carinae with a shallow and indistinct oblique impression, not touch the apex of sublateral carinae, extending from basal 1/3 of pronotum to near anterior angle. Prosternal process (Fig. 6D) with apex weakly rounded, surface distinctly wrinkled sparsely covered with large punctures and long setae.

Scutellum (Fig. 6B) widely triangular, approximately as long as wide, widest at base; surface weakly wrinkled, with several large punctures, each bearing seta which in different length. Lateral margins finely curved, apex obtuse.

Elytra (Fig. 6C) ~ 1.5 × as long as wide, widest at base, narrowed to apex. Surface lighter in color than head and pronotum, shiny, with cupreous metallic luster and rows of sparse long setae. Strial punctures large in basal 2/3, separated by ~ 1.5 × diameters, and much smaller and widely separated in apical 1/3. Granulated carina on interval VIII, other intervals flat. Hind wings well developed.

Metaventrite (Fig. 6D), surface rough and finely with long setae and large round punctures at disc. Median sulcus distinct, extending from posterior margin to 3/4 length of metaventrite. A pair of small round impression located at basal sides of median sulcus. Lateral sides of disc with series of elliptical shallow impression.

***Abdomen*.** Base of ventrite I (Fig. 6D) weakly wrinkled, middle portions of ventrites I–IV and anterior part of ventrite V shiny (Fig. 6D), finely covered with large punctures, each puncture bearing a long seta. Other parts of abdomen (Fig. 6D) with plastron and mixed with sparse long setae. Apex of ventrite V weakly curved. Ventrite I with a pair of well-developed admedian carinae, curved at middle, extending from base to apex.

Legs simple, surface granulated; femora widened, surface with plastron; inner side of tibiae with cleaning fringes; tarsi slightly shorter tibiae; tarsal claws simple.

***Genitalia*.** Aedeagus (Fig. 7A–D), long and slender, symmetrical; median lobe slightly longer than parameres, distinctly narrowed at basal 1/5, apical 4/5 finely get narrowed from base to apex, with apex rounded. Parameres (Fig. 7D) thin, weakly curved to inner side, with apex rounded; apical 1/2 with long setae, apex of paramere with several much longer setae.

Female. Externally similar to the male, averagely larger. Ovipositor as in Fig. 12C, H. Stylus short and narrow, very weakly curved at base, ~ 1/4 as long as distal portion of coxite. Coxite long, apex distinctly expanded, roundly broadened at outer margin, and with several short and curved sensilla. Distal portion of coxite nearly straight, surface finely covered with very short and acute setae. Proximal portion of coxite short, ~ 1/2 the length of distal portion, surface finely covered with very short and acute setae. Valvifers longer than coxite, longitudinal baculum curved.

Measurements. Male (*n* = 10): CL: 2.10–2.23 mm (2.18±0.04); PL: 0.60–0.62 mm (0.62±0.01), PW: 0.73–0.82 mm (0.76±0.03); EL: 1.49–1.61 mm (1.56±0.03), EW: 0.95–1.04 mm (0.99±0.03).

Female: CL (*n* = 10): 2.20–2.27 mm (2.24±0.02); PL: 0.56–0.64 mm (0.61±0.03), PW: 0.73–0.78 mm (0.76±0.02); EL: 1.61–1.63 mm (1.62±0.01), EW: 1.02–1.04 mm (1.03±0.01).

Distribution. China: Guizhou.

Biology. All adults were collected from submerged stone in small ravine stream (Fig. 15F).

Etymology. The specific epithet refers to the type locality: Wangmo County (Guizhou, China); the name is treated as an adjective.

Comparative diagnosis. The new species is similar to *Grouvellinus pilosus* Jeng & Yang, 1998, *G. huaxiensis* Jiang, Huang & Chen, 2023, *G. muyinlini* sp. nov., and *G. lihaitaoi* sp. nov. in habitus. *Grouvellinus wangmoensis* sp. nov. can be distinguished from *G. pilosus* by the following characters: 1) base of pronotum with a pair of rounded foveae in middle (vs with a pair of elongate oval impressions), 2) granulated carinae present on elytron strial interval VIII (vs granulated carinae present on elytron strial interval VII). The new species can be easily distinguished from the other three species mentioned above by the sublateral carinae of pronotum being very short, not in contact with the oblique impression, and by the thin slender parameres of the aedeagus.

Grouvellinus lihaitaoi sp. nov.

https://zoobank.org/6C4113AA-FCAF-44D4-845C-F3000D582D0A
Figs 1D, 8, 9, 12D, I
(李氏戈溪泥甲)

Material examined. (82 exs: 19 ♂♂, 13 ♀♀: 50 exs., sex undetermined): ***Holotype*: China** • ♂, labeled ‘China: Guizhou, Qiannan Buyi and Miao Autonomous Prefecture (黔南布依族苗族自治州), Longli (龙里县), Wantanhe Town (湾滩河镇), H: 1136.10±1.08m, 26°12'52"N, 106°59'27"E, 31.VIII.2023, Jiang Ri-Xin, Hai-Tao Li, Pin Li, Yu-Hao Zhang, Yin-Lin Mu & Xiu-Dong Huang leg.’ (GUGC). ***Paratypes*: China** • 18 ♂♂, 13 ♀♀, 50 exs., sex undetermined, with same label data as the holotype (GUGC).

Diagnosis. Body elongate-oval, dark brown, shiny, with weak cupreous metallic luster. Pronotum widest at base, disc covered with dense small round punctures, surface of posterior angles granulated, middle of base a pair of small round foveae. Elytral interval VIII carinated, carina granulated. Median sulcus of metaventrite thin but distinct, extending from base to 1/2 length of mataventrite. Aedeagus with median lobe distinctly longer than parameres, base distinctly narrowed, apex narrowed, subacute. Parameres wide, apex rounded, outer sides weakly sinuate, lateral portion with long setae at apical 1/6.

Description. Male. Body long-oval (Fig. 1D), head, pronotum and femora dark brown, elytra, tibiae, and antennae reddish brown, surface shiny with cupreous metallic luster. Plastron area confined to head, except for frons, vertex, and clypeus, lateral portions of prosternum, ninth elytral interval and epipleura, lateral portions of mesosternum, metaventrite, abdomen, and surfaces of femora.

Head (Fig. 8A) wider than long, dorsal surface shiny, densely covered with short setae (except discal part) and sparse large punctures, each puncture bearing a longer seta. Clypeus with surface shiny, densely covered with short setae (except disc) and sparse long setae. Labrum transverse, narrower than clypeus, surface shiny, basal 1/2 hairless, apical 1/2 with sparse short setae, lateral margins with long bristles, apical margin rounded.

Pronotum (Fig. 8B), slightly wider than long, widest at base, narrowed anteriad. Surface shiny, disc densely punctured, and with punctures in different length, intervals glabrous, shiny; longitudinal impression absent, with a pair of small round foveae located at median of base; surface of posterior angles distinctly granulated. Anterior margin arcuate, anterior angles produced and weakly acutangular with subacute apex; pronotal margins finely curved. Basal margin trisinuate,

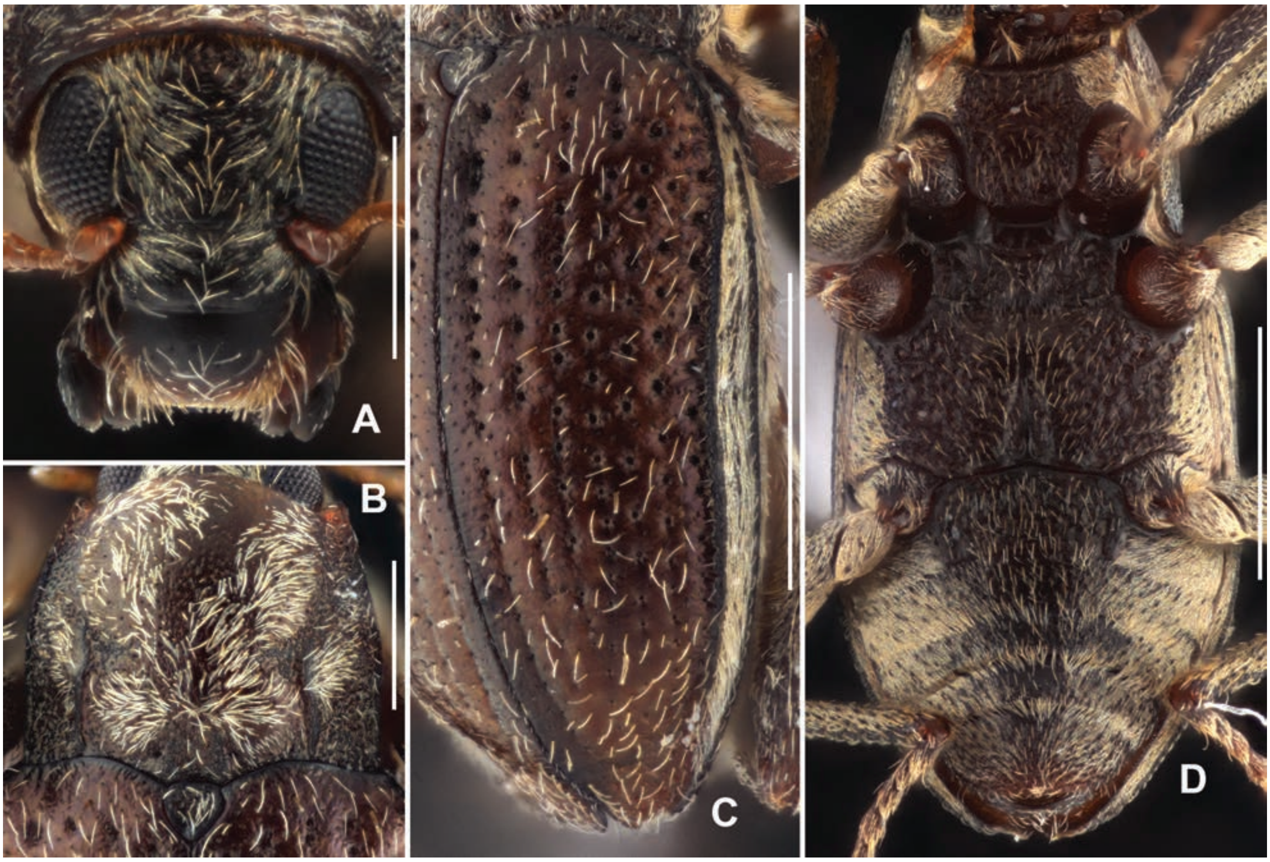

Figure 8. Diagnostic features of *Grouvellinus lihaitaoi* sp. nov., paratype **A** head, dorsal view **B** pronotum, dorsal view **C** elytra, dorsal view **D** ventral habitus. Scale bars: 0.25 mm (**A, B**); 0.5 mm (**C, D**).

posterior angles acutangular. Sublateral carinae distinct, extending from base to ~ 2/5 length of pronotum, each side of sublateral carinae with a shallow and indistinct oblique impression, extending from apex of sublateral carinae to near anterior angle. Prosternal process (Fig. 8D) with apex rounded, surface distinctly wrinkled and sparsely covered with large punctures and long setae.

Scutellum (Fig. 8B) widely triangular, approximately as long as wide, widest at basal 1/3; surface weakly wrinkled, sparsely covered with large punctures, each bearing a long seta. Lateral margins finely curved, apex obtuse.

Elytra (Fig. 8C) ~ 1.5 × as long as wide, widest near apical 1/3. Surface shiny, with sparse long setae. Lateral margins sub-parallel in basal 2/3. Strial punctures larger in basal 2/3, separated by more than twice diameter, and much smaller and widely separated in other portions of elytra. Granulated carina on interval VIII, other intervals flat. Hind wings well developed.

Metaventrite (Fig. 8D), surface rough and finely with long setae and large round punctures at disc. Median sulcus distinct, extending from posterior margin to 1/2 length of metaventrite, base with a pair of round impression. Lateral sides of disc with series of elliptical shallow impression.

***Abdomen*.** Base of ventrite I (Fig. 8D) weakly wrinkled, middle regions of ventrites I–IV and anterior part of ventrite V (Fig. 8D) finely with large round punctures, each puncture bearing a long seta. Other parts of abdomen (Fig. 8D) covered with plastron and mixed with sparse long setae. Apex of ventrite V weakly curved, ventrite I with well-developed pair of admedian carinae, curved at middle, extending from base to apex.

Figure 9. Aedeagus of *Grouvellinus lihaitaoi* sp. nov., paratype **A** dorsal view **B** same, lateral view **C** same, ventral view **D** apex of median lobe and parameres. Scale bars: 0.05 mm (**D**); 0.1 mm (**A–C**).

Legs simple, surface granulated; femora widened, surface with plastron; inner side of tibiae with cleaning fringes; tarsi slightly shorter tibiae; tarsal claws simple.

***Genitalia*.** Aedeagus (Fig. 9A–D), long and slender, symmetrical; median lobe distinctly longer than parameres, widest at basal 2/5, apical 3/5 finely narrowed, with apex rounded. Parameres (Fig. 9D) wide, nearly straight, with apex rounded; apical 1/6 covered with long setae.

Female. Externally similar to the male, averagely larger. Ovipositor as in Fig. 12D, I. Stylus short and narrow, weakly curved near middle, ~ 1/4 as long as distal portion of coxite. Coxite long, with apex expanded, roundly broadened at outer margin, with several short and curved sensilla. Distal portion of coxite nearly straight, surface finely covered with very short and acute setae. Proximal portion of coxite short, longer than 1/2 the length of distal portion, surface finely covered with very short and acute setae. Valvifers slightly longer than coxite, longitudinal baculum weakly curved.

Measurements. Male (*n* = 10): CL: 1.77–2.13 mm (1.88±0.10); PL: 0.49–0.61 mm (0.55±0.04), PW: 0.61–0.77 mm (0.69±0.05); EL: 1.28–1.51 mm (1.38±0.06), EW: 0.78–0.98 mm (0.87±0.06).

Female: CL (*n* = 10): 1.87–1.99 mm (1.93±0.05); PL: 0.52–0.54 mm (0.53±0.01), PW: 0.64–0.67 mm (0.65±0.01); EL: 1.27–1.44 mm (1.38±0.06), EW: 0.84–0.92 mm (0.88±0.03).

Distribution. China: Guizhou.

Biology. All adults were collected from submerged stone in small ravine stream (Fig. 15C–E).

Etymology. The species epithet honors our friend and colleague Dr. Hai-Tao Li (Guizhou University), one of the collectors of the new species; the name is treated as an adjective.

Comparative diagnosis. The new species is most similar to *Grouvellinus muyinlini* sp. nov. It can be distinguished from that species by the following characters: pronotum widest at base (vs widest near middle); median sulcus of metaventrite short, ~ 1/2 the length of metaventrite (vs much longer, ~ 3/4 the length of metaventrite); parameres of aedeagus much wider, apex nearly straight (vs parameres much narrower, apex curved).

Grouvellinus muyinlini **sp. nov.**

https://zoobank.org/84E521A3-CEA7-4C73-9909-B8CAE775C711
Figs 1E, 10, 11, 12E, J
(母氏戈溪泥甲)

Material examined. (40 exs: 20 ♂♂, 20 ♀♀)**:** ***Holotype*****: China** • ♂, labeled ‘China: Guizhou, Guiyang City (贵阳市), Huaxi District (花溪区), Qiantao Buyi and Miao Township (黔陶布依族苗族自治乡), Machang Village (马场村), Raolongxiagu (绕拢峡谷), H: 1084 m, 26°19'12"N, 106°46'19"E, 13.VII.2022, Jiang Ri-Xin, Yin-Lin Mu, Tian-Jun Liu & Feng-E Li leg.’ (GUGC). ***Paratypes*****: China** • 19 ♂♂, 20 ♀♀, with same label data as the holotype (GUGC).

Diagnosis. Body elongate-oval, dark brown with antenna, elytra and tibia pale brown, surface shiny with weak cupreous metallic luster. Elytral interval VIII carinated. Pronotum widest near middle, disc with dense small punctures, portions of posterior angles granulated, base of pronotum with a pair of median foveae. Median sulcus of metaventrite thin but distinct, extending from base to 3/4 length of metaventrite. Aedeagus with median lobe distinctly longer than parameres, constricted at base, finely narrowed from basal 1/5 to apex, apex rounded. Parameres thinner and shorter than

Figure 10. Diagnostic features of *Grouvellinus muyinlini* sp. nov., paratype **A** head, dorsal view **B** pronotum, dorsal view **C** elytra, dorsal view **D** ventral habitus. Scale bars: 0.25 mm (**A, B**); 0.5 mm (**C, D**).

median lobe, weakly sinuated and curved at apex, lateral portion with long setae at apical 1/6.

Description. Male. Body elongate-oval (Fig. 1E), head and elytra dark brown with elytra, tibiae, antennae, and elytra pale brown, dorsal surface shiny with cupreous metallic luster. Plastron area confined to head except for frons, vertex, and clypeus, lateral portions of prosternum, ninth elytral interval and epipleura, lateral portions of mesosternum, metaventrite, abdomen, and femora.

Head (Fig. 10A) wider than long, dorsal surface shiny, densely covered in short setae (except discal part) and sparse longer setae. Clypeus shiny, with dense short setae (except disc) and sparse long setae. Labrum transverse, slightly narrower than clypeus, shiny, basal 1/2 hairless and microreticulated, apical 1/2 with sparse short setae, lateral margins with long bristles, apical margin rounded.

Pronotum (Fig. 10B), slightly wider than long, widest near middle. Disc with dense punctures in different length and long setae, intervals of punctures glabrous, longitudinal impression absent, with a pair of small round foveae located at middle base near posterior margin, surface of posterior angles granulated. Anterior margin arcuate, anterior angles produced and weakly acutangular. Lateral margins finely curved. Basal margin trisinuate, emarginated before scutellum, posterior angles acutangular. Sublateral carinae distinct, extending from base to ~ 2/5 length of pronotum, each side of sublateral carinae with a shallow and indistinct oblique impression, extending from apex of sublateral carinae to near anterior angle. Prosternal process (Fig. 10D) with apex rounded, surface wrinkled and sparsely covered with large punctures and long setae.

Figure 11. Aedeagus of *Grouvellinus muyinlini* sp. nov., paratype **A** ventral view **B** lateral view **C** dorsal view **D** apex of median lobe and parameres. Scale bars: 0.05 mm (**D**); 0.1 mm (**A–C**).

Scutellum (Fig. 10B) widely triangular, approximately as long as wide, widest near middle; surface densely punctured, each puncture bearing a long seta. Lateral margins finely curved, apex obtuse.

Elytra (Fig. 10C) widest near apical 3/7, reddish brown, lateral margins sub-parallel in basal 4/7. Surface shiny, with weakly cupreous metallic luster

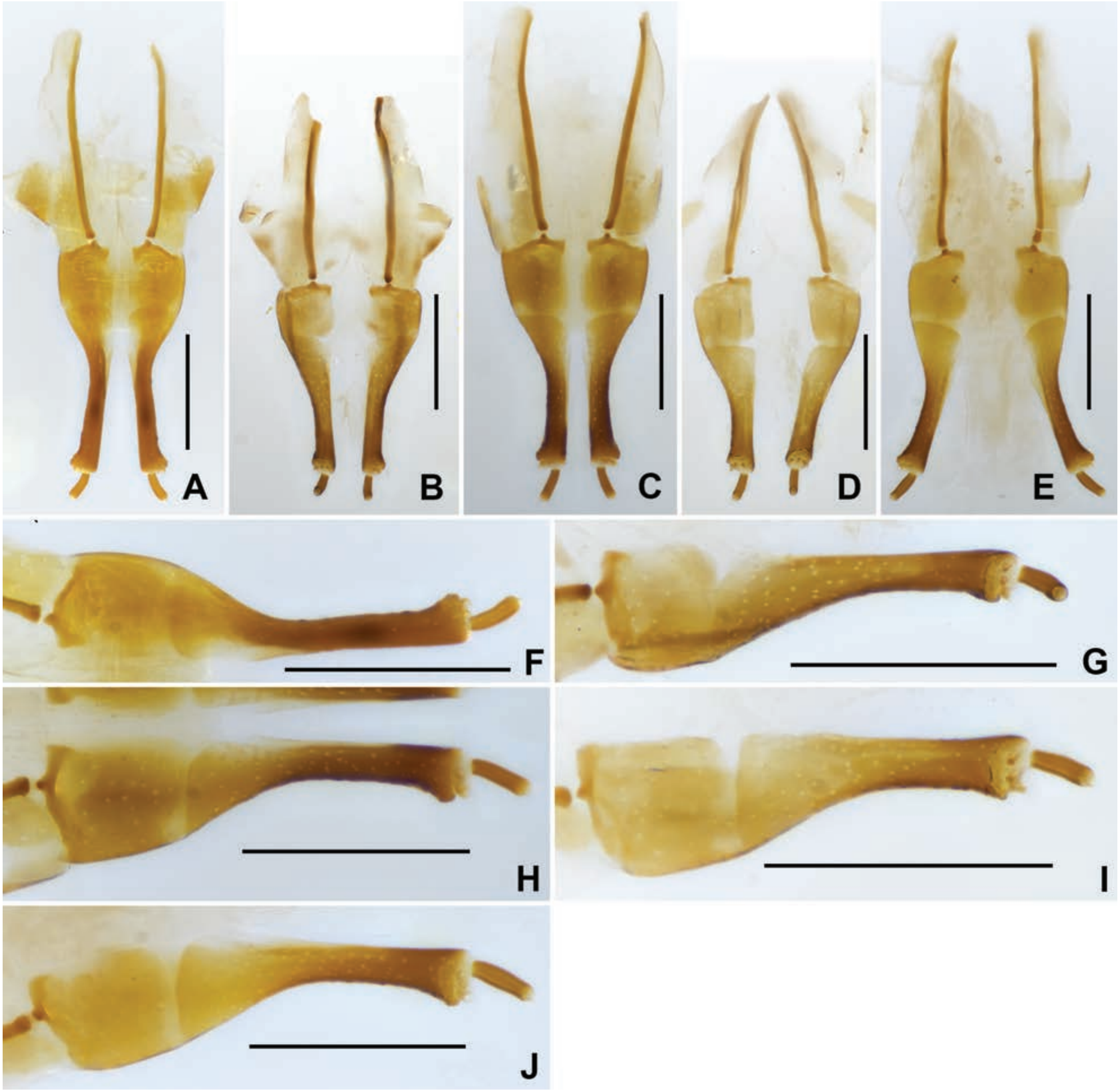

Figure 12. Ovipositor of *Grouvellinus* species **A, F** *G. loong* sp. nov., paratype **B, G** *G. buyi* sp. nov., paratype **C, H** *G. wangmoensis* sp. nov., paratype **D, I** *G. lihaitaoi* sp. nov., paratype **E, J** *G. muyinlini* sp. nov., paratype. Scale bars: 0.1 mm.

and sparse long setae. Granulate carinae on interval VIII, interval VII with a row of sparse and very small granules, extending from base to apex; other intervals flat. Strial punctures larger in basal 4/7, separated by more than 2 × diameter, and much smaller and widely separated in other part of elytra. Hind wings well developed.

Metaventrite (Fig. 10D), surface finely punctured with large punctures and long setae at disc, lateral sides of disc with series of elliptical shallow impression. Median sulcus distinct, extending from posterior margin to 3/4 length of metaventrite, with a pair of round impression at sides of basal median sulcus.

***Abdomen*.** Base of ventrite I (Fig. 10D) weakly wrinkled, middle regions of ventrites I–IV and anterior part of ventrite V (Fig. 10D) punctured with large and round punctures, each puncture bearing a long seta. Other parts of abdomen (Fig. 10D) with plastron and mixed with sparse long setae. Apex of ventrite

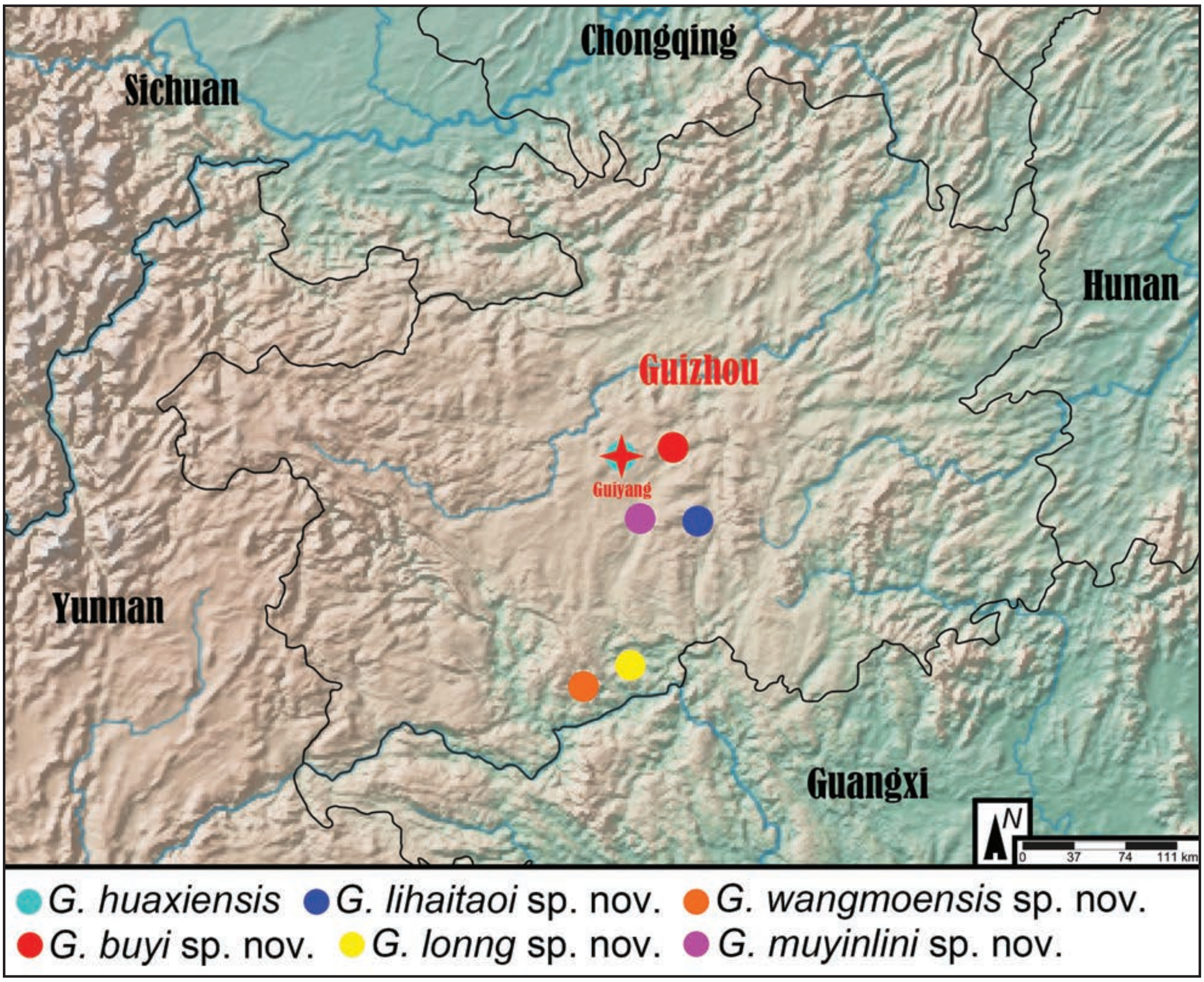

Figure 13. Distribution map of known *Grouvellinus* species from Guizhou Province.

V weakly curved. Ventrite I with a pair of well-developed admedian carinae, curved at middle, extending from base to apex.

Legs simple, surface granulated; femora widened, surface covered with sericeous tomentum; inner side of tibiae with cleaning fringes; tarsi slightly shorter than tibiae; tarsal claws simple.

***Genitalia*.** Aedeagus (Fig. 11A–D), long and wide, symmetrical; median lobe distinctly longer than parameres, constricted at base, finely narrowed from basal 1/5 to apex, with apex rounded. Parameres (Fig. 11D) thinner and shorter than median lobe, weakly sinuated and curved at apex, lateral portion with long setae at apical 1/6.

Female. Externally similar to the male, averagely larger. Ovipositor as in Fig. 12E, J. Stylus short and narrow, nearly straight, weakly expanded at middle, shorter than 1/4 length of distal portion of coxite. Coxite long, apex distinctly expanded, roundly broadened at outer margin, with several short and curved sensilla. Distal portion of coxite nearly straight, surface finely covered with very short and acute setae. Proximal portion of coxite short, ~ 1/2 the length of distal portion, surface finely covered with very short and acute setae which are sparser than setae on distal portion of coxite. Valvifers slightly longer than coxite, longitudinal baculum nearly straight, weakly curved at base.

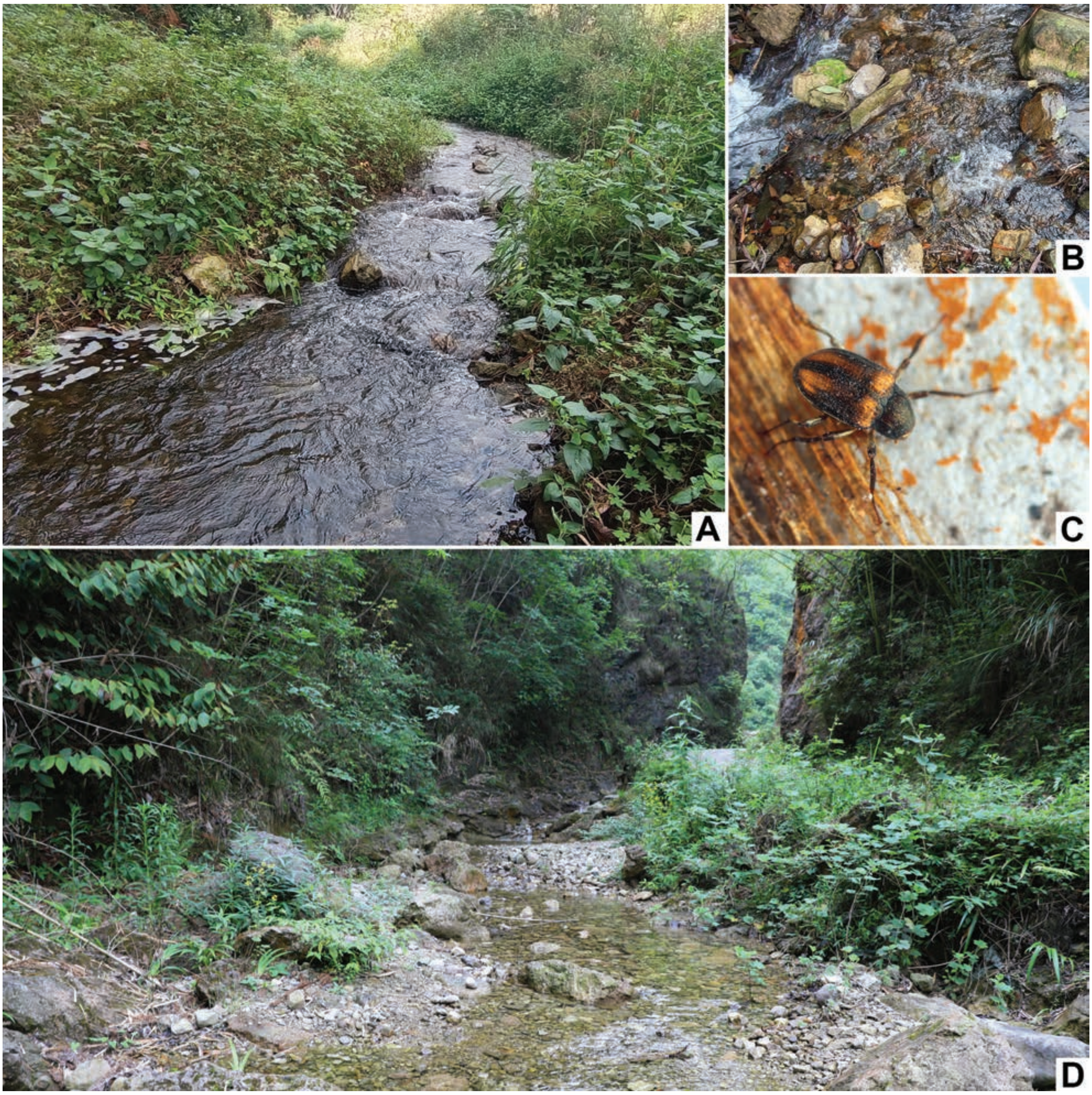

Figure 14. Habitats of *Grouvellinus* species **A** general environment of the type locality of *G. loong* sp. nov. **B** same, microenvironment **C** living adult of *G. loong* sp. nov. **D** general environment of the type locality of *G. buyi* sp. nov.

Measurements. Male (*n* = 10): CL: 1.78–2.09 mm (1.89±0.09); PL: 0.49–0.58 mm (0.53±0.03), PW: 0.62–0.68 mm (0.65±0.02); EL: 1.26–1.52 mm (1.35±0.07), EW: 0.81–0.90 mm (0.86±0.03).

Female (*n* = 10): CL: 1.90–2.11 mm (2.00±0.07); PL: 0.55–0.59 mm (0.57±0.01), PW: 0.68–0.72 mm (0.70±0.01); EL: 1.36–1.52 mm (1.42±0.07), EW: 0.85–1.02 mm (0.92±0.05).

Distribution. China: Guizhou.

Biology. All adults were collected from submerged stone in small ravine stream (Fig. 15C–E).

Etymology. The species epithet honors our friend and colleague Dr. Yin-Lin Mu (Guizhou University), one of the collectors of the new species; the name is treated as an adjective.

Figure 15. Habitat of *Grouvellinus* species **A** general environment of the type locality of *G. lihaitaoi* sp. nov. **B** living adult of *G. lihaitaoi* sp. nov. **C** general environment of *G. muyinlini* sp. nov. **D** dr. Yin-Lin Mu working in the type locality of *G. muyinlini* sp. nov. **E** the first author working in the same locality as ditto **F** general environment of *G. wangmoensis* sp. nov.

Comparative diagnosis. *Grouvellinus muyinlini* sp. nov. is most similar to *G. lihaitaoi* sp. nov. For differences see the comparative diagnosis of *G. lihaitaoi* sp. nov.

Discussion

Recent papers suggested that the genus *Grouvellinus* has a potentially high diversity in Southeast Asia, and particularly in South China (Bian and Sun 2016; Bian and Jäch 2018, 2019; Freitag et al. 2018, 2020; Bian and Zhang 2023; Jiang et al. 2023). Freitag et al. (2020) reported a surprising diversity of *Grou-*

vellinus in a small geographic range of Sabah, and a similar situation can also be found in Guizhou Province, China, where several (three or four) species were collected. On the other hand, some species show stronger adaptation to poor water quality, e.g., *G. huaxiensis* Jiang, Huang & Chen, 2023 was collected in an urban river of Guiyang City.

Some *Grouvellinus* species are highly similar in habitus. However, a simple clustering combined with morphological study is helpful to effectively distinguish species of this group. Moreover, the true diversity of this group in China still needs to be unveiled, especially in the mountain and karst areas of South China.

Acknowledgements

The authors express their sincere gratitude to Mr. Tian-Jun Liu, Miss Yu-Hao Zhang, Drs Yin-Lin Mu, Hai-Tao Li, Pin Li, and Feng-E Li (Guizhou University, Guiyang, China), and Mr. Xiu-Dong Huang (Anshun, China) for their help with our investigation, and to Dr. Zhi-Teng Chen (Jiangsu University of Science and Technology, Zhenjiang, China) for his support of this work. Miss Jade Li (University of Florida, USA) kindly revised the English of this work. We also thank Dr. Zu-Qi Mai (Sun Yat-sen University, Guangdong, China) for his support of this work. Appreciation is also given to Dr. Ján Kodada (Comenius University in Bratislava, Bratislava, Slovakia), Mariano C. Michat (University of Buenos Aires, Buenos Aires, Argentina), and an anonymous referee for providing constructive suggestions.

Additional information

Conflict of interest

The authors have declared that no competing interests exist.

Ethical statement

No ethical statement was reported.

Funding

Financial support was provided by the Program of Excellent Innovation Talents, Guizhou Province (No. 20154021).

Author contributions

Funding acquisition: X-SC. Investigation: P-LW. Writing - original draft: R-XJ, P-LW. Writing - review and editing: X-SC.

Author ORCIDs

Ri-Xin Jiang https://orcid.org/0000-0002-5339-853X
Ping-Lan Wu https://orcid.org/0009-0003-7089-7861
Xiang-Sheng Chen https://orcid.org/0000-0001-9801-0343

Data availability

All of the data that support the findings of this study are available in the main text.

References

Bian D-J, Jäch MA (2018) Revision of the Chinese species of the genus *Grouvellinus* Champion, 1923 (Coleoptera: Elmidae). The *G. acutus* species group. Zootaxa 4387(1): 174–182. https://doi.org/10.11646/zootaxa.4387.1.8

Bian D-J, Jäch MA (2019) Revision of the species *Grouvellinus* Champion, 1923 (Coleoptera: Elmidae) with long median pronotal carina, including descriptions of four new species from China. Zootaxa 4586(1): 127–140. https://doi.org/10.11646/zootaxa.4586.1.6

Bian D-J, Sun H (2016) A key to *Grouvellinus* Champion, 1923 from mainland China with descriptions of two new species (Coleoptera, Elmidae). ZooKeys 623: 89–104. https://doi.org/10.3897/zookeys.623.9610

Bian D-J, Zhang Y (2023) Descriptions of eight new species of *Grouvellinus* from China (Coleoptera, Elmidae). Zootaxa 5254(2): 257–277. https://doi.org/10.11646/zootaxa.5254.2.6

Freitag H, Pangantihon CV, Njunjić I (2018) Three new species of *Grouvellinus* Champion, 1923 from Maliau Basin, Sabah, Borneo, discovered by citizen scientists during the first Taxon Expedition (Insecta, Coleoptera, Elmidae). ZooKeys 754: 1–21. https://doi.org/10.3897/zookeys.754.24276

Freitag H, Molls C, Bouma AM, Garces JM, Rossato M, Cosentino E, Delledonne M (2020) Additional new species of *Grouvellinus* Champion 1923 (Insecta, Coleoptera, Elmidae) discovered by citizen scientists and DNA barcoded in the field applying a novel MinION-based workflow. Journal of Natural History 53(41–42): 2593–2620. https://doi.org/10.1080/00222933.2019.1709669

Jäch MA, Kodada J (1995) Elmidae: 1. Check list and bibliography of the Elmidae of China (Coleoptera). In: Jäch MA, Ji L-Z (Eds) Water beetles of China. Volume 1. Zoologisch-Bota-nische Gesellschaft in Osterreich and Wiener Coleopterologenverein, Vienna, Austria, 289–298.

Jäch MA, Kodada J, Brojer M, Shepard WD, Čiampor F (2016) World Catalogue of Insects. Vol. 14. Coleoptera: Elmidae and Protelmidae. Brill, Leiden and Boston, [XXI +] 318 pp. https://doi.org/10.1163/9789004291775

Jiang R-X, Huang X-D, Chen X-S (2023) Discovery of *Grouvellinus huaxiensis* sp. nov. (Coleoptera: Elmidae) from the urban river Huaxi in Guiyang, China. Zootaxa 5254(4): 585–592. https://doi.org/10.11646/zootaxa.5254.4.10

Jung SW, Jäch MA, Bae YJ (2014) Review of the Korean Elmidae (Coleoptera: Dryopoidea) with descriptions of three new species. Aquatic Insects: International Journal of Freshwater Entomology 36(2): 93–124. https://doi.org/10.1080/01650424.2015.1046457

Junqueira MV, Friedrich G, Araujo PRD (2010) A saprobic index for biological assessment of river water quality in Brazil (Minas Gerais and Rio de Janeiro states). Environmental Monitoring and Assessment 163: 545–554. https://doi.org/10.1007/s10661-009-0857-1

Kodada J, Jäch MA, Čiampor F (2016) Elmidae Curtis, 1830. In: Beutel RG, Leschen RAB. (Eds) Handbook of Zoology. Vol. IV. Part 38. Coleoptera, Beetles. Vol. 1. Morphology and Systematics (Archostemata, Adephaga, Myxophaga, Polyphaga partim). 2nd Ed. Walter de Gruyter, Berlin, 561–589.

Moog O, Jäch MA (2003) Elmidae. In: Moog O (Ed.) Fauna Aquatica Austriaca. Wien: Wasserwirtschaftskataster, Bundesministerium für Land- und Forstwirtschaft, Umwelt und Wasserwirtschaft, 132–158.

ZooKeys 1219: 99–104 (2024)
DOI: 10.3897/zookeys.1219.135654

Research Article

First record of *Mesoscytina* (Hemiptera, Scytinopteroidea, Scytinopteridae) from the Middle Triassic Tongchuan Entomofauna of China

Qianqi Zhang[1,2], Xuheng Du[3], Xiuping Zhu[4], Haichun Zhang[3]

1 *College of Paleontology, Shenyang Normal University, Shenyang 110034, China*
2 *Key Laboratory of Evolution of Past Life in NE Asia, Ministry of Natural Resources, Shenyang 110034, China*
3 *State Key Laboratory of Palaeobiology and Stratigraphy, Nanjing Institute of Geology and Palaeontology, Chinese Academy of Sciences, Nanjing 210008, China*
4 *University of Chinese Academy of Sciences, Beijing 100049, China*
Corresponding author: Qianqi Zhang (qianqizhang@synu.edu.cn)

Abstract

A new scytinopterid species, *Mesoscytina tongchuanensis* **sp. nov.**, is established based on a tegmen collected from the Middle Triassic Tongchuan Formation in Shaanxi Province, NW China. The new species can be easily separated from its congeners by the narrow tegminal apex, less curved terminal branches of stems RP, M and CuA and crossvein *r-m* connected to long vein M_{1+2}. This discovery represents the first record of *Mesoscytina* from the Tongchuan Formation in China and suggests that the genus *Mesoscytina* spread much more widely from Gondwana to northern Pangea in the Middle Triassic.

Key words: Ladinian, *Mesoscytina tongchuanensis* sp. nov., new record, Scytinopteridae, systematics, taxonomy, Tongchuan Formation

Academic editor: Nina Sinichenkova
Received: 27 August 2024
Accepted: 19 October 2024
Published: 27 November 2024

ZooBank: https://zoobank.org/72BBDAA4-2F13-4E09-BCF5-C52FB4C81A93

Citation: Zhang Q, Du X, Zhu X, Zhang H (2024) First record of *Mesoscytina* (Hemiptera, Scytinopteroidea, Scytinopteridae) from the Middle Triassic Tongchuan Entomofauna of China. ZooKeys 1219: 99–104. https://doi.org/10.3897/zookeys.1219.135654

Introduction

The family Scytinopteridae Handlirsch, 1906, an extinct Permian-Triassic hemipteran group widespread in Pangea, is characterized by the costal fracture on the heavily sclerotized punctate tegmen and a hypocostal socket fixed on the thorax (Shcherbakov 1984). Moreover, the basal cell shape, single *r-m* crossvein, very weak or absent nodal groove and vein M bent strongly towards CuA are important common characters among Triassic scytinopterid taxa (Lambkin 2016). As ancestors of true bugs, the scytinopteroids are supposed to inhabit temporary submerged waterside vegetation (Shcherbakov 2022). The taxonomic study of Scytinopteridae is of both evolutionary and ecological significance.

The genus *Mesoscytina* Tillyard, 1919 was originally assigned to Scytinopteridae, then to the cercopoid family Archijassidae Becker-Migdisova, 1962 (Hamilton 1992). Lambkin (2016) re-assigned *Mesoscytina* to Scytinopteridae, re-studied the four species of *Mesoscytina* and further proposed the genus *Triassoscarta* being synonymous with *Mesoscytina*. Lara et al. (2021) established the new combination *Mesoscytina forsterae* (Martins-Neto & Gallego,

2003) (Martins-Neto et al. 2003). Here, we describe a new *Mesoscytina* species from the Tongchuan Entomofauna, which is the fourth Triassic scytinopteroid species discovered in China (Lin 1986; Zhang et al. 2022).

Material and methods

The entire tegmen was collected from the Tongchuan Formation of Hejiafang Village, Jinsuoguan Town, Yintai District, Tongchuan City, Shaanxi Province, NW China. A U-Pb geochronology study confirms the insect-bearing layer is dated to 238–237 Ma, as Ladinian of the Middle Triassic (Zheng et al. 2018).

The holotype (NIGP205761) is housed at the Nanjing Institute of Geology and Palaeontology (**NIGPAS**), Chinese Academy of Sciences (**CAS**), Nanjing, China. Photographs were taken using a stereomicroscope system (ZEISS Stereo Discovery V16) in NIGPAS. Images of the part and counterpart of the tegmen were corrected and stacked using Adobe Photoshop 2021, and line drawings were made through software CorelDRAW 2019. The vein nomenclature follows Shcherbakov (1984, 1996). The nomenclatural acts established herein are registered under ZooBank LSID urn:lsid:zoobank.org:pub:72BB-DAA4-2F13-4E09-BCF5-C52FB4C81A93.

Systematic palaeontology

Order Hemiptera Linnaeus, 1758
Infraorder Cicadomorpha Evans, 1946
Superfamily Scytinopteroidea Handlirsch, 1906
Family Scytinopteridae Handlirsch, 1906

Mesoscytina Tillyard, 1919

Type species. *Mesoscytina australis* Tillyard, 1919.

Mesoscytina tongchuanensis Q. Zhang, Du & H. Zhang, sp. nov.

https://zoobank.org/871B77B9-0162-476B-B3C9-EE1BA18F3D8A
Figs 1, 2A

Type material. ***Holotype*:** No. NIGP205761a, b, an isolated complete tegmen, part and counterpart. Housed at NIGPAS. South of Hejifang Village, Jinsuoguan Town, Yintai District, Tongchuan City, Shaanxi Province, China.

Age and horizon. Ladinian, late Middle Triassic; top of the lower Tongchuan Formation.

Etymology. The specific epithet is from the city of Tongchuan, where the holotype was collected.

Diagnosis. Small tegmen (6–11 mm in length), punctate, quite broad (length/width ratio less than 2.5), broadest on its middle area, with apical area contracted; postcostal area wide; costal fracture curved and single; vein R with two terminal branches; stem M partly curved, with three terminal branches, vein M_{1+2} long; end of vein CuA_2 beyond vein CuP; terminal branches of stems RP, M and CuA not more or less parallel; crossvein *cua-cup* long, less curved veins

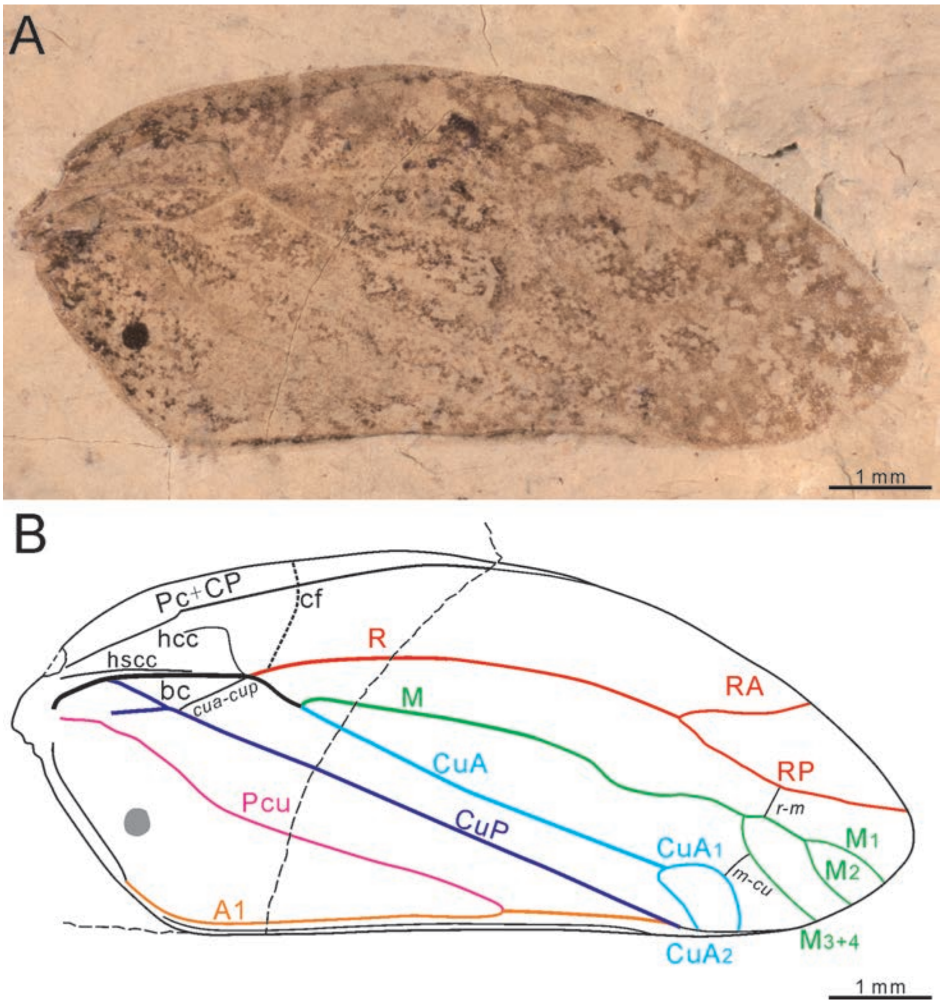

Figure 1. *Mesoscytina tongchuanensis* Q. Zhang, Du & H. Zhang, sp. nov., holotype (NIGP205761), tegmen **A** photograph **B** reconstruction and venation (granules ignored).

M_{3+4} and CuA_1 smoothly connected at crossvein *m-cu*. Clavus developed and convex, veins Pcu and A1 forming a "Y" fork; color patterns small and irregular.

Description. ***Tegmen*** convex with clavus attached, punctate more distinct on basal tegmen surface. Tegmen length 8.9 mm, maximum width 3.75 mm, length/width ratio 2.37. Tegmen apex asymmetric, gradually narrowed posteriorly. Costa anterior strongly arched, posterior margin more or less straight; tegmen broadest near middle part. Vein Pc+CP curved and merged into anterior margin at basal 3/5 tegmen length. Costal area widest near basal cell; postcostal area much wider than costal area. Hypocostal carina sigmoid, merged into stem R+M+CuA, hyposubcostal carina straight, close to stem R+M+CuA gradually; costal fracture curved apically, originating from stem R, stretched cross vein Pc+CP vertically. Basal cell closed, nearly triangle in shape. Vein R slightly curved, first forked into veins RA and RP at apical 1/4 of tegmen length; vein RA shorter than vein RP in length; vein RP curved posteriorly. Stem M+CuA strong and short, bifurcated first near basal 1/3 of tegmen length. Vein M curved anteriorly first, extending straight on middle membrane, then strongly bent towards vein CuA before reaching level of stem R forking. Vein M first forked into veins M_{1+2} and M_{3+4} at apical 1/5 tegmen length; veins M_1, M_2 and M_{3+4} single; crossvein *r-m* connected veins RP and M_{1+2}; crossvein *m-cu* connected to evenly curved

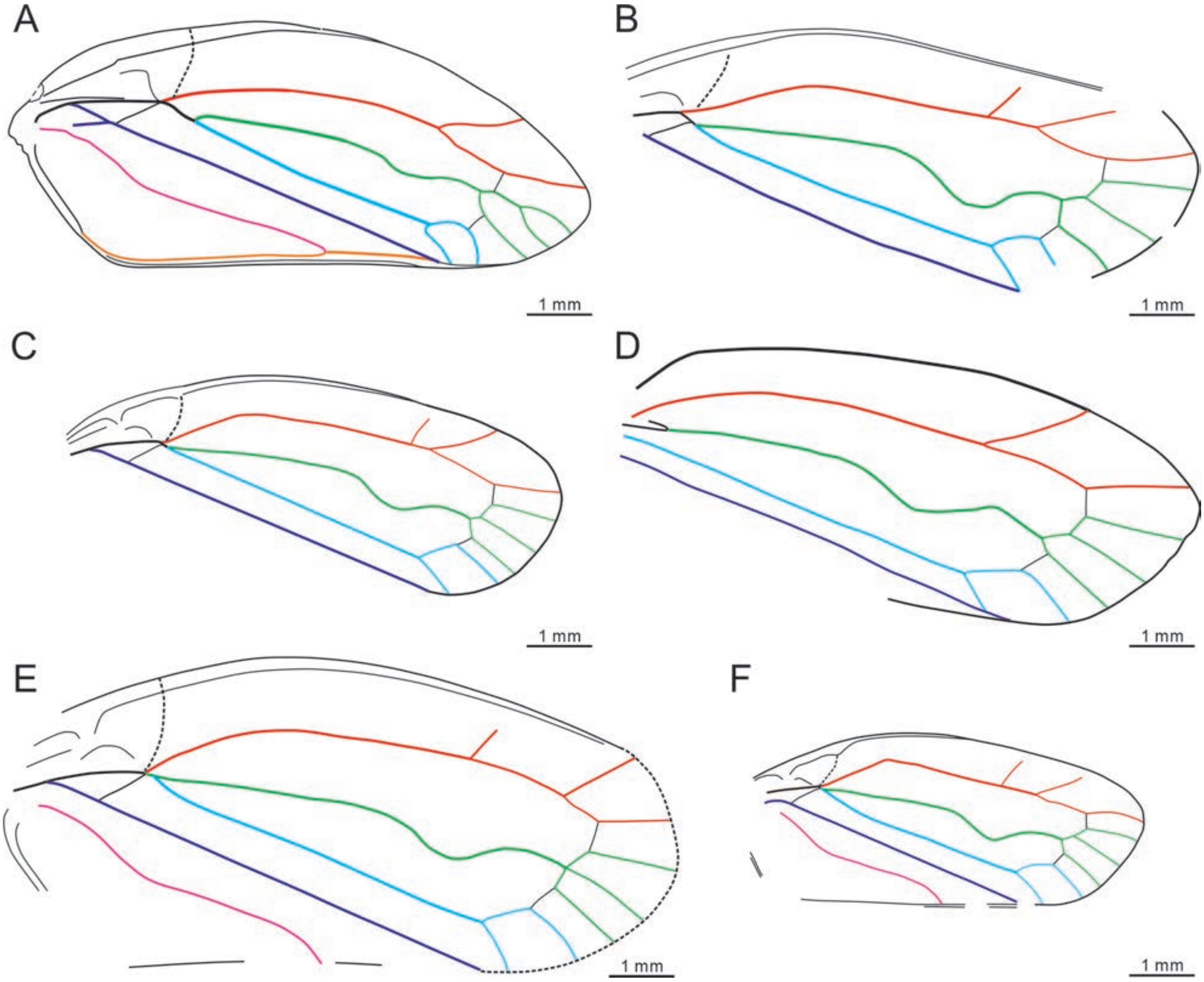

Figure 2. Comparison of tegminal venation in *Mesoscytina* Tillyard, 1919 **A** *M*. *tongchuanensis* Q. Zhang, Du & H. Zhang, sp. nov. **B** *M*. *australis* Tillyard, 1919 **C** *M*. *fistulae* Lambkin, 2016 **D** *M*. *forsterae* (Martins-Neto & Gallego) Lara et al. 2021 **E** *M*. *magna* Lambkin, 2016 **F** *M*. *woodsi* Lambkin, 2016.

M_{3+4} and CuA_1. Vein CuA single and straight, extending in direction of stem M+CuA; vein CuA divided into veinlets CuA_1 and CuA_2 near same level of vein R fork; vein CuA_1 curved strongly towards posterior margin, vein CuA_2 shorter than vein CuA_1, merely just extending beyond clavus apex. Vein CuP single, slightly curved basally before leaving basal cell, then extending straight towards clavus apex after connecting with long crossvein *cua-cup*. Clavus large and convex, with anal angle about 120°; vein Pcu single, curved posteriorly, forming a "Y" fork with vein A1. Vein A2 close to A1, parallel with postclaval margin and merged before end level of vein CuP. Small, irregular, dark-colored patterns shown on tegmen.

Discussion

According to the key to genera of Scytinopteridae proposed by Zhang et al. (2022), the new species is placed within the genus *Mesoscytina* Tillyard, 1919 by the punctate tegmen, curved vein M, apically forked vein R and three terminal branches of vein M.

So far, there are only five species of *Mesoscytina* Tillyard, 1919 (*M. australis* Tillyard, 1919, *M. fistulae* Lambkin, 2016; *M. forsterae* (Martins-Neto & Gallego, 2003) Lara et al. 2021; *M. magna* Lambkin, 2016 and *M. woodsi* Lambkin, 2016) reported from the Triassic at Mount Crosby, Denmark Hill, Gayndah and Dinmore (Queensland, NE Australia) (Tillyard 1919; Lambkin 2016) and of Tongchuan (Shaanxi, NW China). The notable differences between *Mesoscytina tongchuanensis* Q. Zhang, Du et H. Zhang, sp. nov. and its congeners lie in a lower length/width ratio (at least 2.6 in its congeners), a much longer length of stem M_{1+2}, apical terminals of RP, M and CuA less parallel, crossvein *r-m* connected to vein M_{1+2} and the apical shape of the tegmen.

Specifically, the new species (Fig. 2A) roughly differentiates from *M. australis* Tillyard, 1919 (Fig. 2B) by a wider but shorter costal area, a narrower apex and less developed R branches. It can also be easily distinguished from *M. fistulae* (Fig. 2C) by the more curved branches of veins M and CuA; from *M. forsterae* (Fig. 2D) in the presence of a larger basal cell, and crossvein *r-m* connected to vein M_{1+2} (to M_1 in *M. forsterae*); from *M. magna* (Fig. 2E) by the shorter tegmen, the less developed areola postica (wider than medial area cells in *M. magna*), three M branches that forked twice (forked into three branches at the same level in *M. magna*); and from *M. woodsi* (Fig. 2F) in having a larger tegmen with base of vein R slightly curved (angulate at base in *M. woodsi*).

Conclusion

As the first record of *Mesoscytina* from the Middle Triassic Tongchuan Entomofauna in China, *M. tongchuanensis* Q. Zhang, Du & H. Zhang, sp. nov. is unique by its lateral narrowed apex, less curved terminal branches of stems RP, M and CuA and crossvein *r-m* connected to vein M_{1+2}. Its establishment not only extends the palaeogeographical record of *Mesoscytina* Tillyard, 1919 from Gondwana to northern Pangea supercontinents of the Northern Hemisphere in the Middle Triassic (Ladinian) but provides the most complete tegminal venation information (especially the clavus) in this genus to date.

Additional information

Conflict of interest

The authors have declared that no competing interests exist.

Ethical statement

No ethical statement was reported.

Funding

This research is supported by the National Natural Science Foundation of China (42293280), the Fundamental Research Funds for the Liaoning Universities and the Shenyang Normal University (BS202209).

Author contributions

Funding acquisition: QZ, HZ. Investigation: XZ. Software: XD. Writing - original draft: QZ. Writing - review and editing: HZ, XD.

Author ORCIDs

Qianqi Zhang https://orcid.org/0000-0001-9354-4610
Xuheng Du https://orcid.org/0000-0002-3476-5074
Xiuping Zhu https://orcid.org/0009-0001-3200-5864
Haichun Zhang https://orcid.org/0000-0003-4553-8317

Data availability

All of the data that support the findings of this study are available in the main text.

References

Hamilton KGA (1992) Lower Cretaceous Homoptera from the Koonwarra Fossil Bed in Australia, with a New Superfamily and Synopsis of Mesozoic Homoptera. Annals of the Entomological Society of America 85(4): 423–430. https://doi.org/10.1093/aesa/85.4.423

Handlirsch A (1906) Die Fossilen Insekten und die Phylogenie der Rezenten Formen, parts I-IV. Ein Handbuch für Paläontologen und Zoologen. Verlag von Wilhelm Engelmann, Leipzig, 640 pp.

Lambkin KJ (2016) Revision of the Scytinopteridae (Hemiptera: Cicadomorpha: Scytinopteroidea) of the Queensland Triassic. Zootaxa 4117: 580–590. https://doi.org/10.11646/zootaxa.4117.4.9

Lara MB, Bustos-Escalona EL, Mancuso AC, Arcucci A (2021) Upper Triassic hemipterans from the south-western Gondwana: taxonomical, paleobiological, and paleogeographical implications. Journal of South American Earth Sciences 107(103119). https://doi.org/10.1016/j.jsames.2020.103119

Lin QB (1986) Early Mesozoic fossil insects from South China. Palaeontologica Sinica (n. s.) Series B, 21. Science Press, Beijing, 112 pp. [in Chinese with English abstract]

Martins-Neto RG, Gallego OF, Melchor RN (2003) The Triassic insect fauna from South America (Argentina, Brazil and Chile): a checklist (except Blattoptera and Coleoptera) and descriptions of new taxa. Acta Zoologica Cracoviensia 46(suppl.– Fossil Insects): 229–256.

Shcherbakov DE (1984) Systematics and phylogeny of Permian Cicadomorpha (Cimicida and Cicadina). Paleontological Journal 1984(2): 87–97.

Shcherbakov DE (1996) Origin and evolution of the Auchenorrhyncha as shown by the fossil record. In: Schaefer CW (Ed.) Studies on Hemipteran Phylogeny. Entomological Society of America, Lanham, Maryland, 31–45. https://doi.org/10.4182/AMYC5234.1996.31

Shcherbakov DE (2022) A peculiar new genus of Scytinopteridae (Hemiptera, Cicadomorpha) from the Permian-Triassic boundary beds of Mongolia. Palaeoentomology 5(3): 218–221. https://doi.org/10.11646/palaeoentomology.5.3.2

Tillyard RJ (1919) Mesozoic insects of Queensland. No. 7. Hemiptera Homoptera; with a note on the phylogeny of the Suborder. Proceedings of the Linnean Society of New South Wales 44: 857–896.

Zhang QQ, Zheng DR, Teng X, Zhang HC (2022) New Scytinopteridae (Hemiptera: Scytinopteroidea) from the middle Triassic Tongchuan Entomofauna of NW China. Historical Biology 34(11): 2259–2264. https://doi.org/10.1080/08912963.2021.2010194

Zheng DR, Chang S-C, Wang H, Fang Y, Wang J, Feng CQ, Xie GW, Jarzembowski EA, Zhang HC, Wang B (2018) Middle-Late Triassic insect radiation revealed by diverse fossils and isotopic ages from China. Science Advances 4: eaat1380. https://doi.org/10.1126/sciadv.aat1380

ZooKeys 1219: 105–122 (2024)
DOI: 10.3897/zookeys.1219.121027

Research Article

A new species of the genus *Leptobrachella* (Amphibia, Anura, Megophryidae) from Dayaoshan National Nature Reserve, Guangxi, China

Gui-Dong Yu[1], Kun Qin[2,3], Tao Meng[1], Peng Li[4], Wan-Xiao Peng[4], Wei-Cai Chen[4,5]

1 *Guangxi Forest Inventory and Planning Institute, Nanning 530001, China*
2 *Guangxi Dayaoshan Forest Ecosystem Research Station, Jinxiu 545700, China*
3 *Laibin Jinxiu Dayaoshan Forest Ecosystem Observation and Research Station of Guangxi, Jinxiu 545700, China*
4 *Key Laboratory of Environment Change and Resources Use in Beibu Gulf Ministry of Education, Nanning Normal University, Nanning 530001, China*
5 *Guangxi Key Laboratory of Earth Surface Processes and Intelligent Simulation, Nanning Normal University, Nanning 530001, China*
Corresponding authors: Wei-Cai Chen (chenweicai2003@126.com); Tao Meng (gxmengtao@163.com)

Academic editor: Angelica Crottini
Received: 16 February 2024
Accepted: 16 October 2024
Published: 27 November 2024

ZooBank: https://zoobank.org/BC0D5160-30A3-4F4F-8C2A-467690E85E3C

Citation: Yu G-D, Qin K, Meng T, Li P, Peng W-X, Chen W-C (2024) A new species of the genus *Leptobrachella* (Amphibia, Anura, Megophryidae) from Dayaoshan National Nature Reserve, Guangxi, China. ZooKeys 1219: 105–122. https://doi.org/10.3897/zookeys.1219.121027

Abstract

A new species of the Asian leaf litter toad genus *Leptobrachella*, *L. dayaoshanensis* **sp. nov.**, is described based on phylogenetic analysis, morphological characters, and bioacoustic data. This species occurs in the Dayaoshan National Nature Reserve located in Jinxiu County, Guangxi, China. Phylogenetic analysis indicates that this new species is closely related to *L. verrucosa*, as demonstrated by phylogenetic trees. The new species can be distinguished from its congeners by a combination of the following characters: (1) medium size (mean snout–vent length (SVL) of 27.9 ± 0.7 mm, range 26.6–28.9 mm in males; 34.4 mm in female); (2) rough dorsal surface featuring small, raised tubercles and ridges; (3) flanks adorned with irregular black spots and creamy white glands; (4) creamy white ventral surface with sparse light-brown spots and irregular tiny textures; (5) brown throat and chest; (6) rudimentary toe webbing; (7) wide lateral fringes on toes; (8) distinct continuous ventrolateral glandular line; (9) tibiotarsal articulation reaching the midpoint of eye when the leg is extended forward; (10) heels that do not meet when thighs are appressed at right angles to body; (11) bicolored iris, with the upper half being copper and gradually transitioning to silver in the lower half; and (12) advertisement calls consisting of two model types, with dominant frequencies of 4.2–6.8 kHz at 21.0 °C. The new species has a breeding season that occurs from March to April and is found in evergreen forests at elevations between 1,000 and 1,600 m.

Key words: Bioacoustics, cryptic diversity, morphology, phylogeny, taxonomy

---

Introduction

Leptobrachella liui (Fei & Ye, 1990) is known to have a wide distribution in eastern and southern China (AmphibiaChina 2024; Frost 2024). In 1931, Pope collected 13 specimens from Chong’an (now Wuyishan City), Fujian, China, and initially classified them as *Megophrys pelodytoides*. Later, they were transferred to the genus *Leptolalax* Dubois, 1980, and then to *Leptobrachella* Smith, 1925 (Chen et al. 2018). However, Pope (1931) also noted that the Fujian specimens differed from the holotype (Boulenger 1893; Smith 1930), mainly in the number of law teeth of tadpoles (4 lines vs 5–6 lines). In 1950, Liu (1950) examined the Fujian specimens collected by Pope and argued that they belonged to an unknown species in the genus *Megophrys* (Liu 1950; Fei et al. 1992). In 1990, Fei et al. (1990) classified the Fujian specimens as a new species, *Leptobrachella liui*, and subsequently redescribed them (Fei et al. 1992). They also assigned specimens from Dayaoshan and Longsheng, Guangxi, Leishan, Guizhou, Yizhang, Hunan, and Zhejiang provinces to *L. liui*, despite some morphologic variations. Later reports indicated that *L. liui* was widely distributed in Fujian, Zhejiang, Jiangxi, Hunan, Guangdong, and Guangxi provinces (Fei et al. 2012; Mo et al. 2014; Shen 2014; Fei and Ye 2016; Chen et al. 2018). Based on molecular data, Chen et al. (2018) initially discovered that specimens of *L. liui* from various geographic populations can be categorized into three distinct lineages, forming the *L. liui* species complex. The first lineage, found in the Mangshan Nature Reserve, Yizhang County, Hunan, China, was identified as *L. mangshanensis*, representing the first cryptic species (Chen et al. 2018; Hou et al. 2018). The second lineage, discovered in the Dawuling Forest Station, Maoming City, Guangdong, China, was named *L. yunkaiensis*, corresponding to the second cryptic species (Chen et al. 2018; Wang et al. 2018). The third lineage was identified as *L. liui*, representing the sensu stricto *L. liui*. Interestingly, within the second lineage, a specific sequence (GenBank no. EF544238) from Dayaoshan, Jinxiu County, Guangxi, China, exhibited a significantly shorter evolutionary branch and a relatively larger genetic divergence compared to *L. yunkaiensis*, indicating the presence of an unknown species within *Leptobrachella*. Recently, we collected 16 specimens from Dayaoshan, Jinxiu County, Guangxi. Through thorough examination of morphology, phylogeny, and bioacoustics, we observed distinct differences between these specimens, previously classified as *L. liui*, and both the sensu stricto *L. liui* from the type locality and *L. yunkaiensis*. Therefore, we propose the classification of these specimens as a new species within the genus *Leptobrachella*.

Material and methods

Sampling

Sixteen specimens were collected from Dayaoshan (**DYS**), Jinxiu County, Guangxi, China (Fig. 1). All specimens were initially fixed in 10% formalin for 48 h and subsequently transferred to 75% ethanol for permanent storage at Nanning Normal University (**NNU**). Prior to fixation, muscle tissues were extracted and stored in 100% ethanol for molecular analysis.

Morphometrics and morphological comparisons

All specimens were measured following the methodology described in Rowley et al. (2016). Measurements were taken using a digital caliper with an accuracy of 0.1 mm. The following morphological characters were measured: snout–vent length (**SVL**), head length (**HL**) from the tip of the snout to the rear of the jaws, head width (**HW**) at the commissure of the jaws, snout length (**SNT**) from the tip of the snout to the anterior eye corner, diameter of the exposed portion of the eyeball (**ED**), interorbital distance (**IOD**), which is the shortest distance

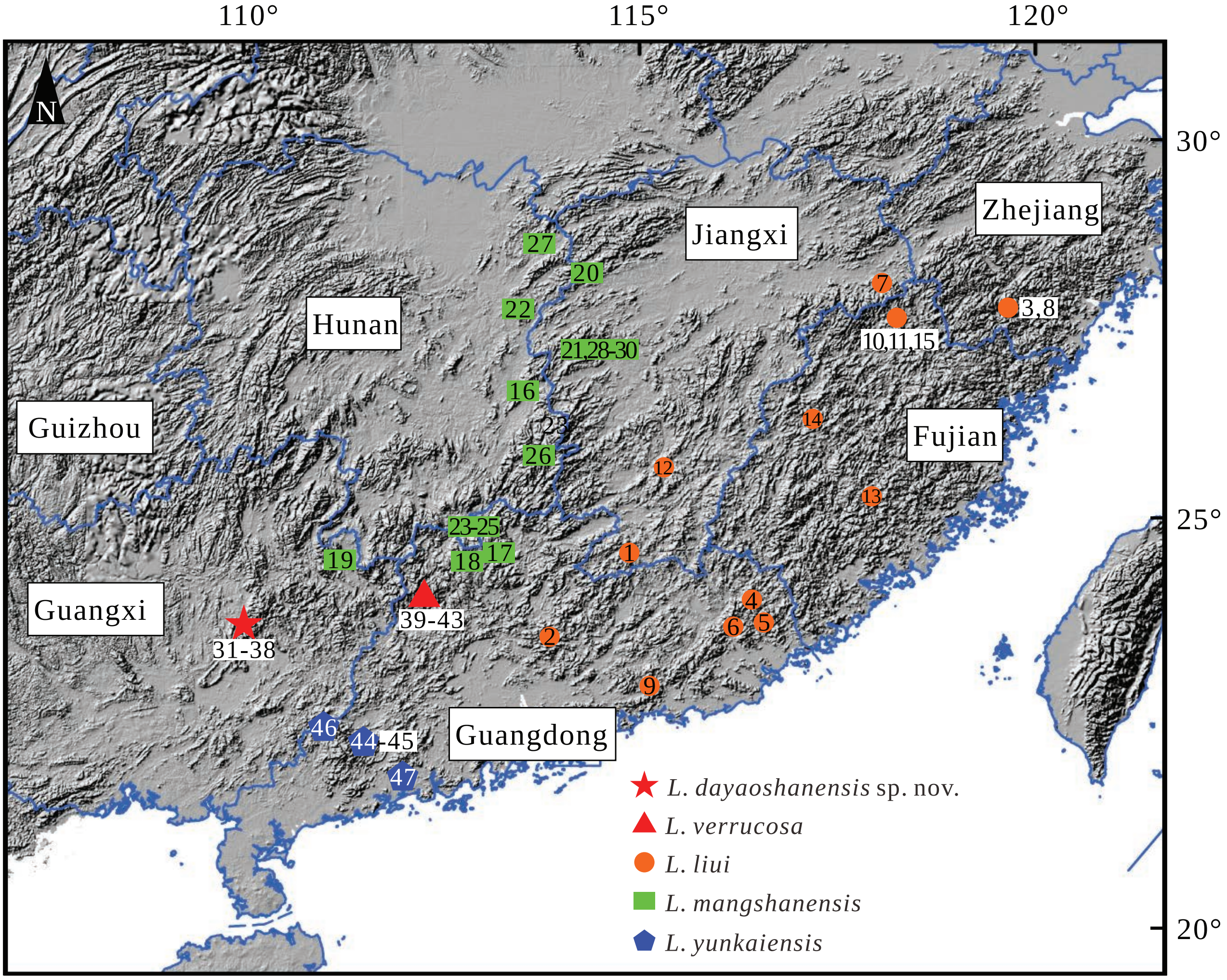

Figure 1. Localities of the new species and its sister taxa.

between the anterior corners of the orbits, horizontal diameter of the tympanum (**TD**), distance from the anterior edge of the tympanum to the posterior eye corner (**TED**), internarial space distance (**IN**), tibia length (**TIB**) with flexed hindlimb, forelimb length (**FLL**) from the elbow to the tip of the third finger, length of the foot and tarsus (**TFL**) from the tibiotarsal articulation to the distal end of toe IV, manus length (**ML**) from the tip of the third digit to the proximal edge of the inner palmar tubercle, hindlimb length (**HLL**) from the tip of the fourth toe to the vent, and the distance from the proximal edge of the femoral gland to the knee (**FG-knee**). Gender was determined through direct observation of calls in life or the presence of internal vocal sac openings.

Comparative morphological data were obtained from the references (Suppl. material 2: table S1) and museum specimens (Suppl. material 2: table S2). For morphological comparisons, we used 15 adult males from the new specimens to compare with their closely related species, including *Leptobrachella liui* (type locality, male, *n* = 6), *L. mangshanensis* (type locality, male, *n* = 6), and *L. verrucosa* (holotype and paratypes, male, *n* = 5), based on the results of phylogenetic analyses. We performed Principal Component Analyses (PCA) and the Mann-Whitney *U* test using SPSS v. 20. Before analysis, the measurements were transformed as follows: we calculated the ratio of each morphometric character (except SVL itself) to SVL, and then log-transformed them for morphometric analyses.

Molecular analyses

Genomic DNA was isolated from muscle tissue using tissue extraction kits (Tiangen Biotech Co. Ltd., Beijing, China). Mitochondrial fragments of the 16S gene were amplified and sequenced using the primers: 16Sar_L, 5'–CGCCTGTTTACCAAAAA CAT–3'; 16Sbr_H, 5'–CCGGTCTGAACTCAGATCACGT–3') (Palumbi et al. 1991). Polymerase chain reaction (PCR) amplification was performed as described by Chen et al. (2021). The fragments were sequenced on an automated DNA sequencer (ABI Prism 3730, Applied Biosystems, USA). The newly obtained sequences were deposited in GenBank (accession numbers: PQ476281–PQ476287). Phylogenetic relationships were reconstructed using maximum-likelihood (ML) and Bayesian-inference (BI) analyses. The sequence information used in the molecular analysis is provided in Table 1. The best-fit nucleotide substitution models (GTR+F+I) were selected using ModelFinder v. 2.2.0 (Kalyaanamoorthy et al. 2017; Zhang et al. 2020) based on the Bayesian information criterion (BIC). ML analyses were performed in IQ-tree v. 2.2.2 (Nguyen et al. 2015) with 2000 ultrafast bootstrap replicates. BI was conducted using MrBayes v. 3.2 (Ronquist et al. 2012). Two independent runs with four Markov Chain Monte Carlo simulations were performed for 30 million iterations, and trees were sampled every 1,000th generation. The first 25% of trees were discarded as burn-in. Uncorrected pairwise distances were calculated using Mega v. 7 with the default settings (Kumar et al. 2016).

Table 1. DNA sequences used in this study. '*' represents type locality. '#' means the sequences named *Leptobrachella liui* from Chen et al. (2018).

ID	Species	Locality	Voucher no.	16S	Note#
1	*L. liui*	Jiulian Shan, Jiangxi, China	SYS a002105	MH055911	*L. liui*
2	*L. liui*	Nankunshan Nature Reserve, Guangdong, China	SYS a004497	MH055924	*L. liui*
3	*L. liui*	Dongkeng Town, Jingning County, Zhejiang, China	SYSa002732	MH605575	*L. liui*
4	*L. liui*	Tongguzhang, Guangdong, China	SYS a004733	MH055912	*L. liui*
5	*L. liui*	Jiaoshuikeng, Guangdong, China	SYS a003698	MH055913	*L. liui*
6	*L. liui*	BaiTang, Guangdong, China	KIZ018349	MH055914	*L. liui*
7	*L. liui*	Tongba Shan, Jiangxi, China	SYS a001702	KM014548	*L. liui*
8	*L. liui*	Dongkeng, Zhejiang, China	SYS a002733	MH055909	*L. liui*
9	*L. liui*	Gutian Nature Reserve, Guangdong, China	SYS a002650	MH055910	*L. liui*
10	*L. liui*	Wuyishan, Fujian, China *	SYS a001597	KM014547	*L. liui*
11	*L. liui*	Wuyishan, Fujian, China *	SYS a002478	MH605573	*L. liui*
12	*L. liui*	Huanggangshan, Jiangxi, China	SYS a001620	KM014549	*L. liui*
13	*L. liui*	Daiyunshan, Fujian, China	SYS a001736	KM014550	*L. liui*
14	*L. liui*	Longqishan, Fujian, China	SYS a002506	MH055907	*L. liui*
15	*L. liui*	Wuyishan, Fujian, China *	ZYCA907	MH055908	*L. liui*
16	*L. mangshanensis*	Longzha, Hunan, China	SYS a002539	MH055918	*L. liui*
17	*L. mangshanensis*	Tianjingshan National Forest Park, Guangdong, China	SYS a002805	MH055921	*L. liui*
18	*L. mangshanensis*	Nanling National Forest Park, Guangdong, China	SYS a002829	MH055920	*L. liui*
19	*L. mangshanensis*	Dadong Shan, Guangxi, China	SYS a002848	MH055922	*L. liui*
20	*L. mangshanensis*	Wugongshan, Jiangxi, China	SYS a004035	MH055916	*L. liui*
21	*L. mangshanensis*	Jinggangshan, Jiangxi, China	SYS a004051	MH055917	*L. liui*
22	*L. mangshanensis*	Yunyangshan, Hunnan, China	SYS a002540	MH055923	*L. liui*
23	*L. mangshanensis*	Mangshan, Hunan, China*	MSZTC201701	MG132196	*L. liui*
24	*L. mangshanensis*	Mangshan, Hunan, China*	MSZTC201702	MG132197	*L. liui*
25	*L. mangshanensis*	Mangshan, Hunan, China*	MSZTC201703	MG132198	*L. liui*

ID	Species	Locality	Voucher no.	16S	Note#
26	*L. mangshanensis*	Guidong, Hunan, China	SYS a002521	MH055919	*L. liui*
27	*L. mangshanensis*	Yangxi, Jiangxi, China	SYS a002578	MH055915	*L. liui*
28	*L. mangshanensis*	Mt. Jinggang, Jiangxi, China	SYSa004044	MH406906	*L. liui*
29	*L. mangshanensis*	Mt. Jinggang, Jiangxi, China	SYSa004045	MH406907	*L. liui*
30	*L. mangshanensis*	Mt. Jinggang, Jiangxi, China	SYSa004052	MH406908	*L. liui*
31	*L. dayaoshanensis* sp. nov.	Dayaoshan, Jinxiu County, Guangxi, China*	ZYC A100	EF544238	*L. liui*
32	*L. dayaoshanensis* sp. nov.	Dayaoshan, Jinxiu County, Guangxi, China*	NNU202103018	PQ476281	
33	*L. dayaoshanensis* sp. nov.	Dayaoshan, Jinxiu County, Guangxi, China*	NNU202103019	PQ476282	
34	*L. dayaoshanensis* sp. nov.	Dayaoshan, Jinxiu County, Guangxi, China*	NNU202103021	PQ476283	
35	*L. dayaoshanensis* sp. nov.	Dayaoshan, Jinxiu County, Guangxi, China*	NNU202103022	PQ476284	
36	*L. dayaoshanensis* sp. nov.	Dayaoshan, Jinxiu County, Guangxi, China*	NNU202103027	PQ476285	
37	*L. dayaoshanensis* sp. nov.	Dayaoshan, Jinxiu County, Guangxi, China*	NNU202103028	PQ476286	
38	*L. dayaoshanensis* sp. nov.	Dayaoshan, Jinxiu County, Guangxi, China*	NNU202103032	PQ476287	
39	*L. verrucosa*	Lianshan Bijiashan Nature Reserve, Guangdong, China	GEP a059	OP279589	
40	*L. verrucosa*	Lianshan Bijiashan Nature Reserve, Guangdong, China	GEP a060	OP279590	
41	*L. verrucosa*	Lianshan Bijiashan Nature Reserve, Guangdong, China	GEP a061	OP279591	
42	*L. verrucosa*	Lianshan Bijiashan Nature Reserve, Guangdong, China	GEP a062	OP279592	
43	*L. verrucosa*	Lianshan Bijiashan Nature Reserve, Guangdong, China	GEP a063	OP279593	
44	*L. yunkaiensis*	Dawushan, Guangdong, China*	SYS a004666	MH055933	*L. liui*
45	*L. yunkaiensis*	Dawushan, Guangdong, China*	SYS a004663	MH605584	
46	*L. yunkaiensis*	Lidong, Guangxi, China	KIZ018211	MH055931	*L. liui*
47	*L. yunkaiensis*	Ehuangzhang Nature Reserve, Guangdong, China	KIZ047782	MH055932	*L. liui*
48	*L. aerea*	Quang Binh, Vietnam	ZFMK 86362	JN848409	
49	*L. alpina*	Caiyanghe, Yunnan, China	KIZ049024	MH055867	
50	*L. applebyi*	Phong Dien Nature Reserve, Thua Thien-Hue, Vietnam	KIZ010701	MH055947	
51	*L. arayai*	Borneo, Malaysia*	AE100/S9	DQ642119	
52	*L. ardens*	Kon Ka Kinh National Park, Gia Lai, Vietnam*	ZMMU-NAP-06099	MH055949	
53	*L. aspera*	Huanglianshan Nature Reserve, Lyuchun, Yunnan, China*	SYS a007743	MW046199	
54	*L. baluensis*	Sabah, Borneo, Malaysia*	SP 21604	LC056792	
55	*L. bashaensis*	Basha Nature Reserve, Guizhou, China*	GIB196404	MW136295	
56	*L. bidoupensis*	Bidoup-Nui Ba National Park, Lam Dong, Vietnam*	ZMMU-A-4797-01454	MH055945	
57	*L. bijie*	Bijie City, Guizhou, China*	SYS a007313	MK414532	
58	*L. botsfordi*	Lao Cai, Vietnam*	AMS R 176540	MH055952	
59	*L. bourreti*	Mao'ershan, Guangxi, China	KIZ019389	MH055869	
60	*L. brevicrus*	Sarawak, Borneo, Malaysia*	ZMH A09365	KJ831302	
61	*L. chishuiensis*	Guizhou, China*	CIBCS20190518047	MT117053	
62	*L. crocea*	Thua Thien-Hue, Vietnam	ZMMU-NAP-02274	MH055955	
63	*L. damingshanensis*	Wuming County, Guangxi, China*	NNU202103281	MZ145229	
64	*L. dong*	Tongdao County, Hunan, China*	CIB SSC1757	OP764530	
65	*L. dorsospina*	Yushe Forest Park, Shuicheng, Guizhou, China*	SYS a004961	MW046194	
66	*L. dringi*	Borneo, Malaysia*	KUHE:55610	AB847553	
67	*L. eos*	Phongsaly, Laos*	MNHN 2004.0274	JN848452	
68	*L. feii*	Yunnan, China*	KIZ048894	MT302634	
69	*L. firthi*	Kon Tum, Vietnam*	AMS: R 176524	JQ739206	
70	*L. flaviglandulosa*	Xiaoqiaogou Nature Reserve, Yunnan, China*	KIZ016072	MH055934	
71	*L. fritinniens*	Danum Valley Field Center, Sabah, Malaysia	FMNH 244800	MH055971	
72	*L. fuliginosa*	Phetchaburi, Thailand	KUHE:20197	LC201988	
73	*L. gracilis*	Bukit Kana, Sarawak, Malaysia	FMNH 273682	MH055972	
74	*L. guinanensis*	Shangsi County, Guangxi, China*	NNU00557	OP548561	
75	*L. hamidi*	Borneo, Malaysia*	KUHE 17545	AB969286	
76	*L. heteropus*	Peninsular, Malaysia	KUHE 15487	AB530453	
77	*L. isos*	Gia Lai, Vietnam*	AMS R 176480	KT824769	
78	*L. itiokai*	Gunung Mulu National Park, Sarawak, Malaysia*	KUHE:55897	LC137805	
79	*L. jinshaensis*	Lengshuihe Nature Reserve, Jinsha County, Guizhou, China*	CIBJS20200516001	MT814014	
80	*L. jinyunensis*	Mt. Jinyun, Beibei District, Chongqing, China*	CIB 119039	OQ024778	

ID	Species	Locality	Voucher no.	16S	Note[#]
81	*L. juliandringi*	Sarawak, Borneo, Malaysia*	KUHE 17557	LC056784	
82	*L. kajangensis*	Tioman, Malaysia*	LSUHC:4439	LC202002	
83	*L. kalonensis*	Binh Thuan, Vietnam*	IEBR A.2014.15	KR018114	
84	*L. kecil*	Cameron, Malaysia *	KUHE:52439	LC202003	
85	*L. khasiorum*	Meghalaya, India*	SDBDU 2009.329	KY022303	
86	*L. korifi*	Doi Inthanon, Thailand*	KUHE 19134	LC741033	
87	*L. laui*	Wutongshan, Shenzhen city, China*	SYS a001507	KM014544	
88	*L. macrops*	Dak Lak, Vietnam*	AMS R177663	KR018118	
89	*L. maculosa*	Ninh Thuan, Vietnam*	AMS: R 177660	KR018119	
90	*L. maoershanensis*	Mao'er Shan, Guangxi, China	KIZ07614	MH055927	
91	*L. marmorata*	Borneo, Malaysia*	KUHE 53227	AB969289	
92	*L. maura*	Borneo, Malaysia	SP 21450	AB847559	
93	*L. melanoleuca*	Kapoe, Ranong, Thailand	KIZ018031	MH055967	
94	*L. melica*	Ratanakiri, Cambodia*	MVZ 258198	HM133600	
95	*L. minima*	Doi Phu Fa, Nan, Thailand	KIZ024317	MH055852	
96	*L. mjobergi*	Sarawak, Borneo, Malaysia*	KUHE 47872	LC056787	
97	*L. nahangensis*	Tuyen Quang, Vietnam*	ROM 7035	MH055853	
98	*L. namdongensis*	Thanh Hoa, Vietnam*	VNUF A.2017.95	MK965390	
99	*L. neangi*	Veal Veng District, Pursat, Cambodia*	CBC 1609	MT644612	
100	*L. niveimontis*	Yongde County, Yunnan, China *	KIZ028276	MT302620	
101	*L. nyx*	Ha GiangProv., Vietnam*	AMNH A 163810	DQ283381	
102	*L. oshanensis*	Emei Shan, Sichuan, China*	Tissue ID: YPX37492	MH055896	
103	*L. pallida*	Lam Dong, Vietnam*	UNS00510	KR018112	
104	*L. parva*	Mulu National Park, Sarawak, Malaysia*	KUHE:55308	LC056791	
105	*L. pelodytoides*	NA	TZ819	AF285192	
106	*L. petrops*	Ba Vi National Park, Ha Tay, Vietnam	ROM 13483	MH055901	
107	*L. phiadenensis*	Phia Oac-Phia Den NP, Cao Bang Prov., Vietnam*	IEBR A.5205	OR405872	
108	*L. phiaoacensis*	Phia Oac-Phia Den NP, Cao Bang Prov., Vietnam*	IEBR A. 5195	OR405871	
109	*L. picta*	Borneo, Malaysia	UNIMAS 8705	KJ831295	
110	*L. pluvialis*	Lao Cai, Vietnam*	MNHN:1999.5675	JN848391	
111	*L. puhoatensis*	Nghe An, Vietnam*	VNMN 2016 A.22	KY849586	
112	*L. purpurus*	Yunnan, China *	SYSa006530	MG520354	
113	*L. purpuraventra*	Guizhou, China *	SYSa007281	MK414517	
114	*L. pyrrhops*	Loc Bac, Lam Dong, Vietnam*	ZMMU-A-4873-00158	MH055950	
115	*L. rowleyae*	Da Nang City, Vietnam*	ITBCZ2783	MG682552	
116	*L. sabahmontanus*	Borneo, Malaysia*	BORNEENSIS 12632	AB847551	
117	*L. shangsiensis*	Shangsi County, China*	NHMG1401032	MK095460	
118	*L. shimentaina*	Shimentai Nature Reserve, Guangdong, China*	SYS a004712	MH055926	
119	*L. shiwandashanensis*	Shangsi, Guangxi, China*	NNU202103261	MZ326695	
120	*L. sinorensis*	Mae Hong Son, Thailand*	KUHE 19816	LC741036	
121	*L. sola*	Gunung Stong, Kelantan, Malaysia	KU RMB20973	MH055973	
122	*L. suiyangensis*	Guizhou, China *	GZNU20180606005	MK829649	
123	*L. sungi*	Vinh Phuc, Vietnam *	ROM 20236	MH055858	
124	*L. tadungensis*	Dak Nong, Vietnam*	UNS00515	KR018121	
125	*L. tengchongensis*	Yunnan, China *	SYSa004598	KU589209	
126	*L. tuberosa*	Kon Ka Kinh National Park, Gia Lai, Vietnam*	ZMMU-NAP-02275	MH055959	
127	*L. ventripunctata*	Zhushihe, Yunnan, China *	SYSa004536	MH055831	
128	*L. wuhuangmontis*	Pubei County, Guangxi, China *	SYS a003486	MH605578	
129	*L. wulingensis*	Hunan, China *	CSUFT194	MT530316	
130	*L. wumingensis*	Wuming County, Guangxi, China*	NNU 01058	OR194551	
131	*L. yeae*	Mount Emei, Sichuan, China *	CIBEMS20190422HLJ1-6	MT957019	
132	*L. yingjiangensis*	Yunnan, China *	SYSa006532	MG520351	
133	*L. yunkaiensis*	Yunyang County, Chongqing, China *	GZNU20210622001	OL800364	
134	*L. zhangyapingi*	Chiang Mai, Thailand *	KIZ07258	MH055864	
135	*Xenophrys major*	Kon Tum Province, Vietnam	AMS R173870	KY476333	
136	*Leptobrachium chapaense*	Lao Cai Province, Vietnam	AMS R 171623	KR018126	

Bioacoustics analyses

Advertisement calls were recorded using a SONY PCM-A10 recorder at a distance of approximately 0.5 m. Four individuals were recorded in the field, and ambient temperatures were measured immediately after the recordings using a Deli LE505 hand-held weather meter. The call recordings were analyzed using the software Raven Pro v. 1.6 (Cornell Laboratory of Ornithology, Ithaca, NY, USA), following the method described by Köhler et al. (2017). Audio-spectrograms were generated by applying a fast-Fourier transform to 512 points with a 50% overlap and a grid-spacing of 172 Hz, using Hanning windows.

Results

Morphology

The Mann-Whitney *U* test revealed that the DYS specimens differed significantly from *Leptobrachella liui*, *L. mangshanensis*, and *L. verrucosa* (Table 2) in terms of various morphological characters, such as SVL, HL, HW, SNT, TD, IN, TIB, FLL, ML, and HLL. This finding was further supported by the results of the PCA analysis, which demonstrated that the DYS specimens were distinct from *L. liui*, *L. mangshanensis*, and *L. verrucosa* (Fig. 2). In terms of morphology, the DYS specimens exhibited differences compared to *L. liui* in body size, ventral surface textures, and dermal ridges of toes. Additionally, they differed from *L. mangshanensis* in dorsal surface, lateral fringes of toes, and iris color, and from *L. verrucosa* in lateral fringes of toes, relative finger lengths, and ventrolateral glandular line. For more detailed comparisons, please refer to the "Comparisons" section.

Table 2. Measurements and morphometric comparisons between *Leptobrachella dayaoshanensis* sp. nov., *L. liui*, *L. mangshanensis*, and *L. verrucosa*. "*" stands for *p*-value < 0.05.

	***L. dayaoshanensis* sp. nov.**			***p*-value from Mann-Whitney *U* test**		
	Males (*n* = 15) Ranges (mm)	**Mean ± SD (mm)**	**Female (*n* = 1)**	**New species vs *L. liui***	**New species vs *L. mangshanensis***	**New species vs *L. verrucosa***
SVL	26.6–28.9	27.9 ± 0.7	34.4	0.000*	0.000*	0.001*
HL	7.8–9.1	8.4 ± 0.3	9.8	0.000*	0.000*	0.001*
HW	9.1–9.9	9.5 ± 0.2	10.9	0.000*	0.000*	0.001*
SNT	3.3–4.1	3.7 ± 0.2	4.1	0.001*	0.001*	0.026*
ED	3.0–4.0	3.5 ± 0.3	4.1	0.020*	0.020*	0.010*
IOD	2.6–3.3	2.9 ± 0.2	3.1	1.000	1.000	0.965
TD	1.3–1.8	1.5 ± 0.1	2.0	0.000*	0.000*	0.002*
TED	0.9–1.4	1.1 ± 0.1	1.4	0.010*	0.010*	0.032*
IN	2.4–2.9	2.6 ± 0.1	2.8	0.000*	0.000*	0.001*
TIB	11.7–13.7	12.9 ± 0.5	15.0	0.001*	0.001*	0.005*
FLL	11.4–13.1	12.4 ± 0.5	13.5	0.000*	0.000*	0.001*
TFL	16.8–19.4	17.8 ± 0.6	20.6	0.003*	0.001*	unknown
ML	6.0–6.9	6.6 ± 0.3	7.1	0.000*	0.000*	0.001*
HLL	36.7–41.2	38.9 ± 1.0	46.2	0.000*	0.000*	0.001*
FG-knee	4.1–5.6	5.0 ± 0.4	5.9	0.000*	0.001*	unknown

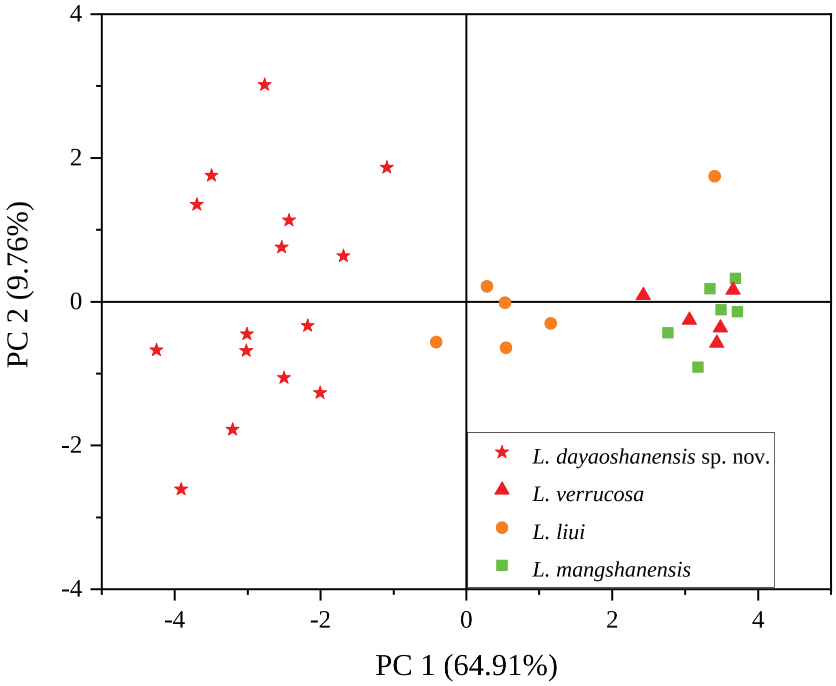

Figure 2. Scatter plot of PC1 and PC2 of PCA based on the morphometric measurements, separating *Leptobrachella dayaoshanensis* sp. nov., *L. liui*, *L. mangshanensis*, and *L. verrucosa*.

Phylogenetic analyses and genetic divergence

About 530 base pairs were included in the matrix of 136 sequences based on the 16S gene. The phylogenetic relationships within *Leptobrachella* remain unresolved in the 16S gene trees. Both ML and BI analyses resulted in similar topological trees (Fig. 3). The phylogenetic trees suggest that the DYS specimens form a monophyletic group and are genetically closest to *L. verrucosa*. Additionally, *L. liui* and *L. mangshanensis* are monophyletic to each other. The genetic divergences between the DYS specimens and *L. verrucosa* range from 2.3% to 2.8%, while for *L. liui* it ranges from 2.6% to 4.1%, and for *L. mangshanensis* it ranges from 2.1% to 2.8% (Suppl. material 2: table S3).

Bioacoustics

The ambient temperature was recorded at approximately 21.0 °C. The calls of DYS specimens consist of two types: Type A and Type B, as illustrated in Fig. 4. Type A calls have durations ranging from 68 to 88 ms (mean ± SD: 78.1 ± 4.4 ms, n = 58) and intervals of 110 to 170 ms (134.6 ± 13.7 ms, n = 58), with dominant frequencies between 4.2 and 6.8 kHz. In contrast, Type B calls have durations ranging from 261 to 361 ms (298.5 ± 25.4 ms, n = 14) and dominant frequencies also ranging from 4.5 to 6.8 kHz (Fig. 4). These call characters, including durations, intervals, number of notes per call, and dominant frequencies, differentiate the calls of DYS specimens from those of *L. liui* (Ding et al. 2019). Moreover, the calls of DYS specimens also exhibit differences from those of other known species within the *Leptobrachella* genus (Suppl. material 2: table S4). Based on the results of phylogenetic analysis, morphology, and bioacoustics, the DYS specimens are described as a new species within the genus *Leptobrachella*.

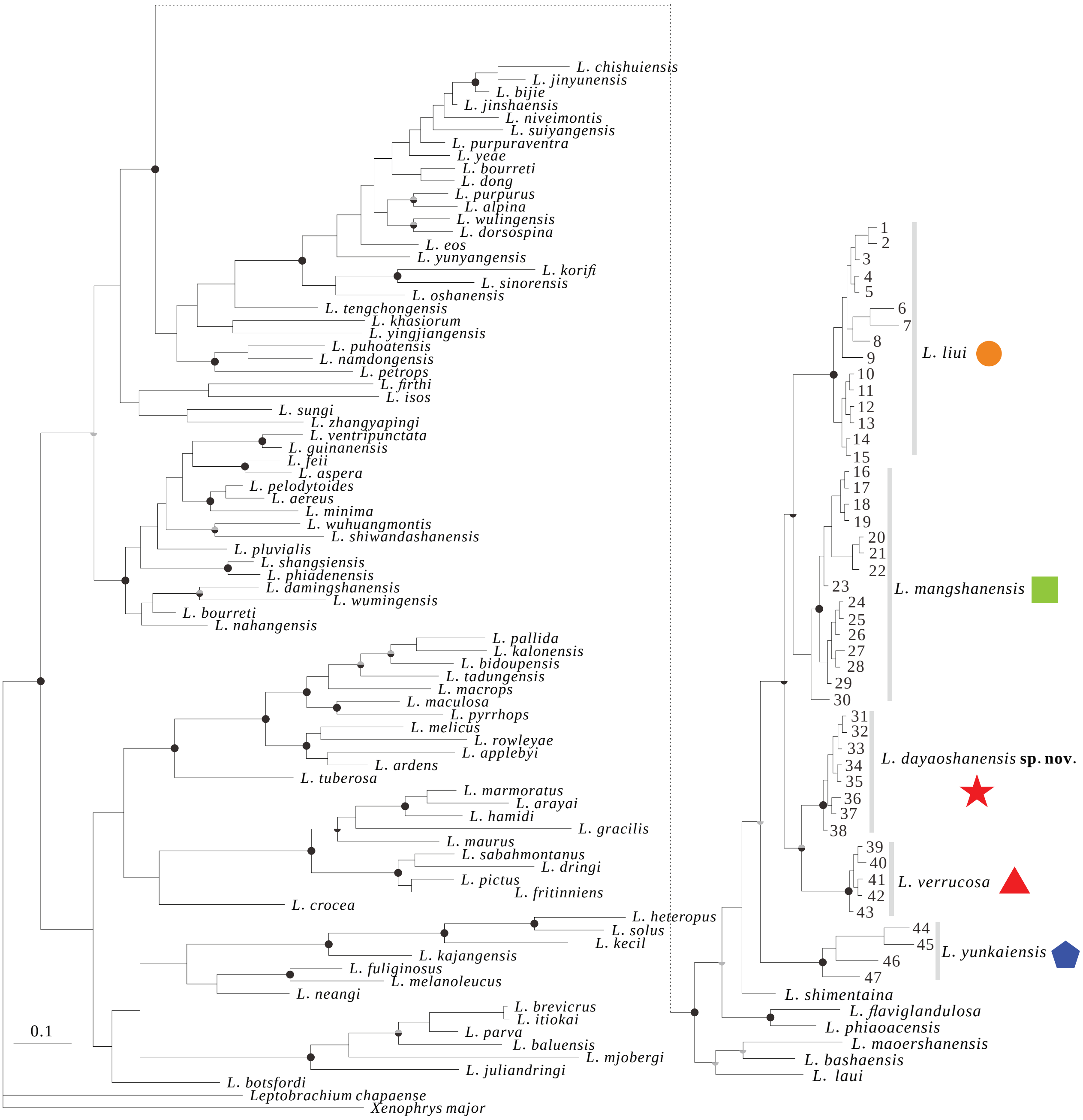

Figure 3. BI trees based on 16S fragments with Bayesian posterior probabilities/bootstrap supports on branches. Bayesian posterior probabilities, upper half, >0.95 = grey, 1 = black; bootstrap supports, lower half, >70%<90% = grey, >90% = black).

Taxonomic account

***Leptobrachella dayaoshanensis* Chen, Yu, Meng & Qin, sp. nov.**
https://zoobank.org/FB15638D-4519-4DDA-A95A-007DAEDCEBB7
Fig. 5A–E

Leptolalax liui Fei & Ye, 1990 (Chresonymy): Fei et al. 1992; Fei et al. 2012; Mo et al. 2014.

Type material. ***Holotype*** • NNU 20210318, adult male, collected at the Dayaoshan National Nature Reserve (DYS), Jinxiu County, Guangxi, China (24.153°N,

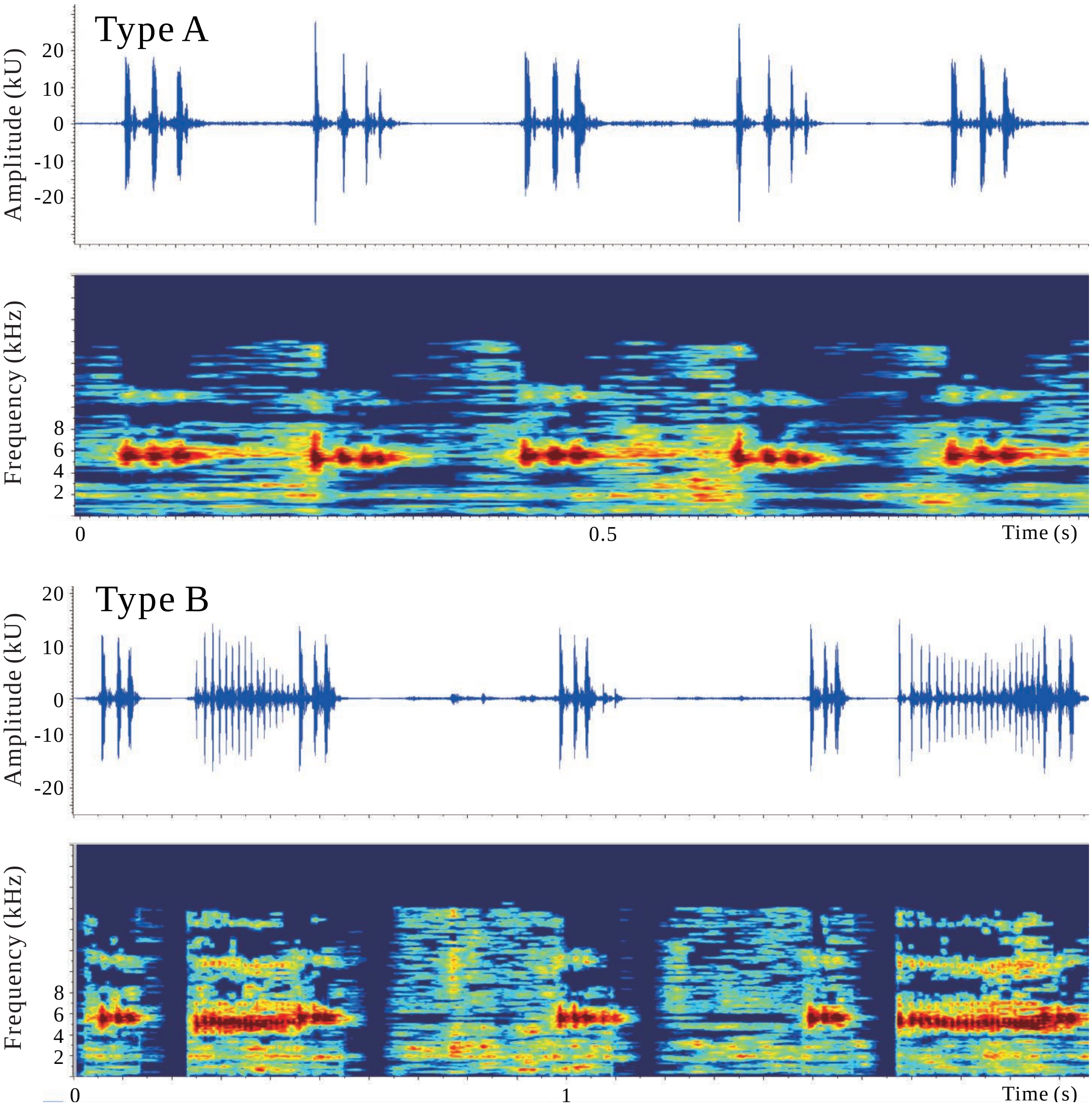

Figure 4. Advertisement call spectrograms of *Leptobrachella dayaoshanensis* sp. nov.

110.213°E; elevation 1132 m), collected by Wei-Cai Chen on 12 March 2021. ***Paratypes*** • NNU 20210319–26, NNU 20210328–33, 14 adult males, and NNU 20210327, one adult female, collected at the same locality as holotype on 12 March 2021 by Wei-Cai Chen.

Etymology. The species name *dayaoshanensis* refers to the type locality, Mount Dayaoshan. The suggested English name is Dayaoshan Leaf Litter Toad, and the Chinese name is Da Yao Shan Zhang Tu Chan (大瑶山掌突蟾).

Diagnosis. *Leptobrachella dayaoshanensis* sp. nov. can be distinguished from its congeners by a combination of the following characters: (1) medium size (SVL mean 27.9 ± 0.7 mm, range 26.6–28.9 mm in males; 34.4 mm in female); (2) dorsal surface rough with small, raised tubercles and ridges; (3) flanks with irregular black spots and creamy-white glands; (4) ventral surface creamy-white with sparse, light-brown spots and irregular, tiny textures; (5) brown throat and chest; (6) rudimentary toe webbing; (7) wide toes lateral fringes; (8) distinct continued ventrolateral glandular line; (9) tibiotarsal articulation reaching the midpoint of eye when the leg is pressed forward; (10) heels not meeting when thighs are appressed at right angles to body; (11) bicolored iris, with upper half copper, gradually transitioning to silver in lower half; and (12) advertisement calls consisting of two types models, with dominant frequencies of 4.2–6.8 kHz (21.0 °C).

Description of holotype. Adult male, head width larger than length (HW/HL = 1.08); snout protruding, projecting over the lower jaw; nostril oval, closer to tip of snout than eye; canthus rostralis rounded; loreal region sloping; interorbital area flat; pupil vertical; eye diameter less snout length (ED/SNT = 0.75); internarial distance less than interorbital distance (IN/IOD = 0.77); tympanum distinct, rounded and concave, significantly less than eye diameter, TD/ED = 0.43; distinct and raised supratympanic fold from the corner of eye to supra-axillary gland; vomerine teeth absent; tongue with a shallow notch at the posterior tip (Fig. 5A–F).

Tips of fingers slightly swollen; relative finger lengths I < II < IV < III; nuptial pad absent; subarticular tubercles absent; prominent inner palmar tubercle and very small outer palmar tubercle; finger webbing and dermal fringes absent. Tips of toes rounded, slightly swollen but less than toe width; relative toe lengths I < II < V < III < IV; subarticular tubercles absent, instead by consecutive dermal ridges; large and elongated inner metatarsal tubercle; outer metatarsal tubercle absent; toe webbing rudimentary; toes lateral fringes well-developed, half of phalange in width; TIB/SVL = 0.42; tibia–tarsal articulation reaching the medium of eye when the leg is pressed forward; heels not meeting when thighs are appressed at right angles to body.

Dorsal surface rough with small, raised tubercles and ridges; ventral surface smooth without tubercles; pectoral glands oval and creamy white, ~1.2 mm in diameter; femoral glands oval, ~1.3 mm in diameter, closer to knee than to vent; supra-axillary glands distinct and rounded, ~1.0 mm in diameter; continued ventrolateral glandular line distinct; limbs surface without tubercles (Fig. 5A–F).

Color of holotype in life. Dorsum saffron yellow with distinct brown markings, a brown triangle between eyes, a brown “W” marking on shoulder, and a brown “Λ” marking on lower back; tympanum pale brown; supratympanic line brown from posterior corner of eye to supra-axillary glands; brown bars on upper lip wide; flanks with irregular black spots and creamy yellow glands; three transverse, dark-brown bars distinct on dorsal surface of hindlimbs; elbows, upper arms and tibiotarsal surfaces light tangerine; ventral surface creamy white, with sparse, light-brown spots and irregular, tiny textures; throat and chest brown; pectoral and femoral glands creamy white, supra-axillary glands light tangerine; pupil black; iris bicolored, upper half copper, gradually transitioning to silver in lower half (Fig. 5A–F).

Color of holotype in preservative. Dorsum and limbs surfaces faded to uniform grey; brown triangular marking distinctly visible between eyes; irregular black spots on flanks distinct; throat, chest grey, and belly creamy white; pectoral, femoral, supra-axillary, and ventrolateral glands creamy white; dark bars on limbs, fingers, and toes distinct; elbow pale orange; upper arm and tibiotarsus faded to grey.

Variation. Measurements of the type series are presented in Table 2. The presence of tubercles or ridges on the dorsum varies, as do the irregular markings (Suppl. material 1: fig. S1). Certain specimens exhibit a lighter mustard

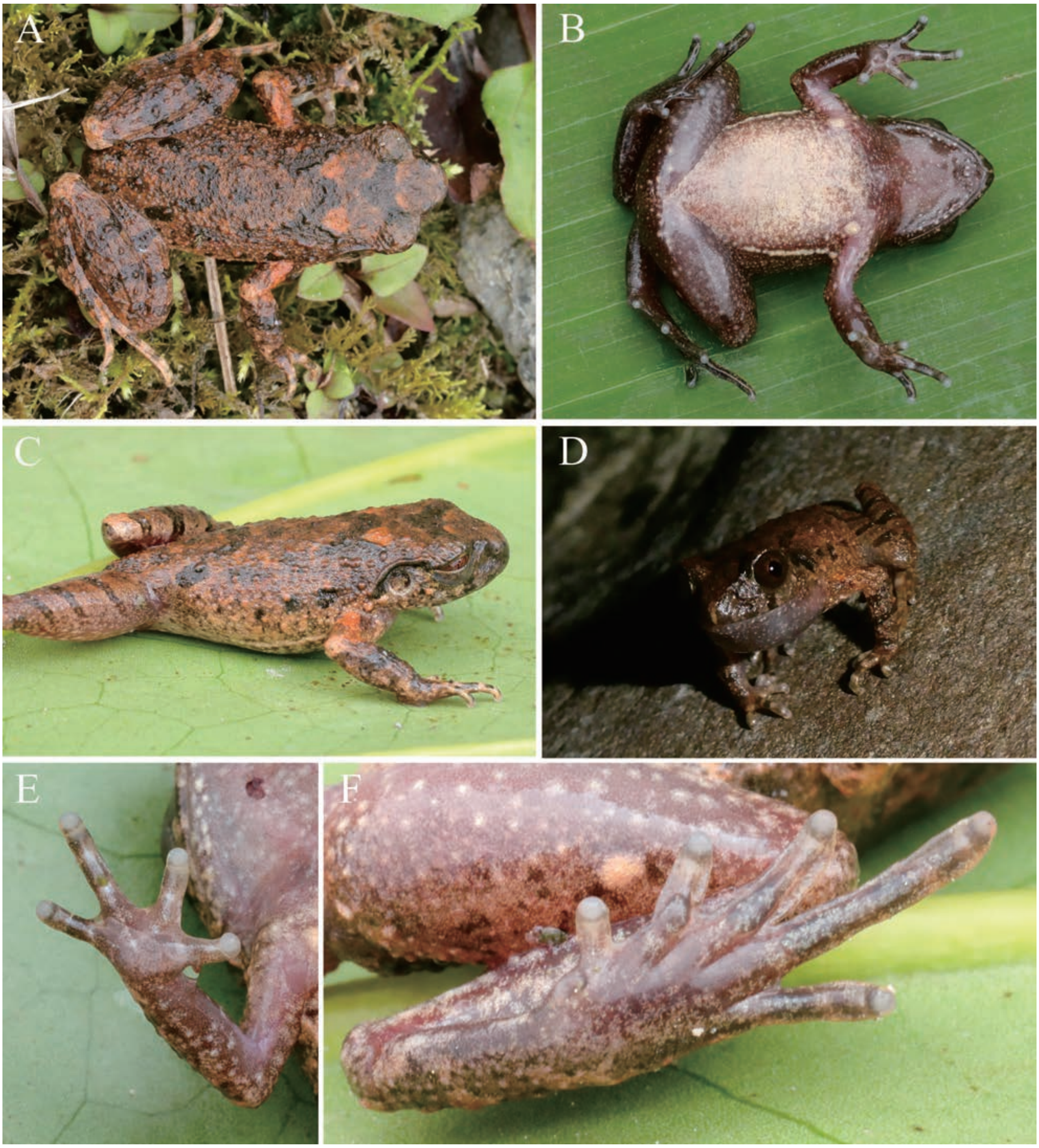

Figure 5. The holotype of *Leptobrachella dayaoshanensis* sp. nov. **A** dorsal view **B** ventral view **C** dorsolateral view **D** calling in the field **E** ventral view of hand **F** ventral view of foot.

color. Additionally, the margin of the throat displays creamy-white tubercles in some individuals (Suppl. material 1: fig. S2).

Measurements of holotype (in mm). SVL 27.6, HL 8.6, HW 9.3, SNT 4.0, ED 3.0, IOD 3.1, TD 1.3, TED 1.2, IN 2.4, TIB 11.7, FLL 12.2, THL 17.8, ML 6.7, HLL 39.4, FG-knee 4.7.

Ecology and distribution. *Leptobrachella dayaoshanensis* sp. nov. was discovered in the evergreen forest at Mount Dayaoshan, at elevations between 1,000 and 1,600 m. Our observations revealed that adult males of this species were found calling near rocky streams between 19:00 and 24:00 h during our survey. Interestingly, there were also instances where advertisement calls could be heard during the daytime. We noted that the advertisement calls were audible from early March until the end of April. Presently, *L. dayaoshanensis* sp. nov. is only found within the Dayaoshan National Nature Reserve.

Comparisons. *Leptobrachella dayaoshanensis* sp. nov. can be distinguished from other *Leptobrachella* species by its body size (males: SVL 26.6–28.9 mm; female: 34.4 mm); small, raised tubercles and ridges on dorsum; presence of irregular black spots on flanks; creamy-yellow ventral surface with sparse, light-brown spots and irregular textures; rudimentary toe webbing; wide lateral fringes; tongue with a shallow notch; brown throat and chest; distinct continued ventrolateral glandular line; tibiotarsal articulation reaching the midpoint of eye; heels not meeting when thighs are appressed at right angles to body; and bicolored iris, with the upper half being copper, gradually transitioning to silver in the lower half. Furthermore, the species can be identified by its unique advertisement calls (Fig. 4, Suppl. material 2: table S4).

Phylogenetically, *L. dayaoshanensis* sp. nov. is closely related to *L. liui*, *L. mangshanensis*, and *L. verrucosa* (Fig. 3). Morphologically, *L. dayaoshanensis* sp. nov. differs from *L. liui* in having a relatively larger body size in female (SVL 34.4 mm vs SVL 23.1–28.1 mm); HL/HW = 0.92 (vs HL/HW = 1.01); ventral surface creamy yellow, with sparse, light-brown spots and irregular textures, brown throat and chest with scattered, light, creamy spots (vs chest and margins creamy white with dark-brown spots); heels not meeting when thighs are appressed at right angles to body (vs overlapped); consecutive dermal ridges under toes (vs discrete dermal ridges); different call durations (68–88 ms vs 26–78 ms) and dominant frequencies (4.2–6.8 kHz vs 4.8–5.5 kHz). *Leptobrachella dayaoshanensis* sp. nov. differs from *L. mangshanensis* in having a rough dorsal surface with small, raised tubercles and ridges (vs dorsal skin smooth with small orange tubercles and irregular, dark-brown stripes); wide toe lateral fringes (vs narrow toe lateral fringes); distinct longitudinal ridges under toes (vs indistinct longitudinal ridges under toes); tibiotarsal articulation reaching the medium of eye (vs tibiotarsal articulation reaching anterior margin of snout); brown throat and chest, and creamy-white belly with sparse, light-brown spots and irregular, tiny textures (vs greyish-white throat and belly with little white speckles); bicolored iris, upper half copper, gradually transitioning to silver in lower half (vs bright-orange upper, greyish cream below). *Leptobrachella dayaoshanensis* sp. nov. differs from *L. verrucosa* in having relatively larger body size in males (SVL 26.6–28.9 mm vs SVL 23.2–25.9 mm); head width larger than length (HW/HL = 1.08) (vs head length slightly larger than head width, HW/HL = 0.95); eye diameter less snout length (SNT/ED = 1.33) (vs SNT/ED = 1.03); tongue with a shallow notch at the posterior tip (vs tongue deeply notched distally); tibiatarsal articulation reaching the medium of eye when the leg is pressed forward (vs tibiotarsal articulation reaches to anterior corner of eye); rough dorsal surface with small, raised tubercles and ridges (vs shagreened dorsal surface with numerous conical tubercles, lacking spines, enlarged warts, or skin ridges); brown supratympanic line (vs black supratympanic line); wide toe lateral fringes (vs narrow toe lateral fringes); brown throat and chest (vs creamy white); relative finger lengths I < II < IV < III (vs I = II = IV < III); bicolored iris, upper half copper, gradually transitioning to silver in lower half (vs upper half coppery orange, lower half greyish brown); distinct continued ventrolateral glandular line (vs discrete ventrolateral gland line). Furthermore, *L. dayaoshanensis* sp. nov. is found at elevations over 1,000 m, whereas *L. verrucosa* inhabits elevations of 500–600 m. The advertisement calls of the new species can be heard from early March to the end of April, while the breeding season of *L. verrucosa* lasts from April to June according to Lin et al. (2022).

Leptobrachella dayaoshanensis sp. nov. differs from *L. shimentaina* and *L. yunkaiensis* in lacking lateral fringes on fingers (vs presence of lateral fringes on fingers), heels not meeting when thighs are appressed at right angles to body (vs overlapped); from *L. flaviglandulosa* in having heels not meeting when adpressed (vs overlapped), consecutive dermal ridges under toes (vs discrete dermal ridges); from *L. bashaensis* in having relatively larger body size (SVL 26.6–28.9 mm in males, 34.4 mm in female vs SVL 22.9–25.6 mm in males, 27.1 mm in female); wide toe lateral fringes (vs narrow toe lateral fringes); from *L. maoershanensis* in having wide toe lateral fringes (vs narrow toe lateral fringes), distinct consecutive dermal ridges under toes (vs indistinct longitudinal ridges under toes); from *L. laui* in lacking finger lateral fringes (vs presence of moderate lateral fringes), creamy-yellow ventral surface with sparse, light-brown spots and irregular textures, brown throat and chest with scattered, light-creamy spots (vs near immaculate creamy-white chest and belly); from *L. phiaoacensis* in having wide toe lateral fringes (vs narrow toe lateral fringes), heels not meeting when thighs are appressed at right angles to body (vs overlapped), continued ventrolateral glandular line (vs discrete ventrolateral gland line), brown throat and chest (vs creamy white).

In having supra-axillary and ventrolateral glands, *L. dayaoshanensis* sp. nov. differs from its congeners from South of the Isthmus of Kra, *L. arayai*, *L. dringi*, *L. fritinniens*, *L. gracilis*, *L. hamidi*, *L. heteropus*, *L. kajangensis*, *L. kecil*, *L. marmorata*, *L. maura*, *L. melanoleuca*, *L. picta*, *L. platycephala*, *L. sabahmontana*, and *L. sola* (vs absent in the latter species). In having a relatively larger body size (SVL 26.6–28.9 mm in males, 34.4 mm in females), *L. dayaoshanensis* sp. nov. differs from *L. baluensis* (SVL 14.9–15.9 mm in males), *L. bondangensis* (SVL 17.8 mm in male), *L. brevicrus* (SVL 17.1–17.8 mm in males), *L. fusca* (SVL 16.3 mm in male), *L. itiokai* (SVL 15.2–16.7 mm in males), *L. juliandringi* (SVL 17.0–17.2 mm in males), *L. mjobergi* (SVL 15.7–19.0 mm in males), *L. natunae* (SVL 17.6 mm in male), *L. palmata* (SVL 14.4–16.8 mm in males), *L. parva* (SVL 15.0–16.9 mm in males), and *L. serasanae* (SVL 16.9 mm in female).

For the remaining known *Leptobrachella* species from north of the Isthmus of Kra, in having SVL 26.6–28.9 mm in males, *L. dayaoshanensis* sp. nov. differs from the smaller *L. applebyi* (19.6–22.3 mm), *L. ardens* (21.3–24.7 mm), *L. bidoupensis* (18.5–25.4 mm), *L. melica* (19.5–22.7 mm), *L. niveimontis* (22.5–23.6 mm), *L. pluvialis* (21.3–22.3 mm), *L. rowleyae* (23.4–25.4 mm); from the larger *L. dushanensis* (31.9–32.9 mm), *L. nahangensis* (40.8 mm), *L. sungi* (48.3–52.7 mm), and *L. zhangyapingi* (45.8–52.5 mm).

Furthermore, in having wide lateral fringes on toes, *L. dayaoshanensis* sp. nov. differs from *L. applebyi*, *L. ardens*, *L. crocea*, *L. kalonensis*, *L. lateralis*, *L. macrops*, *L. maculosa*, *L. melica*, *L. nahangensis*, *L. namdongensis*, *L. neangi*, *L. nyx*, *L. oshanensis*, *L. pallida*, *L. pluvialis*, *L. pyrrhops*, *L. rowleyae*, *L. shiwandashanensis*, *L. tadungensis*, *L. tuberosa* and *L. ventripunctatus* (vs absent lateral fringes on toes). In having black spots on flanks, *L. dayaoshanensis* sp. nov. differs from *L. aerea*, *L. botsfordi*, *L. crocea*, *L. eos*, *L. firthi*, *L. graminicola*, *L. isos*, *L. pallida*, *L. petrops* and *L. tuberosa* (vs absent).

Leptobrachella dayaoshanensis sp. nov. differs from its congeners in the dominant frequency of 4.2–6.8 kHz (21.0 °C) (Suppl. material 2: table S4).

Discussion

Preprimary phylogenetic trees revealed that sequences named *Leptobrachella liui* downloaded from GenBank (Chen et al. 2018; Frost 2024) did not form a monophyletic group but could be divided into four lineages. Among these lineages, the DYS specimens form a monophyletic group closely related to *L. verrucosa*. Despite the close phylogenetic relationship, the DYS specimens and *L. verrucosa* are distinct, as confirmed by PCA, Man-Whitney *U* test, and morphological characters (see comparison section). Therefore, the DYS specimens can be classified as a new species of *Leptobrachella*. Three sequences named *L. liui* from southwestern Guangdong were clustered with *L. yunkaiensis* (paratype) with well-supported values (Fig. 3). Due to their close geographical distance and low genetic divergence (Suppl. material 2: table S3), we assigned these three sequences to *L. yunkaiensis*. Sequences named *L. liui* but nested within *L. mangshanensis* were treated as *L. mangshanensis*, which are found in the borders between Hunan and Jiangxi, and between Guangxi, Guangdong, and Hunan (Fig. 1). The sensu stricto *L. liui* occurs in and around the type locality (Wuyishan, Fujian, China), as well as northern and eastern Guangdong (Fig. 1). Further field investigations are required to determine whether *L. liui* and *L. mangshanensis* have sympatric distributions.

Additionally, it should be noted that the taxonomy of the population of Leishan, Guizhou reported by Fei et al. (1992) has not been considered within the *L. liui* species complex. In recent years, several new species of *Leptobrachella* have been discovered in Guizhou (AmphibiaChina 2024). However, there is no evidence supporting the existence of *L. liui* in Guizhou. Therefore, we conclude that *L. liui* does not exist in Guizhou.

Acknowledgements

We express our gratitude to the staff of the Dayaoshan National Nature Reserve for their assistance during fieldwork. We also extend our thanks to Zhi-Tong Lyu for providing measurements of certain species. Finally, we would like to acknowledge the contributions of the two reviewers, Chung Hoang and Gang Wei, as well as the academic editor, Angelica Crottini, in enhancing the quality of this manuscript.

Additional information

Conflict of interest

The authors have declared that no competing interests exist.

Ethical statement

No ethical statement was reported.

Funding

This work was supported by the National Natural Science Foundation of China (grant numbers 32360128 and 32060116), Guangxi Natural Science Foundation, China (grant number 2020GXNSFDA238022), and Guangxi Forest Department (grant number 2014–22). Additionally, this research received support from the scientific research capacity building project for Laibin Jinxiu Dayaoshan Forest Ecosystem Observation and Research Station of Guangxi (grant number 22–035–130–01).

Author contributions

CWC conceived and designed the study and prepared the manuscript. YGD and CWC measured the specimens. CWC and LP performed the molecular experiments and analyzed the data. CWC, YGD, MT and QK conducted field surveys. PWX drew the figures. All authors read and approved the final version of the manuscript.

Author ORCIDs

Gui-Dong Yu https://orcid.org/0009-0008-1928-6594
Peng Li https://orcid.org/0000-0001-8311-0544
Wan-Xiao Peng https://orcid.org/0000-0001-5635-9061
Wei-Cai Chen https://orcid.org/0000-0002-2398-4079

Data availability

All of the data that support the findings of this study are available in the main text or Supplementary Information.

References

AmphibiaChina (2024) The database of Chinese amphibians. Kunming Institute of Zoology (CAS), Kunming, Yunnan, China. [Electronic Database accessible at:] http://www.amphibiachina.org/ [accessed 5 Feb. 2024]

Boulenger GA (1893) Concluding report on the reptiles and batrachians obtained in Burma by Signor L. Fea dealing with the collection made in Pegu and the Karin Hills in 1887–88. Annali del Museo Civico di Storia Naturale di Genova 13: 304–347.

Chen JM, Poyarkov Jr NJ, Suwannapoom C, Lathrop A, Wu YH, Zhou WW, Yuan ZY, Jin JQ, Chen HM, Liu HQ, Nguyen TQ, Nguyen SN, Duong TV, Eto K, Nishikawa K, Matsui M, Orlov NL, Stuart BL, Brown RM, Rowley JJL, Murphy RW, Wang YY, Che J (2018) Largescale phylogenetic analyses provide insights into unrecognized diversity and historical biogeography of Asian leaf-litter frogs, genus *Leptolalax* (Anura: Megophryidae). Molecular Phylogenetics and Evolution 124: 162–171. https://doi.org/10.1016/j.ympev.2018.02.020

Chen WC, Peng WX, Pan WH, Liao NY, Liu YJ, Huang Y (2021) A new species of *Leptobrachella* Smith 1925 (Anura: Megophryidae) from southern Guangxi, China. Zootaxa 5020: 581–596. https://doi.org/10.11646/zootaxa.5020.3.8

Ding GH, Chen ZQ, Tang Y, Lin ZH (2019) The advertisement call of *Leptobrachella liui* Fei and Ye, 1990 (Anura: Megophryidae). Zootaxa 4576(3): 588–590. https://doi.org/10.11646/zootaxa.4576.3.11

Dubois A (1980) Notes sur la systematique et la repartition des amphibiens anoures de Chine et des regions avoisinantes IV. Classification generique et subgenerique des Pelobatidae Megophryinae. Bulletin Mensuel de la Société Linnéenne de Lyon 49: 469–482. https://doi.org/10.3406/linly.1980.10444

Fei L, Ye CY (2016) Amphibians of China, Volume 1. Chengdu Institute of Biology, Chinese Academy of Sciences. Science Press, Beijing, 1040 pp.

Fei L, Ye CY, Huang YZ (1990) Key to Chinese Amphibians. Publishing House for Scientific and Technological Literature, Chongqing, 364 pp.

Fei L, Ye CY, Li SS (1992) Two new species of pelobatid toads of genus *Leptolalax* from Yunnan Province of China (Amphibia: Anura). Acta Biologica Plateau Sinica 11: 45–54.

Fei L, Ye CY, Jiang JP (2012) Colored atlas of Chinese Amphibians and their distributions. Sichuan Publishing House of Science and Technology, Chengdu, 619 pp.

Frost DR (2024) Amphibian Species of the World: an Online Reference. Version 6.1. American Museum of Natural History, New York. https://amphibiansoftheworld.amnh.org/index.php [Accessed 25 Jan. 2024]

Hou YM, Zhang MF, Hu F, Li SY, Shi SC, Chen J, Mo XY, Wang B (2018) A new species of the genus *Leptolalax* (Anura, Megophryidae) from Hunan, China. Zootaxa 4444(3): 247–266. https://doi.org/10.11646/zootaxa.4444.3.2

Kalyaanamoorthy S, Minh BQ, Wong TK, Von Haeseler A, Jermiin LS (2017) ModelFinder: fast model selection for accurate phylogenetic estimates. Nature Methods 14(6): 587–589. https://doi.org/10.1038/nmeth.4285

Köhler J, Jansen M, Rodríguez A, Kok PJR, Toledo LF, Emmrich M, Glaw F, Haddad CFB, Rödel MO, Vences M (2017) The use of bioacoustics in anuran taxonomy: Theory, terminology, methods and recommendations for best practice. Zootaxa 4251(1): 1–124. https://doi.org/10.11646/zootaxa.4251.1.1

Kumar S, Stecher G, Tamura K (2016) MEGA 7: Molecular Evolutionary Genetics Analysis Version 7.0 for Bigger Datasets. Molecular Biology and Evolution 33: 1870–1874. https://doi.org/10.1093/molbev/msw054

Lin SS, Li YH, Lu YH, Su HL, Wu SB, Zhang QQ, Mo MJ, Xiao SJ, Pan Z, Pan HJ, Zeng ZC (2022) A new species of the genus *Leptobrachella* (Anura, Megophryidae) from northwestern Guangdong Province, China. Herpetozoa 35: 165–178. https://doi.org/10.3897/herpetozoa.35.e89981

Liu CC (1950) Amphibians of western China. Fieldiana. Zoological Memoires 2: 1–397. https://doi.org/10.5962/bhl.part.4737

Mo YM, Wei ZY, Chen WC (2014) Colored Atlas of Guangxi Amphibians. Guangxi Science and Technology Publishing House, Nanning, 313 pp.

Nguyen LT, Schmidt HA, Von HA, Minh BQ (2015) IQ-TREE: A fast and effective stochastic algorithm for estimating maximum likelihood phylogenies. Molecular Biology and Evolution 32(1): 268–274. https://doi.org/10.1093/molbev/msu300

Palumbi SR, Martin R, Romano S, McMillan WO, Stice L, Grabowski G (1991) The Simple Fool's Guide To PCR, v2.0. Special publication of the University of Hawaii Department of Zoology and Kewalo Marine Laboratory.

Pope CH (1931) Notes on Amphibians from Fukien, Hainan, and other parts of China. Bulletin of the AMNH 61: 8.

Ronquist F, Teslenko M, Van Der Mark P, Ayres DL, Darling A, Höhna S, Larget B, Liu L, Suchard MA, Huelsenbeck JP (2012) Mrbayes 3.2: Efficient bayesian phylogenetic inference and model choice across a large model space. Systematic Biology 61(3): 539–542. https://doi.org/10.1093/sysbio/sys029

Rowley JJL, Tran DTA, Le DTT, Dau VQ, Peloso PLV, Nguyen TQ, Hoang HD, Nguyen TT, Ziegler T (2016) Five new, microendemic Asian Leaf-litter Frogs (*Leptolalax*) from the southern Annamite mountains, Vietnam. Zootaxa 4085(1): 63–102. https://doi.org/10.11646/zootaxa.4085.1.3

Shen YH (2014) Fauna Hunan: Amphibia. Hunan Science and Technology Press, Changsha, China.

Smith MA (1925) Contributions to the herpetology of Borneo. Sarawak Museum Journal 3: 15–34.

Smith MA (1930) The reptiles and amphibians of Malay Peninsula. Bulletin Raffles Museum 3: 1–149.

Wang J, Yang JH, Li Y, Lyu ZT, Zeng ZC, Liu ZY, Ye YH, Wang YY (2018) Morphology and molecular genetics reveal two new *Leptobrachella* species in southern China (Anura, Megophryidae). ZooKeys 776: 105–137. https://doi.org/10.3897/zookeys.776.22925

Zhang D, Gao F, Jakovlić I, Zou H, Zhang J, Li WX, Wang GT (2020) PhyloSuite: An integrated and scalable desktop platform for streamlined molecular sequence data management and evolutionary phylogenetics studies. Molecular Ecology Resources 20(1): 348–355. https://doi.org/10.1111/1755-0998.13096

Supplementary material 1

Supplementary figures

Authors: Gui-Dong Yu, Kun Qin, Tao Meng, Peng Li, Wan-Xiao Peng, Wei-Cai Chen

Data type: pdf

Explanation note: **figure S1.** Dorsal surface compared between holotype and some paratypes. **A** NNU 20210318, **B** NNU 20210322, **C** NNU 20210324, **D** NNU 20210325, **E** NNU 20210330, **F** NNU 20210327; **figure S2.** Ventral surface compared among some paratypes and ventral view of foot. **A** NNU 20210320, **B** NNU 20210322, **C** NNU 20210324, **D** NNU 20210327, **E** NNU 20210330, **F** NNU 20210332, **G** NNU 20210322, **H** NNU 20210325.

Link: https://doi.org/10.3897/zookeys.1219.121027.suppl1

Supplementary material 2

Supplementary tables

Authors: Gui-Dong Yu, Kun Qin, Tao Meng, Peng Li, Wan-Xiao Peng, Wei-Cai Chen

Data type: xlsx

Explanation note: **table S1:** References for morphological characters for congeners of the genus Leptobrachella; **table S2:** Comparative material examined; **table S3:** Uncorrected p-distance in Leptobrachella species based on 16S gene fragments; **table S4:** Dominant frequency of advertisement calls of species available in the genus Leptobrachella.

Link: https://doi.org/10.3897/zookeys.1219.121027.suppl2

ZooKeys 1219: 123–133 (2024)
DOI: 10.3897/zookeys.1219.137409

Research Article

An additional †Archearadinae flat-bug species from Cretaceous Burmese Amber (Hemiptera, Aradidae)

Royce T. Cumming[1,2,3], Julia J. Mlynarek[1]

1 *Montreal Insectarium, 4581 rue Sherbrooke est, Montréal, H1X 2B2, Québec, Canada*
2 *Richard Gilder Graduate School, American Museum of Natural History, New York, NY 10024, USA*
3 *Biology, Graduate Center, City University of New York, New York, USA*
Corresponding author: Royce T. Cumming (phylliidae.walkingleaf@gmail.com)

Abstract

Currently 19 species of Aradidae (flat bugs) are known from the Cretaceous deposits of Burma (Burmese/Kachin amber). In reviewing unidentified aradid species from this deposit, an unnamed species was located. This aradid includes a unique combination of features from several Cretaceous aradid genera coupled with apomorphic antennae morphology allows easy differentiation from other aradids. Therefore, a new genus and species is herein described as *Sauronaradus meganae* **gen. et. sp. nov.** to accommodate these unique features.

Key words: Burma, Cenomanian, extinct, Heteroptera, Myanmar, new species, Pentatomomorpha

Academic editor: Chen-Yang Cai
Received: 18 September 2024
Accepted: 18 October 2024
Published: 28 November 2024

ZooBank: https://zoobank.org/BD49B17B-1B71-4FB2-ABD3-84AEDD7ADB96

Citation: Cumming RT, Mlynarek JJ (2024) An additional †Archearadinae flat-bug species from Cretaceous Burmese Amber (Hemiptera, Aradidae). ZooKeys 1219: 123–133. https://doi.org/10.3897/zookeys.1219.137409

Introduction

The Aradidae is a cosmopolitan family of true bugs with more than 2000 described species in 8 subfamilies and 230 genera (Schuh and Slater 1995). The Aradidae are considered most diverse in Australia but can be found in all biogeographic realms except Antarctica (Schuh and Slater 1995). They are easily recognizable due to their dorsoventrally flattened bodies and rough bark-like texture. Aradid species can be macropterous or apterous. Even though their ecology is not well documented, they are believed to be mycophagous and individuals can generally be found living under bark of dead trees, on fallen branches, or in the leaf litter (Swanson 2020) while some species are associated with clear cutting and forest fires (Deyrup and Mosley 2004; Johansson et al. 2010).

Species of Aradidae are somewhat prevalent in the fossil record. Thirty-nine extinct species have been described from various fossil deposits from the Cretaceous to the present. Deposits include middle-late Eocene Baltic amber (Heiss 2000; Heiss 2002a, b, c), Lower Eocene French amber (Marchal et al. 2011), early to mid-Miocene Dominican amber (Froeschner 1992), early to mid-Miocene Mexican amber (Heiss 2016), Miocene Shangwang formation in China (Zhang et al. 1994), Early Miocene Foulden Maar formation in New Zealand (Kaufuss et al. 2011) and from mid-Cretaceous Burmese/Kachin amber (Heiss and Grimaldi 2001, 2002; Grimaldi et al. 2002).

Kachin amber (found in the Hukawng Basin of Kachin State in northern Myanmar) dates from the mid-Cretaceous around 100 million years ago (Shi et al. 2012). Kachin amber is considered especially important because of the diverse fauna it has preserved from a crucial period in the Cretaceous (Ross 2024). This amber deposit has also been prolific for aradids in particular. Currently there are 19 species from 12 genera of Aradidae described from Kachin amber (Heiss and Chen 2023b; Heiss 2023). In 2001, Aradidae from Kachin amber began to be described and Heiss and Grimaldi (2001) described two species of *Archaearadus* Heiss & Grimaldi, 2001. Grimaldi and Engel (2008) described the new genus, *Cretopiesma.* In 2012, one species of *Myanmezira* Heiss & Poinar, 2012 and one species of *Kachinocoris* Heiss, 2012 were described (Heiss and Poinar 2012; Heiss 2012). Heiss (2016, 2019b, 2019c) added a further three more species, one each of *Aradoleptus* Heiss, 2016, *Archaeneurus* Heiss, 2019a and *Archecalisius* Heiss, 2019a. In 2020, Azar et al. (2020) revised *Cretopiesma* Grimaldi & Engel, 2008 from Kachin amber and described three new species. In 2022, Heiss (2022) described the new genus *Pachytylaradus*. Most recently in 2023, Heiss (2023) described a new species of *Cretozemira* Heiss, 2023 and Heiss and Chen (2023a, 2023b) described two species belonging to the new genus *Archemezira* Heiss & Chen, 2023.

We describe an additional new genus and species in this remarkable family of true bugs belonging to the extinct subfamily †Archearadinae from Kachin amber.

Material and methods

The amber containing the holotype specimen is from the well-known Hukawng Valley in northern Myanmar, a prolific site of amber excavation (Grimaldi et al. 2002). The age of this amber deposit is estimated to be ~98.79 ± 0.62 million years old, within the Cenomanian stage of the Cretaceous (Shi et al. 2012). The specimen described and illustrated herein was morphologically reviewed using a 2x-225x trinocular boom stand stereo microscope (#ZM-4TW3-FOR-20MBI3) and photographs were taken with an attached high-speed 20MP camera (#MU2003-BI-CK) (AmScope, Irvine, USA). Illumination was from a 6-Watt LED dual gooseneck illuminator lit by a #85-265VAC/50-60Hz lighting unit (AmScope, Irvine, USA). Measurements were taken using an AmLite digital camera software for Mac OS X 10.8 64-bit which was calibrated with a 0.01 mm microscope stage calibration slide (#MR095) (AmScope, Irvine, USA). Adobe Photoshop Elements 13 (Adobe Inc., San Jose, USA) was used as post-processing software.

Aradidae head morphology terminology follows Rakitov (2022).

Aradidae currently described from Burmese Amber

†Archearadinae Heiss & Grimaldi, 2002

Archearadus burmensis Heiss & Grimaldi, 2001
Archearadus elongatus Heiss, 2016
Archemezira nuoxichenae Heiss & Chen, 2023*
Archemezira nuoyichenae Heiss & Chen, 2023*

---

* Tentatively assigned to this subfamily in the original description.

Cretopiesma anticum (Heiss & Poinar, 2012)**
Cretopiesma engelgrimaldii Azar, Heiss & Huang, 2020
Cretopiesma inexpectatum Azar, Heiss & Huang, 2020
Cretopiesma lini Azar, Heiss & Huang, 2020
Cretopiesma suukyiae Grimaldi & Engel, 2008***
Cretozemira elongata Heiss, 2023
Sauronaradus meganae gen. et. sp. nov.*

Mezirinae Oshanin 1908

Myanmezira longicornis Heiss & Poinar, 2012

Calisiinae Stål 1873

Calisiomorpha yuripopovi Heiss, 2016*
Calisiomorpha herczeki Heiss, 2023
Archecalisius longiventris Heiss, 2019

Unspecified subfamily

Aradoleptus birmanus Heiss, 2016
Ellenbergeria oviventris Heiss, 2016
Kachinocoris brevipennis Heiss, 2012
Pachytylaradus cretaceous Heiss, 2022
Archeaneurus neli Heiss, 2019

Systematic palaeontology

Order Hemiptera Linnaeus, 1758
Suborder Heteroptera Latreille, 1810
Infraorder Pentatomomorpha Leston, Pendergrast & Southwood, 1954
Family Aradidae Brullé, 1836
Subfamily †Archearadinae Heiss & Grimaldi, 2002 (tentatively placed)

Genus *Sauronaradus* gen. nov.
https://zoobank.org/653B62FB-8028-4D63-9ABA-0B17FB4F2037

Type species. *Sauronaradus meganae* gen. et sp. nov., herein designated.

Etymology. Generic name derived from the epic fantasy novels "The Lord of the Rings" by J. R. R. Tolkien (1892–1973). Both authors independently, upon seeing the spines and armor-like habitus of this species, thought of the armored cinematic depiction of the villainous protagonist Sauron during the "War of the Last Alliance" during the "late Second Age". The name Sauron ([ˈsaʊron] or [ˈθaʊron], is from the language "Quenya" [one of the languages spoken by the

---

** Originally described as *Microaradus anticus* Heiss & Poinar, 2012. Transferred to *Cretopiesma* in Azar et al. (2020).

*** Originally placed in Piesmatidae by Grimaldi and Engel (2008) and subsequently moved to general Aradidae by Cassis and Schuh (2010).

High Elves of Middle-earth]), and he is the eponymous “Lord of the Rings”. The eponym is coupled with árados (Greek: ἄρᾰδος), which is Latinized as “*aradus*”, referencing the relationship to Aradidae. Gender is masculine following -*aradus*.

Diagnosis. Distinguished from all known extant and extinct Aradidae by various features of the exceptionally long and thin antennae. Typically, aradid antennae are stockier and short, with antennomere lengths only 2×–10× the width, but in *Sauronaradus* gen. nov. antennomeres II, III, and IV have lengths ~20–22× their widths (Fig. 1E). Additionally, many aradids often have the terminal antennomere shorter than segments II or III, but in *Sauronaradus* gen. nov. the terminal antennomere is of a similar length and width to antennomeres II and III (Fig. 1E). *Sauronaradus* gen. nov. appears to possibly be related to the co-occurring Cretaceous species *Archemezira nuoxichenae* Heiss & Chen, 2023 and *Archemezira nuoyichenae* Heiss & Chen, 2023 as these also have a long and similarly shaped clypeus and long and slender antennae. *Sauronaradus* gen. nov. can be differentiated from *A. nuoxichenae* and *A. nuoyichenae* however by the terminal antennomere, which is longer than antennomeres II or III (versus *A. nuoxichenae* and *A. nuoyichenae* where the terminal antennomere is shorter than antennomeres II or III). Additionally, *Sauronaradus* gen. nov. can be differentiated from these species by the parallel-sided abdomen (versus broad and rounded) and the overall smaller size (~5 mm versus the massive 23.5 mm (*A. nuoyichenae*) and large 15.4 mm (*A. nuoxichenae*). *Sauronaradus* gen. nov. also shares characters with *Archearadus* Heiss & Grimaldi, 2001; such as the long clypeus, narrow neck, and spiniform tubercles of the pronotum.

Description. Macropterous, medium body size ~5 mm (from the apex of the clypeus to the apex of the abdomen); body flat, lateral margins prominently marked with tubercles (with the pronotum margins with three large spiniform tubercles on each side ranging in length from 0.10–0.15 mm long; abdominal margins with granulation and minor tubercles); coloration dark brown.

Head. Longer than wide, clypeus prominent and boxy, with two clearly defined widths, broad for the first half, then half as wide on the apex; antennae exceptionally long and thin with antennomere lengths ~20× the segment widths, segments II–IV of about equal length. Compound eyes large and bulging. Vertex of head with four spiniform tubercles transversing the compound eyes.

Pronotum. A rounded isosceles trapezoid with three distinct widths from the anterior to the posterior. Lateral margin with three large spiniform tubercles. Surface marked throughout by small divots and four longitudinal carinae (the two in the center are more prominent and run the full length of the pronotum while the exterior carinae are less pronounced, only prominent on the posterior half).

Scutellum. Rounded triangular, with the base width ca. equal to the length; surface flat without carinae, just slight granulation/divots.

Legs. Armed with small granulation throughout (more prominent on femora, less so on the tibiae, with some of the more prominent nodes of the femora including a singular seta). Femora thicker than tibiae. Tibiae with dense, thick setae on the apical ends ventral surface. Tarsi two-segmented, claws with lemniscate pulvilli.

Abdomen. Macropterous, but wing details are not discernable in the holotype. Only slightly wider than the thorax, with lateral margins that are subparallel; segments with weakly undulating margins creating three to five lumps with the posterior-most the most prominent and the others of a similar smaller size.

Remarks. This new genus is tentatively placed in the subfamily †Archearadinae Heiss & Grimaldi, 2002. This subfamily lacks an apomorphic character that easily defines it, but instead has been defined by a set of characters from several extant subfamilies, which are held in a unique combination in the †Archearadinae. The features present in *Sauronaradus* gen. nov. which are known from the †Archearadinae are: clypeus long and prominent, open rostral atrium arising between the compound eyes not at the apex of the clypeus, abdominal tergites III and VI not fused but instead separated by a distinct suture, and the tarsi are two-segmented with claws bearing pulvilli. This tentative subfamilial placement is also supported by the morphological features shared between *Sauronaradus* gen. nov. and the genera *Archemezira* and *Archearadus*.

Sauronaradus meganae **sp. nov.**

https://zoobank.org/CC59C92B-2178-4C3C-B599-2114D420D433
Figs 1, 2

Type material. ***Holotype***: specimen number IMQC-AMB-ara0001; Hukawng Valley, Myanmar, accession c. 2010; male; specimen deposited within the Montreal Insectarium, Montreal, Quebec, Canada (IMQC).

Taphonomy. Ovular piece of clear amber (~15.5 × 10.9 mm), with minimal debris obscuring the holotype (Fig. 2D). The holotype is wholly intact and appears to have little warping. Due to the dark coloration the wings are difficult to discern as they are tucked closely to the abdomen surface. One syninclusion is present, a slightly damaged *Cretopiesma suukyiae* Grimaldi & Engle, 2008.

Type locality and horizon. Latest Albian to lowermost Cenomanian (mid-Cretaceous), Hukawng Valley, northern Myanmar.

Etymology. Patronym, named to honor Megan Solan, environmental toxicologist and entomologist. The first author wishes to thank Megan for her years of friendship and passion for entomology. Her enthusiasm for research is infectious and a positive driving force in the sciences.

Diagnosis. Currently the genus is monotypic. See the above diagnosis of the genus for differentiation of this species from other aradids.

Description (All measurements are in mm and based on the holotype). Macropterous male; large, 5.05 long, 1.88 wide; body flattened (Figs 1, 2).

Head 1.16 long, 0.89 wide (across the compound eyes); dorsally and ventrally rough textured. Compound eyes strongly protruding (Fig. 2A). Ocelli absent. Clypeus long, protruding, and boxy, with two clearly defined widths, broad for the posterior half (loral lobe), then half as wide on the apical half (maxillary lobe; Fig. 2B). Dorsally there is a prominent anteclypeus on the posterior half (Fig. 2A). Clypeus loral lobe with two prominent apically pointing tubercles on each side; clypeus maxillary lobe with nodes on the dorsal and lateral surfaces (Fig. 2B). Ventral surface of head with nodes similar to the dorsal surface nodes, and a narrow median depression of gula (Fig. 2E). Bucculae not prominent. Open rostral atrium arising between the compound eyes, not at the apex of clypeus. Four, prominent, conical tubercles are present on the dorsal surface of the head. One pair are anteorbital tubercles present near the base of the compound eyes, and the second pair are situated evenly between the anteorbital tubercles (Fig. 2A). These four tubercles are of similar size and shapes. Head

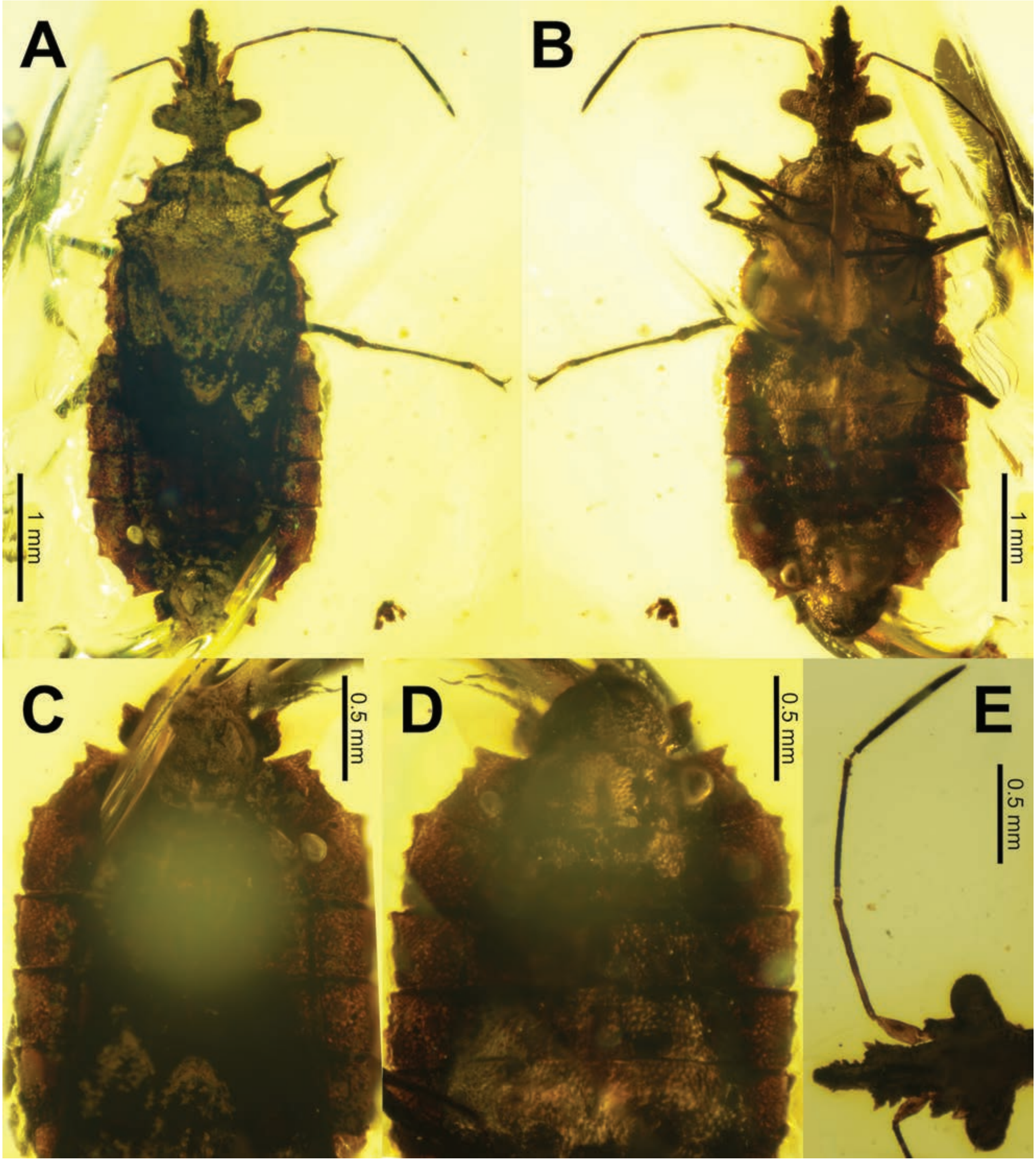

Figure 1. *Sauronaradus meganae* gen. et sp. nov. holotype **A** dorsal habitus **B** ventral habitus **C** abdomen, dorsal **D** abdomen, ventral **E** right antenna, dorsal.

lacking prominent postocular lobes, instead immediately behind the compound eyes is the notably constricted postocciput, which is slightly narrower than the anterior of the pronotum.

Antenna exceptionally long and thin with antennomeres II, III, and IV with lengths c. 20–22× their widths. Antenna with four antennomeres; basal antennomere (scape) the shortest, antennomere lengths: I: 0.27, II: 0.62, III: 0.70, IV: 0.74; antennomeres II, III, and IV tubiform; antennomeres II and III with surface granulation, and antennomere IV densely marked with setae throughout the surface with the seta length slightly less than the antennomere width, with the seta strongly angled apically (Fig. 1E). Antenniferous lobe prominent with a granular surface; stout, not projecting apically beyond the antennal insertion. Antennal insertion one-third of the way between the compound eyes and the apex of the clypeus (Fig. 2B). Rostrum with four segments extending to the posterior margin on the procoxal cavity (~1.73 mm long; Fig. 2E).

Thorax pronotum (0.99 mm long, greatest width 1.44); roughly trapezoidal in shape (increasing in width caudally) but with somewhat undulating margins (approximate widths from the anterior to the posterior: 0.42 mm, 0.99 mm, 1.44 mm, 1.24 mm; Fig. 2C). Pronotum lateral margin armed on the anterior two-thirds with three prominent spiniform tubercles (anterior most 0.11 mm, middle 0.10 mm, posterior-most 0.15 mm long; Fig. 2B). The posterior third of the pronotum bulges out to a width of 1.44 mm, and this bulge is armed with several smaller tubercles (Fig. 2B). Pronotum surface punctate throughout, with two paramedial carinae on each side of the sagittal plane, the central pair of carinae extend the full length of the pronotum and diverge in a similar fashion to the pronotum width, while the exterior carinae are less pronounced and are more prominent on the posterior half (Fig. 2C). Carinae jagged in form, not uniform in intensity throughout the lengths, somewhat rising and falling in rough textures (Fig. 2C). Scutellum long and prominent, 1.24 mm wide, 1.16 mm long; dorsal surface with the anterior third slightly raised above the posterior two-thirds; surface flat but punctate throughout; apex broadly rounded. Prosternum; 0.49 mm long, surface punctate and marked with a moderate rostral groove which continues onto the mesosternum as a broader depression along the sagittal plane (Fig. 2E). Mesosternum maximum width 1.44 mm, length 0.51 mm; ventral surface punctate (Fig. 2E). Metasternum 0.51 mm long, 1.59 mm wide.

Legs long and thin, all with slightly granular surfaces. Profemora 0.90 mm long, thinner on the proximal third. Leg lengths: protibiae 0.75 mm, mesofemora 0.92 mm, mesotibiae 0.60 mm, metafemora 1.16 mm, metatibiae 0.93 mm. Tibiae with sparse setae throughout, with longer and thicker setae on the distal ends (Fig. 2F). Tarsi with two tarsomeres; apical tarsomere is 1.5–2.0 times longer than the previous tarsomere; apical tarsomere thin proximally, widening notably for the proximal half, then a uniform broad width on the distal half (Fig. 2F, G). Apical tarsomere ventrally with few thin setae, previous tarsomere with thicker but sparse setae on the distal end (Fig. 2F). Tarsal claws long and simple; pulvilli approximately lemniscate, slightly shorter than tarsal claws (Fig. 2F, G).

Wings fully developed, but details are indiscernible due to taphonomy of the holotype.

Abdomen broad and flat, all surfaces punctate; length 2.41, greatest width 1.88 mm. Abdominal segment lengths: III = 0.57 mm, IV = 0.34 mm, V = 0.32 mm, VI = 0.37 mm, VII = 0.43 mm, VIII = 0.40 mm. Each abdominal segment has margins which gently undulate, with four or five humps, the posterior-most of which is on the posterior margin and larger than the others (Fig. 1C, D). Male terminalia broad and roughly bell shaped, surfaces rugose, a distinctly raised median ridge protrudes on the dorsal surface (Fig. 1C, D). Paratergite VIII rhomboid, angulated posteriorly, with the lateral margin slightly undulating (Fig. 1C, D).

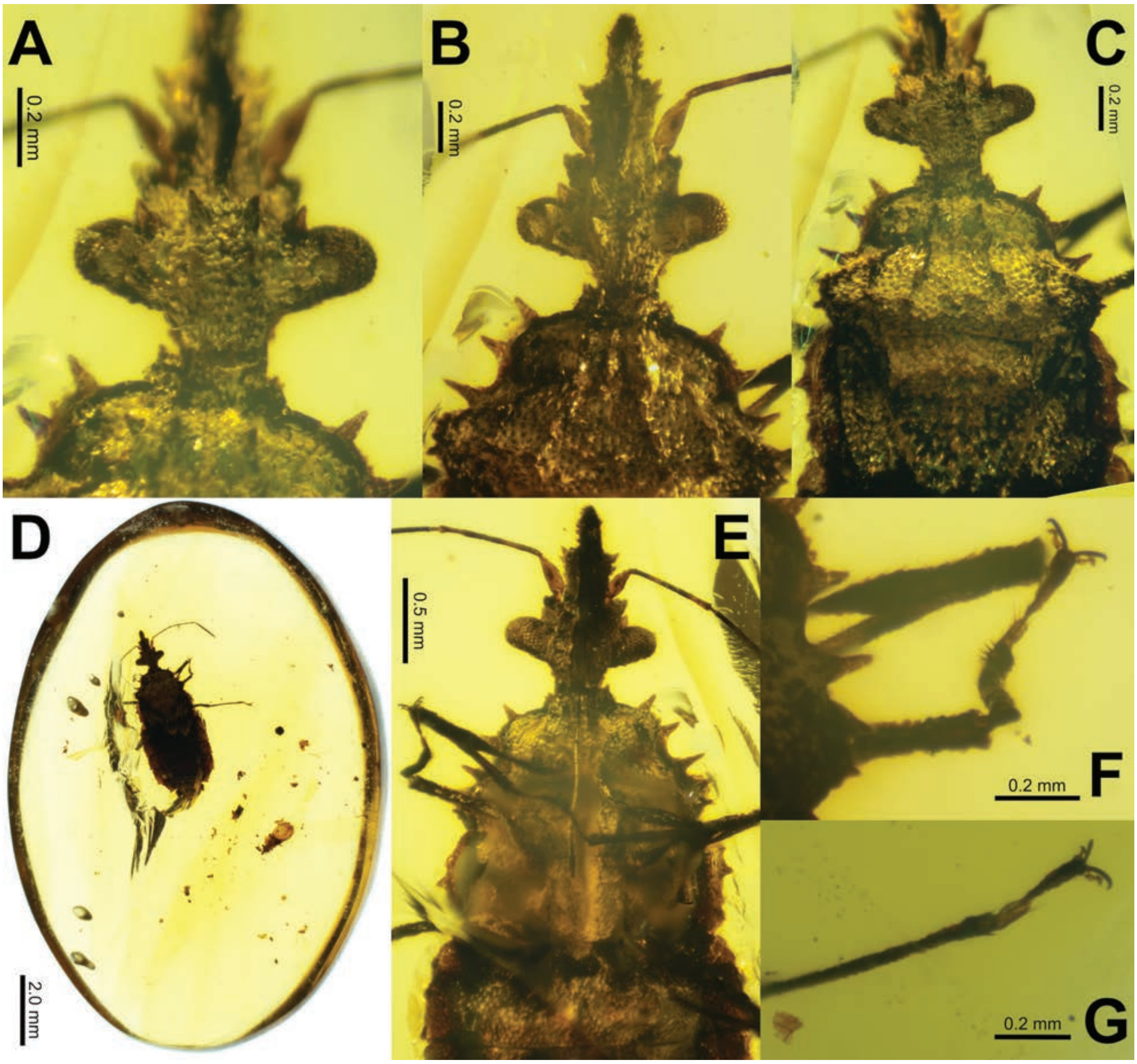

Figure 2. *Sauronaradus meganae* gen. et sp. nov. holotype **A** anterior lit to highlight the spines of the head, dorsal **B** head through thorax, dorsal **C** pronotum, lit to highlight carinae, dorsal **D** full amber piece with holotype inclusion and *Cretopiesma suukyiae* syninclusion to the lower right of *Sauronaradus meganae* gen. et sp. nov. **E** head through thorax, ventral **F** pro- and meso- legs, mesotibia and tarsus visible, dorsal **G** right metatibia, dorsal.

Discussion

Following this description of a new species, there are now 20 Aradidae species described from Cretaceous Kachin amber. Nine of the species have been described since 2020 suggesting that, even though this group is rarely found, it may have been diverse in the mid-Cretaceous, and we are only now beginning to understand this diversity. The morphological uniqueness of the species also demonstrates how little we know about the mid-Cretaceous flat-bug fauna. Goßner et al. (2007) demonstrated with extant fauna that aradid species require specific habitats to survive. As *Sauronaradus meganae* gen. et sp. nov. and the two Cretaceous species of *Archemezira* all have long and thin antennae (when compared with the short, stout antennae typically seen in extant aradids), this suggests that perhaps these extinct species could have inhabited a different micro-habitat than modern aradids prefer. While modern aradids typically inhabit the bark of dead trees or leaf litter, with the flora of the Cretaceous significantly different than that of today this notable habitat difference could be correlated with these macro morphological differences in extant versus extinct aradid taxa. Hopefully, future research into Cretaceous aradid diversity will reveal overarching morphological trends.

Additional information

Conflict of interest

The authors have declared that no competing interests exist.

Ethical statement

No ethical statement was reported.

Funding

No funding was reported.

Author contributions

Both authors have contributed equally.

Author ORCIDs

Royce T. Cumming https://orcid.org/0000-0001-7930-1292
Julia J. Mlynarek https://orcid.org/0000-0002-1569-9403

Data availability

All of the data that support the findings of this study are available in the main text

References

Azar D, Heiss E, Huang D (2020) Review of the flat bug genus *Cretopiesma* Grimaldi & Engel, 2008 from mid-Cretaceous Burmese amber and description of three new species (Hemiptera: Heteroptera: Aradidae: Archearadinae). Palaeoentomology 3(1): 6–31. https://doi.org/10.11646/palaeoentomology.3.1.2

Brullé A (1836) Histoire naturelle des insectes, traitant de leur organisation et des leurs moers en géneral, et comprenant leur classification et la description des espèces. Orthoptéres et Hémiptères IX (2): 1–415.

Cassis G, Schuh RT (2010) Systematic methods, fossils, and relationships within Heteroptera (Insecta). Cladistics 26: 262–280. https://doi.org/10.1111/j.1096-0031.2009.00283.x

Deyrup M, Mosley JG (2004) Natural history of the flat bug *Aradus gracilicornis* in fire-killed pines (Heteroptera: Aradidae). Florida Entomologist 87(1): 79–81. https://doi.org/10.1653/0015-4040(2004)087[0079:NHOTFB]2.0.CO;2

Froeschner RC (1992) The flat bug genus *Calisiopsis* Champion: a review with descriptions of three new species, including one from Dominican Republic amber (Heteroptera: Aradidae). Proceedings of the Biological Society of Washington 105: 32–39.

Goßner MM, Engel H, Blaschke M (2007) Factors determining the occurrence of Flat Bugs (Aradidae) in beech dominated forests. Naturnähe-Indikatoren 4: 59–89. https://d-nb.info/1209916339/34

Grimaldi DA, Engel MS (2008) An unusual, primitive Piesmatidae (Insecta: Heteroptera) in Cretaceous amber from Myanmar (Burma). American Museum Novitates 3611: 117. https://doi.org/10.1206/0003-0082(2008)3611[1:AUPPIH]2.0.CO;2

Grimaldi DA, Engel MS, Nascimbene PC (2002) Fossiliferous Cretaceous amber from Myanmar (Burma): Its rediscovery, biotic diversity, and paleontological significance. American Museum Novitates 3361: 1–71. https://doi.org/10.1206/0003-0082(2002)361<0001:FCAFMB>2.0.CO;2

Heiss E (2000) Revision der Familie Aradidae des Baltischen Bernsteins II. Drei neue Calisius Arten (Insecta, Heteroptera). Carolinea 58: 195–201.

Heiss E (2002a) Revision der Familie Aradidae des Baltischen Bernsteins V. Eine neue Gattung und zwei neue Arten der Unterfamilie Calisiinae (Heteroptera, Aradidae). Linzer biologische Beiträge 34: 1127–1136.

Heiss E (2002b) Revision of the family Aradidae in Baltic Amber IV: Two new *Aradus* from the collection of the Institut für Paläontologie, Museum für Naturkunde, Berlin (Heteroptera, Aradidae). Mitteilungen des Naturkundemuseums Berlin, Deutsche Entomologische Zeitschrift 49: 221–225. https://doi.org/10.1002/mmnd.20020490207

Heiss E (2002c) Revision der Familie Aradidae des Baltischen Bernsteins VI: Neue Arten der Gattung Aradus Fabricius 1803 (Heteroptera, Aradidae). Linzer biologische Beiträge 34(2): 1137–1150.

Heiss E (2012) *Kachinocoris brevipennis* n. gen., n. sp. in Cretaceous Burmese amber (Hemiptera: Heteroptera). Zootaxa 3227: 64–68. https://doi.org/10.11646/zootaxa.3227.1.4

Heiss E (2016) New genera and species of Aradidae in Cretaceous Burmese amber. (Hemiptera: Heteroptera). Linzer biologische Beiträge 48: 419–429.

Heiss E (2019a) *Archeaneurus neli* gen. et. sp. nov. from Cretaceous Burmese amber (Heteroptera, Aradidae). Palaeoentomology 2: 566–569. https://doi.org/10.11646/palaeoentomology.2.6.4

Heiss E (2019b) New genus and species of Calisiinae from Cretaceous Burmese amber (Hemiptera, Heteroptera, Aradidae). Linzer Biologische Beiträge 51: 83–87.

Heiss E (2019c) *Archeaneurus neli* gen. et sp. nov. from Cretaceous Burmese amber (Heteroptera, Aradidae). Palaeoentomology 2: 566–569. https://doi.org/10.11646/palaeoentomology.2.6.4

Heiss E (2022) *Pachytylaradus cretaceous* gen. et. sp. nov. from Burmese amber (Heteroptera, Aradidae). Palaeoentomology 5: 294–297. https://doi.org/10.11646/palaeoentomology.5.4.1

Heiss E (2023) A new species, a new synonymy, a revised generic assignment and new records in some African and Palaearctic Aradidae (Hemiptera: Heteroptera). Zootaxa 5315: 469–478. https://doi.org/10.11646/zootaxa.5315.5.3

Heiss E, Chen H-R (2023a) A striking new XXL-size flat bug from mid-Cretaceous Burmese amber: *Archemezira nuoyichenae* sp. nov. (Heteroptera, Aradidae). Palaeoentomology 6: 527–532. https://doi.org/10.11646/palaeoentomology.6.5.11

Heiss E, Chen H-R (2023b) *Archemezira nuoxichenae* gen. et sp. nov. from Burmese amber (Heteroptera, Aradidae). Palaeoentomology 6: 17–21. https://doi.org/10.11646/palaeoentomology.6.1.5

Heiss E, Grimaldi D (2001) *Archearadus burmensis* gen., sp. n., a remarkable Mesozoic Aradidae in Burmese amber (Heteroptera, Aradidae). Carolinea 59: 99–102.

Heiss E, Grimaldi D (2002) The first known female of *Archearadus burmensis* Heiss & Grimaldi, 2001 in Cretaceous Burmese amber (Heteroptera: Aradidae). Zeitschrift der Arbeitsgemeinschaft Österreichischer Entomologen 54: 55–59.

Heiss E, Poinar Jr G (2012) New Aradidae in Mesozoic Burmese amber (Hemiptera, Heteroptera). Annalen des Naturhistorischen Museums Wien, Serie A 114: 307–316.

Johansson T, Hjältén J, Stenbacka F, Dynesius M (2010) Responses of eight boreal flat bug (Heteroptera: Aradidae) species to clear-cutting and forest fire. Journal of Insect Conservation 14: 3–9. https://doi.org/10.1007/s10841-009-9218-1

Kaulfuss U, Wappler T, Heiss E, Larivière MC (2011). *Aneurus* sp. from the early Miocene Foulden Maar, New Zealand: the first Southern Hemisphere record of fossil Aradidae (Insecta: Hemiptera: Heteroptera). Journal of the Royal Society of New Zealand 41: 279–285. https://doi.org/10.1080/03036758.2011.559665

Latreille PA (1810) Considérations générales sur l'ordre natural des animaux composant les classes des Crustacés, des Arachnides et des Insectes; avec un tableau méthodique de leurs genres, disposés en familles. F. Schoell, Paris, 444 pp. https://doi.org/10.5962/bhl.title.39620

Leston D, Pendergrast JD, Southwood TRE (1954) Classification of the terrestrial Heteroptera (Geocorisae). Nature 174: 91–92. https://doi.org/10.1038/174091b0

Linnaeus C (1758) Systema naturae per regna tria naturae, secundum classes, ordines, genera, species, cum characteribus, differentiis, synonymis, locis. Editio decima, reformata. Laurentii Salvii; Stockholm, 824 pp. https://doi.org/10.5962/bhl.title.542

Marchal L, Guilbert E, Brisac P, Nel A (2011) A new record and a new species of Aradidae fossils (Hemiptera: Heteroptera). Zootaxa 2832: 56–62. https://doi.org/10.11646/zootaxa.2832.1.4

Oshanin BF (1908) Verzeichnis der paläarktischen Hemipteren mit besonderer Berücksichtigung ihrer Verteilung im Russischen Reiche. Buchdruckerei der Kaiserlichen Akademie der Wissenschaften, St. Petersburg 1: 395–586. https://www.biodiversitylibrary.org/page/12713295

Rakitov R (2022) The mouthparts of the Aradidae (Insecta: Hemiptera: Heteroptera). Arthropod Structure & Development 71(101211): 1–29. https://doi.org/https://doi.org/10.1016/j.asd.2022.101211

Ross AJ (2024) Complete checklist of Burmese (Myanmar) amber taxa 2023. Mesozoic 1(1): 21–57. https://doi.org/10.11646/mesozoic.1.1.4

Schuh RT, Slater JA (1995) True Bugs of the World (Hemiptera: Heteroptera): Classification and Natural History. Cornell University Press, Ithaca, New York, 337 pp.

Shi G, Grimaldi DA, Harlow GE, Wang J, Wang J, Yang M, Lei W, Li Q, Li X (2012) Age constraint on Burmese amber based on U-Pb dating of zircons. Cretaceous Research 37: 155–163. https://doi.org/10.1016/j.cretres.2012.03.014

Stål C (1873) Enumeratio Hemipterorum. Bidrag till en förteckning öfver aller hittills kända Hemiptera, jemte systematiska meddelanden (Enumeratio Hemipterorum. Contribution to a list of the most hitherto known Hemiptera, also systematic notices). Kongliga Svenska Vetenskaps-Academiens Nya Handlingar, Stockholm (New Proceedings of the Royal Swedish Academy of Sciences, Stockholm) 11(2): 1–163. https://doi.org/10.5962/bhl.title.12549

Swanson DR (2020) A Synopsis of the Flat Bugs (Heteroptera: Aradidae) of Michigan. The Great Lakes Entomologist 53(2): 83–104. https://doi.org/10.22543/0090-0222.2354

Zhang JF, Sun B, Zhang XY (1994) Miocene insects and spiders from Shanwang, Shandong. Science Press, Beijing, 298 pp.

ZooKeys 1219: 135–142 (2024)
DOI: 10.3897/zookeys.1219.131379

Research Article

A new species of the Neotropical genus *Smilidarnis* Andrade (Hemiptera, Membracidae), with a new country record for the genus

Stuart H. McKamey[1]

1 *Systematic Entomology Laboratory, Agricultural Research Service, U.S. Department of Agriculture, c/o National Museum of Natural History, P.O. Box 37012, Washington, D.C. 20013, USA*
Corresponding author: Stuart H. McKamey (stuart.mckamey@usda.gov)

Abstract

Smilidarnis is **fixed as the correct original spelling**. *Smilidarnis similifasciatus*, **sp. nov.**, from Bolivia and French Guiana, closely resembles *S. fasciatus* Andrade in being brightly colored but differs in the metathoracic tibial chaetotaxy, the male pygofer, first anal segment, aedeagus, and color pattern. In this new species, which is larger than *S. fasciatus*, females are larger than males. Photographs of the male and female adults and genitalia of the new species are provided. Bolivia is a new country record for the genus. A key to all species is provided.

Key words: Bolivia, French Guiana, Neotropical, spelling fixation

Introduction

Membracid treehoppers are famous for their hyperdeveloped pronotum, which is usually expanded to cover much of the body or projected upwards and posteriorly over it. Many species are cryptically colored yet others exhibit the classic aposematic coloration, such as bright red, orange, or yellow, sometimes over a black ground color, advertising their presence to potential predators (Joron 2009).

The higher taxa of Membracidae are largely based on forewing venation, leg chaetotaxy, and coverage of scutellum and wings by the pronotum. Andrade (1989) established the genus *Smilidarnis* for two new species without placing the genus to higher taxon because they display features of both Smiliinae and Darninae. His diagnosis was expanded slightly by McKamey (2023) to accommodate the new variation found among three new species. Specifically, Andrade reported metathoracic tibial cucullate rows II and III double and, by implication, row I single, but *S. duocornus* McKamey has row I absent and *S. robustus* McKamey has rows I and III double and row II absent. In addition, two of the new species described by McKamey (2023) have suprahumeral horns. *Smilidarnis* is still unplaced within the family. Features indicating placement in Smiliinae include Andrade's species having metathoracic tibial chaetotaxy matching that of Ceresini, and in *S. concolor* Andrade the forewing veins R and M are confluent near its apex, which is a diagnostic feature of Smiliinae (Deitz 1975). *Smilidarnis* also has features of Darninae: some *Smilidarnis* have the metathoracic tibia with setal row I or II absent

OPEN ACCESS

Academic editor: Christopher H. Dietrich
Received: 5 July 2024
Accepted: 22 October 2024
Published: 28 November 2024

ZooBank: https://zoobank.org/B8C2A765-B22B-4B18-B9A8-421340767C35

Citation: McKamey SH (2024) A new species of the Neotropical genus *Smilidarnis* Andrade (Hemiptera, Membracidae), with a new country record for the genus. ZooKeys 1219: 135–142. https://doi.org/10.3897/zookeys.1219.131379

(Hemikypthini and some Darnini lacking row I, some Hemikypthini lacking row II); and R_{4+5} and M_{1+2} are separate throughout (Fig. 2), which occurs in all Darninae and no Smiliinae. Consequently, leg chaetotaxy and forewing venation do not provide evidence resolving the relationship of *Smilidarnis* to other treehoppers. Based on morphology, the phylogenetic estimate by Dietrich et al. (2001) placed Smilidarnis as the sister-group to seven tribes of Smiliinae. A more recent, unpublished molecular phylogeny by Evangelista et al. (2017) placed *Smilidarnis* as the sister group of Ceresini (Smiliinae). No other phylogenetic estimates have included *Smilidarnis*.

Until now, *S. fasciatus* Andrade (1989) was the only brightly colored species in the genus. It is recorded only from French Guiana and Peru. Lapèze (2021) collected three specimens of *S. fasciatus* at lights in two localities in French Guiana. He noted that in contrast to most membracids, the female was smaller than the male. The female habitus photographs by Lapèze (2021, p. 118) match the line drawing by Andrade (1989; Figs 1, 2) in every respect. A newly discovered species closely allied to *S. fasciatus*, and as brightly colored, is represented by a series of six specimens of males and females, from Bolivia, which were also collected at lights. The series of the new species provides an opportunity to investigate male vs. female variation in size, morphology, and coloration. The color pattern in the photograph by Sakakibara of a specimen from French Guiana (Deitz and Wallace 2010; distribution by Dr. A. M. Sakakibara, pers. comm.) is consistent with that of the new species.

Materials and methods

In quoting labels, quotation marks separate labels and a vertical line separates lines on a label.

Terminology for general morphology, forewing venation (except crossvein s), and leg chaetotaxy follows Deitz (1975) except the gonoplac for the female genitalia, which follows Mejdalani (1998).

The abdomen was detached, macerated in a 10% KOH solution at room temperature for 72 hr, bathed in water, then in acetic acid to stop the reaction. After dissection, structures were stored in a glass microvial containing glycerin and pinned beneath the specimen.

A Leica MZ12 stereomicroscope was used to examine structures. All measurements were taken directly from the metadata of images from all specimens.

Images were taken with a Canon 5Dsr camera with an adjustable 65mm lens. Photos were taken using Capture One Pro version 10.1.2, 64 bit, build 10.1.2.23 imaging software, aided by CamLift version 2.9.7.1. The specimen was lit using two adjustable Dynalite MH2050 RoadMax flash heads, each attached to a Manfrotto 244 arm. The light was diffused using a lampshade-style cone of translucent paper between the specimen and light sources. After individual focal planes were photographed, they were compiled into a single, composite image using Zerene Stacker - USDA SI-SEL Lab Bk imaging system, version 1.04, build T201706041920. Stacked images were enhanced and edited in Adobe Photoshop CSS Extended version 12.0. The scale bars were generated through Photoshop directly from the metadata of the photos.

All specimens are deposited in the U.S. National Museum of Natural History, Smithsonian Institution, Washington, DC (**USNM**).

Results

Smilidarnis Andrade (1989) is here fixed as the correct original spelling in accordance with ICZN Article 32.5 (International Commission on Zoological Nomenclature 1999); it was misspelled *Smiliodarnis* in the discussion. The Bolivian specimens of the new species represents a new country record for the genus.

Key to species

1 Pronotum with pair of stout suprahumeral spines.................................... **2**
– Pronotum without suprahumeral spines **3**
2 Breadth across suprahumeral spines distinctly greater than breadth across posterior lateral spines (McKamey 2023; Fig. 2) .... ***S. duocornus* McKamey**
– Breadth across suprahumeral spines subequal, slightly less than breadth across posterior lateral spines (McKamey 2023, fig. 14) .... ***S. robustus* McKamey**
3 Pronotum posteriorly with tips but not bases of lateral spines black; forewing with veins R and M distally fused then separated preapically............ .... ***S. concolor* Andrade**
– Pronotum posteriorly with bases of lateral spines black; forewing with veins R and M not fused at any point.. **4**
4 Pronotum with central apical spine pale throughout; head vertex with ventrolateral margins and frontoclypeus forming evenly convex curve (McKamey 2023; Fig. 9) .... ***S. erwini* McKamey**
– Pronotum with central apical spine black in distal third; head vertex with ventrolateral margins straight and frontoclypeus forming an angle (Fig. 3) **5**
5 Pronotum with lateral margin having an isolated yellow patch .... ***S. fasciatus* Andrade**
– Pronotum with most lateral yellow band bifurcate posteriorly, lower arm running along almost entirety of lateral margin (Figs 2, 5).......................... .... ***S. similifasciatus* sp. nov.**

***Smilidarnis similifasciatus* sp. nov.**
https://zoobank.org/FC4868AC-C340-4292-B7E5-778D81965EC2

Diagnosis. Pronotum without suprahumeral spines; brightly colored with orange, yellow, and black; most lateral yellow band bifurcate posteriorly, lower arm running along almost entirety of lateral margin.

Distribution. Bolivia (**new country record for genus**), French Guiana.

Description. Dimensions (mm). Pronotal length ♀10.3–10.8, ♂9.8–9.9; total length including wings in repose ♀12.1–12.6, ♂11.5; width between humeral angles ♀4.7–4.8, ♂4.5–4.7; head width including eyes ♀3.9–4.0, ♂3.7–3.9, head width excluding eyes ♀2.7–2.8, ♂2.5–2.7; head height ♀1.7–1.8, ♂1.7–1.8; distance between apices of posterolateral spine apices ♀2.6–2.9, ♂2.4–2.6. ***Head*** (Figs 3, 6). Vertex inclined forward, wider than tall, glabrous, vertical dark lines including ocelli depressed; dorsal margin weakly convex, lateral margins straight; ocelli circular, on imaginary middle line between eyes; distance from outer margin of ocellus to eye 1.13 × distance between inner margins of ocelli; frontoclypeal sutures prominent; frontoclypeus in anterior view ventrally convex, in line with vertex ventrolateral margins. ***Pronotum*** (Figs 1–6). Suprahumeral spines absent; weakly elevated immediately behind humeral angles; distally with 3 spines, all directed ventroposteriorly, lateral pair directed weakly laterally; lateral spines reaching to level above r-m crossvein, central spine surpassing forewing vein M_{3+4}. ***Legs.*** All femora lacking cucullate setae and spines; metathoracic tibia row I cucullate setae basally in single row, distally double, row II in single row, sparse and with minute basal hoods, row III cucullate setae in single row. ***Female terminalia.*** Sternite VII deeply emarginate medially; pygofer long; valvula I (Fig. 10) long, with one weak, wide dorsal process distally, apex rounded; valvula II (Figs 11, 12) in lateral view narrow and lanceolate with dorsal margin linear, lacking dorsal dentae or sinuations, apex subacute, ventrally striate; gonoplac (Fig. 13) long, distally wide, apex rounded, bearing macrosetae along entire ventral margin. ***Male terminalia*** (Figs 7–9). Abdominal segment X (1st anal segment) with basaoventral lobe (Fig. 7); pygofer (Fig. 7) including lateral plate subquadrate, lateral plate with weak dorsal lobe, ovate, pilose throughout, subgenital plate fused basally, its sides subparallel, slightly narrowing distally, length in ventral view about 2.3 × width; style (Figs 8, 9) recurved with short acute apex bearing 4 setae preapically; aedeagus (Figs 8, 9) U-shaped in lateral view, shaft subparallel in anterior and lateral views, lacking dentae or other texture on distoanterior face but with minute dentae along lateral margins (Fig. 9); gonopore dorsal. ***Color.*** Male and female alike in color; pronotal color orange with 5 yellow longitudinal bands, medial and most lateral band nearly extending to large yellow spot in posterior fifth, most lateral longitudinal band bifurcate at mid length into 2 solid branches, 1 running along lateral margin, and black at bases and apices of posterior spines; head orange with 3 vertical yellow bands connecting to medial and closest yellow bands of pronotum; forewing anteriorly clear, posteriorly with amber tint.

Material examined. *Smilidarnis similifasciatus*, ***holotype*** • ♂ with labels "BOLIVIA, Dept. Santa Cruz | Prov. Andres Ibañez, Potreillos del Guenda, 17°40.27′ S, | 63°27.45′ W, 370 m, 5 Dec 2008 | T. J. Henry, at MV/black light" and red label "HOLOTYPE | Smilidarnis | similifasciatus | McKamey" (USNM). ***Paratypes*** • 4 ♀, 1 ♂, all same data as holotype but with blue paratype labels (USNM).

Etymology. The specific name is a masculine Latin adjective based on a combination of "*similis*" (similar to) and the allied species "*fasciatus*".

Discussion. *Smilidarnis fasciatus* and *S. similifasciatus* key out in the same couplet because they are superficially similar. Nevertheless, they differ in several respects. Regarding coloration, in the new species all yellow stripes are longer in both males and females than those of *S. fasciatus*. Regarding metathoracic tibia, cucullate setal rows are double rows in *S. fasciatus* but single rows in the new species (row I distally double). Regarding terminalia, in the new species the pygofer and lateral plate combined is more quadrate than in *S. fasciatus*, the lateral plate itself is ovate (vs. subquadrate in *S. fasciatus*), segment X has a basoventral lobe present (vs. absent in *S. fasciatus*), and the aedeagal dentae are lateral (vs. on the face of the shaft in *S. fasciatus*).

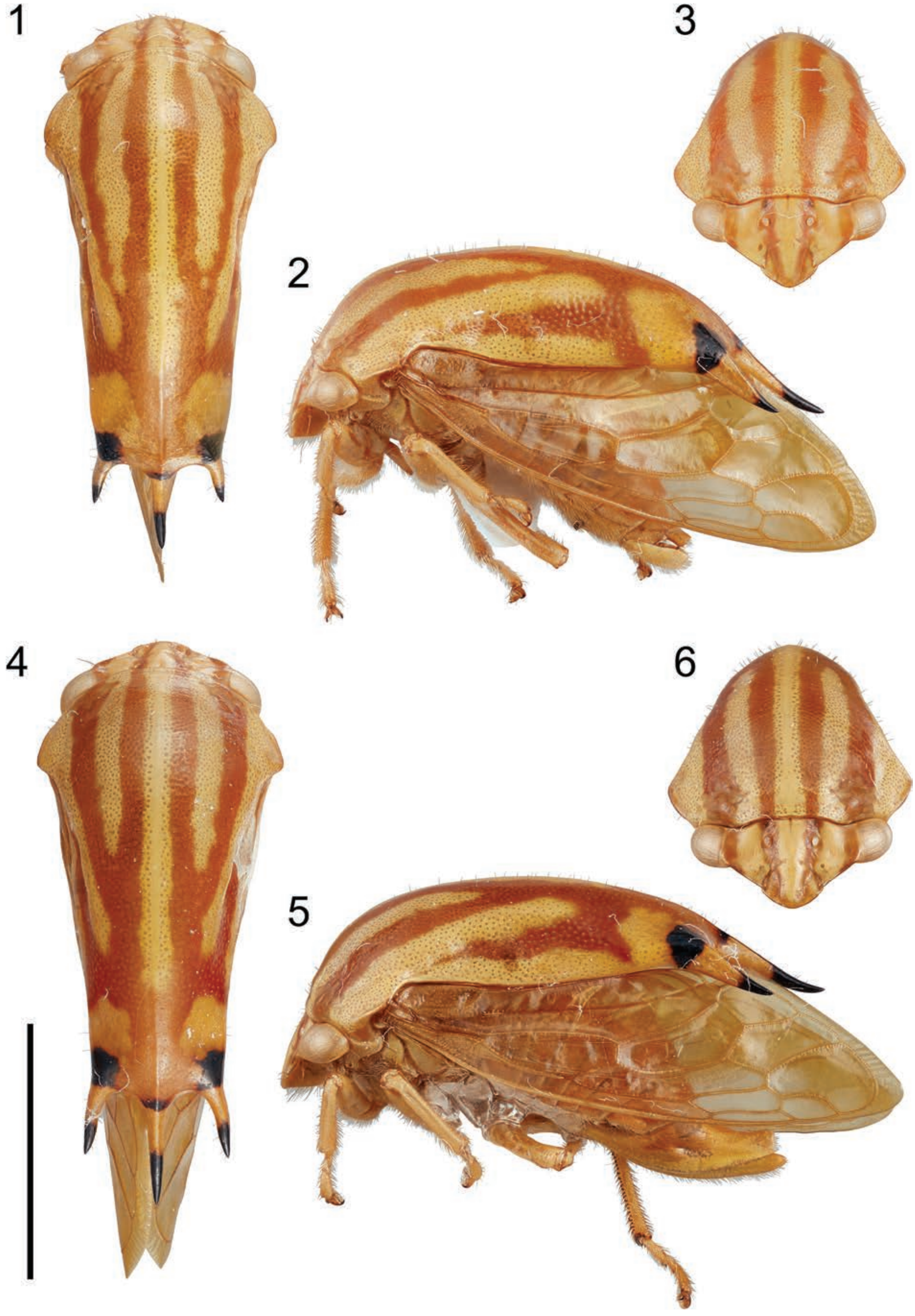

Figures 1–6. *Smilidarnis similifasciatus* sp. nov. **1–3** male habitus in dorsal. lateral, and anterior views, respectively **4–6** female habitus in dorsal, lateral, and anterior views, respectively. Scale bar: 5 mm.

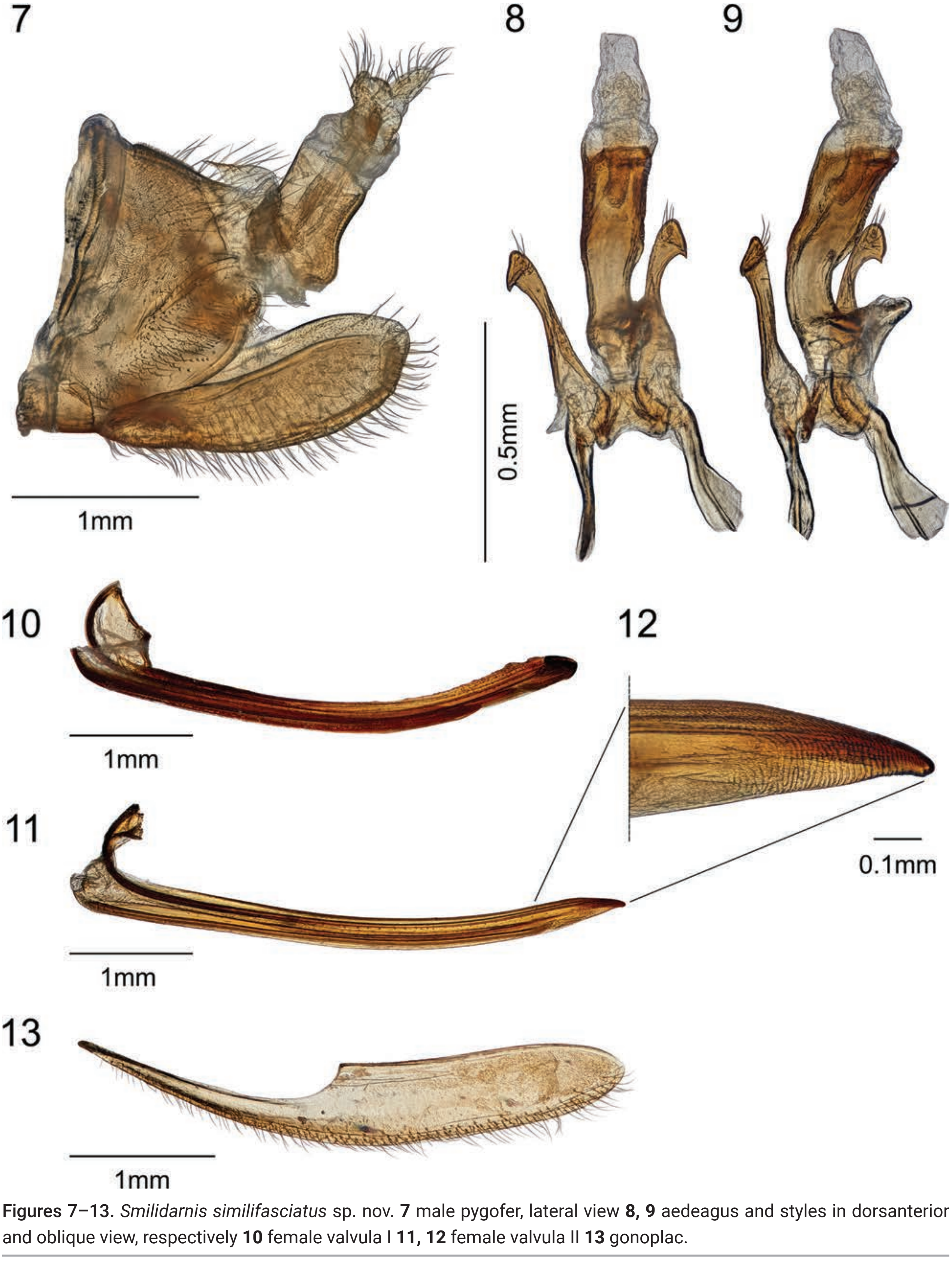

Figures 7–13. *Smilidarnis similifasciatus* sp. nov. **7** male pygofer, lateral view **8, 9** aedeagus and styles in dorsanterior and oblique view, respectively **10** female valvula I **11, 12** female valvula II **13** gonoplac.

The female habitus photographs by Lapèze (2021) match the illustration of *S. fasciatus* by Andrade (1989), while the photograph by Sakakibara (Deitz and Wallace 2010) corresponds to *S. similifasciatus*. Both species, therefore, are recorded from French Guiana. The *S. similifasciatus* male terminalia is most similar to that of *S. erwini* McKamey (2023) in that both have abdominal segment X bearing a basoventral lobe and the aedeagus lacking dentae or other texture on the dorsoanterior face of the shaft. The female genitalia of *S. fasciatus* has not been described so no comparison with that species is possible here, and only the second valvulae of *S. concolor* has been illustrated and described. The female genitalia of *S. similifasciatus* resembles those of *S. duocornus*, *S. robustus* and the second valvulae of *S. concolor*, in having the first valvulae long and narrow with poorly developed dentae distally, the second valvulae lanceolate, and the gonoplac distally wide with long setae ventrally.

Although the Bolivian males of the new species are slightly smaller than the lengths given by Andrade (1989) and Lapèze (2021) for *S. fasciatus*, in *S. similifasciatus* the four females are all larger than both males in every respect except head height, in contrast to Lapèze's (2021) opposite finding about the relative lengths of genders of *S. fasciatus* in French Guiana. Also, the females of *S. similifasciatus* are longer than those of *S. fasciatus* as reported by Lapèze (2021).

Acknowledgements

I thank Alyssa Seemann (USDA Systematic Entomology Laboratory) for taking and processing photographs and compiling plates, and Lewis Deitz (emeritus, North Carolina State University), Olivia Evangelista (CSIRO, Australia), and an anonymous reviewer for comments on an earlier draft of the manuscript. Mention of trade names or commercial products in this publication is solely for the purpose of providing specific information and does not imply recommendation or endorsement by the USDA. The USDA is an equal opportunity provider and employer.

Additional information

Conflict of interest

The author has declared that no competing interests exist.

Ethical statement

No ethical statement was reported.

Funding

United States Department of Agriculture (USDA) Systematic Entomology Laboratory.

Author contributions

The author solely contributed to this work.

Author ORCIDs

Stuart H. McKamey https://orcid.org/0000-0002-9617-0594

Data availability

All of the data that support the findings of this study are available in the main text.

References

Andrade GS (1989) *Smilidarnis*, a new genus with two new species of Membracidae from South America (Homoptera). Revista Brasileira de Zoologia 6(4): 695–699. https://doi.org/10.1590/S0101-81751989000400015

Deitz LL (1975) Classification of the higher categories of the New World treehoppers (Homoptera, Membracidae). North Carolina Agricultural Experiment Station Technical Bulletin 225: 1–177.

Deitz LL, Wallace MS [team leaders] (2010) [and updates] Treehoppers: Aetalionidae, Melizoderidae, and Membracidae (Hemiptera). http://treehoppers.insectmuseum.org

Dietrich CH, McKamey SH, Deitz LL (2001) Morphology-based phylogeny of the treehopper family Membracidae (Hemiptera: Cicadomorpha: Membracoidea). Systematic Entomology 26: 213–239. https://doi.org/10.1046/j.1365-3113.2001.00140.x

Evangelista O, Flórez-V C, Takiya DM, Cryan JR, Dietrich CH, Urban JM (2017) Molecular-based phylogeny of the treehopper family Membracidae: towards a revised classification of higher-level taxa. In: XV International Auchenorrhyncha Congress Abstracts (unpublished), Mendes, Brazil, 1222–1223.

International Commission on Zoological Nomenclature (1999) International Code of Zoological Nomenclature, 4th edition. xxix, 306 pp. The International Trust for Zoological Nomenclature, London. https://code.iczn.org/?frame=1

Joron M (2009) Chapter 10 - Aposematic Coloration. In: Resh VH, Cardé RT (Eds) Encyclopedia of Insects (2nd Edition). Elsevier Inc., 33–38. https://doi.org/10.1016/B978-0-12-374144-8.00010-2

Lapèze J (2021) Guide illustré des membracides de Guyane Version 3, (privately published) 142 pp. https://www.faune-guyane.fr/index.php?mid=20219

McKamey SH (2023) Three new species of the Neotropical genus *Smilidarnis* Andrade (Hemiptera, Membracidae). ZooKeys 1174: 85–95. https://doi.org/10.3897/zookeys.1174.103324

Mejdalani G (1998) Morfologia externa dos Cicadellinae (Homoptera. Cicadellidae): comparaçao entre *Versigonalia ruficauda* (Walker) e *Tretogonia cribrata* Melichar (Proconiini), com notas sobre outras espécies e análise da terrminologia. Revista Brasileira de Zoologia 19(2): 451–544. https://doi.org/10.1590/S0101-81751998000200015

ZooKeys 1219: 143–163 (2024)
DOI: 10.3897/zookeys.1219.129773

Research Article

A new species of *Pristimantis* (Amphibia, Anura, Strabomantidae) from a montane forest of the Pui Pui Protected Forest in central Peru

Edgar Lehr[1,2], Jiří Moravec[3], Yingtong Wang[1], Marek Uvizl[3,4]

1 *Department of Biology, Illinois Wesleyan University, P.O. Box 2900, Bloomington, IL 61701, USA*
2 *Departamento de Herpetología, Museo de Historia Natural, Universidad Nacional Mayor de San Marcos, Av. Arenales 1256, Jesús María, Lima 15072, Peru*
3 *Department of Zoology, National Museum, Cirkusová 1740, 193 00 Prague 9, Czech Republic*
4 *Department of Zoology, Faculty of Science, Charles University, Viničná 7, Praha 2, Czech Republic*
Corresponding author: Edgar Lehr (elehr@iwu.edu)

Abstract

Herpetological inventories conducted in the Pui Pui Protected Forest in the central Peruvian Andes between 2012 and 2014 revealed unusually high local anuran richness and endemism. Herein, we describe a new species of *Pristimantis* discovered in the buffer zone of the protected area between 1550 and 1730 m a.s.l. The description is based on one subadult male (snout–vent length 14.4 mm), one adult female (snout–vent length 26.4 mm), and six juvenile specimens collected in the montane forest between 1550 and 1730 m a.s.l. DNA barcoding placed *P. vrazi* **sp. nov.** as the sister taxon to *P. rhabdocnemus* and in the clade also containing *P. lindae*, *P. sinschi*, *P. quaquaversus*, and one still unnamed *Pristimantis* species. *Pristimantis vrazi* **sp. nov.** differs from all these closely related species by the combination of the following characters: tuberculate dorsum, presence of the tympanum, presence of dentigerous processes on the vomer, absence of vocal slits, a red median horizontal streak across the iris, a narrow black median vertical streak on the lower half of the eye, cream to dark brown dorsal ground coloration, and cream to gray ventral ground coloration.

Key words: Andes, cryptic species diversity, Enrique Stanko Vráz, *Pristimantis vrazi* new species

Academic editor: Luis Ceríaco
Received: 14 June 2024
Accepted: 12 October 2024
Published: 28 November 2024

ZooBank: https://zoobank.org/F229ADA4-C1EC-40D3-8DFA-D087988EC891

Citation: Lehr E, Moravec J, Wang Y, Uvizl M (2024) A new species of *Pristimantis* (Amphibia, Anura, Strabomantidae) from a montane forest of the Pui Pui Protected Forest in central Peru. ZooKeys 1219: 143–163. https://doi.org/10.3897/zookeys.1219.129773

Introduction

The Pui Pui Protected Forest (PPPF, Figs 1, 2), located in eastern Andes of central Peru, was established in 1985 and covers 60,000 ha (45.5% montane forest, 54.5% puna habitats) between 1700 and 4500 m a.s.l. Its herpetofauna was unknown until Lehr and colleagues started surveys between 2012 and 2014 in both upper montane forest and high Andean grasslands (puna). Their expeditions resulted in the recording of 37 species for the PPPF (22 amphibians, 15 reptiles; Lehr and Moravec 2024), including seven new species of amphibians (six species of the genus *Pristimantis* Jiménez de la Espada, 1870, and one *Phrynopus* Peters, 1873), one new species of gymnophthalmid lizard, and two new gymnophthalmid genera (Lehr and Moravec 2017; Lehr and von May 2017; Lehr et al. 2017b, 2017c, 2018, 2020; Moravec et al. 2018, 2020).

A recent DNA barcoding of an undetermined series of *Pristimantis* obtained in 2013 from montane forests of the PPPF buffer zone (*Pristimantis* sp. 1 and *P.* sp. 2 of Lehr and Moravec 2024) revealed the presence of three species: one clustering together with *P. croceoinguinis* (Lynch, 1968), and two unnamed species that are new to science.

Because one of the new species is only presented by a single barcoded specimen, we hesitate to describe it as a new until additional molecular data support its species status. The second new species is represented by a series of eight specimens and distinguished based on two barcoded adult individuals. Therefore, we describe it herein as a new species of *Pristimantis*, which phenotypically resembles *P. croceoinguinis*, *P. lindae* (Duellman, 1978), *P. rhabdocnemus* (Duellman & Hedges, 2005), and *P. sinschi* Lehr, Moravec & Kodejš, 2020.

Material and methods

Morphological characters

The format for the description follows Lynch and Duellman (1997), except that the term "dentigerous processes of vomers" is used instead of "vomerine odontophores" (Duellman et al. 2006), and the diagnostic characters used are those of Duellman and Lehr (2009). Taxonomic classification follows Hedges et al. (2008), except that we followed Pyron and Wiens (2011) for family placement. The holotype was fixed in 96% ethanol and stored in 70% ethanol. Liver tissue of the holotype and paratype were taken for genetic analyses. Sex and maturity of specimens were identified by observing gonads by dissections. Specimens were considered juveniles when gonads were too small to distinguish between sexes. A specimen with clearly identifiable gonads but with only a slightly larger snout-vent length compared to the largest juvenile was considered a subadult. The following measurements were taken by YW to the nearest 0.1 mm with digital calipers under a stereomicroscope: snout–vent length (**SVL**, straight length distance from tip of snout to vent), tibia length (**TL**, distance from the knee to the distal end of the tibia), foot length (**FL**, distance from proximal margin of inner metatarsal tubercle to tip of toe IV), head length (**HL**, from angle of jaw to tip of snout), head width (**HW**, at level of angle of jaw), horizontal eye diameter (**ED**), interorbital distance (**IOD**), upper eyelid width (**EW**), internarial distance (**IND**), eye–nostril distance (**E–N**, straight line distance between anterior corner of orbit and posterior margin of external nares). Fingers and toes are numbered preaxially to postaxially from I–IV and I–V, respectively. We compared the lengths of toes III and V by adpressing both toes against toe IV; lengths of fingers I and II were compared by adpressing the fingers against each other. Drawings were made by YW using a stereomicroscope and a camera lucida. Photographs taken by EL and JM were used for descriptions of coloration in life. Coloration refers to coloration in life unless otherwise stated. Holotype was photographed by YW submersed in ethanol to avoid reflections. Comparisons of congeners focused on phenotypically similar species from Ecuador and Peru, those with close phylogenetic relationships as recovered in our tree, and species known from the PPPF and its buffer zone. Information on species for comparative diagnoses was obtained from Duellman and Lehr (2009), from original species descriptions, and from examined specimens. For specimens

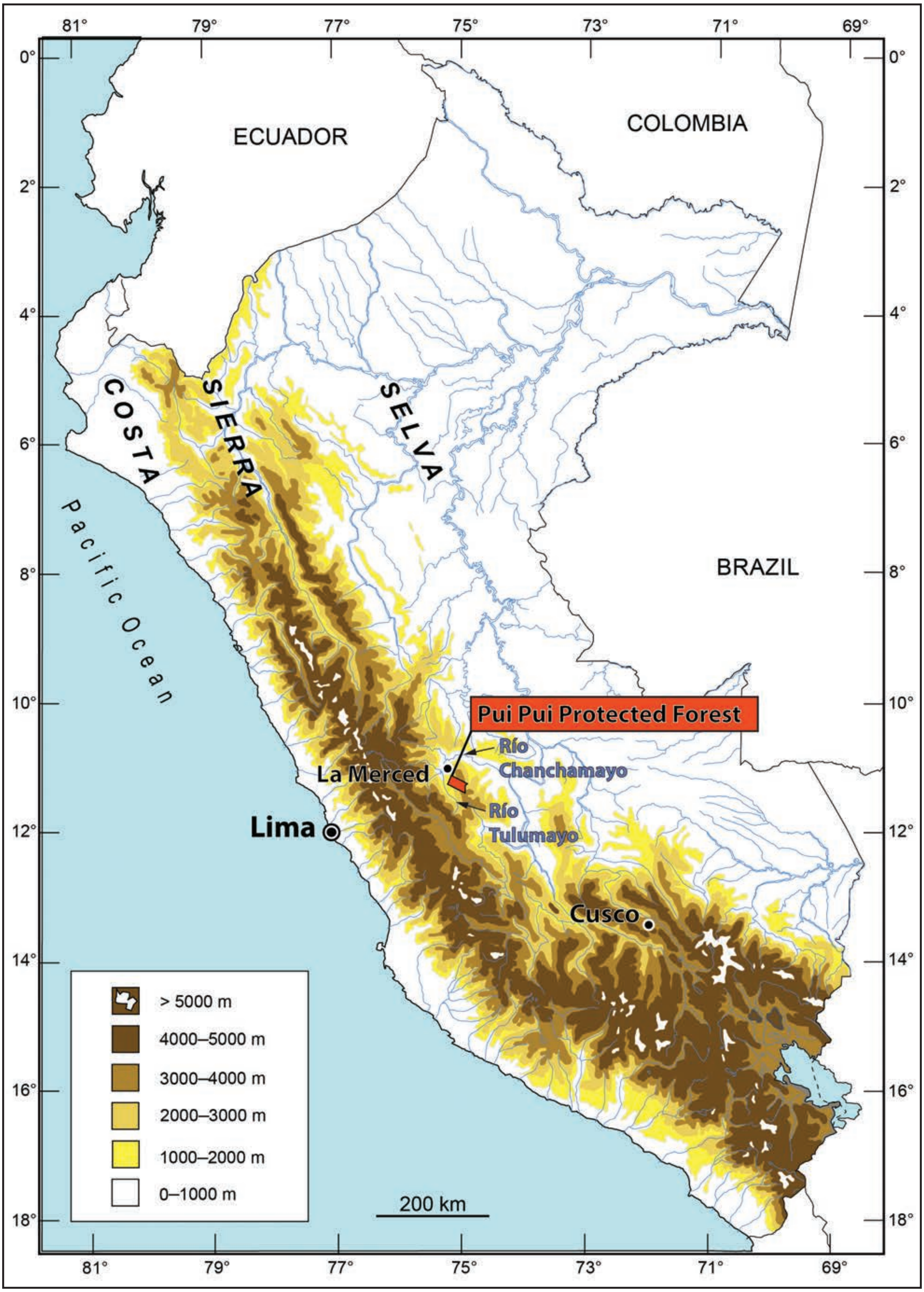

Figure 1. Map of Peru with the Pui Pui Protected Forest (Junín Region) in red.

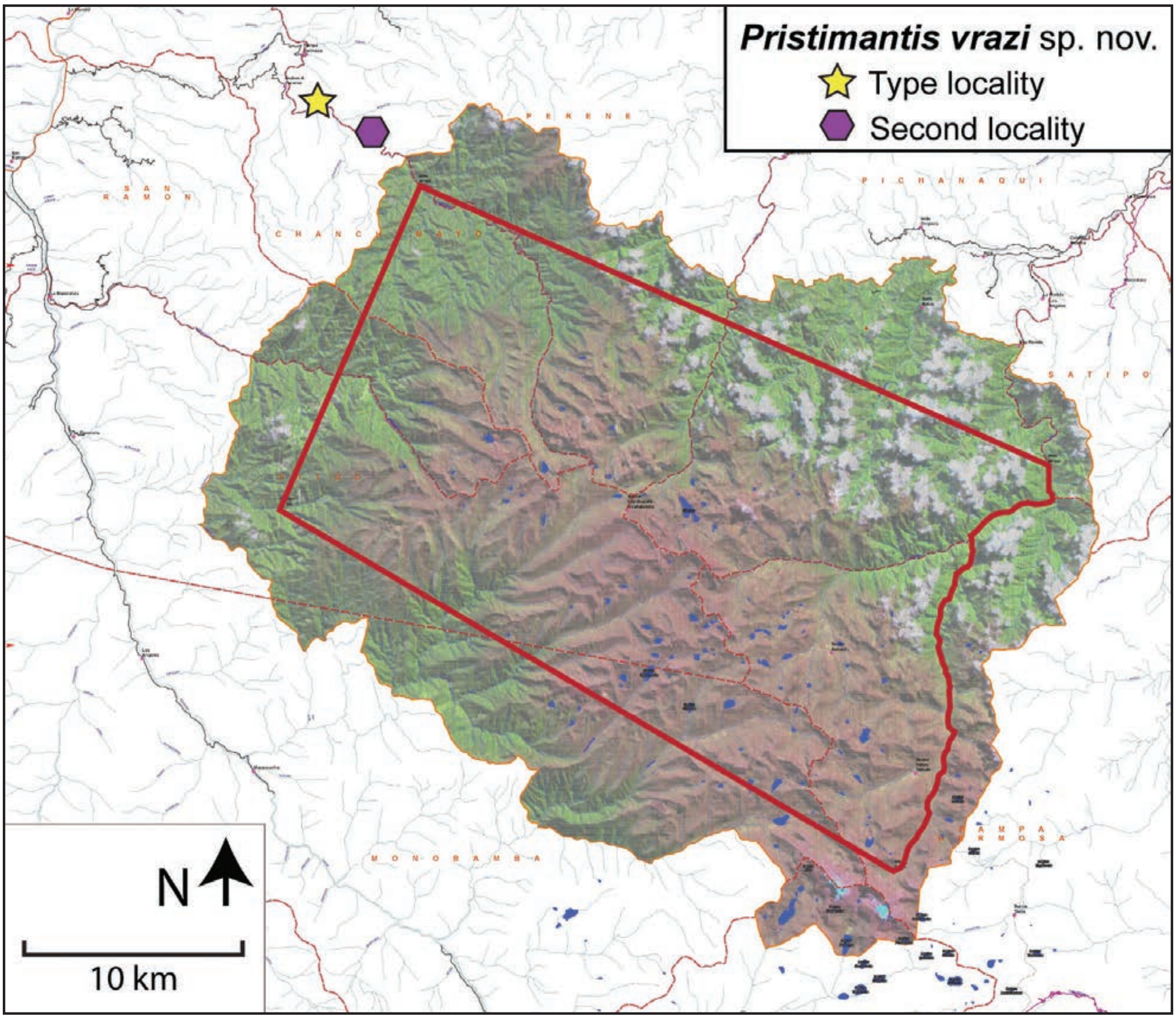

Figure 2. Map of the Pui Pui Protected Forest with the collecting sites of *Pristimantis vrazi* sp. nov.

examined, see Appendix 1 "Comparative specimens examined". Codes of collections are: **IWU** (field number) = Illinois Wesleyan University, Bloomington, USA; **MUSM** = Museo de Historia Natural Universidad Nacional Mayor de San Marcos, Lima, Peru; **NMP-P6V** = National Museum Prague, Prague, Czech Republic. Threat status was assessed using the IUCN criteria (IUCN 2016).

Molecular analysis

Taxon sampling

In this study, we used liver samples of three *Pristimantis* species collected by us in the buffer zone of the PPPF in 2013 to extract DNA. A list of the newly genetically investigated material and its GenBank accession numbers is in Table 1. For the final dataset, we retrieved sequences of numerous additional species of *Pristimantis* from the central Peru stored in the GenBank to show phylogenetic position of our new material in relation to DNA sequences published earlier (most importantly in Duellman and Hedges 2007;

Table 1. Names of taxa, museum numbers, field data, and GenBank accession numbers of the newly genetically investigated material. PPPF = Pui Pui Protected Forest.

Species	Museum number	Locality	Coordinates	Elevation (m)	Collectors; year	GenBank accession number	
						16S	***12S***
P. vrazi sp. nov. (holotype)	MUSM 41581	PPPF buffer zone, Peru	11°05'44.2"S, 75°13'39.8"W	1550	E. Lehr, J. C. Cusi, R. von May, J. Moravec; 2013	PQ330255	PQ345842
P. vrazi sp. nov.	MUSM 41582	PPPF buffer zone, Peru	11°05'44.2"S, 75°13'39.8"W	1550	E. Lehr, J. C. Cusi, R. von May, J. Moravec; 2013	PQ330256	PQ345843
P. croceoinguinis	MUSM 31930	PPPF buffer zone, Peru	11°05'44.2"S, 75°13'39.8"W	1550	E. Lehr, J. C. Cusi, R. von May, J. Moravec; 2013	PQ330254	PQ345841
Pristimantis sp.	MUSM 32735	PPPF buffer zone, Peru	11°12'38.5"S, 74°57'28.9"W	1800	E. Lehr, J. Moravec; 2014	PQ330257	PQ345844

Hedges et al. 2008; Lehr and Moravec 2017; Lehr and von May 2017; Lehr et al. 2017b; Moravec et al. 2020). To obtain more general phylogeny, we also selected and included into our dataset sequences of species representing all main evolutionary lineages and species groups of *Pristimantis* (Padial et al. 2014). As an outgroup, we included GenBank sequences of *Phrynopus*, *Oreobates* Jiménez de la Espada, 1872, *Tachiramantis* Heinicke, Barrio-Amorós & Hedges, 2015, and *Yunganastes* Padial, Castroviejo-Fisher, Köhler, Domic & De la Riva, 2007.

DNA extraction, PCR, sequencing, and sequence alignment

The genomic DNA was extracted from the tissues stored in 96% ethanol using Geneaid Genomic DNA Mini Kit. Two mitochondrial markers, fragments of the genes for 12S rRNA (*12S*) and 16S rRNA (*16S*), that are commonly used in the amphibian DNA barcoding (Vences et al. 2012), were targeted. The primer sequences and PCR conditions were adapted after previous studies (Kocher et al. 1989; Palumbi et al. 1991; Moravec et al. 2009, 2020). The PCR products were subjected to Sanger sequencing forward and reverse directions at Macrogen, Inc. (Amsterdam, the Netherlands), using the PCR primers. The multiple sequence alignment was performed using the implemented MAFFT plugin (Katoh and Standley 2013) in Geneious v. 11.0.5 (https://www.geneious.com), that was subsequently manually edited. The final concatenated alignment was 1850 bp long, consisting of 860 bp from *12S* and 990 bp from *16S*. The aligned matrix was uploaded to Zenodo (https://doi.org/10.5281/zenodo.13934869).

Phylogenetic analysis

The phylogenetic tree was constructed using maximum likelihood (ML). The nucleotide substitution model for each partition, GTR+F+I+R7 for *12S* and TIM2+F+R7 for *16S*, was selected based on the Bayesian information criterion using ModelFinder (Kalyaanamoorthy et al. 2017). The ML analysis was done in IQ-TREE (Chernomor et al. 2016; Nguyen et al. 2015). The search for the best-scoring ML was performed by ultrafast bootstrap (UFBoot; Hoang et al. 2018) with 1000 bootstrap and 1000 topology replicates. The ML analysis was run on the CIPRES Science Gateway (Miller et al. 2010). Uncorrected *p*-distances between haplotypes were calculated in MEGA11 (Tamura et al. 2021).

Results

Molecular phylogenetic analyses

In this study, we generated four new sequences of both *12S* and *16S* for three species of the genus *Pristimantis* from central Peru. Combined with the GenBank sequences, the final dataset comprised 2,394 unique concatenated sequences (1,057 of *12S*, and 2,253 of *16S*) for ingroup *Pristimantis* genus and outgroup *Oreobates*, *Phrynopus*, *Tachiramantis*, and *Yunganastes*.

The final dataset was comprised of 1,306 parsimony informative positions (70.59% of the total length) and missing data accounted for 29.09% bases of the dataset.

The obtained phylogenetic tree (Fig. 3) shows up to 11 clades within the highly supported genus *Pristimantis*. In general, the structure is consistent with clades/species groups reconstructed in our previous studies based on less numerous datasets (Lehr et al. 2017a; Moravec et al. 2020). The newly recognized species, *Pristimantis vrazi* sp. nov., belongs to a well-supported subclade with *P. lindae*, *P. quaquaversus* (Lynch, 1974), *P. rhabdocnemus*, *P. sinschi*, and *Pristimantis* sp. as closest relatives (*P. rhabdocnemus* in sister position). The mean uncorrected genetic *p*-distances values of 16S rRNA barcode between the new species and other members of this subclade vary between 5.01% and 7.52% (Table 2).

The previous undetermined PPPF *Pristimantis* sp. 1 (sensu Lehr and Moravec 2024) clusters together with *P. croceoinguinis* and belongs to a different species-rich clade containing, for example, *P. altamazonicus* (Barbour & Dunn, 1921), *P. ashaninka* Lehr & Moravec, 2017, *P. cruciocularis* (Lehr, Lundberg,

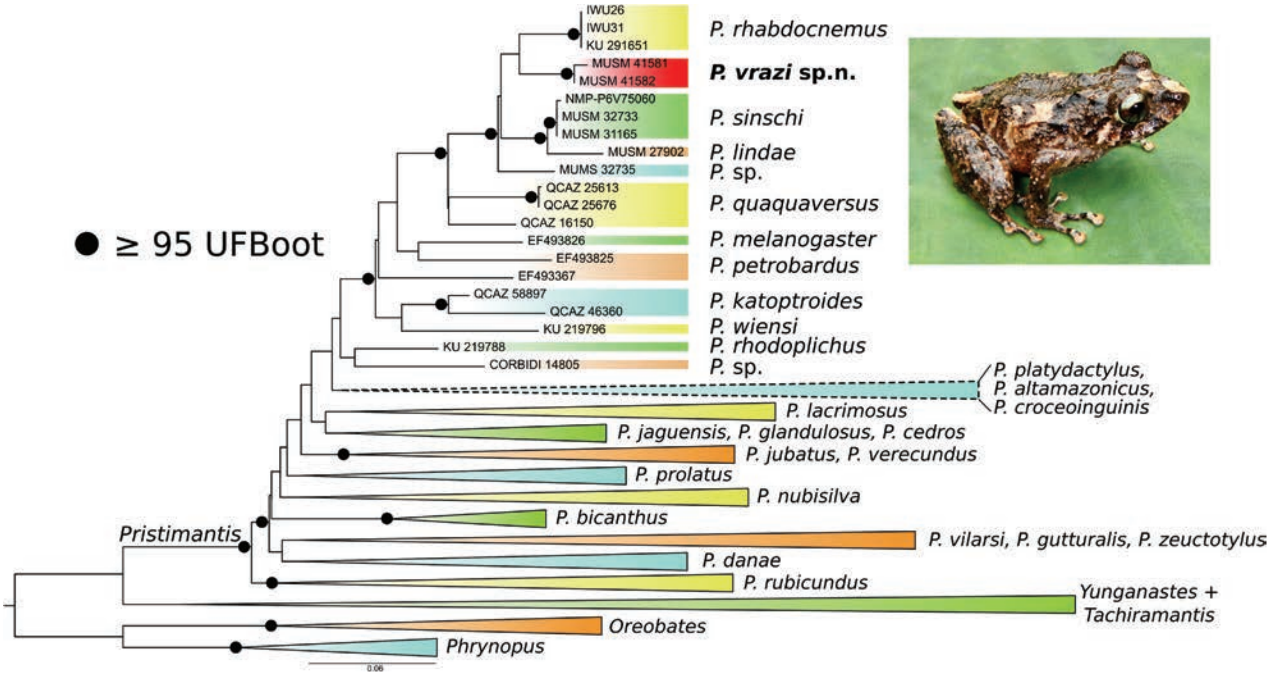

Figure 3. Maximum-likelihood tree of reconstructed phylogenetic relationships of the *Pristimantis* frogs based on the concatenated dataset *12S* and *16S* sequences. Branch support values are shown by black dots on the nodes. The numbers at the tips represent either voucher numbers or GenBank accession numbers. Branch support values are shown by black dots on the nodes. The clade outlined with a dotted line includes the fourth sample molecularly processed in this study, along with other species such as *P. croceoinguinis*, *P. altamazonicus*, *P. ashaninka*, *P. cruciocularis*, and *P. platydactylus*.

Table 2. Mean uncorrected genetic *p*-distance values of 16S rRNA barcode for species from the clade containing *Pristimantis vrazi* sp. nov. and for *P. croceoinguinis*. The distances are shown as percentages.

	Species	1	2	3	4	5	6	7	8	9	10	11
1	*P. rhabdocnemus*	0.00										
2	*P. vrazi* sp. nov.	5.01–5.20	0.46									
3	*P. sinschi*	5.02–5.33	6.34–7.08	0.00								
4	*P. lindae*	6.80–7.22	7.08–7.52	3.05–3.06	–							
5	*Pristimantis* sp.	5.93–6.11	5.61–6.18	4.82	6.11	–						
6	*P. quaquaversus*	8.38–9.64	8.79–12.30	8.18–9.11	9.18–10.36	6.91–9.18	0.00–1.90					
7	*P. melanogaster*	10.05–10.69	10.65–11.21	8.81–8.86	9.16	10.22	7.40–8.88	–				
8	*P. petrobardus*	10.97–11.68	10.53–10.66	8.68–9.74	10.59	10.60	8.20–10.20	7.64	–			
9	*P. katoproides*	8.57–12.74	5.23–11.85	5.71–11.17	5.71–10.55	6.86–11.30	7.48–12.43	4.00–9.87	7.43–10.04	4.00		
10	*P. wiensi*	9.66–10.27	11.55–12.30	8.96–9.01	9.48	11.11	8.18–10.73	8.08	8.92	5.71–9.66	–	
11	*P. croceoinguinis*	16.13–16.95	16.98–17.81	13.46–13.54	14.70	14.84	12.00–14.34	11.51	11.17	12.00–15.41	13.08	–

Aguilar & von May, 2006), *P. platydactylus* (Boulenger, 1903), and many other species (Fig. 3; Lehr et al. 2017a; Moravec et al. 2020).

Taxonomy

Pristimantis vrazi **Moravec, Lehr, Wang & Uvizl, sp. nov.**
https://zoobank.org/BF790673-89B1-45ED-A8B6-51660A874404
Figs 4–8, Tables 1, 2
Suggested English name: Vráz's Robber Frog
Suggested Spanish name: Rana cutín de Vráz

Type material. ***Holotype*****.** MUSM 41581 (field number IWU 200, Figs 4, 5, 7), GenBank accession numbers PQ330255 (*16S*), PQ345842 (*12S*); adult ♀; from buffer zone of the Pui Pui Protected Forest (11°05'44.2"S, 75°13'39.8"W), 1550 m a.s.l., property of Abelardo Cabrejos Vega, Distrito Pichanaqui, Provincia Chanchamayo, Región Junín, Peru; Edgar Lehr, Juan Carlos Cusi, Rudolf von May & Jiří Moravec leg., 10 June 2013.

Paratype**.** MUSM 41582 (IWU 205, Fig. 6), GenBank accession numbers PQ330256 (*16S*), PQ345843 (*12S*); 1 subadult ♂; from the type locality; Edgar Lehr, Juan Carlos Cusi, Rudolf von May & Jiří Moravec leg., 10 June 2013.

Referred specimens. MUSM 31929 (IWU 197), MUSM 41583 (IWU 201), MUSM 31932 (IWU 204), MUSM 31933 (IWU 206) (Fig. 8), 4 juveniles; all from the type locality; Edgar Lehr, Juan Carlos Cusi, Rudolf von May, and Jiří Moravec leg.; 10 June 2013 • MUSM 31937 (IWU 214), MUSM 31983 (IWU 215), 2 juveniles; from the buffer zone of the Pui Pui Protected Forest (11°06'17.0"S, 75°12'26.2"W); 1730 m a.s.l.; Edgar Lehr, Juan Carlos Cusi, Rudolf von May, and Jiří Moravec leg.; 11 June 2013.

Generic placement. We assign this species to *Pristimantis* based on our molecular data (Fig. 3) and the general morphological similarity to other members of the genus.

Diagnosis. A new species of *Pristimantis* not assigned to any species group having the following combination of characters: (1) skin on dorsum shagreen with scattered conical tubercles; skin on venter areolate; weak

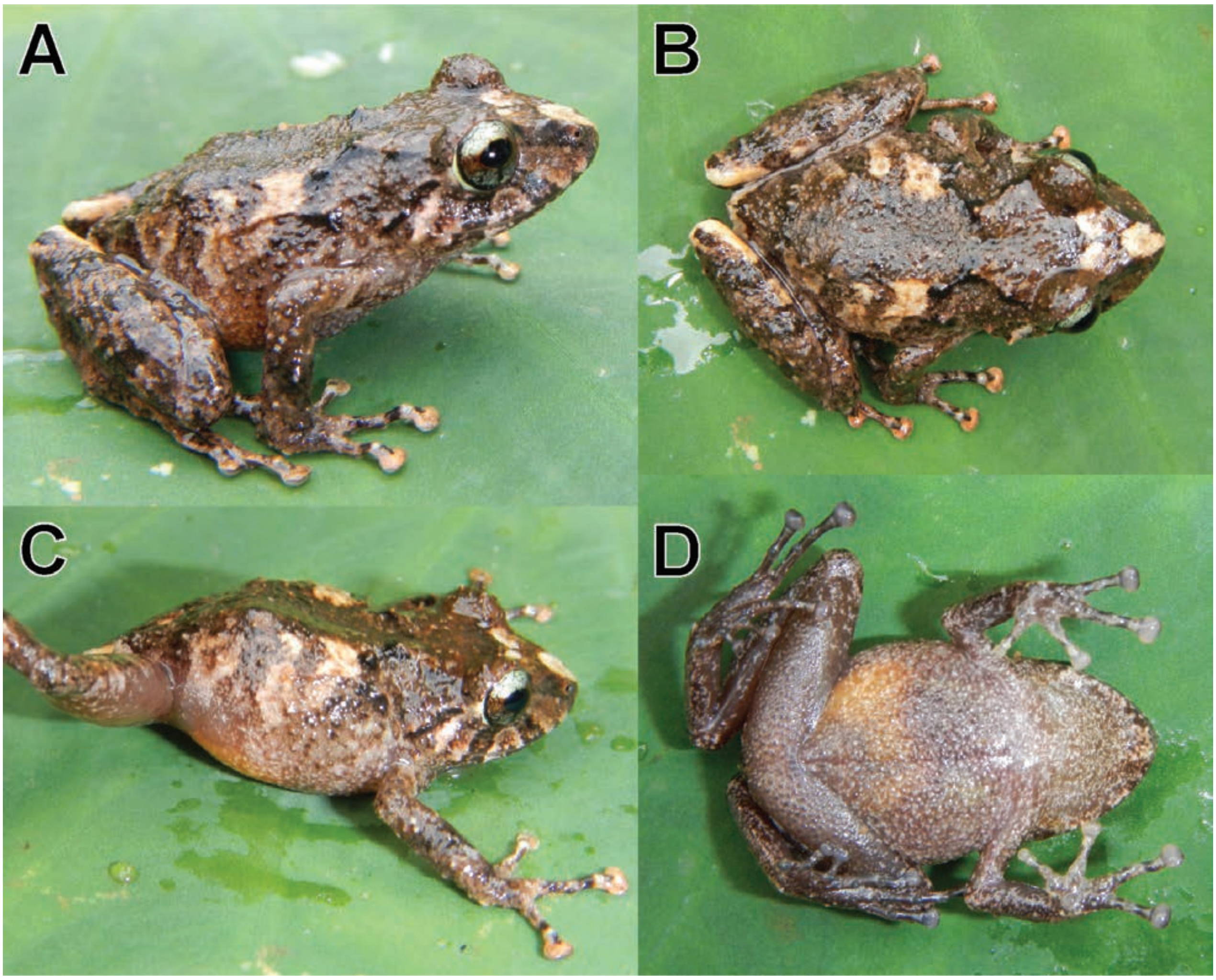

Figure 4. Life adult female holotype (MUSM 41581, SVL = 26.4 mm) of *Pristimantis vrazi* sp. nov. **A** dorsolateral view **B** dorsal view **C** lateral view **D** ventral view. Photos by E. Lehr.

discoidal fold present; short dorsolateral ridges present; (2) tympanic membrane and tympanic annulus present; (3) snout moderately long, acutely rounded in dorsal view, rounded in profile; (4) upper eyelid bearing small conical tubercles; EW narrower than IOD; cranial crest absent; (5) dentigerous processes of vomers present, oblique; (6) vocal slits and nuptial pads absent; (7) finger I shorter than finger II; discs of digits broadly expanded, round, bearing circumferential grooves; (8) fingers with narrow lateral fringes; (9) ulnar tubercles small, round; (10) heel without tubercles; inner tarsal fold absent; inner edge of tarsus with low, elongated tubercles; (11) inner metatarsal tubercle ovoid, 4–5 times larger than outer elongated metatarsal tubercle; numerous supernumerary plantar tubercles; (12) toes with weak lateral fringes; basal toe webbing present; toe V longer than toe III; toe discs smaller than those on fingers, circumferential grooves present; (13) in life, the dorsum ranges from cream to dark grayish brown with a black W-shaped scapular fold, with or without cream blotches; anterior and posterior surfaces of thighs grayish brown with pale gray spots; groin grayish brown with pale-gray spots with or without a hint of olive-green; venter cream to gray with or without numerous small, brown, dark dots; iris pale bronze with fine

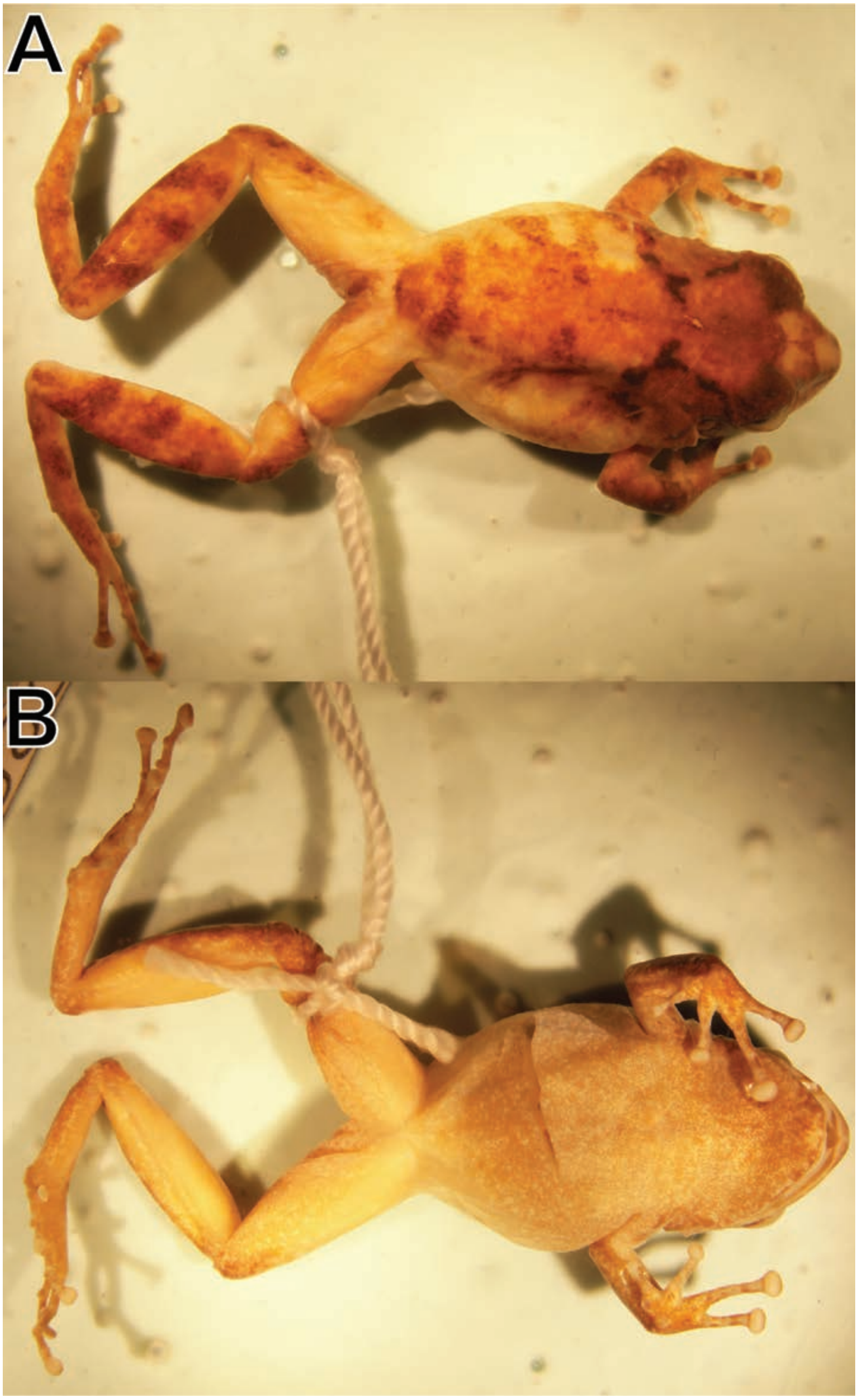

Figure 5. Preserved holotype (MUSM 41581, SVL = 26.4 mm) of *Pristimantis vrazi* sp. nov. **A** dorsal view **B** ventral view. Photos by Y. Wang.

black reticulation, a reddish brown median horizontal streak, and a narrow black median vertical streak on lower half of eye; head light to dark brown dorsally, with or without brown or black interorbital bar and canthal stripes, with or without white spot at dorsal tip of snout; (14) SVL in single subadult male 14.4 mm, in single adult female 26.4 mm.

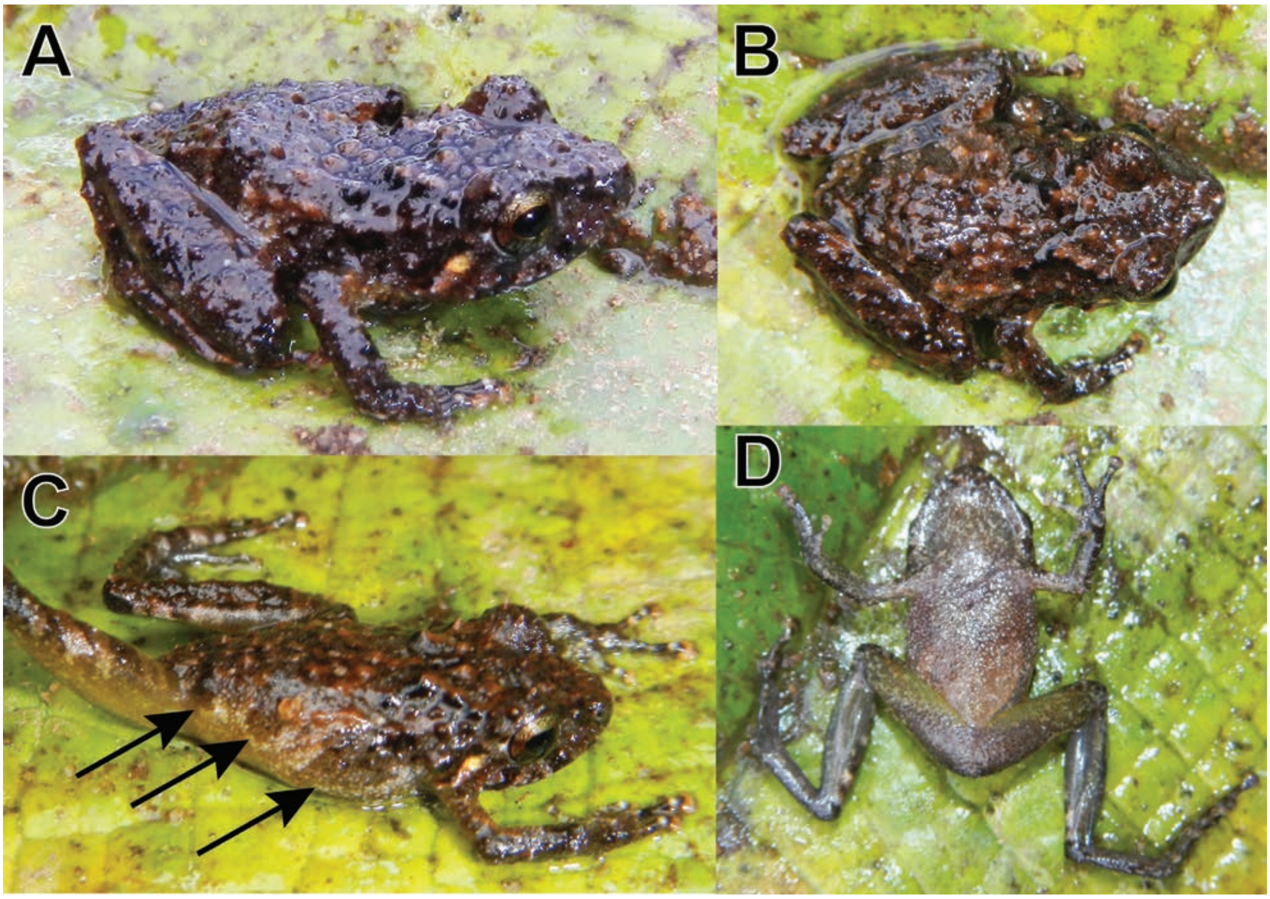

Figure 6. Life subadult male paratype (MUSM 48582, SVL = 14.4 mm) of *Pristimantis vrazi* sp. nov. **A** dorsolateral view **B** dorsal view **C** lateral view **D** ventral views. Arrows indicate the three dark grayish-brown bars on the flank. Photos by E. Lehr.

Comparison. *Pristimantis vrazi* is distinguished from its congeners in Peru (152 species; AmphibiaWeb 2024) by the following combination of characters: dorsum with conical tubercles and short dorsolateral ridges, tympanic membrane and tympanic annulus present, males without vocal slits and nuptial pads, dentigerous processes of vomer present, groin grayish brown with or without a hint of pale olive-green, and iris pale bronze with fine black reticulation, a reddish-brown median horizontal streak, and a narrow black median vertical streak on lower half of eye. The following 11 species of *Pristimantis* have been recorded from montane forests in the PPPF and its surroundings including the Distrito de Pampa Hermosa (Moravec et al. 2020; Venegas et al. 2023; Lehr and Moravec 2024; this paper): *Pristimantis albertus* Duellman & Hedges, 2007, *P. aniptopalmatus* (Duellman & Hedges, 2005), *P. ashaninka*, *P. bipunctatus* (Duellman & Hedges, 2005), *P. clarae* Venegas, García-Ayachi, Marchelie, Ormeño & Catenazzi, 2023, *P. croceoinguinis*, *P. cruciocularis*, *P. sagittulus* (Lehr, Aguilar & Duellman, 2004), *P. sinschi*, *P.* cf. *stictogaster* (Duellman & Hedges, 2005), and *P.* sp.

Comparing to *Pristimantis vrazi* (characters in parentheses), *P. albertus* has distinct dorsolateral folds (short ridges), males with vocal slits (absent), and a yellow groin (grayish brown with pale-gray spots with or without a hint of olive-green) (Duellman and Hedges 2007; Moravec et al. 2020). *Pristimantis aniptopalmatus* has females with SVL up to 22.0 mm (26.4 mm), males have vocal slits (absent), and the iris is grayish white (pale bronze with reddish-brown streak) (Duellman and Hedges 2005). *Pristimantis ashaninka* is only known from the northeastern corner of the PPPF (northwestern corner), and both species have the dorsum with conical tubercles and the venter pale gray and mottled grayish brown. However, *P. ashaninka* lacks a tympanum (present), has the dorsum with a reddish-brown blotch in shape of an hourglass (absent), and the iris with a black narrow upper and lower streak (only lower streak present) (Lehr and Moravec 2017). *Pristimantis vrazi* and *P. bipunctatus* have the iris bronze, with a median horizontal reddish-brown streak. However, *P. bipunctatus* has females with SVL up to 41.5 mm (26.4 mm), males with vocal slits and nuptial pads (absent), and the scapular with a pair of black warts (absent) (Duellman and Lehr 2009). *Pristimantis clarae* was recently described from the Distrito de Pampa Hermosa, but it is a member of the *P. danae* group and differs in having distinct dorsolateral folds (short ridges), heals with low conical tubercles (absent), males with vocal slits (absent), coppery iris (pale bronze with reddish-brown streak), and dorsum with triangular blotches (dorsum dark grayish brown) (Venegas et al. 2023). *Pristimantis croceoinguinis* is known from montane forests in the north-central buffer zone and the eastern corner of the PPPF, and it also has the iris with a reddish-brown median streak and a vertical dark-brown streak at lower half of the eye. However, *P. croceoinguinis* lacks a tympanum (present), and has the groin yellow (grayish brown) (Lynch 1968). *Pristimantis vrazi* and *P. cruciocularis* occur syntopically in the surroundings of the PPPF. However, *P. cruciocularis* lacks a tympanum (present), fingers and toes lack lateral fringes (present), has a red or orange groin (cream to dark brown with or without a hint of olive-green), and has the iris with a dark-brown cross (vertical streak at lower half or iris) (Lehr et al. 2006).

Pristimantis sagittulus from the northwestern part of the PPPF has dentigerous processes of vomers absent (present), males with vocal slits and nuptial pads (both absent), and posterior surfaces of thighs with longitudinal red stripes (no red skin coloration) (Duellman and Lehr 2009). *Pristimantis stictogaster* has vocal slits present (absent), and dark-brown groin with white spots (grayish brown with pale-gray spots with or without a hint of olive-green), and white belly with dark-brown spots (venter cream to gray with or without numerous small dark-brown dots) (Duellman and Lehr 2009). *Pristimantis platydactylus* is known for its remarkable variation in color pattern (De la Riva 1998; Lehr et al. 2006; Duellman and Lehr 2009). However, *P. platydactylus* has the tympanic annulus barely evident (distinct), and males have vocal slits and nuptial pads (both absent).

Our phylogeny (Fig. 3) revealed close phylogenetic similarities of *P. vrazi* with *P. lindae*, *P. quaquaversus*, *P. rhabdocnemus*, *P. sinschi*, and *P.* sp. *Pristimantis vrazi* and *P. lindae* have the iris with a red median horizontal streak and fingers and toes with lateral fringes. However, *P. lindae* has the dorsum shagreen (tuberculate), males with nuptial pads and vocal slits (absent), and a prominent tympanum (not prominent) (Duellman 1978). *Pristimantis quaquaversus* has males with vocal slits (absent), heel with a conical tubercle (absent), tympanic membrane absent (present), and the venter white with or without brown spots (gray and brown mottled) (Lynch 1974). *Pristimantis vrazi* and *P. rhabdocnemus* are related as sister taxa in our phylogeny (Fig. 3), are of similar size, and have a grayish-brown dorsal ground coloration. However, *P. rhabdocnemus* lacks a tympanum (present), lacks dentigerous processes of vomers (present), and has a grayish-tan iris (iris pale bronze with fine black reticulation, a reddish-brown median horizontal streak, and a narrow black median vertical streak on lower half of eye) (Duellman and Hedges 2005). *Pristimantis vrazi* and *P. sinschi* have the dorsum with conical tubercles, the venter areolate, and males that lack vocal slits and nuptial pads, and the iris pale bronze with fine black reticulation and broad median red or reddish-brown band through pupil and a narrow black vertical streak from pupil across lower half of iris (Moravec et al. 2020; this paper). However, *P. sinschi* lacks a tympanum (present), lacks a pale brown tympanic stripe (present), has the groin black with cream blotches (cream to dark brown with or without a hint of olive-green), and venter mottled black and cream (pale gray and brown mottled).

Holotype description. Adult female (Figs 4, 5); head narrower than body, slightly longer than wide; head width 36.4% of SVL; head length 33.3% of SVL; cranial crest absent; snout acutely rounded in dorsal view, round and moderate in length in lateral view, E–N 78.3% of eye diameter; nostrils protuberant, directed dorsolaterally; canthus rostralis straight in dorsal view, rounded in profile; loreal region slightly concave; lips rounded; upper eyelid bearing several small, conical tubercles; EW 85.2% of IOD; supratympanic fold distinct, short, extending diagonally from posterior margin of upper eyelid towards insertion of arm, covering upper and posterior margin of the tympanum; tympanic membrane and tympanic annulus present, more distinct on the right side of head, tympanum 29.3% of ED; several conical postrictal tubercles present bilaterally, some fusing to short ridges. Choanae small, ovoid; dentigerous processes of vomers oblique and round; tongue longer than wide, not notched posteriorly, posterior one-third free.

Skin on dorsum (Fig. 4B) shagreen, with many scattered tubercle, with short, weakly defined dorsolateral fold on anterior half of body (Fig. 4A); skin on flanks shagreen with scattered tubercles (Fig. 4C); skin on throat and chest smooth, belly areolate (Fig. 4D); discoidal and thoracic folds weakly defined; cloacal sheath short.

Outer ulnar surface with numerous minute tubercles; outer palmar tubercle round and slightly bifid, inner palmar tubercle ovoid, approximately one-half size of outer tubercle; distinct supernumerary tubercles, ovoid, approximately one-half size of subarticular tubercles; subarticular tubercles well defined, round in ventral view, conical in lateral view; fingers with narrow lateral fringes; finger I shorter than finger II; discs on fingers broadly expanded, rounded, bearing circumferential grooves (Fig. 7A).

Hind limbs long, slender, tibia length 53.1% of SVL; foot length 43.6% of SVL; upper surface of hind limbs shagreen with many scattered tubercles; anterior surface of thighs smooth, posterior and ventral surfaces of the thighs areolate; heels without conical tubercles; outer surface of tarsus with minute tubercles; inner tarsal fold not present; inner metatarsal tubercle ovoid, 4–5 times size of ovoid outer metatarsal tubercle; subarticular tubercles well defined, round in ventral view, conical in lateral view; few plantar supernumerary tubercles distinct, about one-fourth size of subarticular tubercles; toes with narrow lateral fringes; basal webbing present, most prominent between toes IV and V; discs expanded, slightly truncated, slight smaller as discs on fingers, bearing circumferential grooves; relative length of toes: I <II<III<V<IV (Fig. 7B).

In life (Fig. 4), dorsum dark grayish brown with a black W-shaped scapular fold; head dorsally with a pale brown interorbital bar and a pale cream blotch on snout, head laterally grayish brown with a dark-brown canthal stripe, a dark-brown supratympanic stripe, two dark-brown labial bars below eye and distinct

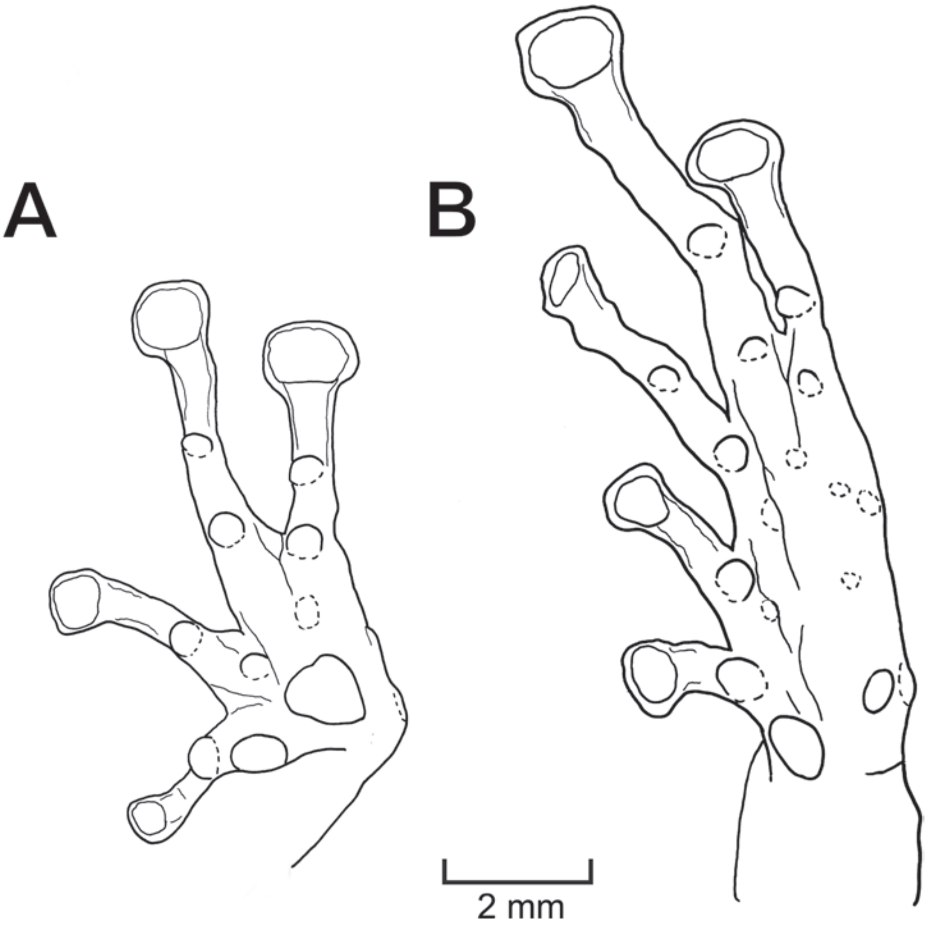

Figure 7. Holotype (MUSM 41581) of *Pristimantis vrazi* sp. nov. **A** ventral view of hand **B** ventral view of foot, preserved toes are not on the same plane, resulting in an artifact with toe V appearing thinner than it is. Drawings by Y. Wang.

pale brown tympanic stripe from posterior outer corner of upper eyelid to corner of mouth; arms dorsally grayish brown with a dark-brown diagonal bar on lower arm; hind limbs dorsally grayish brown with three dark-brown diagonal bars; flanks pale brown with three diagonal dark grayish-brown bars alternating with three pale-brown diagonal to vertical bars; groin, anterior and posterior surfaces of thighs grayish brown with pale-gray spots; throat, chest, belly, and extremities pale-gray and dark-brown mottled; finger and toe discs dorsally pale reddish brown; iris pale bronze with fine black reticulation, a reddish-brown median horizontal streak, and a narrow black median vertical streak at lower half of eye.

In alcohol (Fig. 5) after 10 years, the dorsal ground coloration is pale brown with dark-brown flecks, dark brown W-shaped ridge in scapular area, cream interorbital bar and cream blotch on snout; flanks cream with three pale-brown stripes; groin, anterior and posterior surfaces of thighs cream; thighs and tibias ventrally cream, throat, chest, and belly cream and pale grayish-brown mottled; iris pale gray.

Holotype measurements (in mm). SVL 26.4; TL14.0; FL 11.5; HL 8.8; HW 9.6; ED 3.7; TY 1.1; IOD 2.7; EW 2.3; IND 2.1; E–N 2.9.

Variation. The single subadult male paratype MUSM 41582 (Fig. 6) has following measurements (in mm): SVL 14.4; TL 8.2; FL 6.3; HL 5.0; HW 5.4; ED 2.3; TY 0.4; IOD 2.2; EW 1.2; IND 1.2; E–N 1.6. It has strongly tuberculated dorsum (tubercles of conical shape), dark grayish-brown dorsum with reddish-brown flecks. The flanks bear three dark grayish-brown bars (Fig. 6C). The six juvenile referred specimens (Fig. 8, SVL = 11.9–14.3 mm) have the dorsum tuberculate, the venter pale to dark gray, with brown mottling, the iris pale bronze with fine black reticulation, a reddish-brown median horizontal streak, and a narrow black median vertical streak on lower half of the eye, and a distinct pale-cream tympanic stripe (Fig. 8C). One specimen (MUSM 31929, Fig. 8A) has a middorsal pale cream stripe that is narrow on the head and wider on its back.

Etymology. We dedicate this new species to the Czech explorer and patriot Enrique Stanko Vráz (1860–1932), who explored Africa, South America, and eastern Asia (Todorová 2006). In South America, he spent several years

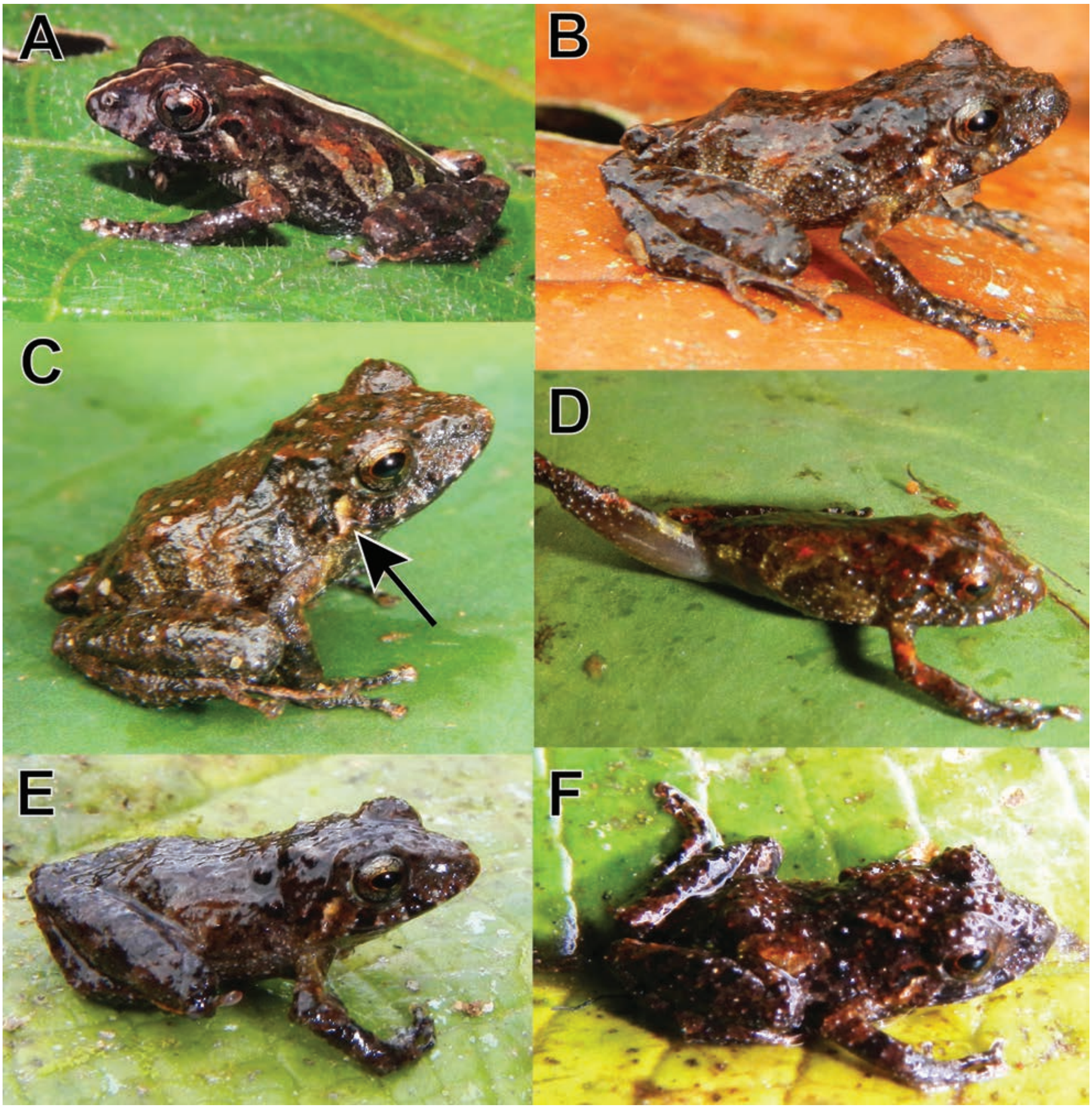

Figure 8. Juvenile referred specimens of *Pristimantis vrazi* sp. nov. **A** MUSM 31929, SVL = 12.3 mm **B** MUSM 31933, SVL = 12.0 mm **C** MUSM 41583, SVL = 14.1 mm **D** MUSM 31937, SVL = 11.9 mm **E** MUSM 31932, SVL = 14.3 mm **F** MUSM 31938, SVL = 12.1 mm. Photo A by J. Moravec, all others by E. Lehr.

Figure 9. Valley of the Rio Huatziroqui in the buffer zone of the Pui Pui Protected Forest, type locality of *Pristimantis vrazi* sp. nov. Type specimens were collected along the river at elevations between 1550 m and 1730 m a.s.l. Photo by J. Moravec.

working in Venezuela and traveling by boat from Venezuela to Peru via the Rio Orinoco, Rio Negro, and Rio Amazonas before crossing the Andes and working around Cajamarca. His specimen collections (animals, artifacts) were sent to the National Museum in Prague. He published his travels and observations in South America in a book (Vráz 1900) that provides valuable original insights into South American nature and indigenous peoples at the end of the 19th century and still inspires people. The specific epithet is used as a noun in apposition.

Distribution and natural history. *Pristimantis vrazi* is only known from two localities of the northwestern corner of the buffer zone of the Pui Pui Protected Forest (Fig. 2) between 1550 and 1730 m a.s.l. The type locality lies in the valley of Rio Huatziroqui (Fig. 9). The slopes of the valley are covered by primary mountain rainforest characterized by a 15–20 m high canopy. The type specimens were collected on the right bank of the river. They inhabited a disturbed forest that was interspersed with small coffee plantations, solitary houses of local coffee farmers, and various forest paths. All specimens were found at night on low vegetation (up to 80 cm above ground). The holotype was found at 8:55 p.m. on a leaf 80 cm above ground. Other syntopic frogs include *Pristimantis bipunctatus*, *P. cruciocularis*, and the hylid *Boana aguilari*. Considering the sparse data available, we here classify *P. vrazi* as Data Deficient according to the IUCN Red List criteria.

Discussion

It is a common practice for taxonomists to describe at first the “easy” new species, those that are easily recognized based on unique characters, and leave the more challenging taxa for later. Lehr and colleagues followed this approach and described six new species from the PPPF in 2017, one new reptile species and genus in 2018, a new reptile genus in 2019, and one new species in 2020 (Lehr and von May 2017; Lehr and Moravec 2017; Lehr et al. 2017b, 2017c, 2018, 2020; Moravec et al. 2018, 2020). A series of 11 specimens of *Pristimantis* sp. that were difficult to identify were kept in a jar, and we assumed that they represented one new species. Hence, we collected tissues selectively to cover the different collecting sites. Surprisingly, our molecular phylogeny (Fig. 3) revealed three species of *Pristimantis*. One is *P. croceoinguinis* (listed as *Pristimantis* sp. 1 and shown in photos 63 and 64 in Lehr and Moravec (2024). Two other species are new to science. The first of them is named *Pristimantis* sp. 2 by Lehr and Moravec (2024; photos 65 and 66) and *Pristimantis* sp. in this paper; at present, it is represented by a single barcoded sample, and more robust molecular data support is necessary for its proper delimitation. The second new species (not pictured by Lehr and Moravec 2024) is described herein as *P. vrazi*. According to Venegas et al. (2023), 34 new *Pristimantis* species were discovered in the Cordillera Oriental in central Peru (Regións Huánuco, Pasco, and Junín) in the last two decades. Including their *P. clarae* and our *P. vrazi*, this number has increased to 36 species. Venegas et al. (2023) pointed out that many species of *Pristimantis* are endemic to small montane areas and valleys where they may be threatened by habitat destruction. Our herpetological surveys show that local endemism of the *Pristimantis* species is very high in the PPPF. Up to date, 15 *Pristimantis* species have been recognized in this protected area (including the puna habitats) and its buffer zone, and eight of them (53%) appear to be endemic. Comparison of *Pristimantis* diversity in three most thoroughly surveyed part of the PPPF—Rio Huatziroqui valley (8 species/2 endemics), Rio Bravo valley (5 species/2 endemics), and central and southeastern part of the puna zone (4 species/4 endemics)—reveals that the local endemism reaches 25–100%. This finding, which underlines the exceptionality of the local anuran fauna, can be explained by the geography of the PPPF. The protected area is located on the northwestern spur of the eastern Andes, which has the character of a mountainous peninsula. The upper part of this peninsula is covered with puna, and its western, northern, and eastern edges descend into deep valleys covered with cloud forests and mountain rainforests. Individual valleys are isolated from each other by mountain ridges. Members of the genus *Pristimantis* generally have low vagility (Duellman and Lehr 2009). They may, therefore, be a case where allopatric speciation contributed to the emergence of many local, geographically isolated species. Similarly, a high rate of local *Pristimantis* endemism can also be detected in other isolated mountain areas in central Peru. For example, data on the anuran diversity of the Cordillera Yanachaga (Pasco Region) available in Angulo et al. (2016) and Frost (2024) show a similar level of local endemism in the genus *Pristimantis*—nine (53%) of the 17 observed species are endemic. Protected areas such as the PPPF or Yanachaga-Chemillén National Park are, therefore, of fundamental importance for the protection of the unique anuran diversity of the eastern Andes of central Peru.

Dedicating new species to people (eponyms), especially in the past or from the past, has caused public protest when their misconduct, racism, or misogyny was revealed, and demands to change the popular names have arose (e.g., North American bird species; Ogden 2024). To avoid such problems, we have carefully reviewed Vráz's biography and publications (e.g., Vráz 1900; Todorová

2006) and did not notice any misconduct or dishonorable behavior. Consequently, we feel reassured to honor Enrique Stanko Vráz for his accomplishments in the exploration of South American nature with this species' dedication. His books, unfortunately not translated into English, still inspire many readers.

Acknowledgements

We thank J.C. Cusi and R. von May for assisting in the fieldwork in 2013. We thank C. Aguilar (MUSM, Lima, Peru) for the loan of specimens. Collecting and export permits were issued by the Ministerio del Ambiente, Lima, Peru. IACUC at IWU approved the research proposal (IACUC 11-003). We thank P. Székely and an anonymous reviewer for their feedback that improved our manuscript.

Additional information

Conflict of interest

The authors have declared that no competing interests exist.

Ethical statement

No ethical statement was reported.

Funding

The work by EL was funded by a Northern European Explorers Grant (GEFNE13-11) funded by National Geographic Society Science and Exploration Europe. The work of JM and MU was financially supported by the Ministry of Culture of the Czech Republic (DKRVO 2024–2028/6.I.a, National Museum of the Czech Republic, 00023272).

Author contributions

EL, JM collected specimens, EL, JM, YW, performed morphological comparisons, all authors contributed figures. JM and MU obtained genetic data and performed phylogenetic analyses. All authors analyzed the data and wrote the manuscript.

Author ORCIDs

Edgar Lehr https://orcid.org/0000-0002-0517-390X
Jiří Moravec https://orcid.org/0000-0003-4114-7466
Marek Uvizl https://orcid.org/0000-0001-6366-8567

Data availability

All of the data that support the findings of this study are available in the main text or Supplementary Information.

References

AmphibiaWeb (2024) AmphibiaWeb. Information on amphibian biology and conservation. http://amphibiaweb.org/ [Accessed 21 September 2024]

Angulo A, von May R, Icochea J, Chaparro JC, Hedges SB, Lehr E, López DG, Lundberg M, Moravec J (2016) Parque Nacional Yanachaga-Chemillén, Pasco, Perú. Anfibios del bosque de nubes y su zona de amortiguamiento. Field Guides, no. 738. The Field Museum, Chicago, USA, 6 pp.

Chernomor O, von Haeseler A, Minh BQ (2016) Terrace aware data structure for phylogenomic inference from supermatrices. Systematic Biology 65: 997–1008. https://doi.org/10.1093/sysbio/syw037

De la Riva I (1998) Redescription, variation, biology, and distribution of *Eleutherodactylus platydactylus* (Boulenger, 1903) (Amphibia: Anura: Leptodactylidae), the taxonomic status of *E. bockermanni* Donoso-Barros, 1970, and comments on polymorphism in anurans. Revista Española de Herpetologia 11: 71–90.

Duellman WE (1978) New species of leptodactylid frogs of the genus *Eleutherodactylus* from the Cosñipata Valley, Perú. Proceedings of the Biological Society of Washington 91: 418–430.

Duellman WE, Hedges SB (2005) Eleutherodactyline frogs (Anura: Leptodactylidae) from the Cordillera Yanchaga in central Peru. Copeia 2005: 526–538. https://doi.org/10.1643/CH-05-019R

Duellman WE, Hedges SB (2007) Three new species of *Pristimantis* (Lissamphibia, Anura) from montane forests of the Cordillera Yanachaga in Central Peru. Phyllomedusa 6: 119–135. https://doi.org/10.11606/issn.2316-9079.v6i2p119-135

Duellman WE, Lehr E (2009) Terrestrial-breeding Frogs (Strabomantidae) in Peru. Natur und Tier-Verlag, Münster, 382 pp.

Duellman WE, Lehr E, Venegas PJ (2006) Two new species of *Eleutherodactylus* (Anura: Leptodactylidae) from northern Peru. Zootaxa 1285: 51–64. https://doi.org/10.11646/zootaxa.1285.1.4

Frost DR (2024) Amphibian species of the world: an online reference. [Downloadable from] http://research.amnh.org/herpetology/amphibia/index.html [Accessed 18 May 2024]

Hedges SB, Duellman WE, Heinicke H (2008) New world direct-developing frogs (Anura: Terrarana): molecular phylogeny, classification, biogeography, and conservation. Zootaxa 1737: 1–182. https://doi.org/10.11646/zootaxa.1737.1.1

Hoang DT, Chernomor O, von Haeseler A, Minh BQ, Vinh LS (2018) UFBoot2: improving the ultrafast bootstrap approximation. Molecular Biology and Evolution 35: 518–522. https://doi.org/10.1093/molbev/msx281

IUCN [Standards and Petitions Subcommittee] (2016) Guidelines for using the IUCN Red List categories and criteria. Version 12. Prepared by the Standards and Petitions Subcommittee. http://www.iucnredlist.org/documents/RedListGuidelines.pdf [Accessed 10 June 2024]

Kalyaanamoorthy S, Minh BQ, Wong TKF, von Haeseler A, Jermiin LS (2017) ModelFinder: Fast model selection for accurate phylogenetic estimates. Nature Methods 14: 587–589. https://doi.org/10.1038/nmeth.4285

Katoh K, Standley DM (2013) MAFFT Multiple Sequence Alignment Software Version 7: improvements in performance and usability. Molecular Biology and Evolution 30: 772–780. https://doi.org/10.1093/molbev/mst010

Kocher TD, Thomas WK, Meyer A, Edwards SV, Pääbo S, Villablanca FX, Wilson AC (1989) Dynamics of mitochondrial DNA evolution in animals: amplification and sequencing with conserved primers. Proceedings of the National Academy of Sciences of the United States of America 86: 6196–6200. https://doi.org/10.1073/pnas.86.16.6196

Lehr E, Moravec J (2017) A new species of *Pristimantis* (Amphibia, Anura, Craugastoridae) from a montane forest of the Pui Pui Protected Forest in central Peru (Región Junín). ZooKeys 645: 85–102. https://doi.org/10.3897/zookeys.645.11221

Lehr E, Moravec J (2024) Región Junín, Peru. Amphibians and Reptiles of the Pui Pui Protected Forest. Field Guides, no. 1672. The Field Museum, Chicago, USA, 7 pp.

Lehr E, von May R (2017) A new species of terrestrial-breeding frog (Amphibia, Craugastoridae, *Pristimantis*) from high elevations of the Pui Pui protected Forest in central Peru. ZooKeys 660: 17–42. https://doi.org/10.3897/zookeys.660.11394

Lehr E, Aguilar C, Duellman WE (2004) A striking new species of *Eleutherodactylus* from Andean Peru (Anura: Leptodactylidae). Herpetologica 60: 275–280. https://doi.org/10.1655/03-24

Lehr E, Moravec J, von May R (2020) A new cryptic genus of terrestrial lizard (Gymnophthalmidae, Cercosaurinae) from the eastern Andes of central Peru. Salamandra 56: 1–15.

Lehr E, Lundberg M, Aguilar C, von May R (2006) New species of *Eleutherodactylus* (Anura: Leptodactylidae) from the eastern Andes of central Peru with comments on central Peruvian *Eleutherodactylus*. Herpetological Monographs 20: 105–128. https://doi.org/10.1655/0733-1347(2007)20[105:NSOEAL]2.0.CO;2

Lehr E, Moravec J, Cusi JC, Gvoždík V (2017a) A new minute species of *Pristimantis* (Amphibia: Anura: Craugastoridae) with a large head from the Yanachaga-Chemillén National Park in central Peru, with comments on the phylogenetic diversity of *Pristimantis* occurring in the Cordillera Yanachaga. European Journal of Taxonomy 325: 1–22. https://doi.org/10.5852/ejt.2017.325

Lehr E, von May R, Moravec J, Cusi JC (2017b) Three new species of *Pristimantis* (Amphibia, Anura, Craugastoridae) from upper montane forests and high Andean grasslands of the Pui Pui Protected Forest in central Peru. Zootaxa 4299: 301–336. https://doi.org/10.11646/zootaxa.4299.3.1

Lehr E, von May R, Moravec J, Cusi JC (2017c) A new species of *Phrynopus* (Amphibia, Anura, Craugastoridae) from upper montane forests and high Andean grasslands of the Pui Pui Protected Forest in central Peru. ZooKeys 713: 131–157. https://doi.org/10.3897/zookeys.713.20776

Lehr E, Moravec J, Whitworth A, Villacampa J, Cusi JC, von May R (2018) New distribution records for *Euspondylus excelsum* Chávez, Catenazzi & Venegas, 2017 (Reptilia, Gymnophthalmidae, Cercosaurinae) in Peru. Check List 14: 1141–1149. https://doi.org/10.15560/14.6.1141

Lynch JD (1968) Two new frogs of the genus *Eleutherodactylus* from eastern Ecuador (Amphibia: Leptodactylidae). Journal of Herpetology 2: 129–135. https://doi.org/10.2307/1563112

Lynch JD (1974) New species of frogs (Leptodactylidae: *Eleutherodactylus*) from the Amazonian lowlands of Ecuador. Occasional Papers of the Museum of Natural History, University of Kansas 31: 1–22. https://doi.org/10.5962/bhl.part.29037

Lynch JD, Duellman WE (1997) Frogs of the genus *Eleutherodactylus* in western Ecuador: systematics, ecology, and biogeography. Special Publication Natural History Museum University of Kansas 23: 1–236. https://doi.org/10.5962/bhl.title.7951

Miller MA, Pfeiffer W, Schwartz T (2010) Creating the CIPRES Science Gateway for inference of large phylogenetic trees. In: Anonymous (Ed.) Gateway Computing Environments Workshop (GCE), 14 Nov. 2010. Curran Associates, New Orleans, 1–8. https://doi.org/10.1109/GCE.2010.5676129

Moravec J, Aparicio J, Guerrero-Reinhard M, Calderon G, Jungfer KH, Gvoždík V (2009) A new species of *Osteocephalus* (Anura: Hylidae) from Amazonian Bolivia: first evidence of tree frog breeding in fruit capsules of the Brazil nut tree. Zootaxa 2215: 37–54. https://doi.org/10.11646/zootaxa.2215.1.3

Moravec J, Šmíd J, Štundl J, Lehr E (2018) Systematics of Neotropical microteiid lizards (Gymnophthalmidae, Cercosaurinae), with the description of a new genus and species from the Andean montane forests. ZooKeys 774: 105–139. https://doi.org/10.3897/zookeys.774.25332

Moravec J, Lehr E, Kodejš K (2020) A new species of *Pristimantis* (Amphibia, Anura, Strabomantidae) from the Pui Pui Protected Forest (central Peru), with comments on *Pristimantis albertus* Duellman & Hedges, 2007. ZooKeys 994: 125–148. https://doi.org/10.3897/zookeys.994.56277

Nguyen L, Schmidt HA, von Haesler A, Minh BQ (2015) IQ-TREE: a fast and effective stochastic algorithm for estimating maximum likelihood phylogenies. Molecular Biology and Evolution 32: 268–274. https://doi.org/10.1093/molbev/msu300

Ogden LE (2024) Inclusive language in biological sciences: A work in progress. BioScience 74(4): 232–237. https://doi.org/10.1093/biosci/biae005

Padial JM, Grant T, Frost DR (2014) Molecular systematics of terraranas (Anura: Brachycephaloidea) with an assessment of the effects of alignment and optimality criteria. Zootaxa 3825: 1–132. https://doi.org/10.11646/zootaxa.3825.1.1

Palumbi S, Martin A, Romano S, McMillan WO, Stice L, Grabowski G (1991) The Simple Fool’s Guide to PCR. Version 2. University of Hawaii, Honolulu, 47 pp.

Pyron RA, Wiens JJ (2011) A large-scale phylogeny of Amphibia including over 2800 species, and a revised classification of extant frogs, salamanders, and caecilians. Molecular Phylogenetics and Evolution 61: 543–583. https://doi.org/10.1016/j.ympev.2011.06.012

Tamura K, Stecher G, Kumar S (2021) MEGA11: molecular evolutionary genetics analysis version 11. Molecular Biology and Evolution 38: 3022–3027. https://doi.org/10.1093/molbev/msab120

Todorová J (2006) Enrique Stanko Vráz. Záhadný cestovatel fotograf. [Enrique Stanko Vráz. Mysterious traveller photographer]. National Museum, Prague, 186 pp. [In Czech with English summary]

Vences M, Nagy ZT, Sonet G, Verheyen E (2012) DNA barcoding amphibians and reptiles. In: Kress WJ, Erickson DL (Eds) DNA Barcodes: Methods and Protocols. Methods in Molecular Biology 858. Springer Nature, Cham, 79–107. https://doi.org/10.1007/978-1-61779-591-6_5

Venegas PJ, García-Ayachi LA, Marchelie A, Ormeño JR, Catenazzi A (2023) A new species of terrestrial-breeding frog, genus *Pristimantis* (Anura: Strabomantidae), from the Peruvian Yungas of Central Peru. Taxonomy 3: 331–1345. https://doi.org/10.3390/taxonomy3020019

Vráz ES (1900) Napříč rovníkovou Amerikou. [Across Equatorial America]. Bursík and Kohout, Prague, [v–xv, 940 +] 86 pp. [In Czech]

Appendix 1

Comparative specimens examined.

Pristimantis albertus (5): Peru, Junín: Pui Pui Protected Forest (Rio Huatziroqui valley, 11°07'37.2"S, 75°10'37.0"W), 1970 m a.s.l., MUSM 31953, 31956, 31959, NMP-P6V 75067, 76021.

Pristimantis aniptopalmatus (2): Peru, Junín: buffer zone of the Pui Pui Protected Forest, 1970 m a.s.l., MUSM 33996, NMP-P6V 75055.

Pristimantis bipunctatus (2): Peru, Junín: buffer zone of the Pui Pui Protected Forest (11°05'44.2"S, 75°13'39.8"W), 1550 m a.s.l., MUSM 31926, 31931.

Pristimantis cruciocularis (2): Peru, Junín: buffer zone of the Pui Pui Protected Forest (11°06'17.0"S, 75°12'26.2"W), 1730 m a.s.l., MUSM 31935, 31939.

Pristimantis croceoinguinis (3): Peru, Junín: buffer zone of the Pui Pui Protected Forest (11°05'44.2"S, 75°13'39.8"W), 1550 m a.s.l., MUSM 31930; buffer zone of the Pui Pui Protected Forest (11°06'17.0"S, 75°12'26.2"W), 1730 m a.s.l., MUSM 31958; buffer zone of the Pui Pui Protected Forest, San Juan de Miraflores (11°06'19.3"S, 75°00'02.5"W), 1400 m a.s.l., MUSM 31154.

Pristimantis lindae (3): Peru, Cusco: Alto Shima, 1785 m a.s.l., MUSM 26528, 26542; Alto Shima, 1790 m a.s.l., MUSM 26540.

Pristimantis sagittulus (2): Peru: Junín: from the Pui Pui Protected Forest (Rio Huatziroqui valley, 11°07'37.2"S, 75°10'37.0"W), 1970 m a.s.l., MUSM 31952.

Pristimantis sinschi (2): Peru: Junín: from the Pui Pui Protected (Rio Bravo valley, 11°12'38.5"S, 74°57'28.9"W), 1800 m a.s.l., MUSM 32733, NMP-P6V 75060.

Pristimantis cf. *stictogaster* (2): Peru, Junín: from the Pui Pui Protected Forest (Rio Bravo valley, 11°12'38.5"S, 74°57'28.9"W), ca. 1800 m a.s.l., NMP-P6V 75061, 76024.

Pristimantis sp. (1): Peru, Junín: from the Pui Pui Protected Forest (Rio Bravo valley, 11°12'38.5"S, 74°57'28.9"W), ca. 1800 m a.s.l., MUSMS 32735.

Supplementary material 1

Large tree figure

Authors: Edgar Lehr, Jiří Moravec, Yingtong Wang, Marek Uvizl

Data type: pdf

Explanation note: Large tree figure: Maximum-likelihood tree showing the reconstructed phylogenetic relationships of *Pristimantis* frogs based on concatenated *12S* and *16S* sequences. The numbers at the tips represent GenBank accession numbers, except for the four samples used in this study, which are represented by voucher numbers..

Link: https://doi.org/10.3897/zookeys.1219.129773.suppl1

ZooKeys 1219: 165–174 (2024)
DOI: 10.3897/zookeys.1219.126777

Research Article

Chromis abadhah (Teleostei, Pomacentridae), a new species of damselfish from mesophotic coral ecosystems of the Maldives

Luiz A. Rocha[1], Hudson T. Pinheiro[1,2], Ahmed Najeeb[1,3], Claudia R. Rocha[1,4], Bart Shepherd[5]

1 *Department of Ichthyology, California Academy of Sciences, San Francisco, CA 94118 USA*
2 *Center for Marine Biology, University of São Paulo, São Sebastião, SP 11600, Brazil*
3 *Maldives Marine Research Institute, Ministry of Fisheries, Marine Resources and Agriculture, Malé 20025, Maldives*
4 *Department of Microbiology, California Academy of Sciences, San Francisco, CA 94118 USA*
5 *Steinhart Aquarium, California Academy of Sciences, San Francisco, CA 94118 USA*
Corresponding author: Luiz A. Rocha (LRocha@calacademy.org)

Abstract

A new species of *Chromis* (Teleostei, Pomacentridae) is described from four specimens collected between 95 and 110 m depth in mesophotic coral ecosystems in the Maldives, Indian Ocean. *Chromis abadhah* **sp. nov.** can be distinguished from all of its congeners by the following combination of characters: dorsal-fin rays XIII, 12–13; anal-fin rays II,11–12; pectoral-fin rays 17–18; tubed lateral-line scales 17; gill rakers 7+17–18 = 24–25; pearly white body with a large black marking covering the anterior two-thirds of the anal fin. The closest DNA barcode sequence (5.1% average uncorrected genetic distance on the mitochondrial *COI* gene), among those available, is *Chromis woodsi*, a similar mesophotic species known from the coastal western Indian Ocean (Somalia to South Africa). The new species is easily distinguished from *C. woodsi* by having 13 dorsal spines (versus 14 in *C. woodsi*), the absence of a black band on the base of the tail (present in *C. woodsi*), and by the genetic difference.

Key words: *COI*, deep reefs, ichthyology, Indian Ocean, rebreather diving, taxonomy

Academic editor: Tihomir Stefanov
Received: 3 May 2024
Accepted: 14 October 2024
Published: 29 November 2024

ZooBank: https://zoobank.org/C6875778-70CD-49A8-8EDC-CD891F8E906D

Citation: Rocha LA, Pinheiro HT, Najeeb A, Rocha CR, Shepherd B (2024) *Chromis abadhah* (Teleostei, Pomacentridae), a new species of damselfish from mesophotic coral ecosystems of the Maldives. ZooKeys 1219: 165–174. https://doi.org/10.3897/zookeys.1219.126777

Introduction

The family Pomacentridae (damselfishes and anemonefishes) is one of the largest and most conspicuous families of fish inhabiting tropical shallow coral reefs (Allen 1991). One of the key elements of their evolutionary success in coral reefs is resource partitioning, both at the spatial and trophic axes, with species falling into three main trophic levels: herbivores, zooplanktivores, and omnivores (Frédérich and Parmentier 2016). Despite its recent splitting into three genera (*Azurina* Jordan & McGregor, 1898, *Pycnochromis* Fowler, 1941, and *Chromis* Cuvier, 1814 sensu stricto; Tang et al. 2021), *Chromis* still is the most species-rich genus within Pomacentridae, comprising 78 valid species, all zooplanktivorous, at least 10 of which, including several recently described, are found only below 60 m (Pyle et al. 2008; Arango et al. 2019; Tea et al. 2019; McFarland et al. 2020). They are conspicuous residents of mesophotic coral ecosystems (coral reef habitats occurring at depths from 30–150 m) across all tropical seas, and are often seen in high numbers where they occur. *Chromis* is also the only genus of Pomacentridae that occurs below 80 m and down to at least 180 m depth (McFarland et al. 2020; Shepherd et al. 2020).

Because they are much harder to explore than their shallow-water counterparts, deep reefs are home to many undescribed species (Pyle et al. 2019). Their relative inaccessibility initially led scientists to consider deep reefs as potential refuges for threatened shallow-water species; however, the general consensus now is that species assemblages in mesophotic ecosystems are very different from shallow-water ones, and that deep reefs are also heavily impacted (Rocha et al. 2018; Pinheiro et al. 2023).

Exploration of the planet's mesophotic ecosystems has been uneven. Hawaii and some locations in the Caribbean, the South Pacific and the Red Sea are relatively well-known, whereas the eastern Pacific, eastern Atlantic and Indian Ocean are largely unexplored (Bongaerts et al. 2019). Aiming to fill this gap through a partnership between the California Academy of Sciences, the Maldives Marine Research Institute, and Rolex, we conducted ichthyological surveys to depths of 150 meters at 21 locations across five atolls in the Maldives, Indian Ocean between January 2022 and October 2023. Several new species of fishes were discovered during these surveys, of which this is the first to be described.

Material and methods

Specimens were collected with hand nets and immediately transported to a field laboratory where they were photographed, tissue sampled, and fixed in 10% formalin. Measurements and x-radiographs were made at the California Academy of Sciences after fixation and preservation in 75% ethanol. Counts were made with the aid of a microscope; measurements were made with digital calipers to the nearest 0.01 mm and rounded to one decimal place, following the conventions described in Allen and Randall (2004) and Pyle et al. (2008). Spiniform procurrent caudal-fin rays are those situated anteriorly to segmented procurrent caudal-fin rays, especially visible in radiographs. Vertebral counts include the first vertebra fused to the skull, and the last vertebra fused to the hypural plate; vertebral counts are presented as precaudal + caudal, where the first caudal vertebrae is the anteriormost vertebrae having its haemal spine associated with the anal fin pterygiophore, and the last caudal vertebrae is fused to the hypural plate. Gill-raker counts are presented as upper (epibranchial) + lower (ceratobranchial) rakers on the anterior face of the first arch; the angle raker is included in the second count. Counts and measurements for the holotype and paratypes are presented in Table 1. Measurements in the text are given as percent standard length (**SL**), unless otherwise noted. Data are presented first for the holotype, followed by a range of values for the paratypes, in parenthesis, where variation was noted. The holotype and paratypes were deposited at the California Academy of Sciences (**CAS**) and at the Smithsonian Institution's National Museum of Natural History (**USNM**) ichthyological collections.

In December 2022, four individuals were collected with hand nets by members of our team diving on mixed-gas, closed-circuit rebreathers (Hollis Prism 2). Molecular analysis and PCR amplification of the standard barcode fragment of the mitochondrial cytochrome *c* oxidase subunit I gene (*COI*) were performed following protocols described by Arango et al. (2019) using BOLFishF1/BOLFishR1 primers. Alignments of DNA sequences were done using a standard

Geneious global alignment with free end gaps and 65% similarity in the program Geneious Prime 2020.0.3 (Kearse et al. 2012). Our genetic dataset contains sequences of only one mitochondrial DNA marker. Therefore, we did not attempt to perform a phylogenetic reconstruction, and genetic distances are uncorrected. We used all available *Chromis COI* sequences from GenBank and the Barcode of Life databases for genetic comparisons.

Results

Chromis abadhah **sp. nov.**

https://zoobank.org/885AA4D1-AFF6-4CBF-91B7-EBBA49760C18
Figs 1–3, Table 1
Suggested Maldivian name: Abadhah Chromis
Suggested English name: Perpetual Chromis

Type material. ***Holotype*** (Figs 1, 2) • CAS 248401 (field code LAR2969), 68.7 mm SL, GenBank PQ410417, Maafilaafushi, Faadhippolhu Atoll, 5°21'40"S, 73°24'45"E, hand nets 101 m, H.T. Pinheiro, B. Shepherd, L.A. Rocha, 15.XII.2022. ***Paratypes*** • CAS 248403 (field code LAR2968), 66.1 mm SL, GenBank PQ410416, same data as holotype • USNM 470765 (field code LAR2970), 64.5 mm SL, GenBank PQ410418, same data as holotype • CAS 248402 (field code LAR2965), 50.2 mm SL, Maafilaafushi, Faadhippolhu Atoll, 5°21'40"S, 73°24'45"E, hand nets 118 m, H.T. Pinheiro, B. Shepherd, L.A. Rocha, 14.XII.2022.

Diagnosis. The following combination of characters distinguishes *Chromis abadhah* sp. nov. from all of its congeners: dorsal-fin rays XIII, 12–13; anal-fin rays II,11–12; pectoral-fin rays 17–18; tubed lateral-line scales 17; gill rakers 7+17–18 = 24–25; body pearly white; large black marking covering anterior two-thirds of anal fin; small black spot on upper edge of pectoral-fin base; no markings on caudal peduncle.

Figure 1. Holotype of *Chromis abadhah*, CAS 248401, 68.7 mm SL, shortly after collection. Photo by Luiz Rocha.

Table 1. Counts and measurements for *Chromis abadhah* sp. nov., holotype and paratypes.

	Holotype	Paratypes		
	CAS 248401	**CAS 248403**	**USNM 470765**	**CAS 248402**
TL (mm)	92.6	90.1	87.1	67.4
Standard length (mm)	68.7	66.1	64.5	50.2
Counts:				
Dorsal-fin rays	XIII, 12	XIII, 13	XIII, 12	XIII, 12
Anal-fin rays	II, 11	II, 12	II, 11	II, 11
Pectoral-fin rays	18 | 18	18 | 18	18 | 18	17 | 18
Pelvic-fin rays	I, 5	I, 5	I, 5	I, 5
Principal caudal rays	7 + 6	7 + 6	7 + 6	6 + 6
Procurrent segmented caudal rays	3 | 3	3 | 3	3 | 3	3 | 3
Procurrent spiniform caudal rays	3 | 3	3 | 3	3 | 3	3 | 3
Tubed lateral-line scales	17	17	17	17
Posterior mid-lateral pored scales	8	9	9	9
Scales above l.l.	3	3	3	3
Scales below l.l.	9	9	9	9
Circumped. scales	16	16	17	18
Gill rakers	7 + 17	7 + 18	7 + 18	7 + 17
Supraneural bones	3	3	3	3
Vertebrae	26 (11+15)	26 (11+15)	26 (11+15)	26 (11+15)
Measurements:				
Body depth	56.3	59.0	55.5	55.0
Body width	21.1	20.2	18.3	19.6
Head length	35.6	35.6	36.0	36.8
Snout length	9.6	8.9	9.3	9.8
Orbit diameter	15.0	14.2	12.6	14.2
Interorbital width	14.3	12.7	13.4	12.2
Caudal-peduncle depth	14.3	15.4	15.4	15.7
Caudal-peduncle length	7.7	7.8	10.3	8.6
Upper jaw length	12.6	11.5	10.5	10.6
Pre-dorsal length	41.9	42.7	42.1	42.8
Spinous dorsal-fin base	49.4	50.9	49.3	46.2
Soft dorsal-fin base	15.6	16.3	15.2	14.5
Dorsal-fin base	65.0	67.2	62.9	46.0
1st dorsal spine	6.7	8.7	10.3	8.5
2nd dorsal spine	13.4	13.2	15.9	14.9
3rd dorsal spine	15.8	16.8	18.0	18.4
4th dorsal spine	17.5	17.7	19.4	21.4
5th dorsal spine	17.1	17.7	18.8	21.0
6th dorsal spine	18.3	17.6	18.6	20.5
Last dorsal spine	12.1	11.8	11.9	14.4
Longest dorsal ray	25.8 (4th)	20.8 (4th)	21.7 (4th)	28.2 (3rd)
Preanal length	73.9	72.4	69.1	67.2
1st anal spine	7.5	7.5	7.2	7.1
2nd anal spine	23.5	22.2	21.9	23.3
Longest anal ray	22.2 (1st)	19.4 (1st)	19.6 (1st)	20.2 (1st)
Anal-fin base	21.3	24.7	24.2	21.1
Caudal-fin length	33.9	32.1	39.2	34.7
Caudal concavity	15.0	15.4	20.3	16.4
Longest pectoral ray	34.6 (1st)	34.5 (1st)	31.6 (1st)	32.9 (1st)
Prepelvic length	41.3	42.4	40.9	43.0
Pelvic-spine length	20.1	20.6	20.6	23.2
1st pelvic soft ray	29.5	30.4	32.6	29.5

Description. Dorsal-fin rays XIII, 12 (XIII, 12–13); anal-fin rays II, 11 (II, 12); all soft dorsal- and anal-fin rays branched, the last to base, the last two soft rays associated with a single complex pterygiophore; fourth (third) dorsal ray longest, 25.8% (20.8–28.2) SL; pectoral-fin rays 18|18 (17|18), the uppermost and lowermost unbranched; first pectoral ray the longest, 34.6% (31.6–34.5) SL; pelvic-fin rays I,5; principal caudal-fin rays 7+6 (6–7+6), the uppermost and lowermost unbranched; upper and lower procurrent caudal-fin rays 6, the anteriormost 3 rays (dorsally and ventrally) spiniform; tubed lateral-line scales 17; scales above lateral line to origin of dorsal fin 3; scales below lateral line to origin of anal fin 9; circumpeduncular scales 16 (16–18); gill rakers 7+17 = 24 (7+17–18 = 24–25); supraneural bones 3; vertebrae 11 precaudal + 15 caudal = 26.

Body moderately deep, depth 56.3% (55.0–59.0) SL, and compressed, the width 21.1% (18.3–20.2) SL; head length 35.6% (35.6–36.8) SL; profile of head slightly convex above orbit, nape slightly convex; snout length 9.6% (8.9–9.8) SL; eye large, orbit diameter 15.0% (12.6–14.2) SL; interorbital width 14.3% (12.2–13.4) SL; caudal-peduncle depth 14.3% (15.4–15.7) SL; caudal-peduncle length 8.0% (7.8–10.3) SL.

Mouth terminal, oblique, upper jaw angle about 45° to the horizontal axis of head and body; posterior edge of maxilla extending slightly beyond vertical at anterior edge of eye, upper jaw length 12.6% (10.5–11.5) in head length; teeth multi-serial, outer row of conical teeth in each jaw, much larger anteriorly; narrow band of villiform teeth lingual to outer row, in three irregular rows anteriorly, narrowing to a single row on side of jaws; tongue triangular with rounded tip; gill rakers long and slender, longest on lower limb near angle about half the length of gill filaments; anterior nostril relatively large with a short fleshy rim, more elevated on posterior edge and located at level of horizontal line through middle of pupil, slightly less than halfway between front of snout and anterior edge of orbit; posterior nostril much smaller and slit-shaped, located above and behind anterior nostril, close to edge of orbit. Opercle ending posteriorly in flat spine, the tip relatively acute and not obscured by scales; preopercular margin smooth, posterior margin extending dorsally to almost level of upper edge of orbit; suborbital with free lower margin extending nearly to a vertical at posterior edge of orbit.

Scales finely ctenoid; tubed portion of lateral line ending beneath rear portion of spinous dorsal fin (base of 13th dorsal-fin spine); head scaled except lips; scaly sheath at base of dorsal and anal fins, progressively thicker towards body; column of scales on each membrane of dorsal fin, narrowing distally, those on spinous portion of dorsal fin progressively longer, reaching about two-thirds the distance to spine tips on posterior membranes; two or three columns of scales on anal-fin membranes, progressively smaller distally; small scales on caudal fin extending about one-third distance to posterior margin; small scales only on base of pectoral fins; median scaly process extending posteriorly from between bases of pelvic fins, its length about half that of pelvic spine; axillary scale above base of pelvic spine about half the length of pelvic spine. Origin of dorsal fin above second lateral-line scale; pre-dorsal length 41.9% (42.1–42.7) SL; spinous dorsal-fin base length 49.4% (46.2–50.9) SL; soft dorsal-fin base length 15.6% (14.5–16.3) SL; first dorsal spine 6.7% (8.5–10.3) SL; second dorsal spine 13.4% (13.2–15.9) SL; third dorsal spine 15.8% (16.8–18.4) SL; fourth dorsal spine 17.5% (17.7–21.4) SL; fifth dorsal spine 17.1% (17.7–21.0) SL; sixth dorsal spine 18.3% (17.6–20.5) SL; last dorsal spine 12.1% (11.8–14.4) SL; fourth dorsal ray

Figure 2. Preserved holotype and x-ray of *Chromis abadhah*, CAS 248401, 68.7 mm SL. Photo and x-ray by Jon Fong.

longest, 25.8% (20.8–28.2) SL; first anal spine 7.5% (7.1–7.5) SL; second anal spine 23.5% (21.9–23.3) SL; longest anal-fin ray first, 22.2% (19.4–20.2); caudal fin forked, with filamentous extensions, its length 33.9% (32.1–39.2) SL, and concavity 15.0% (15.4–20.3) SL; first pectoral-fin ray longest, 34.6% (31.6–34.5) SL; pelvic spine 20.1% (20.6–23.2) SL; first pelvic soft ray 29.5% (29.5–32.6) SL.

***Color*.** In life (Fig. 3): Body pearly white with pale blue undertones, darker dorsally, with light gray pigment, especially between lateral line and dorsal fin. Belly and cheeks bright white. Row of scales below bottom half of eye very reflective. Bright silvery-blue circle surrounds darker, central part of iris. Area on head between eyes and above iris greenish silver. Lips pale blue. Anterior two-thirds of anal fin black.

Figure 3. *Chromis abadhah* in its natural habitat in Faadhippolhu Atoll, Maldives, at approximately 110 m depth. Photo by Luiz Rocha.

Distal portions of the soft dorsal, caudal, and posterior third of anal fin transparent. Small black spot on upper margin of pectoral-fin base. Pelvic fins pale blue to pearly white. Recently deceased and in alcohol (Figs 1, 2): Head and body overall gray in color (brown in alcohol), lighter ventrally. Dorsal, caudal, ventral, and pectoral fins pale gray (brown in alcohol) with distal portions translucent. Anal fin dark brown to black (black in alcohol); other black markings as described in life.

Habitat and distribution. *Chromis abadhah* is only known from the Maldives. It has been recorded at eight locations spanning 180 km (from Faadhippolhu to Dhaalu Atoll) so we presume it should be widely distributed across the Maldivian Archipelago. The type specimens were collected on a steep slope between 101 and 118 m depth off Maafilaafushi Island, and other individuals were observed elsewhere between 80 and 120 m depth. Habitat complexity was medium to high (small crevices and caves) but of low relief, with an apparently high diversity of encrusting sponges.

Etymology. The work that led to the discovery of this species was funded by the Rolex Perpetual Planet initiative through a Rolex Award for Enterprises to LAR. To honor this initiative, we name this species “abadhah” (pronounced aa-BAH-duh), which means “perpetual” in Dhivehi, the local language of the Maldives. We also hope that this species and its habitat remain perpetual. To be treated as a noun in apposition.

Discussion

In addition to *Chromis abadhah*, three other species of *Chromis* have an overall pearly white body with black markings in life: *Chromis axillaris* (Bennett, 1831), *Chromis pelloura* Randall & Allen, 1982, and *Chromis woodsi* Bruner & Arnam, 1979. All are mesophotic, having only been recorded below 30 m depth. *Chromis axillaris* is the most widely distributed, being recorded in various locations between the western Indian Ocean and the western Pacific at depths of 60 to 100 m (Bruner and Arnam 1979; Allen 1991). *Chromis pelloura* is found in the Red Sea at depths of 30 to 80 m, and is very similar in color and morphology to *C. axillaris* (Randall and Allen 1982). In addition to the black bar covering the caudal peduncle (also in the previous two species), the distal half of the anal fin of *C. woodsi* (found at 50 to 175 m depth in the coastal western Indian Ocean) also is solid black (Bruner and Arnam 1979). *Chromis abadhah* differs from all of these by lacking a black bar on the caudal peduncle, having 13 dorsal spines (all others have 14), and by a distribution apparently restricted to the Maldives.

Recently, Tang et al. (2021) revised the taxonomy of *Chromis* and reassigned several species to the genera *Azurina* and *Pycnochromis*. All mesophotic species remained in *Chromis* stricto sensu, and several authors have pointed out that most of them have 14 dorsal-fin spines (Pyle et al. 2008; Allen and Erdmann 2009; Tea et al. 2019). *Chromis abadhah* is unusual among mesophotic species by having 13; therefore, the number of dorsal-fin spines does not appear to diagnose a deep-reef clade, and a comprehensive molecular analysis that includes more species is needed to better understand the relationships among shallow and deep lineages.

Acknowledgements

We are grateful to JD Fong for pictures and x-rays of the type specimens and D Pitassy for providing the USNM collection number, and to the CalAcademy dive operations team for dive training and support in the field. We are also thankful to many colleagues who helped in the field and with discussions, including B Greene, K Lev, T Phelps, R Pyle, Y-K Tea, and M Zahuwaan. Hollis and Carpe Diem Maldives provided gear and logistical support respectively. The Maldivian Coast Guard authorized and supervised the technical diving and provided nautical support in all expeditions. Research and collecting permits were provided by the Maldives Ministries of Fisheries Marine Resources and Agriculture and of Environment, Climate Change and Technology. This is a collaborative research initiative with the Maldives Marine Research Institute, and we especially thank MMRI Director S Naeem for her support.

Additional information

Conflict of interest

The authors have declared that no competing interests exist.

Ethical statement

No ethical statement was reported.

Funding

This work was funded by a Rolex Award for Enterprises to LAR, and by the generous support of donors who endorsed the California Academy of Sciences' Hope for Reefs Initiative. HTP thanks FAPESP (The São Paulo Research Foundation) for funding and fellowship (2019/24215-2 and 2021/07039-6).

Author contributions

L Rocha, H Pinheiro, and B Shepherd discovered and collected the new species. L Rocha and A Najeeb took specimen data and obtained all collecting permits. C Rocha did the DNA sequencing. All authors contributed to manuscript writing and editing.

Author ORCIDs

Luiz A. Rocha https://orcid.org/0000-0003-4011-569X
Hudson T. Pinheiro https://orcid.org/0000-0002-3143-1474
Claudia R. Rocha https://orcid.org/0000-0001-8069-6535
Bart Shepherd https://orcid.org/0000-0002-8918-1551

Data availability

All of the data that support the findings of this study are available in the main text.

References

Allen GR (1991) Damselfishes of the world. Mergus Publishers, Melle, Germany, 271 pp.

Allen GR, Erdmann MV (2009) Two new species of damselfishes (Pomacentridae: *Chromis*) from Indonesia. Aqua, Journal of Ichthyology and Aquatic Biology 15: 3–20.

Allen GR, Randall JE (2004) Two new species of damselfishes (Pomacentridae: *Chromis*) from Indonesian seas. Aqua, Journal of Ichthyology and Aquatic Biology 9: 17–24.

Arango BG, Pinheiro HT, Rocha C, Greene BD, Pyle RL, Copus JM, Shepherd B, Rocha LA (2019) Three new species of *Chromis* (Teleostei, Pomacentridae) from mesophotic coral ecosystems of the Philippines. ZooKeys 835:1–15. https://doi.org/10.3897/zookeys.835.27528

Bongaerts P, Perez-Rosales G, Radice VZ, Eyal G, Gori A, Gress E, Hammerman NM, Hernandez-Agreda A, Laverick J, Muir P, Pinheiro HT, Pyle RL, Rocha LA, Turner JA, Booker R (2019) Mesophotic.org: a repository for scientific information on mesophotic ecosystems. Database 2019: baz140. https://doi.org/10.1093/database/baz140

Bruner JC, Arnam S (1979) *Chromis woodsi*, a new species of damselfish (Pomacentridae) from the western Indian Ocean with a redescription of *Chromis axillaris* (Bennett), 1831. Fieldiana Zoology 73(3): 49–63. https://doi.org/10.5962/bhl.title.2856

Frédérich B, Parmentier E (2016) Biology of Damselfishes. CRC Press, Boca Raton, Florida, 340 pp. https://doi.org/10.1201/9781315373874

Kearse M, Moir R, Wilson A, Stones-Havas S, Cheung M, Sturrock S, Buxton S, Cooper A, Markowitz S, Duran C, Thierer T, Ashton B, Meintjes P, Drummond A (2012) Geneious Basic: An integrated and extendable desktop software platform for the organization and analysis of sequence data. Bioinformatics 28: 1647–1649. https://doi.org/10.1093/bioinformatics/bts199

McFarland EP, Baldwin CC, Robertson DR, Rocha LA, Tornabene L (2020) A new species of *Chromis* damselfish from the tropical western Atlantic (Teleostei, Pomacentridae). Zookeys 1008: 107–138. https://doi.org/10.3897/zookeys.1008.58805

Pinheiro HT, MacDonald C, Santos RG, Bobat A, Cresswell BJ, Francini-Filho R, Galbraith GF, Musembi P, Phelps TA, Quimbayo JP, Quiros TEAL, Shepherd B, Stefanoudis PV, Teixeira JB, Woodall LC, Rocha LA (2023) Plastic pollution on the world's coral reefs. Nature 619: 311–316. https://doi.org/10.1038/s41586-023-06113-5

Pyle RL, Earle JL, Greene BD (2008) Five new species of the damselfish genus *Chromis* (Perciformes: Labroidei: Pomacentridae) from deep coral reefs in the tropical western Pacific. Zootaxa 1671: 3–31. https://doi.org/10.11646/zootaxa.1671.1.2

Pyle RL, Kosaki RK, Pinheiro HT, Rocha LA, Whitton RK, Copus JM (2019) Fishes: Biodiversity. In: Loya Y, Puglise KA, Bridge TCL (Eds) Mesophotic Coral Ecosystems. Springer, New York, 749–777. https://doi.org/10.1007/978-3-319-92735-0_40

Randall JE, Allen GR (1982) *Chromis pelloura* a new species of damselfish from the Northern Red Sea. Aquarium 5(11): 15–19.

Rocha LA, Pinheiro HT, Shepherd BS, Papastamatiou YP, Luiz OJ, Pyle RL, Bongaerts P (2018) Mesophotic coral ecosystems are threatened and ecologically distinct from shallow water reefs. Science 361(6399): 281–284. https://doi.org/10.1126/science.aaq1614

Shepherd B, Pinheiro HT, Phelps TAY, Easton EE, Perez-Matus A, Rocha LA (2020) A New Species of *Chromis* (Teleostei: Pomacentridae) from Mesophotic Coral Ecosystems of Rapa Nui (Easter Island) and Salas y Gómez, Chile. Copeia 108(2): 326–332. https://doi.org/10.1643/CI-19-294

Tang KL, Stiassny MLJ, Mayden RL, DeSalle R (2021) Systematics of Damselfishes. Ichthyology & Herpetology 109(1): 258–318. https://doi.org/10.1643/i2020105

Tea, YK, Gill AC, Senou H (2019) *Chromis tingting*, a new species of damselfish from mesophotic coral ecosystems of southern Japan, with notes on *C. mirationis* Tanaka (Teleostei: Pomacentridae). Zootaxa 4586(2): 249–260. https://doi.org/10.11646/zootaxa.4586.2.2

ZooKeys 1219: 175–194 (2024)
DOI: 10.3897/zookeys.1219.131102

Research Article

The new genus *Purpurata* (Lepidoptera, Crambidae, Spilomelinae), with descriptions of two new species from China

Xin-Lei Xue[1,2], Xiao-Qiang Lu[1,3], Xi-Cui Du[1,2]

1 *College of Plant Protection, Southwest University, Chongqing 400715, China*
2 *Yibin Academy of Southwest University, Yibin, Sichuan 644000, China*
3 *Guangyuan Center for Disease Control and Prevention, Guangyuan, Sichuan 628040, China*
Corresponding author: Xi-Cui Du (duxicui@swu.edu.cn, duxicui@hotmail.com)

Abstract

The male genitalia characters of four species, *Botys iopasalis* Walker, 1859, *Pleuroptya obfuscalis* Yamanaka, 1998, *Botys plagiatalis* Walker, 1859 and *Patania shompen* Singh et Ahmad, 2022, placed in the genus *Patania* Moore, 1888 before the present study, do not conform to the diagnosis of *Patania*. A new genus, *Purpurata* **gen. nov.**, is established for these four species, and two new species, *Purpurata directa* **sp. nov.** and *Purpurata lurida* **sp. nov.** are described based on their external morphology and genitalia characters. *Purpurata directa* **sp. nov.** is designated as the type species of the new genus. Five species of the new genus were clearly separated from *Patania* species in the Maximum likelihood phylogenetic tree constructed based on COI sequence data. Compared to *Patania*, the new genus *Purpurata* exhibits distinctive characters in male genitalia: the uncus is short, broad, and arc-shaped posteriorly; the gnathos is present and setose, or reduced; and the fibula is very small and setose. In addition, *Patania clava* (Xu & Du), **syn. nov.** is synonymized with *Purpurata iopasalis* **comb. nov.** An identification key to species of the new genus is presented based on morphological characters of habitus and genitalia. Images of the habitus and genitalia are provided.

Key words: DNA barcode, identification key, morphology, moths, taxonomy

Academic editor: Richard Mally
Received: 3 July 2024
Accepted: 28 October 2024
Published: 2 December 2024

ZooBank: https://zoobank.org/A7CEF41B-6FE9-48DF-87BD-7474CD8AEAB7

Citation: Xue X-L, Lu X-Q, Du X-C (2024) The new genus *Purpurata* (Lepidoptera, Crambidae, Spilomelinae), with descriptions of two new species from China. ZooKeys 1219: 175–194. https://doi.org/10.3897/zookeys.1219.131102

Introduction

The genus *Patania* Moore, 1888 was assigned to the Spilomelinae tribe Agroterini Acloque, 1897 by Mally et al. (2019). Many species of *Patania* were previously recorded in *Pleuroptya* Meyrick, 1890 (Munroe 1983, 1995; Shaffer et al. 1996; Leraut 2005; Du 2009; Kirpichnikova 2009; Heppner 2012; Sasaki and Yamanaka 2013), which was synonymized with *Patania* by Kirti and Gill (2007). During our study of the genus *Patania*, we found that four species, *P. iopasalis* (Walker, 1859), *P. obfuscalis* (Yamanaka, 1998), *P. plagiatalis* (Walker, 1859) and *P. shompen* Singh et Ahmad, 2022, exhibited some distinctive characters in the genitalia, such as on the uncus, gnathos, fibula, and apophyses anteriores, which did not correspond to the diagnostic characters of *Patania*. Additionally, some genitalia characters of these four species, such as the fibula, cornutus, and corpus bursae, did not correspond to the characters of another similar genus, i.e., *Nagiella* Munroe, 1976. Therefore, after systematically comparing the morphological characters of these four species with *Patania* and *Nagiella* species, and based on the phylogenetic analysis of DNA barcode data, we establish a new genus, *Purpurata* gen. nov., for these four known species and describe two new species.

Materials and methods

Taxon sampling

Specimens were collected by light trap at night and killed by ammonium hydroxide or ethyl acetate. The examined pinned specimens, including all type specimens of the new species, are deposited in the Insect Collection, Southwest University, Chongqing, China (**SWU**), except for six specimens of two known species, which are deposited in the Insect Collection of Nankai University (**NKU**). The corresponding author examined comparative specimens of *Botys iopasalis* and some *Patania* species, which were deposited in the Natural History Museum, London, United Kingdom (**NHMUK**). We extracted and obtained 11 sequences from five species of the new genus *Purpurata*, seven sequences from three *Patania* species, and five sequences from two *Nagiella* species (Table 1). All these sequences have been uploaded to NCBI. In addition, four sequences of two *Agrotera* species, one sequence of one *Patania* species, two sequences of one *Pycnarmon* species and six sequences of two *Nosophora* species were downloaded from NCBI and BOLD. Among them, *Agrotera* is the type genus of Agroterini (Mally et al. 2019), *Patania* and *Nagiella* are similar genera to *Purpurata*, and *Pycnarman pantherata* (Butler, 1878) and *Nosophora* are closely related to *Botys iopasalis* (Matsui et al. 2022), one of the focal taxa in the present study. We included the type species of *Patania*, *Botys concatenalis* Walker, 1866, in the analysis to deduce the monophyly of the new genus *Purpurata*. Therefore, the five genera *Patania*, *Nagiella*, *Agrotera*, *Pycnarmon*, and *Nosophora* are used as outgroups in this study. The information on specimens used for mitochondrial COI gene sequencing and phylogenetic analysis is provided in Table 1.

The preparation of genitalia slides primarily followed Li and Zheng (1996). The habitus images were taken with a digital camera (Canon EOS 5D), and the genitalia images were taken with a digital camera (Leica DFC 450) attached to a stereomicroscope (Leica M205 A).

DNA extraction, PCR amplification, sequencing

A total of 15 species, including five species of *Purpurata* gen. nov. and ten outgroup species, were included for PCR analysis and DNA sequencing (Table 1). Total DNA was extracted from dried legs using the TIANGEN DNA extraction kit according to the manufacturer's instructions. The 658-base pair (bp) barcode region of COI was PCR amplified using primers LepF1 and LepR1 (Hajibabaei et al. 2006). After verifying PCR products by running them on a 1% agarose gel, sequencing was conducted by Shanghai Sangon Biotechnology Co., Ltd (Shanghai, China) using the same primers as those used in PCR.

Table 1. Sample information for species of *Purpurata* gen. nov. and the outgroups.

Species	Sequence ID	Location (China, except for last four)	NCBI and BOLD accession no.
Purpurata iopasalis comb. nov.	XD1401067	Wuzhishan, Hainan	PQ463661
	LXQ180076	Diaoluoshan, Hainan	PQ463660
	XD1401014	Diaoluoshan, Hainan	PQ463662
Purpurata directa sp. nov.	XD1401032	Wuzhishan, Hainan	PQ463664
	XD1401110	Diaoluoshan, Hainan	PQ463663
Purpurata plagiatalis comb. nov.	XD1500022	Mulun, Guangxi	PP865067
Purpurata obfuscalis comb. nov.	LXQ180070	Haugaoxi, Sichuan	PP865068
	LXQ180071	Haugaoxi, Sichuan	PP865069
	XD1405336	Huagaoxi, Sichuan	KU143853
Purpurata lurida sp. nov.	XD1401079	Diaoluoshan, Hainan	PP865070
	LXQ180262	Changyang, Hubei	PP865071
Patania balteata	XD1405399	Haugaoxi, Sichuan	KU143838
	XD1405300	Haugaoxi, Sichuan	KU143837
	XD1405441	Haugaoxi, Sichuan	KU143839
Patania chlorophanta	XD1404265	Jinzhongshan, Guangxi	KU058652
	XD1404239	Jinzhongshan, Guangxi	KU058653
	XD1401035	Wuzhishan, Hainan	KU058654
Patania concatenalis	XD1401058	Diaoluoshan, Hainan	KU143840
	Pyr000116	Lingshui, Hainan	CNPYA116-10
Pycnarmon pantherata	Pyr000126	Yuanqu, Shanxi	CNPYA126-10
	Pyr000127	Yuanqu, Shanxi	CNPYA127-10
Nagiella hortulatoides	LXQ180100	Huanglianshan, Yunnan	PQ463665
	LXQ180099	Huanglianshan, Yunnan	PQ463666
	LXQ180217	Huanglianshan, Yunnan	PQ463667
Nagiella quadrimaculalis	XD1405327	Haugaoxi, Sichuan	KU143854
	XD1402131	Bawangling, Hainan	PP865072
Nosophora dispilalis	Pyr001429	Nanning, Guangxi	CNPYD1429-10
	Pyr001430	Nanning, Guangxi	CNPYD1430-10
	Pyr001431	Nanning, Guangxi	CNPYD1431-10
Nosophora semitritalis	Pyr000949	Yuanqu, Shanxi	CNPYD949-10
	Pyr000950	Yuanqu, Shanxi	CNPYD950-10
	Pyr000951	Yichang Wufeng, Hubei	CNPYD951-10
Agrotera nemoralis	ODOPE217-11	Bavaria, Germany	KX045648
	PHLAC175-10	South Tyrol, Italy	JF859792
Agrotera basinotata	ANICN229-10	Queensland, Australia	HQ952613
	ANICN230-10	Queensland, Australia	HQ952614

Data analysis

All COI sequences were aligned manually using Align-Muscle in MEGA 7.0, and were translated into amino acid sequences for visual correction. Intraspecific and interspecific genetic distances were calculated based on the Kimura 2-parameter (K2P) distance model (Kimura 1980). Phylogenetic analysis was performed based on a phylogenetic tree constructed using the Maximum likelihood (ML) method with 1,000 bootstrap replications (Saitou and Nei 1987), in which three *Patania* species, two *Nagiella* species, one *Pycnarmon* species, two *Nosophora* species and two *Agrotera* species were chosen as the outgroups.

Table 2. Kimura 2-parameter genetic distances (as percent) calculated within (in bold) and between *Purpurata* species and the outgroups.

	1	2	3	4	5	6	7	8	9	10	11	12	13	14	15
1. *Purpurata iopasalis* comb. nov.	**0.00**														
2. *Purpurata obfuscalis* comb. nov.	8.72	**0.01**													
3. *Purpurata directa* sp. nov.	6.93	9.49	**0.00**												
4. *Purpurata plagiatalis* comb. nov.	6.84	8.36	5.45	**0.00**											
5. *Purpurata lurida* sp. nov.	3.58	6.52	8.28	7.85	**0.00**										
6. *Patania concatenalis*	9.91	12.76	10.90	10.80	11.87	**0.00**									
7. *Patania balteata*	10.59	13.09	10.25	9.38	12.36	10.60	**0.00**								
8. *Patania chlorophanta*	9.15	12.50	11.36	11.06	12.07	12.07	8.53	**0.00**							
9. *Nosophora dispilalis*	10.95	11.72	11.40	10.94	11.31	10.25	12.01	10.53	**0.00**						
10. *Nosophora semitritalis*	10.77	11.14	10.34	10.07	10.25	11.51	12.36	11.41	7.20	**0.00**					
11. *Pycnarmon pantherata*	10.42	12.23	11.21	10.95	11.30	10.77	8.87	9.39	10.07	11.84	**0.00**				
12. *Nagiella hortulatoides*	11.30	11.43	12.47	10.43	12.85	10.90	9.21	10.95	10.89	11.84	9.40	**0.00**			
13. *Nagiella quadrimaculalis*	11.39	12.29	11.58	10.68	12.64	10.69	8.95	10.98	10.33	11.58	8.96	4.47	**0.00**		
14. *Agrotera nemoralis*	11.92	13.54	12.29	11.21	13.18	10.86	9.81	11.98	11.56	11.03	11.21	11.03	11.65	**0.00**	
15. *Agrotera basinotata*	10.24	12.92	10.43	10.25	10.94	9.74	7.18	11.15	11.93	10.96	9.22	10.43	9.46	8.37	**0.00**

Results

DNA sequence analysis

A total of 11 COI sequences from five species of *Purpurata* gen. nov. were obtained. In total, 36 COI sequences from *Purpurata* species and the outgroup species were analyzed. The dataset contained no obvious pseudogenes, indicating the correct target gene sequence was amplified and sequenced.

The ML phylogenetic tree shows five monophyletic branches for *Purpurata* gen. nov., corresponding to the five morphological species *P. iopasalis* comb. nov., *P. lurida* sp. nov., *P. obfuscalis* comb. nov., *P. directa* sp. nov., and *P. plagiatalis* comb. nov. (Fig. 1). These branches form a well-supported (98% Bootstrap support) monophylum that is sister to *Nosophora*. *Patania*, with three sampled species, including the type species *P. concatenalis,* is polyphyletic, with *Nagiella*, *Pycnarmon*, and *Agrotera* nested within. The intraspecific genetic distances within *Purpurata* range from 0.00% to 0.01%, and interspecific genetic distances range from 3.58% to 9.49% (Table 2). The interspecific genetic distances between the ingroup species and outgroup species range from 9.15% to 13.54% (Table 2).

Taxonomic account

Purpurata gen. nov.

https://zoobank.org/B30E1964-1BD5-47CD-9196-BA496B0FA390

Type species. *Purpurata directa* sp. nov., here designated.

Diagnosis. *Purpurata* is readily distinguished from its phylogenetic sister genus *Nosophora* (type species: *Botys dispilalis* Hampson, 1896) by the yellow wings with their purple-brown lines and patches, while in *Nosophora*, the wings are dark shiny brown and feature a large, comma-shaped spot in the

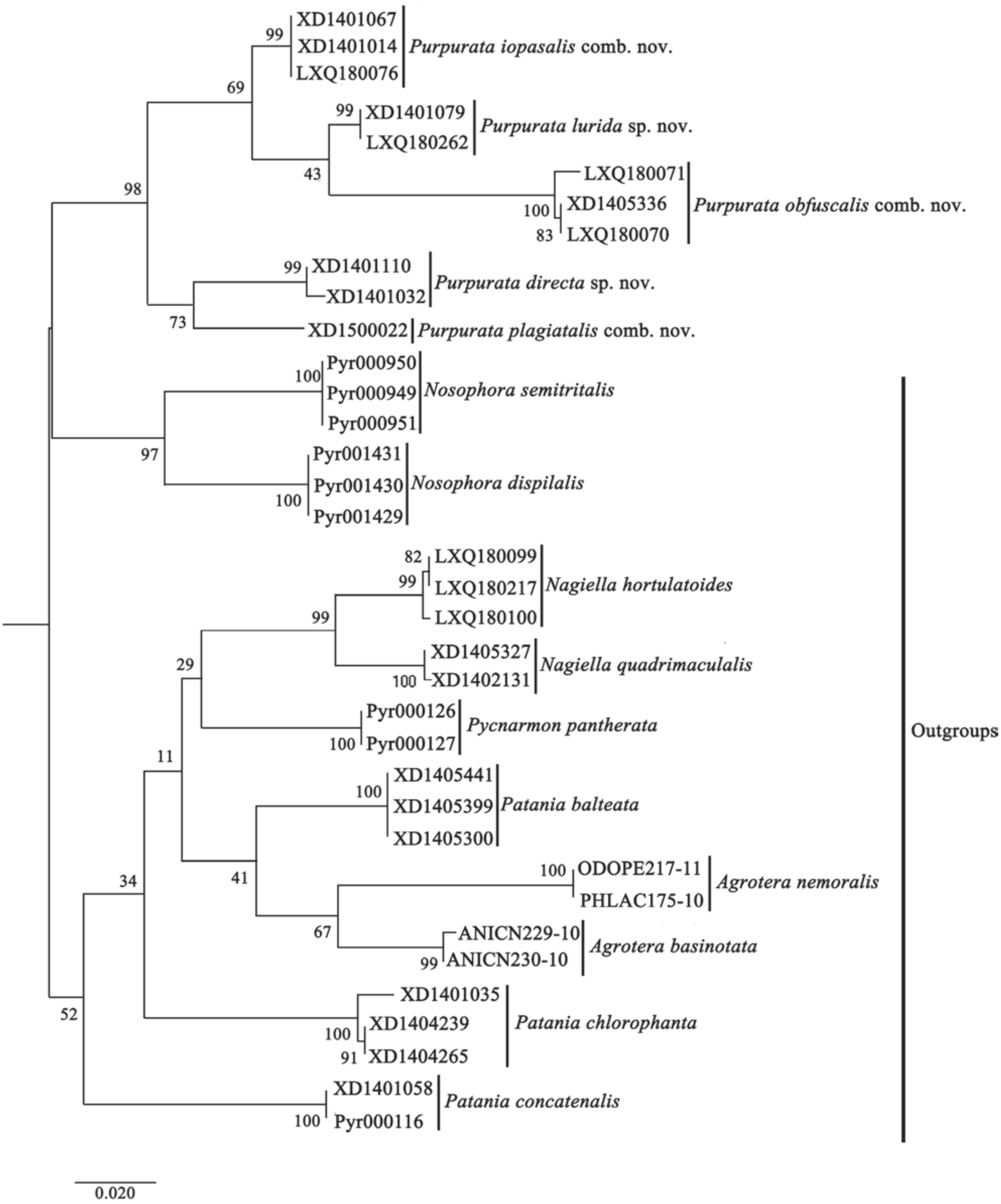

Figure 1. Phylogenetic hypothesis of relationships among five species of *Purpurata* gen. nov. and ten species of five outgroup genera inferred from a Maximum likelihood (ML) analysis of the DNA barcode data. Numbers near the branches are bootstrap support values based on 1000 replicates.

forewing. Furthermore, the vertex of the head is hollowed out in males of *N. dispilalis* (see Lederer 1863: pl. 4 fig. 24 (misidentified as *N. chironalis*); Hampson 1896: 288), whereas it is rounded in *Purpurata* species (Fig. 2). In *Purpurata*, compared to the similar genera *Patania* and *Nagiella*, the uncus is arc-shaped on the posterior margin, the valva is shorter and broader than those of the latter two, and the fibula is shorter and smaller in male genitalia; the apophyses anteriores is not broadened or very slightly broadened near the base in the female genitalia. Comparatively, in *Patania* and *Nagiella*, the uncus is generally trapezoidal (except that *N. bispina* has a rather short and broad uncus, with rounded posterior margin), and the fibula are generally well developed and sclerotized; the apophyses anteriores broaden rhomboidally near the base. In addition, in *Purpurata*, the gnathos is present and setose apically, generally undeveloped (except that *P. iopasalis* and *P. shompen* have well-developed gnathos). *Patania* species usually lack a gnathos, and a few species have a gnathos but no setae at the apex. *Nagiella* species generally have a gnathos, but no setae at the apex. In *Purpurata*, the phallus has a protruding sclerotized structure at the posterior end, with a thick needle-like or spine-like cornutus and a brush-like cornutus. Comparatively, the phallus of *Patania* and *Nagiella* lack a protruding sclerotized structure posteriorly. *Patania* species have, or lack, a cornutus (if present, diverse morphologically), and *Nagiella* species generally lack a cornutus (except for *N. bispina* with a curved hook cornutus). The compared characters here are present in the type species of *Patania* and *Nagiella*, *Botys concatenalis*, and *Nagia desmialis* respectively, which were fully investigated in our study.

Description. *Habitus*. Body and wings yellow, with purple-brown wing markings. Frons rounded. Labial palpus upturned, exposed 3rd joint short and blunt (Fig. 2). Antenna filiform, male with ventral cilia. Forewing with length of cell ~ 1/2 of wing; discocellulars incurved; R from cell at ~ 5/6 above; Rs_2 anastomosed with Rs_3 ~ 3/5 of Rs_3 beyond cell; Rs_1 close to Rs_2+s_3; Rs_4 slightly curved towards Rs_2+s_3 at base; M_2, M_3 and CuA_1 from posterior angle of cell and uniformly spaced at the base; CuA_2 from cell at ~ 2/3 below. Hindwing with length of cell ~ 1/3 of wing; discocellulars incurved; Sc+R anastomosed with Rs ~ 1/5 beyond the cell; M_2, M_3 and CuA_1 separately from posterior angle cell; CuA_2 from cell at 2/3 below (Figs 3, 4). Abdomen yellow dorsally; 1st and 2nd tergites with black spots laterally and 7th tergites black posteriorly in male. Tympanal organs with praecinctorium strongly bifid (Fig. 5).

***Male genitalia*.** Uncus short and broad, with arc-shaped posterior margin, except for *P. iopasalis* with narrowed apex of uncus. Gnathos present and bearing setae apically, or vestigial to a transverse band. Valva ligulate, relatively broad and short generally. Fibula small and membranous, with setae. Sacculus undeveloped. Phallus cylindrical, with a protruding sclerotized structure posteriorly, with a thick needle-like or spine-like cornutus and a brush-like cornutus composed of a spine cluster, and a granular sclerotized area near the middle.

***Female genitalia*.** Apophyses anteriores longer than apophyses posteriores, occasionally slightly broadened near base. Antrum sclerotized. Ductus bursae usually long and slender. Corpus bursae round or oval, usually with a round signum.

Distribution. This genus is mainly distributed in the Palaearctic and Oriental realms. And *P. plagiatalis* is also found in the Neotropical and Australasian realms, *P. iopasalis* is also found in the Australasian realms.

Etymology. The genus name *Purpurata* is derived from the Latin word *purpuratus* meaning purple, indicating the distinctive purple-brown coloration of wing markings. The gender is feminine.

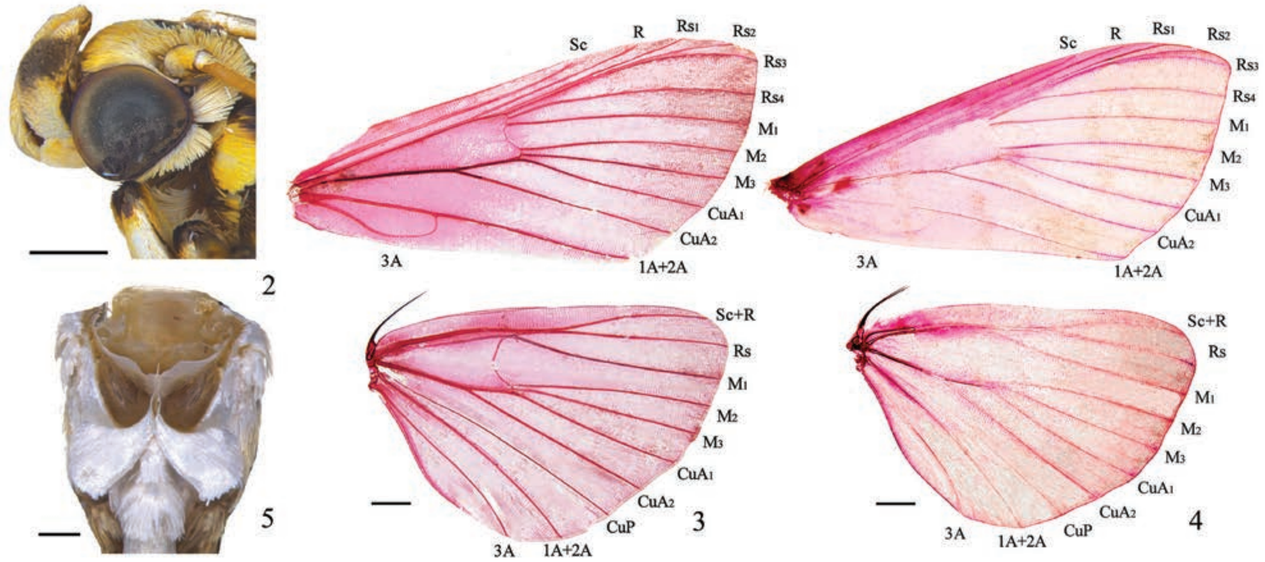

Figures 2–5. *Purpurata directa* sp. nov. **2** head ♂ **3** wing venation ♂ **4** wing venation ♀ **5** tympanal organ. Scale bars: 0.5 mm (**2, 5**); 1.0 mm (**3, 4**).

Remarks. This new genus comprises four known species from the genus *Patania* of Spilomelinae, and two new species described in the present study. It corresponds to the main diagnostic characters of Crambidae: forewing with vein R_{S4} free and with oval sclerotization costad at base of vein 1A+2A; bullae tympani open cephalad; tympanum and conjunctivum lying at a blunt angle; praecinctorium present; and male genitalia without uncus arms. Further, it corresponds to the main diagnostic characters of Spilomelinae: fornix tympani projecting ventrad from tympanic frame; praecinctorium bilobed; retinacular hook absent; and females with two frenular bristles. Moreover, based on the Agroterini characters stated in Mally et al. (2019), labial palps upturned and 3rd labial palpomere directed dorsally; uncus with a broad base, head chaetae simple and unsplit; the ratio between saccus length and sacculus breadth > 1, we place this genus in the tribe Agroterini.

Key to *Purpurata* species based on morphology of habitus and genitalia

1 Postmedial line of forewing punctiform between M_2 and CuA_2 (Figs 7, 11); phallus posteriorly with a nail head-like, rectangular, or rounded protruding sclerite (Figs 14c, 19c) **2**

– Postmedial line of forewing dentate or linear between M_2 and CuA_2 (Figs 6, 8–9, 10); phallus posteriorly with a finger-like or oval protruding sclerite (Figs 12c, 15c, 17c) **4**

2 Gnathos vestigial to a narrow band (Fig. 19a); sacculus with a lamellar projection near distal end (Fig. 19); phallus posteriorly with a rounded protruding sclerite, and a short thorn-like cornutus near end, besides needle-like cornutus and brush-like cornutus (Fig. 19c) .... ***P. plagiatalis* comb. nov.**

– Gnathos thick finger-like (Fig. 14a); sacculus without lamellar projection; phallus posteriorly with a nail head-like or rectangular sclerite, and without short thorn-like cornutus near distal end, besides needle-like cornutus and brush-like cornutus (Fig. 14c) **3**

3 Postmedial line of hindwing punctiform between M_2 and CuA_2 (Fig. 7); phallus posteriorly with a nail head-like sclerite (Fig. 14c)........ ***P. iopasalis* comb. nov.**

– Postmedial line of hindwing linear between M_2 and CuA_2; phallus posteriorly with a rectangular sclerite .... ***P. shompen* comb. nov.**

4 Postmedial line of forewing linear between M_2 and CuA_2 (Figs 8, 9); phallus posteriorly with an oval sclerite (Fig. 15c); gnathos transverse lamina (Fig. 15a)...***P. directa* sp. nov.**

– Postmedial line of forewing dentate between M_2 and CuA_2 (Figs 6, 10); phallus posteriorly with a finger-like sclerite (Figs 12c, 17c); gnathos vestigial to a narrow band (Figs 12a, 17a) **5**

5 Uncus short and broad (Fig. 17a), triangular; valva with distal 1/3 narrowed very gradually and rounded apically (Fig. 17)..........***P. lurida* sp. nov.**

– Uncus semicircular (Fig. 12a); valva with distal 1/3 narrowed gradually and pointed apically (Fig. 12) .... ***P. obfuscalis* comb. nov.**

Purpurata obfuscalis (Yamanaka, 1998), comb. nov.

Figs 6, 12, 12a–c, 13

Pleuroptya obfuscalis Yamanaka, 1998: 106. Type locality: Nepal.

Patania obfuscalis: Nuss et al. 2003–2024. Global Information System on Pyraloidea.

Material examined. China • Chongqing Municipality, 2 ♂♂, 1 ♀, Jinyun Mountain, alt. 550 m, 29 July 2010, Xi-Cui Du & Chao-Wei Bi leg., genitalia slide no.: XLJ14221 ♀ • 1 ♂, Simian Mountain, alt. 1120 m, 17 July 2010, Xi-Cui Du & Li-Fang Song leg. • 2 ♂♂, JinYin Mountain, Qianjiang District, alt. 1100 m, 25–26 July 2012, Jun Zhang & Li-Jun Xu leg. • 1 ♂, Small South Sea, Qianjiang District, alt. 370 m, 21 July 2012, Jun Zhang & Li-Jun Xu leg. • **Sichuan Prov.**, 4 ♂♂, Huagaoxi Nature Reserve, Guandou Village, alt. 763 m, 30 August 2014, Dan-Xu & Xue-Li Wei leg., genitalia slide no.: XDJ15048 ♂ • **Gansu Prov.**, 2 ♂♂, Bifeng Valley, Wen County, alt. 860 m, 2005. 9–10 July 2012, Hai-Li Yu leg. (NKU) • **Yunnan Prov.**, 2 ♂♂, Pianma Village, Lushui County, Nujiang Prefecture, alt. 1889 m, 18 August 2015, Xue-Li Wei leg., genitalia slide no.: LXQ18279 • 2 ♂♂, Cangyuan County, Lincang City, alt. 1242 m, 25 July 2015, Xue-Li Wei leg. • 1 ♂, Jinuo Township, Xishuangbanna, alt. 1100 m, 15 May 2018, Xi-Cui Du leg. • 2 ♂♂, Xishuangbanna Tropical Botanical Garden, alt. 659 m, 28 May 2015, Man-Fei Tao leg. • 2 ♂♂, Daxichang Village, Malipo County, alt. 1465 m, 5 June 2015, Man-Fei Tao leg. • 2 ♂♂, Huanglian Mountain, Honghe Prefecture, alt. 900 m, 23 May 2018, Xi-Cui Du & Xiao Qiang-Lu leg. • **Xizang Autonomous Region**, 1 ♂, Zhangmu Town, alt. 2300 m, 5 August 2017, Jian-Yue Qiu & Hao Xu leg., genitalia slide no.: XXL23275 ♂ • **Guangxi Zhuang Autonomous Region**, 1 ♂, Nonggang National Nature Reserve, Longzhou County, alt. 188 m, 3 August 2011, GuiQing-He leg. • **Guizhou Prov.**, 2 ♂♂, 3 ♀♀, Baishao, Kuankuoshui, alt. 800 m, 10–11, 13 August 2010, Xi-Cui Du leg. • 1 ♂, WengAng village, LiBo County, alt. 1345 m, 20 July 2015, Ji-Ping Wan leg. • **Hainan Prov.**, 4 ♀♀, Wuzhi Mountain, alt.795 m, 18 May 2014, Li-Jun Xu & Dan Xu leg. • 1♂, Diaoluo Mountain, alt. 500 m, 23 May 2014, Li-Jun Xu & Dan Xu leg. • **Shaanxi Prov.**, 1 ♂, Ningshan County, Xunyangba Town, alt. 1400 m, 3 August 2014, Hai-Li Yu leg. • **Hubei Prov.**, 1♂, Pingbaying

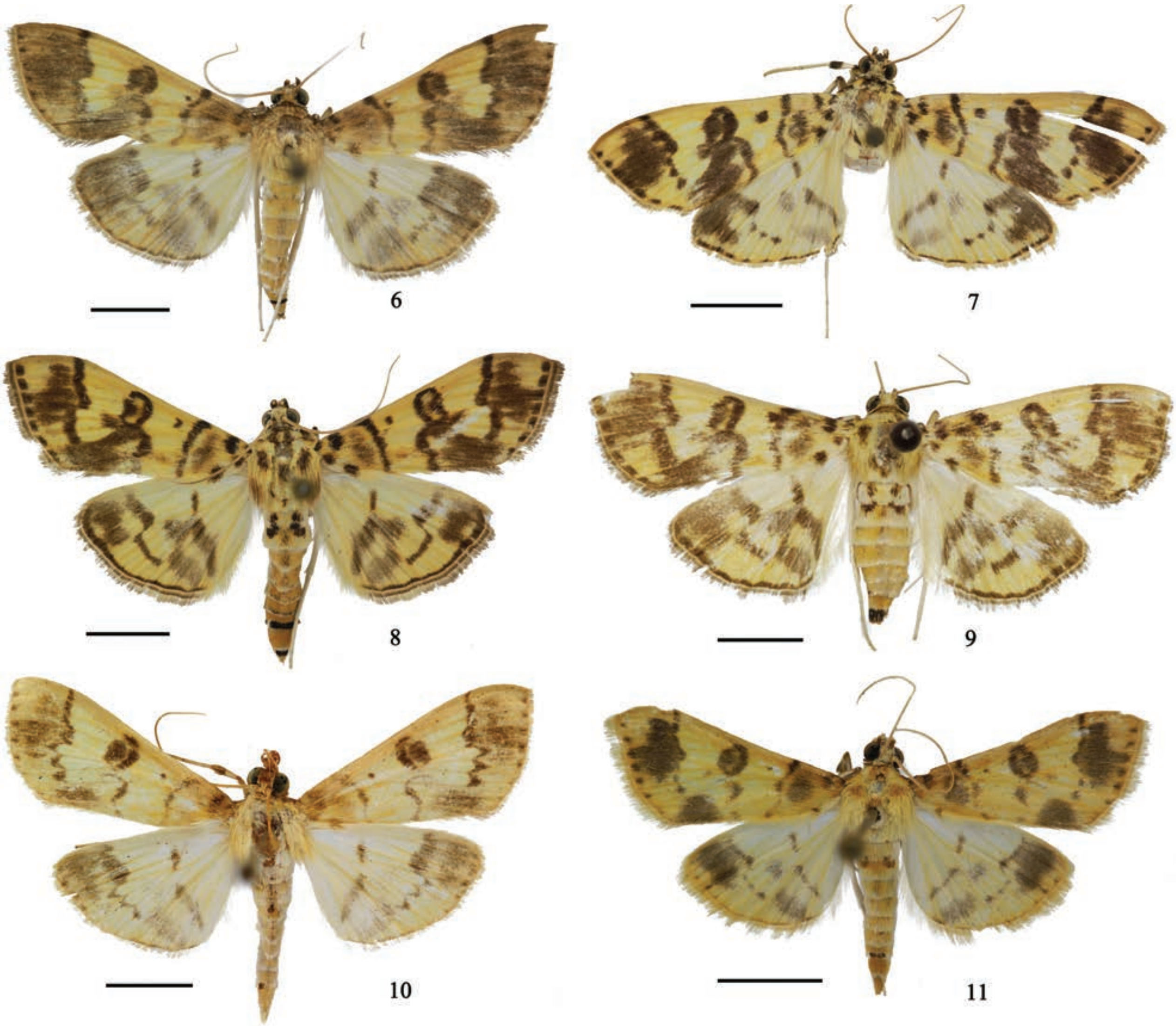

Figures 6–11. Habitus of *Purpurata* species **6** *P. obfuscalis* ♂ **7** *P. iopasalis* ♂ **8** *P. directa* sp. nov. holotype ♂ **9** *P. directa* sp. nov. paratype ♀ **10** *P. lurida* sp. nov. holotype ♂ **11** *P. plagiatalis* ♂. Scale bars: 0.5 cm.

National Forest Park, Xianfeng County, alt. 280 m, 21 July 1999, Hou-Hun Li leg. (NKU) • 5 ♂♂, 2 ♀♀, Hejiaping Town, Changyang County, alt. 800 m, 18 June 2018, Xi-Cui Du & Xiao Qiang-Lu leg., genitalia slide no.: LXQ18140 ♀ • **Anhui Prov.**, 1 ♂, Tang Kou Town, Huangshan City, 4 August 2004, Jia-Sheng Xu & Jia-Liang Zhang leg. (NKU) • **Zhejiang Prov.**, 1 ♂, Longtang Mountain, alt. 500 m, 22 May 2012, Xiao-Bing Fu leg. • 2 ♂♂, Tianmu Mountain, alt. 400 m, 24–25 July 2011, Xi-Cui Du & Xiao Bing-Fu leg. • **Hong Kong Special Administrative Region**, 1 ♂, Kadoorie Farm, alt. 21 m, 13 April 2007, Hou-Hun Li leg. (NKU).

Diagnosis. This species is distinguished by wings with postmedial line dentate and excurved between M_2 and CuA_2 (Fig. 6); gnathos vestigial to a narrow band (Fig. 12a); valva with distal 1/3 narrowed gradually and pointed apically, costa arched medially and bearing a cluster of long setae (Fig. 12); fibula a triangular lamina, with setae medially (Fig. 12b); phallus posteriorly with a finger-like protruding sclerite, a thick, spine-like cornutus and a brush-like cornutus (Fig. 12c).

Redescription. ***Habitus* (Fig. 6).** Forewing length 8.0–15.0 mm, wingspan 25.0–33.0 mm. Frons and vertex yellowish brown. Labial palpus with 1st segment yellowish white ventrally, the remainder yellowish brown. Maxillary palpus brown. Antenna yellowish brown, with ventral cilia ~ 1/3 in length of diameter of flagellomere in male. Patagium and tegula yellow, with brown patches. Thorax yellow dorsally, white ventrally. Legs yellowish white, distal end of front tibia black. Wings yellow, with purple-brown lines and patches. Forewing with three small spots at base, another spot near basal dorsum; antemedial line slightly wavy, accompanied by a large elliptical pale patch inside; orbicular stigma a dark brown dot; discoidal stigma reniform, yellow centrally; postmedial line obliquely inward from costa, dentate and excurved between M_2 and CuA_2, then incurved to discoidal stigma below and sinuous to inner margin; an irregular large patch between anterior postmedial line and terminal margin, another irregular large patch below discoidal stigma and extended to tornus; a line of small spots along terminal margin. Hindwing with discoidal stigma a short oblique stripe; postmedial line same as forewing before CuA_2, not apparent afterwards; an irregular large patch near apex beyond anterior postmedial line; a misty band below discoidal stigma, accompanied by another irregular misty wide band extended to tornus. Abdomen yellow dorsally; 1st and 2nd tergites with pale black spots laterally; 7th tergites black posteriorly in male; terminally black in some female individuals.

Male genitalia (Fig. 12). Uncus semicircular. Gnathos vestigial to a narrow band (Fig. 12a). Valva with distal 1/3 narrowed gradually, and pointed apically; costa arched medially and bearing a cluster of long setae. Fibula a triangular lamina, with setae medially (Fig. 12b). Saccus oval. Juxta a broad plate, invaginated anteriorly. Phallus posteriorly with a finger-like protruding sclerite, with a thick spine-like cornutus and a brush-like cornutus composed of a spine cluster (Fig. 12c).

Female genitalia (Fig. 13). Apophyses anteriores ~ 2 × length of apophyses posteriores. Ostium bursae relatively large, antrum broad. Ductus bursae ~ 2 × length of corpus bursae. Corpus bursae nearly rounded, with a round signum.

Distribution. China (Chongqing, Sichuan, Gansu, Xizang, Yunnan, Guangxi, Guizhou, Hainan, Shanaxi, Hubei, Anhui, Zhejiang, Xianggang), Nepal (Yamanaka 1998).

Purpurata iopasalis **(Walker, 1859), comb. nov.**

Figs 7, 14, 14a–c

Botys iopasalis Walker, 1859: 652. Type locality: India (Hindustan). Type depository: NHMUK.
Boty boteralis Walker, 1859: 716. Type locality: Malaysia (Sarawak).
Sylepta [sic] *marcidalis* Swinhoe, 1906: 382.
Pleuroptya iopasalis: Inoue 1982: 1: 343, 2: 234, 454.
Patania clava Xu & Du, 2016: 130, figs 1–4, 9–10. Syn. nov. Type locality: China (Hainan).

Material examined. ***Holotype*** of *Patania clava* • 1 ♂, **China, Hainan Prov.,** Diaoluo Mountain, alt. 900 m, 23 May 2014, Li-Jun Xu & Dan Xu leg., genitalia slide number XD15056. ***Paratype*** of *P. clava* • 1 ♀, same data as holotype, genitalia slide number XD15050.

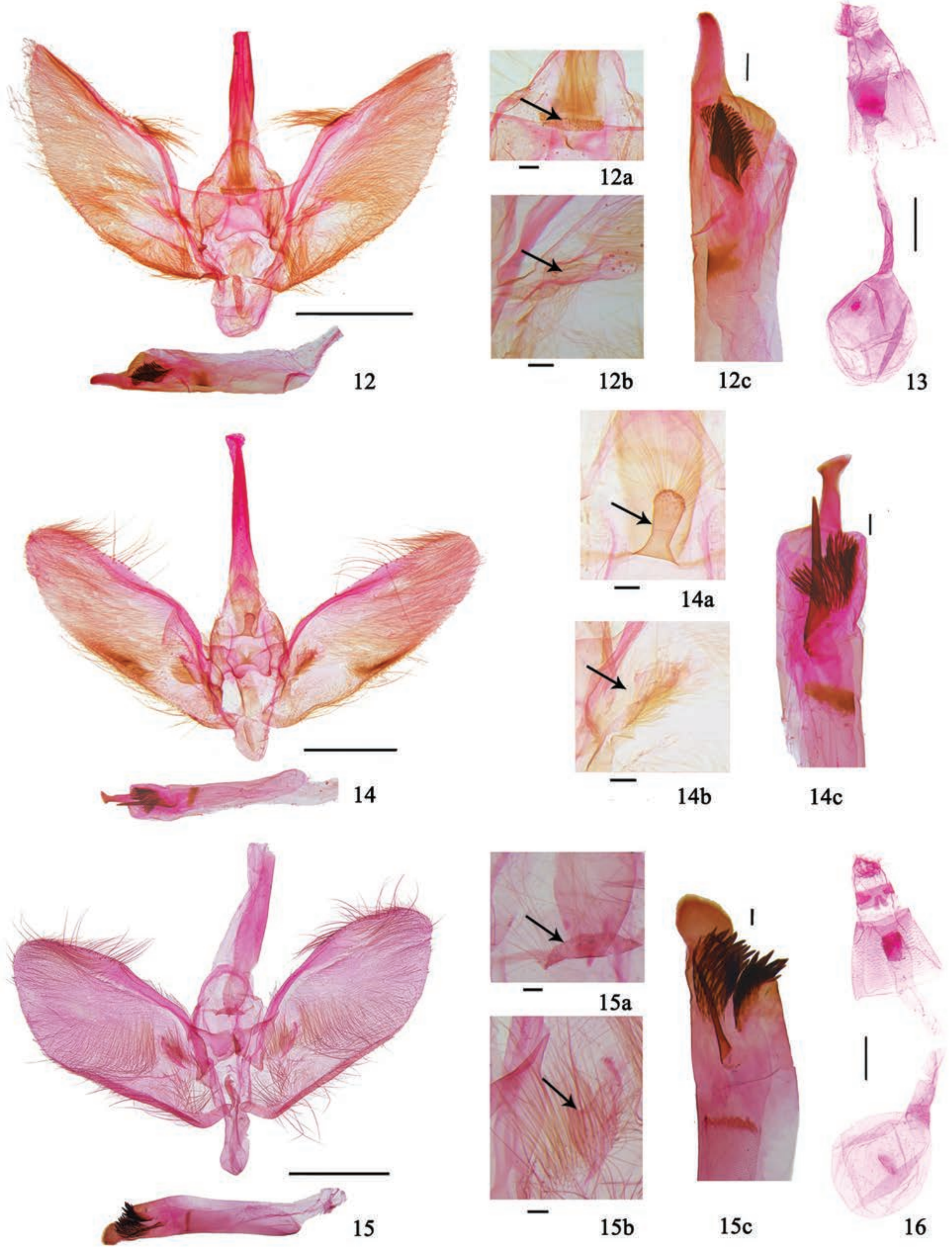

Figures 12–16. Genitalia of *Purpurata* species **12, 13** *P. obfuscalis* **12** male, genitalia slide no. XXL23275 **13** female, genitalia slide no. XLJ14221 **14** *P. iopasalis*, male, genitalia slide no. XXL23277 **15, 16** *P. directa* sp. nov. **15** male, holotype, genitalia slide no. LXQ18315 **16** female, paratype, genitalia slide no. XLJ14147 **12a, 14a, 15a** gnathos **12b, 14b, 15b** fibula **12c, 14c, 15c** cornuti and posterior protrusion of phallus. Scale bars: 1.0 mm (**12–16**); 0.1 mm (**12a–c, 14a–c, 15a–c**).

Additional material. **China** • **Hainan Prov.,** 1 ♂, Wuzhi Mountain, alt. 795 m, 20 May 2014, Li-Jun Xu & Dan Xu leg., genitalia slide no.: XXL23277.

Diagnosis. This species is similar to *P. obfuscalis* in appearance, but can be distinguished by the larger size (forewing length 13.0–19.0 mm, wingspan 33.0–35.0 mm), antenna with ventral cilia approximately as long as flagellomere diameter in male, postmedial line of fore and hind wings punctiform between M_2 and CuA_2 (Fig. 7); uncus nearly triangular (Fig. 14), gnathos thick, finger-like (Fig. 14a), costa of valva without a cluster of setae medially, fibula densely covered with setae (Fig. 14b), phallus posteriorly with a nail head-like protruding sclerite (Fig. 14c) in male genitalia (Fig. 14); ductus bursae ~ 4 × length of corpus bursae, signum absent in female genitalia. In *P. obfuscalis*, the forewing length is 8.0–15.0 mm and wingspan is 25.0–33.0 mm, the ventral cilia of antenna is ~ 1/3 length of flagellomere diameter in male, the postmedial lines of the fore and hind wings are dentate between M_2 and CuA_2 (Fig. 6). In male genitalia, the uncus of *P. obfuscalis* is semicircular (Fig. 12), the gnathos is reduced to a narrow band (Fig. 12a), the costa of valva bears a cluster of long setae medially (Fig. 12), the fibula bears setae medially (Fig. 12b), the phallus posteriorly has a finger-like protruding sclerite (Fig. 12c); in female genitalia, the ductus bursae is ~ 2 × as long as the corpus bursae and a rounded signum is present (Fig. 13).

Distribution. China (Yunnan, Hainan, Fujian, Guangdong, Taiwan) (Lu and Guan 1953; Xu and Du 2016), Japan, Indonesia, India, Myanmar, Sri Lanka, Malaysia, Thailand, Timor Leste, Philippines, Caroline Islands, Papua New Guinea, Pakistan, Australia (Hampson 1896; Shibuya 1928, 1929; Klima 1939; Inoue 1982; Wang and Speidel 2000).

Remarks. The uncus and fibula of this species are narrower than in other species of this genus. We found that the external morphology and male genitalia characters of *Patania clava* were the same as those of *Purpurata iopasalis*. Their distinctive characters were that the postmedial lines of the fore and hind wings were punctiform between M_2 and CuA_2, the gnathos was thick finger-like and setose apically (Walker 1859; Inoue 1982, Yamanaka 1998; Xu and Du 2016). Therefore, *Patania clava* is synonymized with *Botys iopasalis*. For a detailed description of this species see Walker (1859) and Xu and Du (2016). Moreover, Xu and Du (2016) described that the labial palpus of *Patania clava* was pale yellow with a brown patch near the base, while we observed that this species had a subapical brown spot beside this basal spot, and the subapical brown spot was obscured in some individuals.

Purpurata directa **sp. nov.**

https://zoobank.org/2C6FEFF3-EB2B-466D-B087-81CBBB2D6E51
Figs 2, 8, 9, 15, 15a–c, 16

Patania iopasalis: Xu and Du 2016: 132, figs 5–8. Type locality: India (misidentification).

Diagnosis. This species is very similar to *P. iopasalis* in appearance, but can be distinguished by ventral cilia ~ 1/3 length of flagellomere diameter in male, antemedial line of forewing relatively straight and slightly inclined outward, postmedial line of fore and hind wings smooth linear between M_2 and CuA_2 (Figs 8, 9); uncus semicircular, gnathos a transverse lamina, and valva broader than the latter in male genitalia (Fig. 15); a signum present in female genitalia (Fig. 16). In *P. iopasalis*, the ventral cilia are approximately equal in length of flagellomere diameter in male, the antemedial line is slightly wavy, the postmedial line of fore and hind wings punctiform between M_2 and CuA_2 (Fig. 7); the uncus is nearly triangular, and the gnathos is finger-like in the male genitalia (Fig. 14a); and the signum is absent in the female genitalia.

Type material. ***Holotype*:** ♂ pinned, with genitalia in a separate slide. **CHINA** • **Hunan Prov.**, Huping Mountain, Shimen County, alt. 350 m, 6 June 2017, Jian-Yue Qiu & Hao Xu leg., genitalia slide number: LXQ18315. ***Paratypes*:** pinned, some with genitalia in the separate slides, respectively. **CHINA** • 6 ♂♂, same data as holotype • **Hubei Prov.**, 1 ♂, Hejiaping Town, Changyang County, alt. 800 m, 18 May 2018, Xian-Qiang Lu & Xi-Cui Du leg. • **Chongqing Municipality**, 2 ♀♀, Daheba, Jinfo Mountain, alt. 600 m, 14, 17 July 2017, Shi-Man Bu leg • **Sichuan Prov.**, 2 ♂♂, Emei Mountain, alt. 863 m, 17 July 2011, Jian-Bo Cao leg. • **Guizhou Prov.**, 3 ♂♂, Baishao, Kuankuoshui, alt. 800 m, 10 August 2010, Xi-Cui Du leg., genitalia slide number: HGQ13018, HGQ13019 • 3 ♂♂, 1 ♀, Wengang village, Libo County, alt. 1345 m, 20 July 2015, Ji-Ping Wan leg. • **Yunnan Prov.**, 1 ♂, Baihualing Village, Baoshan City, alt. 1520 m, 13 July 2007, Dan-Dan Zhang leg. • 1 ♂, Daxichang Village, Malipo County, alt. 1465 m, 7 August 2007, Man-Fei Tao leg. • **Hainan Prov.**, 1 ♂, Bawangling National Forest Park, 11 June 2010, Li Kang leg., genitalia slide number: XLJ14105 • 3 ♂♂, 1 ♀, Wuzhi Mountain, alt. 795 m, 18, 19, 21 May 2014, Li-Jun Xu & Dan Xu leg., genitalia slide number: XD15024 ♂, XLJ14146 ♂, XLJ14147 ♀ • 1 ♂, Diaoluo Mountain, alt. 500 m, 25 May 2014, Li-Jun Xu & Dan Xu leg., genitalia slide number: XD15049 • **Guangxi Zhuang Autonomous Region**, 3 ♂♂, Nonggang National Nature Reserve, Longzhou County, alt. 188 m, 25, 27, 30 July 2011, Gui-Qing He leg., genitalia slide number: XLJ14083 (being identified as *Patania iopasalis* by Xu and Du (2016)), XLJ13199 • 3 ♂♂, Nonggang National Nature Reserve, Longzhou County, alt. 188 m, 2 August 2011, Gui-Qing He leg., genitalia slide number: XLJ13164 • 5 ♂♂, Mulun Nature Reserve, alt. 288 m, 21 July 2015, Dan Xu leg. • **Guangdong Prov.**, 5 ♂♂, Renhua County, Danxia Mountain, alt. 408 m, 31 May 2018, Feng-Xia He leg.

Description. ***Habitus*** (Figs 2, 8, 9). Forewing length 9.0–13.5 mm, wingspan 21.0–30.0 mm. Frons and vertex yellow. Labial palpus yellowish white, with distal part of 2nd segment brown. Maxillary palpus yellowish white basally, brown near distal end. Antenna yellowish brown, with brown spots on scape, ventral cilia ~ 1/3 in length of diameter of flagellomere in male. Patagium and tegula yellow, with brown patches. Thorax yellowish brown dorsally, white ventrally. Legs pale yellow, front coxa and middle tibia with outer sides black at the base and distal end, front tibia with distal end black. Wings yellow, with purple-brown lines and patches. Forewing with three small spots at base, another spot near basal dorsum; antemedial line relatively straight, slightly inclined outward, accompanied by a large elliptical pale patch inside; orbicular stigma a dark brown dot; discoidal stigma reniform, yellow centrally, connected to postmedial line posteriorly; postmedial line slightly obliquely inward from costa, straightly excurved between M_2 and CuA_2, then incurved to discoidal stigma below and sinuous to inner margin; an irregular large patch between anterior postmedial line and terminal margin, another irregular large patch below discoidal stigma and extended to tornus; a line of small spots along terminal margin. Hindwing with discoidal stigma a short oblique stripe; postmedial line same as forewing before CuA_2, not apparent afterwards; an irregular large patch near apex beyond anterior postmedial line; a band below discoidal stigma slightly inclined towards tornus, accompanied by another irregular misty wide band extended to tornus. Cilia of fore and hind wings purple-brown, white basally. Abdomen yellow dorsally, white ventrally; 1st and 2nd tergites with black spots laterally; 7th and 8th tergites black posteriorly in male; terminally black in female.

Male genitalia (Fig. 15). Uncus semicircular. Gnathos a transverse lamina, with posterior end arc-shaped and setose (Fig. 15a). Valva broad tongue-shaped, with long setae along distal costa; sacculus a narrowed band; fibula a triangular lamina, setose basally (Fig. 15b). Saccus cylindrical, with rounded end. Juxta a narrowed plate. Phallus posteriorly with an oval protruding sclerite, with a thick, needle-like cornutus and a brush-like cornutus composed of a spine cluster (Fig. 15c).

Female genitalia (Fig. 16). Apophyses anteriores ~ 2 × length of apophyses posteriores. Ductus seminalis originating from antrum. Ductus bursae ~ 2 × length of corpus bursae. Corpus bursae nearly rounded, with a short transverse bar-like signum.

Distribution. China (Chongqing, Sichuan, Guizhou, Yunnan, Hainan, Hubei, Hunan, Guangdong, Guangxi).

Etymology. The species name *directa* is derived from the Latin word *directus*, an adjective, meaning straight, indicating the antemedial line of forewing relatively straight.

Purpurata lurida **sp. nov.**

https://zoobank.org/04DDE7A6-D2E1-40AC-8D98-C6D9A526BB55
Figs 10, 17, 17a–c, 18

Diagnosis. This species is similar to *P. obfuscalis* in appearance and genitalia, but can be distinguished by the body color paler than the latter (Fig. 10); uncus short and broad triangular (Fig. 17a); valva shorter and broader than the latter, with distal 1/3 narrowed very gradually and rounded apically (Fig. 17). In *P. obfuscalis*, the uncus is semicircular (Fig. 12a); the distal 1/3 of the valva is narrowed gradually and pointed apically (Fig. 12).

Type material. ***Holotype*:** ♂ pinned, with genitalia in a separate slide. **China** • **Guizhou Prov.**, Kuankuoshui Nature Reserve, alt. 1500 m, 15 August 2010, Xi-Cui Du leg., genitalia slide number: XLJ14084. ***Paratypes*:** pinned, some with genitalia in separate slides. **China** • **Hubei Prov.**, 2 ♂♂, Hejiaping Town, Changyang County, alt. 800 m, 18 June 2018, Xiao-Qiang Lu & Xi-Cui Du leg. • 2 ♂♂, Xingdou Mountain, Maoba Town, Enshi, alt. 780 m, 30 July 2012, Jun Zhang & Xiao-Bing Fu leg. • **Chongqing Municipality**, 2 ♂♂, Jinyun Mountain, alt. 550 m, 22, July 2010, Li Kang & Xing-Fu Fu leg., genitalia slide number: XLJ14103 • 2 ♂♂, 1 ♀, Jinyun Mountain, 29 July 2010, Xi-Cui Du & Chao-Wei Bi leg., genitalia slide number: XLJ14104 ♀ • 1♂, Jinyun Mountain, 30 July 2012, Li-Jun Xu & Jian-Bo Cao leg. • 2 ♂♂, Jinyin Mountain, Qianjiang District, alt. 1100 m, 26 July 2012, Li-Jun Xu & Jun-Zhang leg. • **Yunnan Prov.**, 1 ♂, Daxichang village, Malipo

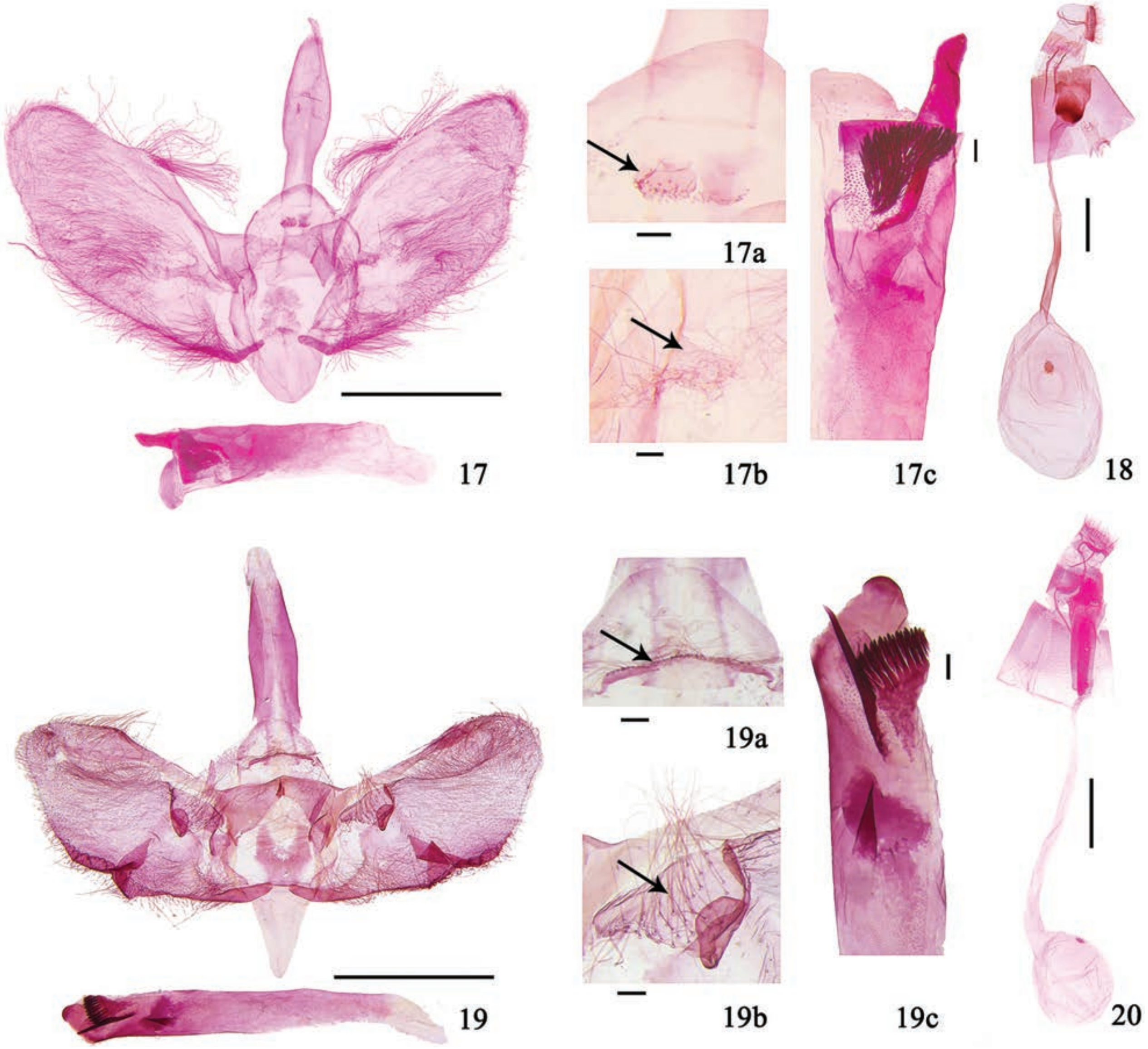

Figures 17–20. Genitalia of *Purpurata* species **17, 18** *P. lurida* sp. nov. **17** male, holotype, genitalia slide no. XLJ14084 **18** female, paratype, genitalia slide no. LXQ18316 **19, 20** *P. plagiatalis* **19** male, genitalia slide no. HGQ13237 **20** female, genitalia slide no. XLJ14204 **17a, 19a** gnathos **17b, 19b** fibula **17c, 19c** cornuti and posterior protrusion of phallus. Scale bars: 1.0 mm (**17–20**); 0.1 mm (**17a–c, 19a–c**).

County, alt. 1465 m, 5 June 2015, Man-Fei Tao leg. • 2♀♀, Xishuangbanna Tropical Botanical Garden, alt. 659 m, 28 May 2015, Man-Fei Tao leg., genitalia slide number: LXQ18316 • **Hainan Prov.**, 1♂, Diaoluo Mountain vocational village, alt. 500 m, 23 May 2014, Li-Jun Xu & Dan Xu leg. • **Zhejiang Prov.**, 3♂♂, Tianmu Mountain, alt. 400 m, 24, 25, 30 July 2011, Xi-Cui Du & Xiao-Bing Fu leg.

Description. ***Habitus*** (Fig. 10). Forewing length 11.0–13.5 mm, wingspan 24.0–30.0 mm. Frons and vertex yellowish brown. Labial palpus with 1st segment yellowish white ventrally, the remainder yellowish brown. Maxillary palpus brown. Antenna yellowish brown, with ventral cilia ~ 1/3 in length of diameter of flagellomere in male. Patagium and tegula yellow. Thorax yellow dorsally, white ventrally. Legs yellowish white, distal end of front tibia black. Wings pale yellow, with purple-brown lines and patches. Forewing with three small spots at base, another spot near basal dorsum; antemedial line slightly wavy, accompanied by a large elliptical pale patch inside; orbicular stigma a dark brown dot; discoidal stigma reniform, yellow centrally; postmedial line slightly obliquely inward from costa, dentate and excurved between M_2 and CuA_2, then incurved to discoidal stigma below and sinuous to inner margin; an irregular large patch near apex beyond anterior postmedial line, another misty patch near tornus below CuA_2; a line of spots along marginal line. Hindwing with discoidal stigma a short oblique stripe; postmedial line same as forewing before CuA_2, not apparent afterwards; an irregular large patch near apex beyond anterior postmedial line; a band below discoidal stigma, accompanied by another irregular misty wide band extended to tornus. Cilia of fore and hind wings yellowish white. Abdomen yellow dorsally, white ventrally; 1st and 2nd tergites with pale black spots laterally and 7th tergites black posteriorly in male.

Male genitalia (Fig. 17). Uncus short and broad triangular. Gnathos vestigial to a narrow band and bearing a few short setae (Fig. 17a). Valva broad tongue-shaped, with distal 1/3 narrowed very gradually, and rounded apically; costa arched medially and bearing a cluster of long setae; fibula a short lamina, setose basally (Fig. 17b). Saccus oval. Juxta a broad plate. Phallus posteriorly with a finger-like protruding sclerite, with a thick, needle-like cornutus and a brush-like cornutus composed of a spine cluster (Fig. 17c).

Female genitalia (Fig. 18). Apophyses anteriores ~ 2 × length of apophyses posteriores. Antrum broad, ductus seminalis originating from antrum. Ductus bursae ~ 2 × length of corpus bursae. Corpus bursae nearly oval, with a round signum.

Distribution. China (Chongqing, Guizhou, Yunnan, Hainan, Hubei, Zhejiang).

Etymology. The species name *lurida* is derived from the Latin word *luridus*, an adjective, meaning pale yellow, indicating the pale wing color.

Purpurata plagiatalis **(Walker, 1859), comb. nov.**

Figs 11, 19, 19a–c, 20

Botys plagiatalis Walker, 1859: 673. Type locality: Sri Lanka.
Pleuroptya plagiatalis: Inoue 1982: 1: 343, 2: 234.
Patania plagiatalis: Nuss et al. 2003–2024. Global Information System on Pyraloidea.

Material examined. Guangxi Zhuang Autonomous Region • 1 ♂, Nonggang National Nature Reserve, Longzhou County, alt. 188 m, 27 July 2011, Gui-Qing He leg., genitalia slide number: HGQ13237 • 1 ♂, Mulun National Nature Reserve, alt. 288 m, 22 July 2015, Dan Xu leg. • **Hainan Prov.**, 1 ♀, Jianfengling Nature Reserve, alt. 770 m, 13 July 2014, Pei-Xin Cong, Lin-Jie Liu & Sha Hu leg. (NKU), genitalia slide number: XLJ14204.

Diagnosis. This species is distinguished by wings with postmedial line punctiform and excurved between M_2 and CuA_2 (Fig. 11); gnathos vestigial to a narrow band (Fig. 19a); sacculus narrowed medially, with a lamellar projection near distal end (Fig. 19); fibula ear-shaped, with long setae (Fig. 19b); phallus posteriorly with a rounded protruding sclerite, with a thick needle-like cornutus and a brush-like cornutus, and a short thorn-like cornutus near posterior end (Fig. 19c).

Redescription. *Habitus* (Fig. 11). Forewing length 8.0–9.5 mm, wingspan 18.0–22.0 mm. Frons and vertex yellowish brown. Labial palpus yellowish white, pale brown at distal end of 2nd segment. Maxillary palpus brown. Antenna yellowish brown, with ventral cilia ~ ½ in length of diameter of flagellomere in male. Patagium and tegula yellow, with pale yellowish brown patches centrally and basally respectively. Thorax yellow dorsally, white ventrally. Legs yellowish white, distal end of front tibia black. Wings yellow, with purple-brown lines and patches. Forewing with three small spots at base, another spot near basal dorsum; antemedial line slightly wavy, accompanied by a large elliptical patch inside; orbicular stigma a dark brown dot; discoidal stigma reniform, yellow centrally; postmedial line punctiform and excurved between M_2 and CuA_2; an irregular large patch near apex beyond anterior postmedial line, a nearly semicircular patch near tornus below CuA_2; a line of small spots along terminal margin. Hindwing with discoidal stigma a short oblique stripe; postmedial line same as forewing before CuA_2, not apparent afterwards; a large patch near apex beyond anterior postmedial line; a thin band below discoidal stigma, accompanied by an irregular misty wide band extended to tornus. Cilia of fore and hind wings yellowish white. Abdomen yellow dorsally, 1st and 2nd tergites with pale black spots laterally and 7th tergites black posteriorly in male.

Male genitalia (Fig. 19). Uncus short and broad. Gnathos vestigial to a narrow band and setose (Fig. 19a). Valva broad tongue-shaped with long setae along distal costa; fibula ear-shaped with long setae (Fig. 19b). Sacculus narrowed medially, with a lamellar projection near distal end. Saccus triangular. Juxta forcipate. Phallus posteriorly with a rounded protruding sclerite, with a thick needle-like cornutus and a brush-like cornutus composed of a spine cluster, and a short thorn-like cornutus near posterior end (Fig. 19c).

Female genitalia (Fig. 20). Apophyses anteriores ~ 2 × as long as apophyses posteriores. Antrum relatively long, with a long, sclerotized band. Ductus bursae ~ 4 × as long as corpus bursae. Corpus bursae nearly rounded, with a round signum.

Distribution. China (Xizang, Yunnan, Guangxi, Guangdong, Hainan, Fujian) (Lu and Guan 1953; Wang et al. 2003), Australia, Guatemala, Japan, India, Sri Lanka (Walker 1859; Inoue 1982; Klima 1939).

Host plants. *Ipomoea* spp. (Wang et al. 2003).

Purpurata shompen (Singh & Ahmad, 2022), comb. nov.

Patania shompen Singh & Ahmad in Singh et al. 2022: 14, figs 1–2, 5–7. Type locality: India (Great Nicobar Island).

Diagnosis. This species is similar to *P. iopasalis*, but can be distinguished by the postmedial line of forewing punctiform between M_2 and CuA_2, and the postmedial line of hindwing linear between M_2 and CuA_2 (Singh et al. 2022: fig. 1); phallus posteriorly with a rectangular protruding sclerite in male genitalia (Singh et al. 2022: fig. 7). In *P. iopasalis*, the postmedial line of the fore and hind wings are punctiform between M_2 and CuA_2 (Fig. 7); and phallus posteriorly with a nail head-like protruding sclerite in male genitalia (Fig. 14c).

Distribution. India (Great Nicobar Island) (Singh et al. 2022).

Remarks. This species is not found in China. The diagnosis is summarized based on the description and images of habitus and genitalia by Singh et al. (2022).

Discussion

According to the description and habitus images by Moore (1888), we found the external morphology of *Syllepte leopardalis* (Moore, 1888), distributed in India, very similar to the new genus *Purpurata*, especially in wing color and markings. But its antennae do not seem to be filiform according to the habitus illustration provided by Moore. The genitalia of *S. leopardalis* were not described or illustrated, so further study is needed to confirm its morphological characters and affiliation.

Acknowledgments

We are grateful to Li-Jun Xu for her preliminary work about the genus *Patania*, and the other graduate students and undergraduate in Laboratory of Lepidoptera Systematics (Southwest University, Chongqing, China) for their contributions to the specimen collection. We also give our thanks to Dr Jian-Yue Qiu and Dr Hao Xu (Mianyang Teachers' College, Sichuan, China), to Dr Dan-Dan Zhang (Sun Yat-Sen University, China) for providing some specimens, to Prof. Hou-Hun Li (Nankai University, Tianjing, China) for lending us specimens, and to NHMUK for providing access to the corresponding author for examining some relevant specimens. We would also like to thank the language editor Dr Christopher Glasby for proofreading our manuscript. And special thanks are given to Dr Richard Mally (Czech University of Life Sciences, Czech Republic), Dr Bernard Landry (Muséum d'histoire naturelle, Switzerland), and another anonymous reviewer for reviewing our manuscript and their helpful suggestions. Cordial thanks are given to Dr Richard Mally again for professionally supplementing some important information to our revised manuscript.

Additional information

Conflict of interest

The authors have declared that no competing interests exist.

Ethical statement

No ethical statement was reported.

Funding

This study is sponsored by Natural Science Foundation of Chongqing, China (No. CSTB2022NSCQ-MSX1164), National Natural Science Foundation of China (No. 31772500), Shuangcheng cooperative agreement research grant of Yibin, China (No. XNDX2022020011) and Joint Fund of Henan Science and Technology R&D program (Advantageous Discipline De-velopment) (NO. 232301420119).

Author contributions

Conceptualization: XLX, XCD, XQL. Data curation: XLX, XCD. Funding acquisition: XCD. Investigation: XLX, XQL. Methodology: XLX, XCD, XQL. Project administration: XCD. Resources: XCD. Supervision: XCD. Writing - original draft: XQL, XLX. Writing - review and editing: XLX, XCD.

Author ORCIDs

Xin-Lei Xue https://orcid.org/0009-0000-5697-0872
Xiao-Qiang Lu https://orcid.org/0009-0009-3696-7778
Xi-Cui Du https://orcid.org/0000-0002-7796-7303

Data availability

All of the data that support the findings of this study are available in the main text.

References

Du XC (2009) Spilomelinae. In: Li HH, Ren YD, Zhang DD, Du XC, Li WC, You P (Eds) Insect Fauna of Henan (Lepidoptera: Pyraloidea). Science Press, Beijing, 282–288.

Hajibabaei M, Janzen DH, Burns JM, Hallwachs W, Hebert PDN (2006) DNA barcodes distinguish species of tropical Lepidoptera. Proceedings of the National Academy of Sciences of the United States of America 103(4): 968–971. https://doi.org/10.1073/pnas.0510466103

Hampson GF (1896) Moths Vol. IV. The Fauna of British India, including Ceylon and Burma, [i–xxviii] 1–594.

Heppner JB (2012) Taiwan Lepidoptera Catalog. Supplement 1. Corrections and Additions. Lepidoptera Novae 5(1): 1–84.

Inoue H (1982) Pyralidae. In: Inoue H, Sugi S, Kuroko H, Moriuti S, Kawabe A, Owada M (Eds) Moths of Japan. Kodansha, Tokyo, 1: 307–404, 2: 223–254.

Kimura M (1980) A simple method for estimating evolutionary rates of base substitutions through comparative studies of nucleotide sequences. Journal of Molecular Evolution 16: 111–120. https://doi.org/10.1007/BF01731581

Kirpichnikova VA (2009) Pyralids (Lepidoptera, Pyraloidea: Pyralidae, Crambidae) of the Fauna of Russian Far East. Dalnauka, Vladivostok, 518 pp.

Kirti JS, Gill NS (2007) Revival of genus *Patania* Moore and reporting of a new species *menoni* (Pyraustinae: Pyralidae: Lepidoptera). Journal of Entomological Research 31(3): 265–275. https://www.indianjournals.com/ijor.aspx?target=ijor:jer&volume=31&issue=3&article=020

Klima A (1939) Pyralidae: subfamily: Pyraustinae I. In: Bryk F (Ed.) Lepidopterorum Catalogous. Dr. W. Junk, Gravenhage, 89: 186–224.

Lederer J (1863) Beitrag zur Kenntniss der Pyralidinen. Wiener Entomologische Monatschrift 7(8, 10–12): 243–280, 331–504 [pls 2–18].

Leraut P (2005) Contribution à l'étude des genres *Pyralis* Linnaeus, *Pleuroptya* Meyrick et *Haritalodes* Warren (Lepidoptera, Pyraloiden). Revue Francaise d' Entomologie (N.S.) 27(2): 77–94.

Li HH, Zheng ZM (1996) Methods and techniques of specimens of Microlepidoptera. Journal of Shaanxi Normal University (Natural Science Edition) 24(3): 63–70.

Lu JR, Guan ZH (1953) List of Chinese Pyralid insects, addendum of Hu "List of Chinese Insects", Part II. Nymphulinae, Scopariinae, Pyraustinae. Acta Entomologica Sinica 3(2): 203–244.

Mally R, Hayden J, Neinhuis C, Jordal B, Nuss M (2019) The phylogenetic systematics of Spilomelinae and Pyraustinae (Lepidoptera: Pyraloidea: Crambidae) inferred from DNA and morphology. Arthropod Systematics & Phylogeny 77(1): 141–204. https://doi.org/10.26049/ASP77-1-2019-07

Matsui Y, Mally R, Kohama S, Aoki I, Azuma M, Naka H (2022). Molecular phylogenetics and tribal classification of Japanese Pyraustinae and Spilomelinae (Lepidoptera: Crambidae). Insect Systematics & Evolution 54: 77–106. https://doi.org/10.1163/1876312X-bja10037

Moore F (1888) Descriptions of new Indian lepidopterous insects from the collection of the late Mr. WS Atkinson. Heterocera (continued) (Pyralidae, Crambidae, Geometridae, Tortricidae, Tineidae). In: Hewitson WC, Moore F (Eds) Descriptions of new Indian lepidopterous Insects from the collection of the late Mr. WS Atkinson. Asiatic Society of Bengal / Taylor & Francis, Calcutta / London, 199–299. https://www.biodiversitylibrary.org/bibliography/5528

Munroe EG (1983) Pyralidae (except Crambinae). In: Hodges RW, Dominick T, Davis DR, Ferguson DC, Franclemont JG, Munroe EG, Powell JA (Eds) Check List of the Lepidoptera of America north of Mexico including Greenland. E. W. Classey Ltd. and the Wedge Entomological Research Foundation, London, 67–76, 78–85.

Munroe EG (1995) Crambidae. In: Heppner JB (Eds) Atlas of Neotropical Lepidoptera, Volume 3. Checklist: Part 2. Hyblaeoidea - Pyraloidea - Tortricoidea. Association for Tropical Lepidoptera & Scientific Publishers, Gainesville, 34–79. https://doi.org/10.1093/aesa/90.5.706

Nuss M, Landry B, Mally R, Vegliante F, Tränkner A, Bauer F, Hayden J, Segerer A, Schouten R, H Li, Trofimova T, Solis MA, Prins JD, Speidel W (2003–2024) Global Information System on Pyraloidea. http://globiz.pyraloidea.org

Saitou N, Nei M (1987) The neighbor-joining method: a new method for reconstructing phylogenetic trees. Molecular Biology and Evolution 4(4): 406–425. https://doi.org/10.1093/oxfordjournals.molbev.a040454

Sasaki A, Yamanaka H (2013) Spilomelini. In: Nasu Y, Hirowatari T, Kishida Y (Eds) The Standard of Moths in Japan IV. Gakken Education Publishing, Tokyo, 74–84, 415–478.

Shaffer M, Nielsen ES, Horak M (1996) Pyraloidea. In: Nielsen, ES, Edwards, ED, Rangsi, TV (Eds) Checklist of the Lepidoptera of Australia. In: Nielsen ES (Eds) Monographs on Australian Lepidoptera 4. CSIRO Division of Entomology, Canberra, 164–199.

Shibuya J (1928) The systematic study on the Formosan Pyralidae. Journal of the Faculty of Agriculture, Hokkaido Imperial University 22(1): 217–229. https://eprints.lib.hokudai.ac.jp/dspace/handle/2115/12624

Shibuya J (1929) On the known and unrecorded species of the Japanese Pyraustinae (Lepid.). Journal of the Faculty of Agriculture, Hokkaido Imperial University 25(3): 182–183. https://eprints.lib.hokudai.ac.jp/dspace/handle/2115/12650

Singh N, Ahmad J, Chandra K (2022) A new species of genus *Patania* Moore, 1888 from India (Lepidoptera: Crambidae, Spilomelinae). Shilap-Revista de Lepidopterologia 50(197): 13–17. https://doi.org/10.57065/shilap.178

Walker F (1859) Pyralides. List of Specimens of Lepidopterous Insects in the Collection of the British Museum. Printed by order of the Trustees, London, 18: 509–798.

Wang XZ, Speidel W (2000) Pyraloidea (Pyralidae, Crambidae). Guide book to insects in Taiwan (19). Shu Shin Books, Taipei, 295 pp.

Wang JS, Song SM, Wu YY, Chen TM (2003) Fauna of Pyralidae of Wuyishan Nature Reserve in China. China Science and Technology Press, Beijing, 324–326.

Xu D, Du XC (2016) A new species of Patania from the Hainan Island, China (Lepidoptera, Crambidae). ZooKeys 614: 129–135. https://doi.org/10.3897/zookeys.614.8810

Yamanaka H (1998) Pyralidae of Napal (II). Tinea 15(suppl. 1): 99–115.

ZooKeys 1219: 195–214 (2024)
DOI: 10.3897/zookeys.1219.133899

Research Article

Four new species of *Tapinocyba* Simon, 1884 (Araneae, Linyphiidae) from Jiangjin District of Chongqing, China

Muhammad Irfan[1,2*], Dai Yun[3*], Wang Lu-Yu[1], Zhang Zhi-Sheng[1]

1 *Key Laboratory of Eco-environments in Three Gorges Reservoir Region (Ministry of Education), School of Life Sciences, Southwest University, Chongqing 400715, China*
2 *College of Plant Protection, Southwest University, Chongqing 400715, China*
3 *Forestry Bureau of Jiangjin District, Chongqing 402262, China*
Corresponding authors: Zhang Zhi-Sheng (zhangzs327@qq.com); Wang Lu-Yu (wangluyu1989@163.com)

Abstract

Four new species of the genus *Tapinocyba* Simon, 1884 are described from Jiangjin, Chongqing: *T. centralis* **sp. nov.** (♂), *T. denticulata* **sp. nov.** (♂♀), *T. triangularis* **sp. nov.** (♂♀), and *T. virga* **sp. nov.** (♂♀). The new species exhibit distinctive genital features, such as a bifurcated embolus tip in the male palp of *T. denticulata* **sp. nov.** and *T. virga* **sp. nov.**, and embolus tip unbifurcated in *T. centralis* **sp. nov.** The epigynes display more unique characteristics, such as epigynal plate with a pit ventrally on its frontal face in *T. triangularis* **sp. nov.** and *T. virga* **sp. nov.**, which is absent in all other known *Tapinocyba* species. Detailed descriptions, along with photographs of genital characters, somatic features, and a distribution map, are provided.

Key words: Description, Erigoninae, morphology, sheet-web, taxonomy

Academic editor: Dragomir Dimitrov
Received: 4 August 2024
Accepted: 27 October 2024
Published: 3 December 2024

ZooBank: https://zoobank.org/40631DBF-34FF-4C81-A6A4-8C940FBA1E69

Citation: Irfan M, Yun D, Lu-Yu W, Zhi-Sheng Z (2024) Four new species of *Tapinocyba* Simon, 1884 (Araneae, Linyphiidae) from Jiangjin District of Chongqing, China. ZooKeys 1219: 195–214. https://doi.org/10.3897/zookeys.1219.133899

Introduction

The family Linyphiidae is one of the most diverse spider families worldwide, comprising 634 extant genera and 4,858 species, including 11 fossil genera and 62 species (WSC 2024). Currently, 532 species in 175 genera have been reported from China (Tanasevitch 2024), of which 37 species in 22 genera have been recorded in Chongqing Municipality (Irfan et al. 2022, 2023a, 2023b). *Tapinocyba* Simon, 1884, is a small genus consisting of 41 species, primarily distributed across Nearctic and Palearctic regions (WSC 2024). In the Chinese fauna, three species have been recorded, specifically from the provinces of Jilin, Sichuan, and Taiwan (Sha et al. 1994; Tanasevitch 2011, 2018).

Jiangjin District is located in the southwest of Chongqing, China, along the upper section of the Yangtze River. This work is the first study on Linyphiidae spiders collected in Jiangjin. As a result, four new species belonging to the genus *Tapinocyba* have been identified and described here.

---

* These authors contributed equally to this work.

Materials and methods

The specimens were collected using Malaise traps and sieving leaf litter methods. All specimens were preserved in 75% ethanol. Left male palps were examined and photographed after dissection. After dissection, epigynes were cleared in trypsin enzyme solution before examination and photography. The specimens were examined and measured using Leica M205A stereomicroscope equipped with Leica DFC450 camera and LAS v. 4.6 software. All the photos of habitus and genitalia were taken with Kuy Nice CCD mounted on an Olympus BX53 compound microscope. Compound focus images were generated using Helicon Focus v. 6.7.1. Eye sizes were measured at the maximum dorsal diameter. Leg measurements are shown as total length (femur, patella, tibia, metatarsus, tarsus). All measurements are given in millimeters. Map was created using the online mapping software SimpleMappr (Shorthouse 2010) (Fig. 12). Specimens are deposited in the School of Life Sciences, Southwest University, Chongqing (**SWUC**), China. The terminology used in figures legend follows Hormiga (2000). In text "Fig." and "Figs" refer to figures herein, while "fig." and "figs" refer to figures published elsewhere.

The following abbreviations are used in the text and figures: **a.s.l.** = above sea level; **AER** = anterior eye row; **ALE** = anterior lateral eyes; **AME** = anterior median eyes; **AME–ALE** = the distance between AME and ALE; **AME–AME** = the distance between AMEs; **ARP** = anterior radical process; **CD** = copulatory ducts; **CO** = copulatory openings; **DP** = dorsal plate; **DSA** = distal suprategular apophysis; **DTA** = dorsal tibial apophysis; **E** = embolus; **FD** = fertilization ducts; **MM** = median membrane sensu van Helsdingen (1965) = embolic membrane sensu van Helsdingen (1986) and Hormiga (1994); **MSA** = marginal suprategular apophysis; **PC** = paracymbium; **PER** = posterior eye row; **PLE** = posterior lateral eyes; **PME** = posterior median eyes; **PME–PLE** = distance between PME and PLE; **PME–PME** = distance between PMEs; **PT** = protegulum; **R** = radix; **S** = spermatheca; **SPT** = suprategulum; **ST** = subtegulum; **T** = tegulum; **TmI** = position of trichobothrium on metatarsus I; **TP** = tailpiece; **VP** = ventral plate.

Taxonomy

Family Linyphiidae Blackwall, 1859
Subfamily Erigoninae Emerton, 1882

Genus *Tapinocyba* Simon, 1884
(盾大蛛属)

Type species. *Walckenaera praecox* O. Pickard-Cambridge, 1873; gender feminine.

Tapinocyba centralis sp. nov.
https://zoobank.org/101F9F9F-3E08-47D8-A050-6C5A6ABFC7BA
Figs 1, 2, 12
(中盾大蛛)

Type material. ***Holotype:*** China • ♂; Chongqing Municipality, Jiangjin District, Zhuyang Town, Yunwuping, Guanyin Valley; 29°9'1.38"N, 105°57'28.18"E, 558 m a.s.l.,

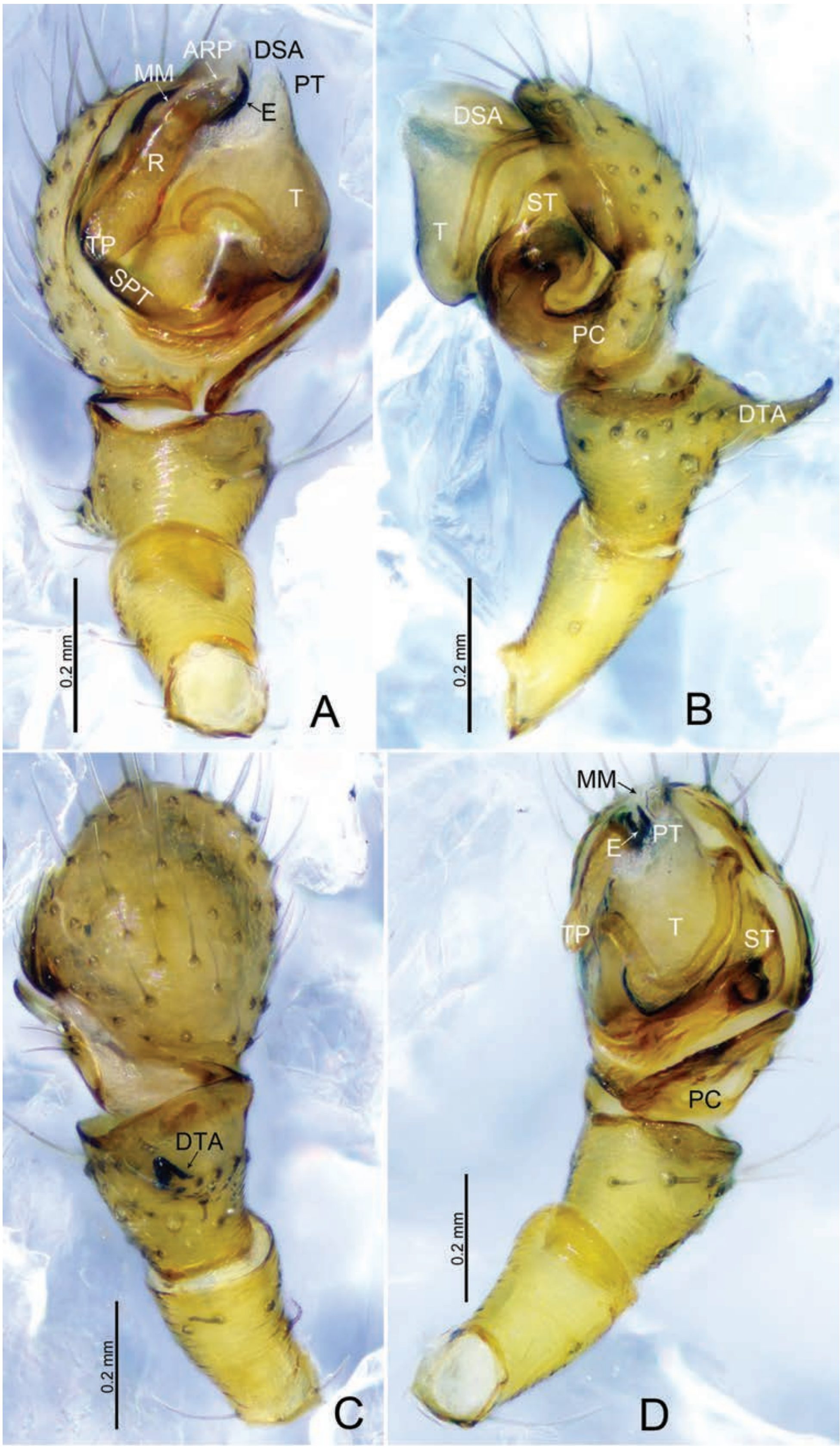

Figure 1. *Tapinocyba centralis* sp. nov., male holotype **A** palp, prolateral view **B** palp, retrolateral view **C** palp, dorsal view **D** palp, ventral view. Abbreviations: ARP = anterior radical process; DSA = distal suprategular apophysis; DTA = dorsal tibial apophysis; E = embolus; MM = median membrane; MSA = marginal suprategular apophysis; PC = paracymbium; PT = protegulum; R = radix; SPT = suprategulum; ST = subtegulum; T = tegulum; TP = tailpiece.

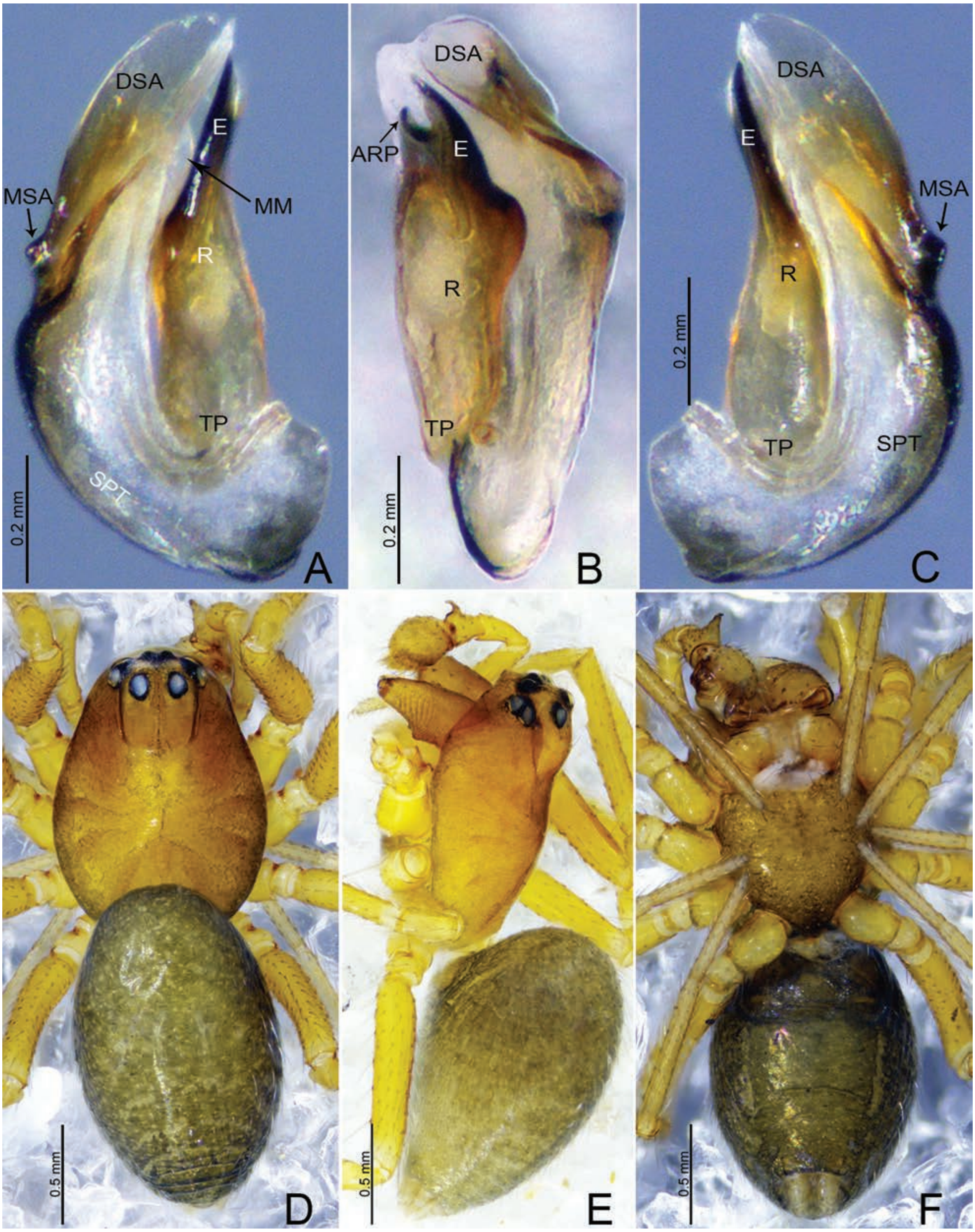

Figure 2. *Tapinocyba centralis* sp. nov., male paratype (**A–C**) and male holotype (**D–F**). **A–C** Embolic division **D** habitus, dorsal view **E** habitus, lateral view **F** habitus, ventral view. Abbreviations: ARP = anterior radical process; DSA = distal suprategular apophysis; E = embolus; MM = median membrane; MSA = marginal suprategular apophysis; R = radix; SPT = suprategulum; TP = tailpiece.

2023.I.7, Wang L.Y. et al. leg.; SWUC-T-LIN-26-01. ***Paratypes:*** 3♂; same location data as holotype; SWUC-T-LIN-26-02 to SWUC-T-LIN-26-04 • 2♂; same location data as holotype; SWUC-T-LIN-26-02 & SWUC-T-LIN-26-03 • 1♂; Zhuyang Town, Yunwuping, Dashibao; 29°9'6.99"N, 105°57'34.51"E; 542 m a.s.l.; 2023.I.7; Wang L.Y. et al. leg.; SWUC-T-LIN-26-04.

Etymology. The specific epithet is derived from the Latin adjective *centralis*, meaning "median" and referring to the dorsal tibial apophysis, which is located dorsally in almost median of the tibia in dorsal view of the male palp.

Diagnosis. The male of *Tapinocyba centralis* sp. nov. resembles *T. praecox* (O. Pickard-Cambridge, 1873) in having the similar cephalic lobe and embolic division (Figs 1A–D, 2A–C; Hormiga 2000: fig. 27A–E, pl. 62A–F) and can be distinguished by the dorsal tibial apophysis located almost in median of tibia in dorsal view in *T. centralis* sp. nov. (Fig. 1C; vs located at the tip of tibia); anterior radical process present in *T. centralis* sp. nov. (Fig. 1C; vs absent).

Description. Male (holotype, Fig. 2D–F): total length: 1.40. Carapace 0.76 long, 0.53 wide, brown, cephalic region strongly elevated, cephalic pits present behind the PLEs, fovea, cervical and radial grooves distinct. Clypeus 0.20 high. Chelicerae with five promarginal and five retromarginal teeth. Sternum yellowish brown as long as wide, shield-like, with microsetae. Eyes: AER recurved, PER procurved, slightly wider than AER, PMEs present on cephalic lobe. Eye sizes and interdistances: AME 0.03, ALE 0.06, PME 0.05, PLE 0.05, AME–AME 0.01, PME–PME 0.05, AME–ALE, 0.02, PME–PLE 0.06, AME–PME 0.08, ALE–ALE 0.24, PLE–PLE 0.25, ALE–PLE 0.01. Length of legs: I 1.93 (0.55, 0.20, 0.48, 0.38, 0.32), II 1.73 (0.47, 0.19, 0.40, 0.36, 0.31), III 1.46 (0.43, 0.17, 0.29, 0.32, 0.25), IV 1.97 (0.54, 0.18, 0.50, 0.41, 0.34). TmI 0.41 and TmIV absent. Tibial spine formula: 1-1-1-1. Opisthosoma 0.81 long, 0.52 wide, oval, greenish.

Palp (holotype, Fig. 1A–D; a paratype, Fig. 2A–C). Femur unmodified, almost as long as both patella and tibia. Patella longer than tibia. Tibia widest at distal end, with one retrolateral and one dorsal trichobothria, dorsal tibial apophysis half the length of tibia, tapering towards tip with blunt end; paracymbium U-shaped, basally with setae, distal arm tip with blunt end; tegulum almost round, ventrally bulging above subtegulum, protegulum distinct, membranous; suprategulum small, with small median suprategular apophysis, invisible on unexpanded palp, distal suprategular apophysis membranous; embolic division simple, consisting of a radix longer than wide; tailpiece round; median membrane short; anterior radical process somewhat triangular with pointed end; embolus short, horn-shaped, slightly curved with pointed end.

Female. Unknown.

Distribution. Known only from the type locality (Fig. 12).

Tapinocyba denticulata **sp. nov.**

https://zoobank.org/F4C75A35-DB03-4B3F-9F54-4F640463163F
Figs 3–5, 12
(齿盾大蛛)

Type material. ***Holotype:*** China • ♂; Chongqing Municipality, Jiangjin District, Simian Mountain, Zhengtian Valley, 28°36'46.97"N, 106°25'54.77"E, 1170 m a.s.l., 2023.III.02, Wang L.Y. et al. leg.; SWUC-T-LIN-27-01. ***Paratypes:*** 1♀; same loca-

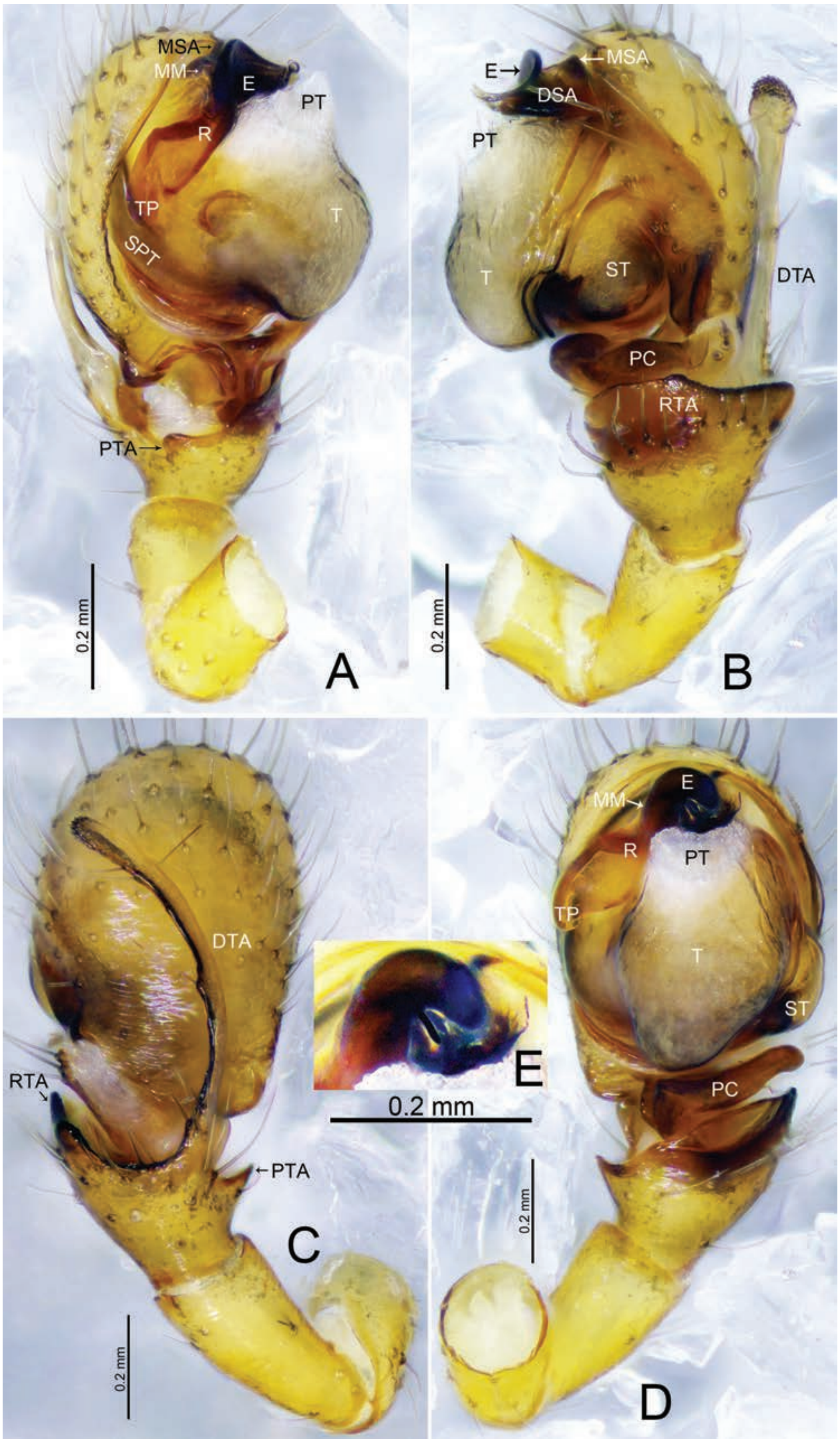

Figure 3. *Tapinocyba denticulata* sp. nov., male holotype **A** palp, prolateral view **B** palp, retrolateral view **C** palp, dorsal view **D** palp, ventral view **E** embolus, ventral view. Abbreviations: DSA = distal suprategular apophysis; DTA = dorsal tibial apophysis; E = embolus; MM = median membrane; MSA = marginal suprategular apophysis; PC = paracymbium; PT = protegulum; PTA = prolateral tibial apophysis; R = radix; RTA = retrolateral tibial apophysis; SPT = suprategulum; ST = subtegulum; T = tegulum; TP = tailpiece.

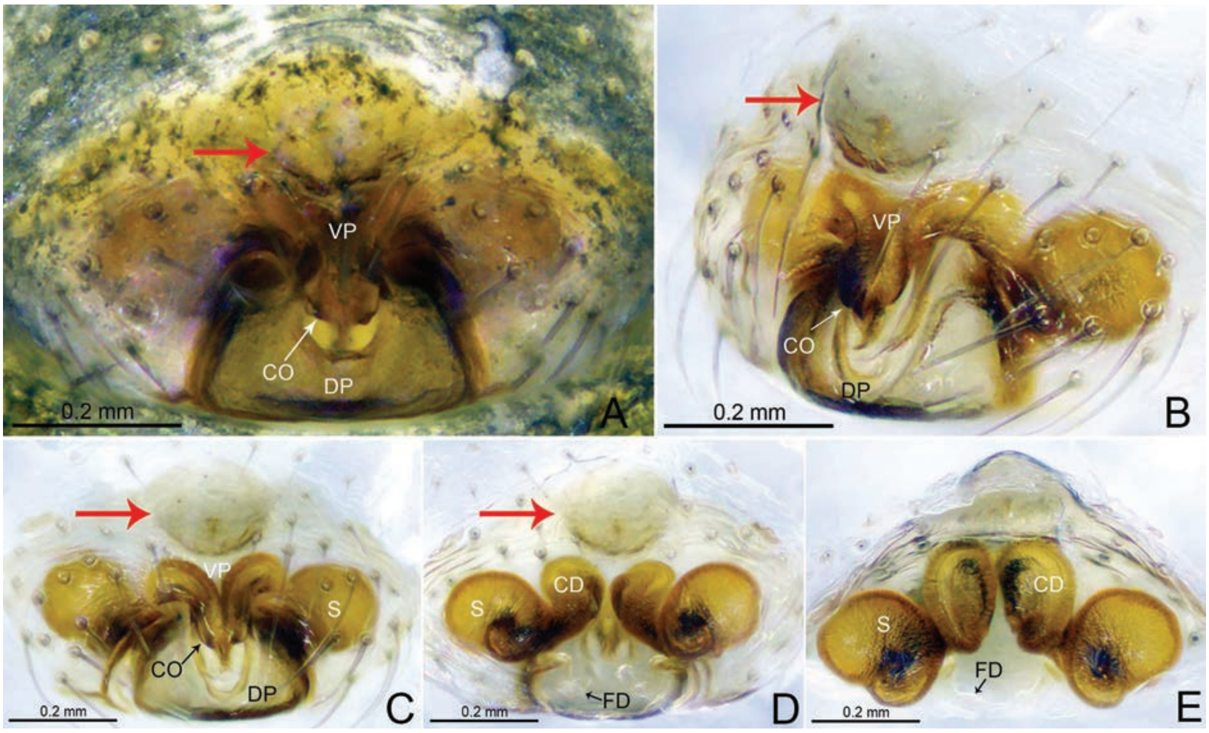

Figure 4. *Tapinocyba denticulata* sp. nov., female paratype **A, C** epigyne, ventral view **B** epigyne, lateral view **D** vulva, dorsal view **E** vulva, anterior view **A–D** red arrow indicating epigynal plate mid ventrally with a conspicuous round patch anteriorly. Abbreviations: CD = copulatory duct; CO = copulatory opening; DP = dorsal plate; FD = fertilization duct; S = spermathecae; VP = ventral plate.

tion data as holotype; SWUC-T-LIN-27-02 • 1♀: Simian Mountain, Chaoyuanguan, 28°38'53.38"N, 106°20'23.84"E, 920 m a.s.l., 2023.I.22, Wang B. et al. leg.; SWUC-T-LIN-27-03 • 1♂; Simian Mountain, Qinjiagou, 28°37'6.32"N, 106°23'53.40"E, 1131 m a.s.l., 2023.III.2, Zhang Z.G. et al. leg.; SWUC-T-LIN-27-04.

Etymology. The specific epithet is derived from the Latin adjective *denticulatus*, meaning "teeth" and referring to the small teeth at the tip of dorsal tibial apophysis of the male palp.

Diagnosis. The male of *Tapinocyba denticulata* sp. nov. resembles *T. praecox* (O. Pickard-Cambridge, 1873) in having the similar embolic division (Fig. 3A–D; Hormiga 2000: fig. 27A–E, pl. 62A–F) and can be distinguished by the ocular region strongly curved, making right-angle with cephalothorax, extending above the clypeus in *T. denticulata* sp. nov. (Fig. 5B; vs ocular region not modified); dorsal tibial apophysis as long as cymbium, tip with small teeth, extending above the cymbium in *T. denticulata* sp. nov. (Fig. 3C; vs half the length of tibia, with blunt tip, extending away from cymbium); retrolateral tibial apophysis present in *T. denticulata* sp. nov. (Fig. 3C; vs absent); embolus curved clockwise with bifurcated tip in *T. denticulata* sp. nov. (Fig. 3A, B, E; vs slightly curved with blunt tip). The female of *T. denticulata* sp. nov. resembles *T. affinis* Lessert, 1907 in having the similar copulatory ducts and spermathecae (Fig. 4A–E; Wiehle 1960: figs 984a, b, 985) and can be distinguished by the tapering part of ventral plate as long as wide in *T. denticulata* sp. nov. (Fig. 4A, B, E; vs somewhat triangular). The epigyne of *Tapinocyba denticulata* sp. nov. can be distinguished from *T. praecox* by the dorsal plate ventrally grooved in *T. denticulata* sp. nov. (Fig. 4A–C; vs not grooved).

Description. Male (holotype, Fig. 5A–C): total length 1.74; carapace 0.87 long, 0.60 wide, brown, cephalic region slightly elevated, cephalic pits absent,

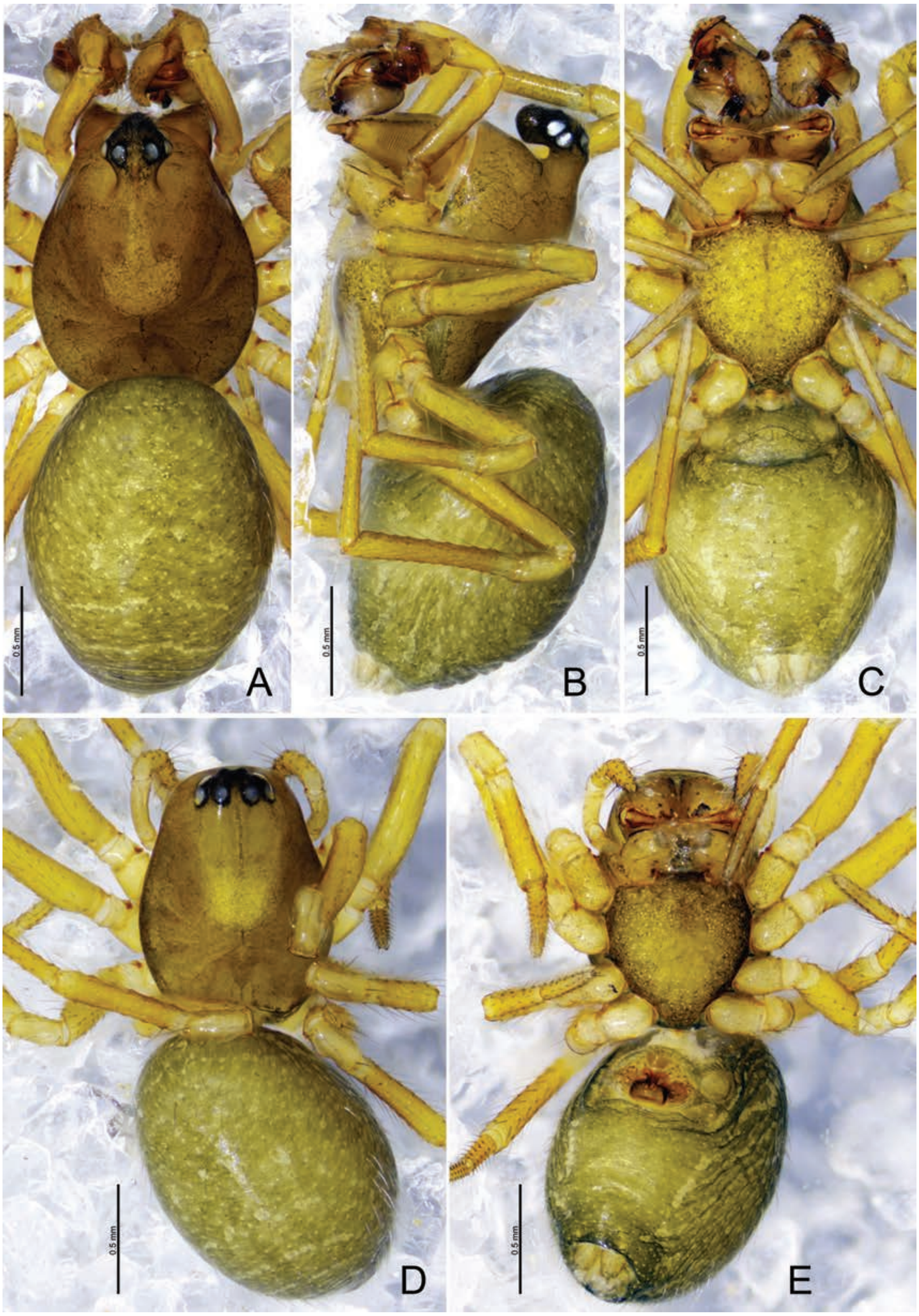

Figure 5. *Tapinocyba denticulata* sp. nov., male holotype (**A–C**) and female paratype (**D, E**) **A**, **D** habitus, dorsal view **B** habitus, lateral view **C, E** habitus, ventral view.

fovea, cervical and radial grooves distinct. Clypeus 0.20 high. Chelicerae with five promarginal and five retromarginal teeth. Sternum yellowish brown, as long as wide, shield-like, with microsetae. Ocular region strongly curved, extending above clypeus, eyes: AER recurved, PER procurved, slightly wider than AER. Eye sizes and interdistances: AME 0.03, ALE 0.06, PME 0.04, PLE 0.05, AME–AME 0.02, PME–PME 0.07, AME–ALE, 0.02, PME–PLE 0.03, AME–PME 0.06, ALE–ALE 0.19, PLE–PLE 0.20, ALE–PLE contiguous. Length of legs: I 1.97 (0.59, 0.21, 0.48, 0.36, 0.33), II 1.82 (0.56, 0.19, 0.43, 0.35, 0.29), III 1.68 (0.58, 0.15, 0.45, 0.28, 0.22), IV 2.00 (0.58, 0.19, 0.48, 0.38, 0.39). TmI 0.63 and TmIV absent. Tibial spine formula: 1-1-1-1. Opisthosoma 0.97 long, 0.71 wide, oval, greenish.

Palp (Fig. 3A–D). Femur unmodified, almost as long as both patella and tibia. Patella as long as tibia. Tibia widest at distal end, with one retrolateral and one dorsal trichobothria, with three apophyses; dorsal tibial apophysis almost as long as cymbium, slightly curved, tip with teeth; prolateral tibial apophysis (PTA) small, somewhat triangular in dorsal view; retrolateral tibial apophysis sclerotized, tip with serrated margin; paracymbium J-shaped, basally with setae, distal arm tip with blunt end; tegulum almost round, ventrally bulging above the subtegulum, protegulum distinct, membranous; suprategulum small, with small median suprategular apophysis, distal suprategular apophysis membranous; embolic division simple, consisting of a radix longer than wide; tailpiece slightly curved with blunt tip; median membrane short, present in between embolus and distal suprategular apophysis; embolus curved, with bifurcated tip.

Female (paratype SWUC-T-LIN-27-02, Fig. 5D, E): total length 1.64; carapace 0.76 long, 0.51 wide, cephalic region slightly elevated, brown, fovea, cervical and radial grooves distinct. Clypeus 0.11 high. Chelicerae with six promarginal and five retromarginal teeth. Sternum shield-shaped, as wide as long, greenish brown, with microsetae. Eyes: AER recurved, PER straight, slightly wider than AER. Eye sizes and interdistances: AME 0.04, ALE 0.06, PME 0.04, PLE 0.05, AME–AME 0.01, PME–PME 0.04, AME–ALE, 0.01, PME–PLE 0.02, AME–PME 0.05, ALE–ALE 0.21, PLE–PLE 0.23, ALE–PLE contiguous. Length of legs: I 1.73 (0.40.53, 0.20, 0.42,0.30, 0.28), II 1.59 (0.50, 0.19, 0.35, 0.29, 0.26), III 1.32 (0.39, 0.16,0.28, 0.27, 0.22), IV 1.74 (0.53, 0.16, 0.42,0.34, 0.29). TmI 0.64 and TmIV absent. Tibial spine formula: 1-1-1-1. Opisthosoma 0.96 long, 0.64 wide, oval, greenish.

Epigyne (Fig. 4A–E). Epigynal plate twice as wide as long, anteriorly with round patch; ventral plate tapering ventrally; dorsal plate almost rectangular, with small groove at the center; copulatory opening located mid-ventrally at the junction of dorsal and ventral plates; copulatory ducts large, curving into one loop; spermathecae large and kidney-shaped, located anterior to the epigynal transverse slit, spaced by two diameters; fertilization ducts large and sinuous.

Distribution. Known only from the type locality (Fig. 12).

Tapinocyba triangularis **sp. nov.**

https://zoobank.org/423E1D35-63A9-4C2A-ACDC-B5675DE3F080
Figs 6–8, 12
(三角盾大蛛)

Type material. ***Holotype:*** China • ♂; Chongqing Municipality, Jiangjin District, Tanghe Town, Gunziping Jianshanzi, Dayuandong, 28°55'46.81"N, 106°5'13.45"E, 752 m a.s.l., 2023.III.25, Wang L.Y. et al. leg.; SWUC-T-LIN-28-01. ***Paratypes:*** 6♂6♀; same location data as holotype; SWUC-T-LIN-28-02 to SWUC-T-LIN-28-13 • 5♂4♀; Tanghe Town, Gunziping, Jianshanzi, Dayuandong, 28°55'46.81"N, 106°5'13.45"E, 752 m a.s.l., 2023.4.15 and 2023.IV.30., Wang L.Y. et al. leg.;

SWUC-T-LIN-28-14 to SWUC-T-LIN-28-22 • 1♂; Simian Mountain, Tudi Yan Guard Management Station, 28°37'24.45"N, 106°24'6.69"E, 1126 m a.s.l., 2023.IV.27, Zhang Z.G et al. leg.; SWUC-T-LIN-28-23.

Etymology. The specific epithet is derived from the Latin adjective *triangularis*, meaning "triangular" and referring to the somewhat triangular ventral part of the dorsal tibial apophysis of the male palp in retrolateral view.

Diagnosis. The male of *Tapinocyba triangularis* sp. nov. resembles *T. emei* Tanasevitch, 2018 in having the similar cephalic lobe, tibial apophyses, distal suprategular apophysis (Figs 6A–D, 7A–C; Tanasevitch 2018: figs 1–5) and resembles *T. algirica* Bosmans, 2007 in having the similar anterior radical process and embolus in male palp (Bosmans 2007: figs 153–156), but it can be distinguished by the horn-shaped embolus in *T. triangularis* sp. nov. (Fig. 8A; vs claw-shaped in *T. emei*), anterior radical apophysis present in *T. triangularis* sp. nov. (Figs 6B, 7B; vs absent in *T. emei*), and tibial apophyses present in *T. triangularis* sp. nov. (Fig. 8A; vs absent in *T. algirica*). The female of *T. triangularis* sp. nov. resembles *T. virga* sp. nov. in having the similar ventral and dorsal plate (Figs 7D–H, 10D–H) and can be distinguished by the spermathecae globular in *T. triangularis* sp. nov. (Fig. 7G, H; vs oval); copulatory opening as long as wide in *T. triangularis* sp. nov. (Fig. 7D vs longer than wide).

Description. Male (holotype, Fig. 8A–C): total length 1.98; carapace 0.94 long, 0.75 wide, brown, cephalic lobe 0.35 long, 0.15 wide, strongly elevated, cephalic pits present at the base of cephalic lobe, fovea, cervical and radial grooves distinct. Clypeus 0.29 high. Chelicerae with five promarginal and five retromarginal teeth. Sternum yellowish brown as long as wide, shield-like, with microsetae. Eyes: AER recurved, PER procurved, slightly wider than AER, PMEs present on cephalic lobe. Eye sizes and interdistances: AME 0.05, ALE 0.07, PME 0.05, PLE 0.06, AME–AME 0.01, PME–PME 0.11, AME–ALE, 0.07, PME–PLE 0.15, AME–PME 0.13, ALE–ALE 0.37, PLE–PLE 0.39, ALE–PLE 0.01. Length of legs: **I** 2.49 (0.72, 0.25, 0.61, 0.50, 0.41), **II** 2.23 (0.66, 0.22, 0.54, 0.45, 0.36), **III** 1.9 (0.56, 0.22, 0.41, 0.40, 0.31), **IV** 2.51 (0.72, 0.23, 0.62, 0.55, 0.39). TmI 0.43 and TmIV absent. Tibial spine formula: 1-1-1-1. Opisthosoma 0.98 long, 0.72 wide, oval, greenish.

Palp (holotype, Fig. 6A–D, a paratype SWUC-T-LIN-28-02, Fig 7A–C). Femur unmodified, almost as long as both patella and tibia. Patella longer than tibia. Tibia widest at distal end, with one retrolateral and one dorsal trichobothria, with two apophyses; dorsal tibial apophysis broad, tip curved ventrally pointing towards paracymbium in retrolateral view; retrolateral tibial apophysis small, somewhat triangular; paracymbium J-shaped, basally with setae, distal arm tip with blunt end; tegulum almost round, ventrally bulging above the subtegulum, protegulum distinct, membranous; suprategulum small, with distinct median suprategular apophysis, distal suprategular apophysis membranous; embolic division simple, consisting of a radix longer than wide; tailpiece tapering with blunt tip; anterior radical process half the length of embolus, sharp with pointed end; median membrane short, present in between embolus and distal suprategular apophysis; embolus slightly curved, with pointed tip.

Female (paratype SWUC-T-LIN-28-03, Fig. 8D, E): total length 1.76; carapace 0.84 long, 0.60 wide, cephalic region slightly elevated, brown, fovea, cervical and radial grooves distinct. Clypeus 0.10 high. Chelicerae with six promarginal and five retromarginal teeth. Sternum shield-shaped, longer than wide, yellowish

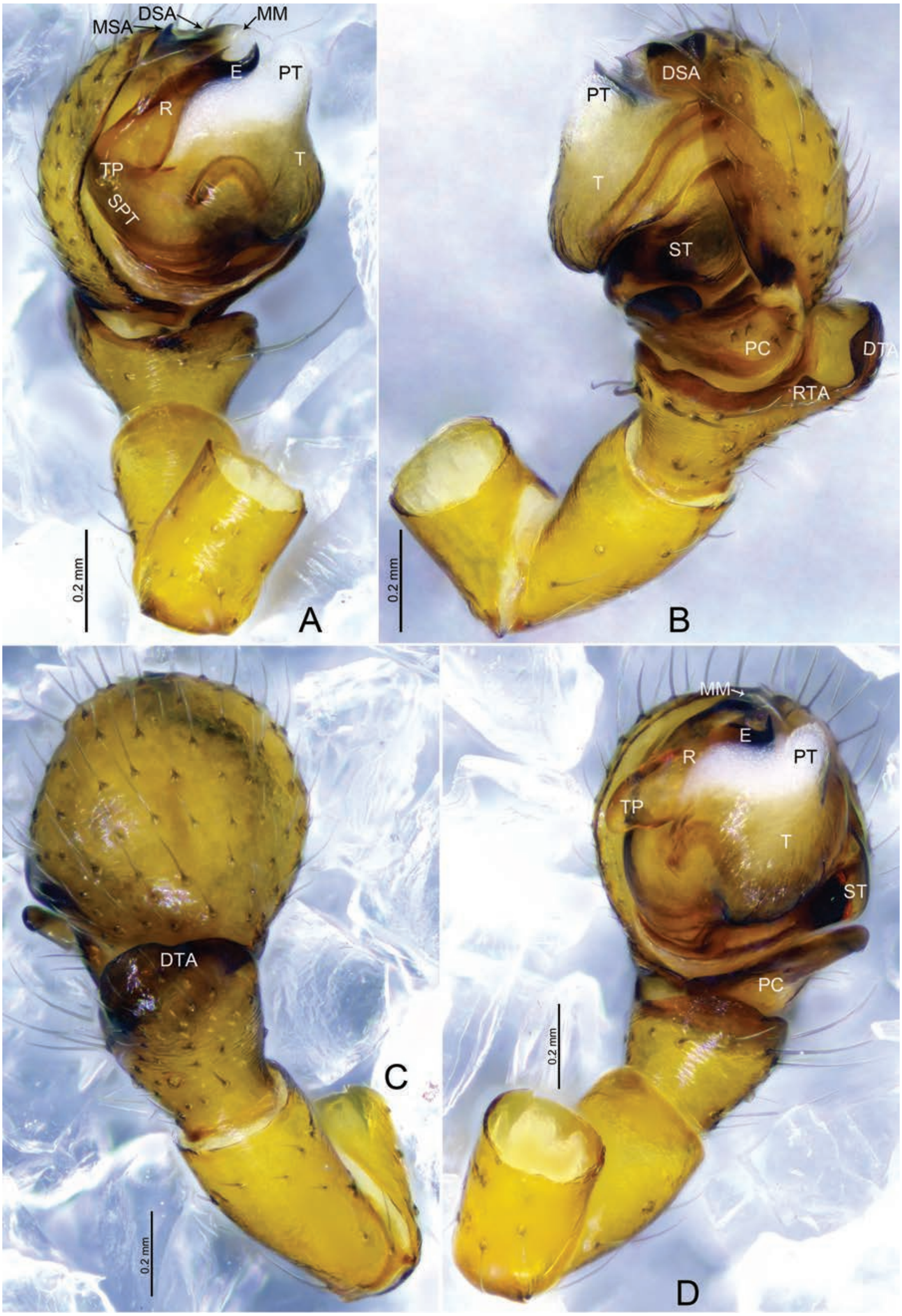

Figure 6. *Tapinocyba triangularis* sp. nov., male holotype **A** palp, prolateral view **B** palp, retrolateral view **C** palp, dorsal view **D** palp, ventral view. Abbreviations: DSA = distal suprategular apophysis; DTA = dorsal tibial apophysis; E = embolus; MM = median membrane; MSA = marginal suprategular apophysis; PC = paracymbium; PT = protegulum; R = radix; RTA = retrolateral tibial apophysis; SPT = suprategulum; ST = subtegulum; T = tegulum; TP = tailpiece.

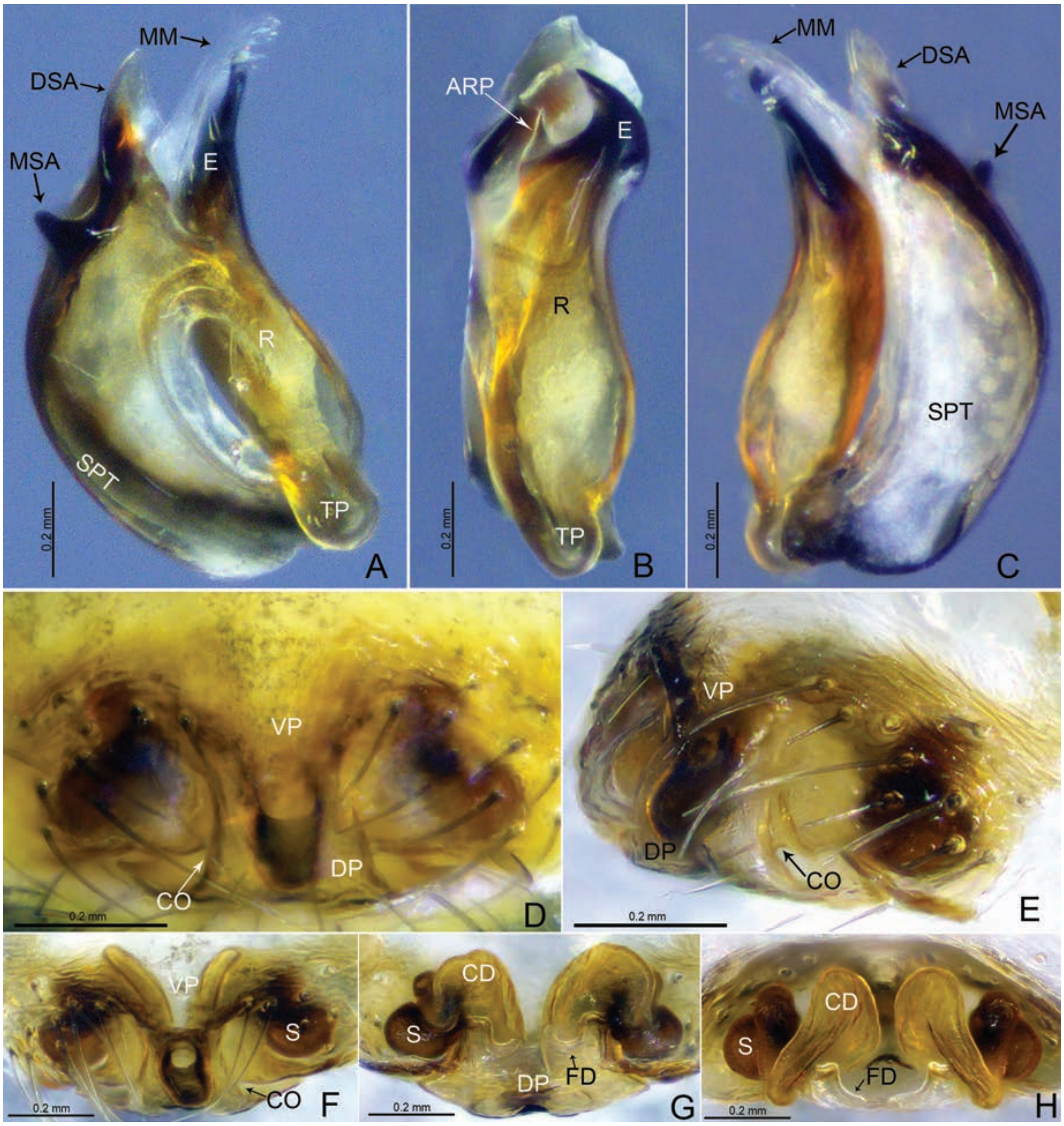

Figure 7. *Tapinocyba triangularis* sp. nov., male paratype (**A–C**), female paratype (**D–H**) **A–C** embolic division **D, F** epigyne, ventral view **E** epigyne, lateral view **G** vulva, dorsal view **H** vulva, anterior view. Abbreviations: ARP = anterior radical process; CD = copulatory duct; CO = copulatory opening; DP = dorsal plate; DSA = distal suprategular apophysis; E = embolus; FD = fertilization duct; MM = median membrane; MSA = marginal suprategular apophysis; R = radix; S = spermathecae; SPT = suprategulum; TP = tailpiece; VP = ventral plate.

brown, with microsetae. Eyes: AER recurved, PER slightly procurved, slightly wider than AER. Eye sizes and interdistances: AME 0.03, ALE 0.06, PME 0.06, PLE 0.06, AME–AME 0.02, PME–PME 0.04, AME–ALE, 0.03, PME–PLE 0.04, AME–PME 0.04, ALE–ALE 0.26, PLE–PLE 0.29, ALE–PLE contiguous. Length of legs: **I** 2.1 (0.57,0.22, 0.51, 0.43, 0.37), **II** 1.94 (0.56, 0.18,0.47,0.39, 0.34), **III** 1.68 (0.51,0.21, 0.32,0.36,0.28), **IV** 2.21 (0.64,0.20, 0.57,0.44, 0.36). TmI 0.46 and TmIV absent. Tibial spine formula: 1-1-1-1. Opisthosoma 1.10 long, 0.75 wide, oval, greenish, dorsally with a pair of sigillae.

Epigyne (Fig. 7D–H). Epigynal plate twice as wide as long; ventral plate tapering ventrally, posteriorly with round hole followed by sclerotized ventral pit

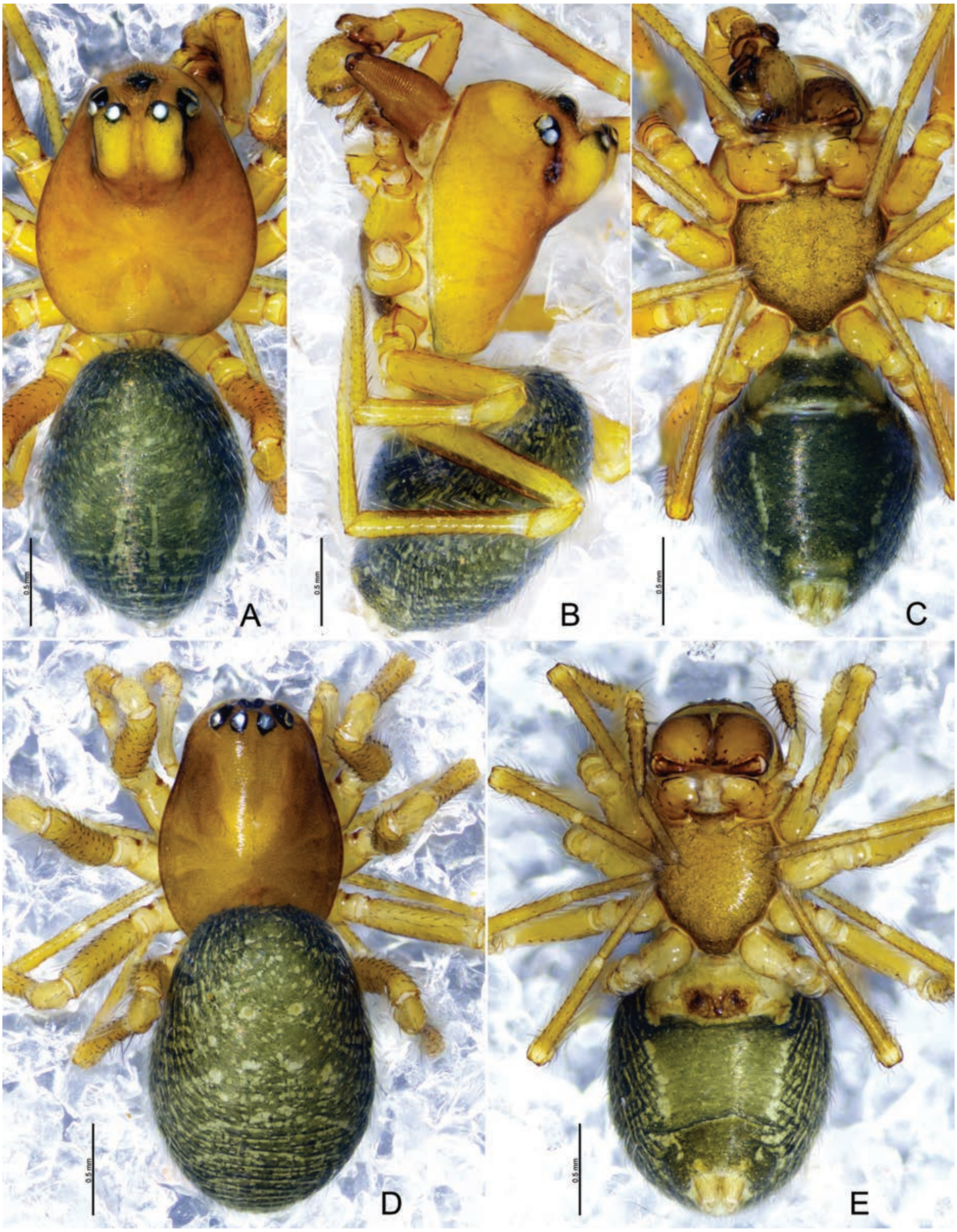

Figure 8. *Tapinocyba triangularis* sp. nov., male holotype (**A–C**) and female paratype (**D, E**) **A, D** habitus, dorsal view **B** habitus, lateral view **C, E** habitus, ventral view.

on it frontal face; dorsal plate almost rectangular, longer than wide; copulatory opening located posteriorly at the base of dorsal plate; copulatory ducts large, curving into two loops; spermathecae located dorsolaterally, spaced by three diameters; fertilization ducts large and sinuous.

Distribution. Known only from the type locality (Fig. 12).

Tapinocyba virga sp. nov.

https://zoobank.org/6C72739C-2035-4788-B65B-1E72FCB0520A
Figs 9–12
(棒盾大蛛)

Type material. ***Holotype:*** China • ♂; Chongqing Municipality, Jiangjin District, Tanghe Town Gunziping Jianshanzi, Dayuandong, 28°55'46.81"N, 106°5'13.45"E, 752 m a.s.l., 2023.III.5, Wang L.Y. et al. leg.; SWUC-T-LIN-29-01. ***Paratypes:*** 1♂3♀; same location data as holotype; SWUC-T-LIN-29-02 to SWUC-T-LIN-29-05 • 1♂; Tanghe Town Gunziping Jianshanzi, Dayuandong, 28°55'46.81"N, 106°5'13.45"E, 752 m a.s.l., 2023.III.25, Wang L.Y. et al. leg.; SWUC-T-LIN-29-06 • 2♂; Baisha Town, Zhang Gongshan, Xiannu Cave, 28°57'10.27"N, 106°8'57.34"E, 809 m a.s.l., 2023.III.5, Wang L.Y. et al. leg.; SWUC-T-LIN-29-07 & SWUC-T-LIN-29-08 • 2♂; Tanghe Town Gunziping Jianshanzi, Dayuandong, 28°55'46.81"N, 106°5'13.45"E, 752 m a.s.l., 2023.II.5, Wang L.Y. et al. leg.; SWUC-T-LIN-29-09 & SWUC-T-LIN-29-10 • 1♀; Tanghe Town, Longyuemen, Dayuandong, Gunziping Management Station, 28°55'43.93"N, 106°5'20.81"E, 773 m a.s.l., 2023.II.5, Wang L.Y. et al. leg.; SWUC-T-LIN-29-11.

Etymology. The specific epithet is derived from the Latin noun *virga*, meaning “rod” and referring to the somewhat rod-like dorsal tibial apophysis of the male palp.

Diagnosis. The male of *Tapinocyba virga* sp. nov. resembles *T. praecox* (O. Pickard-Cambridge, 1873) in having the similar embolic division (Figs 9A–D, 10A–C; Hormiga 2000: fig. 27A–E, pl. 62A–F) and can be distinguished by the ocular region modified in *T. virga* sp. nov. (Fig. 11B; vs not modified); tibia with three apophyses (DTA, PTA and RTA) in *T. virga* sp. nov. (Fig. 9A, B, D; vs tibia with one apophysis); anterior radical apophysis present in *T. virga* sp. nov. (Figs 10A, C; vs absent); and embolus as long as radix with bifurcated tip in *T. virga* sp. nov. (Figs 9A, 10A; vs much shorter than radix with pointed tip). The female of *T. virga* sp. nov. resembles *T. triangularis* sp. nov. in having the similar ventral and dorsal plate (Fig. 10D–H; Fig. 7D–H) and can be distinguished by the spermathecae oval in *T. virga* sp. nov. (Fig. 10G, H; vs globular); copulatory opening longer than wide in *T. virga* sp. nov. (Fig. 10D vs as long as wide).

Description. Male (holotype, Fig. 11A–C): total length 1.69; carapace 0.79 long, 0.59 wide, brown, cephalic region slightly elevated, cephalic pits absent, fovea, cervical and radial grooves distinct. Clypeus 0.20 high. Chelicerae with six promarginal and five retromarginal teeth. Sternum yellowish brown longer than wide, shield-like with microsetae. Ocular region strongly curved, extending above clypeus, eyes: AER recurved, PER procurved, slightly wider than AER. Eye sizes and interdistances: AME 0.03, ALE 0.04, PME 0.06, PLE 0.05, AME–AME 0.03, PME–PME 0.07, AME–ALE, 0.01, PME–PLE 0.02, AME–PME 0.07, ALE–ALE 0.19, PLE–PLE 0.21, ALE–PLE contiguous. Length of legs: I 1.88 (0.55, 0.21,0.46, 0.39,0.27), II 1.73 (0.52, 0.19, 0.41,0.33, 0.28), III 1.44 (0.41, 0.17, 0.31, 0.30, 0.25), IV 2.51 (0.56, 0.20, 0.48, 0.36,0.29). TmI 0.54 and TmIV absent. Tibial spine formula: 1-1-1-1. Opisthosoma 0.96 long, 0.66 wide, oval, greenish.

Palp (holotype, Fig. 9A–D, a paratype SWUC-T-LIN-29-02, Fig. 10A–C). Femur unmodified, almost as long as both patella and tibia. Patella longer than tibia. Tibia widest at distal end, with one retrolateral and one dorsal trichobothria, with two apophyses; dorsal tibial apophysis rod-like, two-third length of tibia; prolateral tibial apophysis (PTA) thumb-shaped with tapering tip in dorsal view; retrolateral

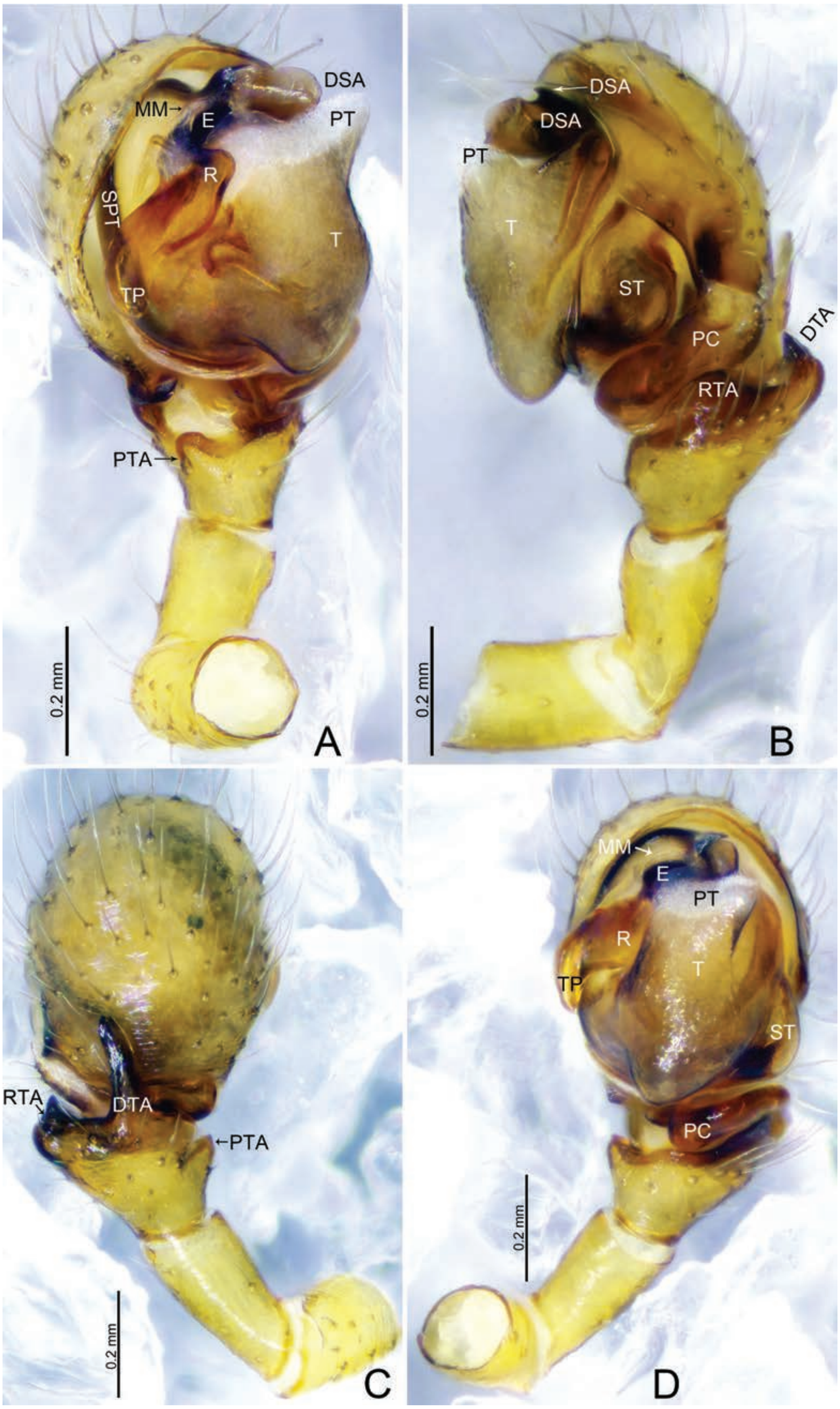

Figure 9. *Tapinocyba virga* sp. nov., male holotype **A** palp, prolateral view **B** palp, retrolateral view **C** palp, dorsal view **D** palp, ventral view. Abbreviations: DSA = distal suprategular apophysis; DTA = dorsal tibial apophysis; E = embolus; MM = median membrane; MSA = marginal suprategular apophysis; PC = paracymbium; PT = protegulum; PTA = prolateral tibial apophysis; R = radix; RTA = retrolateral tibial apophysis; SPT = suprategulum; ST = subtegulum; T = tegulum; TP = tailpiece.

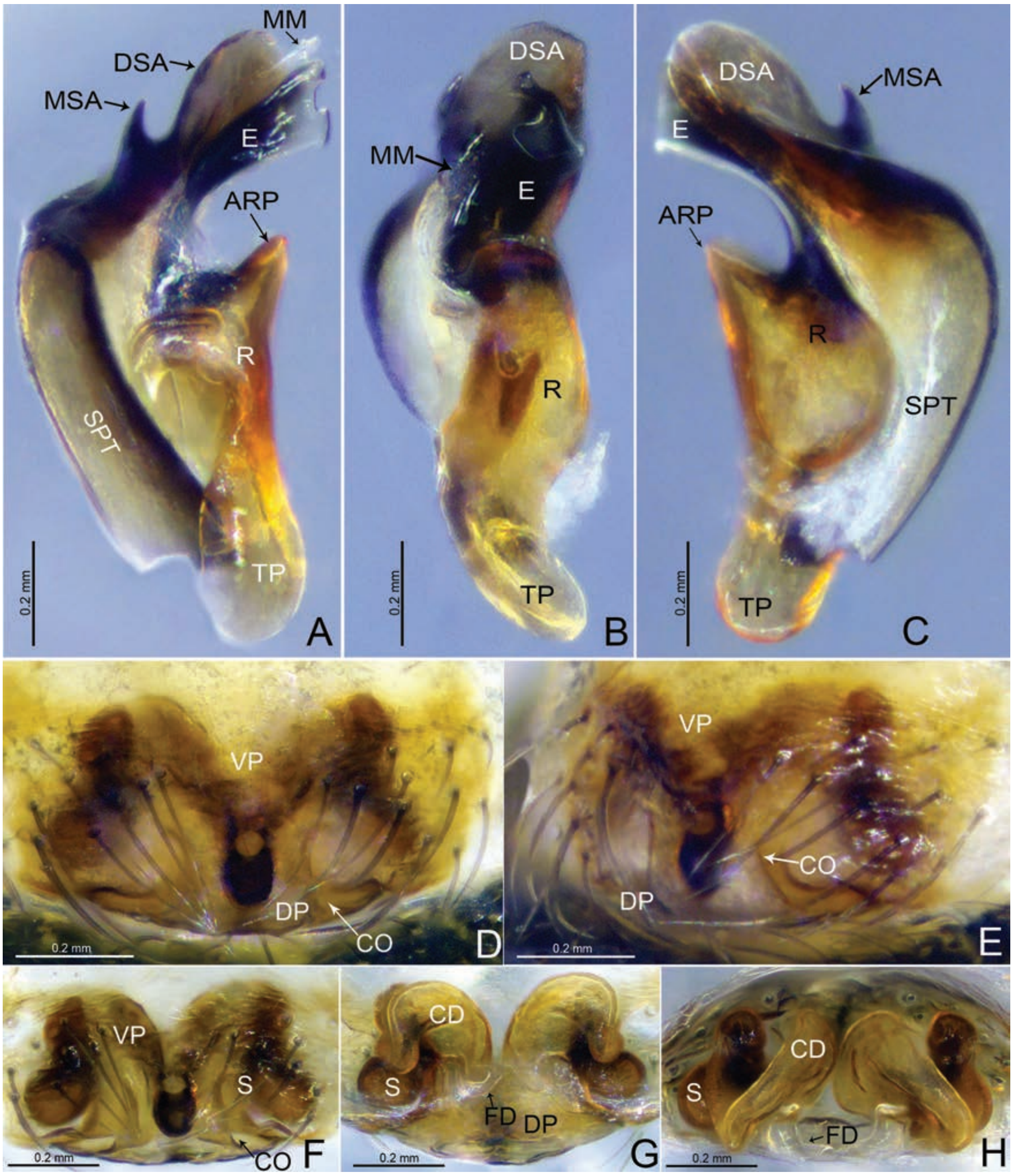

Figure 10. *Tapinocyba virga* sp. nov., male paratype (**A–C**), female paratype (**D–H**) **A–C** embolic division **D, F** epigyne, ventral view **E** epigyne, lateral view **G** vulva, dorsal view **H** vulva, anterior view. Abbreviations: ARP = anterior radical process; CD = copulatory duct; CO = copulatory opening; DP = dorsal plate; DSA = distal suprategular apophysis; E = embolus; FD = fertilization duct; MM = median membrane; MSA = marginal suprategular apophysis; R = radix; S = spermathecae; SPT = suprategulum; TP = tailpiece; VP = ventral plate.

tibial apophysis D-shaped; paracymbium J-shaped, basally with setae, distal arm tip hook-shaped with blunt end; tegulum almost round, ventrally bulging above the subtegulum, protegulum distinct, membranous; suprategulum small, with distinct median suprategular apophysis, distal suprategular apophysis membranous; embolic division simple, consisting of a radix longer than wide; tailpiece slightly curved with blunt tip; anterior radical process one-third the length of embolus, with blunt tip; median membrane short, present in between embolus and distal suprategular apophysis; embolus almost as long as radix, with bifurcated tip.

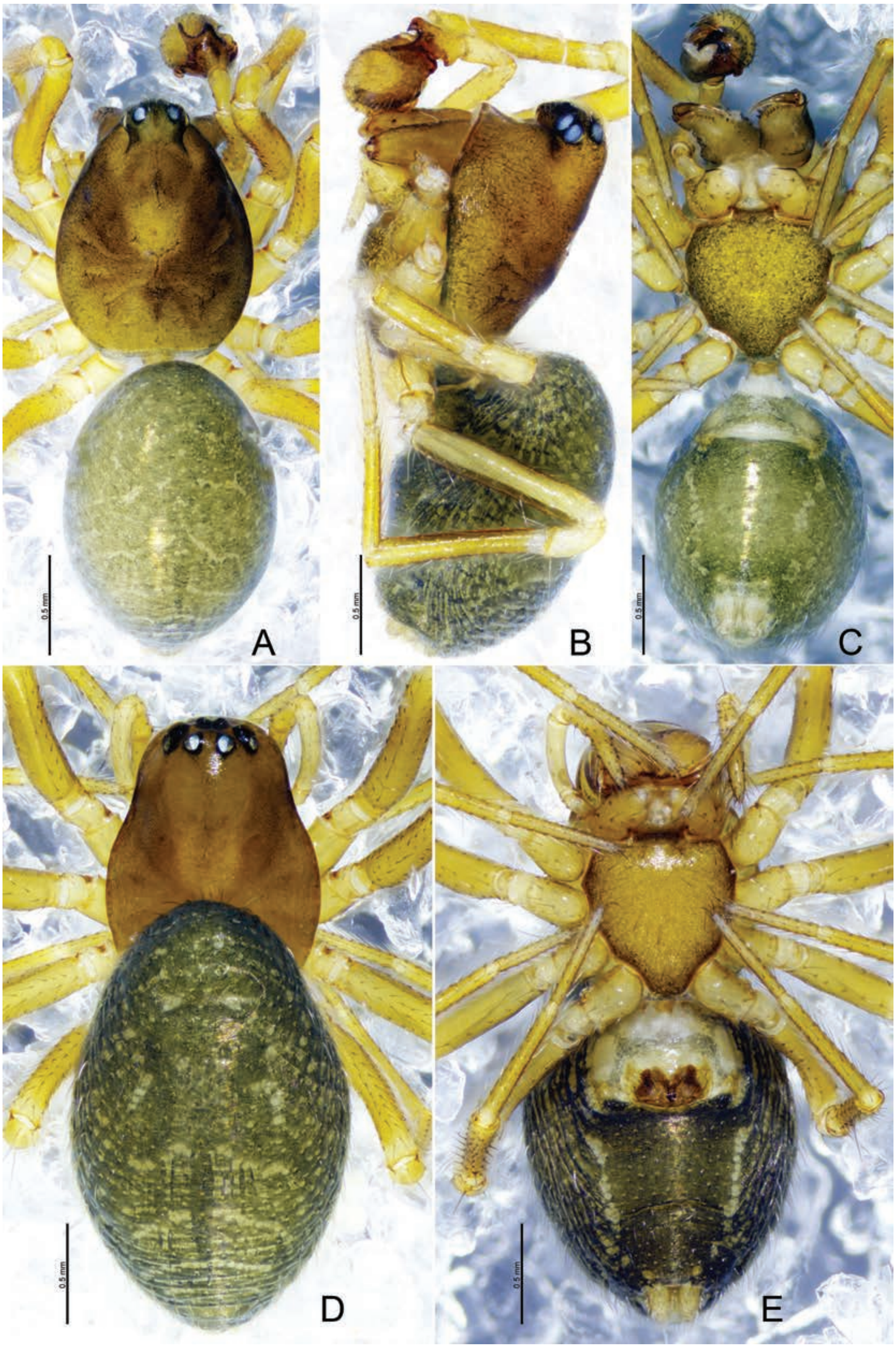

Figure 11. *Tapinocyba virga* sp. nov., male holotype (**A–C**) and female paratype (**D, E**) **A, D** habitus, dorsal view **B** habitus, lateral view **C, E** habitus, ventral view.

Female (paratype SWUC-T-LIN-29-03, Fig. 11D, E): total length 1.86; carapace 0.91 long, 0.62 wide, cephalic region slightly elevated, brown, fovea, cervical and radial grooves distinct. Clypeus 0.10 high. Chelicerae with six promarginal

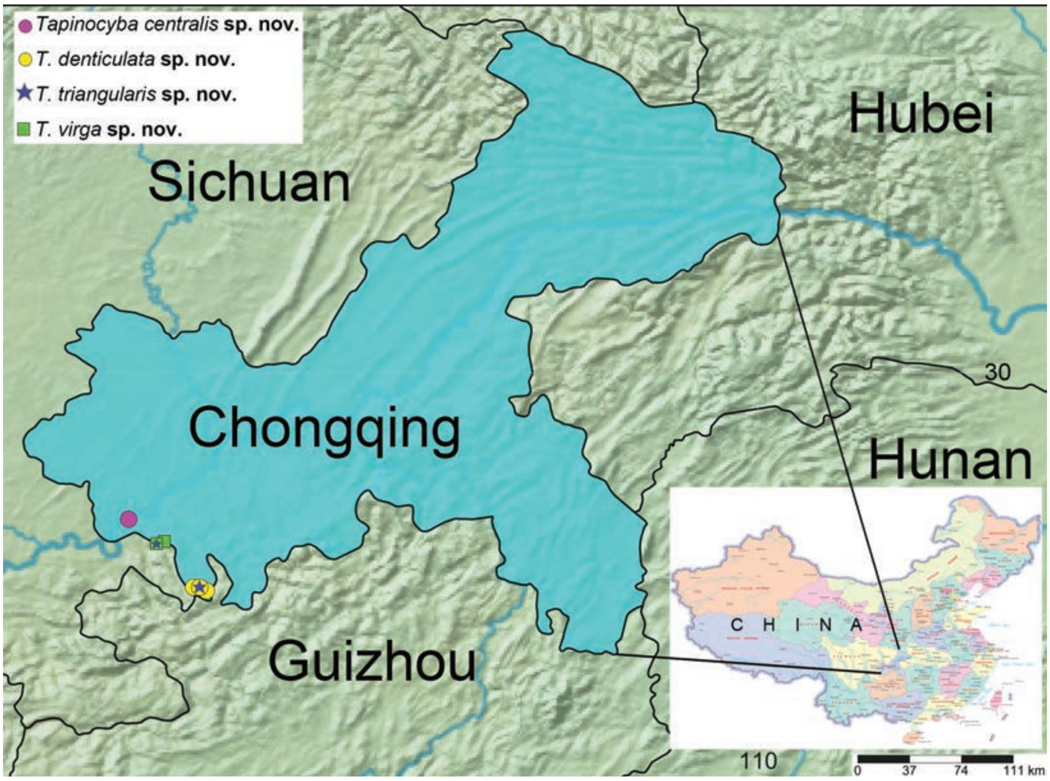

Figure 12. Distribution of *Tapinocyba* species in Jiangjin, Chongqing.

and five retromarginal teeth. Sternum shield-shaped, longer than wide, yellowish brown with microsetae. Eyes: AER recurved, PER slightly procurved, slightly wider than AER. Eye sizes and interdistances: AME 0.03, ALE 0.06, PME 0.06, PLE 0.05, AME–AME 0.03, PME–PME 0.06, AME–ALE, 0.02, PME–PLE 0.02, AME–PME 0.05, ALE–ALE 0.26, PLE–PLE 0.28, ALE–PLE 0.01. Length of legs: I 2.1 (0.57,0.22, 0.51, 0.43, 0.37), II 1.99 (0.60, 0.23, 0.45, 0.38, 0.33), III 1.67 (0.52, 0.18, 0.36,0.35, 0.26), IV 2.22 (0.66, 0.19, 0.55, 0.46, 0.33). TmI 0.50 and TmIV absent. Tibial spine formula: 1-1-1-1. Opisthosoma 1.10 long, 0.75 wide, oval, greenish, dorsally with a pair of sigillae, ventral side greenish black.

Epigyne (Fig. 10D–H). Epigynal plate two times wider than long; ventral plate tapering ventrally, posteriorly with round hole followed by sclerotized ventral pit on its frontal face; dorsal plate almost rectangular, longer than wide; copulatory opening located posteriorly at the base of dorsal plate; copulatory ducts large, curving into two loops; spermathecae located dorsolaterally, spaced by three diameters; fertilization ducts large and sinuous.

Distribution. Known only from the type locality (Fig. 12).

Habitat. The specimens of the species described here were collected from leaf litter in broad-leaved and coniferous forests.

Remarks

After examining and comparing the new species with the type species of the genus *Tapinocyba* and other related species, we conclude that they share both somatic and genital similarities. The male palps exhibit comparable embolic divisions, featuring a small embolus and an anterior radical process, as described by Millidge (1979). The epigynes also display almost identical structures and shapes, except for the epigynal plate with a pit ventrally on its frontal face in *T. triangularis* sp. nov. and *T. virga* sp. nov. that is absent in all other known *Tapinocyba* species. Based on these structural and morphological affinities, we propose that all the new species presented here belong to the genus *Tapinocyba*.

Acknowledgements

The manuscript benefited greatly from comments by Andrei V. Tanasevitch (Russian Academy of Sciences, Russia). We are thankful to Zhang Zheng-Gui, Cai You-Guo, Yuan Zhi-Hui, Cheng Lei, Wang Bo, Cheng Jun, Luo Ping, Lu Qian-Le, Chen Xu-Long, and Ren Tian-Yu for help in specimen collection.

Additional information

Conflict of interest

The authors have declared that no competing interests exist.

Ethical statement

No ethical statement was reported.

Funding

This study is supported by the Chongqing Provincial Funding Postdoc Award 2021 to Muhammad Irfan (cstc2021jcyj-bsh0237), National Natural Sciences Foundation of China Research Fund for International Young Scientists to Muhammad Irfan (W2433063) and fund in survey of wild protected animals of Jiangjin District.

Author contributions

All authors have contributed equally.

Author ORCIDs

Muhammad Irfan https://orcid.org/0000-0003-0445-9612
Dai Yun https://orcid.org/0009-0005-2709-5788
Wang Lu-Yu https://orcid.org/0000-0002-5250-3473
Zhang Zhi-Sheng https://orcid.org/0000-0002-9304-1789

Data availability

All of the data that support the findings of this study are available in the main text.

References

Bosmans R (2007) Contribution to the knowledge of the Linyphiidae of the Maghreb. Part XII. Miscellaneous erigonine genera and additional records (Araneae: Linyphiidae: Erigoninae). Bulletin & Annales de la Société Entomologique de Belgique 143: 117–163.

Emerton JH (1909) Supplement to the New England Spiders. Transactions of the Connecticut Academy of Arts and Sciences 14: 171–236. https://doi.org/10.5962/bhl.title.36049

Helsdingen PJ van (1965) Sexual behaviour of *Lepthyphantes leprosus* (Ohlert) (Araneida, Linyphiidae), with notes on the function of the genital organs. Zoologische Mededelingen 41: 15–42.

Helsdingen PJ van (1986) The *Porrhomma microphthalmum* species-group. Bulletin of the British Arachnological Society 7(1): 11–16.

Hormiga G (1994) Cladistics and the comparative morphology of linyphiid spiders and their relatives (Araneae, Araneoidea, Linyphiidae). Zoological Journal of the Linnean Society 111(1): 1–71. https://doi.org/10.1111/j.1096-3642.1994.tb01491.x

Hormiga G (2000) Higher level phylogenetics of erigonine spiders (Araneae, Linyphiidae, Erigoninae). Smithsonian Contributions to Zoology 609: 1–160. https://doi.org/10.5479/si.00810282.609

Irfan M, Wang LY, Zhang ZS (2022) Two new species of Micronetinae Hull, 1920 spiders (Araneae: Linyphiidae) from Yintiaoling Nature Reserve, Chongqing, China. Acta Arachnologica Sinica 31(1): 17–26. https://doi.org/10.3969/j.issn.1005-9628.2022.01.003

Irfan M, Wang LY, Zhang ZS (2023a) One new genus and nine new species of Linyphiidae spiders from Yintiaoling Nature Reserve, Chongqing of China. Zootaxa 5257(1): 82–114. [incl. Erratum: Zootaxa 5263(4): 575–600. https://doi.org/10.11646/zootaxa.5263.4.9] https://doi.org/10.11646/zootaxa.5257.1.7

Irfan M, Wang LY, Zhang ZS (2023b) Survey of Linyphiidae spiders (Arachnida: Araneae) from Wulipo National Nature Reserve, Chongqing, China. European Journal of Taxonomy 871: 1–85. https://doi.org/10.5852/ejt.2023.871.2129

Lessert R de (1907) Notes arachnologiques. Revue Suisse de Zoologie 15: 93–128. https://doi.org/10.5962/bhl.part.7899

Millidge AF (1979) Some erigonine spiders from southern Europe. Bulletin of the British Arachnological Society 4(7): 316–328.

Pickard-Cambridge O (1873) On new and rare British spiders (being a second supplement to “British spiders new to science”, Linn. Trans. vol xxvii, p. 393). Transactions of the Linnean Society of London 28(4): 523–555 [pl. 46]. https://doi.org/10.1111/j.1096-3642.1873.tb00231.x

Sha YH, Gao JC, Zhu CD (1994) Three new generic records and five new record species of Erigoninae from China (Araneae: Linyphiidae). Acta Arachnologica Sinica 3: 14–20.

Shorthouse DP (2010) SimpleMappr, an online tool to produce publication-quality point maps. https://www.simplemappr.net [Accessed 02 August 2024]

Simon E (1884) Les arachnides de France. Tome cinquième, deuxième et troisième partie. Roret, Paris, 180–885 [pl. 26–27].

Tanasevitch AV (2011) On some linyphiid spiders from Taiwan (Araneae: Linyphiidae). Zootaxa 3114: 31–39. https://doi.org/10.11646/zootaxa.3114.1.3

Tanasevitch AV (2018) A new *Tapinocyba* Simon, 1884 from southern China (Aranei: Linyphiidae). Arthropoda Selecta 27(2): 169–171. https://doi.org/10.15298/arthsel.27.2.08

Tanasevitch AV (2024) Linyphiidae Spiders of the World. http://old.cepl.rssi.ru/bio/tan/linyphiidae/ [Accessed 02 August 2024]

Wiehle H (1960) Spinnentiere oder Arachnoidea (Araneae). XI. Micryphantidae-Zwergspinnen. Die Tierwelt Deutschlands 47: 1–620.

WSC (2024) World Spider Catalog. Version 25.0. Natural History Museum Bern. http://wsc.nmbe.ch [Accessed 02 August 2024]

ZooKeys 1219: 215–231 (2024)
DOI: 10.3897/zookeys.1219.134005

Research Article

Description of a new *Osedax* (Annelida, Polychaeta, Siboglinidae) species colonizing cow bones in the South Atlantic Ocean

Thammy Gularte[1], Paulo Y. G. Sumida[1], Gilberto Bergamo[1], Greg W. Rouse[2]

1 *Biological Oceanography Department, Oceanographic Institute – University of São Paulo, Praça do Oceanográfico, 191, 05508-120, São Paulo, SP, Brazil*
2 *Scripps Institution of Oceanography, UC San Diego, La Jolla CA, 92093-0202, USA*
Corresponding author: Greg W. Rouse (grouse@ucsd.edu)

Abstract

A new species of *Osedax* is described here using molecular and morphological data. It was found at the depth of 550 m off the Brazilian coast through experimental deployment of cow bones. *Osedax nataliae* **sp. nov.** is the second *Osedax* species from the Southwest Atlantic Ocean and had been previously reported as *Osedax* 'BioSuOr-4'. Phylogenetic analysis of five concatenated genetic makers (28S rDNA, Histone H3, 18S rDNA, 16S rDNA, and cytochrome c oxidase I) placed *Osedax nataliae* **sp. nov.** within a well-supported *Osedax* Clade V, nested within a clade of Pacific Ocean *Osedax* though with poor support. The minimum interspecific COI distance between *O. nataliae* **sp. nov.** and another known *Osedax* was 13.92% (closest to *O.* 'sagami-3'). The maximum intraspecific COI diversity (uncorrected) within *O. nataliae* **sp. nov.** sampled here was 2.44% and population structure was visualized via haplotype network analysis. Morphologically, *O. nataliae* **sp. nov.** is characterized by its reddish orange crown of palps and a ventral yellowish collar on the anterior trunk where it meets the base of the crown. *Osedax nataliae* **sp. nov.** shares features with other Clade V species, notably pinnules inserted on the outer margin of palps. Additionally, the presence of dwarf males within the tube lumen of females was documented. Further sampling and research in the Southern Hemisphere are needed to understand the diversity and biogeography of *Osedax* across the world's oceans.

Key words: New species, phylogeny, taxonomy, whale falls

Academic editor: Christopher Glasby
Received: 6 August 2024
Accepted: 26 October 2024
Published: 3 December 2024

ZooBank: https://zoobank.org/09E12217-61BB-4875-8F37-42B274290D21

Citation: Gularte T, Sumida PYG, Bergamo G, Rouse GW (2024) Description of a new *Osedax* (Annelida, Polychaeta, Siboglinidae) species colonizing cow bones in the South Atlantic Ocean. ZooKeys 1219: 215–231. https://doi.org/10.3897/zookeys.1219.134005

Introduction

Dead whale carcasses are one of the most remarkable energy sources for a plethora of deep-sea organisms as they sink and reach the deep seafloor, known as whale falls, becoming a habitat island for many species during decomposition, which can last for a few years to decades (Lundsten et al. 2010; Smith et al. 2015). The enormous input of organic matter from whale falls supports diverse ecosystems, rich in opportunistic species capable of tolerating the organic matter decomposition (Smith and Baco 2003; Gaudron et al. 2010). Still, as with vents and seeps, these ecosystems can have unique and specialized species and communities (Smith and Baco 2003; Braby et al. 2007; Lundsten et al. 2010; Smith et al. 2015).

The study of these communities revealed some remarkable new species, including the annelid genus *Osedax* Rouse, Goffredi & Vrijenhoek, 2004 (Siboglinidae), a group of organisms specialized to exploit bones and teeth of dead marine vertebrates (Rouse and Goffredi 2023). *Osedax* taxa lack a digestive system and have a particular endosymbiotic relationship with heterotrophic bacteria hosted in the branching root system that excavates the bone. The symbiotic bacteria are capable of metabolizing complex carbon compounds within the bones yielding nutrition to both symbionts and the *Osedax* hosts (Goffredi et al. 2005, 2007; Katz et al. 2010; Tresguerres et al. 2013). *Osedax* specimens also usually exhibit a marked sexual dimorphism, in which the females can reach 1–10 cm and the males are microscopic dwarfs (paedomorphic) and live in harems attached to the female trunk (Rouse et al. 2004, 2008; Vrijenhoek et al. 2008, 2009). The genus currently has 33 described species in all the ocean basins, with a wide bathymetric range, varying from 21 to 4204 meters (Rouse et al. 2018; Fujiwara et al. 2019; Eilertsen et al. 2020; Georgieva et al. 2023; Berman et al. 2024). More than half of the named species were first collected from the California margin, where whale-fall studies are most numerous and long-standing (Smith et al. 2015).

As in most deep-sea exploration areas of knowledge, the data on whale-fall associated species in the Global South is still limited, and it is predicted that many hundreds of whale-fall species remain to be discovered in these ocean regions (Smith et al. 2015). This prediction relies on the high abundance of large marine mammals in this region (Laws 1977) and their seasonal migratory routes between high-latitude feeding grounds and low-latitude breeding grounds (Dawbin 1966). This knowledge gap is particularly pronounced for *Osedax* species, as *Osedax braziliensis* Fujiwara, Jimi, Sumida & Kitazato, 2019 is the only described species for the South Atlantic Ocean (excluding Antarctic and subantarctic species) and it was found inhabiting the first reported natural whale carcass in the deep Southwest Atlantic Ocean at 4204 m depth during an expedition with the human-occupied submersible Shinkai 6500 in 2018 (Fujiwara et al. 2019).

Aiming to reduce the knowledge gap regarding the organic falls community diversity in the South Atlantic Ocean and its global connectivity, the project BioSuOr ("Biodiversity and connectivity of benthic communities in organic substrates in the deep southwest Atlantic") was conducted between 2016 and 2017, implanting mammalian bones and wood samples in Brazilian deep waters. These samples were implanted at multiple sites across three different depths: 550, 1500 and 3300 m. The deployment of the organic falls was achieved using free-fall landers equipped with acoustic releases for recovery and were subsequently colonized by a variety of polychaetes, crustaceans and mollusks. Some of the results from this project in the Southwest Atlantic Ocean have been documented (Shimabukuro and Sumida 2019; Shimabukuro et al. 2019, 2022; Souza et al. 2021; Avila et al. 2023; Bergamo et al. 2024), reporting the occurrence of 24 animal species (Shimabukuro et al. 2022), including potential new species.

During the sampling of BioSuOr project material, numerous *Osedax* specimens were observed colonizing the implanted cow bones (Fig. 1). Four *Osedax* species were recovered from this project and their mitochondrial cytochrome *c* oxidase subunit I (COI) sequences were reported and lodged on GenBank as

Figure 1. Cow femur colonized by *Osedax* individuals in an implanted free-fall lander after recovery.

BioSuOr-1, 2, 3, and 4 (Shimabukuro and Sumida 2019). Here, we use molecular phylogenetic and morphological data to formally describe *Osedax* 'BioSuOr-4', which was recovered on bones at a depth of 550 m, along with an assessment of its intraspecific diversity. Additionally, we documented the occurrence of dwarf males in this species.

Materials and methods

Sample collection and morphological analysis

Osedax specimens investigated in this study were obtained through an in-situ experiment that involved implanting bovine bones using experimental autonomous structures (landers) equipped with acoustic releases (see Saeedi et al. 2019) in the Southwest Atlantic Ocean, off the Brazilian continental margin (26°36'13.44"S, 46°09'9.29"W) at 550 m depth (Fig. 2). Landers were deployed in July 2016 using the R/V Alpha Crucis and recovered in May 2017 with the R/V Alucia. Once onboard bones were placed in sea water at 4 °C to photograph living *Osedax*. Bones with worms were then fixed in 96% ethanol. *Osedax* specimens were later extracted at Laboratório de Mar Profundo (**LAMP**), Instituto Oceanográfico, Universidade de São Paulo, with 115 female specimens and tubes extracted using a stereomicroscope. The holotype and attached dwarf males were imaged from fixed material with Leica MZ12.5 (+ Canon Rebel T6i camera), or Leica M205C (+ Leica MC170HD camera) stereomicroscopes. A dwarf male was imaged with a Leica DMR compound microscope and Canon Rebel T6i camera.

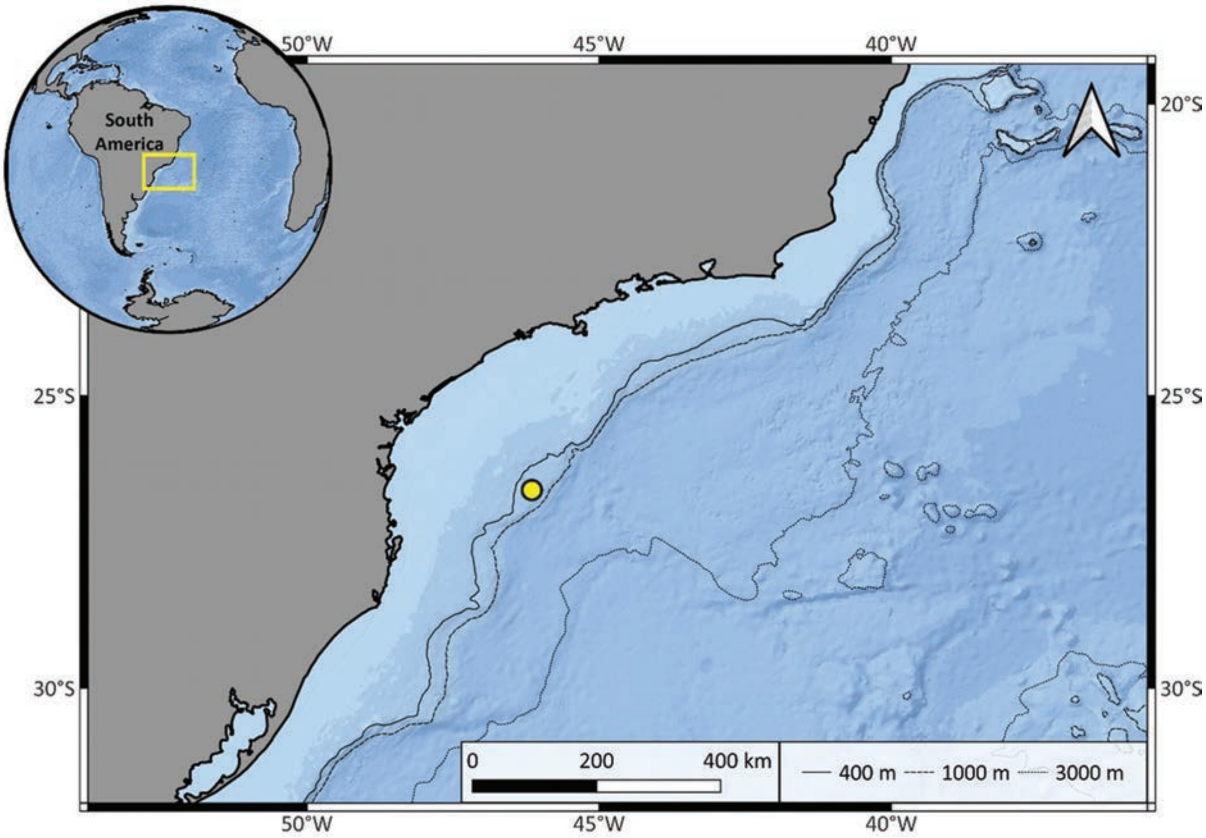

Figure 2. The yellow circle indicates exact position of the lander at 550 m depth off the Brazilian continental margin recovered in May 2017 with the R/V Alucia.

For scanning electron microscopy (SEM) analysis, female specimens were dehydrated in absolute ethanol. They were then rinsed in two 10-min baths in a solution consisting of 50% ethanol and 50% Hexamethyldisilazane (HMDS), followed by an additional two 10-min baths in HMDS alone. Specimens were left to dry overnight, then mounted on stubs using carbon adhesive tape, sputter-coated with gold, and examined and photographed under a Zeiss Sigma VP SEM at Laboratório de Microscopia Eletrônica, Instituto de Biociências, Universidade de São Paulo.

DNA preparation, amplification, and sequencing

DNA of 37 female specimens was extracted from their root regions using Zymo Research DNA-tissue miniprep kits, following the manufacturer's provided protocol. Extracted DNA was utilized as template for the polymerase chain reaction (PCR) amplification of fragments of mitochondrial cytochrome *c* oxidase subunit I (COI) and 16S rRNA (16S) genes, and the nuclear 18S rRNA (18S), 28S rRNA (28S) and Histone H3 (H3) genes, using primers shown in Table 1. COI was sequenced for all specimens initially for species delimitation. Subsequently, other markers were sequenced from a single representative specimen.

PCR amplification was conducted using a mixture consisting of 12.5 µl Apex™ 2.0× Taq Red DNA polymerase Master Mix (Genesee Scientific), 1 µl of each appropriate forward and reverse primers (10 µM), 8.5 µl of ddH2O, and 2 µl of eluted DNA. PCR cycling was conducted in a thermal cycler following specific

Table 1. List of genes, primers and PCR temperature profiles used in the present study.

Gene	Primer set	Reference	Cycle
Cytochrome *c* oxidase subunit I (COI)	OsCO1r/OsCO1f	Glover et al. 2005	120s at 95 °C, 35 cycles of 60s at 94 °C, 60s at 50 °C and 60s at 72 °C, 420s at 72 °C
16S rRNA (*16S*)	16SarL/16SbrH	Palumbi 1996	180s at 95 °C, 35 cycles of 40s at 95 °C, 40s at 50 °C and 50s at 72 °C, 300s at 72 °C
18S rRNA (*18S*)	18S-1F/18S-5R	Giribet et al. 1996	180s at 95 °C, 40 cycles of 30s at 95 °C, 30s at 50 °C and 90s at 72 °C, 480s at 72 °C
	18S-a2.0/18S-9R	Giribet et al. 1996; Whiting et al. 1997	180s at 95 °C, 40 cycles of 30s at 95 °C, 30s at 50 °C and 90s at 72 °C, 480s at 72 °C
	18S-3F/18S-bi	Giribet et al. 1996; Whiting et al. 1997	180s at 95 °C, 40 cycles of 30s at 95 °C, 30s at 52 °C and 90s at 72 °C, 480s at 72 °C
28S rRNA (*28S*)	D1F/D3R	Brown et al. 1999	180s at 94 °C, 35 cycles of 60s at 94 °C, 30s at 55 °C and 110s at 72 °C, 240s at 72 °C
Histone H3 (*H3*)	H3F/H3R	Colgan et al. 1998	180s at 95 °C, 40 cycles of 30s at 95 °C, 45s at 53 °C and 45s at 72 °C, 300s at 72 °C

profiles and temperatures for each primer, as indicated in Table 1. Following confirmation of appropriate bands via gel electrophoresis, PCR products were purified using ExoSAP-IT following the manufacturer's protocol, and sent to Eurofins Genomics Company (Louisville, Kentucky, USA) for sequencing. Resulting sequences were assembled and edited in Geneious Prime R11.5.1 (Kearse et al. 2012) before deposition in GenBank under accession numbers shown in Table 2.

Phylogenetic analysis

Assembled sequences were align using MAFFT (Katoh and Standley 2013; Rozewicki et al. 2019) in the program Mesquite (Maddison and Maddison 2019), including sequences from 41 *Osedax* named and unnamed species and members of three other Siboglinidae genera as outgroups (Table 2).

The most appropriate evolutionary model for each marker was recovered using ModelTest-NG (Darriba et al. 2020). The best models chosen (based on AICc) were COI = GTR+I+G4, 16S = TIM2+I+G4, 18S = GTR+I+G4, 28S = TIM3+I+G4, and H3 = TVMef+I+G4. A maximum likelihood (ML) phylogenetic tree using the concatenated sequences of all five markers was generated using the RAxML GUI program (Edler et al. 2021). Node support was assessed through bootstrapping with 1000 replicates. We chose not to conduct a Bayesian phylogenetic analysis of the data as it would yield very similar estimate of the molecular phylogeny as the maximum likelihood results. Also, as pointed out in Berman et al. (2024), missing data for many *Osedax* terminals is likely responsible for the lack of well-supported relationships rather than any particular analytical method.

Minimum genetic distance based on uncorrected *p*–distance of COI was calculated using PAUP* (Swofford 2002) between the sampled specimens and the other 44 sequences from reported *Osedax* and non-*Osedax* species. These distances were calculated using the COI alignment employed in the phylogenetic analyses.

To provide insights into the genetic relationships at the population level of the new *Osedax* species described here, a TCS haplotype network (Clement et al. 2000) using a 426 bp alignment of the COI marker was recovered for the 37 specimens sequenced using the program PopART (Leigh and Bryant 2015).

Table 2. List of species and GenBank accession numbers for sequences in this study. New sequences in bold.

Taxa	Source/Authority	COI	16S	18S	28S	H3
Outgroup						
Lamellibrachia columna	Webb 1969	DQ996645	FJ347646	FJ347679	MG264417	FJ347696
Riftia pachyptila	Jones 1981	KP119562	KP119573	KP119591	KP119582	KP119555
Sclerolinum brattstromi	Webb 1964	FJ347644	FJ347644	FJ347680	FJ347677	FJ347697
Osedax						
O. antarcticus	Glover et al. 2013	KF444422	KF444418	KF444420	–	–
O. 'BioSuOr-1'	Shimabukuro and Sumida 2019	MH616036	–	–	–	–
O. 'BioSuOr-2'	Shimabukuro and Sumida 2019	MH616081	–	–	–	–
O. 'BioSuOr-3'	Shimabukuro and Sumida 2019	MH616075	–	–	–	–
O. nataliae sp. nov.	This study; Shimabukuro and Sumida 2019	MH616012–MH616016, **PP765811–PP765827, PP982821–PP982840**	**PP669598**	**PP669599**	**PP669600**	**PP766874**
O. bozoi	Berman et al. 2024	ON357627	ON261606	ON261611	ON261610	ON254806
O. braziliensis	Fujiwara et al. 2019	LC381421	–	LC381424	–	–
O. bryani	Rouse et al. 2018	KP119563	KP119574	KP119597	KP119584	KP119561
O. byronbayensis	Georgieva et al. 2023	OQ801427	OQ820973	OQ803227	–	–
O. craigmcclaini	Berman et al. 2024; McClain et al. 2019	MN258704	ON217799	ON220153	ON226742	ON254807
O. crouchi	Amon et al. 2014	KJ598038	KJ598032	KJ598035	–	–
O. deceptionensis	Taboada et al. 2015	KF444428	KF444419	KF444421	MG264418	KT860546
O. docricketts	Rouse et al. 2018	FJ347626	FJ347650	FJ347688	FJ347666	FJ347710
O. estcourti	Berman et al. 2024	ON211943	ON217536	ON220129	ON220739	ON254809
O. fenrisi	Eilertsen et al. 2020	MT556178	–	MT556473	–	–
O. frankpressi	Rouse et al. 2004	FJ347607	FJ347658	FJ347682	FJ347674	FJ347705
O. jabba	Rouse et al. 2018	FJ347638	FJ347647	FJ347693	FJ347676	FJ347703
O. japonicus	Fujikura et al. 2006	FM998111	–	FM995535	–	–
O. knutei	Rouse et al. 2018	FJ347635	FJ347648	FJ347692	FJ347664	FJ347700
O. lehmani	Rouse et al. 2018	DQ996634	FJ347660	FJ347689	FJ347672	FJ347706
O. lonnyi	Rouse et al. 2018	FJ347643	FJ347651	FJ347695	FJ347663	FJ347699
O. 'MB16'	Salathé and Vrijenhoek 2012	JX280613	KP119581	KP119592	KP119588	KP119560
O. 'mediterranea'	Taboada et al. 2015	KT860548	KT860551	KT860550	KT860549	KT860547
O. mucofloris	Glover et al. 2005	AY827562	–	–	AY941263	–
O. nordenskjoeldi	Amon et al. 2014	KJ598039	KJ598033	KJ598036	–	–
O. packardorum	Rouse et al. 2018	FJ347629	FJ347661	FJ347690	FJ347673	FJ347707
O. priapus	Rouse et al. 2015	KP119564	KP119575	KP119594	KP119585	KP119556
O. randyi	Rouse et al. 2018	FJ347615	FJ347659	FJ347684	FJ347675	FJ347712
O. rogersi	Amon et al. 2014	KJ598034	KJ598037	KJ598040	–	–
O. roseus	Rouse et al. 2008	FJ347609	FJ347657	FJ347683	FJ347670	FJ347709
O. rubiplumus	Rouse et al. 2004	EU852488	FJ347656	FJ347681	FJ347671	FJ347704
O. ryderi	Rouse et al. 2018	KP119563	KP119574	KP119597	KP119584	KP119561
O. 'sagami-3'	Pradillon et al. unpublished	FM998081	–	FM995537	–	–
O. 'sagami-4'	Pradillon et al. unpublished	FM998082	–	FM995541	–	–
O. 'sagami-5'	Pradillon et al. unpublished	FM998083	–	FM995539	–	–
O. sigridae	Rouse et al. 2018	FJ347642	FJ347655	FJ347694	FJ347669	FJ347711
O. talkovici	Rouse et al. 2018	FJ347621	FJ347654	FJ347685	FJ347668	FJ347698
O. tiburon	Rouse et al. 2018	FJ347624	FJ347653	FJ347687	FJ347662	FJ347702
O. traceyae	Berman et al. 2024	ON211990	ON212680	ON10988	ON220740	ON254808
O. ventana	Rouse et al. 2018	EU236218	FJ347652	FJ347686	FJ347665	FJ347701
O. westernflyer	Rouse et al. 2018	FJ347631	FJ347649	FJ347691	FJ347667	FJ347708
O. waadjum	Georgieva et al. 2023	OQ801430	OQ820974	OQ803228	–	–

Results

Taxonomy

Siboglinidae Caullery, 1914
***Osedax* Rouse, Goffredi & Vrijenhoek, 2004**

***Osedax nataliae* Gularte, Sumida, Bergamo & Rouse, sp. nov**
https://zoobank.org/ED3DE09A-776C-46FF-8418-59881D751365
Figs 3–5

Osedax 'BioSuOr-4' sec. Shimabukuro and Sumida 2019.

Type material. *Holotype*: MZUSP 6201, Female, preserved in ethanol, derived from an experimentally deployed cow bones (*Bos taurus*) at a depth of 550 m, collected with *R/V Alucia* on the continental margin off São Paulo state, Brazil (26°36'13.44"S, 46°09'9.29"W) on 18 May 2017. ***Paratypes***: MZUSP 6203–6204, all females (30), preserved in ethanol, collected on cow bones deployed at the same locality and date as the holotype. Two dwarf male (allotypes), fixed in ethanol from tube of holotype: MZUSP 6202, same date and locality as holotype.

Diagnosis and description. Holotype female (Fig. 3A–C); body length ~ 14.7 mm; gelatinous tube (removed) 0.2 wide, longer than trunk and crown; crown of palps, ~ 2.8 mm long; trunk length ~ 7.4 mm, width ~ 0.5 mm; root structure ~ 4.5 mm long; width ~ 2.4 mm; Crown of four pinnulated palps, with the pinnules arranged along the outer margin of the palps (Figs 3B, 4). Conspicuous oviduct shorter than palps (Figs 3B, 4A–D). Collar ventrally along the margin of anterior trunk, except for the dorsal portion (Figs 3B, 4B–E). Live specimens with palps bright red-orange distally, becoming yellow and then white proximally to the boundary with the trunk (Fig. 5). No obvious pigmentation on trunk or demarcation into upper and lower trunk. Root structure missing in holotype, bulbous or lobulate in paratypes. Ovisac an ellipsoidal mass contain oocytes at various stages of development (Fig. 3A). Dwarf male ~ 170 μm in length, fusiform, no appendage organs (Fig. 3C); posterior hooks present (Fig. 3D).

Distribution. Known from the continental margin off São Paulo state, Santos basin, Brazil, at a depth of 550 m; on experimentally deployed cow bones.

Molecular results. The final lengths of sequences for the different genetic markers were 482–600 bp (COI), 454 bp (16S), 1769 bp (18S), 997 bp (28S) and 309 bp (H3). Uncorrected intraspecific divergence of *O. nataliae* sp. nov. for COI was up to 2.44%. In terms of distance, the most closely related species to *O. nataliae* sp. nov. was *O.* 'sagami-3', with a minimum interspecific distance for COI of 13.92% (Suppl. material 1). The phylogenetic analysis of the concatenated dataset of the five markers placed *Osedax nataliae* sp. nov. in the well-supported Clade V (see Rouse et al. 2018) although relationships within the clade were poorly supported. The new species was recovered as sister species to the clade formed by *O*. 'sagami-3', known from NW Pacific at unknown depth, and *Osedax roseus*, from NW and NE Pacific at depths of 633 to 1820 m (Fig. 6). A total of 22 distinct haplotypes were recovered for the COI dataset (*n* = 38), with the most common one being shared by ten individuals (Fig. 7). Despite originating from a single experimental lander, the network reveals a central and more common haplotype surrounded by several closely related and some more distant haplotypes with numerous nucleotide substitutions.

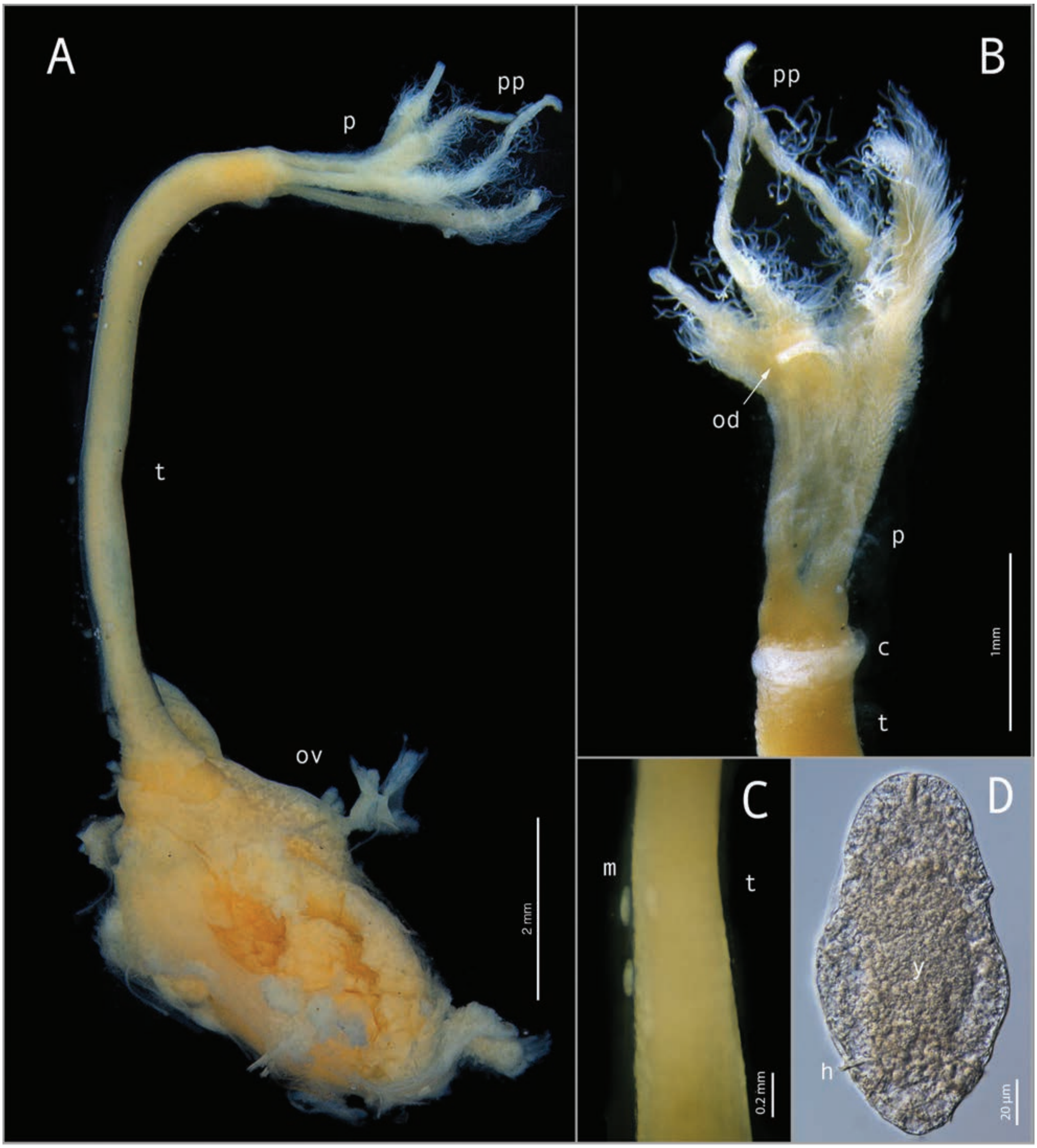

Figure 3. *Osedax nataliae* sp. nov. Preserved female holotype (MZUSP 6201) **A–C** and male specimens (MZUSP 6202) **D**: **A** lateral view of the entire specimen **B** detail of palps and trunk **C** detail of trunk with male attached to the surface **D** light microscope of individual male (preserved). Abbreviations: c, collar; m, male; od, oviduct; ov, ovisac; p, palps; pp, pinnules; t, trunk; h, hooks; y, yolk.

Remarks. *Osedax nataliae* sp. nov. is part of the Clade V according to the phylogenetic analysis (Fig. 6) and shares some important morphological features with the other taxa within this clade, such as pinnules inserted on the outer margin of palps (Fig. 4D, E) and a collar at the base of the crown (Figs 4B, 5B–E). The collar of *Osedax nataliae* sp. nov. and *Osedax roseus* (the closest species in molecular phylogeny that has a morphological description) are

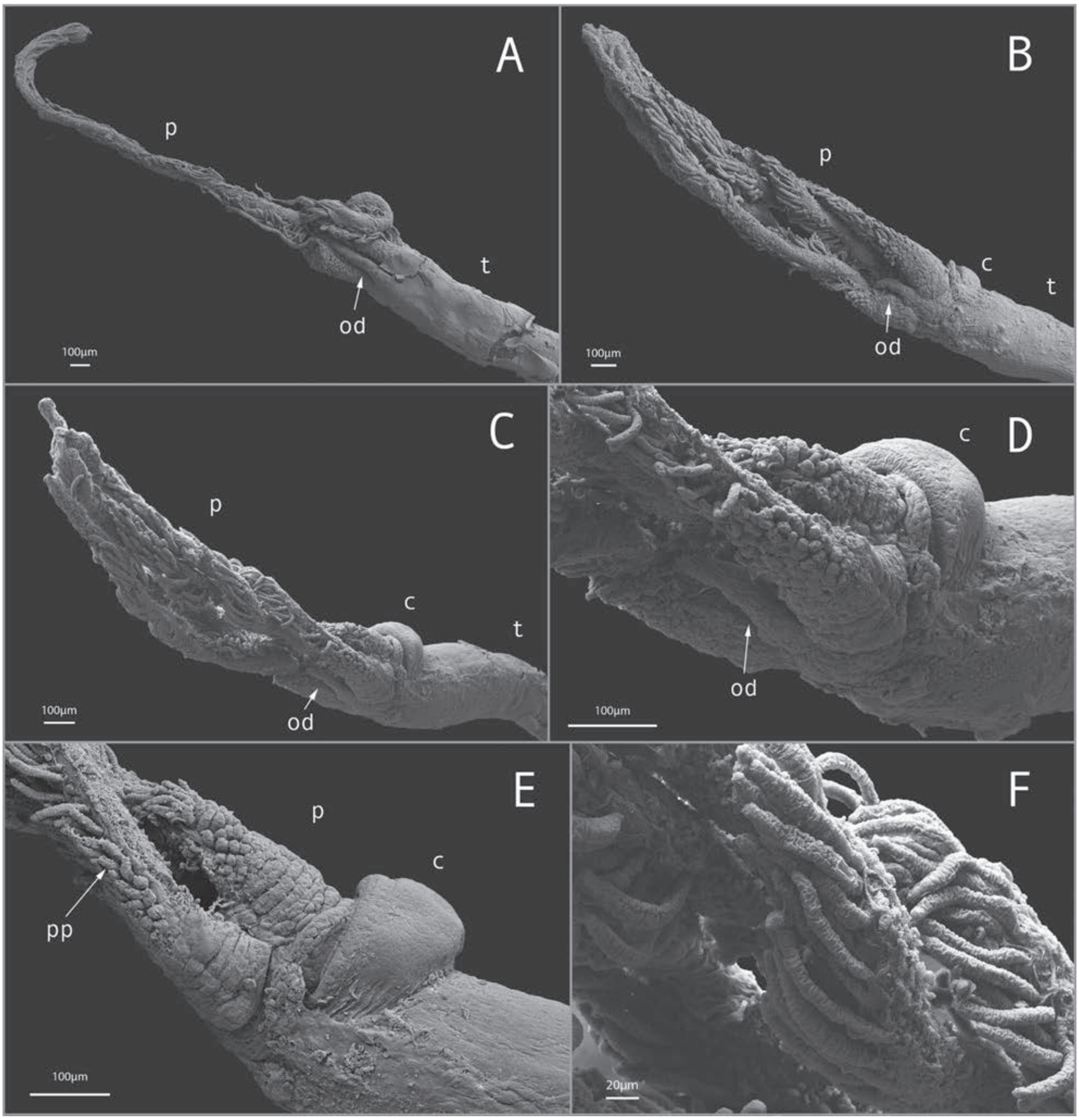

Figure 4. *Osedax nataliae* sp. nov. Scanning Electron Microscopy (SEM) of two paratypes. Paratype (MZUSP 6204) **A** dorsal view of palps and trunk end of paratype 1. Paratype (MZUSP 6205) **B** dorsal view of palps and trunk end **C** lateral view highlighting oviduct and collar position **D** detail of the base of the palps **E** lateral view of the collar **F** detail of the pinnules in the palps. Abbreviations: c, collar; od, oviduct; p, palps; pp, pinnules; t, trunk.

similar in shape and position, though more inflated in *O. nataliae* sp. nov. Some specimens of *Osedax nataliae* sp. nov. appear to lack a collar, which could be an artifact of fixation. The dwarf males of *O. nataliae* sp. nov., with a length of 170 µm, are notably smaller than the males of *O. rubiplumus* (400 µm–1.1 mm long) but similar in size to those of *O. roseus* (130–210 µm) and *O. frankpressi* (150–250 µm). The body size (length of crown + trunk) of *Osedax nataliae* sp. nov. females varied markedly among the individuals examined, ranging from 4 mm to 15 mm, with a mean value of 6.76 mm. When compared with groups from the same clade, the body size is like *O. roseus*, *O. bryani*, and *O. fenrisi*

Figure 5. *Osedax nataliae* sp. nov. Live specimens photographed alive onboard R/V Alucia after recovery from the lander. Red palps and trunk are partially extended in gelatinous tubes.

females but much smaller than *O. rubiplumus*. *Osedax nataliae* sp. nov. is not obviously distinguishable from its relatives on morphology. Its notable features such as the red-orange distal crown of pinnulate palps, yellowing towards the base, collar, and long trunk (Fig. 3) may occur in other species of Clade V, such as *O. roseus*. However, molecular data from both the phylogenetic analysis (Fig. 6) and COI distance (Suppl. material 1) confirm *Osedax nataliae* sp. nov. as a new species.

Etymology. This species is named after Natalia Gularte, mother of the first author, in recognition of her long and continued support in this research effort.

Discussion

This study formally describes a second species of *Osedax* from the South Atlantic Ocean, combining both morphological and molecular approaches. *Osedax nataliae* sp. nov. was previously reported under the informal epithet of ‘BioSuOr-4’ (see Shimabukuro and Sumida 2019) based on COI alone though its phylogenetic placement was not clear based on such limited data. With the additional data of five molecular markers, *O. nataliae* sp. nov. joins *O. bryani*, *O. fenrisi*, *O. craigmcclaini*, *O. rubiplumus*, *O.* ‘sagami-4’, *O. roseus*, and *O.* ‘sagami-3’, to supplement the membership of the well-supported Clade V (Vrijenhoek et al. 2009; Rouse et al. 2015, 2018; Eilertsen et al. 2020; Berman et al. 2024). However, relationships within clade V are poorly supported likely owing to the lack of DNA data for most of the molecular markers used here for terminals

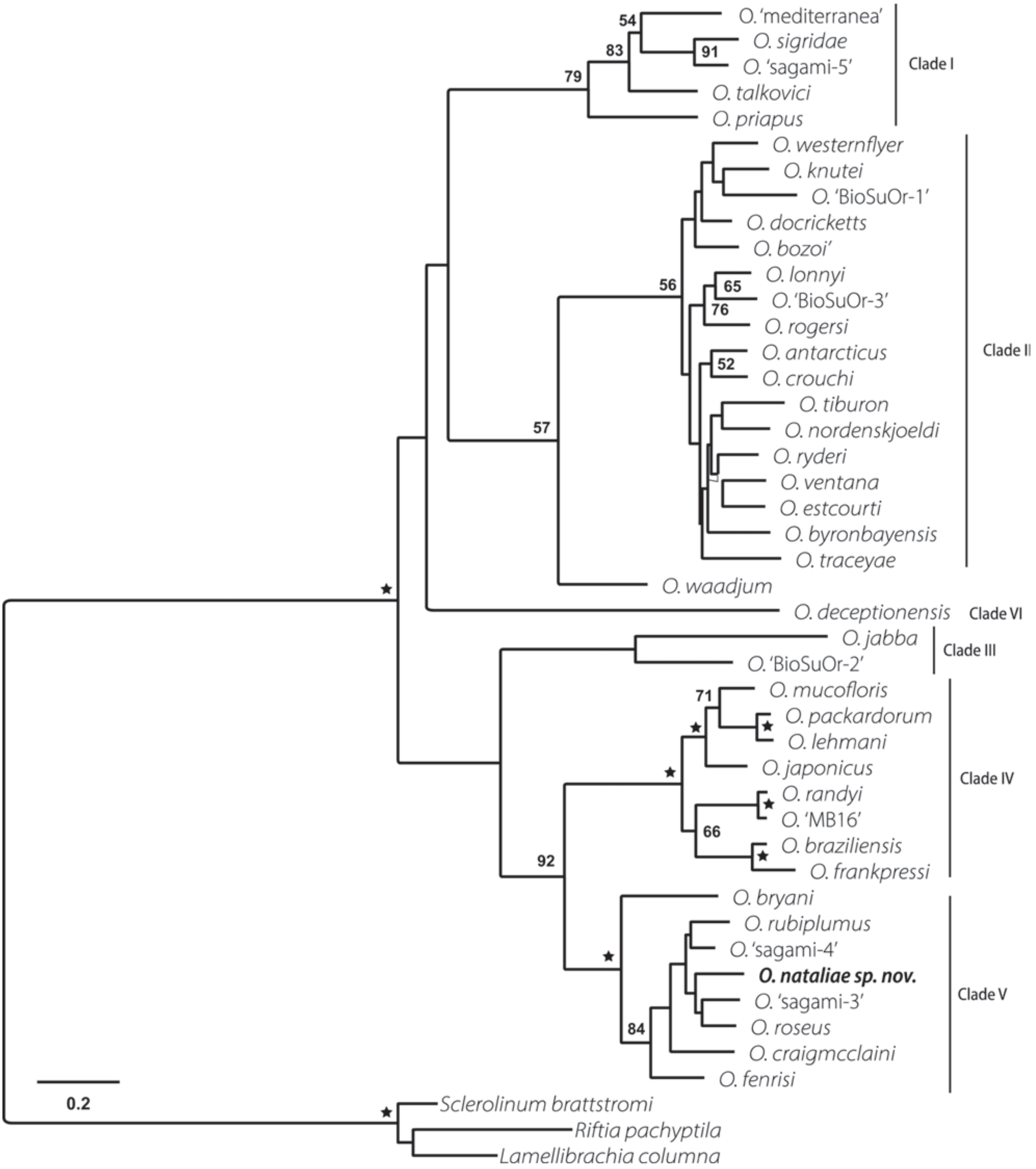

Figure 6. *Osedax* phylogenetic analysis. Maximum likelihood phylogenetic tree based on a partitioned concatenated dataset of COI, 16S, 18S, 28S, and H3 markers (MAFFT-aligned) for the data shown in Table 2. Bootstrap support values are indicated. Black star values were ≥ 95% (BS). Missing values indicate BS < 50%.

such as *O.* 'sagami-3', *O.* 'sagami-4', and *O. fenrisi*. The present results suggest *O. nataliae* sp. nov. is nested among a Pacific clade of *Osedax* (Fig. 5), but sampling of *Osedax* diversity is presently biased towards that ocean basin.

The migratory routes of many species of whales through the Atlantic Ocean, including the sub-Atlantic populations of humpback whale (*Megaptera novaeangliae*) which migrate from South Georgia Islands through Rio Grande Rise and northwards to Abrolhos Bank (Best et al. 1993; Zerbini et. al 2006;

Santos et al. 2010; Wedekin et al. 2014) suggest that the deep-sea oceans in the Southern Hemisphere may provide a rich supply of whale carcasses to support *Osedax* species. The report of 16 whale-fall-associated new species, including four *Osedax* species from the BioSuOr project conducted in the Southwest Atlantic Ocean (Shimabukuro et al. 2022) supports this hypothesis.

The haplotype network for *O. nataliae* sp. nov. (Fig. 7) reveals high genetic diversity within the study area, with 22 haplotypes recovered from the 37 specimens sequenced. This network also shows no evidence of any population 'bottleneck', which would have been indicated by a much lower diversity of haplotypes for the number of specimens sequenced (Avise 2000). This diverse haplotype network aligns with observations seen previously in other *Osedax* species (Glover et al. 2005; Rouse et al. 2008; Amon et al. 2014).

As part of the BioSuOr project, *O. nataliae* sp. nov. was exclusively reported from cow bones deployed at a depth of 550 m. No information is available regarding the possibility of this species colonizing only small bones nor is there data on its depth range capability. Further research is needed to investigate the potential substrate preferences and depth range of *O. nataliae* sp. nov. to better understand its ecological niche and distribution in deep-sea ecosystems.

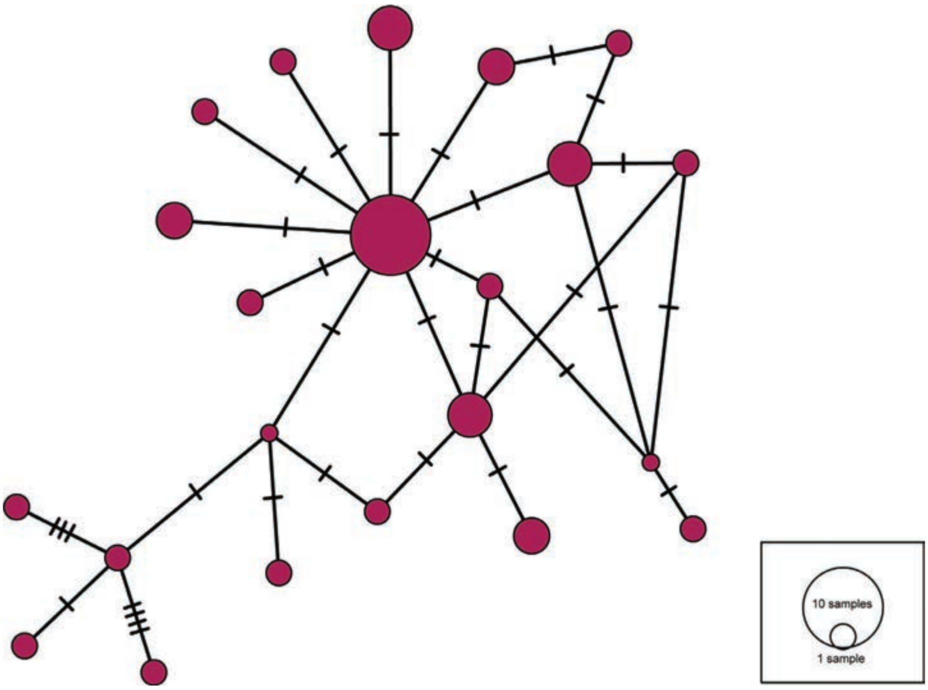

Figure 7. Haplotype network using COI for 37 *Osedax nataliae* sp. nov. Circles are haplotypes and crosshatches are single nucleotide substitutions.

Acknowledgments

We are thankful to the captains and crews of R/V Alpha Crucis and R/V Alucia for the deployment and recovery of the lander. We would also like to extend our thanks to Mauricio Shimabukuro, Orlemir Carrerette, Daniel M. Couto, Avery S. Hiley, and Sonja Huč for their training contributions and assistance during sample analyses. Thanks also to reviewers Thomas Dahlgren and Sergio Taboada for their valuable critiques.

Additional information

Conflict of interest

The authors have declared that no competing interests exist.

Ethical statement

No ethical statement was reported.

Funding

The authors would like to acknowledge the funding support provided by Fundação de Amparo à Pesquisa do Estado de São Paulo (FAPESP) through grants 2011/50185-1, 2022/04019-7 and 2022/12683-4, and Conselho Nacional de Desenvolvimento Científico e Tecnológico (CNPq) through grant 301554/2019-6.

Author contributions

Conceptualization: TG, PYGS, GWR. Methodology: TG, GB, PYGS, GWR. Formal analysis: TG, GB, GWR. Investigation: TG, GB, GWR. Resources: PYGS, GWR. Writing - Original draft: TG, GB. Writing - Review and Editing: TG, PYGS, GB, GWR. Visualization: TG, GB, GWR. Supervision: PYGS, GWR. Funding Acquisition: PYGS, GWR.

Author ORCIDs

Thammy Gularte https://orcid.org/0000-0002-3121-1973
Paulo Y. G. Sumida https://orcid.org/0000-0001-7549-4541
Gilberto Bergamo https://orcid.org/0000-0001-5464-909X
Greg W. Rouse https://orcid.org/0000-0001-9036-9263

Data availability

All data generated during this study are included in this article. Sequences are published in GenBank and BOLD.

References

Amon DJ, Wiklund H, Dahlgren TG, Copley JT, Smith CR, Jamieson AJ, Glover AG (2014) Molecular taxonomy of *Osedax* (Annelida: Siboglinidae) in the Southern Ocean. Zoologica Scripta 43: 405–417. https://doi.org/10.1111/zsc.12057

Avila AKF, Shimabukuro M, Couto DM, Alfaro-Lucas JM, Sumida PYG, Gallucci F (2023) Whale falls as chemosynthetic refugia: a perspective from free-living deep-sea nematodes. Frontiers in Marine Science 10: 1111249. https://doi.org/10.3389/fmars.2023.1111249

Avise JC (2000) Phylogeography: the history and formation of species. Harvard University Press, Cambridge, USA, 447 pp. https://doi.org/10.2307/j.ctv1nzfgj7

Bergamo G, Carrerette O, Shimabukuro M, Santos CSG, Sumida PYG (2024) Revealing a new eyeless *Nereis* (Nereididae: Annelida) clade from deep-sea organic falls. Zoological Journal of the Linnean Society 201: 1–31. https://doi.org/10.1093/zoolinnean/zlad122

Berman GH, Hiley AS, Read GB, Rouse GW (2024) New species of *Osedax* (Siboglinidae: Annelida) from New Zealand and the Gulf of Mexico. Zootaxa 5443: 337–352. https://doi.org/10.11646/zootaxa.5443.3.2

Best PB, Payne R, Rowntree V, Palazzo JT, Both MDC (1993) Long-range movements of South Atlantic right whales *Eubalaena australis*. Marine Mammal Science 9: 227–234. https://doi.org/10.1111/j.1748-7692.1993.tb00451.x

Braby CE, Rouse GW, Johnson SB, Jones WJ, Vrijenhoek RC (2007) Bathymetric and temporal variation among *Osedax* boneworms and associated megafauna on whale-falls in Monterey Bay, California. Deep-Sea Deep-Sea Research Part I Oceanographic Research Papers 54: 1773–1791. https://doi.org/10.1016/j.dsr.2007.05.014

Brown S, Rouse G, Hutchings P, Colgan D (1999) Assessing the usefulness of histone *H3*, *U2* snRNA and *28S* rDNA in analyses of polychaete relationships. Australian Journal of Zoology 47: 499–516. https://doi.org/10.1071/ZO99026

Clement M, Posada D, Crandall KA (2000) TCS: a computer program to estimate gene genealogies. Molecular Ecology 9: 1657–1659. https://doi.org/10.1046/j.1365-294x.2000.01020.x

Colgan DJ, McLauchlan A, Wilson GDF, Livingston SP, Edgecombe GD, Macaranas J, Cassis G, Gray MR (1998) Histone *H3* and *U2* snRNA DNA sequences and arthropod molecular evolution. Australian Journal of Zoology 46: 419–437. https://doi.org/10.1071/zo98048

Darriba D, Posada D, Kozlov AM, Stamatakis A, Morel B, Flouri T (2020) ModelTest-NG: a new and scalable tool for the selection of DNA and protein evolutionary models. Molecular Biology and Evolution 37: 291–294. https://doi.org/10.1093/molbev/msz189

Dawbin WH (1966) 9. The seasonal migratory cycle of humpback whales. In: Whales, Dolphins, and Porpoises University of California Press, 145–170. https://doi.org/10.1525/9780520321373-011

Edler D, Klein J, Antonelli A, Silvestro D (2021) raxmlGUI 2.0: a graphical interface and toolkit for phylogenetic analyses using *RAxML*. https://doi.org/10.1101/800912

Eilertsen MH, Dahlgren TG, Rapp HT (2020) A new species of *Osedax* (Siboglinidae: Annelida) from colonization experiments in the Arctic deep sea. Frontiers in Marine Science 7: 443. https://doi.org/10.3389/fmars.2020.00443

Fujikura K, Fujiwara Y, Kawato M (2006) A New species of *Osedax* (Annelida: Siboglinidae) associated with whale carcasses off Kyushu, Japan. Zoological Science 23: 733–740. https://doi.org/10.2108/zsj.23.733

Fujiwara Y, Jimi N, Sumida PYG, Kawato M, Kitazato H (2019) New species of bone-eating worm *Osedax* from the abyssal South Atlantic Ocean (Annelida, Siboglinidae). ZooKeys 814: 53–69. https://doi.org/10.3897/zookeys.814.28869

Gaudron SM, Pradillon F, Pailleret M, Duperron S, Le Bris N, Gaill F (2010) Colonization of organic substrates deployed in deep-sea reducing habitats by symbiotic species and associated fauna. Marine Environmental Research 70: 1–12. https://doi.org/10.1016/j.marenvres.2010.02.002

Georgieva MN, Wiklund H, Ramos DA, Neal L, Glasby CJ, Gunton LM (2023) The annelid community of a natural deep-sea whale fall off eastern Australia. In: Kupriyanova EK, Gunton LM (Eds) RV Investigator—Abyssal Annelida. Records of the Australian Museum 75: 167–213. https://doi.org/10.3853/j.2201-4349.75.2023.1800

Giribet G, Carranza S, Baguna J, Riutort M, Ribera C (1996) First molecular evidence for the existence of a Tardigrada + Arthropoda clade. Molecular Biology and Evolution 13: 76–84. https://doi.org/10.1093/oxfordjournals.molbev.a025573

Glover AG, Källström B, Smith CR, Dahlgren TG (2005) World-wide whale worms? A new species of *Osedax* from the shallow north Atlantic. Proceedings of the Royal Society B: Biological Sciences 272: 2587–2592. https://doi.org/10.1098/rspb.2005.3275

Glover AG, Wiklund H, Taboada S, Avila C, Cristobo J, Smith CR, Kemp KM, Jamieson AJ, Dahlgren TG (2013) Bone-eating worms from the Antarctic: the contrasting fate of whale and wood remains on the Southern Ocean seafloor. Proceedings of the Royal Society B: Biological Sciences 280: 20131390. https://doi.org/10.1098/rspb.2013.1390

Goffredi SK, Orphan VJ, Rouse GW, Jahnke L, Embaye T, Turk K, Lee R, Vrijenhoek RC (2005) Evolutionary innovation: a bone-eating marine symbiosis. Environmental Microbiology 7: 1369–1378. https://doi.org/10.1111/j.1462-2920.2005.00824.x

Goffredi SK, Johnson SB, Vrijenhoek RC (2007) Genetic diversity and potential function of microbial symbionts associated with newly discovered species of *Osedax* polychaete worms. Applied and Environmental Microbiology 73: 2314–2323. https://doi.org/10.1128/AEM.01986-06

Jones ML (1981) *Riftia pachyptila* Jones: Observations on the vestimentiferan worm from the Galápagos Rift. Science 213: 333–336. https://doi.org/10.1126/science.213.4505.333

Katoh K, Standley DM (2013) MAFFT Multiple sequence alignment software Version 7: improvements in performance and usability. Molecular Biology and Evolution 30: 772–780. https://doi.org/10.1093/molbev/mst010

Katz S, Klepal W, Bright M (2010) The skin of *Osedax* (Siboglinidae, Annelida): An ultrastructural investigation of its epidermis. Journal of Morphology 271: 1272–1280. https://doi.org/10.1002/jmor.10873

Kearse M, Moir R, Wilson A, Stones-Havas S, Cheung M, Sturrock S, Buxton S, Cooper A, Markowitz S, Duran C, Thierer T, Ashton B, Meintjes P, Drummond A (2012) Geneious Basic: An integrated and extendable desktop software platform for the organization and analysis of sequence data. Bioinformatics 28: 1647–1649. https://doi.org/10.1093/bioinformatics/bts199

Laws RM (1977) Seals and whales of the Southern Ocean. Philosophical Transactions of the Royal Society of London. B, Biological Sciences 279: 81–96. https://doi.org/10.1098/rstb.1977.0073

Leigh JW, Bryant D (2015) PopART: full-feature software for haplotype network construction. Methods in Ecology and Evolution 6: 1110–1116. https://doi.org/10.1111/2041-210X.12410

Lundsten L, Schlining KL, Frasier K, Johnson SB, Kuhnz LA, Harvey JBJ, Clague G, Vrijenhoek RC (2010) Time-series analysis of six whale-fall communities in Monterey Canyon, California, USA. Deep Sea Research Part I: Oceanographic Research Papers 57: 1573–1584. https://doi.org/10.1016/j.dsr.2010.09.003

Maddison WP, Maddison DR (2019) Mesquite Project. Mesquite: A modular system for evolutionary analysis. https://www.mesquiteproject.org/ [accessed 8 July2024]

McClain CR, Nunnally C, Dixon R, Rouse GW, Benfield M (2019) Alligators in the abyss: The first experimental reptilian food fall in the deep ocean. PLoS ONE 14: e0225345. https://doi.org/10.1371/journal.pone.0225345

Palumbi SR (1996) Nucleic acids II: The polymerase chain reaction. In: Hillis DM, Moritz C, Mable BK (Eds) Molecular Systematics. Sinauer Associates, Sunderland, Massachusetts, 205–247.

Rouse GW, Goffredi SK (2023) *Osedax* (Siboglinidae: Annelida) utilizes shark teeth for nutrition. Journal of the Marine Biological Association of the United Kingdom 103: e35. https://doi.org/10.1017/S0025315423000243

Rouse GW, Goffredi SK, Vrijenhoek RC (2004) *Osedax* : Bone-eating marine worms with dwarf males. Science 305: 668–671. https://doi.org/10.1126/science.1098650

Rouse GW, Worsaae K, Johnson SB, Jones WJ, Vrijenhoek RC (2008) Acquisition of dwarf male “harems” by recently settled females of *Osedax roseus* n. sp. (Siboglinidae; Annelida). The Biological Bulletin 214: 67–82. https://doi.org/10.2307/25066661

Rouse GW, Wilson NG, Worsaae K, Vrijenhoek RC (2015) A Dwarf male reversal in bone-eating worms. Current Biology 25: 236–241. https://doi.org/10.1016/j.cub.2014.11.032

Rouse GW, Goffredi SK, Johnson SB, Vrijenhoek RC (2018) An inordinate fondness for *Osedax* (Siboglinidae: Annelida): Fourteen new species of bone worms from California. Zootaxa 4377: 451–489. https://doi.org/10.11646/zootaxa.4377.4.1

Rozewicki J, Li S, Amada KM, Standley DM, Katoh K (2019) MAFFT-DASH: integrated protein sequence and structural alignment. Nucleic Acids Research: gkz342. https://doi.org/10.1093/nar/gkz342

Saeedi H, Bernardino AF, Shimabukuro M, Falchetto G, Sumida PYG (2019) Macrofaunal community structure and biodiversity patterns based on a wood-fall experiment in the deep South-west Atlantic. Deep Sea Research Part I: Oceanographic Research Papers 145: 73–82. https://doi.org/10.1016/j.dsr.2019.01.008

Salathé RM, Vrijenhoek RC (2012) Temporal variation and lack of host specificity among bacterial endosymbionts of *Osedax* bone worms (Polychaeta: Siboglinidae). BMC Evolutionary Biology 12: 189. https://doi.org/10.1186/1471-2148-12-189

Santos MC de O, Siciliano S, Vicente AF de C, Alvarenga FS, Zampirolli É, Souza SP de, Maranho A (2010) Cetacean records along São Paulo state coast, Southeastern Brazil. Brazilian Journal of Oceanography 58: 123–142. https://doi.org/10.1590/S1679-87592010000200004

Shimabukuro M, Sumida PYG (2019) Diversity of bone-eating *Osedax* worms on the deep Atlantic whale falls—bathymetric variation and inter-basin distributions. Marine Biodiversity 49: 2587–2599. https://doi.org/10.1007/s12526-019-00988-2

Shimabukuro M, Carrerette O, Alfaro-Lucas JM, Rizzo AE, Halanych KM, Sumida PYG (2019) Diversity, distribution and phylogeny of Hesionidae (Annelida) colonizing whale falls: new species of *Sirsoe* and connections between ocean basins. Frontiers in Marine Science 6: 478. https://doi.org/10.3389/fmars.2019.00478

Shimabukuro M, Couto DM, Bernardino AF, Souza BHM, Carrerette O, Pellizari VH, Sumida PYG (2022) Whale bone communities in the deep Southwest Atlantic Ocean. Deep Sea Research Part I: Oceanographic Research Papers 190: 103916. https://doi.org/10.1016/j.dsr.2022.103916

Smith CR, Baco AR (2003) Ecology of whale falls at the deep sea floor. Oceanography and Marine Biology: an Annual Review 41: 311–354. https://doi.org/10.1201/9780203180594.ch6

Smith CR, Glover AG, Treude T, Higgs ND, Amon DJ (2015) Whale-Fall Ecosystems: Recent Insights into Ecology, Paleoecology, and Evolution. Annual Review of Marine Science 7: 571–596. https://doi.org/10.1146/annurev-marine-010213-135144

Souza BHM, Passos FD, Shimabukuro M, Sumida PYG (2021) An integrative approach distinguishes three new species of Abyssochrysoidea (Mollusca: Caenogastropoda) associated with organic falls of the deep south-west Atlantic. Zoological Journal of the Linnean Society 191: 748–771. https://doi.org/10.1093/zoolinnean/zlaa059

Swofford D. L. (2002) PAUP*: Phylogenetic analysis using parsimony (*and other methods). https://paup.phylosolutions.com

Taboada S, Riesgo A, Bas M, Arnedo MA, Cristobo J, Rouse GW, Avila C (2015) Bone-eating worms spread: Insights into shallow-Water *Osedax* (Annelida, Siboglinidae) from Antarctic, Subantarctic, and Mediterranean Waters. PLoS ONE 10: e0140341. https://doi.org/10.1371/journal.pone.0140341

Tresguerres M, Katz S, Rouse GW (2013) How to get into bones: proton pump and carbonic anhydrase in *Osedax* boneworms. Proceedings of the Royal Society B: Biological Sciences 280: 20130625. https://doi.org/10.1098/rspb.2013.0625

Vrijenhoek RC, Johnson SB, Rouse GW (2008) Bone-eating *Osedax* females and their "harems" of dwarf males are recruited from a common larval pool. Molecular Ecology 17: 4535–4544. https://doi.org/10.1111/j.1365-294X.2008.03937.x

Vrijenhoek RC, Johnson SB, Rouse GW (2009) A remarkable diversity of bone-eating worms (*Osedax*; Siboglinidae; Annelida). BMC Biology 7: 74. https://doi.org/10.1186/1741-7007-7-74

Webb M (1964) A new bitentaculate pogonophoran from Hardangerfjorden, Norway. Sarsia 15: 49–56. https://doi.org/10.1080/00364827.1964.10409528

Webb M (1969) *Lamellibrachia barhami*, gen. nov., sp. nov. (Pogonophora), from the northeast Pacific. Bulletin of Marine Science 19: 18–47.

Wedekin LL, Rossi-Santos MR, Baracho C, Cypriano-Souza AL, Simões-Lopes PC (2014) Cetacean records along a coastal-offshore gradient in the Vitória-Trindade Chain, western South Atlantic Ocean. Brazilian Journal of Biology 74: 137–144. https://doi.org/10.1590/1519-6984.21812

Whiting MF, Carpenter JC, Wheeler QD, Wheeler WC (1997) The Strepsiptera problem: Phylogeny of the holometabolous Insect orders inferred from *18S* and *28S* ribosomal DNA sequences and morphology. Farrell B (Ed). Systematic Biology 46: 1–68. https://doi.org/10.1093/sysbio/46.1.1

Zerbini AN, Andriolo A, Heide-Jørgensen MP, Pizzorno JL, Maia YG, VanBlaricom GR, DeMaster DP, Simões-Lopes PC, Moreira S, Bethlem C (2006) Satellite-monitored movements of humpback whales *Megaptera novaeangliae* in the Southwest Atlantic Ocean. Marine Ecology Progress Series 313: 295–304. https://doi.org/10.3354/meps313295

Supplementary material 1

Minimum genetic distance based on uncorrected p–distance between species within Clade V

Authors: Thammy Gularte, Paulo Y. G. Sumida, Gilberto Bergamo, Greg W. Rouse

Data type: xlsx

Explanation note: The maximum intraspecific divergences among *Osedax nataliae* sp. nov. specimens are in bold.

Link: https://doi.org/10.3897/zookeys.1219.134005.suppl1

ZooKeys 1219: 233–248 (2024)
DOI: 10.3897/zookeys.1219.130895

Research Article

The first report of two new janiroid isopod species (Asellota, Janiroidea) from the western Indian Ocean

Valiallah Khalaji-Pirbalouty[1], Manal Abdulrahman Al-Kandari[2]

1 *Department of Biology, Faculty of Basic Science, Shahrekord University, Shahrekord, Iran*
2 *Coastal and Marine Research Program, Environment and Life Sciences Research Center, Kuwait Institute of Scientific Research, Hamad Al-Mubarak Street, Building 900004, Area 1, Raas Salmiya, Kuwait*
Corresponding author: Valiallah Khalaji-Pirbalouty (khalajiv@yahoo.com)

Abstract

Two new janiroid isopod species, *Heterosignum behbehanii* **sp. nov.** and *Uromunna alyamanii* **sp. nov.**, are described from the Kuwaiti waters, representing the first record of the genera in the western Indian Ocean. *Heterosignum behbehanii* **sp. nov.** is distinguished from its congeners by pereonites 2–7 with a pair of short single lateral spine-like processes; the relatively short length of the anterior part of its pleotelson, which accounts for about 0.1 of the total length of the pleotelson; and the stylet with an elongate, downwardly curved, and distally pointed apex. *Uromunna alyamanii* **sp. nov.** is equally unique, with the pleotelson bearing two denticles on each lateral margin, pleopod 2 endopod stylet extending beyond the apex of the protopod, and pleopod 4 exopod distal tip with a long plumose seta. This discovery of unique characteristics of the new species significantly enhances our understanding of marine biodiversity in the western Indian Ocean and underscores the importance of further research in this area. The identification keys are provided to all known species of *Heterosignum* and Indian Ocean *Uromunna* species.

Key words: *Heterosignum*, identification key, Indian Ocean, Kuwait, Munnidae, new record, new species, Paramunnidae, taxonomy, *Uromunna*

Academic editor: Saskia Brix
Received: 1 July 2024
Accepted: 6 November 2024
Published: 3 December 2024

ZooBank: https://zoobank.org/2B55BA1C-2E86-4471-997B-624F508870A7

Citation: Khalaji-Pirbalouty V, Al-Kandari MA (2024) The first report of two new janiroid isopod species (Asellota, Janiroidea) from the western Indian Ocean. ZooKeys 1219: 233–248. https://doi.org/10.3897/zookeys.1219.130895

Introduction

The superfamily Janiroidea Sars, 1897 is composed of 25 families, with Paramunnidae Vanhöffen, 1914 and Munnidae Sars, 1897, standing out as the two largest and most diverse families within the suborder Asellota (Boyko et al. 2008, onwards). The isopod family Paramunnidae consists of about 195 described species classified into 45 genera, all of which are tiny benthic dwellers known worldwide, from shallow tidal zones to abyssal depths (Just and Wilson 2007; Boyko et al. 2008, onwards). Within Paramunnidae, the genus *Heterosignum* Gamô, 1976, comprises seven valid species. Apart from *Heterosignum unicornis* (Kensley, 1976), found in the Amsterdam Islands in the southern Indian Ocean, the remaining *Heterosignum* species have been exclusively reported in the areas around Japan (Shimomura 2009, 2011).

The family Munnidae Sars, 1897, with its 114 described species distributed across six genera (Boyko et al. 2008, onwards), is a testament to the adaptability of these small, free-living isopods. They thrive in diverse environments, ranging from shallow waters to abyssal depths spanning tropical and polar regions across the globe. Their remarkable adaptability allows them to thrive in various habitats, including mud and sand flats, intertidal rock pools, seagrass meadows, sponges, and coral reefs (Wilson 1980). This adaptability is a fascinating aspect of their biology that continues to intrigue researchers in the field. Within Munnidae, the genus *Munna* Krøyer, 1839, is the most species-rich and is currently composed of 79 valid species (Boyko et al. 2008 onwards). The genus *Uromunna* Menzies, 1962, is the second known genus with the highest species diversity of 28 recorded species (Boyko et al. 2008, onwards).

To date, 15 *Uromunna* species have been reported from the Atlantic Ocean, primarily in the northern regions, and 10 species in the Pacific Ocean. Notably, the eastern Indian Ocean, particularly the Australian region, is home to three *Uromunna* species: *U. brevicornis* (Thomson, 1946) from Swan River, Western Australia; *U. humei* Poore, 1984 from Apollo Bay, Victoria, and *U. phillipi* Poore, 1984 from Port Phillip Bay, Victoria. However, no *Uromunna* species have been reported from the western, northern, and southern regions of the Indian Ocean. This absence makes our discovery of two new species, one each from *Heterosignum* and *Uromunna* in the western Indian Ocean, particularly significant.

Materials and methods

Sample collection was conducted during sampling trips (2013–2017), focusing on the littoral zone along Kuwait's coastline and offshore islands (Al-Kandari et al. 2022). All material was fixed and preserved in 96% ethanol.

The specimens' sorting, dissection and imaging were performed using a Leica® M125 stereomicroscope equipped with a DFC450 camera. Dissected appendages were mounted onto glass slides in stained antibacterial glycerine-gelatine (Merck). Pencil appendage drawings were made using a Leica (DM1000) compound microscope equipped with camera lucida. All illustrations were electronically inked with Corel Draw (version X6). The specimens were prepared for SEM photographs using previously described techniques (Khalaji-Pirbalouty et al. 2022) and examined with a Vega3 SBU scanning electron microscope (TESCAN Brno, Czech Republic).

The morphological terminology used herein is a comprehensive compilation from established sources such as Poore (1984), Shimomura and Mawatari (2002), and Esquete and Wilson (2016). All the material used in this study is deposited in the Museum of Nature, Hamburg, the Leibniz Institute for the Analysis of Biodiversity Change (**LIB**).

Results

Taxonomy

Suborder Asellota Latreille, 1802
Superfamily Janiroidea Sars, 1897
Family Paramunnidae Vanhöffen, 1914

Genus *Heterosignum* Gamô, 1976

Type species. *Heterosignum mutsuensis* Gamô, 1976 (original designation).

Diagnosis. The most recent revision and diagnosis of the genus is that of Shimomura and Mawatari (2002).

Heterosignum behbehanii sp. nov.

https://zoobank.org/38B4B177-F22A-42D0-A139-61D9D21B8F38
Figs 1–4, 5A, B

Etymology. The species is named in honour of Dr Abdulmanaf Behbehani, a respected figure who taught Marine Biology and Ecology at Kuwait University and researched Kuwait's marine environment and Kuwait's intertidal macrofauna for over four decades.

Type material. ***Holotype*:** • ♂, 1.12 mm (ZMH-K-64934), KUWAIT, Al-Salam Beach; 29°21.631'N, 47°57.204'E; 28.X.2014; V. Grintsov leg. ***Paratypes*:** • 1♀, 1.34 mm (ZMH-K-64935), same data as the holotype • 1 ♂ 1.1 mm; 4 ♀♀ up to 1.25 mm (ZMH-K-64936), Umm Al-Maradim Island; 28°40.778'N, 48°39.207'E; 11.XI.2014; V. Grintsov leg.

Diagnosis. Eyes with 3 ommatidia; eyestalks with medium length, reaching proximal half of peduncular article 2 of antenna 2. Pereonites 2–7 with a pair of relatively short single lateral spine-like processes. The pleotelson has a relatively short anterior neck, length about 0.1 pleotelson length, lateral margins with 6 denticles each. Male pleopod 2 with an elongate, downwardly curved and distally pointed apex endopodal stylet.

Description. Male: Body (Fig. 1B) length 1.28 mm; about 2 times as long as wide, widest at pereonite 3.

Head (Fig. 1B) 0.36 times as long as wide (including eyestalks); frontal margin convex, having pair of weak preocular lobes. ***Eyestalks*** (Figs 1B, 4A) arising from posterior half of head, reaching proximal half of peduncular article 2 of antenna 2, 0.62 length of head, eyes with 3 ommatidia.

Pereon (Figs 1B, 4A, 5A) dorsal surface smooth; ***pereonite 1*** laterally rounded, without lateral spine-like processes; ***pereonites*** 2–7 with a pair of short single lateral spine-like processes; ***pereonites*** 1–3 increasing in width and ***pereonites*** 4–7 decreasing in width. ***Pleonite 1*** small, 0.26 times as long as wide, with pair of fine dorsal setae.

Pleotelson (Fig. 1B, J) about 1.3 times longer than wide, anterior part narrow, about 0.13 times of total length of pleotelson, posterior part bulbous, tapering posteriorly, lateral margins each with 6 denticles, posterior margin rounded, ventral margins with a raw of small submarginal simple setae. ***Uropod*** (Fig. 1I) cylindrical, endopod with 2 lateral and 6 apical setae; exopod about 0.3 length of endopod, with 3 apical setae.

Antennula (Fig. 1C) peduncular article 1 shorter than article 2; article 2 with 1 simple and 3 small sensory palmate setae distodorsally; article 3 about 0.5 length of article 2, with 1 simple seta distally; flagellum with three articles, article 1 shortest, with 1 distoventral seta; article 3 subequal to article 2, distally with 1 long, 2 short setae and 1 aesthetasc.

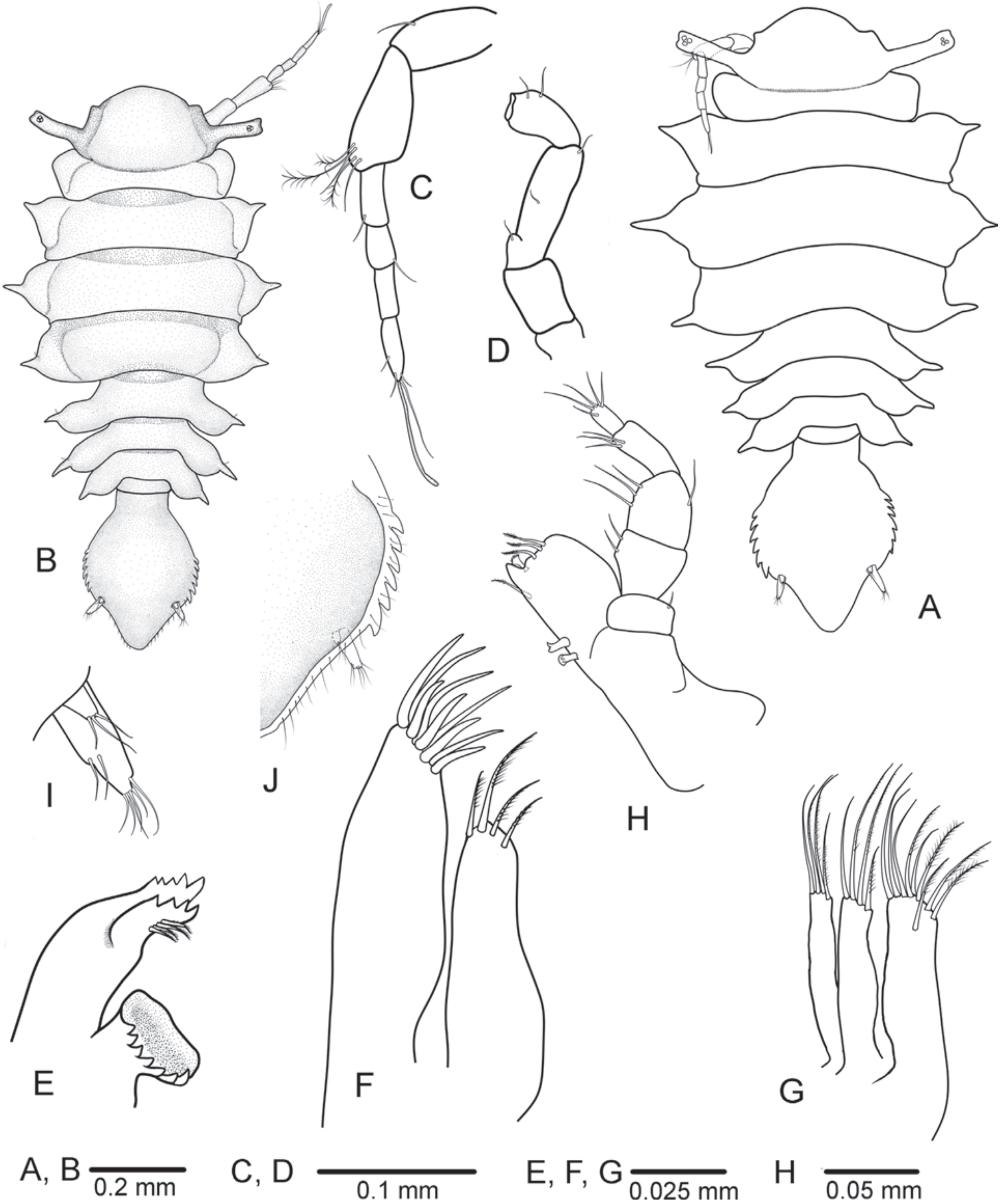

Figure 1. *Heterosignum behbehanii* sp. nov. **A** female habitus **B–J** male holotype (ZMH-K-64934) **B** habitus **C** antennula **D** antenna **E** mandible **F** maxillula **G** maxilla **H** maxilliped **I** uropod **J** pleotelson lateral margin, ventral view.

Antenna (Fig. 1D) with peduncle articles 1 and 2 combined about 0.8 length of article 3; peduncle article 3 with convex proximal protrusion bearing single seta, with 1 simple seta medially and 1 simple seta distally; article 4 about half length of article 3, with 2 distolateral setae.

Mandible (Fig. 1E) incisor process with 5 and ***lacinia mobilis*** with 4 cusps; spine row with 4 robust serrate setae.

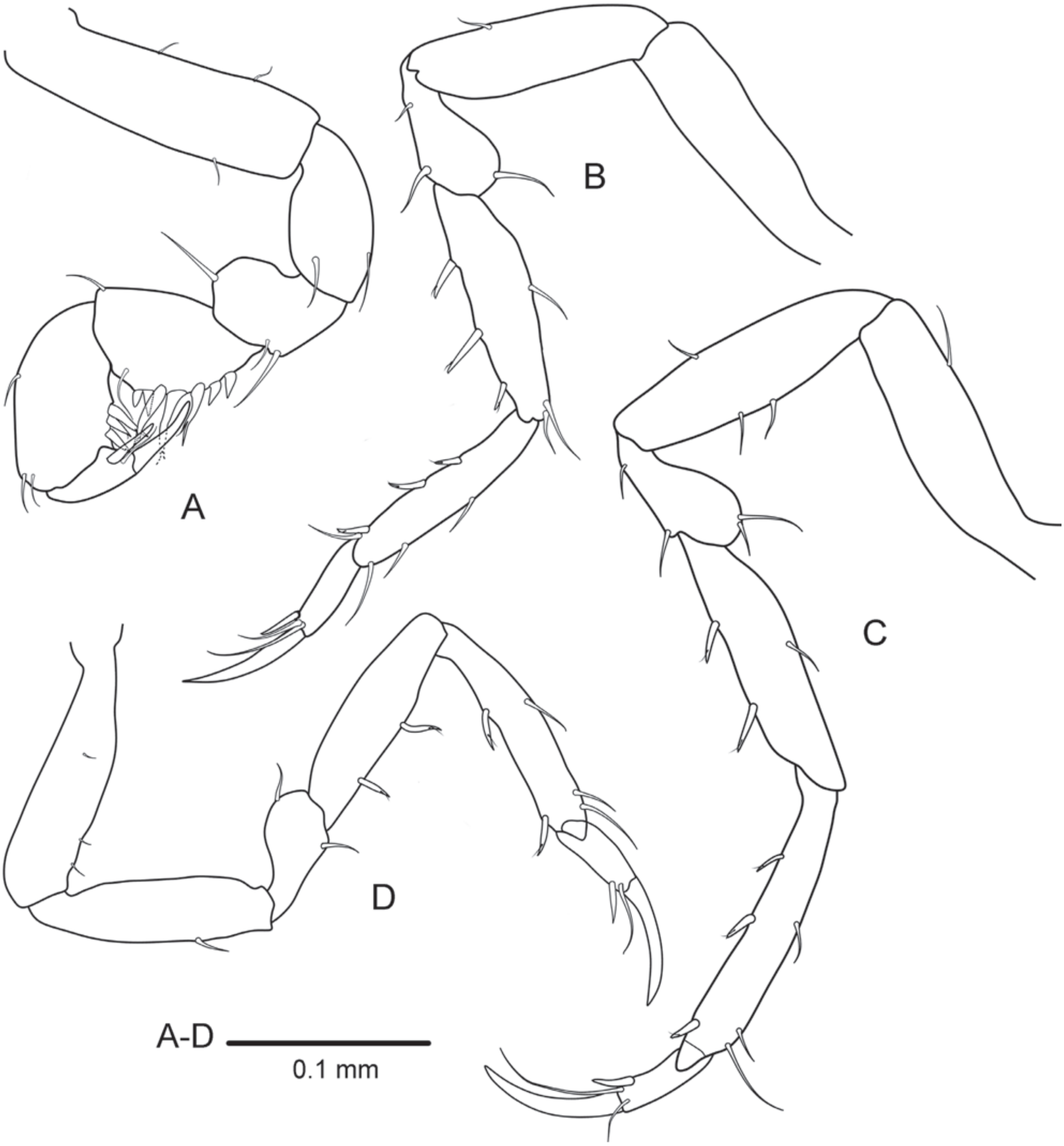

Figure 2. *Heterosignum behbehanii* sp. nov. (ZMH-K-64934), male holotype **A** pereopod 1 **B** pereopod 2 **C** pereopod 5 **D** pereopod 7.

Maxillula (Fig. 1F): lateral lobe with 9 robust apical setae; medial lobe with 4 robust serrate setae on distal margin.

Maxilla (Fig. 1G) lateral and mesial lobes, each with 4 pectinate robust apical setae; medial lobe with 9 robust setae along distal margin, some of them serrated.

Maxilliped (Fig. 1H) endite distal margin with 1–2 fan-shaped setae, 3 serrate setae, and 1 sub marginal seta medially, mesial margin with 2 coupling hooks; palp article 1 with 1 short seta laterally; article 2 shorter than article 3 with 2 setae medially; article 3 with 3 setae medially and 1 seta laterally; article 4 subequal in length to article 3, with 3 setae distomedially; article 5 narrowest, with 5 setae distally.

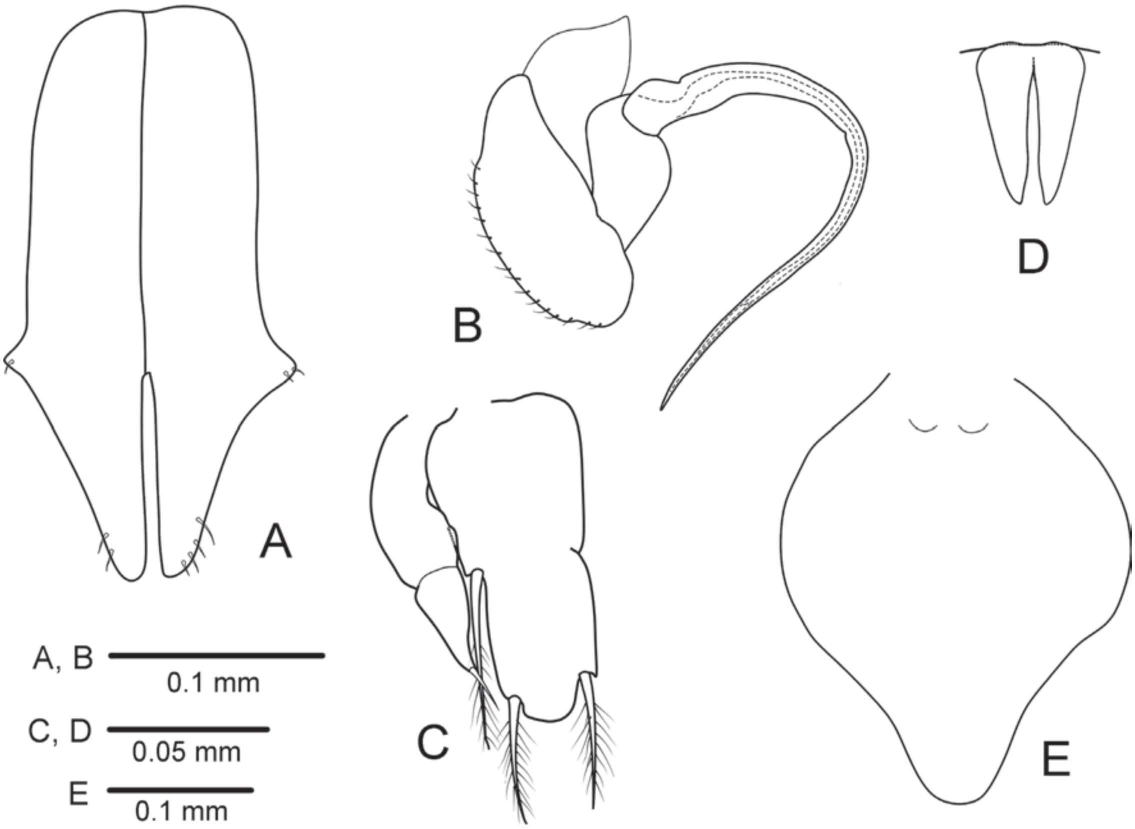

Figure 3. *Heterosignum behbehanii* sp. nov. (ZMH-K-64934), male holotype **A** pleopods 1 **B** pleopod 2 **C** pleopod 3 **D** penial processes **E** female operculum.

Pereopod 1 (Fig. 2A) shorter than ***pereopods 2–7***: basis 3.6 times as long as greatest width, superior margin with 1 and inferior margin with 2 small setae; ischium 0.5 times as long as basis, with 2 long setae distally; merus shorter than carpus, superior margin with 1 robust seta medially, with 2 robust setae on inferodistal corner; carpus inferior margin with 4 denticles, 3 robust setae and 1 submarginal simple seta, superior margin with 1 simple seta on distal corner; propodus longer than carpus, with 3 robust setae on inferior margin; dactylus with 1 subapical simple seta, unguis subequal in length to dactylus, accessory claw length 0.6 unguis length.

Pereopod 2 (Fig. 2B) basis about 3.5 times as long as greatest width; ischium about 0.9 times as long as basis, with 1 long seta on inferior margin; merus about 0.5 times as long as carpus, inferior margin with 2 and superior margin with 1 long simple setae; carpus and propodus subequal in length, carpus inferior margin with 3 robust setae, superior margin with 1 seta medially and 2 simple long setae on distal corner; propodus inferior margin with 3 robust setae and 1 long simple seta, superior margin with 3 long simple setae; dactylus with 2 subapical simple setae, a small accessory claw, unguis 1.5 times as long as dactylus.

Pereopod 5 (Fig. 2C) basis about 3.8 times as long as greatest width; ischium about 0.92 times as long as basis, with 1 long seta on inferior margin and 2 long setae on superior margin; merus about 0.46 times as long as carpus, inferior and superior margin with 2 simple setae each; carpus shorter than propodus, with 2 robust setae on inferior margin and 1 simple seta on superior margin medially; propodus inferior margin with 3 robust setae, superior margin with 3 simple setae; dactylus with 2 subapical simple setae; unguis 1.4 times as long as dactylus.

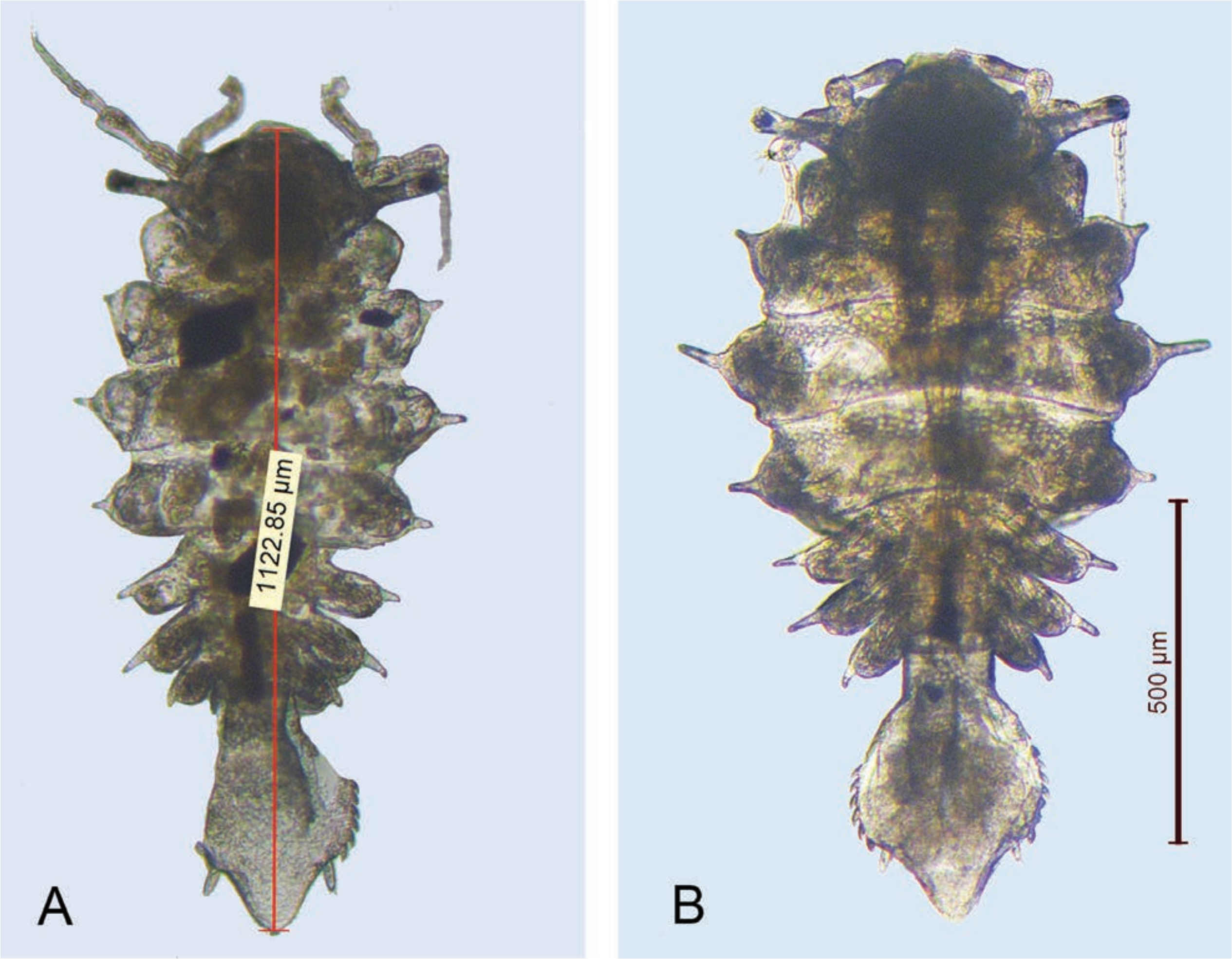

Figure 4. *Heterosignum behbehanii* sp. nov. Al-Khiran, Kuwait (28°38.484'N, 48°23.287'E) **A** male **B** female.

Pereopod 7 (Fig. 2D) basis about 3.8 times as long as greatest width; ischium about 0.85 times as long as basis, with 1 long seta on inferior margin; merus about 0.47 times as long as carpus, inferior and superior margins with 1 long simple seta; carpus shorter than propodus, with 2 robust setae on inferior margin; propodus inferior margin with 2 robust setae, superior margin with 3 simple setae; unguis 1.5 times as long as dactylus.

Pleopod 1 (Fig. 3A) distally separate, with 2–4 apical setae; short lateral projections present, each projection with 1–2 setae.

Pleopod 2 (Fig. 3B) protopod length 2.4 width, with 16 simple marginal setae; second article of endopod elongate, downwardly curved, proximally swollen, becoming narrower until distal pointed apex, about 2.4 as long as protopod, without any ornamentation.

Pleopod 3 (Fig. 3C), endopod with 2 long plumose setae apically and 1 long plumose seta laterally; exopod composed of two articles, narrower than endopod; article 2 with 1 terminal seta.

Penes (Fig. 3D) fused along basal part, well separated at distal part, tapering to narrowly rounded apices.

Female (Figs 1A, 4B, 5A, B). Similar to males in the morphology of all pereonal appendages. Body broader than in males, about 1.8 times as long as

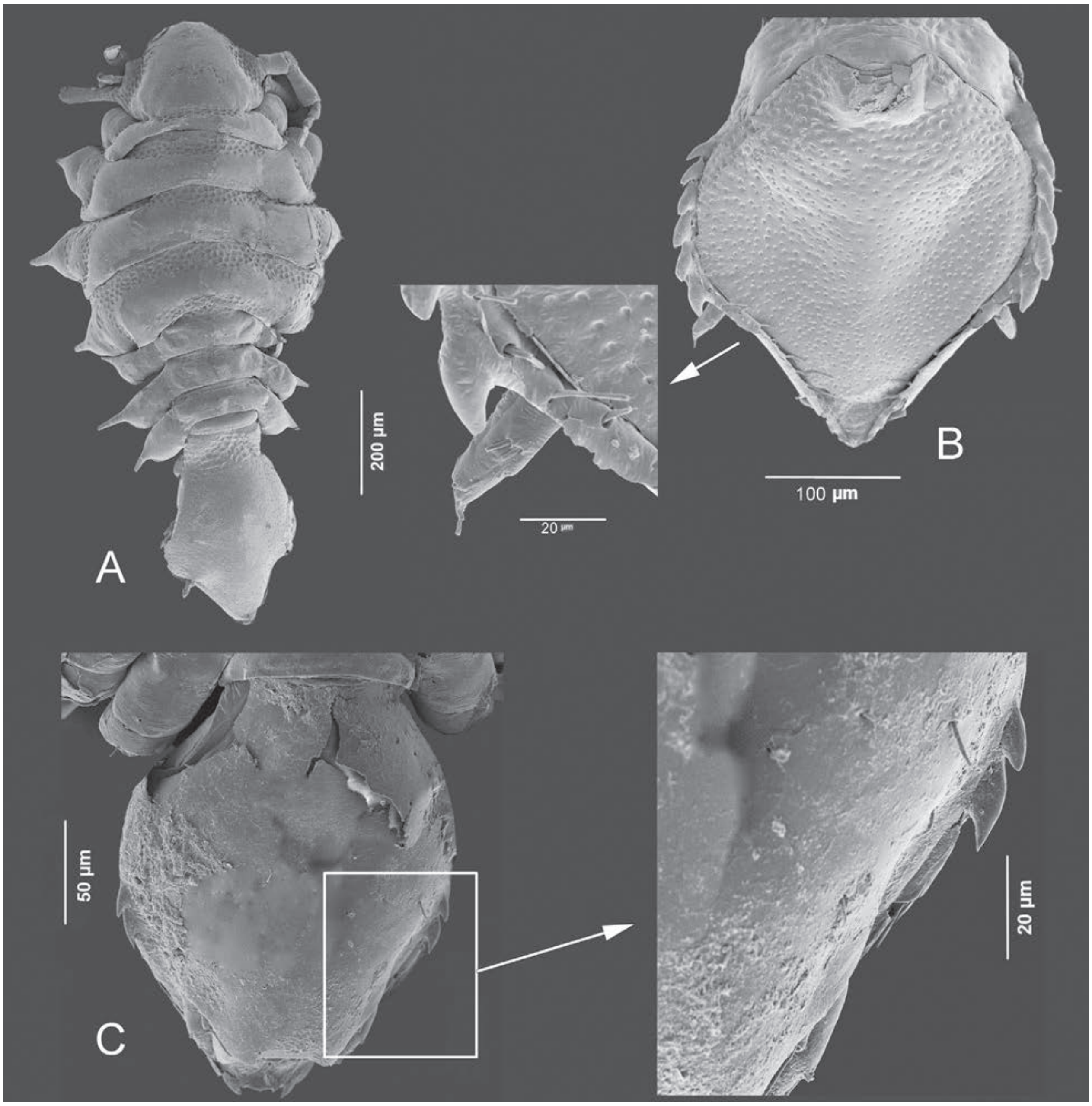

Figure 5. Scanning electron micrographs **A, B** *Heterosignum behbehanii* sp. nov. (Al-Khiran, Kuwait: 28°38.484'N, 48°23.287'E) **A** female habitus **B** pleotelson, ventral view **C** *Uromunna alyamanii* sp. nov. (Al-Nuwaseeb, Kuwait: 28°34.792'N, 48°24.078'E), female pleotelson.

wide; widest at pereonite 3. The largest female length is 1.34 mm. ***Operculum*** (Fig. 3E) ovate, 1.2 times as long as broad, without any marginal setae.

Remarks. *Heterosignum behbehanii* sp. nov. is most similar to *H. elegans* Shimomura & Mawatari, 2002 from Japan, as both of these species have lateral spine-like processes on pereonites 2–7, a pleotelson with 6 denticles on its lateral margins of the posterior part, and pleopod 2 with a slender very long, curved second article of the endopod. However, the new species is distinguished from *H. elegans* in having its notably shorter lateral spine-like processes on pereonites 2–7, a smaller anterior part of the pleotelson (about 0.1 vs. 0.4 times the total length of pleotelson), and the first pleopod being distally separate instead of distally connected.

The new species differs from *Heterosignum unicornis* (Kensley, 1976), the only species reported from the Indian Ocean (southern Indian Ocean, Amsterdam Island). *Heterosignum unicornis* has a stout mid-dorsal spine (horn) on the first pereonite, lacking lateral spine-like processes on pereonites 5–7, and a pleotelson with 4 denticles on its lateral margins.

Key to species of *Heterosignum* (males)

1 Pereonite 1 with strong mid-dorsal horn-shape spine **2**
– Pereonite 1 without mid-dorsal horn-shape spine ***3***
2 Head with one stout mid-dorsal horn-shape spine; pereonite 1 with lateral spine-like processes................. ***H. ohtsukai* Shimomura & Mawatari, 2002**
– Head without mid-dorsal horn-shape spine; pereonites 1 and 7 without lateral spine-like processes .... ***H. unicornis* (Kensley, 1976)**
3 Head without long anteriorly directed processes on the anterior margin... **4**
– Head with 2 long anteriorly directed processes on the anterior margin...... .... ***H. bicornis* Shimomura, 2011**
4 Eyestalks slender, medium or long, with a few ommatidia......................... **5**
– Eyestalks stout, short, without ommatidia ... ***H. hashimotoi* Shimomura, 2009**
5 Pereonites 2–4 and 6 with a pair of relatively short single lateral spine-like processes or not; anterior part of the pleotelson short, cylindrical, about 0.1 of the total length **6**
– Pereonites 2–4 and 6 with a pair of very long single lateral spine-like processes; anterior part of the pleotelson long, cylindrical, about 0.4 of the total length.................................. ***H. elegans* Shimomura & Mawatari, 2002**
6 Pereonites 4, 5 and 7 without lateral spine-like processes; pleopod 2 with broad protopod, bearing 12 marginal setae, endopodal second article about 1.1 as long as protopod.......................... ***H. mutsuensis* Gamô, 1976**
– Pereonites 2–7 with short lateral spine-like processes; pleopod 2 with broad protopod, bearing 16 marginal setae, endopodal second article about 2.4 as long as protopod.................................. ***H. behbehanii* sp. nov.**

Family Munnidae Sars, 1897

Genus *Uromunna* Menzies, 1962

Type species. *Uromunna ubiquita* (Menzies, 1952), by original designation.

Diagnosis. The most recent diagnosis to the genus is that of Esquete and Wilson (2016).

Uromunna alyamanii sp. nov.

https://zoobank.org/383D6E48-C576-431E-92C8-29C99BE55CBD
Figs 5C, 6–8

Etymology. The species is named in honour of Dr Faiza Yousef Al-Yamani, a pioneering figure who established the Oceanography Program at the Environment and Life Sciences Research Center at Kuwait Institute for Scientific Research (KISR) in 1991.

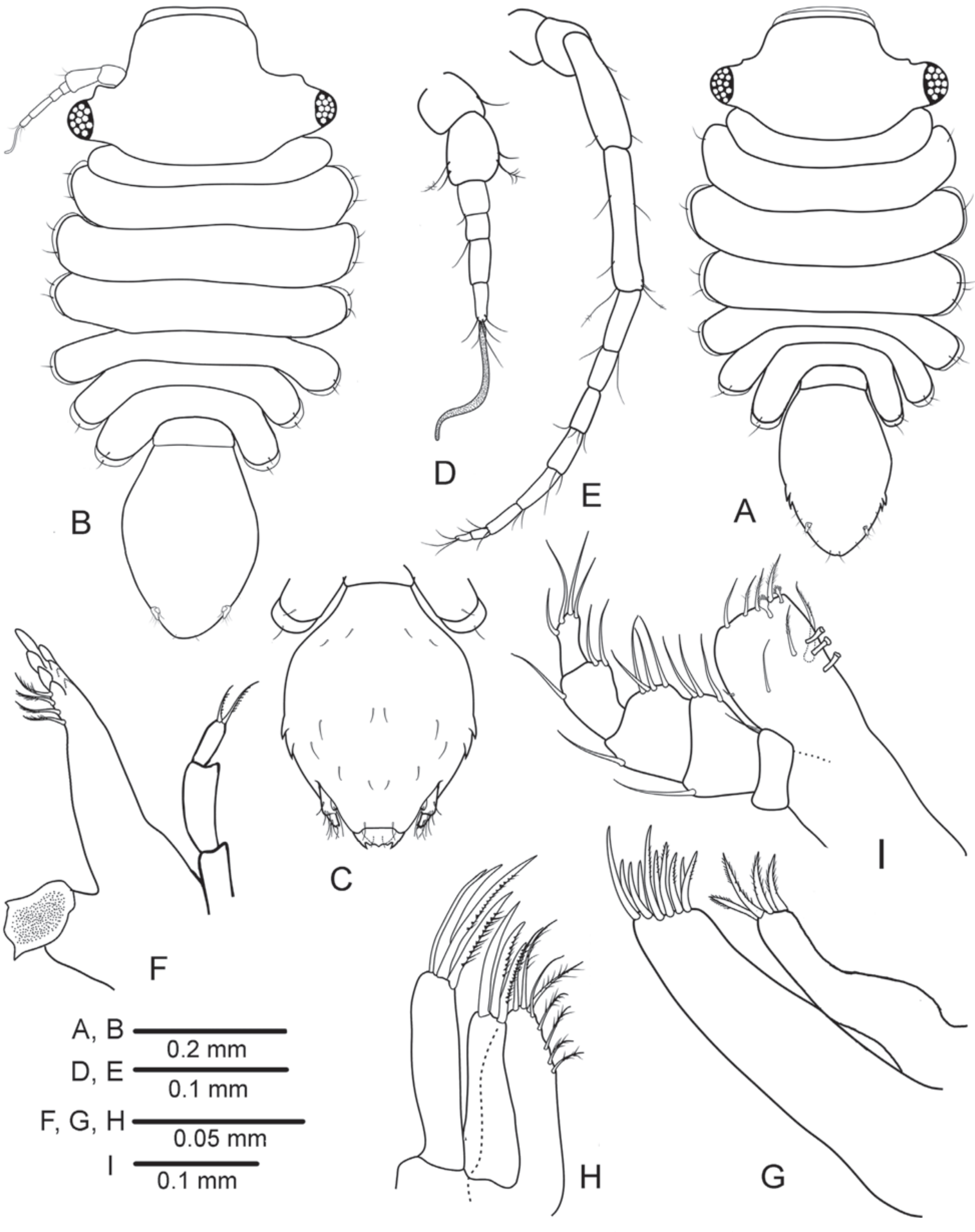

Figure 6. *Uromunna alyamanii* sp. nov. **A** female habitus **B–I** male holotype (ZMH-K-64937) **B** habitus **C** pleotelson **D** antennula **E** antenna **F** mandible **G** maxillula **H** maxilla **I** maxilliped.

Type material. ***Holotype*:** • ♂, 0.78 mm (ZMH-K-64937); KUWAIT. Quaruh Island; 28°49.105'N, 48°46.553'E; 10. XI. 2014; V. Grintsov leg. ***Paratypes*:** • 1♀, 0.88 mm (ZMH-K-64938), same data as the holotype • 1♀, 0.78 mm (ZMH-K-64939), Al-Khiran; 29°38'48.47"N, 48°23'28.68"E; 05. I.2015; V. Grintsov leg. • 2 ♀♀, up

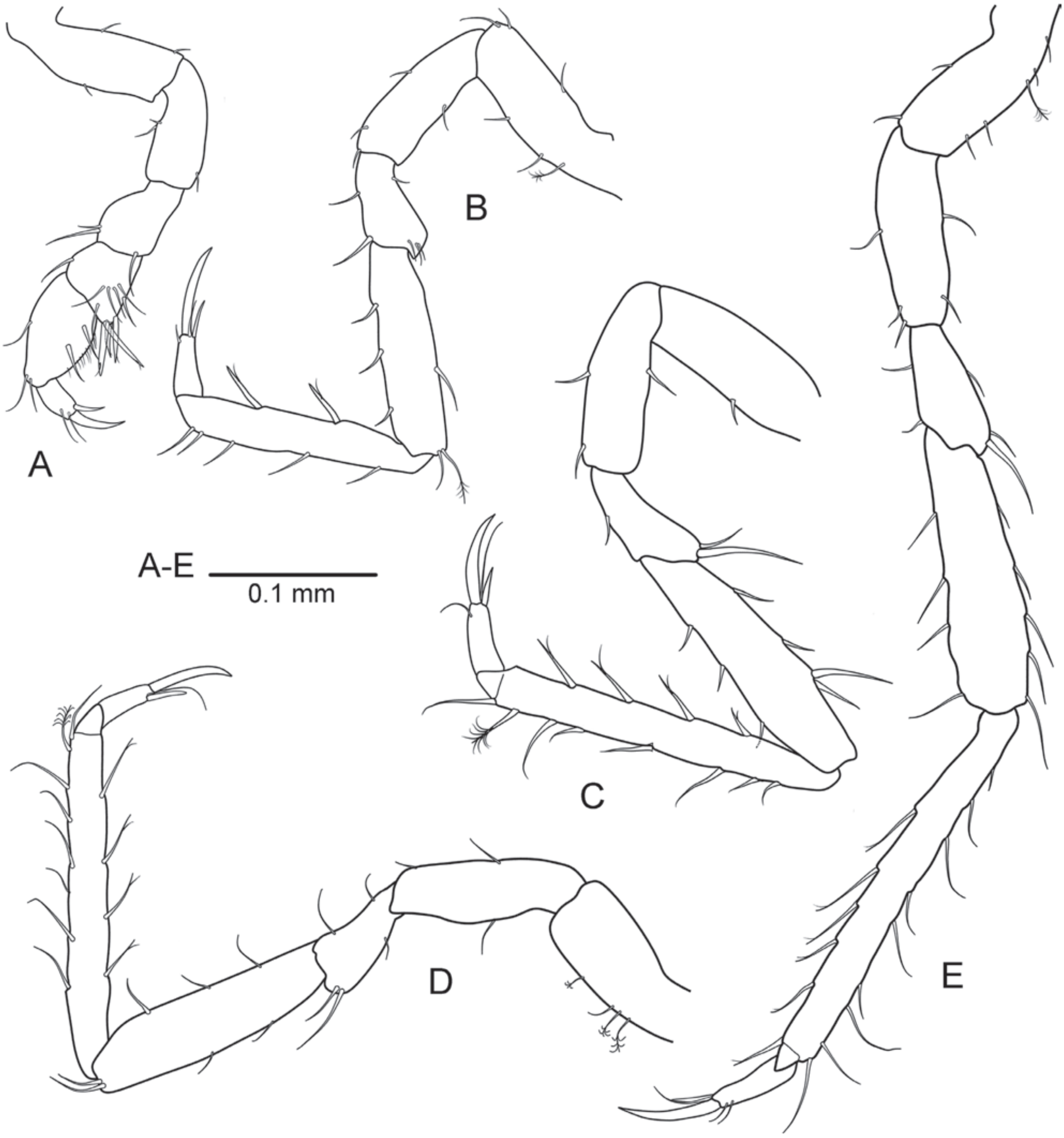

Figure 7. *Uromunna alyamanii* sp. nov. male holotype (ZMH-K-64937) **A** pereopod 1 **B** pereopod 2 **C** pereopod 4 **D** pereopod 5 **E** pereopod 7.

to 0.75 mm (ZMH-K-64940), Auha Island; 29°22.32'N, 48°26.27'E; 10. II.2016; V. Grintsov leg. • 2 ♀♀, up to 0.8 mm, 1♂, 0.725 mm, 1 slide (ZMH-K-64941), Al-Nuwaiseeb; 28°34.792'N, 48°24.078'E; 07.I.2015; V. Grintsov leg. • 1♀, 0.787 mm, 1 slide (ZMH-K-64941), Failaka Island; 29°28.049'N, 48°17.838'E; 22.XII.2014; V. Grintsov leg.

Diagnosis. Pleotelson 1.26 times longer than wide, 0.31 times of whole body, and lateral margins each with 2 denticles. Maxillipedal endite with three coupling hooks. Male pleopod 1 distal margin medial lobes convex, each lobe with three setae. Pleopod 2 protopod elongate, with distally rounded apex; endopod

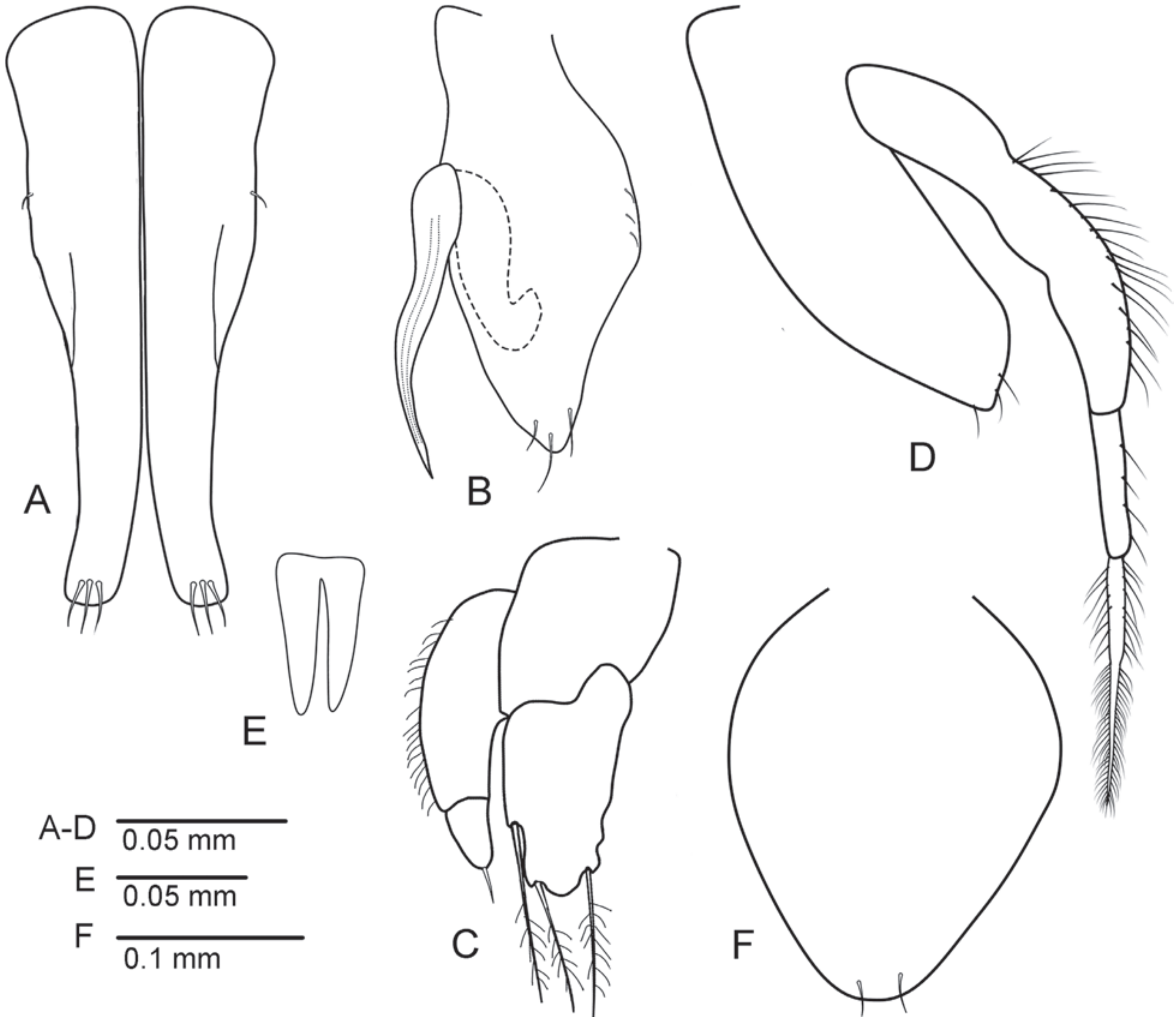

Figure 8. *Uromunna alyamanii* sp. nov. male holotype (ZMH-K-64937) **A** pleopods 1 **B** pleopod 2 **C** pleopod 3 **D** pleopod 4 **E** penial processes **F** female operculum.

stylet extending just beyond apex of protopod, about 0.7 times as long as protopod. Pleopod 4 exopod distal tip with 1 elongate plumose seta.

Description. Male: ***Body*** (Fig. 6B) length 0.78 mm; about 2.1 times as long as wide.

Head (Fig. 6B) 0.65 times as long as wide; anterior margin straight; preocular lobes distinct and projecting. ***Eyes*** present, ommatidia on eye lobe outer margin, with 12 ommatidia.

Pereon (Fig. 6B) dorsal surface smooth; ***pereonite 1*** narrowest; ***pereonite 3*** widest and longest; coxae visible on pereonites 2–7, each with 1–2 small setae; ***pereonites 5–7*** turned back; lateral margins rounded; ***pereonite 7*** longer then pereonite 6, about 1.5 times as long as pereonite 6.

Pleonite 1 small, about 0.4 times as long as wide, without dorsal setae.

Pleotelson (Figs 6B, 5C, 6C) about 1.26 times longer than wide, pyriform, lateral margins each with 2 small lateral denticles; dorsal surface covered with 16 simple setae.

Uropod (Fig. 6C) cylindrical, endopod bearing 6 lateral and apical setae; exopod minute, with one simple seta.

Antennula (Fig. 6D) peduncular article 1 shorter than article 2; article 2 with 2 simple and 2 small sensory palmate setae sub distally; article 3 about 0.5 length of article 2, with 1 simple seta distally; flagellum with three articles, article 2 longest; article 3 distally with 1 long aesthetasc.

Antenna (Fig. 6E) about 0.8 times as long as body; antennal flagellum shorter than peduncular articles, with 8 articles.

Mandible (Fig. 6F) incisor process and ***lacinia mobilis*** with 4 cusps; spine row with 4 robust serrate setae. Palp articles 1 and 2 without setae, third article 0.55 times as long as article 2, with 2 serrated setae apically.

Maxillula (Fig. 6G) lateral lobe with 10 robust apical setae; medial lobe with 4 robust serrate setae on distal margin.

Maxilla (Fig. 6H) lateral and mesial lobes each with 4 and 3 pectinate robust apical setae; medial lobe with 8 robust setae along distal margin, some of them serrated.

Maxilliped (Fig. 6I) endite distal margin with 2 fan-shaped setae, 4 serrate setae, and 3 sub marginal serrated setae dorsally; mesial margin with 3 coupling hooks; palp article 1 bearing short seta on distomesial corner; article 2 sub equal length to article 3, with 3 setae medially and 1 seta on distolateral corner; article 3 with 4 setae medially and 1 seta laterally; article 4 subequal in length to article 3, with 2 setae distomedially and 1 seta laterally; article 5 with 4 setae distally.

Pereopod 1 (Fig. 7A) shorter than ***pereopods 2–7***; basis 2.6 times as long as greatest width, superior margin with 1 and inferior margin with 2 small setae; ischium about 0.7 times as long as basis, superior margin with 2 and inferior margin with 1 small setae; merus longer than carpus, 0.75 times as long as ischium, superior margin with 2 and inferior margin with 1 robust setae distally; carpus with 4 robust bifid setae on inferodistal corner, inferior margin with 1 marginal and 4 submarginal long simple setae, superior margin with 1 long simple seta medially; propodus 1.75 times as long as carpus, inferior margin fringed with fine setae, bearing 2 robust submarginal setae, superior margin with 1 long simple seta medially and 2 simple setae distally; dactylus with 2 subapical simple setae, a long unguis, and a long accessory claw.

Pereopod 2 (Fig. 7B) basis about 3.1 times as long as greatest width; ischium about 0.7 times as long as basis, with 3 long setae on inferior margin and 1 long seta on superior margin; merus about 0.45 times as long as carpus, inferior margin with 2 and superior margin with 4 simple setae; carpus about 0.9 times as long as propodus, inferior margin with 3 robust setae, superior margin with 1 seta medially and 1 simple and 1 plumose setae distally; propodus inferior margin with 2 robust bifid setae, superior margin with 5 long simple setae; dactylus with a narrow accessory claw, unguis longer than dactylus.

Pereopod 4 (Fig. 7C) similar to ***pereopod 5*** (Fig. 7D), propodus about 1.5 times as long as carpus, with 4 robust bifid setae on inferior margin and 7 long simple setae and 1 sensory palmate seta on superior margin.

Pereopod 7 (Fig. 7E) basis about 2.8 times as long as greatest width; ischium about 0.86 times as long as basis, with 3 long setae on inferior margin and 2 long setae on superior margin; merus about 0.46 times as long as carpus; carpus with 4 robust setae on inferior margin and 5 robust setae on superior margin; propodus about 1.5 times as long as carpus, inferior margin with 6 robust bifid setae, superior margin with 8 long simple setae and 1 sensory palmate seta; unguis 1.24 times as long as dactylus.

Pleopod 1 (Fig. 8A) consists of two coalescent halves, each half 4.5 times longer than maximum width; proximal part enlarged and tapering distally, distal margin narrowly rounded, each lobe with three setae distally.

Pleopod 2 (Fig. 8B) protopod elongate, with distally rounded apex, about 2.2 times longer than wide, with 3–4 subapical setae; endopodal stylet, elongate, medially swollen but becoming narrower until distal tip, without ornamentation, extending just beyond apex of protopod, endopod stylet length about 0.7 protopod lengths.

Pleopod 3 (Fig. 8C) protopod as long as width; endopod 1.8 times longer than wide, with three plumose setae apically; exopod with two articles, proximal article 2.4 longer than wide, lateral margin fringed with fine setae, distal article 1.6 times longer than wide, with 1 simple seta distally.

Pleopod 4 (Fig. 8D) exopod with 2 articles, article 1 lateral margin fringed with dense fine setae, article 2 lateral margin with a few fine setae; with 1 elongate plumose seta distally.

Penes (Fig. 8E) fused along basal part, well separated at distal part, tapering to rounded apices.

Female (Figs 5C, 6A) body about 1.9 times longer than wide; widest at pereonite 3. Largest female length 0.74 mm. Female operculum (Fig. 8A) length 1.25 width, with one pair of subterminal elongate setae.

Remarks. *Uromunna alyamanii* sp. nov. shares similarities with *U. naherba* Esquete, Wilson & Troncoso, 2014 from NW Iberian Peninsula, Spain, and *U. jejuensis* Kim, Lee & Karanovic, 2023 from the Mun Island, Sea of Japan. These similarities include the appearance of mouthparts, pereopods, and pleopods, especially a round distal apex of male pleopod 1 with three pairs of apical setae, the presence of denticles on the pleotelsonic lateral margins, and a female operculum with a terminal pair of setae. However, the present species also have distinct differences, such as a pleotelson with 2 lateral margin denticles on each side, a feature not found in the latter species.

The new species differs from *U. sheltoni* (Kensley, 1977) from South Africa, which has the distally concave pleopod 1, with 4 short apical setae (vs. distally rounded, with 3 short setae in the present species), and the shorter endopodal stylet of pleopod 2, which does not reach beyond the apex of the ramus.

Key to species of the Indian Ocean species of *Uromunna* (males)

1 Pleotelson lateral margins denticles absent **2**
– Pleotelson lateral margins denticles present, 2 denticles on each side...... .... ***U. alyamanii* sp. nov.**
2 Pleopod 1 strongly curving laterally at apices, each apex with 2 pairs of setae along free mesial margin................ ***U. brevicornis* (Thomson, 1946)**
– Pleopod 1 evenly tapering to apices; each apex with 3 subterminal setae. **3**
3 Pleopod 1 with rounded-truncate apices; pleopod 2 with acute apex, bearing 2 setae along mesial edge.................................. ***U. humei* Poore, 1984**
– Pleopod 1 with obliquely truncate apices; pleopod 2 with rounded-acute apex, bearing 1 subterminal seta ....***U. phillipi* Poore, 1984**

Acknowledgements

We would like to extend our special thanks to all the KISR staff for their invaluable assistance in collecting isopod samples in the field and processing them in the laboratory. We are also profoundly grateful for the crucial financial support from the Kuwait Petroleum Company (KPC) and the Kuwait Institute for Scientific Research (KISR); without them, this research would not have been possible. PLZ replace by: This publication is supported by a special fund provided by Kuwait Science Company (KSC). We would like to thank Dr Saskia Brix (Senckenberg Research Institute, Germany), Dr Brenda Doti (Universidad de Buenos Aires, Argentina) and one anonymous reviewer for their constructive suggestions and helpful comments. Finally, we thank Dr Maria Saburova (KISR) for her valuable support and assistance with the scanning electron microscope.

Additional information

Conflict of interest

The authors have declared that no competing interests exist.

Ethical statement

No ethical statement was reported.

Funding

No funding was reported.

Author contributions

Writing - original draft: VKP. Writing - review and editing: MAAK.

Author ORCIDs

Valiallah Khalaji-Pirbalouty https://orcid.org/0000-0002-0892-7463
Manal Abdulrahman Al-Kandari https://orcid.org/0000-0003-0073-7929

Data availability

All of the data that support the findings of this study are available in the main text.

References

Al-Kandari MA, Khalaji-Pirbalouty V, Abdulkhaliq H, Chen W (2022) Diversity and distribution of the Isopoda (Crustacea, Peracarida) of Kuwait, with an updated checklist. ZooKeys 1080: 107–133. https://doi.org/10.3897/zookeys.1080.71370

Boyko C, Bruce N, Hadfield K, Merrin K, Ota Y, Poore G, Taiti S, Schotte M, Wilson G (2008, onwards) World Marine, Freshwater and Terrestrial Isopod Crustaceans. Database. [https://www.marinespecies.org/isopoda on 2024-06-07] https://doi.org/10.14284/365

Esquete P, Wilson GDF (2016) The genus *Uromunna* (Crustacea: Isopoda: Munnidae) in New South Wales, Australia, with a key for all known species. Marine Biology Research 12(5): 488–512. https://doi.org/10.1080/17451000.2015.1131298

Esquete P, Wilson GDF, Troncoso JS (2014) Ecology and systematics of a new species of *Uromunna* (Crustacea: Isopoda) from Spanish eelgrass beds. Helgoland Marine Research 68(2): 329–339. https://doi.org/10.1007/s10152-014-0393-4

Gamô S (1976) *Heterosignum mutsuensis* gen. nov., sp. nov., a new Isopod Crustacea from Mutsu Bay, Northern Japan (Paraselloidea, Munnidae). Proceedings of the Japanese Society of Systematic Zoology 12: 39–45.

Just J, Wilson GDF (2007) Revision of *Austrosignum* Hodgson and *Munnogonium* George & Stromberg (Paramunnidae) with descriptions of eight new genera and two new species, (Crustacea: Isopoda: Asellota). Zootaxa 1515: 1–29. https://doi.org/10.11646/zootaxa.1515.1.1

Kensley B (1976) Isopodan and Tanaidacean Crustacea from the St Paul and Amsterdam Islands, Southern Indian Ocean. Annals of the South African Museum 69: 261–323.

Khalaji-Pirbalouty V, Oraie H, Santamaria CA, Wägele JW (2022) Redescription of *Tylos maindroni* Giordani Soika, 1954 (Crustacea, Isopoda, Oniscidea) based on SEM and molecular data. ZooKeys 1087: 123–139. https://doi.org/10.3897/zookeys.1087.76668

Menzies RJ (1952) Some marine asellote isopods from northern California, with descriptions of nine new species. Proceedings of the United States National Museum 102 (3293): 117–159. https://doi.org/10.5479/si.00963801.102-3293.117

Menzies RJ (1962) The zoogeography, ecology, and systematics of the Chilean marine isopods. Lunds Universitets Årsskrift N.F. Avd 2 57(11): 1–162.

Poore GCB (1984) Redefinition of *Munna* and *Uromunna* (Crustacea: Isopoda: Munnidae), with descriptions of five species from coastal Victoria. Proceedings of the Royal Society of Victoria 96 (2): 61–81.

Shimomura M (2009) Ten new species of paramunnid isopods (Peracarida: Asellota: Paramunnidae) from Kyushu, southern Japan. Bulletin of the National Museum of Natural Sciences, Series A, Suppl. 3: 47–88.

Shimomura M (2011) A new paramunnid isopod of the genus *Heterosignum* Gamô, 1976 (Crustacea: Asellota) from central Japan. Kitakyushu Museum of Natural History and Human History, Series A 9: 3–7.

Shimomura M, Mawatari SF (2002) A revision of *Heterosignum* (Asellota, Isopoda, Paramunnidae) with descriptions of three new species. Journal of Natural History 36: 2103–2126. DOI: https://doi.org/10.1080/00222930110088734

Thomson JM (1946) New Crustacea from the Swan River estuary. Journal of the Royal Society of Western Australia 30: 35–53.

VanHöffen E (1914) Die Isopoden der Deutschen Südpolar-Expedition 1901–1903. Deutsche südpolar-Expedition 1901–1903 25: 447–598. https://doi.org/10.5962/bhl.title.10649

Wilson GD (1980) New insights into the colonization of the deep sea: Systematics and zoogeography of the Munnidae and the Pleurogoniidae comb. nov. (Isopoda; Janiroidea). Journal of Natural History 14: 215–236. https://doi.org/10.1080/00222938000770201

ZooKeys 1219: 249–270 (2024)
DOI: 10.3897/zookeys.1219.130546

Research Article

Morphometric and phylogenetic analysis of a commercial fish *Leiognathus equula* (Teleostei, Leiognathidae)

Jiajie Chen[1,2*], Xiaodong Wang[1*], Sheng Zeng[3], Wei Tian[2], Deyuan Yang[3,4], Jinqing Ye[5], Junsheng Zhong[1], Chaopeng Jiang[6]

1 *Shanghai Universities Key Laboratory of Marine Animal Taxonomy and Evolution, Shanghai Ocean University, 201306, Shanghai, China*
2 *East China Sea Fisheries Research Institute, Fisheries Science of Chinese Academy, 200090, Shanghai, China*
3 *College of the Environment and Ecology, Xiamen University, 361102, Xiamen, China*
4 *National Taiwan Ocean University, Keelung, 202301, Taiwan*
5 *National Marine Environment Monitoring Center, 116023, Dalian, China*
6 *College of Marine Living Resource Sciences and Management, Shanghai Ocean University, 201306, Shanghai, China*
Corresponding authors: Jinqing Ye (jqye@nmemc.org.com); Junsheng Zhong (jszhong@shou.edu.cn); Chaopeng Jiang (cpjiang@shou.edu.cn)

Abstract

The complete mitochondrial genome and phylogenetic analysis for *Leiognathus equula* from the South China Sea was performed using shallow genome skimming. For accurate species identification and redescription, morphometric and meristic characters were examined and compared with previous descriptions. To facilitate the identification of species and to enable comparison with the mitochondrial genome phylogeny, molecular comparisons were conducted using three mitochondrial genes: large ribosomal RNA (*16S* rRNA), cytochrome c oxidase subunit 1 (*COX1*), and NADH dehydrogenase (*ND5*). The mitogenome (16 398 bp) comprised 38 mitochondrial genes, similar to most bony fishes: 13 protein-coding genes (PCGs), 2 rRNA and 22 transfer RNA genes, and 1 non-coding region. The complete mitogenome comprised 30.7% A, 24.2% T, 15.0% G, and 30.1% C. The A+T content (54.9%) was higher than the G+C content (45.1%). All PCGs started with the typical ATG codon, except *COX1*, which started with GTG. Seven PCGs ended with incomplete stop codons (TA or T). The Ka/Ks ratios of all PCGs were < 1, indicating purifying selection. The phylogenies of Leiognathidae, both based on the amino acid sequences of the 13 PCGs and the single genes *16S* RNA and *COX1*, were monophyletic with high nodal support (> 75%). *L. brevirostris* (NC 026232) is believed to be a *Nuchequula* species, whereas *L. ruconius* (NC 057225) is not classified under *Leiognathus* in the NCBI database. The phylogenetic trees divided the Leiognathidae family into three clades. The mitogenome phylogeny suggested that the Leiognathidae and Chaetodontidae clades are sister groups. These findings provide important genetic data for population genetics research and a phylogenetic analysis of Leiognathidae.

Key words: Leiognathidae, *Leiognathus equula*, mitochondrial genome, phylogenetic tree, South China Sea

OPEN ACCESS

Academic editor: Nina Bogutskaya
Received: 26 June 2024
Accepted: 18 October 2024
Published: 4 December 2024

ZooBank: https://zoobank.org/45499302-A547-4F31-BF85-5CD1D9BA0381

Citation: Chen J, Wang X, Zeng S, Tian W, Yang D, Ye J, Zhong J, Jiang C (2024) Morphometric and phylogenetic analysis of a commercial fish *Leiognathus equula* (Teleostei, Leiognathidae). ZooKeys 1219: 249–270. https://doi.org/10.3897/zookeys.1219.130546

---

[*] These authors contributed equally to this work.

Introduction

Leiognathids (family Leiognathidae), commonly known as ponyfishes or slipmouths, are characterized by their highly protractile mouths that extend dorsorostrally, rostrally, or ventrorostrally. The relationship of Leiognathidae—an ex-perciform—with the order Perciformes is currently under debate. In the new taxonomical classification, Leiognathidae were reclassified from Perciformes to Chaetodontiformes (Betancur-R et al. 2017; Schoch et al. 2020). However, osteological evidence suggests that Leiognathidae should be classified as Acanthuriformes (Gill and Leis 2019; Gill and Michalski 2020).

All members of the family Leiognathidae possess a distinctive circumesophageal light organ that houses bioluminescent bacteria belonging to the genus *Photobacterium*. Males possess a larger light organ and associated features that intensify light during sexual displays for photic communication (Sparks et al. 2005). Many species of leiognathid fish exhibit strong sexual dimorphism in relation to their light organ system (LOS), except *Aurigequula* and *Leiognathus* species. Leiognathids are difficult to distinguish and identify if the features of the LOS are not considered. This difficulty may be due to the fact that both internal and external characteristics are coservative. As a result, there are several putatively widespread “wastebasket” species, such as *Aurigequula fasciata* (Lacepède, 1803) and *Leiognathus equula* (Forsskål, 1775) (Sparks et al. 2005).

Leiognathus equula is a tropical inshore bottom-dwelling panfish with a large, robust, and rhomboid-shaped body (Chakrabarty et al. 2008). It is widely distributed in both the Red Sea and the Indo-West Pacific Ocean (Masuda et al. 1984; Chakrabarty and Sparks 2022). In China, *L. equula* is known to be found from coastal regions of Taiwan (Shen 1993; Chakrabarty et al. 2010; Shen and Wu 2011; Gao et al. 2020) and Taiwan Strait (Chen and Fang 1999; Chen and Yang 2013; Liu et al. 2014) to the South China Sea, including coastal areas of Nansha Islands (Chen et al. 1997; Chen and Ni 2021), Hainan Island (Zheng 1962; Gao et al. 2020; this study), Guangdong (Yan et al. 2021), Beibu Gulf, Guangxi (Liu et al. 2016; Lai and He 2016). *Leiognathus equula* is a senior synonym of *Leiognathus argenteus* Lacepède, 1802, which is the type species of *Leiognathus*. It is significantly larger and more robust than other Leiognathidae species, but it can still be confused with other species due to its conservative morphology (Chen and Yang 2013).

The species is fished commercially in South China; it is one of the most economically important species in Hainan and is often sold together with silver pomfret (*Pampus argenteus*) but at approximately half the price of the latter (Suppl. material 1: fig. S1). However, to date, the species has not received sufficient research attention. Currently, *L. equula* has the conservation status of “Least Concern (LC)” (Larson et al. 2017). In the field of conservation biology, one of the most challenging aspects of species conservation is the effective identification of species. From a commercial perspective, it is of significant interest to identify species for traceability and to enhance the accuracy of their labelling. The mitogenome may prove useful in the design of molecular tools for both objectives.

In recent studies, some species previously classified as *Leiognathus* have been reclassified as belonging to other genera (Ikejima et al. 2004; Sparks and Dunlap 2004; Sparks et al. 2005; Chakrabarty and Sparks 2007, 2008, 2022;

Chakrabarty et al. 2008, 2011; Kimura et al. 2008a, 2008b, 2008c; Sparks and Chakrabarty 2015; Suzuki and Kimura 2023). There are currently ten monophyletic genera in Leiognathidae, which is now widely accepted (see Sparks and Chakrabarty 2015). They appear to be almost identical in terms of their morphology, but there are significant genetic differences between them (Seah et al. 2008). Consequently, genetic analyses constitute an invaluable tool for the identification of species (Seishi Kimura, pers. comm.). Nevertheless, previous phylogenetic studies of the family Leiognathidae have been based on a single gene (Chakrabarty et al. 2011; Ikejima et al. 2004; Sparks and Dunlap 2004; Sparks et al. 2005; Dunlap et al. 2007; Seah et al. 2008; Seth and Barik 2021). The complete mitochondrial genome of Leiognathidae species has yet to be the subject of extensive research. The addition of further species data on mitochondrial genomes will enable more accurate delineation of the family phylogeny.

The objective of this paper is to provide a description of the mitochondrial hologeny of *L. equula*, a basal species of Leiognathidae (Ikejima et al. 2004). However, published whole-gene data could cause confusion and errors in phylogenetic analyses if specimens were not reviewed and the most recent taxonomic status studies were not identified. The authors of this study have taken the initiative to present a basis for morphological identification and to demonstrate the reliability of species identification with the results of a single-gene study, thereby enhancing the credibility of the mitochondrial whole-gene data.

To achieve this objective, eight specimens were collected from the South China Sea and identified as *L. equula* following a process of careful documentation and morphometric comparison. To identify the species accurately, we compared the mitochondrial DNA sequence data of 16S rRNA, COX1, and ND5 fragments and compared the results of the phylogenetic relationships among Leiognathidae species. The genetic relationships within Leiognathidae were analyzed by assembling the mitochondrial genome of *L. equula* and selecting one of the three mitochondrial genome datasets for description. The present findings enhance the understanding of the mitochondrial genome features of the Leiognathidae and its taxonomic classification. Furthermore, they provide crucial genetic data for phylogenetic and population genetic studies of the family Leiognathidae.

Materials and methods

Sample collection and DNA extraction

Eight specimens morphologically identified as *L. equula* were collected from various sources in China, including landing points, fish markets, and onboard commercial and research vessels (Suppl. material 1: table S1, Fig. 1A). They were subsequently stored in 70% ethanol at the East China Sea Fisheries Research Institute, Fisheries Science of Chinese Academy. Before DNA isolation, the surface of the specimens was cleaned with 100% ethanol. Muscle tissue measuring approximately 10 × 10 mm^2 (Fig. 1B) was collected from below the right lateral dorsal fin of the three of eight specimens (voucher numbers DHS14327, DHS19056, and DHS22490) for subsequent DNA extraction. Whole genomic DNA was extracted using the TIANamp Genomic DNA kit (TIANGEN, Beijing, China).

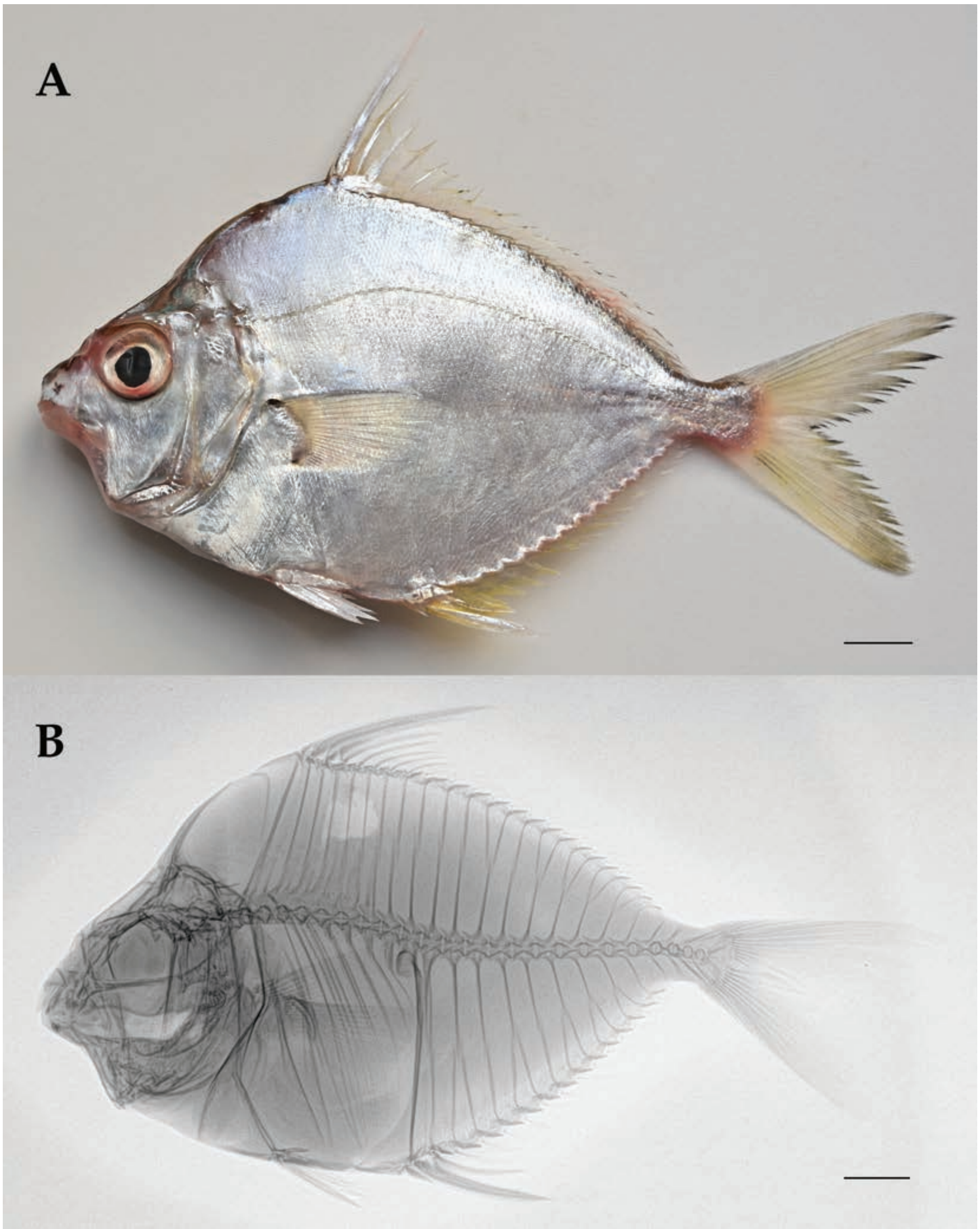

Figure 1. Left lateral view of *L. equula* specimen DHS19056 (SL 105.8 mm) **A** showing color in life (photo by Weiyue Zhang) and **B** radiograph. The whitish area below the dorsal fin indicates where the muscle tissue was sampled. Body depth **A** was measured at the anal-fin origin, and body depth **B** was measured at the dorsal-fin origin. Scale bars: 10 mm.

Species identification

Morphological identification was performed following the original description (Niebuhr 1775), in comparison with other published descriptions (Bloch 1795; Lacepède 1802; Cuvier 1829; James 1975; Masuda et al. 1984) and recent publications (Chen and Fang 1999; Kimura and Peristiwady 2000; Carpenter and Niem 2001; Chakrabarty et al. 2008, 2010; Kimura et al. 2009, 2018; Shen and Wu 2011; Chen and Yang 2013; White et al. 2013; Liu et al. 2014; Psomadakis et al. 2015, 2019; Lai and He 2016; Liu et al. 2016; Yan et al. 2021; Gloerfelt-Tarp and Kailola 2022). Counts and measurements were taken following Sparks and

Dunlap (2004) and Hubbs and Lagler (2004). All measurements were taken using digital calipers accurate to within 0.01 mm. Radiographs were used to examine osteological features. Standard length and head length are abbreviated as SL and HL, respectively. The scales were examined and counted using cyanine blue (Saruwatari et al. 1997). Scale counts are approximations owing to high intraspecific and interspecific variability, irregular arrangements, and the small size of scales, which makes accurate counting challenging.

The assembled sequence was subjected to BLAST using the NCBI BLAST similarity search tool. Subsequently, the *16S*, *COX1*, and *ND5* sequences from NCBI (Suppl. material 1: tables S2, S3) were selected for alignment with mitochondrial fragments, with the objective of verifying species accuracy. In light of the limited availability of mitogenome data for *Leiognathus*, the *16S rRNA*, *COX1*, and *ND5* sequences were also employed to investigate the phylogenetic position of *L. equula*, with a view to comparing the results with those of phylogenetic analyses of the mitogenome.

Mitogenome sequencing and assembly

The DNA library was prepared by the Illumina TruseqTM DNA Sample Preparation Kit (Illumina, San Diego, USA) using the manufacturer's instructions. The prepared library was sequenced by Novogene Bioinformatics Technology Co., Ltd. (Beijing, China) using the DNBSEQ-T7 platform to generate 150 bp paired-end reads. In total, ~ 5 Gb of raw sequence data were generated for each sample. Data cleaning was performed using Fastp v. 0.23.2 with default parameters (Chen et al. 2018). FastQC v. 0.11.5 (http://www.bioinformatics.babraham.ac.uk/projects/fastqc/) was used to assess the quality of raw data and cleaned data (Suppl. material 1: table S4). The assembly pipeline FastMitoAssembler (https://github.com/suqingdong/FastMitoAssembler) was used to assemble the mitochondrial genome, and then GetOrganelle v. 1.7.6.1 (Jin et al. 2020) and NovoPlasty v. 4.3.1 (Dierckxsens et al. 2017) are two commonly used organelle genome assemblers.

Mitogenome annotation and sequence analyses

The mitochondrial genome was annotated using MITOS2 (Donath et al. 2019) and the Mitoz annotation module (Meng et al. 2019). Geneious v. 2021.0.3 was used to check the annotated sequences manually. The base composition and codon usage were calculated, and the relative synonymous codon usage (RSCU) of each protein-coding gene (PCG) was analyzed using PhyloSuite 1.2.3 (Zhang et al. 2020). The following general formulae were applied to estimate A+T skew and G+C skew, respectively: A+T skew = (A% – T%)/(A% + T%) and G+C skew = (G% – C%)/(G% + C%) (Perna and Kocher 1995). To investigate the selective pressure, we calculated the ratios of nonsynonymous and synonymous substitutions (Ka/Ks) in the mitogenomes of all Leiognathidae species using DnaSP 6.0 (Lowe and Chan 2016). tRNA genes were plotted in the ViennaRNA Web Services (http://rna.tbi.univie.ac.at/forna/) according to the secondary structure predicted by tRNAscan-SE 2.0 (Lowe and Chan 2016; Chan et al. 2021) and MITOS Web Server (Bernt et al. 2013) using the vertebrate mitochondrial genetic code. The sequences of the termination-associated sequence (TAS), central conserved sequence blocks (CSB-F, CSB-E, CSB-D, CSB-B, CSB-A), and conserved sequence block domains (CSB-2, CSB-3) in the control region were identified using the Basic Local Alignment Search Tool (BLAST) against the sequences of the reported fish.

Phylogenetic analysis

In order to guarantee the greatest possible accuracy in species identification, a random selection of three regions was tested from a sample of eight. The results were consistent across the three sample assemblies, and we selected OR344340 for description. In order to ascertain the phylogenetic position of species within the Leiognathidae family, we reconstructed a phylogeny of the family Leiognathidae using the mitogenome sequences from the GenBank database (https://ncbi.nlm.nih.gov/) for 36 species (accessed 6 February 2024), including *Lagocephalus gloveri* (Abe and Tabeta 1983) and *Amblygobius phalaena* (Valenciennes, in Cuvier and Valenciennes 1837), which were used as outgroups (Suppl. material 1: table S5). Sequences were downloaded from GenBank (Suppl. material 1: table S5) to establish the database for phylogenetic analysis using PhyloSuite 1.2.3 (Zhang et al. 2020). Next, 13 PCGs of these mitogenomes were extracted, and each coding gene was aligned using the codon alignment mode in Mafft v. 7.313 (Katoh and Standley 2013). Ambiguous regions were removed using Gblocks 0.91 (Castresana 2000), and the best-fit partition models—(GTR+F+I+G4) for maximum likelihood (ML) and (GTR+F+I+G) for Bayesian inference (BI)—were selected by ModelFinder (Kalyaanamoorthy et al. 2017) using the BICc and AICc criterion, respectively.

The ML analysis was performed in IQ-TREE v. 2.2.2 (Nguyen et al. 2015), under the Edge-linked partition model for 200 000 ultrafast bootstraps. The BI analysis was performed in MrBayes v. 3.2.7a (Ronquist et al. 2012), under the partition model (two parallel runs, 2 000 000 generations). Finally, iTOL v. 6 (Letunic and Bork 2021) was used to visualize the ML and BI phylogenetic trees.

Results

Species description based on morphological identification

Description based on eight specimens ranging 81.33–144.02 mm in standard length (SL; Suppl. material 1: table S6). Counts and proportional measurements are given in Table 1. D VIII 16; A III 14; P 20; V I–6; C 17; pored scales in lateral line 63–70; vertebrae (precaudal 9 + caudal 14) = 23 (Fig. 1).

Body robust and large, laterally compressed, rhomboid and deep. Dorsal profile more convex than ventral profile. Greatest body depth at vertical from dorsal fin origin to abdomen. Dorsal fin origin posterior to pelvic fin origins. Anal fin origin vertical through first dorsal fin ray (Fig. 1B). Dorsal head slightly triangular in shape, enclosed by 2 supraorbital ridges, apposed nuchal spine which exceeds eye diameter (Suppl. material 1: fig. S2); back typically slightly to strongly arched (Fig. 1). Snout truncated; length slightly equal to eye diameter. Gill opening large. Lower preopercular right-angled, margin weakly serrate. Branchiostegals 5, branchiostegal membrane attached along lateral margin of isthmus. Caudal peduncle short and shallow. Vertebral count: 9 precaudal + 14 caudal = 23. Neural and hemal spines of vertebral centrum PU4 expanded and bladelike (Fig. 1B).

Table 1. Comparison of morphometric and meristic characters of *L. equula* in the present study and previous studies.

Counts and measurements	Present study (*n* = 8)	Sparks and Dunlap (2004) (*n* = 22)	Chakrabarty et al. (2008) (*n* = 7)	Zheng (1962) (*n* = 10)
Standard length (mm)	105.99 (81.33–144.02)	110.6 (69.0–177.8)	92–128.8	60–232
Counts				
Dorsal fin rays	VIII 16	VII–VIII 12–17	–	VIII 16
Anal fin rays	III 14	III 14	–	III 14
Pectoral fin rays	20	19	–	20
Pored scales in lateral line	63–70	56–65	50–60	58–67
Vertebrae (precaudal+caudal)	9+14 = 23	9+14 = 23	–	–
Measurements				
As % of SL				
Head length	33.21 (31.47–35.91)	30.3 (28.6–33.1)	31.8 (29.8–34.5)	28.74–31.65
Body depth A (origin anal fin)	55.61 (52.95–59.56)	56.2 (51.2–60.5)	–	51.81–57.80
Body depth B (origin dorsal fin)	57.08 (54.76–60.38)	55.1 (49.5–58.3)	57.3 (53.9–61.8)	–
Head width (max.)	12.29 (11.52–13.22)	–	16.1 (15.2–17.6)	–
Caudal peduncle length	5.52 (4.66–6.73)	11.1 (9.4–13.7)	8.3 (6.8–10.6)	–
Caudal peduncle depth	7.57 (7.08–8.25)	6.7 (5.9–7.4)	6.9 (6.5–7.1)	–
Caudal peduncle width	4.26 (3.42–5.10)	4.0 (3.3–4.7)	4.2 (3.6–4.7)	–
Pectoral fin length	25.73 (23.20–27.18)	23.9 (21.2–26.2)	22.0 (20.1–24.1)	–
Pelvic fin length	15.64 (12.58–17.24)	15.5 (11.4–16.8)	16.6 (15.0–18.1)	–
Dorsal fin base length	57.79 (56.34–59.70)	56.2 (53.2–59.1)	–	–
Anal fin base length	47.08 (45.05–50.79)	45.6 (42.3–48.8)	–	–
Predorsal length	52.49 (50.22–54.32)	50.8 (48.4–53.3)	52.5 (50.5–54.0)	–
Prepelvic length	41.04 (37.62–44.85)	37.3 (35.1–40.2)	43.1 (37.2–50.5)	–
Preanal length	57.16 (54.71–59.36)	54.1 (50.2–58.5)	58.2 (56.6–60.2)	–
As % of HL				
Snout length	36.37 (33.26–40.37)	37.0 (33.7–39.6)	34.9 (33.3–37.3)	26.11–32.79
Head width (max.)	37.05 (35.02–42.00)	50.9 (47.9–54.4)	–	–
Upper jaw length	40.48 (38.26–43.04)	25.4 (23.1–27.6)	38.9 (35.0–41.3)	–
Lower jaw length	36.85 (34.90–38.84)	52.0 (48.0–57.4)	40.0 (25.7–60.0)	–
Interorbital width	32.02 (25.31–38.48)	34.3 (31.7–36.6)	36.8 (25.7–43.5)	–
Orbital diameter	31.12 (28.58–33.54)	37.3 (33.3–41.7)	34.6 (30.0–37.6)	29.67–35.34
Preorbital depth	54.00 (48.60–58.99)	22.7 (19.6–25.9)		–

Mouth small and terminal, directed slightly downward, forming tube when protruded. Cleft slightly sloping downward. Lower jaw strongly concave, forming 45° angle when mouth closed. Gape horizontal with inferior eye margin. Lips fleshy but thin. Maxilla exposed, through orbital anterior margin.

Eye moderately large, placed high, lower margin above body axis. Preorbital spine with ridge serrated. Adipose eye lid underdeveloped. Interorbital slightly convex. One short spine on anterior superior margin of eye and posterior of nostril. Nostrils above eyes, two on each side. Anterior nasal pore small and round, posterior large and oblong.

Fins: Dorsal fin 1, with eight spines and 16 rays. First dorsal fin spine very short; second dorsal fin spine longest; 80.35 (77.50–86.39) %HL and 25.26 (15.09–27.83) %SL. Third and fourth dorsal fin spine margin anteriorly serrate. Anal fin with three spines and 14 rays. Second anal fin spine longest; 59.06 (51.79–65.10) %HL and 19.61 (16.98–21.43) %SL. The anal fin spine margin anteriorly serrate. Both dorsal and anal fin base anteriorly covered by membranous sheaths. Pectoral fins rounded and wide. Subthoracic ventral fin shorter than pectoral fin; large axillary scale on pelvic fins; spines retract when laid flat.

Terminal ventral fin reached anal fin origin in juveniles (DHS14500, DHS22489, DHS22490). Caudal fin forked, tips of both lobes round and blunt.

Squamation: Lateral line slightly arched posteriorly from the pectoral fin base to the caudal peduncle, continuing horizontally along the caudal peduncle. Head and chest asquamate, body cycloid scales. Lateral line slightly curved and complete, includes 63–70 pored scales.

Dentition: Teeth pointed and bristled, with three or four tooth rows on upper and lower jaw, with incurve, banded arrangement. Vomer, palatine, and tongue toothless.

Fresh coloration: Body greyish to silvery, with compact grey-black narrow band on back and sides; a dark brown saddle on caudal peduncle. Axil of pectoral fins grey to black. Pelvic fins white. Margin of soft dorsal fin black; no dark spots. Margin of soft anal fin yellow. Caudal fin yellowish with black margin. Concentration of melanophores on snout side (Suppl. material 1: fig. S2). Large axillary scales on pelvic fins silvery (Fig. 1A).

Coloration in preservative: Body yellowish. Color pattern of fins similar to fresh coloration but with a yellowish tinge.

Molecular identification and analysis

Owing to the limited availability of mitochondrial genome data in Leiognathidae, single mitochondrial genes were chosen as the basis for molecular identification. Phylogenetic reconstruction of the family Leiognathidae on the basis of mitochondrial genes *16S* rRNA, *COX1*, and *ND5* was performed using BI and ML methods. The sequences of *L. equula* from different waters clustered together in all three single-gene phylogenetic trees (Suppl. material 1: figs S3–S5), suggesting that the molecular findings are consistent with the morphological results.

The Hongsha (PP551518) sequences clustered with those from the Philippines (AY541653) and Malaysia (EU366341) in the *16S* rRNA BI tree and with those from the Philippines in the *16S* rRNA ML tree (Suppl. material 1: fig. S3). The Yangxi (PP551517) and Changjiang (OR344340) sequences clustered with those from India (MK644023) in the *16S* rRNA BI tree. In both the BI and ML trees based on the *COX1* gene (Suppl. material 1: fig. S4), Hongsha (PP551518) sequences clustered with sequences from India (MK689371) and Taiwan, China (DQ028018) as sister branches. In addition, Yangxi (PP551517) and Changjiang (OR344340) clustered together in the BI tree, while they were sister branches in the ML tree. In both the BI and ML trees based on the *ND5* gene, the Philippines sequence (AB100017) clustered with the Yangxi (PP551517) and Changjiang (OR344340) sequences (Suppl. material 1: fig. S5), respectively. Additionally, Changjiang (OR344340) and Hongsha (PP551518) were sister branches in the BI tree, whereas Yangxi (PP551517) and Hongsha (PP551518) were sister branches in the ML tree.

Mitochondrial genomic structure and base composition

The mitochondrial genome of *L. equula* (GenBank accession number: OR344340) was 16,398 bp (Fig. 2), in accordance with other Leiognathidae species (Suppl. material 1: table S5). Similar to the mitogenome of most fish, the *L. equula* mitogenome contained 37 mitochondrial genes (13 typical PCGs, 22 tRNA genes, and 2 rRNA genes) and a control region (Fig. 2, Suppl. material 1: table S7).

The ND6 gene and eight tRNA genes (*trnS*[uga], *trnE*[uuc], *trnP*[ugg], *trnQ*[uug], *trnA*[ugc], *trnN*[guu], *trnC*[gca] and *trnY*[gua]) were located on the L chain. The remaining mitochondrial genes were located on the H chain (Fig. 2, Suppl. material 1: table S7). There were six overlapping regions (1–10 bp in size) in the mitogenome. The longest overlapping regions (10 bp) were located between *trnK*(uuu)/ATP8. Furthermore, the mitochondrial genome included 12 gene spacers, which exhibited a size range of 1–40 bp. The longest gap (40 nucleotides) was identified between *trnA*(ugc) and *trnN*(guu) at.

The *L. equula* mitogenome showed a slight bias towards A and T nucleotides, which comprised 54.9% of the total base composition (A = 30.7%, T = 24.2%, G = 15.0%, and C = 30.1%). This was accompanied by a positive A+T skew

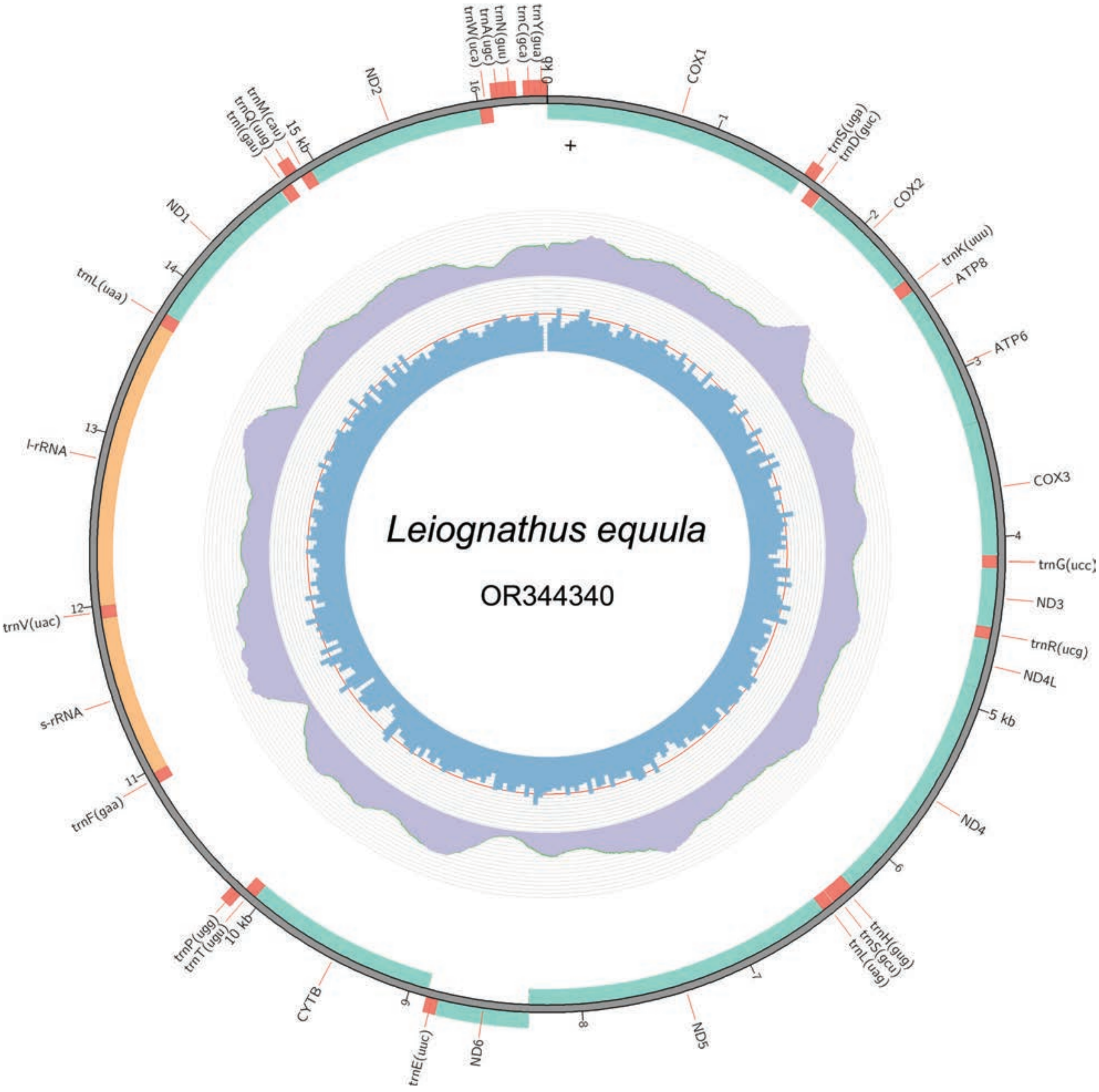

Figure 2. Complete mitogenome of *L. equula*. The middle and innermost circles represent depth distribution and GC content, respectively. The outermost circle shows gene arrangement, with green, orange, and red depicting protein-coding gene fragments, rRNA genes, and tRNA genes, respectively.

(0.117) and a negative G+C skew (−0.334) (Suppl. material 1: table S8). Thus, the *L. equula* mitogenome exhibited a clear A+T preference in its base composition, which is consistent with that in other Leiognathidae species (Suppl. material 1: table S5). Compared with the whole genome, the control region had the highest A+T content (approximately 62.8%; Suppl. material 1: table S8), which is a typical feature of the mitochondrial genomes of animals (Zhang and Hewitt 1997; Satoh et al. 2016). In contrast, the first codon position of the PCGs had the lowest A+T content, 49.0% (Suppl. material 1: table S8).

Protein-coding genes and codon usage

The total length of PCGs was 11,421 bp, with gene length ranging from 177 bp (*ATP8*) to 1830 bp (*ND5*). In total, 12 PCGs had canonical ATG start codons, whereas the *COX1* gene had a GTG start codon. A complete stop codon was observed in seven PCGs, whereas the remaining six PCGs exhibited an incomplete stop codon (TA or T) at their respective termini—*ATP6* and *COX3* were terminated by TA and *COX2*, CYTB, *ND3*, and *ND4* were terminated by T (Suppl. material 1: table S7). Furthermore, the values of A+T skew and G+C skew for the PCGs were 0.017 and −0.353, respectively, suggesting a higher abundance of A and C nucleotides than that of their respective counterparts (Suppl. material 1: table S8).

Suppl. material 1: table S9, Fig. 3 provide a summary of the amino acid usage and RSCU values in the PCGs of *L. equula*. In total, 3800 amino acids were encoded in the mitogenome. Of these, leucine (16.84%) and cysteine (0.71%) were the most and least frequently used amino acids, respectively. The six most frequently used codons in *L. equula* were CUA (Leu), AUC (Ile), CUC (Leu), GCC (Ala), ACC (Thr) and AUA (Met).

Selection pressure analysis

The selection pressure on 13 PGCs of six Leiognathidae species was quantified by computing the ratio of non-synonymous substitutions to synonymous substitutions (Ka/Ks). The Ka/Ks ratios of all PCGs were significantly lower than one (Fig. 4), suggesting that all PCGs were subject to a strong purifying selection pressure in these species (Yang and Bielawski 2000). Among the PCGs, the ATP8 and COX3 genes showed the highest (0.2019) and lowest (0.0265) values of Ka/Ks, respectively.

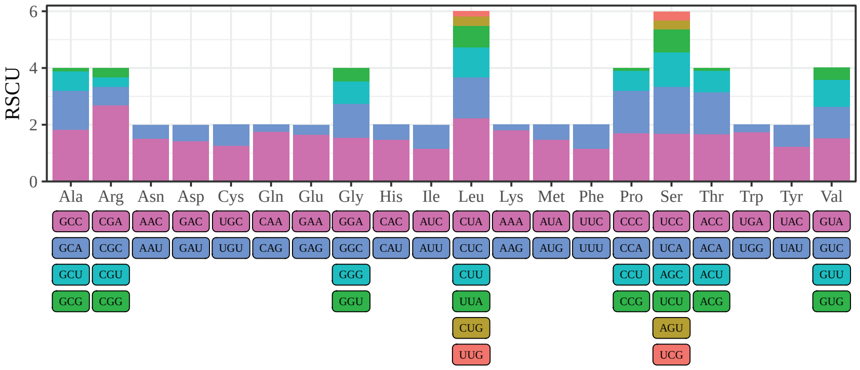

Figure 3. Relative synonymous codon usage (RSCU) of all protein-coding genes in the mitogenome of *L. equula*.

Transfer RNA and ribosomal RNA genes and control region

The mitogenome of *L. equula* contained 22 tRNA genes ranging from 67 to 75 bp in size, representing 9.5% (1552 bp) of the entire mitogenome (Suppl. material 1: table S7). Of the 22 tRNA genes, 14 were located on the H strand, and eight tRNA genes were located on the L strand (Suppl. material 1: table S8). All tRNA genes were predicted to fold into the typical cloverleaf secondary structure, except *trnS*(gcu), which lacked the dihydrouridine (DHU) arm (Fig. 5). The A+T content of the 22 tRNA genes was 57.60%, with a positive A+T skew (0.028) and G+C skew (0.065).

The two rRNA genes, *12S* and *16S* rRNA genes, were 949 bp and 1694 bp in length, respectively (Suppl. material 1: table S7). The rRNA genes were located between *trnF*(gaa) and *trnL*(uaa), separated from each other by *trnV*(uac) (Fig. 2, Suppl. material 1: table S7), as observed in other vertebrates. The A+T and G+C content of the two rRNA genes was 53.69% and 46.31%, respectively, with an A+T skew and a G+C skew of 0.29 and -0.10, respectively. These values indicate a clear bias in favor of the utilization of A and C nucleotides.

The control region of *L. equula* is located between *trnP*(ugg) and *trnF*(gaa), with a total length of 727 bp (Fig. 2, Suppl. material 1: table S7). A termination-associated sequence (TAS), central conserved sequence block (CSB) domains containing five conserved sequence blocks (CSB-F, CSB-E, CSB-D, CSB-B, and CSB-A), and a variable domain consisting of two conserved sequence blocks (CSB-2 and CSB-3) were identified in the control region of the *L. equula* mitogenome through a homology search (Fig. 6). The G-box (GTGGGGG) was identified in the CSB-E, which exhibited the highest conservation across teleost fish. Additionally, a pyrimidine tract (TTCTTTTTTCTCTTACTTTTCATCT) was identified following the CSB-A, which was also present in other Leiognathidae species (Accession numbers from GenBank MG677547 and NC_057225).

Phylogenetic analysis

The position of Leiognathidae in the molecular phylogenetic trees was reconstructed on the basis of 13 concatenated PCGs using the ML and BI methods. Phylogenetic analyses conducted using BI and ML yielded a consistent topology. The phylogenetic trees divided the Leiognathidae family into three

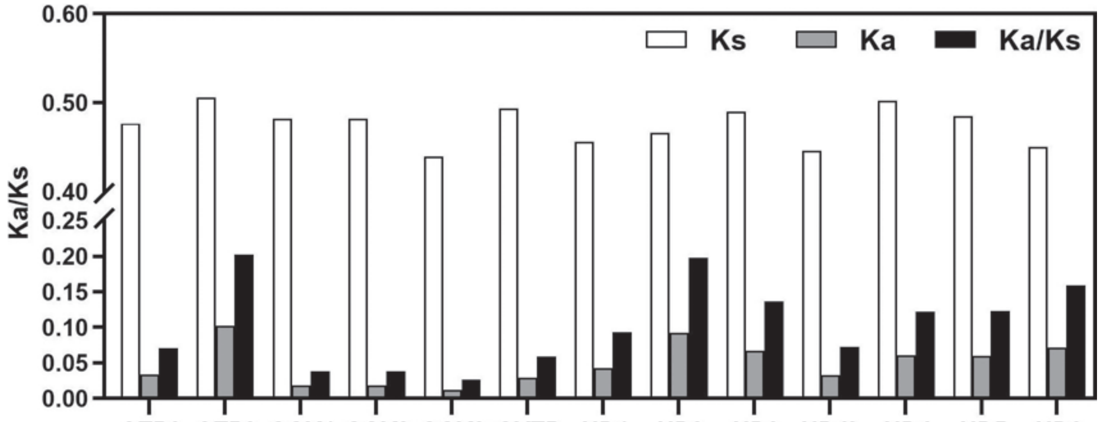

Figure 4. Mean Ka, Ks, and Ka/Ks values of 13 protein-coding genes from six Leiognathidae species.

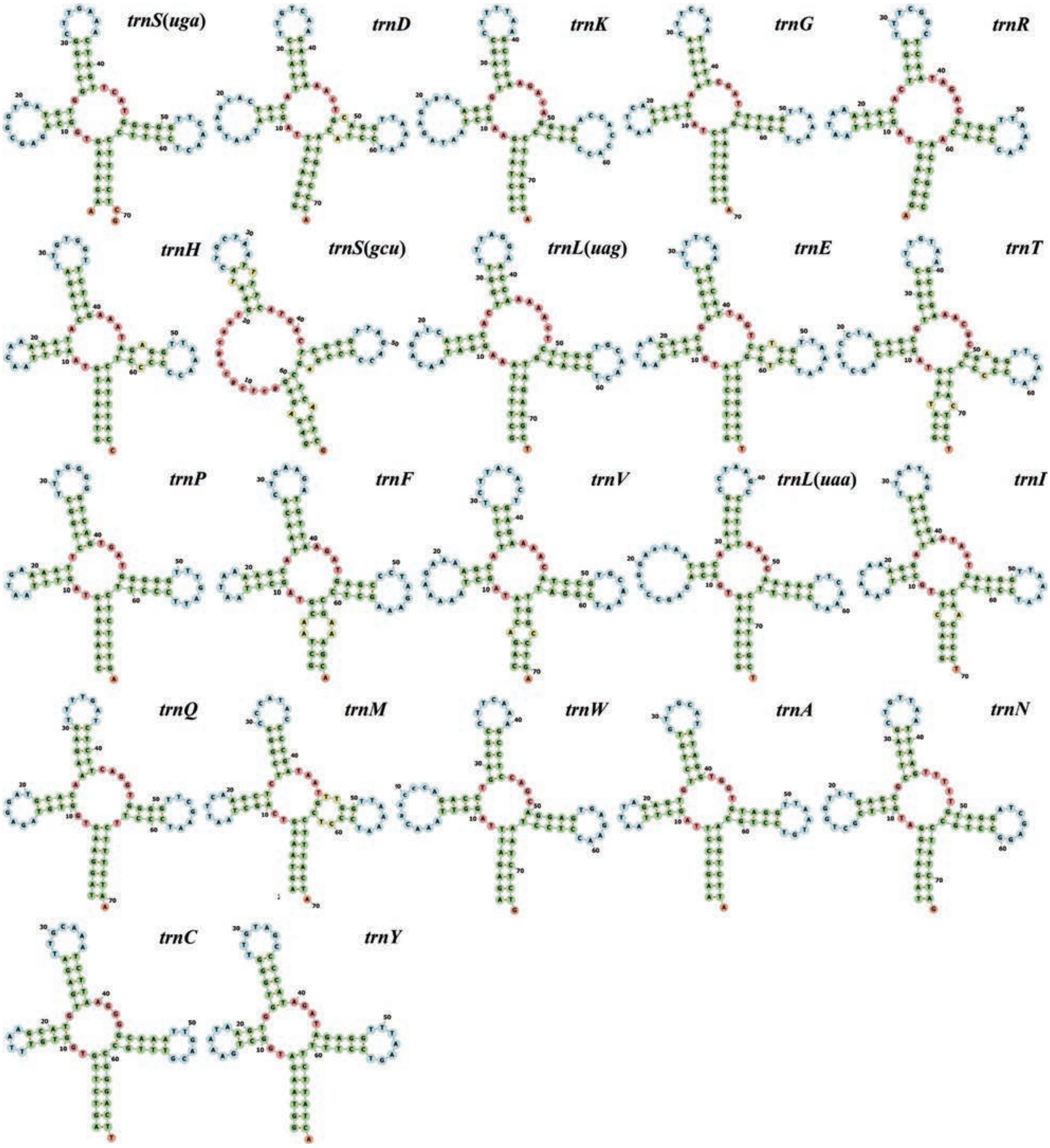

Figure 5. Secondary structure of the 22 tRNA genes in the mitochondrial genome of *L. equula*.

distinct clades (Fig. 7). *Nuchequula nuchalis* (Temminck and Schlegel 1845) and *Leiognathus brevirostris* (Valenciennes, in Cuvier and Valenciennes 1835) are grouped together with nearly equal branch lengths, indicating that the molecular record of *L. brevirostris* is likely also *Nuchequula*, supporting previous studies (Chakrabarty and Sparks 2007; Chakrabarty et al. 2010; Gao et al. 2020). *Nuchequula* spp. and *Photopectoralis bindus* (Valenciennes, in Cuvier and Valenciennes 1835) are sister branches clustered with single branches of *L. equula*. *Leiognathus ruconius* (Hamilton, 1822) (now *Deveximentum ruconius*) and *Gazza minuta* (Bloch, 1795) forms another branch, they are the mandible vertical and presence of strongly caniniform teeth type of the family, respectively.

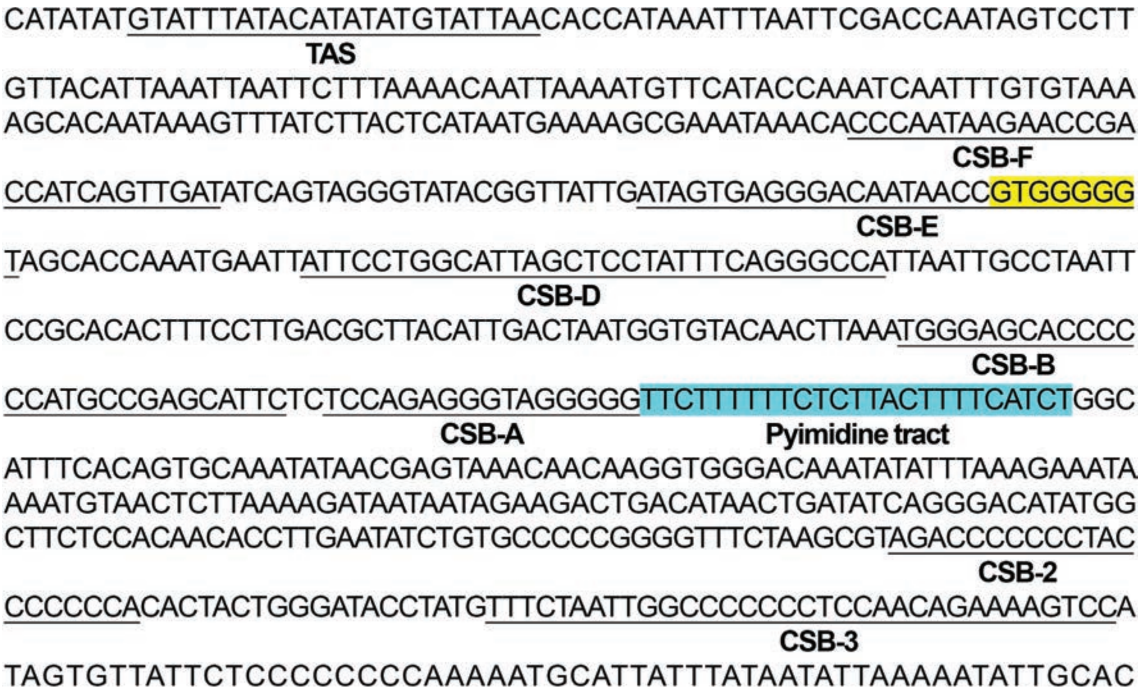

CATATATGTATTTATACATATATGTATTAACACCATAAATTTAATTCGACCAATAGTCCTT
TAS
GTTACATTAAATTAATTCTTTAAAACAATTAAAATGTTCATACCAAATCAATTTGTGTAAA
AGCACAATAAAGTTTATCTTACTCATAATGAAAAGCGAAATAAACACCCAATAAGAACCGA
CSB-F
CCATCAGTTGATATCAGTAGGGTATACGGTTATTGATAGTGAGGGACAATAACCGTGGGGG
CSB-E
TAGCACCAAATGAATTATTCCTGGCATTAGCTCCTATTTCAGGGCCATTAATTGCCTAATT
CSB-D
CCGCACACTTTCCTTGACGCTTACATTGACTAATGGTGTACAACTTAAATGGGAGCACCCC
CSB-B
CCATGCCGAGCATTCTCTCCAGAGGGTAGGGGGTTCTTTTTTCTCTTACTTTTCATCTGGC
CSB-A
Pyimidine tract
ATTTCACAGTGCAAATATAACGAGTAAACAACAAGGTGGGACAAATATATTTAAAGAAATA
AAATGTAACTCTTAAAAGATAATAATAGAAGACTGACATAACTGATATCAGGGACATATGG
CTTCTCCACAACACCTTGAATATCTGTGCCCCCGGGGTTTCTAAGCGTAGACCCCCCCTAC
CSB-2
CCCCCCACACTACTGGGATACCTATGTTTCTAATTGGCCCCCCCTCCAACAGAAAAGTCCA
CSB-3
TAGTGTTATTCTCCCCCCCCAAAAATGCATTATTTATAATATTAAAAATATTGCAC

Figure 6. Structure and sequence of the control region of the *L. equula* mitochondrial genome. The termination-associated sequence (TAS), central conserved blocks (CSB-F, CSB-E, CSB-D, CSB-B, and CSB-A), and conserved sequence block domains (CSB-2 and CSB-3) are underlined.

Discussion

The morphometric and meristic values recorded in the present study were similar to those reported in previous studies on this species. But the number of pored scales in the lateral line (Table 1) was slightly higher than that previously reported. This difference is attributable to the high variability within the species, random pattern of scales, and the deciduous nature of ponyfish scales in preservation (Chakrabarty and Sparks 2007). Furthermore, accurate counting is challenging owing to the small size and degree of embedment of scales. Additionally, the preorbital depth expressed as percent head length (Table 1) is demonstrably higher, which may also be attributed to interspecific differences.

The genus *Leiognathus* currently includes *L. equula* and *L. robustus* (Sparks and Chakrabarty 2015) as well as several undescribed species (Chakrabarty and Sparks 2008; Chakrabarty et al. 2011). Four *Leiognathus* species are currently verified in Eschmeyer's Catalog of Fishes (Fricke et al. 2024): *L. bindoides* (Bleeker, 1851), *L. equula* (Forsskål, in Niebuhr 1775), *L. parviceps* (Valenciennes, in Cuvier and Valenciennes 1835), and *L. robustus* Sparks and Dunlap 2004. However, *L. parviceps* is closely related to or conspecific with *Equulites leuciscus* (Günther, 1860) (Sparks et al. 2005), and *L. bindoides* is considered a junior synonym of *L. bindus* (Weber and de Beaufort 1931) (=*Photopectoralis bindus*). But these species are not as large or strong as *L. equula*. Of the four *Leiognathus* species, *L. equula* and *L. robustus* are the better documented and more recently described species, respectively.

Leiognathus equula, the type species of *Leiognathus*, differs from *L. robustus*, which has been described in various reports (Sparks and Dunlap 2004; Chakrabarty and Sparks 2008, 2022), with respect to the presence of a pronounced hump (vs. absence of an occipital hump), strongly curved, creating the image of an arched back (vs. the presence of a mildly sloping predorsal profile),

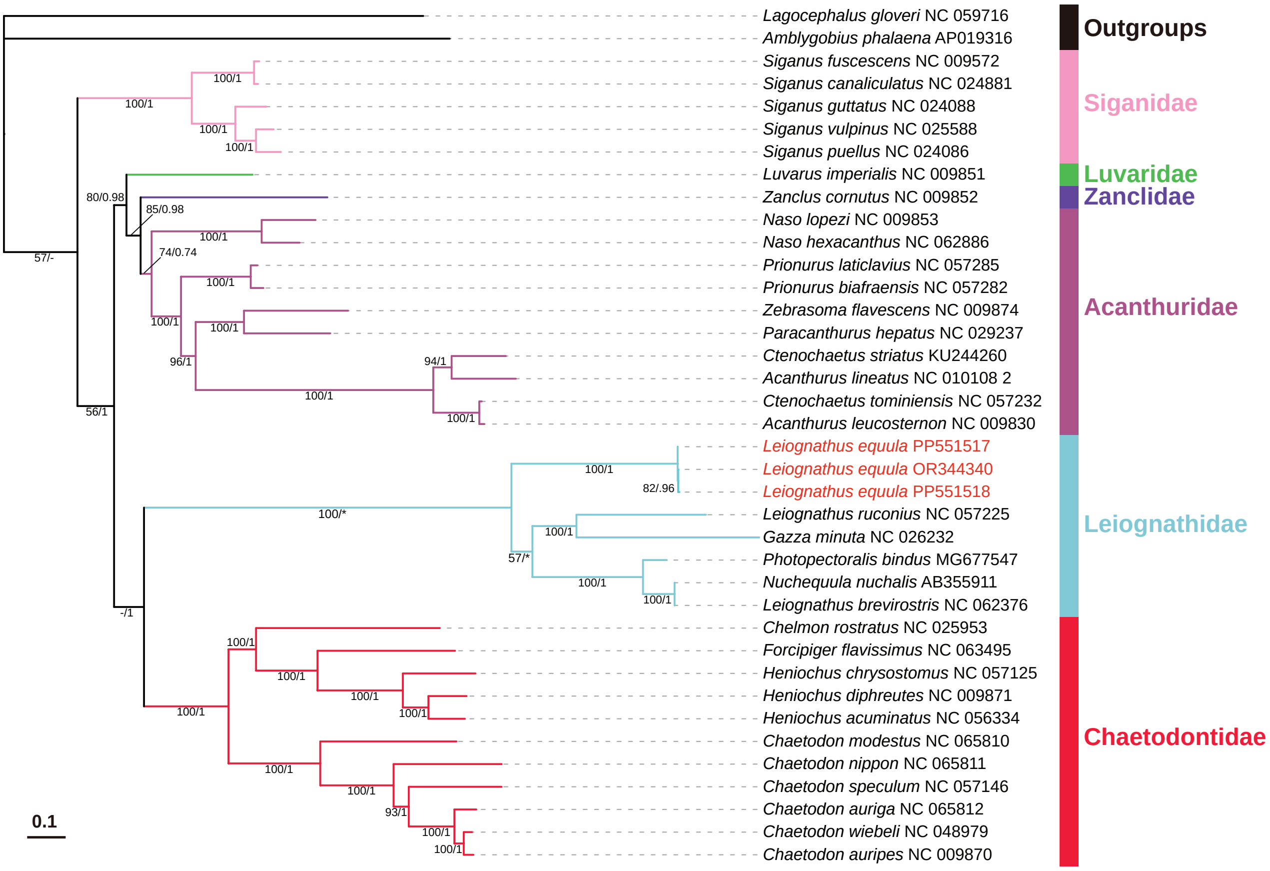

Figure 7. The position of Leiognathidae in the Bayesian inference (BI) and maximum likelihood (ML) phylogenetic tree based on the amino acid sequences of 13 protein-coding genes of the mitochondrial genome and their groupings, clades, ecotypes, and lengths. The numbers above or below branches indicate ML bootstrap values and Bayesian posterior probabilities, respectively; "*" indicates absence from the maximum clade credibility tree; "-" indicates no support value. *L. brevirostris* (NC 026232) should be a species of *Nuchequula*, and *L. ruconius* (NC 057225) is not classified under *Leiognathus* in the NCBI database.

slight bulge above orbit (vs. a distinct preorbital protuberance), and a nuchal spine that is exposed and projecting, particularly distally (vs. not exposed in lateral view). This species can be distinguished from other large leiognathid species such as *Aurigequula fasciata* and *Aurigequula striatus* (James and Badrudeen, 1990) on the basis of its shorter second dorsal and anal fin spines, asquamate scale nuchal region, straighter dorsal head profile, and pigmentation pattern.

The *COX1* gene had a GTG start codon. Other Leiognathidae species have also been reported to use this non-standard start codon (Shi et al. 2018; Sui et al. 2019). Six PCGs exhibited an incomplete stop codon, a common feature of vertebrate PCGs that is thought to be completed by polyadenylation after transcription (Ojala et al. 1981). The 22 tRNA genes exhibited a distribution pattern similar to that observed in other Leiognathidae species (Shi et al. 2018; Sui et al. 2019). The secondary structure of *trnS*(gcu) lacked the dihydrouridine (DHU) arm. This finding is consistent with observations in all bony fish mitogenomes (Yang et al. 2018; Wang et al. 2022).

Previous phylogenetic studies on Leiognathidae did not use the mitochondrial genome. Studies on the mitochondrial genome of Leiognathidae species have been limited. The mitochondrial genome data of only five Leiognathidae species are available in the NCBI database (acquisition number: AB355911, MG677547, NC_026232, NC_057225, NC_062376; accessed February 6, 2024). There are two entries for *Leiognathus*: *L. ruconius* (acquisition number: NC_057225) and *L. brevirostris* (acquisition number: NC_062376). The former was identified as *Deveximentum ruconius* (Sui et al. 2019; Fricke et al. 2024), whereas the latter is actually a species of *Nuchequula* (Chen and Fang 1999; Chakrabarty et al. 2010). The results of the phylogenetic analysis corroborate the aforementioned conclusions. In the present study, the species *L. ruconius* (NC 057225) did not form a clade with *L. equula* but instead formed a sister group with *G. minuta*. The species *L. brevirostris* (NC 026232), which is evidently not a *Leiognathus* species, clustered with *N. nuchalis*. Although the phylogenetic tree in the present study contained only six species, they belong to five different genera of the Leiognathidae. The phylogenetic characteristics above are consistent with previous findings (Sparks and Chakrabarty 2015).

Previous single-gene phylogenetic studies suggest that most genera within the family Leiognathidae are monophyletic (Ikejima et al. 2004; Sparks and Dunlap 2004; Sparks et al. 2005; Seah et al. 2008; Chakrabarty et al. 2011; Seth and Barik 2021). However, they are still nested within *Aurigequula* and *Leiognathus* (Sparks and Chakrabarty 2015). The phylogenetic analysis based on mitochondrial genome sequences (Fig. 7) and single gene sequences (*16S* RNA and *COX1*, Suppl. material 1: figs S3, S4) showed that the family Leiognathidae is monophyletic, whereas the phylogenetic analysis based on the single gene *ND5* (Suppl. material 1: fig. S5) showed the opposite. This can be attributed to the fact that the sequences of the three unidentified species of *Leiognathus* are not grouped with those of the other known species of Leiognathidae.

In the present study, the phylogenies based on mitochondrial genome sequences showed that Leiognathidae are most closely related to Chaetodontidae, forming a sister group. This finding is consistent with the osteological evidence (Gill and Leis 2019; Gill and Michalski 2020). Moreover, the families Acanthuridae, Luvaridae, and Zanclidae formed a separate clade, which forms a sister group to the Leiognathidae and Chaetodontidae clades. This finding is corroborated by previous findings on the time-calibrated phylogeny of the bony fish species (Betancur-R et al. 2017). Whole mitochondrial genome phylogeny suggested with high support that Leiognathidae and Chaetodontidae comprise the order Chaetodontiformes, whereas Acanthuridae, Luvaridae and Zanclidae comprise the order Acanthuriformes (Fig. 7).

Conclusions

In the present study, samples of *L. equula* were collected from different regions of China. The species were identified using both morphological and molecular characteristics. Phylogenies based on the amino acid sequences of 13 protein-coding genes and two single gene sequences (*16S* RNA and *COX1*) but not that based on the single gene *ND5*, indicated that Leiognathidae is a monophyletic family. The phylogenetic trees show that the family Leiognathidae is divided into three clades. Notably, the family Leiognathidae formed was placed as a sister group to the family Chaetodontidae. In the present study, the mitochondrial genome sequence of *L. equula* in the family Leiognathidae was obtained using shallow genome skimming. *L. equula* occupied a basal branch of the Leiognathidae phylogenetic tree; thus, the study provides essential data for the study of the complete mitochondrial genome phylogeny of Leiognathidae.

Acknowledgments

During the process of specimen collection, we thank Qi Chu and Weiyue Zhang from the National Marine Environment Monitoring Center for their assistance in collecting marine specimens. We are also grateful to Yuange Chen from the East China Sea Fisheries Research Institute for his contribution to sample collection. We are grateful to the reviewers and editors for their many helpful comments and questions, which significantly improved the final version of the manuscript.

Additional information

Conflict of interest

The authors have declared that no competing interests exist.

Ethical statement

No ethical statement was reported.

Funding

No funding was reported.

Author contributions

Conceptualization: JC, DY. Data curation: JC, SZ, DY. Formal analysis: JC, SZ, DY. Funding acqui-sition: JZ, JY, CJ. Investigation: JC, JY, WT. Project administration: JY, XW, JC. Resources: JY, CP, DY. Supervision: JZ, CP. Validation: DY, JC. Visualization: SZ, JC. Writing - original draft: JC, XW, SZ. Writing - review and editing: JC, XW, DY.

Author ORCIDs

Jiajie Chen https://orcid.org/0000-0001-7487-231X
Xiaodong Wang https://orcid.org/0000-0001-9424-7896
Sheng Zeng https://orcid.org/0009-0001-0943-3772
Wei Tian https://orcid.org/0009-0008-5272-0700
Deyuan Yang https://orcid.org/0000-0003-3735-9909
Jinqing Ye https://orcid.org/0009-0009-6503-1477
Junsheng Zhong https://orcid.org/0000-0002-9145-7473
Chaopeng Jiang https://orcid.org/0009-0004-0957-231X

Data availability

All of the data that support the findings of this study are available in the main text or Supplementary Information.

References

Abe T, Tabeta O (1983) Description of a new swellfish of the genus *Lagocephalus* (Tetraodontidae, Teleostei) from Japanese waters and the East China Sea. Uo 32: 1–8.

Bernt M, Donath A, Jühling F, Externbrink F, Florentz C, Fritzsch G, Pütz J, Middendorf M, Stadler PF (2013) MITOS: Improved de novo metazoan mitochondrial genome annotation. Molecular Phylogenetics and Evolution 69(2): 313–319. https://doi.org/10.1016/j.ympev.2012.08.023

Betancur-R R, Wiley EO, Arratia G, Acero A, Bailly N, Miya M. Lecointre G, Ortí G (2017) Phylogenetic classification of bony fishes. BMC Ecology and Evolution 17: 162. https://doi.org/10.1186/s12862-017-0958-3

Bleeker P (1851) Over eenige nieuwe geslachten en soorten van Makreelachtige visschen van den Indischen Archipel. Natuurkundig Tijdschrift voor Nederlandsch Indië 1(4): 341–372. https://www.biodiversitylibrary.org/bibliography/13350

Bloch ME (1795) Naturgeschichte der Ausländischen Fische. Vol. 9. Morinofchen Kunfthandlung, Berlin, 192 pp. https://doi.org/10.5962/bhl.title.63303

Carpenter KE, Niem VH (2001) Species identification guide for fishery purposes. The living marine resources of the western central Pacific. Bony fishes part 3 (Menidae to Pomacentridae). Vol. 5. Food and Agriculture Organization of the United Nations, Rome, 3379 pp.

Castresana J (2000) Selection of conserved blocks from multiple alignments for their use in phylogenetic analysis. Molecular Biology and Evolution 17(4): 540–552. https://doi.org/10.1093/oxfordjournals.molbev.a026334

Chakrabarty P, Sparks JS (2007) Phylogeny and Taxonomic Revision of *Nuchequula* Whitley 1932 (Teleostei: Leiognathidae), with the Description of a New Species. American Museum of Natural History 3588: 1–25. https://doi.org/10.1206/0003-0082(2007)3588[1:PATRON]2.0.CO;2

Chakrabarty P, Sparks JS (2008) Diagnoses for *Leiognathus* Lacepède 1802, *Equula* Cuvier 1815, *Equulites* Fowler 1904, *Eubleekeria* Fowler 1904, and a new ponyfish genus (Teleostei: Leiognathidae). American Museum Novitates 3623: 1–11. https://doi.org/10.1206/618.1

Chakrabarty P, Sparks JS (2022) Family Leiognathidae. In: Heemstra PC, Heemstra E, Ebert DA, Holleman W, Randall JE (Eds) Coastal fishes of the western Indian Ocean Vol 3. South African Institute for Aquatic Biodiversity, Makhanda, 469 pp. https://saiab.ac.za/publications/coastal-fishes-of-the-western-indian/

Chakrabarty P, Amarasinghe T, Sparks JS (2008) Rediscription of ponyfishes (Teleostei: Leiognathidae) of Sri Lanka and the status of *Aurigequula* fowler 1918. Ceylon Journal of Science (Biological Sciences) 37(2): 143–161. https://doi.org/10.4038/cjsbs.v37i2.502

Chakrabarty P, Sparks JS, Ho HC (2010) Taxonomic review of the ponyfishes (Perciformes: Leiognathidae) of Taiwan. Marine Biodiversity 40: 107–121. https://doi.org/10.1007/s12526-010-0037-0

Chakrabarty P, Davis MP, Smith WL, Baldwin ZH, Sparks JS (2011) Is sexual selection driving diversification of the bioluminescent ponyfishes (Teleostei: Leiognathidae)? Molecular Ecology 20(13): 2818–2834. https://doi.org/10.1111/j.1365-294X.2011.05112.x

Chan PP, Lin BY, Mak AJ, Lowe TM (2021) tRNAscan-SE 2.0: Improved Detection and Functional Classification of Transfer RNA Genes. Nucleic Acids Research 49(16): 9077–9096. https://doi.org/10.1093/nar/gkab688

Chen IS, Fang LS (1999) The freshwater and estuarine fishes of Taiwan. National Museum of Marine Biology and Aquarium, Taipei, 287 pp.

Chen J, Ni Y (2021) Leiognathidae. In: Wu HL, Zhong JS (Eds) Key to Marine and Estuarine Fishes of China: Arctic Agricultural Press, Beijing, China, 713–725.

Chen MR, Yang SY (2013) Fishes in the Taiwan Strait and its adjacent waters. China Science and Technology Press: Beijing, 351 pp.

Chen QC, Cai YZ, Ma XM (1997) Fishes from Nansha Islands to South China Coastal Waters 1. Science Press, Beijing, 202 pp.

Chen S, Zhou Y, Chen Y, Gu J (2018) fastp: An ultra-fast all-in-one FASTQ preprocessor. Bioinformatics 34(17): i884–i890. https://doi.org/10.1093/bioinformatics/bty560

Cuvier G (1829) Le règne animal distribué d'après son organisation, pour servir de base à l'histoire naturelle des animaux et d'introduction à l'anatomie comparée. Tom 2. Déterville, Paris, 406 pp. https://doi.org/10.5962/bhl.title.49223

Cuvier G, Valenciennes A (1835) Histoire naturelle des poissons. Tome dixième. Suite du livre neuvième. Scombéroïdes. Livre dixième. De la famille des Teuthyes. Livre onzième. De la famille des Taenioïdes. Livre douzième. Des Athérines 10, 482 pp. https://doi.org/10.5962/bhl.title.12283

Cuvier G, Valenciennes A (1837) Histoire naturelle des poissons. Tome douzième. Suite du livre quatorzième. Gobioïdes. Livre quinzième. Acanthoptérygiens à pectorales pédiculées 12, 507 pp. https://doi.org/10.5962/bhl.title.12283

Dierckxsens N, Mardulyn P, Smits G (2017) NOVOPlasty: de novo assembly of organelle genomes from whole genome data. Nucleic Acids Research 45(4): e18. https://doi.org/10.1093/nar/gkw955

Donath A, Jühling F, Al-Arab M, Bernhart SH, Reinhardt F, Stadler PF, Middendorf M, Bernt M (2019) Improved annotation of protein-coding genes boundaries in metazoan mitochondrial genomes. Nucleic Acids Research 47(20): 10543-10552. https://doi.org/10.1093/nar/gkz833

Dunlap PV, Ast, JC, Kimura S, Fukui A, Yoshino T, Endo H (2007) Phylogenetic analysis of host-symbiont specificity and codivergence in bioluminescent symbioses. Cladistics 23(5): 507–532. https://doi.org/10.1111/j.1096-0031.2007.00157.x

Forsskål P (1775) Descriptiones animalium avium, amphibiorum, piscium, insectorum, vermium; quae in itinere orientali observavit; Post mortem auctoris edidit Carsten Niebuhr. Hauniae, Description Animalium, 167 pp. https://doi.org/10.5962/bhl.title.2154

Fricke R, Eschmeyer WN, Fong JD [Eds] (2024) Catalog of fishes: genera, species, references. http://researcharchive.calacademy.org/research/ichthyology/catalog/fishcatmain.asp [accessed 6 February 2024]

Gao T, Gao B, Li Z, Shan B, Song N (2020) Population genetics study of *Leiognathus equulus* based on the control region fragment of mitochondrial DNA. Journal of fisheries of China 44(5): 715–722. https://doi.org/10.11964/jfc.20190411734

Gill AC, Leis JM (2019) Phylogenetic position of the fish genera Lobotes, Datnioides and Hapalogenys, with a reappraisal of acanthuriform composition and relationships based on adult and larval morphology. Zootaxa 4680(1): 1–81. https://doi.org/10.11646/zootaxa.4680.1.1

Gill AC, Michalski S (2020) Osteological evidence for monophyly of the Leiognathidae (Teleostei: Acanthomorpha: Acanthuriformes). Zootaxa 4732(3): 409–421. https://doi.org/10.11646/zootaxa.4732.3.4

Gloerfelt-Tarp T, Kailola PJ (2022) Trawled fishes of southern Indonesia and northwestern Australia. Australian Development Assistance Bureau, Australia, Directorate General of Fisheries, Indonesia, German Agency for Technical Cooperation, Federal Republic of Germany, 422 pp. https://mail.asianfisheriessociety.org/news.php?id=trawled-fishes-of-southern-indonesia-and-northwestern-australia

Günther A (1860) Catalogue of the fishes in the British Museum (Vol. 2). Catalogue of the acanthopterygian fishes in the collection of the British Museum. Squamipinnes, Cirrhitidae, Triglidae, Trachinidae, Sciaenidae, Polynemidae, Sphyraenidae, Trichiuridae, Scombridae, Carangidae, Xiphiidae. British Museum, London, 548 pp. https://doi.org/10.5962/bhl.title.8809

Hamilton F (1822) An account of the fishes found in the river Ganges and its branches. Archibald Constable and Company, Edinburgh, 405 pp. https://doi.org/10.5962/bhl.title.59540

Hubbs CL, Lagler JF (2004) revised by Smith GR. Fishes of the Great Lakes region. University of Michigan Press, Ann Arbor, Michigan, 332 pp. https://doi.org/10.3998/mpub.17658

Ikejima K, Ishiguro NB, Wada M, Kita-Tsukamoto K, Nishida M (2004) Molecular phylogeny and possible scenario of ponyfish (Perciformes: Leiognathidae) evolution. Molecular Phylogenetics and Evolution 31(3): 904-909. https://doi.org/10.1016/j.ympev.2003.10.006

James PSBR (1975) A systematic review of the fishes of the family Leiognathidae. Journal of the Marine Biological Association of India 17(1): 138–172. https://eprints.cmfri.org.in/1445/

James PSBR, Badrudeen M (1990) A new species of silverbelly *Leiognathus striatus* (Family: Leiognathidae: Pisces) from the Gulf of Mannar, India and redescription of *Leiognathus fasciatus* (Lacepede). Journal of Marine Biological Association of India, 32(1–2): 217–226. http://eprints.cmfri.org.in/1126/

Jin JJ, Yu WB, Yang JB, Song Y, DePamphilis CW, Yi TS, Li DZ (2020) GetOrganelle: A fast and versatile toolkit for accurate de novo assembly of organelle genomes. Genome Biology 21: 241. https://doi.org/10.1186/s13059-020-02154-5

Kalyaanamoorthy S, Minh BQ, Wong TKF, Von Haeseler A, Jermiin LS (2017) ModelFinder: Fast model selection for accurate phylogenetic estimates. Nature Methods 14: 587–589. https://doi.org/10.1038/nmeth.4285

Katoh K, Standley DM (2013) MAFFT multiple sequence alignment software version 7: improvements in performance and usability. Molecular Biology and Evolution 30(4): 772–780. https://doi.org/10.1093/molbev/mst010

Kimura S, Peristiwady T (2000) Leiognathidae. In: Matsuura K, Sumadhiharga OK, Tsukamoto K (Eds) Field guide to Lombok Island: identification guide to marine organisms in seagrass beds of Lombok Island, Indonesia. Ocean Research Institute, University of Tokyo, Tokyo, 449 pp.

Kimura S, Ikejima K, Iwatsuki Y (2008a) Eubleekeria Fowler 1904, a valid genus of Leiognathidae (Perciformes). Ichthyological Research 55: 202–203. https://doi.org/10.1007/s10228-007-0025-y

Kimura S, Kimura R, Ikejima K (2008b) Revision of the genus *Nuchequula* with descriptions of three new species (Perciformes: Leiognathidae). Ichthyological Research 55: 22–42. https://doi.org/10.1007/s10228-007-0011-4

Kimura S, Motomura H, Iwatsuki Y (2008c) Equulites Fowler 1904, a senior synonym of Photoplagios Sparks, Dunlap, and Smith 2005 (Perciformes: Leiognathidae). Ichthyological Research 55: 204–205. https://doi.org/10.1007/s10228-008-0041-6

Kimura S, Satapoomin U, Matsuura K (2009) Fishes of Andaman Sea, west coast of southern Thailand. National Muesum of Nature and Science, Tokyo, 346 pp.

Kimura S, Imamura H, Nguyen VQ, Pham TD (2018) Fishes of Ha Long Bay, the natural world heritage site in northern Vietnam. Fisheries Research Laboratory, Mie University, Shima, Japan, 314 pp.

Lacepède BGE (1802) Histoire naturelle des poisons. Vol. 4. Plassan, Paris, 728 pp. https://doi.org/10.5962/bhl.title.11645

Lacepède BGE (1803) Histoire naturelle des poissons. Vol. 5. Plassan, Paris, 803 pp. https://doi.org/10.5962/bhl.title.12463

Lai TH, He BY (2016) Marine Osteichthyes fishes in Guangxi Beibu Gulf of China. Science Press, Beijing, 453 pp.

Larson H, Kaymaram F, Hartmann S, Al-Husaini M, Almukhtar M, Alam S, Sparks JS (2017) *Leiognathus equulus*. The IUCN Red List of Threatened Species 2017: e.T196417A53990344. https://doi.org/10.2305/IUCN.UK.2017-3.RLTS.T196417A53990344.en

Letunic I, Bork P (2021) Interactive Tree of Life (iTOL) v5: An online tool for phylogenetic tree display and annotation. Nucleic Acids Research 49(W1): W293–W296. https://doi.org/10.1093/nar/gkab301

Liu M, Chen X, Yang SY (2014) Marine Fishes of Southern Fujian, China. Vol. 2. China Ocean Press, Beijing, 294 pp.

Liu J, Wu RX, Kang B, Ma L (2016) Fishes of Beibu Gulf. Science Press, Beijing, 420 pp.

Lowe TM, Chan PP (2016) tRNAscan-SE on-line: Integrating search and context for analysis of transfer RNA genes. Nucleic Acids Research 44(W1): W54-W57. https://doi.org/10.1093/nar/gkw413

Masuda H, Amaoka K, Araga C, Uyeno T, Yoshino T (1984) The fishes of the Japanese Archipelago. Tokai University Press, Tokyo, 437 pp.

Meng G, Li Y, Yang C, Liu S (2019) MitoZ: a toolkit for animal mitochondrial genome assembly, annotation and visualization. Nucleic Acids Research 47(11): e63. https://doi.org/10.1093/nar/gkz173

Nguyen L-T, Schmidt HA, Von Haeseler A, Minh BQ (2015) IQ-TREE: A Fast and Effective Stochastic Algorithm for Estimating Maximum-Likelihood Phylogenies. Molecular Biology and Evolution 32(1): 268–274. https://doi.org/10.1093/molbev/msu300

Niebuhr C (1775) Descriptiones animalium avium, amphibiorum, piscium, insectorum, vermium; quae in itinere orientali observavit; Post mortem auctoris edidit Carsten Niebuhr. Hauniae, Description Animalium, 167 pp. https://doi.org/10.5962/bhl.title.2154

Ojala D, Montoya J, Attardi G (1981) tRNA punctuation model of RNA processing in human mitochondria. Nature 290: 470–474. https://doi.org/10.1038/290470a0

Perna NT, Kocher TD (1995) Patterns of nucleotide composition at fourfold degenerate sites of animal mitochondrial genomes. Journal of Molecular Evolution 41: 353–358. https://doi.org/10.1007/BF01215182

Psomadakis PN, Osmany HB, Moazzam M (2015) Field identification guide to the living marine resources of Pakistan. FAO Species Identification Guide for Fishery Purposes. Food and Agriculture Organization of the United Nations, Rome, 386 pp. https://www.fao.org/3/i4932e/i4932e.pdf

Psomadakis PN, Thein H, Russell BC, Tun MT (2019) Field identification guide to the living marine resources of Myanmar. FAO Species Identification Guide for Fishery Purposes. Food and Agriculture Organization of the United Nations and Department of Fisheries, Ministry of Agriculture, Livestock and Irrigation Republic of the Union of Myanmar, Rome, 694 pp. https://www.fao.org/3/ca7180en/CA7180EN.pdf

Ronquist F, Teslenko M, van der Mark P, Ayres DL, Darling A, Höhna S, Larget B, Liu L, Suchard MA, Huelsenbeck JP (2012) MrBayes 3.2: Efficient Bayesian Phylogenetic Inference and Model Choice across a Large Model Space. Systematic Biology 61(3): 539–542. https://doi.org/10.1093/sysbio/sys029

Saruwatari T, López JA, Pietsch TW (1997) Cyanine blue: a versatile and harmless stain for specimen observation. Copeia, 1997: 840–841. https://doi.org/10.2307/1447302

Satoh TP, Miya M, Mabuchi K, Nishida M (2016) Structure and variation of the mitochondrial genome of fishes. BMC Genom 17: 719. https://doi.org/10.1186/s12864-016-3054-y

Schoch CL, Ciufo S, Domrachev M, Hotton CL, Kannan S, Khovanskaya R, Leipe D, Mcveigh R, O'Neill K, Robbertse B, Sharma S, Soussov V, Sullivan JP, Sun L, Turner S, Karsch-Mizrachi I (2020) NCBI taxonomy: a comprehensive update on curation, resources and tools. Database (Oxford) 2020: baaa062. https://doi.org/10.1093/database/baaa062

Seah YG, Ghaffar MA, Usup G (2008) Phylogeny of Ponyfishes from Coastal Waters of the South China Sea. Journal of Applied Biological Sciences 2(3): 125–132. https://dergipark.org.tr/en/pub/jabs/issue/34967/387982

Seth JK, Barik TK (2021) DNA barcoding of the family: Leiognathidae in the water of Bay of Bengal, Odisha coast, India based on 16s rRNA and COI gene sequences. Thalassas: An International Journal of Marine Sciences 37: 831-840. https://doi.org/10.1007/s41208-021-00324-1

Shen SC (1993) Fishes of Taiwan. Department of Zoology, National Taiwan University, Taipei, 960 pp.

Shen SJ, Wu GY (2011) Atlas of fishes in Taiwan. Taiwan University, Taipei, 896 pp.

Shi W, Wu B, Yu H (2018) The complete mitochondrial genome sequence of *Photopectoralis bindus* (Perciformes: Leiognathidae). Mitochondrial DNA, Part B, Resources 3(1): 71–72. https://doi.org/10.1080/23802359.2017.1422404

Sparks JS, Chakrabarty P (2015) Description of a new genus of ponyfishes (Teleostei: Leiognathidae), with a review of the current generic-level composition of the family. Zootaxa 3947(2): 181–190. https://doi.org/10.11646/zootaxa.3947.2.2

Sparks JS, Dunlap PV (2004) A clade of non-sexually dimorphic ponyfishes (Teleostei: Perciformes: Leiognathidae): phylogeny, taxonomy, and description of a new species. American Museum Novitates 3459: 1–21. https://doi.org/10.1206/0003-0082(2004)459<0001:ACONDP>2.0.CO;2

Sparks JS, Dunlap PV, Smith WL (2005) Evolution and diversification of a sexually dimorphic luminescent system in ponyfishes (Teleostei: Leiognathidae), including diagnoses for two new genera. Cladistics, 21(4), 305–327. https://doi.org/10.1111/j.1096-0031.2005.00067.x

Sui Y, Qin B, Song X, Sheng W, Zhang B (2019) Complete mitochondrial genome of the deep pugnose ponyfish *Secutor ruconius* (Perciformes: Leiognathidae) in the East China Sea. Mitochondrial DNA, Part B, Resources 4(2): 3563–3564. https://doi.org/10.1080/23802359.2019.1670108

Suzuki H, Kimura S (2023) Taxonomic revision of the genus *Equulites* Fowler 1904 (Acanthuriformes: Leiognathidae). Ichthyological Research 71: 213–259. https://doi.org/10.1007/s10228-023-00935-z

Temminck CJ, Schlegel H (1845) Pisces. In: Siebold PF de (Ed.) Fauna Japonica, sive descriptio animalium, quae in itinere per Japoniam suscepto annis 1823–1830 collegit, notis observationibus et adumbrationibus illustravit Ph. Fr. de Siebold. Lugduni Batavorum, Batavia, 324 pp.

Wang C, Ye P, Liu M, Zhang Y, Feng H, Liu J, Zhou H, Wang J, Chen X (2022) Comparative Analysis of Four Complete Mitochondrial Genomes of Epinephelidae (Perciformes). Genes 13(4): 660. https://doi.org/10.3390/genes13040660

Weber M, de Beaufort LF (1931) The fishes of the Indo-Australian Archipelago, Vol. 6. Perciformes (continued) Family: Serranidae, Theraponidae, Sillaginidae, Emmelichthyidae, Carangidae, Rachycentridae, Pomatomidae, Lactariidae, Menidae, Leiognathidae, Mullidae. EJ Brill, Leiden, 448 pp. https://doi.org/10.1163/9789004590144

White WT, Last PR, Dharmad, D, Faizah R, Chodriaah U, Prisantoso BI, Pogonoski JJ, Puckridge M, Blaber SJM (2013) Market fishes of Indonesia. Australian Centre for International Agricultural Research: Canberra, 438 pp.

Yan YR, Yi MR, Feng B (2021) Atlas Guide to Economic Fishes of South China Sea. Science Press, Beijing, 417 pp.

Yang Z, Bielawski JP (2000) Statistical methods for detecting molecular adaptation. Trends in Ecology & Evolution 15: 496–503. https://doi.org/10.1016/S0169-5347(00)01994-7

Yang H, Xia J, Zhang JE, Yang J, Zhao H, Wang Q, Sun J, Xue H, Wu Y, Chen J, Huang J, Liu L (2018) Characterization of the Complete Mitochondrial Genome Sequences of

Three Croakers (Perciformes, Sciaenidae) and Novel Insights into the Phylogenetics. International Journal of Molecular Sciences 19(6): 1741. https://doi.org/10.3390/ijms19061741

Zhang D, Gao F, Jakovlić I, Zhou H, Zhang J, Li WX, Wang GT (2020) PhyloSuite: An integrated and scalable desktop platform for streamlined molecular sequence data management and evolutionary phylogenetics studies. Molecular Ecology Resources 20(1): 348–355. https://doi.org/10.1111/1755-0998.13096

Zhang DX, Hewitt GM (1997) Insect mitochondrial control region: A review of its structure, evolution and usefulness in evolutionary studies. Biochemical Systematics and Ecology 25(2) 99–120. https://doi.org/10.1016/S0305-1978(96)00042-7

Zheng WL Leiognathidae (1962) The fishes of South China Sea. In: Institute Zoologica Academia Sinica, Institute Oceanology Academia Sinica, Shanghai Fish Collection (Eds) The fishes of South China Sea: Science Press, Beijing, 438–455.

Supplementary material 1

Supplementary file

Authors: Jiajie Chen, Xiaodong Wang, Sheng Zeng, Wei Tian, Deyuan Yang, Jinqing Ye, Junsheng Zhong, Chaopeng Jiang

Data type: zip

Explanation note: **figure S1.** *Leiognathus equula* was on sale at the landing ports (above) and fish markets (below) in Qinglan, Hainan, on November 9, 2023. **figure S2.** Dorsal head slightly triangular, *L. equula* DHS14327. Arrow indicates the nuchal spine. **figure S3.** Phylogenetic trees of Leiognathidae based on the *16S rRNA* dataset constructed using the Bayesian inference and maximum likelihood methods. **figure S4.** Phylogenetic trees of Leiognathidae based on the *COX1* dataset constructed using the Bayesian inference and maximum likelihood methods. **figure S5.** Phylogenetic trees of Leiognathidae based on the *ND5* dataset constructed using the Bayesian inference and maximum likelihood methods. **table S1.** Collection data for eight specimens of *L. equula*. **table S2.** Taxa used in the *16S rRNA* and *COX1* molecular phylogenetic analysis. **table S3.** Taxa sampled for the *ND5* phylogenetic analysis. **table S4.** Information on raw data and cleaned data from three specimens. **table S5.** List of mitogenomes included in the present study and their base composition and GenBank accession numbers. **table S6.** Morphometric and meristic data of *L. equula* in this study. **table S7.** Information on each gene fragment of *L. equula*. **table S8.** Base composition of the *L. equula* mitochondrial genome. **table S9.** Codon number and relative synonymous codon usage of *L. equula* mitochondrial protein-coding genes.

Link: https://doi.org/10.3897/zookeys.1219.130546.suppl1

ZooKeys 1219: 271–285 (2024)
DOI: 10.3897/zookeys.1219.134970

Research Article

Redescription of *Parascorpaena moultoni* (Whitley, 1961) (Actinopterygii, Scorpaenidae), with new distribution records for the species

Roxanne Cabebe-Barnuevo[1], Kunto Wibowo[2], Hiroyuki Motomura[3]

1 The United Graduate School of Agricultural Sciences, Kagoshima University, 1-21-24 Korimoto, Kagoshima 890-0065, Japan
2 Museum Zoologicum Bogoriense, Research Center for Biosystematics and Evolution, National Research and Innovation Agency, Cibinong 16911, Indonesia
3 The Kagoshima University Museum, 1-21-30 Korimoto, Kagoshima 890-0065, Japan
Corresponding author: Roxanne Cabebe-Barnuevo (k4964780@kadai.jp)

Abstract

Although the status of *Parascorpaena moultoni* (Whitley, 1961) is now well established, the morphology of the species has been re-examined, with new diagnostic features identified. Typically 15 or 16 pectoral-fin rays are present, together with two suborbital ridges, each with a single spine and the origin of the first ridge posterior to the second, well-developed interorbital ridges forming a loop, an undeveloped occipital pit, no scales on the dorsal- and anal-fin soft ray bases. The known range of the species includes Taiwan, the Philippines, Micronesia, Indonesia, Timor-Leste, Papua New Guinea, Solomon Islands, Vanuatu, and Fiji in addition to previously reported Australia, New Caledonia, and Japan.

Key words: COI, morphology, new record, *Scorpaena mcadamsi*, *Scorpaena moultoni*, scorpionfish

Academic editor: Tihomir Stefanov
Received: 18 August 2024
Accepted: 21 October 2024
Published: 4 December 2024

ZooBank: https://zoobank.org/ED2EB481-A793-4E06-8E8E-4778B77B1CA1

Citation: Cabebe-Barnuevo R, Wibowo K, Motomura H (2024) Redescription of *Parascorpaena moultoni* (Whitley, 1961) (Actinopterygii, Scorpaenidae), with new distribution records for the species. ZooKeys 1219: 271–285. https://doi.org/10.3897/zookeys.1219.134970

Introduction

Scorpaena moultoni Whitley, 1961 was originally described from a single specimen collected north of Wilson Island, Capricorn Group, Queensland, Australia, in a depth of ca 15 m. Allen and Cross (1989) later reported the species from the Great Barrier Reef, Queensland. Although Allen et al. (2006) synonymized *S. moultoni* with *Parascorpaena mcadamsi* (Fowler, 1938), without significant justification, Motomura et al. (2011) later validated the taxonomic status of the former, reinstating it as a distinct species, and reported an additional record which extended the known distribution range to New Caledonia. Fricke et al. (2011) provided a detailed distribution within New Caledonia, encompassing Grand Passage (Îles Bélep and northern lagoon) and Grande Terre (northern and southern regions), and subsequent reports from Japan (Tsuno et al. 2022; Mochizuki et al. 2023) have further documented the species off various islands. Based on these published reports, *P. moultoni* has been considered as widely distributed in the western Pacific, from the Ryukyu Islands north to Kochi Prefecture in Japan, and southward to northern Australia and New Caledonia.

This study addresses discrepancies between the original description of *P. moultoni* by Whitley (1961) and features observed in examined specimens, so as to provide a revised morphological description for more accurately distinguishing *P. moultoni* from other valid species within the genus *Parascorpaena*. The examination of many voucher specimens confirmed the wide distribution of *P. moultoni* across the western Pacific Ocean (see below).

Materials and methods

Counts and measurements followed Motomura (2004a, 2004b), Motomura et al. (2005a, 2005b, 2005c, 2006a, 2006b, 2009), and Motomura and Johnson (2006). Standard length (**SL**), head length (**HL**), and morphometrics were measured to the nearest 0.1 mm using digital calipers. Head spine terminology follows Motomura et al. (2009) and Wibowo and Motomura (2021). Curatorial procedures for KAUM specimens followed Motomura and Ishihara (2013).

Phylogenetic relationships among the two closely related species, *Parascorpaena mcadamsi* and *P*. *moultoni*, with *Caracanthus maculatus* (Gray, 1831) serving as the outgroup, were elucidated using MEGA 11 software (Tamura et al. 2021). Analysis applied the Kimura 2-parameter model (Kimura 1980) with 1000 bootstrap replications (Felsenstein 1985) to construct a maximum likelihood tree. All cytochrome oxidase subunit I (COI) sequences used in this study were obtained from BOLD (Barcode of Life Data System) and GenBank databases, including some generated from our previous study (Cabebe-Barnuevo et al. 2024), with accession and voucher numbers listed in Table 1.

Table 1. List of COI sequences utilized in the study.

Species identification	BOLD/GenBank accession number	Specimen voucher code
Caracanthus maculatus	PP683413	KAUM–I. 169070
Parascorpaena mcadamsi	LC745944	KAUM–I. 115044
*Parascorpaena mcadamsi**	PHILA1448-15	USNM 431877
*Parascorpaena mcadamsi**	PHILV495-15	USNM 436361
Parascorpaena moultoni	LC745946	KAUM–I. 72114

* Re-identified as *P. moultoni* based on morphological and molecular data (see Discussion).

Comparative material

Caracanthus maculatus: KAUM–I. 169070, 22.8 mm SL, Nazumado, Okago, Hachijo-jima Island, Izu Islands, Tokyo, Japan, 33°08'25"N, 139°44'11"E, 5–20 m, Y. Dewa and M. C. Sato, 10 June 2022. *Parascorpaena armata* (Sauvage, 1873): KAUM–I. 66443, 82.1 mm SL, off Maigo Fishing Port, Tanegashima Island, Osumi Islands, Kagoshima, Japan, 30°37'24"N, 130°56'31"E 2–8 m. *Parascorpaena aurita* (Rüppell, 1838): KAUM–I. 161814, 44.2 mm SL, off Bandokorobana National Park, Beppu, Ei, Minami-kyushu, Kagoshima, Japan, 31°14'50"N, 130°26'E, 0.3 m, N. Kukita, 23 Oct. 2021; MZB 5564, 79.3 mm SL, off Baluran, Situbondo Regency, East Java, Indonesia, July 1984. *Parascorpaena maculipinnis* Smith, 1957: SAIAB 395, paratype of *Parascorpaena maculipinnis*, 43.5 mm SL, Mozambique, Sept. 1953. *Parascorpaena mcadamsi*: KAUM–I. 115044, 43.7 mm

SL, south of Kiriishi Port, Suwanee-jima Island, Tokara Islands, Ryukyu Islands, Japan, 29°36'34"N, 129°42'50"E, 15–18 m, S. Tashiro et al., 26 Apr. 2018; MZB 26976, 37.1 mm SL, Batu Lompa Island, Tulehu, Ambon Island, Maluku, Indonesia, 03°35'41.2"S, 128°21'16.1"E, 15 m, K. Wibowo, 7 Nov. 2023; MZB 26978, 27.6 mm SL, Hukurila, Ambon Island, Maluku, Indonesia, 03°44'36.4"S, 128°14'29.0"E, 10 m, 12 Nov. 2023, K. Wibowo, 12 Nov. 2023; USNM 98904, holotype of *Scorpaena mcadamsi*, 37.6 mm SL, vicinity of Jola Island, Sulu Archipelago, Philippines, 06°03'45"N, 120°57'E, 36.6 m, RV *Albatross*, 5 Mar. 1908. *Parascorpaena mossambica* (Peters, 1855): ANSP 162881, 2 specimens, 25.2–38.4 mm SL, off north end of West Island, Cocos (Keeling) Islands, 12°08'36"S, 96°48'55"E, 7–8 m, W. F. Smith-Vaniz et al., 24 Feb. 1974. *Parascorpaena picta* (Cuvier, 1829): MZB 26990, 82.4 mm SL, Nusi Island, Biak Islands, West Papua, Indonesia, 8 Aug. 1961; NSMT-P 100290, 36.0 mm SL, Dadonghai, Hainan, China, K. Matsuura. *Parascorpaena poseidon* Chou & Liao, 2022: ANSP 51367, 95.2 mm SL, Vigan, Ilocos Sur, Luzon, Philippines, 17°34'13"N, 120°23'01"E, J. Clemens, 1923.

Museum acronyms

AMS	Australian Museum, Sydney
ANSP	Academy of Natural Sciences of Drexel University, Philadelphia
BPBM	Bernice P. Bishop Museum, Honolulu
CAS/SU	California Academy of Sciences, San Francisco
KAUM	Kagoshima University Museum, Kagoshima
MZB	Museum Zoologicum Bogoriense, Cibinong
NSMT	National Museum of Nature and Science, Tsukuba
ROM	Royal Ontario Museum, Toronto
SAIAB	South African Institute for Aquatic Biodiversity, Makhanda
URM	Department of Marine Sciences, Faculty of Science, University of the Ryukyus, Okinawa
USNM	Museum Support Center, Smithsonian Institute, National Museum of Natural History, Suitland

Results

Parascorpaena moultoni **(Whitley, 1961)**

Figs 1–3; Tables 1, 2
Moulton's Scorpionfish

Scorpaena moultoni Whitley, 1961: 9, fig. 1 (type locality: north of Wilson Island, Capricorn Group, Queensland, Australia).

Material examined. ***Holotype.*** AMS IB. 5062 (Fig. 1A), female, 38.1 mm SL, north of Wilson Island, Capricorn Group, Queensland, Australia, 23°18'S, 151°54'E, 15 m, J. Moulton, 19 Oct. 1960. ***Paratype.*** USNM 99013, female, 27.5 mm SL, Davao Gulf, Mindanao, Philippines, 17°05'42"N, 125°39'42"E, 38 m, RV *Albatross*, 18 Mar. 1908.

Non-type specimens. 46 specimens, 20.4–57.1 mm SL. **Japan:** KAUM–I. 72114, male, 60.9 mm SL, north of Sanekumisaki, Setouchi, Amami-oshima Island, Amami Islands, Ryukyu Islands, 28°11'43"N, 129°11'32"E, 10–24 m;

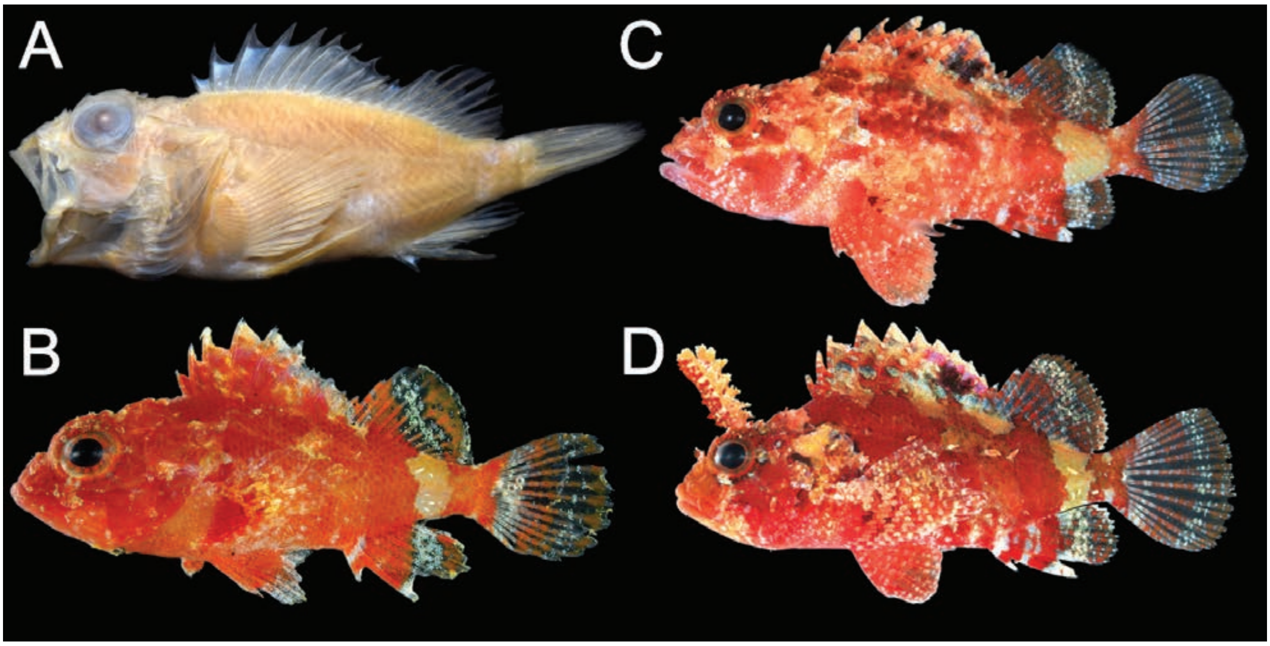

Figure 1. *Parascorpaena moultoni* **A** AMS IB. 5062 (holotype of *Scorpaena moultoni*), female, 38.1 mm SL, Australia **B** KAUM–I. 82275, female, 16.7 mm SL, Japan **C** MZB 26975, male, 35.5 mm SL, Indonesia **D** KAUM–I. 124499, male, 37.0 mm SL, Japan.

KAUM–I. 82275, female, 16.7 mm SL, San, Tokunoshima, Tokuno-shima Island, Amami Islands, 27°51'22"N, 128°58'02"E, 1–18 m, H. Motomura et al., 25 Nov. 2015; KAUM–I. 124499, male, 37.0 mm SL, off Segaura, Kushi, Bounotsu, Minami-satsuma, Kagoshima, 31°15'12"N, 130°13'35"E, 6 m, S. Morishita, 17 Dec. 2018; URM-P 4243, female, 21.1 mm SL, southwest reef off Sesoko Island, Okinawa Islands, Ryukyu Islands, 25 Oct. 1974. **Taiwan:** BPBM 23054, 43.5 mm SL, Yeh-liu, 17 m, J. E. Randall, 26 June 1978; BPBM 23385, 44.4 mm SL, southern end of Mao Pi Tou, 15 m, J. E. Randall et al., 18 July 1978. **Philippines:** BPBM 22133, male, 39.2 mm SL, Sumilon Island, Cebu, 24–26 m, J. E. Randall, 26 Aug. 1977; BPBM 22456, male, 27.8 mm SL, southwest side of Caban, Luzon, 30 m, J. E. Randall et al., 28 July 1978; BPBM 26511, female, 57.1 mm SL, Negros, south of Dumaguete, 22 m, J. E. Randall and G. W. Tribble, 9 Aug. 1978; USNM 372639, male, 26.9 mm SL, Sombrero Island, Batangas, 13°42'N, 120°49'12"E, 6 m, C. J. Ferraris, 24 Apr. 1980; USNM 372667, 37.7 mm SL, Apo Island, Negros Oriental, 09°04'38"N, 123°16'44"E, 0–40 m, V. Springer et al., 7 June 1978; USNM 372668, 2, 30.6–44.6 mm SL, Bararin Island, Palawan, 10°52'42"N, 120°56'46"E, 0–17 m, V. Springer et al., 24 May 1978; USNM 372704, 24.2 mm SL, Siquijor Island, Visayas, 09°08'30"N, 123°29'20"E, 0–6 m, V. Springer et al., 9 May 1978; USNM 431877, male, 20.4 mm SL, Maricaban Island, Batangas, 13°40'12"N, 120°51'04"E, 3–6 m, K. Carpenter et al., 29 Apr. 2014; USNM 436361, 38.2 mm SL, Verde Island, Batangas, 13°34'02"N, 121°02'31"E, 15–20 m, J. T. Williams et al., 23 Apr. 2015. **Micronesia:** BPBM 24669, 5, 20.7–31.8 mm SL, Condor Reef, Caroline Islands, 20–25 fa (36.6–45.6 m), R/V *Townsend Cromwell*, cruise 57, 23 Mar. 1972; CAS 66742, 31.8 mm SL, Ulithi Atoll, Fassarao Island, 09°55'05"N, 139°40'E, 7–25 ft (2.1–7.6 m), B. Daniel, 23 Sept. 1956. **Indonesia:** MZB 26975, male, 35.5 mm SL, Liran Island, Wetar Islands, Maluku, 08°03'03"S, 125°44'52"E, 12 m, K. Wibowo, 1 Mar. 2022; USNM 218670, 3, 23.9–26.9 mm SL, Kasa Island, Maluku, 03°18'S, 128°07'48"E, 0–1 m, V. Springer et al., 4 Mar. 1974; USNM 218671, 2, 25.4–32.1 mm SL, same data as USNM 218670; USNM

372620, 32.0 mm SL, Halmahera, North Maluku, 01°04'12"N, 127°58'48"E, H. Singou, Apr.–May 1978. **Timor-Leste:** AMS I. 46120-045, female, 34.2 mm SL, east of Dili, halfway between Hera and Metinaro, 08°31'01"S, 125°42'05"E, M. McGrouther, 23 Sept. 2012; AMS I. 46119-039, 2, female, 27.1–30.7 mm SL, off Metinaro, 08°30'25"S, 125°45'59"E, M. McGrouther, 22 Sept. 2012. **Papua New Guinea:** CAS 207711, 25.6 mm SL, Madang Harbor, Madang Province, 05°10'51"S, 145°49'41"E, 30–35 ft (9.1–10.7 m), B. Collette, 26 May 1970; USNM 380287, 40.1 mm SL, Massas Island, 05°10'18"S, 145°51'25"E, 0–18 m, V. Springer et al., 6 Nov. 1978. **Solomon Islands:** ROM 42275, male, 37.1 mm SL, Guadalcanal Island, 09°20'S, 159°45'E, P. Nichols and D. Evans, 24 Apr. 1983; USNM 266477, 32.1 mm SL, New Georgia, W. M. Chapman, 4 June 1944. **Vanuatu:** AMS I. 17472-048, female, 29.9 mm SL, Efate Island, Malapoa Peninsula, 17°44'S, 168°17'E, G. R. Allen, 22 June 1973. **Fiji:** BPBM 11354, female, 47.2 mm SL, Viti Levu Island, 18°08'28"S, 178°22'52"E, 8–20 ft (2.4–6.1 m), J. E. Randall et al., 7 Aug. 1971; BPBM 39774, male, 48.0 mm SL, Viti Levu Island, 18°09'35"S, 178°23'58"E, 35–47 ft (10.7–14.3 m), R. L. Pyle et al., 29 Jan. 2002; BPBM 39891, female, 27.7 mm SL, Viti Levu Island, 18°09'51"S, 178°24'01"E, 60 ft (18.3 m), J. L. Earle and D. F. Pence, 31 Jan. 2002; CAS 206979, female, 41.1 mm SL, Viwa Island, 17°12'S, 176°54'E, 70–100 ft (21.3–30.5 m), V. Springer et al., 27 May 1982; CAS 214143, male, 52.5 mm SL, female, 42.8 mm SL, Viti Levu Island, 18°08'38"S, 178°22'49"E, 63 ft (19.2 m), D. W. Greenfield and K. Cole, 2 June 1999; CAS 218624, male, 39.3 mm SL, female, 24.5 mm SL, Viti Levu Island, 18°09'02"S, 178°21'37"E, 10–26 ft (3.0–7.9 m), D. W. Greenfield et al., 12 Feb. 2002; ROM 51930, female, 35.5 mm SL, Great Astrolabe Reef, 18°46'S, 178°28'05"E, R. Winterbottom et al., 5 Apr. 1983.

Diagnosis. A species of *Parascorpaena* with the following characters: pectoral-fin rays 15–17 (usually 15 or 16); pored lateral-line scales 20–22 (mode 21); scale rows in longitudinal series 40–48 (41); scale rows above lateral line 5–8 (7); scale rows below lateral line 10–12 (12); scale rows between sixth dorsal-fin spine base and lateral line 5 or 6 (6); scale rows between last dorsal-fin spine base and lateral line 5 or 6 (5); total gill rakers 12–14 (12); two suborbital ridges, each with one spine; origin of first suborbital ridge posterior to origin of second ridge; interorbital ridges well developed posteriorly from middle of eye, forming a broad loop on rear end, enclosed concavity relatively shallow; occipital pit not developed, almost flat; no scales along dorsal- and anal-fin soft ray bases; black botch on spinous portion of dorsal fin in males, usually found along 7th–10th spines.

Description. Measurements of examined specimens, expressed as percentages of SL and HL, provided in Table 2. Body size small, compressed, with numerous widely scattered papillae; body depth greatest at pelvic-fin spine base. Lateral line complete, pored lateral-line scales continuing onto caudal-fin base (except in small specimens). Head size moderate, length less than half SL, with scattered papillae. Snout moderately blunt; dorsal profile steep. Eyes large, diameter slightly greater than snout length. Mouth large, maxilla extending just below posterior margin of eye. Four prominent pairs of mandibular pores on dentary, first pore positioned just behind tip of lower jaw, second along anterior lacrimal spine, third along posterior lacrimal spine, and fourth behind posterior lacrimal spine (before posterior end of maxilla). Teeth on upper jaw villiform; teeth on lower jaw varying among specimens, from entirely villiform to villiform with enlarged or canine-like teeth on frontal area; teeth on palatines small, villiform, in

Table 2. Counts and proportional measurements (expressed as percentages of standard and head lengths) of *Parascorpaena moultoni*.

	AMS IB 5062 Holotype of *S. moultoni*	**USNM 99013 Paratype of *S. mcadamsi***	**Non-type specimens (*n* = 23)**
Standard length (SL)	38.1	27.5	20.7–57.1
Head length (HL)	17.4	11.4	9.8–25.2
Counts			
Dorsal-fin rays	XII, 9	XII, 9	XII, 9
Anal-fin rays	III, 5	III, 5	III, 5
Pectoral-fin rays (left/right sides)	15/15	16/damaged	15–17/15–17 (mode 16/16)
Pored lateral-line scales	21	20	20–22 (21)
Scale rows in longitudinal series	43	42	40–48 (43)
Scale rows above lateral line	7	6	5–8 (6)
Scale rows below lateral line	10	10	10–12 (11)
Scale rows between 6th dorsal-fin spine base and lateral line	5	5	5–6 (6)
Scale rows between last dorsal-fin spine base and lateral line	5	5	5–6 (5)
Pre-dorsal-fin scale rows	3	4	3–4 (3)
Total gill rakers	11	13	11–14 (12)
Gill rakers (lower + hypobranchial)	7	8	7–10 (8)
Gill rakers (upper)	4	5	4–5 (4)
Measurements (% SL)			
Body depth at pelvic-fin spine base	36.2	36.5	32.4–38.2
Body depth at first anal-fin spine base	30.2	28.3	26.2–33.7
Body width	15.8	13.7	8.2–20.1
Predorsal-fin length	39.4	38.0	36.5–49.3
Preanal-fin length	73.4	73.8	66.3–76.1
Prepelvic-fin length	52.2	41.3	35.2–49.3
Pectoral-fin ray length	32.8	damaged	28.7–45.0
1st dorsal-fin spine length	4.8	8.5	3.5–9.7
2nd dorsal-fin spine length	8.8	13.0	9.2–13.9
3rd dorsal-fin spine length	14.8	17.3	14.2–20.3
4th dorsal-fin spine length	17.6	20.1	15.1–21.1
5th dorsal-fin spine length	17.8	19.4	15.6–20.9
11th dorsal-fin spine length	9.7	10.3	7.6–12.7
12th dorsal-fin spine	14.4	16.3	12.1–17.5
Longest dorsal-fin soft ray length	18.4	damaged	16.9–22.4
1st anal-fin spine length	7.0	10.5	8.5–12.3
2nd anal-fin spine length	21.2	23.0	16.9–27.1
3rd anal-fin spine length	16.5	18.7	15.5–21.2
Longest anal-fin soft ray length	20.2	21.0	18.7–24.9
Pelvic-fin spine length	16.5	17.4	15.7–19.2
Longest pelvic-fin soft ray length	25.2	26.1	22.1–30.2
Caudal-fin length	23.1	24.1	24.8–32.1
Caudal-peduncle depth	9.5	9.8	7.5–11.5

	AMS IB 5062 **Holotype of *S. moultoni***	**USNM 99013** **Paratype of *S. mcadamsi***	**Non-type specimens (*n* = 23)**
Caudal-peduncle length	13.4	18.2	9.6–16.7
Head length	45.6	41.4	42.2–51.6
Measurements (% HL)			
Head width	49.4	55.8	31.4–50.0
Snout length	35.6	27.2	23.4–33.5
Eye diameter	33.2	34.5	28.7–38.8
Interorbital width at vertical midline of eye	12.4	15.4	10.9–17.2
Interorbital width at posterior end of preocular spine base	9.8	14.8	9.7–14.7
Upper-jaw length	46.7	53.3	44.2–55.2
Maxillary depth	14.0	15.6	14.8–20.5
Postorbital length	42.2	46.7	45.7–53.8
Distance between opercular spine tips	13.4	14.5	11.1–15.3
Supraocular-tentacle length	6.9	absent	3.2–30.6

bands; teeth on vomerine villiform, in V-shaped patch. Body entirely covered with cycloid scales (rarely with weak ctenii); body scales not extending to dorsal- and anal-fin soft ray membranes; head mostly naked, a few, small scales behind posterior margin of eye, along posterior end of operculum, and just behind opercular spines; dentary smooth, naked.

Dorsal-fin spines usually 12 (rarely 13) connected to soft rays; fourth or fifth spine longest; sixth to 11th spine gradually decreasing in size; 12th spine elongated, followed by nine (rarely 8) branched soft rays; second dorsal-fin soft ray usually longest; 7th–10th dorsal spines bearing black blotch in male specimens. Anal-fin spines three, second spine longest; five branched soft rays. Bases of both dorsal- and anal-fin soft rays without scales. Pectoral-fin rays usually 15 or 16 (rarely 17); first (uppermost) ray simple, unbranched; second to fifth or sixth ray branched; lower rays thickened, unbranched; tips of fins reaching beyond origin of anal-fin spine. All pectoral-fin rays in small specimens (e.g., <20.0 mm SL) unbranched. Pelvic-fin length variable, not or just reaching anal-fin spine base.

Nasal spines positioned bilaterally on nasal ridge, extending slightly beyond rim. Preocular spine relatively thick, with broad base, located anteriorly within orbital region. Interorbital ridge originating either from above anterior half of eye, or along preocular spine base, extending beyond posterior eye margin; rear end of ridge forming a broad, very shallow interorbital loop. Occipital pit indistinct, almost flat. Supraocular and postocular spines situated above orbital region, close to one another. Supraocular spines each occasionally bearing a single, variably sized tentacle, sometimes small but usually longer than eye diameter. Tympanic spines simple, just behind postocular spine, usually separated by distance greater than that between parietal and nuchal spines. Parietal and nuchal spines simple, close to one another; parietal spine originating posterior to origin of pterotic spine; nuchal spine originating just behind parietal spine. Sphenotic spine just behind posterior margin of eye, small, usually as unevenly sized pair (rarely single). Pterotic spine simple, attached to skin, situated just behind sphenotic spine. Upper and lower post-temporal spines well-developed, upper spine shorter than and positioned just above lower spine, lower spine situated between pterotic and supracleithral spines. Suborbital with two distinct ridges, a suborbital spine on each ridge. Lacrimal bone dorsally with two distinct ridges; anterior lacrimal ridge located before anterior eye margin, longer than posterior lacrimal ridge; posterior ridge located just behind origin of first suborbital ridge (just below ventral eye margin). Anterior and posterior lacrimal spines located along ventral region of lacrimal bone, simple with no additional spinous points; anterior lacrimal spine prominently antrorse, tip not extending beyond lower lip; posterior lacrimal spine distinctly anteriorly oriented in larger specimens (>24.5 mm SL), ventrally oriented with forward curvature in smaller specimens to ~ 20 mm SL, postero-ventrally oriented in specimens <20 mm SL. Preopercular spines five; first and second along posterior margin of maxilla, covered with thick skin, usually with small tentacles; third to fifth exposed, progressively longer, fifth longest with small anterior supplemental preopercular spine. Opercular spines just behind pre-opercular margin; upper opercular spine slightly longer than lower opercular spine. Supracleithral spine single, short, located between upper and lower post-temporal spines (closer to latter). Cleithral spine simple, base covered by operculum; spinous point not extending beyond posteriormost tip of operculum. Postorbital spine usually absent; if present, lump-like, lacking a spinous point. Median interorbital ridge, coronal spine, ridge on lateral surface of maxilla, antero-dorsal lacrimal spines, and lateral lacrimal spine all absent.

Color of fresh specimens. Based on color photographs of three specimens deposited at KAUM and MZB (Fig. 1B–D). Body variegated, predominantly orange-red with interspersed darker red and white blotches. White areas particularly apparent near dorsal region and caudal peduncle. Head predominantly reddish, with numerous orange and white blotches; underside white with reddish mottling along jawline. Spinous portion of dorsal fin variegated orange, reddish, and white; a distinct black blotch on 7th–10th spines in males. Soft-rayed portion of dorsal fin translucent white, with poorly defined orange-red and white blotches. Pectoral fin translucent with poorly defined reddish and white blotches. Pelvic fin orange-red at base, transitioning to white distally. Anal fin primarily orange-red, with poorly defined white blotches. Caudal fin translucent with three orange-red bands; first band on base, second in middle, and third on distal margin.

Color of preserved specimens. Body and ventral surface yellowish-white. Head typically white; some specimens with poorly defined dark blotches. Spinous portion of dorsal fin translucent; distinct black blotch retained in males. Soft-rayed portion of dorsal fin usually translucent; some specimens with poorly defined dark blotches. Anal, pectoral, and pelvic fins usually entirely translucent, with poorly defined dark blotches in some specimens. Caudal fin generally translucent, dark bands apparent in some specimens.

Distribution. *Parascorpaena moultoni* has been previously recorded from Queensland, Australia (Whitley 1961; Allen and Cross 1989), New Caledonia (Motomura et al. 2011; Fricke et al. 2011, 2015), and Japan (Motomura 2013, 2019, 2022, 2023; Motomura and Harazaki 2017; Kimura et al. 2017; Nakae et al. 2018; Mochida and Motomura 2018; Tanaka et al. 2020; Jeong and Motomura 2021; Tsuno et al. 2022; Mochizuki et al. 2023). The voucher specimens examined here extended the confirmed distribution of the species to include Taiwan, the Philippines, Micronesia, Indonesia, Timor-Leste, Papua New Guinea, the Solomon Islands, Vanuatu, and Fiji (Fig. 2).

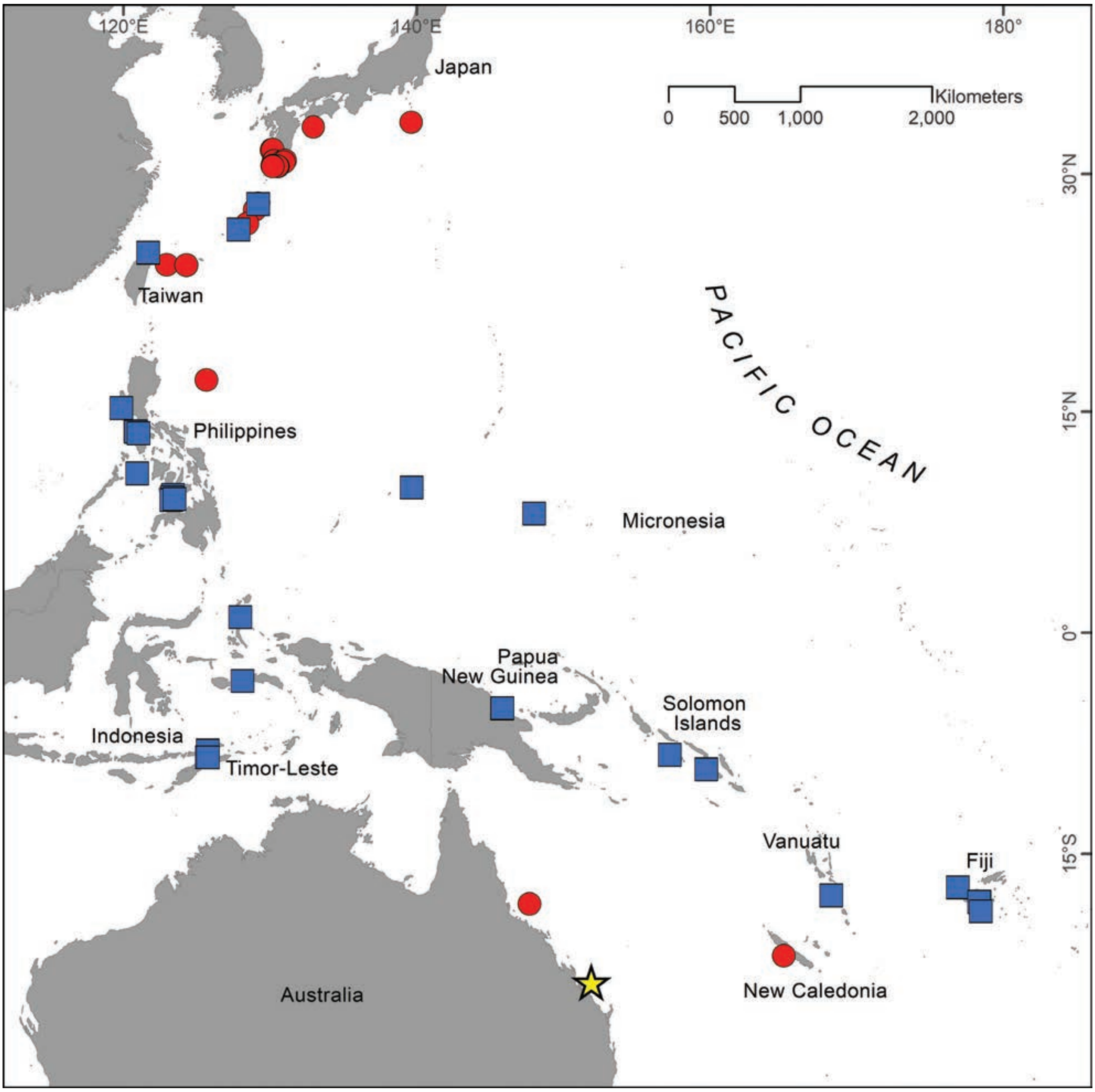

Figure 2. Geographic distribution of *Parascorpaena moultoni* in the Pacific Ocean. Type locality (star); previous reports (circles); new records (squares; this study).

Discussion

This study largely corroborated Whitley's (1961) original description of *Scorpaena moultoni*. However, although Whitley (1961) described the holotype of *Scorpaena moultoni* as lacking supraorbital tentacles (supraocular tentacles in this study), examination of the holotype revealed the presence of short tentacles. Furthermore, the condition of the supraocular tentacles varied among other specimens, sometimes being small but more commonly elongated, usually exceeding the eye diameter. Dental morphology also varied among specimens, the upper-jaw teeth being consistently villiform, whereas those on the lower jaw varied from entirely villiform to enlarged or canine-like teeth anteriorly. The sexual dimorphism seen in *P. mcadamsi*, male specimens having canine-like teeth anteriorly and females only villiform teeth, was not apparent in *P. moultoni* (see Mochizuki et al. 2023). Although Whitley (1961) described undeveloped sphenotic spines, the holotype of *P. moultoni* in fact had two well-developed sphenotic spines. Moreover, the non-type specimens examined typically exhibited one or two sphenotic spines, being unequally-sized in the case of two present. Whitley (1961) also noted that the "upper profile behind the eye is not deeply notched", which refers to the occipital pit, described here as indistinct.

Whitley (1961) initially differentiated *P. moultoni* from its congeners based on several features, including pale coloration, naked head, short maxillary, large scales, absence of dermal flaps, and presence of a few predorsal scales. However, these characters also occur in other species of *Parascorpaena*, making them unsuitable for reliable identification of the former. Although Whitley (1961) also mentioned that *P. moultoni* had two suborbital spines, he did not regard that feature as a significant distinguishing trait. However, after *P. moultoni* had been synonymized with *P. mcadamsi* by Allen et al. (2006), it was later reinstated as a distinct species by Motomura et al. (2011), who emphasized the number of suborbital spines as the key differentiating character from *P. mcadamsi*.

Among the eight valid species of *Parascorpaena* (see Cabebe-Barnuevo et al. 2024), only *P. mcadamsi* and *P. moultoni* exhibit sexual dichromatism, characterized by a black blotch on the 7th–10th dorsal-fin spines in males, such being absent in females (Eschmeyer 1986; Poss 1999; Poss and Motomura 2022; Mochizuki et al. 2023). Examination of the type specimens of *P. mcadamsi* revealed that one of the two paratypes (USNM 99013) was, in fact, *P. moultoni*, distinguishable from the holotype by the number of suborbital spines – two in USNM 99013 and three in the holotype (USNM 98904).

Parascorpaena moultoni is clearly differentiated from *P. armata*, *P. mossambica*, and *P. poseidon* by its two suborbital spines and indistinct occipital pit, whereas the latter three species possess three suborbital spines and a well-developed occipital pit. Although *P. moultoni* shares the same number of suborbital spines with *P. aurita* and *P. picta*, it differs in having a single spine on each suborbital ridge, compared to the absence of a spinous point on the first ridge and presence of two spines on the second ridge in the latter two species, and can further be differentiated by the absence of scales below the dorsal- and anal-fin soft ray bases, which are present in *P*. *aurita* and *P*. *picta*. Moreover, while *P. moultoni* resembles *P. maculipinnis* and *P. mcadamsi* in having an undefined occipital pit, the interorbital ridge posteriorly forming a loop, naked dorsal- and anal-fin soft ray bases, and the origin of the first ridge posterior to the second, the former has only two suborbital spines, compared to the three spines (one on the first ridge and two on the second) found in the latter two species. Consequently, this study affirms that *P. moultoni* can be consistently distinguished from other species of *Parascorpaena* based on occipital pit morphology and the number of suborbital spines.

Cabebe-Barnuevo et al. (2024) compared the orientation of the posterior lacrimal spine (PLS) across differing size categories within the genus *Parascorpaena* and identified three distinct orientations. In the largest individuals, with standard lengths (SLs) of 118.0 mm and 121.4 mm, the PLS was oriented anteriorly. However, in smaller individuals with SLs to 21 mm, the PLS was oriented ventrally with an anterior curvature. The smallest individuals, measuring less than 20 mm SL, exhibited postero-ventral orientation of the PLS. Similar differing orientations of the PLS with size categories were found in *P. moultoni*,

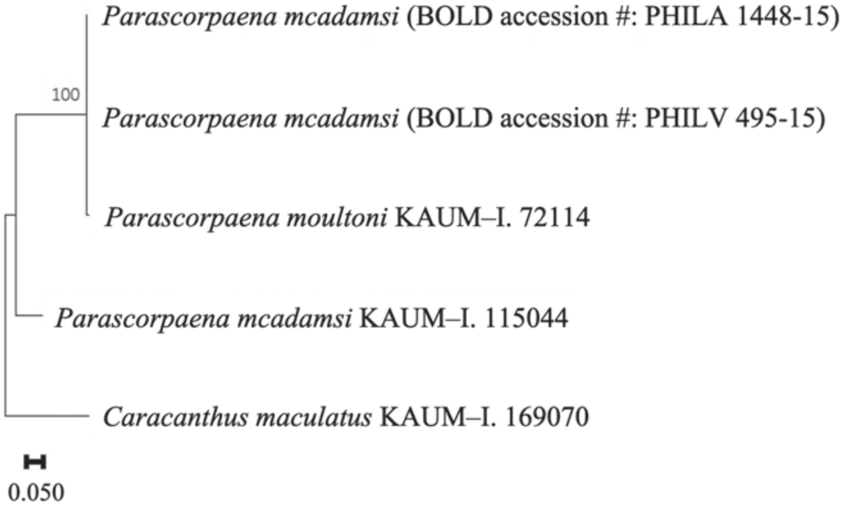

Figure 3. Maximum likelihood phylogenetic tree of COI sequences using the Kimura 2-parameter model, with *Caracanthus maculatus* as outgroup. Node values indicate bootstrap support based on 1,000 replicates.

although the largest recorded specimen of that species was substantially smaller at 57.1 mm SL (this study). Specimens of 24.5–57.1 mm SL had an anteriorly oriented PLS, smaller specimens being characterized by either ventral (e.g., 21.08 mm SL) or postero-ventral (e.g., <20 mm SL) orientation. Clearly, similar growth-related variations in PLS orientation are characteristic of species of *Parascorpaena*, regardless of the maximum size attainable by each.

Cytochrome oxidase subunit I (COI) sequences from KAUM specimens, deposited in GenBank, were utilized to verify the identification of some sequences of *Parascorpaena*. This analysis (Fig. 3) specifically focused on sequences from BOLD and GenBank data originally identified as *P. mcadamsi*, but which were subsequently determined to represent *P. moultoni*. Given that *P. moultoni* was previously regarded as a synonym of *P. mcadamsi*, it is unsurprising that some sequences in public databases (e.g., BOLD) initially identified as *P. mcadamsi* are actually of *P. moultoni*. This study confirmed that sequences with accession numbers PHILA 1448-15 and PHILV 495-15, initially identified as *P. mcadamsi*, represent a single clade together with the sequence of a verified specimen of *P. moultoni* (KAUM–I. 72114), being distinct from the sequence of a verified specimen of *P. mcadamsi* (KAUM–I. 115044). Morphological examination of the voucher specimens for both PHILA 1448-15 and PHILV 495-15 revealed that both specimens had only two suborbital spines, an interorbital ridge forming a loop, an indistinct occipital pit, a black blotch on the 7th–10th dorsal-fin spines, a strongly anteriorly oriented PLS, and cycloid scales, all being consistent with *P. moultoni*. Clearly, gene sequences in public databases, together with associated voucher specimens, should remain under review so as to lessen the likelihood of mistakenly identified sequences and problems arising therefrom.

Acknowledgements

We extend our sincere gratitude to the staff at various institutions for their invaluable contributions to this study. We thank M. McGrouther, A. Hay, K. Parkinso, and S. Reader (AMS), M. Sabaj and M. Arce (ANSP), A. Y. Suzumoto, C. J. Atta, and L. O'Hara (BPBM), D. Catania and M. Hoang (CAS), G. Shinohara,

M. Nakae, K. Fujiwara, and M. Sato (NSMT), R. Winterbottom, D. Stacey, and N. Lujan (ROM), R. Bills, E. Heemstra, O. Gon and M. Dwani (SAIAB), T. Yoshino (formerly URM), and J. Williams, L. Palmer, S. Raredon, K. Murphy, D. Pitassy, K. Bemis, A. Nonaka, and A. Reft (USNM) for opportunities to examine material. We also thank all volunteers, graduates, and students of KAUM for their assistance with specimen collection and curatorial support, and are also grateful to G. Hardy (Ngunguru, New Zealand) for reading the manuscript and assisting with English. We appreciated the invaluable feedback from anonymous reviewers and editors that significantly improved the manuscript. This research forms part of the first author's dissertation. All authors consented to the publication of this article and inclusion in the dissertation submission.

Additional information

Conflict of interest

The authors have declared that no competing interests exist.

Ethical statement

No ethical statement was reported.

Funding

This study was financially supported in part by JSPS KAKENHI Grant Numbers 20H03311, 21H03651, 23K20304, and 24K02087; the JSPS Core-to-core CREPSUM JPJSCCB20200009; and the "Establishment of Glocal Research and Education Network in the Amami Islands" project of Kagoshima University, adopted by the Ministry of Education, Culture, Sports, Science and Technology, Japan.

Author contributions

Conceptualization: RCB, KW, HM. Data curation: RCB, KW, HM. Formal analysis: RCB. Funding acquisition: HM. Investigation: RCB, KW, HM. Resources: KW, HM. Supervision: HM. Visualization: RCB, KW. Project administration: HM. Writing – original draft: RCB. Writing – review and editing: RCB, KW, HM.

Author ORCIDs

Roxanne Cabebe-Barnuevo https://orcid.org/0000-0001-6518-7986
Kunto Wibowo https://orcid.org/0000-0003-4465-3022
Hiroyuki Motomura https://orcid.org/0000-0002-7448-2482

Data availability

All of the data that support the findings of this study are available in the main text.

References

Allen GR, Cross NJ (1989) Scorpaenidae. In: Paxton JR, Hoese DF, Allen GR, Hanley JE (Eds) Zoological catalogue of Australia. Vol. 7. Pisces. Petromyzontidae to Carangidae. Australian Government Publishing Service, Canberra, 438–452.

Allen GR, Cross NJ, Bray DJ, Hoese DF (2006) Scorpaeninae. Scorpionfishes. In: Hoese DF, Bray DJ, Paxton JR, Allen GR (Eds) Zoological Catalogue of Australia. Vol. 35. Fishes. Parts 1–3. CSIRO Publishing, Collingwood, 881–892.

Cabebe-Barnuevo R, Mochizuki K, Motomura H (2024) Monophyly and re-definition of the Indo-Pacific scorpionfish genus *Parascorpaena* Bleeker 1876 (Scorpaenidae). Ichthyological Research, 1–12. https://doi.org/10.1007/s10228-024-00991-z

Chou T-K, Liao T-Y (2022) A new species of *Parascorpaena* Bleeker, 1876 (Teleostei: Scorpaenidae) from Taiwan. Zoological Studies 61: 9. https://doi.org/10.6620/ZS.2022.61-09

Eschmeyer WN (1986) Family no 149: Scorpaenidae. In: Smith MM, Heemstra PC (Eds) Smiths' sea fishes. Springer-Verlag, New York, 463–478.

Felsenstein J (1985) Confidence limits on phylogenies: an approach using the bootstrap. Evolution 39: 783–791. https://doi.org/10.2307/2408678

Fowler HW (1938) Descriptions of new fishes obtained by the United States Bureau of Fisheries steamer "*Albatross*", chiefly in Philippine seas and adjacent waters. Proceedings of the United States National Museum 85: 31–135. https://doi.org/10.5479/si.00963801.85-3032.31

Fricke R, Kulbicki M, Wantiez L (2011) Checklist of the fishes of New Caledonia, and their distribution in the southwest Pacific Ocean (Pisces). Stuttgarter Beiträge zur Naturkunde A, Neue Serie 4: 341–463.

Fricke R, Golani D, Appelbaum-Golani B (2015) New record of the Mozambique scorpionfish, *Parascorpaena mossambica* (Peters, 1855) (Actinopterygii: Scorpaeniformes: Scorpaenidae), from Israel, Gulf of Aqaba, Red Sea. Acta Ichthyologica et Piscatoria 45: 423–425. https://doi.org/10.3750/AIP2015.45.4.12

Gray JE (1831) Description of a new genus of percoid fish, discovered by Mr. Samuel Stutchbury, in the Pacific sea, and now in the British Museum. Zoological Miscellany 1: 20.

Jeong B, Motomura H (2021) An annotated checklist of marine and freshwater fishes of five islands of Mishima in the Osumi Islands, Kagoshima, southern Japan, with 109 new records. Bulletin of the Kagoshima University Museum 16: 1–116.

Kimura M (1980) A simple method for estimating evolutionary rates of base substitutions through comparative studies of nucleotide sequences. Journal of Molecular Evolution 16: 111–120. https://doi.org/10.1007/BF01731581

Kimura Y, Hibino Y, Miki R, Minetoma T, Koeda K (2017) Field guide to fishes of Kuchinoerabu-jima Island in the Osumi Group, Kagoshima, southern Japan, 200 pp.

Mochida I, Motomura H (2018) An annotated checklist of marine and freshwater fishes of Tokunoshima island in the Amami Islands, Kagoshima, southern Japan, with 202 new records. Bulletin of the Kagoshima University Museum 10: 1–80.

Mochizuki K, Oyama K, Kume G, Motomura H (2023) Review of distributional records of *Parascorpaena mcadamsi* and *P. moultoni* (Scorpaenidae) in Japanese waters, and notes on sexual dichromatism and dimorphism of the two species. Ichthy, Natural History of Fishes of Japan 29: 39–57. https://doi.org/10.34583/ichthy.29.0_39

Motomura H (2004a) New species of scorpionfish, *Scorpaena cocosensis* (Scorpaeniformes: Scorpaenidae) from the Cocos Islands, Costa Rica, eastern Pacific Ocean. Copeia 2004: 818–824. https://doi.org/10.1643/CI-04-179R

Motomura H (2004b) Revision of the scorpionfish genus *Neosebastes* (Scorpaeniformes: Neosebastidae) with descriptions of five new species. Indo-Pacific Fishes 37: 1–76.

Motomura H (2013) Scorpaenidae. In: Motomura H, Dewa S, Furuta K, Matsuura K (Eds) Fishes of Iou-jima and Take-shima islands, Mishima, Kagoshima, Japan. The Kagoshima University Museum, Kagoshima and the National Museum of Nature and Science, Tsukuba, 36–66.

Motomura H (2019) Scorpaenidae, Scorpaeninae. Motomura H, Hagiwara K, Senou H, Nakae M (Eds) Identification guide to fishes of the Amami Islands in the Ryukyu Archipelago, Japan. The Minaminippon Shimbun Kaihatsu Center, Kagoshima, 70–78.

Motomura H (2022) Scorpaenidae. In: Iwatsubo H, Itou M, Yamada M, Motomura H (Eds) Field guide to fishes of the East China Sea side of Satsuma Peninsula in Kagoshima, southern Kyushu, Japan. Kagoshima Museum of Aquatic Biodiversity, Kagoshima and the Kagoshima University Museum, Kagoshima, 71–81.

Motomura H (2023) An annotated checklist of marine and freshwater fishes from Tanega-shima and Mage-shima islands in the Osumi Islands, Kagoshima, southern Japan, with 536 new records. Bulletin of the Kagoshima University Museum 20: 1–250.

Motomura H, Harazaki S (2017) Annotated checklist of marine and freshwater fishes of Yaku-shima island in the Osumi Islands, Kagoshima, southern Japan, with 129 new records. Bulletin of the Kagoshima University Museum 9: 1–183.

Motomura H, Ishihara S (2013) Fish collection building and procedures manual. English edn. The Kagoshima University Museum, Kagoshima and the Research Institute for Humanity and Nature, Kyoto, 70 pp.

Motomura H, Johnson JW (2006) Validity of the poorly known scorpionfish, *Rhinopias eschmeyeri*, with redescriptions of *R. frondosa* and *R. aphanes* (Scorpaeniformes: Scorpaenidae). Copeia 2006: 500–515. https://doi.org/10.1643/0045-8511(2006)2006[500:VOTPKS]2.0.CO;2

Motomura H, Fricke R, Eschmeyer WN (2005a) Redescription of a poorly known scorpionfish, *Scorpaena canariensis* (Sauvage), and a first record of *Pontinus leda* Eschmeyer from the Northern Hemisphere (Scorpaeniformes: Scorpaenidae). Stuttgarter Beiträge zur Naturkunde, Serie A (Biologie) 674: 1–15.

Motomura H, Last PR, Yearsley GK (2005b) *Scorpaena bulacephala*, a new species of scorpionfish (Scorpaeniformes: Scorpaenidae) from the northern Tasman Sea. Zootaxa 1043: 17–32. https://doi.org/10.11646/zootaxa.1043.1.2

Motomura H, Paulin CD, Stewart AL (2005c) First records of *Scorpaena onaria* (Scorpaeniformes: Scorpaenidae) from the southwestern Pacific Ocean, and comparisons with the Northern Hemisphere population. New Zealand Journal of Marine and Freshwater Research 39: 865–880. https://doi.org/10.1080/00288330.2005.9517358

Motomura H, Last PR, Gomon MF (2006a) A new species of the scorpionfish genus *Maxillicosta* from the southeast coast of Australia, with a redescription of *M. whitleyi* (Scorpaeniformes: Neosebastidae). Copeia 2006: 445–459. https://doi.org/10.1643/0045-8511(2006)2006[445:ANSOTS]2.0.CO;2

Motomura H, Last PR, Yearsley GK (2006b) New species of shallow water scorpionfish (Scorpaenidae: *Scorpaena*) from the central coast of Western Australia. Copeia 2006: 360–369. https://doi.org/10.1643/0045-8511(2006)2006[360:NSOSWS]2.0.CO;2

Motomura H, Sakurai Y, Senou H, Ho H-C (2009) Morphological comparisons of the Indo-West Pacific scorpionfish, *Parascorpaena aurita*, with a closely related species, *P. picta*, with first records of *P. aurita* from East Asia (Scorpaeniformes: Scorpaenidae). Zootaxa 2191: 41–57. https://doi.org/10.11646/zootaxa.2191.1.2

Motomura H, Béarez P, Causse R (2011) Review of Indo-Pacific specimens of the subfamily Scorpaeninae (Scorpaenidae), deposited in the Muséum national d'Histoire naturelle, Paris, with description of a new species of *Neomerinthe*. Cybium 35: 55–73. https://doi.org/10.26028/cybium/2011-351-006

Nakae M, Motomura H, Hagiwara K, Senou H, Koeda K, Yoshida T, Tashiro S, Jeong B, Hata H, Fukui Y, Fujiwara K, Yamakawa T, Aizawa M, Shinohara G, Matsuura K (2018)

An annotated checklist of fishes of Amami-oshima Island, the Ryukyu Islands, Japan. Memoirs of the National Museum of Nature and Science, Tokyo 52: 205–361.

Peters W (1855) Übersicht der in Mossambique beobachteten seefische. Monatsschr Akad Wiss Berlin 1855: 428–466.

Poss GS (1999) Scorpaenidae. Scorpionfishes (also, lionfishes, rockfishes, stingfishes, stonefishes, and waspfishes). In: Carpenter KE, Niem VH (Eds) FAO species identification guide for fishery purposes. The living marine resources of the western central Pacific. Vol. 4. Bony fishes part 2 (Mugilidae to Carangidae). FAO, Rome, 2291–2352.

Poss SG, Motomura H (2022) Family Scorpaenidae, scorpionfishes and lionfishes. In: Heemstra PC, Heemstra E, Ebert DA, Holleman W, Randall JE (Eds) Coastal fishes of the western Indian Ocean. Vol. 2. South African Institute for Aquatic Biodiversity, Makhanda, 506–549.

Rüppell WPES (1835–1838) Neue wirbelthiere zu der fauna von Abyssinien gehörig. Fische des Rothen Meeres. Siegmund Schmerber, Frankfurt-am-Main, 148 pp. https://doi.org/10.5962/bhl.title.53778

Tamura K, Stecher G, Kumar S (2021) MEGA 11: Molecular evolutionary genetics analysis version 11. Molecular Biology and Evolution 38: 3022–3027. https://doi.org/10.1093/molbev/msab120.

Tanaka S, Shitamitsu T, Senou H, Miyazaki Y (2020) Fish fauna of Tokashiku Bay, Tokashiki, the Kerama Islands, Okinawa Prefecture: Additional records of 144 species. Bulletin of the Kanagawa Prefectural Museum (Natural Science) 49: 107–118.

Tsuno Y, Yuki D, Motomura H, Endo H (2022) First specimen-based records of five species of the family Scorpaenidae from Kochi Prefecture, Japan. Ichthy, Natural History of Fishes of Japan 17: 79–87. https://doi.org/10.34583/ichthy.17.0_79

Whitley GP (1961) A new scorpion fish from Queensland. North Queensland Naturalist 29: 9–10.

Wibowo K, Motomura H (2021) Review of Indo-Pacific species of the scorpionfish genus *Scorpaena* (Teleostei: Scorpaenidae), with descriptions of two new species from the west coast of Australia. Ichthyological Research. https://doi.org/10.1007/s10228-021-00827-0

ZooKeys 1219: 287–302 (2024)
DOI: 10.3897/zookeys.1219.137179

Research Article

Allopachria nigrocatta sp. nov. from Guangxi, with a key and checklist of Chinese species and additional records of *Allopachria* Zimmermann, 1924 from China (Coleoptera, Dytiscidae, Hydroporinae, Hyphydrini)

Zhuo-yin Jiang[1,2], Ya-ru Chen[1], Li-bo Han[1], Feng-long Jia[2], Bei-xin Wang[1]

1 *Department of Entomology, College of Plant Protection, Nanjing Agricultural University, Nanjing 210095, China*
2 *Department of Entomology, College of Life Sciences, Sun Yat-sen University, Guangzhou 510275, China*
Corresponding authors: Feng-long Jia (lssjfl@mail.sysu.edu.cn, fenglongjia@aliyun.com); Bei-xin Wang (wangbeixin@njau.edu.cn)

Abstract

A new species *Allopachria nigrocatta* **sp. nov.** from Guangxi, China is described. New records are provided for the following *Allopachria* species: *A. dudgeoni* Wewalka, 2000 and *A. weinbergeri* Wewalka, 2000 from Zhejiang, and *A. yiae* Bian, Guo & Ji, 2013 from Guizhou. Additional records are also given for some other Chinese species. The habitus and male genitalia of the new species are illustrated. An updated key and a checklist of all Chinese species of *Allopachria* are provided.

Key words: *Allopachria*, checklist, China, Dytiscidae, fauna, Hydroporinae, identification key, new record, new species, Oriental region, taxonomy

Academic editor: Mariano Michat
Received: 16 September 2024
Accepted: 30 October 2024
Published: 4 December 2024

ZooBank: https://zoobank.org/B970895F-E1CE-4F42-81FD-1F03B7DE5680

Citation: Jiang Z-yin, Chen Y-ru, Han L-bo, Jia F-long, Wang B-xin (2024) *Allopachria nigrocatta* sp. nov. from Guangxi, with a key and checklist of Chinese species and additional records of *Allopachria* Zimmermann, 1924 from China (Coleoptera, Dytiscidae, Hydroporinae, Hyphydrini). ZooKeys 1219: 287–302. https://doi.org/10.3897/zookeys.1219.137179

Introduction

Allopachria Zimmermann, 1924, are small to extremely small beetles, most of which bear maculae on their elytra. Male specimens of some species have antennomeres, protibiae or protarsomeres modified in various ways (Wewalka 2000). Species of the genus occur mainly in the Oriental region, from Indonesia in the south to southern China and Japan in the north (Wewalka 2010). *Allopachria* typically live by the margin of flowing waters, usually with a sand or stone bottom. The knowledge of *Allopachria* was very poor until Wewalka (2000) made a comprehensive revision of the genus. Then, the studies increased gradually, and the fauna of Chinese *Allopachria* was also supplemented (Bian and Ji 2010; Wewalka 2010; Bian and Ji 2012; Bian et al. 2013; Ji et al. 2014). Up to now, the genus contains 47 species worldwide (Nilsson and Hájek 2024a), of which 29 species occur in China (Nilsson and Hájek 2024b).

In the present study, we describe a new species from Guangxi, China and provide additional records for some Chinese *Allopachria* species. For the first time, an updated key to all known species from China is provided.

Materials and methods

Specimens were examined and measured under a Nikon SMZ800N stereomicroscope. Some of the specimens were dissected, and the genitalia were put into 10% KOH at room temperature for 8–10 h, then placed in a drop of glycerol on glass slides for photographing. Photographs of habitus and characters were taken with a Nikon DS-Ri2 mounted on a Nikon SMZ25; layers were captured and aligned in the NIS-Elements software. Photographs of genitalia were taken with a Zeiss AxioCam HRc mounted on a Zeiss AX10 microscope with the Axio Vision SE64 software, then stacked in Helicon Focus (ver. 7.0.2). After being photographed, the genitalia were transferred to a transparent plastic plate in a drop of glycerol and attached to the respective specimen. The images were edited and assembled with Adobe Photoshop CS6.

The following abbreviations were used in the descriptions: TL, total length, measurement of length from clypeal margin to apex of elytra; TL-h, total length minus head length, measurement of length from anterior margin of pronotum to apex of elytra; MW, maximum width of body measured at right angle to TL. The terminology follows Wewalka (2000) and Wewalka (2010), and the style of description of the new species follows Jiang et al. (2022). The terminology to denote the orientation of the genitalia follows Miller and Nilsson (2003). Exact label data are cited for the type material and given in quotation marks. Authors' additional remarks are provided in square brackets; [p]–preceding data are printed. Separate label lines are indicated by a slash (/), and separate labels by a double slash (//).

The specimens included in this study are deposited in the following collections:

SYSU	Biological Museum, Sun Yat-sen University, Guangzhou, China.
ZJCQ	Zhuo-yin Jiang collection, Quzhou, China.

Taxonomy

Allopachria nigrocatta Jiang & Jia, sp. nov.

https://zoobank.org/0D13517E-1D9A-4171-AFB3-CD19D5880446

Figs 1A–E, 2A–C, 4A, 6, 7C

Type locality. China, Guangxi Zhuang Autonomous Region, Guilin, Ziyuan County, Maoershan Mt., Huilong Temple, c. 25.9125°N, 110.4656°E; 1557.2 m.

Type material. ***Holotype*** • male (SYSU), labelled: "广西桂林市资源县 / 猫儿山迴龙寺 / 25.9125N，110.4656E / 1557.2m，30.viii.2020 / 姜卓寅 [p] // CHINA: Guangxi, Guilin / Ziyuan County, Maoershan Mt. / Huilong Temple / 25.9125N, 110.4656E / 1557.2m, 30.viii.2020 / Zhuoyin Jiang leg. [p] // HOLOTYPE / *ALLOPACHRIA* / *nigrocatta* sp. nov. / Jiang & Jia det. 2024 [red label, p]". ***Paratype*** • 1 female (SYSU), same label data as holotype, with a paratype label, labelled: "PARATYPE / *ALLOPACHRIA* / *nigrocatta* sp. nov. / Jiang & Jia det. 2024 [red label, p]".

Description of male holotype. ***Habitus*** (Fig. 1A) regularly oval, with continuous outline, broadest in 1/3 of elytral length, moderately convex. ***Colouration.*** Head dark brown to black, somewhat paler at clypeal margin, with small yellowish-brown area behind eyes; pronotum black with lateral margins reddish-brown;

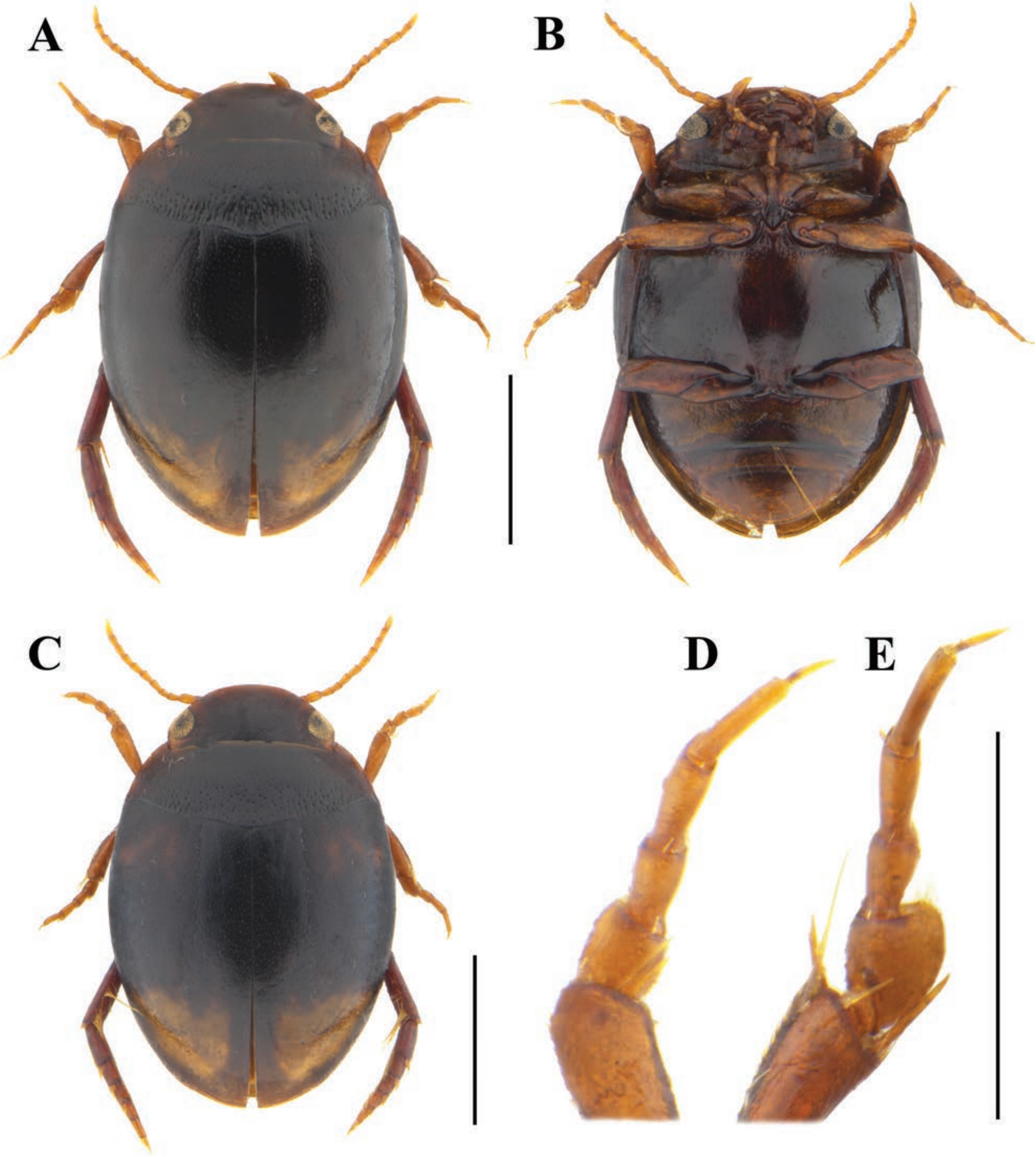

Figure 1. *Allopachria nigrocatta* sp. nov. (Maoershan, Guangxi) **A** habitus in dorsal view (holotype, male) **B** habitus in ventral view (holotype, male) **C** habitus in dorsal view (paratype, female) **D** male protarsus in dorsal view **E** male mesotarsus in dorsal view. Scale bars: 1.0 mm (**A–C**); 0.5 mm (**D, E**).

elytra black, apex with an irregularly shaped yellowish-brown spot not reaching suture; appendages yellowish-brown to reddish-brown; ventral side reddish-brown to black. ***Head*.** Moderately broad, c. 0.67 × width of pronotum, trapezoidal. Anterior margin of clypeus regularly rounded, without bead (Fig. 7C). Antenna with antennomeres long and slender. Shiny, microreticulation presents on anterior half of head and along eyes, consisting of well-impressed polygonal isodiametric meshes. Punctures spread sparsely and more distinct on vertex;

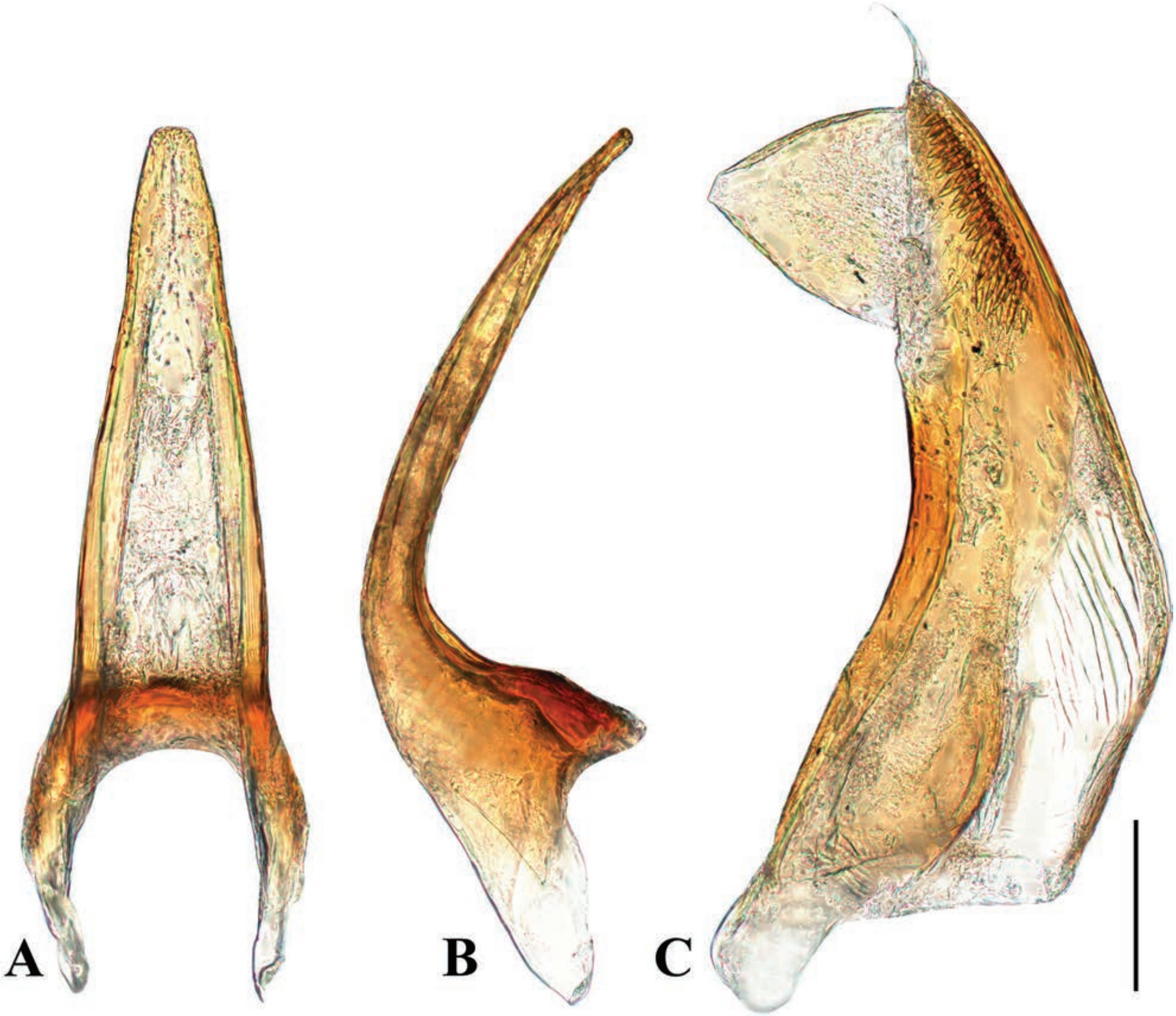

Figure 2. Male genitalia of *Allopachria nigrocatta* sp. nov. (holotype, male; Maoershan, Guangxi) **A** median lobe in ventral view **B** median lobe in lateral view **C** right paramere in lateral view. Scale bar: 0.1 mm.

setigerous punctures present along inner margin of eyes and anterolaterally to eyes in fronto-clypeal depressions. ***Pronotum*.** Strongly transverse (width/length ratio = 2.71), broadest between posterior angles. Lateral margins moderately curved, distinctly beaded. Shiny, microreticulation absent. Punctures and micropunctures spread sparsely and evenly; rows of setigerous punctures present along anterior margin; navel-like punctures present in posterior half. Posterior half also covered with some irregular longitudinal wrinkles. ***Elytra*.** Base as broad as pronotal base; lateral margins moderately curved. Shiny, microreticulation absent. Punctures and micropunctures spread sparsely and evenly; longitudinal rows of setigerous punctures incomplete. ***Legs*.** Protarsomere 1 minimally enlarged (Fig. 1D), mesotarsomere 1 distinctly enlarged (Fig. 1E), with adhesive setae on their ventral side; claws simple, metatarsal claws unequal. ***Ventral side*** (Fig. 1B). Prosternum sinuate anteriorly. Prosternal process heart-shaped, with distinct wide lateral beads in basal two thirds, apex obtuse; surface distinctly punctured. Metaventrite distinctly beaded on anterior margin; lateral parts of metaventrite (“metasternal wings”) narrow. Metacoxal lines prominent, divergent anteriorly. Metacoxal plates with some indistinct wrinkles. Metacoxal processes with a small triangular lobe, obscuring part of metatrochanter. Abdomen with five ventrites (III–IV fused). Microreticulation presents on abdominal ventrites, consisting of well-impressed polygonal isodiametric meshes. Punctures and micropunctures spread sparsely and evenly on metaventrite, metacoxae and abdominal ventrites; setigerous punctures present along anterior margin of metaventrite and medially on ventrites II–IV. ***Male genitalia*.** Median lobe of aedeagus gradually narrowing from base to apex in ventral view, apex truncate (Fig. 2A); 'L'-shaped in lateral view, moderately curved, apex obtuse (Fig. 2B). Parameres moderately broad, distal portion with a large triangular process on dorsal side, with a tuft of setae apically (Fig. 2C).

Female (Fig. 1C). Identical to male in habitus. Dorsal surface submatt, microreticulation presents on head, pronotum and elytra, more densely and longitudinally stretched on elytra. Pro- and mesotarsomeres not enlarged, without adhesive setae.

Variability. Minor variability can be seen in dorsal colouration; there is an indistinct irregular reddish-brown spot on each elytral base in the paratype.

Measurements. TL: 2.5–2.7 mm (mean value: 2.6 ± 0.1 mm); holotype: 2.7 mm. TL-h: 2.2–2.4 mm (mean value: 2.3 ± 0.1 mm); holotype: 2.4 mm. MW: 1.7–1.8 mm (mean value: 1.75 ± 0.05 mm); holotype: 1.8 mm.

Differential diagnosis. *Allopachria nigrocatta* sp. nov. can be distinguished from other *Allopachria* species by its black colour pattern with a yellowish-brown spot on elytral apex. The shape of the median lobe and paramere is also unique. Female specimens can be easily identified by the submatt appearance.

Collection details. On Maoershan Mt., *Allopachria nigrocatta* sp. nov. was collected syntopically with *Platambus punctatipennis* Brancucci, 1984 from a pool with decaying leaves under a rock wall covered with flowing water (Fig. 4A).

Etymology. The species name is a combination of "*nigro*-" from Latin "*nigriculus*" (= blackish) and "*-catta*" (= cat, in Chinese "mao" means cat), referring to its black appearance and the fact that it was collected from Maoershan Mt. The gender of the name is feminine.

Distribution. So far, known only from the type locality on Maoershan Mt., northern Guangxi, China (Fig. 6).

Additional records of Chinese *Allopachria*

Allopachria bianae Wewalka, 2010

Figs 3A, 4B, 6

Allopachria bianae Wewalka, 2010: 31 (orig. descr.).

Material studied. China: Guangdong • 11 spec. (SYSU, ZJCQ), Zhaoqing, Dinghu Distr., Dinghushan Mt., Qingyunsi management station, 23.1737°N, 112.5361°E, 241.2 m, 12.vii.2021, Z.Y. Jiang, Z.Q. Mai & Z.L. Liang leg. • 5 spec. (SYSU, ZJCQ), Zhaoqing, Dinghu Distr., Dinghushan Mt., Qingyunsi management station, 23.1732°N, 112.5354°E, 256.9 m, 17.x.2021, Z.Y. Jiang, Z.Q. Mai & W.C. Xie leg. • 5 spec. (SYSU, ZJCQ), Zhaoqing, Dinghu Distr., Dinghushan Mt., Dizhi management station, 23.1609°N, 112.5323°E, 88.7 m, 14.ix.2022, Z.Y. Jiang & W.C. Xie leg. • 18 spec. (SYSU, ZJCQ), Zhaoqing, Dinghu Distr., Ding-

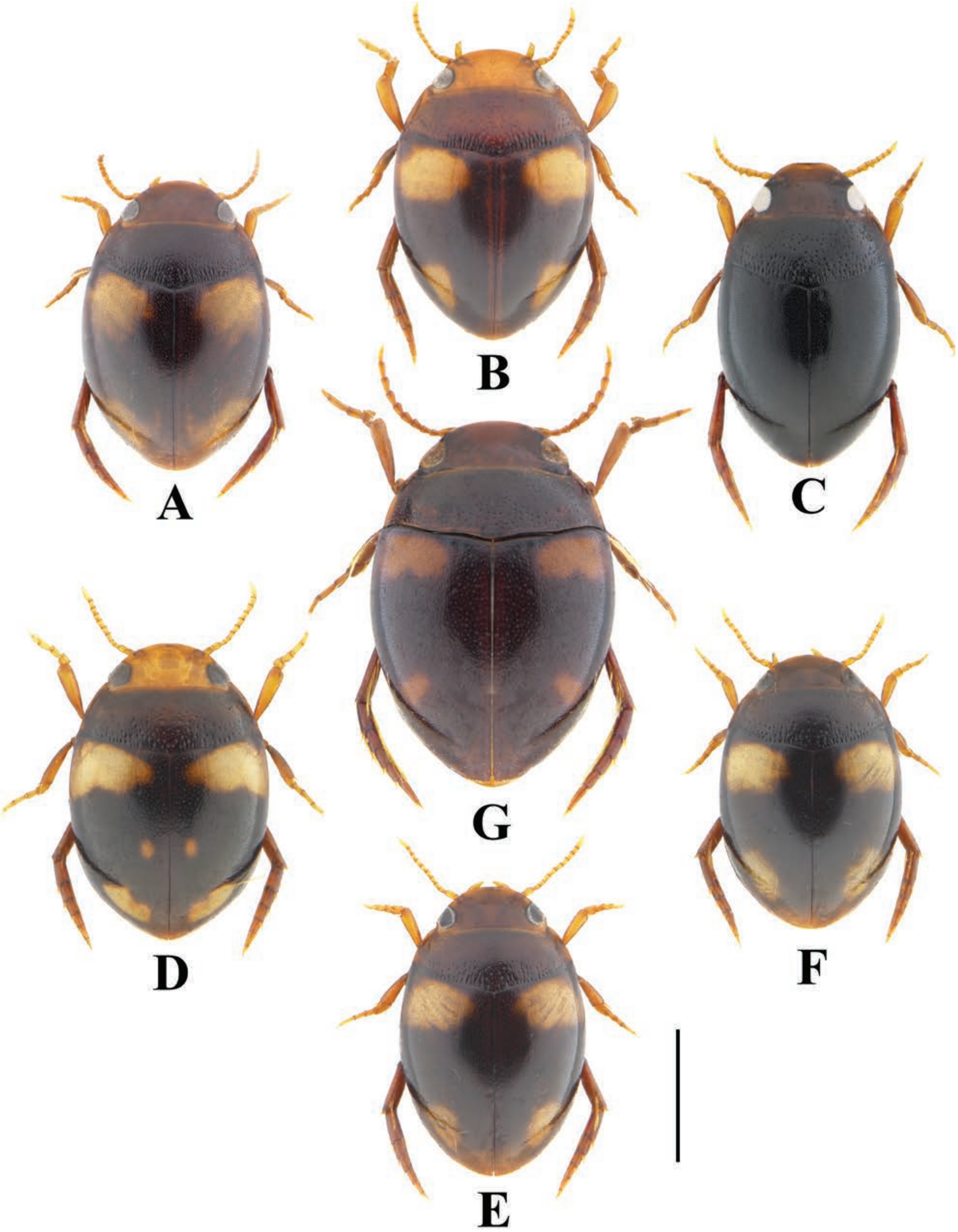

Figure 3. Habitus of *Allopachria* species **A** *Allopachria bianae* (male; Dinghushan, Guangdong) **B** *Allopachria dudgeoni* (male; Tianmushan, Zhejiang) **C** *Allopachria jendeki* (male; Baihualing, Yunnan) **D** *Allopachria miaowangi* (male; Lingwei, Zhejiang) **E** *Allopachria schoenmanni* (male; Tianmushan, Zhejiang) **F** *Allopachria weinbergeri* (male; Lingwei, Zhejiang) **G** *Allopachria yiae* (male; Machang Town, Guizhou). Scale bar: 1.0 mm.

Figure 4. Habitat of *Allopachria* species **A** pool with decaying leaves under rock wall covered with flowing water, Maoershan, Guangxi (*A. nigrocatta* sp. nov.) **B** stream pool with decaying leaves, Dinghushan, Guangdong (*A. bianae*) **C** small stream with decaying leaves, Baihualing, Yunnan (*A. jendeki*) **D** small pool with flowing water surrounded by large stones, Tianmushan, Zhejiang (*A. schoenmanni*).

hushan Mt., Qingyunsi management station, 23.1732°N, 112.5354°E, 256.9 m, 15.ix.2022, Z.Y. Jiang & W.C. Xie leg.

Distribution. So far known only from its type locality on Dinghushan Mt. (Guangdong) (Fig. 6).

Collection details. On Dinghushan Mt., *Allopachria bianae* was collected syntopically with *Neptosternus coomani* Peschet, 1923 and *Neptosternus punctatus* Zhao, Hájek, Jia & Pang, 2012 among decaying leaves in a stream pool (Fig. 4B).

Allopachria dudgeoni **Wewalka, 2000**

Figs 3B, 6, 7E

Allopachria dudgeoni Wewalka, 2000: 117 (orig. descr.); Wewalka 2010: 36 (fauna), Bian and Ji 2010: 64 (fauna), Bian and Ji 2012: 31 (fauna).

Material studied. CHINA: Zhejiang • 1 male (ZJCQ), Hangzhou, Lin'an Distr., Tianmushan Mt., Xiguan Stream S02, 30.3579°N, 119.4487°E, 609 m, x.2023, H.M. Zang & L.B. Han leg. • 1 female (ZJCQ), Hangzhou, Lin'an Distr., Tianmushan Mt., Waijunling, 30.3750°N, 119.4854°E, 537 m, xii.2023, H.M. Zang & L.B. Han leg.

Distribution. Southeastern China (Guangdong, Guangxi, Hong Kong, Jiangxi, Zhejiang). First record from Zhejiang Province (Fig. 6).

Allopachria jendeki **Wewalka, 2000**

Figs 3C, 4C, 6, 7A

Allopachria jendeki Wewalka, 2000: 116 (orig. descr.); Wewalka 2010: 36 (fauna).

Material studied. CHINA: Yunnan • 1 male, 2 females (SYSU, ZJCQ), Baoshan, Baihualing Mt., Zaotang Stream, 25.3087°N, 98.7936°E, 1481.4 m, 11.v.2021, Z.Y. Jiang, Z.M. Yang, Z.Q. Mai & B.P. Huang leg.

Distribution. Southwestern China (Yunnan) (Fig. 6).

Collection details. The specimens were collected among decaying leaves and sand in a small stream on Baihualing Mt. (Fig. 4C).

Allopachria miaowangi **Wewalka, 2010**

Figs 3D, 5A, B, 5Ca, 6, 7F

Allopachria miaowangi Wewalka, 2010: 29 (orig. descr.); Bian and Ji 2012: 34 (fauna).

Allopachria dieterlei Wewalka, 2000: Bian and Ji 2010: 64 (misidentification).

Material studied. CHINA: Zhejiang • 4 males, 1 female (SYSU, ZJCQ), Quzhou, Kecheng Distr., Lingwei, 28.8507°N, 118.9372°E, 177.4 m, 2.v.2024, Z.Y. Jiang & Z.X. Mao leg. • 1 female (ZJCQ), Quzhou, Kecheng Distr., Lingwei, 28.8507°N, 118.9372°E, 177.4 m, 13.iv.2020, Z.Y. Jiang & Z.X. Mao leg.

Figure 5. Habitat and live specimens of *Allopachria miaowangi* and *Allopachria weinbergeri* **A** small stream under the forest (Lingwei, Zhejiang) **B** sand and stones by the margin of the stream (Lingwei, Zhejiang) **C** live specimens of *Allopachria* (**a** *A. miaowangi* **b** *A. weinbergeri*).

Distribution. Eastern China (Hunan, Jiangxi, Zhejiang) (Fig. 6).

Collection details. *Allopachria miaowangi* was collected syntopically with *Allopachria weinbergeri* under sand and stones by the margin of a small stream in Lingwei (Zhejiang) (Fig. 5A, B).

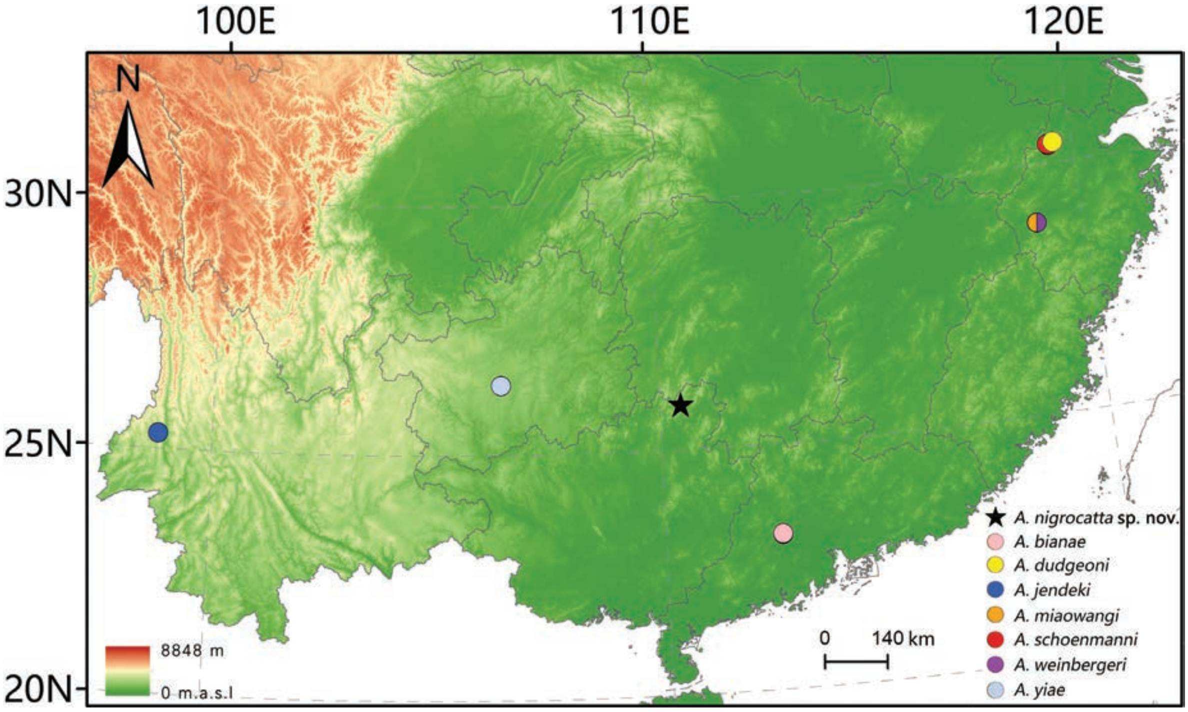

Figure 6. Map of distribution of *Allopachria nigrocatta* sp. nov. and additional records of other *Allopachria* species in China.

***Allopachria schoenmanni* Wewalka, 2000**
Figs 3E, 4D, 6

Allopachria schoenmanni Wewalka, 2000: 113 (orig. descr.).

Material studied. China: Zhejiang • 6 males, 2 females (SYSU, ZJCQ), Hangzhou, Lin'an Distr., Tianmushan Mt., Y437 roadside (Xiguan), 30.3483°N, 119.4509°E, 484.5 m, 20.xi.2023, Z.Y. Jiang leg. • 1 female (ZJCQ), Hangzhou, Lin'an Distr., Tianmushan Mt., Shuiduitang, 30.3682°N, 119.4255°E, 867 m, viii.2023, H.M. Zang & L.B. Han leg.

Distribution. Eastern China (Anhui, Zhejiang) (Fig. 6).

Collection details. Most specimens from Tianmushan Mt. were collected in a small pool with flowing water surrounded by large stones (Fig. 4D).

***Allopachria weinbergeri* Wewalka, 2000**
Figs 3F, 5A, B, 5Cb, 6, 7G

Allopachria weinbergeri Wewalka, 2000: 112 (orig. descr.); Wewalka 2010: 36 (fauna).
Allopachria weinbergerorum Nilsson, 2007: 50 (as unjustified emendation of *weinbergeri*).

Material studied. China: Zhejiang • 4 males, 2 females (SYSU, ZJCQ), Quzhou, Kecheng Distr., Lingwei, 28.8507°N, 118.9372°E, 177.4 m, 2.v.2024, Z.Y. Jiang & Z.X. Mao leg. • 1 female (ZJCQ), Quzhou, Kecheng Distr., Lingwei, 28.8507°N, 118.9372°E, 177.4 m, 13.iv.2020, Z.Y. Jiang & Z.X. Mao leg.

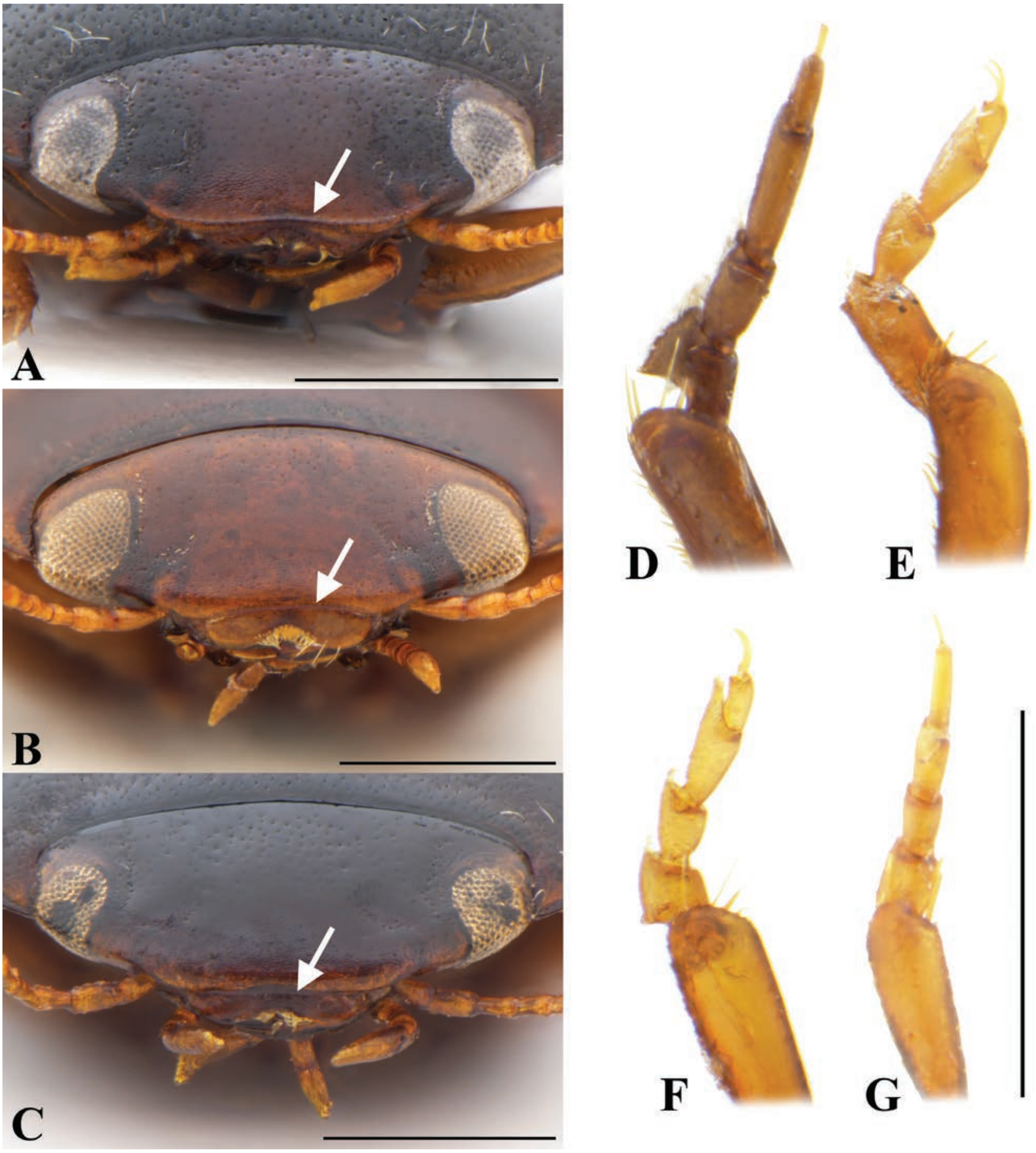

Figure 7. Morphological characters of *Allopachria* spp. **A–C** anterior aspect of head showing clypeus **D–G** male protarsus in dorsal view. **A** *Allopachria jendeki* **B, D** *Allopachria yiae* **C** *Allopachria nigrocatta* sp. nov. **E** *Allopachria dudgeoni* **F** *Allopachria miaowangi* **G** *Allopachria weinbergeri*. Scale bars: 0.5 mm.

Distribution. Eastern China (Fujian, Guangdong, Zhejiang). First record from Zhejiang Province (Fig. 6).

Collection details. *Allopachria weinbergeri* was collected syntopically with *Allopachria miaowangi* under sand and stones by the margin of a small stream in Lingwei (Zhejiang) (Fig. 5A, B).

Allopachria yiae **Bian, Guo & Ji, 2013**

Figs 3G, 6, 7B, 7D

Allopachria yiae Bian, Guo & Ji, 2013: 85 (orig. descr.).

Material studied. China: Guizhou • 3 males, 2 females (SYSU), Pingba, Machang Town, 13.viii.1982, Z.H. Huang leg.

Distribution. Southwestern China (Chongqing, Guizhou). First record from Guizhou Province (Fig. 6).

Key to Chinese *Allopachria* species (appropriate to males only)

1 Anterior margin of clypeus with bead (Fig. 7A, B) **2**

– Anterior margin of clypeus without bead (Fig. 7C) **10**

2 Anterior margin of clypeus with distinct bead (Fig. 7A) **3**

– Anterior margin of clypeus with very fine bead (Fig. 7B) **7**

3 Elytra completely black, without spots (Fig. 3C) .... ***A. jendeki*** **Wewalka, 2000**

– Elytra with two or three yellow to reddish-brown spots **4**

4 Lateral margin of elytron with a longitudinal furrow .... ***A. manfredi*** **Wewalka, 2010**

– Lateral margin of elytron without a longitudinal furrow **5**

5 Male antennae modified, antennomeres 4 and 5 distinctly enlarged .... ***A. scholzi*** **Wewalka, 2000**

– Male antennae not modified, with antennomeres long and slender **6**

6 Size larger (TL: 2.1–2.2 mm); head yellow; elytra with three spots (see Wewalka 2000, fig. 25) .... ***A. ernsti*** **Wewalka, 2000**

– Size smaller (TL: 1.7–1.8 mm); head black; elytra with two spots (see Wewalka 2000, fig. 8) .... ***A. taiwana*** **(Satô, 1990)**

7 Size larger (TL: 2.7–2.9 mm); male protarsomere 1 distinctly enlarged with indention on inner margin at basal half (Fig. 7D) .... ***A. yiae*** **Bian, Guo & Ji, 2013**

– Size smaller (TL: 1.5–1.8 mm); male protarsomere 1 minimally enlarged **8**

8 Male antennomere 5 distinctly enlarged, 'L'-shaped (see Wewalka 2000, fig. 107 .... ***A. froehlichi*** **Wewalka, 2000**

– Male antennomere 5 moderately enlarged, with an obtuse tooth (see Wewalka 2000, fig. 108) **9**

9 Median lobe of aedeagus in lateral view shorter and broader (see Wewalka 2000, fig. 44b) .... ***A. hautmanni*** **Wewalka, 2000**

– Median lobe of aedeagus in lateral view longer and slender (see Wewalka 2000, fig. 43b) .... ***A. schillhammeri*** **Wewalka, 2000**

10 Size smaller (TL: 1.6 mm) .... ***A. jilanzhui*** **Wewalka, 2000**

– Size larger (TL: ≥ 2.0 mm) **11**

11 Apex of median lobe of aedeagus trifid **12**

– Apex of median lobe of aedeagus simple, not trifid **16**

12 Elytra entirely microreticulate **13**

– Elytra without microreticulation **14**

13 Punctation of pronotum regular in size, not navel-like; interstice of the tridentate apex of median lobe narrower (see Wewalka 2000, fig. 63a).. ***A. wangi*** **Wewalka & Nilsson, 1994**

– Punctation of pronotum irregular in size, partly coarse and navel-like; interstice of the tridentate apex of median lobe wider (see Wewalka 2000, fig. 64a)..***A. jaechi*** **Wewalka, 2000**

14 Male protarsomere 1 not modified, minimally enlarged...***A. flavomaculata*** **(Kamiya, 1838)**

– Male protarsomere 1 modified, distinctly enlarged **15**

15 Elytra with two or three spots (see Wewalka 2010, fig. 7a, b); middle part of the tridentate apex of median lobe longer than lateral parts (see Wewalka 2010, fig. 15a)..***A. komareki*** **Wewalka, 2010**

– Elytra with two spots (see Bian and Ji 2010, fig. 1); middle part and lateral parts of the tridentate apex of median lobe equal in length (see Bian and Ji 2010, fig. 3)..***A. wuzhifengensis*** **Bian & Ji, 2010**

16 Male antennomeres 4 and 5 distinctly enlarged (see Wewalka 2000, fig. 113)... ***A. friedrichi*** **Wewalka, 2000**

– Male antenna not or minimally enlarged **17**

17 Male protarsomere 1 modified, distinctly enlarged (Fig. 7E, F)................**18**

– Male protarsomere 1 not modified, minimally enlarged (Fig. 7G)............**22**

18 Male protarsomere 1 elongate (Fig. 7E) **19**

– Male protarsomere 1 short (Fig. 7F)..**20**

19 Male protarsomere 1 about 1.5 times as long as protarsomere 2, insertion of protarsomere 2 at the apical part of protarsomere 1 (Fig. 7E)..***A. dudgeoni*** **Wewalka, 2000**

– Male protarsomere 1 about 2 times as long as protarsomere 2, insertion of protarsomere 2 at the middle of protarsomere 1 (see Bian and Ji 2012, figs 15, 17)..***A. elongata*** **Bian & Ji, 2012**

20 Apex of median lobe of aedeagus pointed in ventral view (see Wewalka 2010, fig. 11a)... ***A. miaowangi*** **Wewalka, 2010**

– Apex of median lobe of aedeagus truncate in ventral view (see Wewalka 2010, fig. 12a)..**21**

21 Punctation of elytra stronger; median lobe of aedeagus in lateral view moderately curved (see Wewalka 2000, fig. 58b)..***A. dieterlei*** **Wewalka, 2000**

– Punctation of elytra finer; median lobe of aedeagus in lateral view almost straight at middle part (see Wewalka 2010, fig. 12b)..***A. guangdongensis*** **Wewalka, 2010**

22 Elytra often completely black, sometimes with two reddish-brown spots (see Wewalka 2010, fig. 6a, b)...............................***A. hajeki*** **Wewalka, 2010**

– Elytra with one or two yellowish-brown to reddish-brown spots.............**23**

23 Size larger (TL: 2.5–2.7 mm); male mesotarsomere 1 distinctly enlarged (Fig. 1E); elytra often with one spot at apex (Fig. 1A).... ***A. nigrocatta*** **sp. nov.**

– Size smaller (TL: 2.0–2.4 mm); male mesotarsomere 1 not or minimally enlarged; elytra with two spots: one at base and one at apex **24**

24 Apex of median lobe of aedeagus rounded or truncate in ventral view ..**25**

– Apex of median lobe of aedeagus pointed in ventral view **27**

25 Apex of median lobe of aedeagus rounded in ventral view (see Wewalka 2000, fig. 51a) .... ***A. liselotteae* Wewalka, 2000**

– Apex of median lobe of aedeagus truncate in ventral view...................... **26**

26 Median lobe of aedeagus in ventral view distinctly narrowed behind apical fourth (see Wewalka 2010, fig. 13a) .... ***A. bianae* Wewalka, 2010**

– Median lobe of aedeagus in ventral view with sides almost parallel over entire length (see Ji et al. 2014, fig. 3) .... ***A. longyanensis* Ji, Guo & Bian, 2014**

27 Median lobe of aedeagus in ventral view broadened in middle, apex slender (see Bian and Ji 2012, fig. 10).................... ***A. yanfengi* Bian & Ji, 2012**

– Median lobe of aedeagus in ventral view narrowed in middle, apex slightly broad **28**

28 Median lobe of aedeagus in ventral view slightly narrowed in middle (see Wewalka 2000, fig. 50a)............................ ***A. schoenmanni* Wewalka, 2000**

– Median lobe of aedeagus in ventral view distinctly narrowed in middle .**29**

29 Median lobe of aedeagus in ventral view broader at apex (see Bian and Ji 2010, fig. 6) .... ***A. grandis* Bian & Ji, 2010**

– Median lobe of aedeagus in ventral view narrower at apex (see Wewalka 2000, fig. 49a)..***A. weinbergeri* Wewalka, 2000**

List of Chinese *Allopachria* Zimmermann species, including their distribution

Allopachria bianae Wewalka, 2010 Guangdong
Allopachria dieterlei Wewalka, 2000 Hunan
Allopachria dudgeoni Wewalka, 2000 Guangdong, Guangxi, Hong Kong, Jiangxi, Zhejiang
Allopachria elongata Bian & Ji, 2012 Guangxi
Allopachria ernsti Wewalka, 2000 Guangxi; North Vietnam
Allopachria flavomaculata (Kamiya, 1838) Guangxi; Japan
Allopachria friedrichi Wewalka, 2000 Hunan
Allopachria froehlichi Wewalka, 2000 Hong Kong
Allopachria grandis Bian & Ji, 2010 Jiangxi
Allopachria guangdongensis Wewalka, 2010 Guangdong, Guangxi
Allopachria hajeki Wewalka, 2010 Yunnan
Allopachria hautmanni Wewalka, 2000 Anhui
Allopachria jaechi Wewalka, 2000 Hainan
Allopachria jendeki Wewalka, 2000 Yunnan
Allopachria jilanzhui Wewalka, 2000 Guangxi, Hunan
Allopachria komareki Wewalka, 2010 Guangdong
Allopachria liselotteae Wewalka, 2000 Guangxi
Allopachria longyanensis Ji, Guo & Bian, 2014 Fujian
Allopachria manfredi Wewalka, 2010 Guangdong
Allopachria miaowangi Wewalka, 2010 Hunan, Jiangxi, Zhejiang
Allopachria nigrocatta sp. nov. Guangxi
Allopachria schillhammeri Wewalka, 2000 Hunan
Allopachria schoenmanni Wewalka, 2000 Anhui, Zhejiang
Allopachria scholzi Wewalka, 2000 Yunnan
Allopachria taiwana (Satô, 1990) Taiwan

Allopachria wangi Wewalka & Nilsson, 1994 Taiwan
Allopachria weinbergeri Wewalka, 2000 Fujian, Guangdong, Zhejiang
Allopachria wuzhifengensis Bian & Ji, 2010 Hunan, Jiangxi
Allopachria yanfengi Bian & Ji, 2012 Guangxi
Allopachria yiae Bian, Guo & Ji, 2013 Chongqing, Guizhou

Acknowledgements

We thank Dr Bing-lan Zhang (SYSU) for guiding us in the use of photography equipment.

Additional information

Conflict of interest

The authors have declared that no competing interests exist.

Ethical statement

No ethical statement was reported.

Funding

This study was supported by GDAS Special Project of Science and Technology Development (2020GDSYL-20200102021, 2020GDASYL-20200301003).

Author contributions

Writing manuscript: Zhuo-yin Jiang, Feng-long Jia. Taking photos and making plates: Zhuo-yin Jiang, Ya-ru Chen, Li-bo Han. Reviewing manuscript: Zhuo-yin Jiang, Bei-xin Wang.

Author ORCIDs

Zhuo-yin Jiang https://orcid.org/0000-0001-6825-4283
Feng-long Jia https://orcid.org/0000-0003-2391-5038
Bei-xin Wang https://orcid.org/0000-0002-5253-8799

Data availability

All of the data that support the findings of this study are available in the main text.

References

Bian DJ, Ji LZ (2010) *Allopachria* Zimmermann, 1924 from Jiangxi, China, with descriptions of two new species (Coleoptera: Dytiscidae). Zootaxa 2350: 59–65. https://doi.org/10.11646/zootaxa.2350.1.6

Bian DJ, Ji LZ (2012) Notes on Chinese *Allopachria* Zimmermann, with descriptions of two new species from Guangxi (Coleoptera: Dytiscidae). Zootaxa 3151: 28–34. https://doi.org/10.11646/zootaxa.3151.1.2

Bian DJ, Guo C, Ji LZ (2013) *Allopachria yiae* sp. n. from Chongqing, China (Coleoptera: Dytiscidae: Hydroporinae). Zootaxa 3681(1): 85–88. https://doi.org/10.11646/zootaxa.3681.1.6

Brancucci M (1984) A new *Platambus* from China (Coleoptera, Dytiscidae). Mitteilungen der Schweizerischen Entomologischen Gesellschaft 57: 153–154.

Ji LZ, Guo C, Bian DJ (2014) *Allopachria longyanensis* sp. n. from China (Coleoptera: Dytiscidae). Zootaxa 3755(2): 194–196. https://doi.org/10.11646/zootaxa.3755.2.5

Jiang ZY, Zhao S, Yang ZY, Jia FL, Hájek J (2022) A review of *Copelatus* Erichson, 1832 of Mainland China, with description of ten new species from the *japonicus* complex (Coleoptera: Dytiscidae: Copelatinae). Zootaxa 5124(3): 251–295. https://doi.org/10.11646/zootaxa.5124.3.1

Miller KB, Nilsson AN (2003) Homology and terminology: Communicating information about rotated structures in water beetles. Latissimus 17: 1–4.

Nilsson AN (2007) Some necessary corrections of the spelling of species-group names within the family Dytiscidae (Coleoptera). Zootaxa 1615: 49–54. https://doi.org/10.11646/zootaxa.1615.1.5

Nilsson AN, Hájek J (2024a) A World Catalogue of the family Dytiscidae, or the Diving Beetles (Coleoptera, Adephaga). Version 1.I.2024. Distributed as a PDF file via Internet. http://www.waterbeetles.eu

Nilsson AN, Hájek J (2024b) Catalogue of Palearctic Dytiscidae (Coleoptera). Version 1.I.2024. Distributed as a PDF file via Internet. http://www.waterbeetles.eu

Peschet R (1923) Dytiscidae et Haliplidae nouveaux (Col.). Bulletin de la Société Entomologique de France 1923: 175–181. https://doi.org/10.3406/bsef.1923.27196

Wewalka G (2000) Taxonomic revision of *Allopachria* (Coleoptera: Dytiscidae). Entomological Problems 31(2): 97–128.

Wewalka G (2010) New species and new records of *Allopachria* Zimmermann (Coleoptera: Dytiscidae). Koleopterologische Rundschau 80: 25–42.

Zhao S, Hájek J, Jia FL, Pang H (2012) A taxonomic review of the genus *Neptosternus* Sharp of China with the description of a new species (Coleoptera: Dytiscidae: Laccophilinae). Zootaxa 3478: 205–212. https://doi.org/10.11646/zootaxa.3478.1.22

ZooKeys 1219: 303–329 (2024)
DOI: 10.3897/zookeys.1219.133132

Research Article

Sipadantonius roihani gen. et sp. nov., a new genus and species of Pseudocyclopidae Giesbrecht, 1893 (Copepoda, Calanoida) from the marine cave "Turtle Tomb" of Sipadan Island, Sabah, Malaysia

Chaichat Boonyanusith[1], Koraon Wongkamhaeng[2], Abdul-Rahim Azman[3]

1 *School of Biology, Faculty of Science and Technology, Nakhon Ratchasima Rajabhat University, Nakhon Ratchasima 30000, Thailand*
2 *Department of Zoology, Faculty of Science, Kasetsart University, Bangkok 10900, Thailand*
3 *Department of Earth Sciences and Environment, Faculty of Science and Technology, Universiti Kebangsaan Malaysia, 43600 UKM Bangi, Selangor, Malaysia*
Corresponding author: Abdul-Rahim Azman (abarahim@gmail.com)

Academic editor: Kai Horst George
Received: 26 July 2024
Accepted: 18 October 2024
Published: 6 December 2024

ZooBank: https://zoobank.org/FEE5F180-FA49-497C-A7C6-AEE122053BCD

Citation: Boonyanusith C, Wongkamhaeng K, Azman A-R (2024) *Sipadantonius roihani* gen. et sp. nov., a new genus and species of Pseudocyclopidae Giesbrecht, 1893 (Copepoda, Calanoida) from the marine cave "Turtle Tomb" of Sipadan Island, Sabah, Malaysia. ZooKeys 1219: 303–329. https://doi.org/10.3897/zookeys.1219.133132

Abstract

A new genus and species of the family Pseudocyclopidae, *Sipadantonius roihani* **gen. et sp. nov.**, was described based on specimens collected using a light trap in the marine cave of Sipadan Island, Sabah, Malaysia. The new genus is most related to *Pinkertonius*, primarily based on the similarity observed in the armament of ancestral segment IV of the male antennules, the armament of the female P5 Exp-3, the segmentation of the male P5, the armament of the maxillular basal exite, and the relative length of the ancestral segment XXVII of the antennules. Nevertheless, it distinguishes itself from *Pinkertonius* and all other genera of the family by the absence of the lateral seta of the basis of all swimming legs, the presence of an inner seta on the coxa of the female P5, the reduction of furcal setae I and III, as well as the specific armament of the ancestral segment XX of the antennules and the maxillular coxal endite. The female of *Sipadantonius roihani* **gen. et sp. nov.** has aesthetascs on the ancestral segments IV and XX of the antennules, as well as six setae on the maxillular coxal endite, exhibiting the most plesiomorphic characteristics of the family Pseudocyclopidae. The latter characteristic has not been recorded in the order Calanoida. It was hypothesised that the new species was a particle feeder living in the pelagic zone of the marine cave. The existence of the new species supported the assumption that the regional distribution of the family Pseudocyclopidae exhibited the Tethyan track, which might have been the subsequent result of the colonisation of the habitats prior to the closure of the Tethys Sea.

Key words: Crustacea, Southeast Asia, systematics, taxonomy, Zooplankton

Introduction

Based on the phylogenetic research conducted by Bradford-Grieve et al. (2014), 14 calanoid genera were recognised as members of the family Pseudocyclopidae Giesbrecht, 1893, which included *Badijella* Kršinic, 2005, *Boholina* Fosshagen, in Fosshagen & Iliffe, 1989, *Brattstromia* Fosshagen, in Fosshagen & Iliffe, 1991, *Exumella* Fosshagen, 1970, *Exumellina* Fosshagen, 1998, *Hondurella* Suárez-Morales & Iliffe, 2007, *Normancavia* Fosshagen & Iliffe, 2003, *Pinkertonius* Bradford-Grieve, Boxshall & Blanco-Bercial, 2014, *Placocalanus* Fosshagen, 1970, *Pseudocyclops* Brady, 1872, *Ridgewayia* Thompson I.C. & Scott A., 1903, *Robpalmeria* Fosshagen & Iliffe, 2003, *Stargatia* Fosshagen & Iliffe, 2003 and *Stygoridgewayia* Tang, Barron & Goater, 2008. The family was united with the family Epacteriscidae Fosshagen, 1973, thereby forming the superfamily Pseudocyclopoidea Giesbrecht, 1893, which was the basal clade of the order Calanoida Sars, 1903, based on molecular phylogenetic study (Bradford-Grieve et al., 2014). Among the listed genera, *Pinkertonius* was regarded as the basal taxon of the family (Bradford-Grieve et al. 2014).

Pseudocyclopid copepods are prevalent in shallow benthopelagic or anchialine cave habitats within tropical and subtropical marine waters globally, as documented by various researchers (e.g., Fosshagen and Iliffe 1989, 1991, 1998, 2003; Boxshall and Jaume 2012; Bradford-Grieve et al. 2014; Ohtsuka et al. 1996, 2000; Suárez-Morales and Iliffe 2007; Figueroa 2011; Moon and Soh 2014). Additionally, some genera and species are recognised from freshwater subterranean habitats, including *Stygoridgewayia trispinisa* Tang, Barron & Goater, 2008, *Boholina laorsriae* Boonyanusith, Wongkamhaeng & Athibai, 2020 and *Boholina reducta* Tran & Chang, 2020 (Tang et al. 2008; Boonyanusith et al. 2020; Tran and Chang 2020).

In the past decade, a great deal of research was conducted regarding the zooplankton ecosystem of Malaysian waters (Rezai et al. 2009; Yoshida et al. 2012; Nakajima et al. 2013; Balqiah and Rahim 2021), resulting in the documentation of more than 230 species. Nevertheless, the documentation regarding the prevalence of endemic zooplankton species remained insufficient. To date, only four species were recognised as endemic or host-specific, namely *Brachiella malayensis* Ohtsuka, Piasecki, Ismail & Kamarudin, 2020, *Kensakia parva* Harris V.A. & Iwasaki, 1997, *Labidocera jaafari* Othman, 1986 and *Sipadania celerinae* Humes & Lane, 1993. A recent biological survey conducted at the Sipadan Turtle Tomb yielded a significant number of specimens of calanoid copepods, which could not be assigned to any described species.

Morphologically, the new species appeared to resemble the genus *Pinkertonius* in the armament of the ancestral segment IV of the male antennule, the armament of the female P5 Exp-3, and the segmentation of both rami of the male P5. However, it bore a specific combination of the characteristics, particularly regarding the armament of the swimming legs and mouthparts; therefore, the status of a new genus was justified for the Malaysian specimens, and the name of *Sipadantonius* gen. nov. was proposed. The description and illustrations of the new taxon were provided hereafter.

Materials and methods

Specimens were collected in the Turtle Tomb of Sipadan Island, Sabah, Malaysia, on 3 August 2023 (Fig. 1). Sampling was conducted utilising a modified light trap at a depth of 20–24 m, which was deployed at the bottom substrate for ~ 24 hours. The specimens utilised for morphological descriptions were preserved in 10% buffered formalin prior to examination. Copepods were meticulously sorted under a stereomicroscope, followed by fixation and storage in 70% ethanol in the laboratory. Subsequently, a few specimens were soaked in the mixture of glycerol and 70% ethanol (approximate ratio 1/10 v/v) for 30 min. After that, animals of both sexes were individually transferred into a drop of 40% glycerol on a glass slide and dissected under a stereomicroscope. The material

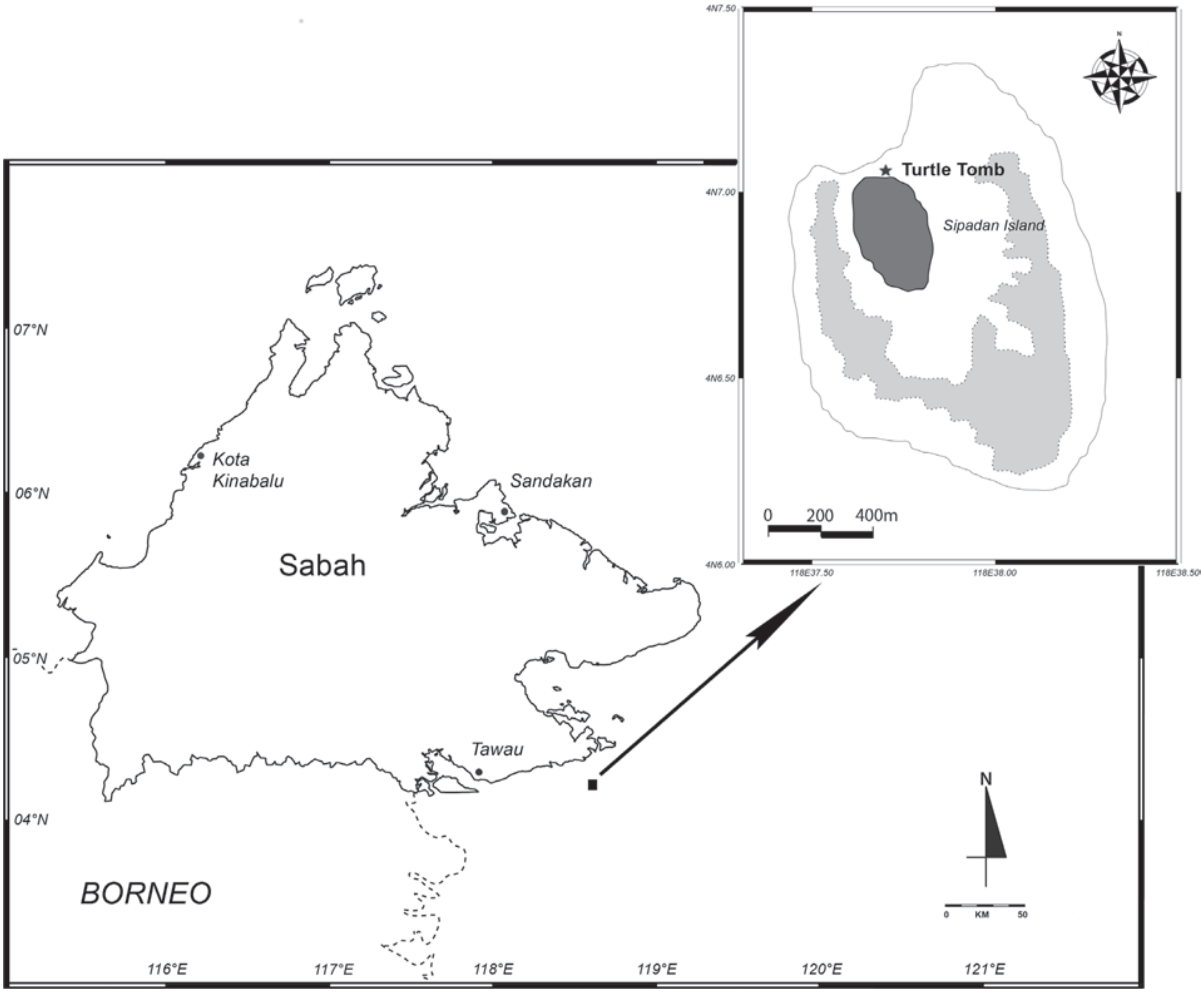

Figure 1. Geographical location of the type locality of *Sipadantonius roihani* gen. et sp. nov.

was ultimately mounted with a coverslip and subsequently examined under a Nikon ECLIPSE E200 compound light microscope at 1000 × magnification.

The habitus and appendages were examined and subsequently drawn utilising a drawing tube attached to a compound microscope at 400 × and 1000 × magnifications, respectively. Description was made by adopting the terminology established by Huys and Boxshall (1991) and employing the following abbreviations: **ae** = aesthetasc, **I** = spine, **Endp** = endopod, **Exp** = exopod, **Endp-1 (2, 3)** = proximal (middle, distal) segment of the endopod of the swimming legs, **Exp-1 (2, 3)** = proximal (middle, distal) segment of the exopod of the swimming legs, **P1–P6** = first to sixth swimming legs, **Seta I–VII** = first to seventh furcal seta, **Seta I** = anterolateral accessory seta, **Seta II** = anterolateral seta, **Seta III** = postereolateral seta, **Seta IV** = outer terminal seta, **Seta V** = inner terminal seta, **Seta VI** = terminal accessory seta, and **Seta VII** = dorsal seta.

Specimen repositories

The type material was deposited at the Universiti Kebangsaan Malaysia Muzium Zoologi (UKMMZ), Malaysia and the Sabah Parks Zoological Collection in Semporna, in accordance with the requirements stated in the Sabah Biodiversity Council – License for Transfer Ref. No. JKM/MBS.1000-2/3 JLD.5 [41].

Taxonomic account

Order Calanoida Sars, 1903
Superfamily Pseudocyclopoidea Giesbrecht, 1893
Family Pseudocyclopidae Giesbrecht, 1893

Genus *Sipadantonius* gen. nov.

https://zoobank.org/EF5F740F-CEAE-4CC4-BD2E-4E4FE621C904

Diagnosis. Female: Elliptical body. Single plate rostrum, with rounded tip, lacking rostral filaments. Six-segmented prosome. Symmetrical and rounded postero-lateral corners of the fifth pedigerous somite. Four-segmented and symmetrical urosome. Double-somite genital with genital operculum ventromedially. Symmetry furcal rami, with serrated hyaline frill on distal margin, armed with five setae on the tip of the ramus, without furcal setae I and III; spiniform seta II; normal-developed seta V, slightly longer than seta IV. Antennule with 26 segments-; ancestral segments II and fused III; ancestral segments X and partly fused XI; relatively short ancestral segment XXVII; with aesthetasc on ancestral segments I, III–XXI, XXV, and XXVII. Antennae with two-segmented Endp and nine-segmented Exp; segments I–VII of Exp each with one seta. Mandibles with un-modified coxal gnathobase, five-segmented Exp and two-segmented Endp; a distal segment of Endp with ten setae. Maxillulae with nine setae on coxal epipodite and six setae on coxal endite; unarmed basal exite; two-segmented, un-modified Endp. Seven-segmented maxillae lack an outer seta on the outer margin of the coxa. Eight-segmented maxillipeds; length of segments II–VI of Endp is equivalent to syncoxa; transformed proximalmost seta on segment III, with feather-like tip. Three-segmented P1–P5 with both rami; coxa with seta on the distomedial corner; the basis of all swimming legs lacking lateral seta, that of P2–P5 with cuticular window representing the remnant of armament on outer margin; the posterior surface of the basis of P1 with the curved hyaline process. Spine and setal complements of Exp-3 of P2–P5: 2.3.3.3 and 5.5.5.4, respectively; setal complement of Endp-3 of P2–P5: 8.7.7.6. Distolateral corner of P1 Endp-1 and Endp-2 of P1–P4 with bifid indentures; distolateral corner of both Endp-1 and Endp-2 of P5 un-fid. *Male*: Body shape, rostrum, prosome, mouthparts, furcal rami, and P1–P4 are identical to those of females. Slightly asymmetrical urosome. The left antennule is identical to that of the female; the 22-segmented right antennule, weakly geniculate; fused ancestral segments II–IV, XXI–XXIII, and XXIV–XXV. P5 is asymmetrical, with both three-segmented rami; basis with cuticular pores representing the remnant of armament on outer margin; Endp-1 of left and right legs lacks inner seta; separated Exp-2 and Exp-3; those of the right leg are modified to function as grasping organ.

Type species. *Sipadantonius roihani* sp. nov.

Etymology. Named after the type locality, Sipadan Island, Sabah, Malaysia, in combination with the *-tonius* stem from the existing generic name *Pinkertonius* Bradford-Grieve, Boxshall & Blanco-Bercial, 2014, alluding to the similarity of the genus *Pinkertonius*. The gender is masculine.

Sipadantonius roihani sp. nov.

https://zoobank.org/C38B34EF-2C23-4A8D-9396-616EAD33D82D
Figs 2–6 (female); 6–8 (male)

Material examined. ***Holotype*** • ♀ (adult), 0.95 mm long; 3 August 2023; coll. Azman, B.A.R.; light trap; UKMMZ-1631. ***Allotype*** • ♂ (adult), 0.87 mm long, collection data for holotype; UKMMZ-1632. ***Paratypes*** • 1 ♀ (adult) and 1 ♂ (adult); each was utterly dissected and mounted on a slide in glycerol and then sealed with nail varnish; the data was identical to that of the holotype; UKMMZ-1633–1634.

Additional material. • 2 ♂♂ (adult); the data was identical to that of the holotype; preserved in 70% ethanol, subsequently retained in collection of the Sabah Parks Zoological Collection in Semporna, Sabah.

Type locality. The marine cave "Turtle Tomb", Sipadan Island, Sabah, Malaysia; the entrance is located at 4°07'04.8"N, 118°37'41.0"E. Samples were collected in the cave at a depth of 22.0 meters below the sea surface, ~ 100 meters from the entrance.

Description of adult female. Body (Fig. 2A, B) with a total length of 0.91–0.95 mm (measured from anterior margin of cephalosome to tip of furcal rami; mean: 0.93 mm; *n* = 3), slightly dorsoventrally flattened; integument covered with hair-like spinules. Prosome six-segmented, elliptical, ~ 70% of body length and 2.2 × as long as urosome, ~ 2.3 × as long as wide, with greatest width at posterior margin of the first pedigerous somite (P1-bearing somite) (Fig. 2A). Cephalosome and all pedigerous somites free, with smooth hyaline frill on posterior margin of cephalosome and first four pedigerous somites (Fig. 2A, B); postero-lateral corners symmetrical and rounded (Fig. 2B). Naupliar eye not discernible. Urosome four-segmented, comprising genital double-somite, and three free abdominal somites; all somites with finely serrated hyaline frill on posterior margin (Fig. 2C–F). Genital double-somite barrel-shaped (Fig. 2E), ~ 27% of urosome length, as long as wide, with greatest width at mid-length of double-somite, with lingual-shaped genital operculum ventromedially; two gonoporal plates triangular-shaped, partially hidden under genital operculum (Fig. 2E). Three free abdominal somites subequal in length. Anal somite with slightly developed anal operculum; posterior margin with serrated hyaline frill dorso-laterally (Fig. 2F, G); anal operculum with smooth free margin, ornamented with row of spinules (Fig. 2F).

Furcal rami (Fig. 2F, G) symmetrical, parallel, each ~ 3 × as long as wide, with serrated hyaline frill on distal margin and two cuticular pores laterally (Fig. 2F, G); furcal setae I and III absent; furcal seta II spiniform, with setulae along inner margin; seta IV shorter than seta V, with breaking planes and plumose; seta V longest, with breaking plane and plumose, sub-equal to urosome length, ~ 1.2 × as long as seta IV; seta VI plumose, ~ 0.8 × as long as seta V; seta VII very short and plumose, inserted beside seta VI (Fig. 3A). Length ratio of furcal setae II to ramus length ~ 0.5 and the ratio of setae to ramus length from seta IV to seta VII: 3.3: 3.9: 3.0: 0.2.

Rostrum (Figs 2B, 3D) well developed, single plate and V-shaped; base broad, completely fused to anterior margin of cephalic shield and tapering to rounded tip between bases of antennules, with two sensillae, lacking rostral filaments.

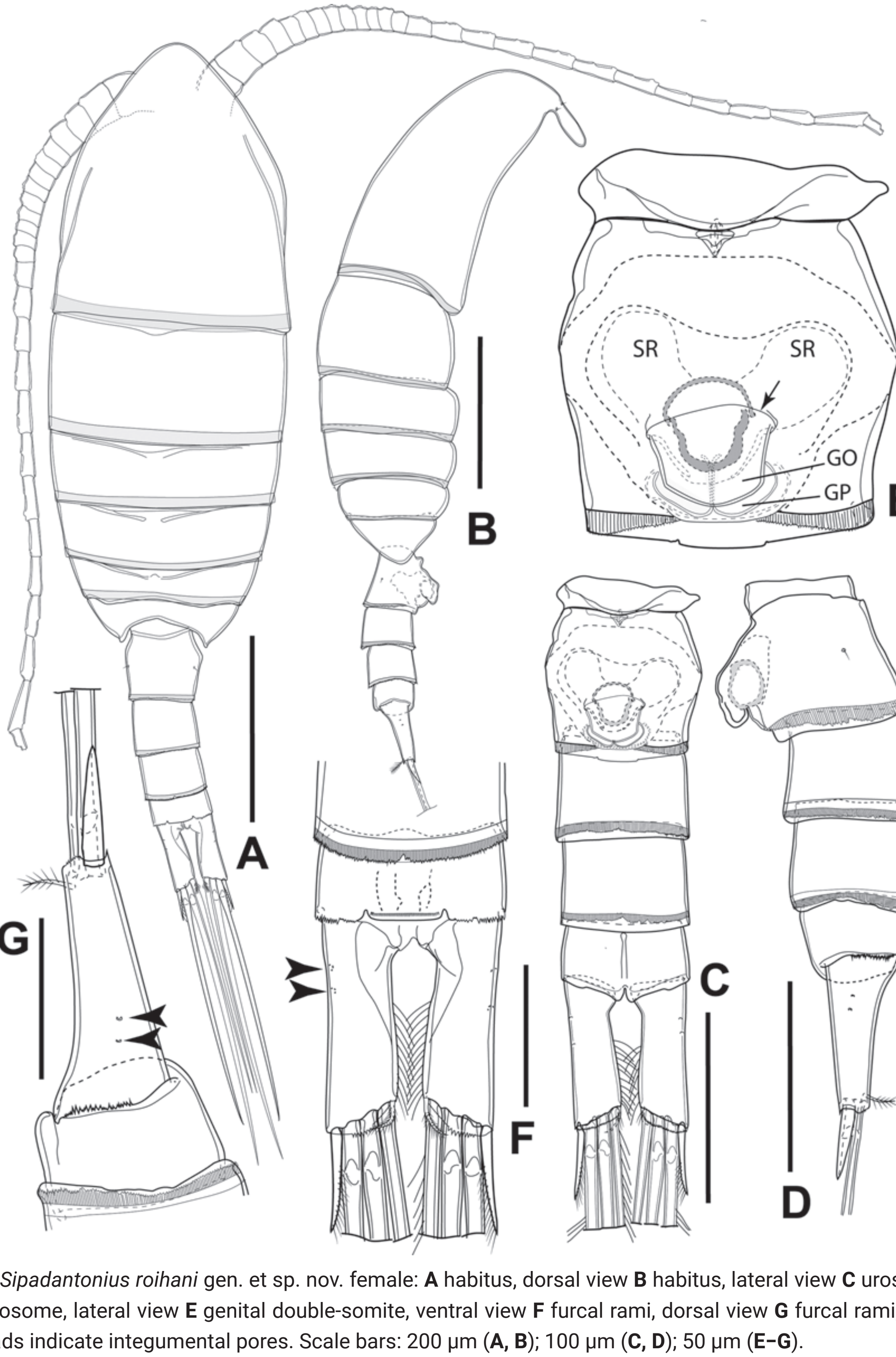

Figure 2. *Sipadantonius roihani* gen. et sp. nov. female: **A** habitus, dorsal view **B** habitus, lateral view **C** urosome, ventral view **D** urosome, lateral view **E** genital double-somite, ventral view **F** furcal rami, dorsal view **G** furcal rami, lateral view. Arrowheads indicate integumental pores. Scale bars: 200 µm (**A, B**); 100 µm (**C, D**); 50 µm (**E–G**).

Antennules (Figs 2A, 3C, D) symmetrical, representing 26-segmented, reaching distal margin of urosomite 2; ancestral segments II and III completely fused, representing evident segment II; ancestral segments X–XI partly fused, with remnant of ancestral articulation; ultimate segments ~ 1/3 of the length of pre-ultimate segment. Armature formula as follows (Roman numerals correspond to ancestral segment): 1+ae (I), 2+ae (II–III), 1+ae (IV), 2+ae (V), 2+ae (VI), 2+ae (VII), 2+ae (VIII), 2+ae (IX), 2+ae (X), 2+ae (XI), 2+ae (XII), 2+ae (XIII), 2+ae

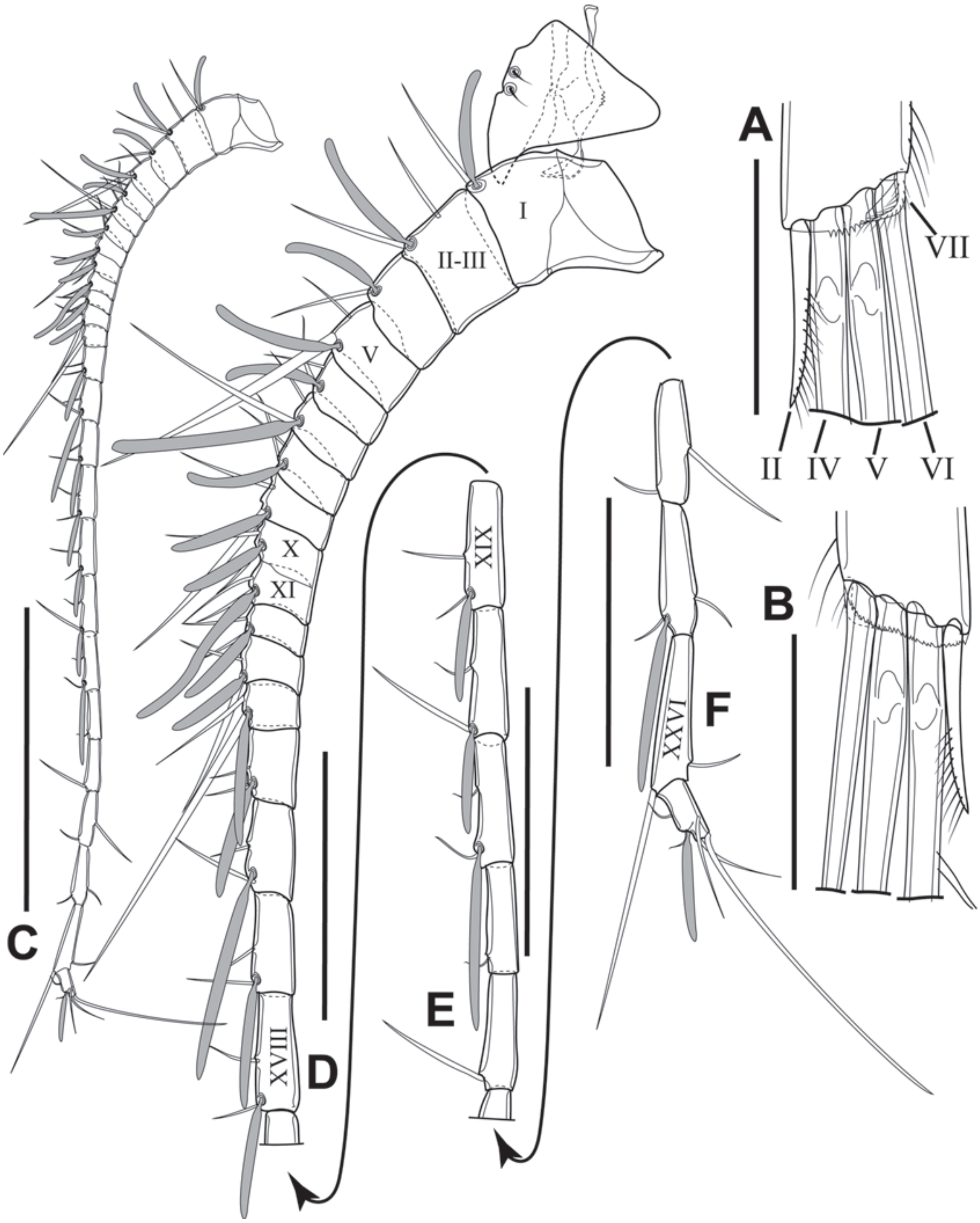

Figure 3. *Sipadantonius roihani* gen. et sp. nov. female: **A** tip of furcal ramus, dorsal view **B** tip of furcal ramus, ventral view **C** antennule **D** rostrum and segments 1–17 of antennule **E** segments 18–22 of antennule **F** segments 23–26 of antennule. Roman numerals on antennule correspond to ancestral segments. Scale bars: 50 μm (**A, B**); 200 μm (**C**); 100 μm (**D–F**).

(XIV), 2+ae (XV), 2+ae (XVI), 2+ae (XVII), 2+ae (XVIII), 2+ae (XIX), 2+ae (XX), 2+ae (XXI), 1 (XXII), 1 (XXIII), 2 (XXIV), 2+ae (XXV), 2 (XXVI), 5+ae (XXVII–XXVIII).

Antennae (Fig. 4A) biramous. Coxa short, bearing one seta on distomedial corner. Basis with two setae on distomedial corner. Exp nine-segmented, setal formula from proximal to distal segments: 1.1.1.1.1.1.1.1.3. Endp two-segmented; proximal segment bearing two setae inserted at the same place on medial margin; distal segment bilobed, bearing nine apical setae on medial lobe and seven apical setae on distal lobe, with curved row of spinules on outer margin.

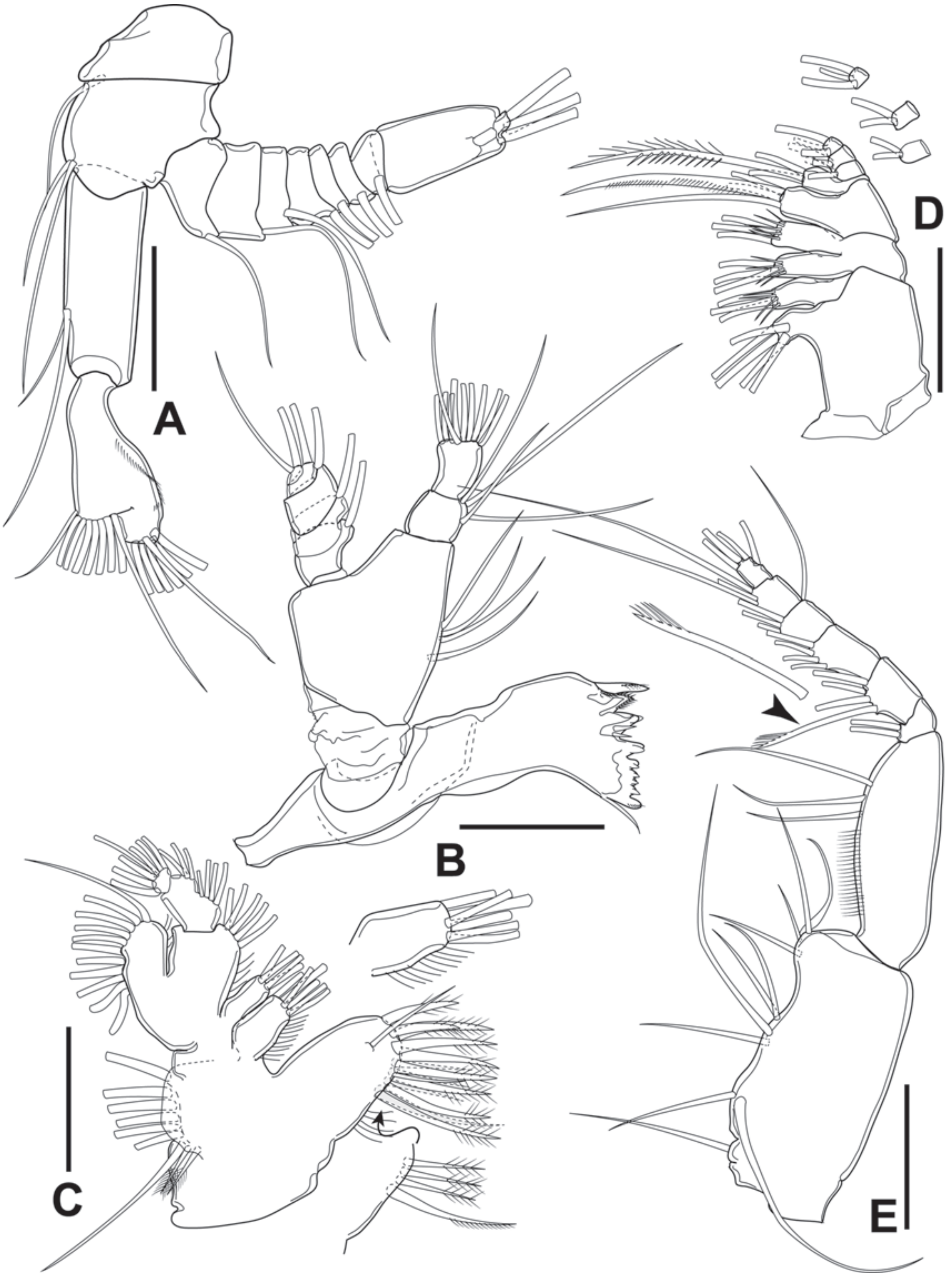

Figure 4. *Sipadantonius roihani* gen. et sp. nov. female: **A** antenna **B** mandible **C** maxillule, with picture of setae on posterior surface of praecoxal arthrite and enlarged picture of coxal endite **D** maxilla **E** maxilliped, with enlarged picture of transformed seta. Arrowhead indicates transformed seta on maxilliped. Scale bars: 50 µm.

Mandibles (Fig. 4B) with sclerotised gnathobase comprising nine cuspidate teeth and one small dorsal seta on cutting edge. Mandibular palp biramous; basis with four setae on inner margin. Exp five-segmented, setal formula from proximal to distal segments: 1.1.1.1.2. Endp two-segmented; proximal segment with four setae on distomedial corner; distal segment short, with ten apical setae.

Maxillulae (Fig. 4C) with praecoxal arthrite bearing nine spinulose and spiniform marginal setae and one smooth marginal seta, with one seta on anterior surface and four setae on posterior surface; proximalmost one on posterior surface longest, unipinnate. Coxal epipodite with nine apical setae; two proximal ones shortest; coxal endite with six apical setae. Basis fused to Endp, proximal and distal endites armed with four and five apical setae, respectively; basal exite knob-like appearance, unarmed. Exp with eleven setae along apical and outer margin. Endp two-segmented, proximal and middle segments completely fused, setal formula: 4.3.7.

Maxillae (Fig. 4D) seven-segmented, comprising praecoxa, coxa, basis and four-segmented Endp. Proximal and distal praecoxal endites with five and three apical setae, respectively. Coxa with two endites, each armed with three apical setae, with long spinules near distal margin of endite. Basis with large basal endite, armed with four apical setae; one of which strong and spiniform. Endp with setal formula: 3.2.2.3.

Maxillipeds (Fig. 4E) eight-segmented, comprising syncoxa, basis, and six-segmented Endp. Syncoxa with four syncoxal endites, setal formula: 1.2.4.4; one seta on second and third endite ~ 2 × as long as seta arising nearby. Basis with three medial setae, with row of spinules on anterior surface. Endp with setal formula: 2.4.4.3.3+1.4; seta 4 on segment II of Endp spiniform, with feather-like tip (Fig. 4G).

P1–P4 (Figs 5A–H, 6A–D) biramous, comprising coxa, basis, and three-segmented rami. Integument ornamented with numerous spinules and short hairs. Intercoxal sclerite sub-rectangular. Coxa with medial seta on distomedial corner. Basis of P2–P4 with cuticular window representing remnant of armament on outer margin (Figs 5G, 6C, D) but the remnant not discernible in P1 (Fig. 6B). Outer spine of P1 Exp setiform; those of Exp of P2–P4 stronger and oar-shaped. Distolateral corner of P1 Exp-2 drawn out into mint leaf-like process; those of Exp-1 and Exp-2 of P2–P4 slightly extended, with two acutely protrusions beside spine; inner protrusion larger and longer than outer one. Anterior surfaces of Exp-1 and Exp-2 with cuticular pores near insertion of outer spine; Exp-2 with acutely minute process near distomedial corner in P2–P4 but not discernible in P1; Exp-3 with cuticular pores near insertion of both proximalmost outer spine and outer apical one. Endp of all swimming legs with cuticular pores near distal margin of Endp-1 and at distal ~ 1/4 of Endp-3. Outer and outer apical spines of all swimming legs relatively short, oar-shaped; inner apical spine with serrated cuticular expansion on outer margin. Armature of swimming legs as presented in Table 1. Some other characteristics of P1–P4 as following described.

Table 1. Armament of P1–P5 in *Sipadantonius roihani* gen. et sp. nov., (Legend: outer-inner element; outer-apical-inner element; Arabic numerals indicate number of setae; Roman numerals indicate number of spines).

Swimming leg	Coxa	Basis	Exopod			Endopod		
			1	2	3	1	2	3
P1	0-1	0-1	I-1	1-1	II-I-4	0-1	0-2	1-2-3
P2	0-1	0-0	I-1	I-1	II-I-5	0-1	0-2	2-2-4
P3	0-1	0-0	I-1	I-1	III-I-5	0-1	0-2	2-2-4
P4	0-1	0-0	I-1	I-1	III-I-5	0-1	0-2	2-2-3
P5 (female)	0-1	0-0	I-1	I-1	III-I-4	0-1	0-1	2-2-2
Left leg of P5 (male)	0-0	0-0	I-0	I-0	0-I-I	0-0	0-1	2-2-2
Right leg of P5 (male)	0-0	0-0	I-0	I-0	I-0-I	0-0	0-1	2-2-2

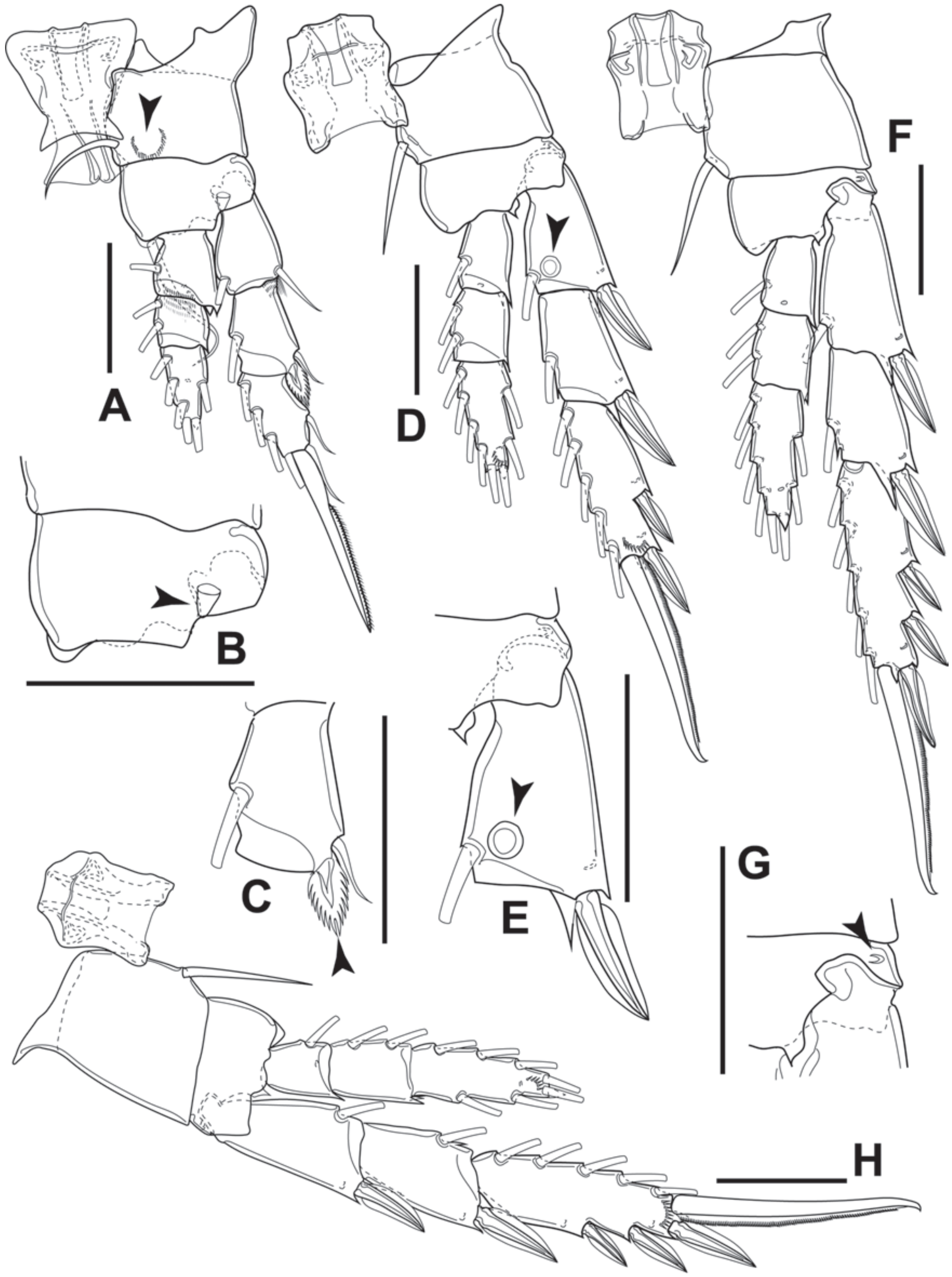

Figure 5. *Sipadantonius roihani* gen. et sp. nov. female: **A** P1 **B** basis of P1, posterior surface **C** P1 Exp-2 **D** P2 **E** P2 Exp-1, posterior surface **F** P3 **G** lateral margin of basis of P3 **H** P4. Arrowheads indicate the important characteristic of the structure. Scale bars: 50 μm.

P1 (Figs 5A–C, 6A, B). Coxa trapezoidal; anterior surface with triangular expansion on proximomedial corner and oval integumental window near distomedial corner; integumental window surrounded by curved spinules. Basis bearing medial seta on distomedial corner but lacking either lateral seta or remnant of armament on outer margin; posterior surface with short curved hyaline

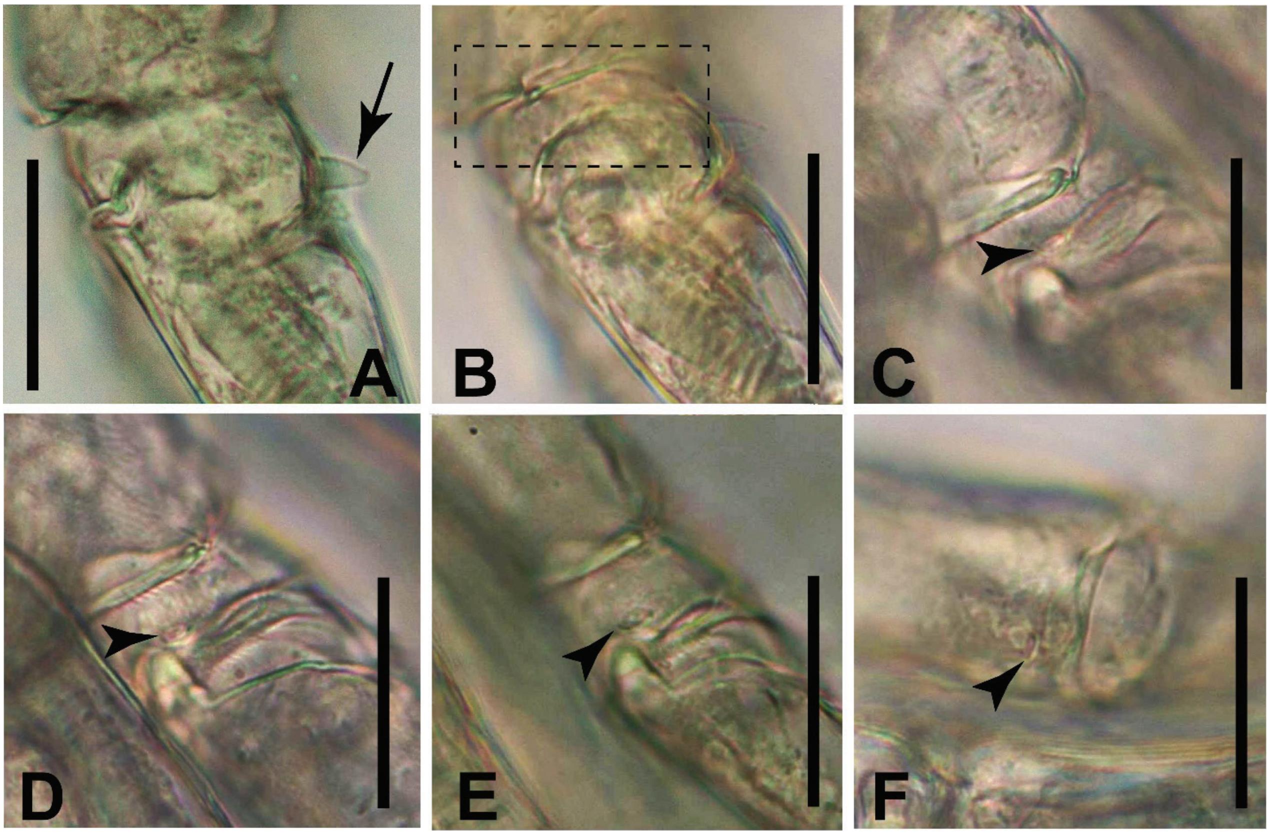

Figure 6. *Sipadantonius roihani* gen. et sp. nov. photographs of lateral surface of basis of swimming legs, female (**A–E**) and male (**F**): **A** posterior hyaline process on basis of P1 (indicated by arrow) **B** P1 **C** P3 **D** P4 **E, F** P5. Arrowheads indicate cuticular windows on lateral margin of basis. Scale bars: 10 µm.

process near insertion of Exp (Fig. 6B). Anterior surface of Exp-1 with row of long spinules on distolateral corner. Endp-1 with bifid indenture on distolateral corner and long spinules along posterior margin; Endp-2 with an acute indenture on distolateral corner.

P2 (Fig. 5D, E). Coxa rectangular. Posterior surface of Exp-1 with circular integumental window near insertion of inner seta; Exp-3 with two outer spines. Endp-1 with an acute indenture on distolateral corner; that of Exp-2 bifid.

P3 (Figs 5F, G, 6C) as that of P2 but Exp-1 lacking integumental window on posterior surfaces and Exp-3 with three outer spines.

P4 (Figs 5H, 6D) Coxa sub-quadrate. Basis and rami as those of P3.

P5 (Figs 6E, 7A) biramous, with both rami three-segmented; armament as in Table 1. Integument and intercoxal sclerite as described for P2–P4. Coxa rectangular, longer than wide; medial seta shorter than those of P1–P4. Basis, Exp-1 and Exp-2 as in P3 and P4, but inner seta on Exp-1 shorter than those of P1–P4. Exp-3 ~ 2.5 × as long as wide, offset on inner side at distal ~ 1/3 of segment. Endp-1 and Endp-2 with an acute indenture on distolateral corner each; Endp-3 longer than length of Endp-1 and Endp-2 combined. Ornamentation as that of P3 and P4.

Description of adult male. Body (Fig. 7B) with a total length of 0.87 and 0.89 mm (measured from anterior margin of cephalosome to tip of furcal rami; mean: 0.89 mm; *n* = 2). Habitus slightly smaller and slenderer than in female (Fig. 7B, C). Prosome six-segmented, elliptical, ~ 70% of body length and 2.2 × as long as urosome, ~ 2.6 ×as long as wide, with greatest width at posterior margin

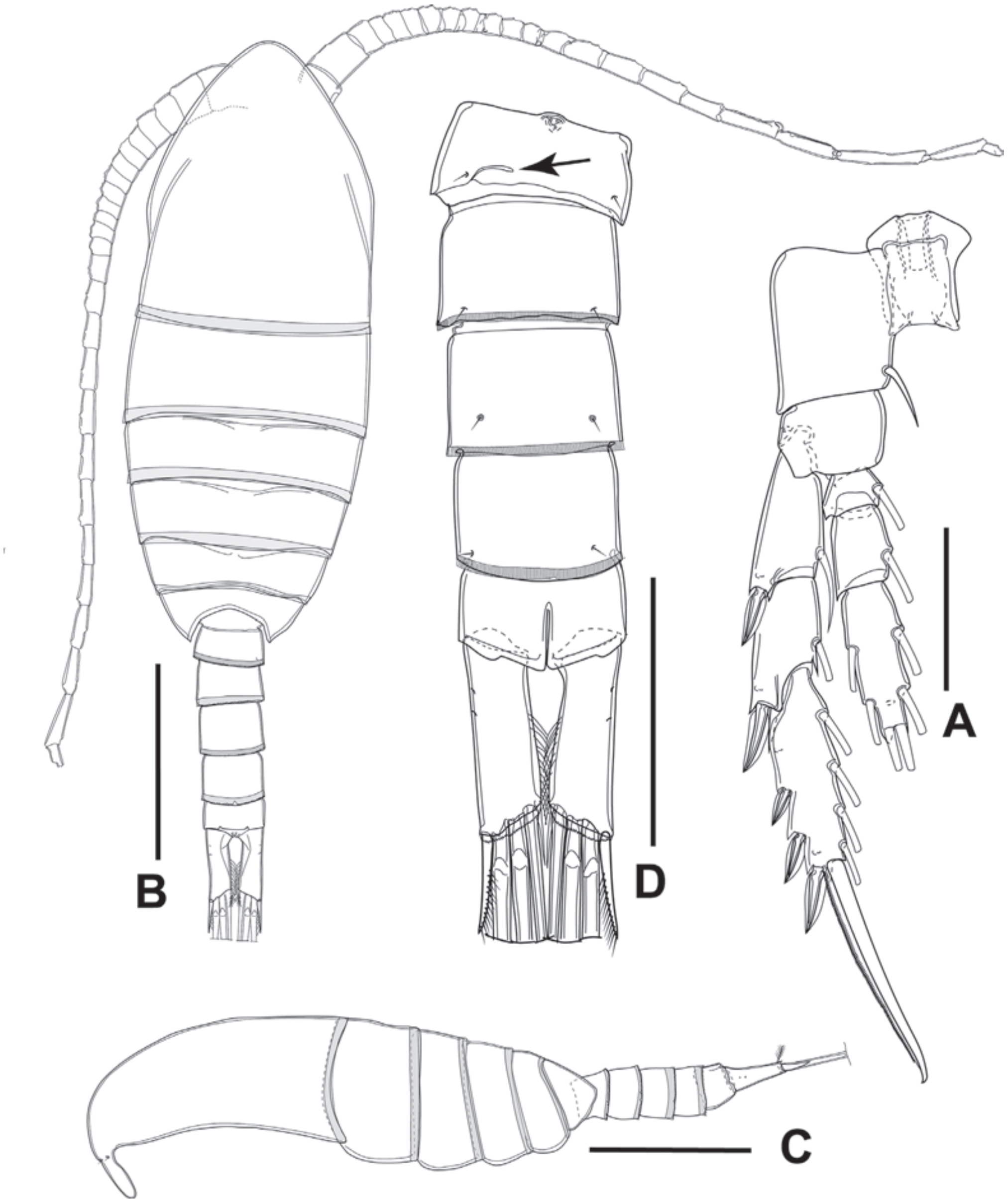

Figure 7. *Sipadantonius roihani* gen. et sp. nov. female **(A)** and male **(B–D)**: **A** P5 **B** habitus, dorsal view **C** habitus, lateral view **D** urosome, ventral view. Arrow indicates the ventral suture on genital somite. Scale bars: 50 µm (**A, D**); 200 µm (**B, C**).

of the first pedigerous somite. Cephalosome and first three pedigerous somites similar to those in female. Naupliar eye not discernible. Urosome five-segmented; comprising genital somite and four free abdominal somites. Genital somite slightly asymmetrical; ventral surface with gonopore on proximal margin. All free abdominal somites similar in length, each with finely serrated hyaline frill on posterior margin. Anal somite identical to that of female (Fig. 7B, D).

Furcal rami (Fig. 7D) identical to that of female, ~ 3 ×as long as wide. Armament and ornamentation identical to that of female.

Antennules asymmetrical. Left antennule non-geniculate, reaching distal margin of urosomite 2; articulation and setation identical to those of female. Right antennule geniculate, representing 22-segmented (Fig. 8A, B); ancestral segments II–IV completely fused, representing evident segment II; ancestral segment XIV with hook-like transformed seta; ancestral segments XXI–XXIII and XXIV–XXV completely fused representing evident segment XIX and XX,

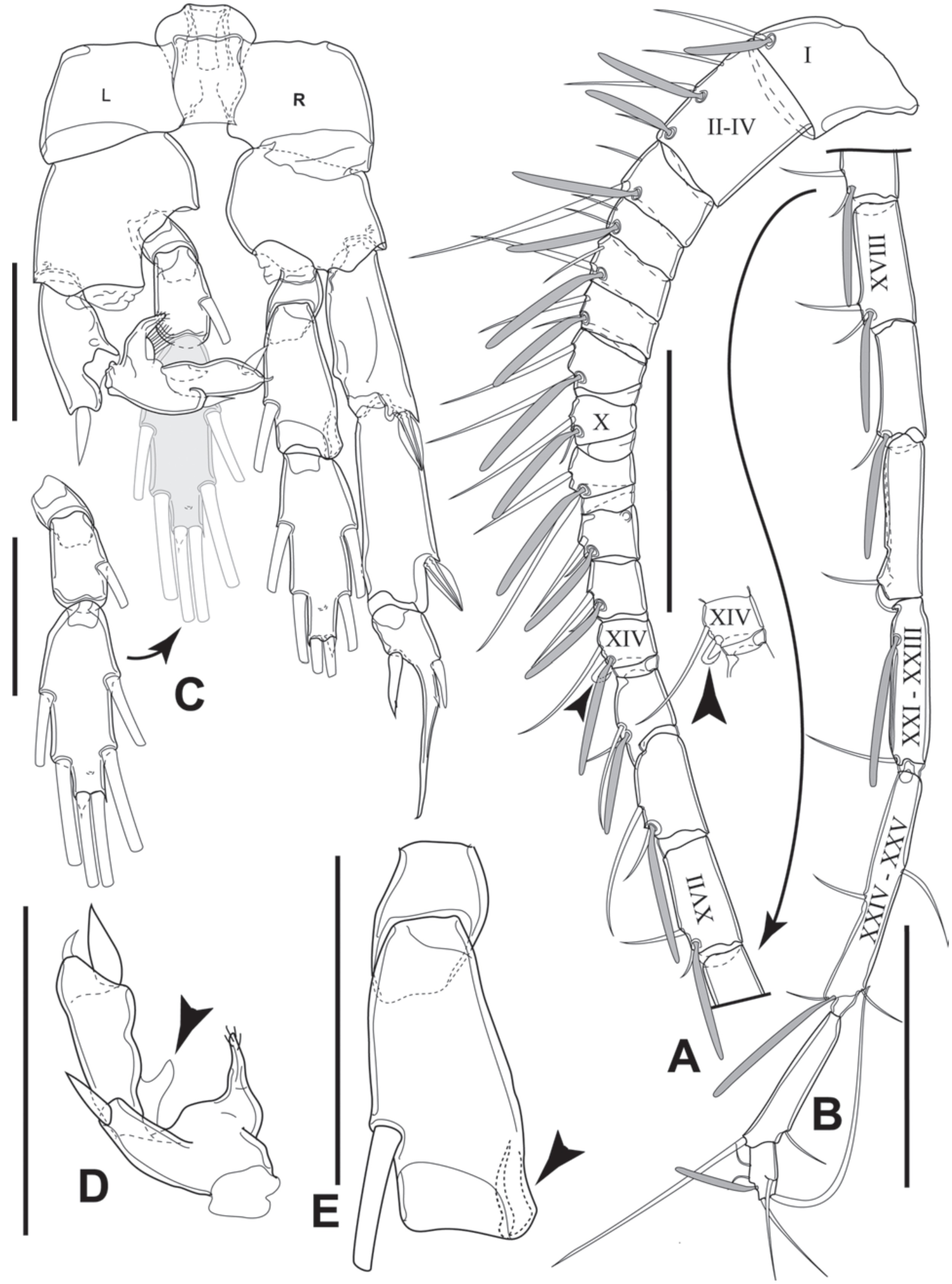

Figure 8. *Sipadantonius roihani* gen. et sp. nov. male: **A** segments 1–15 of antennule, with picture of segment 12 that aesthetasc is removed **B** segments 16–22 of antennule **C** P5 furcal view **D** Exp-2 and Exp-3 of right leg of P5, lateral view **E** Endp-1 and Endp-2 of left leg of P5, posterior surface. Arrowheads indicate the important characteristic of the structure and Roman numerals on antennule correspond to ancestral segments. Scale bars: 200 µm (**A, B**); 50 µm (**C–E**).

respectively; ultimate segments ~ 1/3 of the length of pre-ultimate segment; armature formula as follows (Roman numerals correspond to ancestral segment): 1+ae (I), 3+2ae (II–IV), 2+ae (V), 2 (VI), 2+ae (VII), 2+ae (VIII), 2+ae (IX), 2+ae (X), 2+ae (XI), 2+ae (XII), 2+ae (XIII); 1 hooked seta+1+ae (XIV), 2+ae (XV), 2+ae (XVI), 2+ae (XVII), 2+ae (XVIII), 1+ae (XIX), 1 (XX), 1+ae (XXI–XXIII), 4+ae (XXIV–XXV), 2 (XXVI), 5+ae (XXVII–XXVIII).

Antenna, mandible, maxillula, maxilla, maxilliped, and P1–P4 as those of female.

P5 (Fig. 8C–E) biramous, asymmetrical. intercoxal sclerite as described for female P3; coxa lacking medial seta. Left leg biramous; coxa and basis as shown; Exp and Endp three-segmented each. Exp-1 lacking inner seta, with conical, smooth outer spine; Exp-2 transformed, with claw-like extension on medial margin and conical, smooth outer spine; Exp-3 with conical, smooth subapical spine and minute apical spine, with claw-like cuticular expansion at base (Fig. 8C, D); Endp inserted on medial socket of basis; Endp-1 without inner seta, anterior surface longer than posterior one; Endp-2 shorter than that of right leg, with inner seta; Endp-3 with six marginal setae and cuticular pore on anterior surface. Right leg biramous; coxa and basis as shown; Exp and Endp three-segmented each; Exp-1 and Exp-2 elongate, each with one outer spine, but lacking inner seta each; Exp-3 with apical spine fused to segment bearing it, with spine on both lateral and medial margin; Endp-1 as that of right leg; Endp-2 longer than that of left leg, with longitudinal groove on distolateral corner and inner seta; Endp-3 as that of right leg.

Variability. Based on three male specimens, including the allotype, the inner seta was absent from the right P4 Exp-1 in the allotype. There was no additional remarkable variation between the females and males.

Abnormality. There was a curved suture on the right side of the ventral surface of the genital somite in one male (Fig. 7D).

Etymology. The specific epithet was conferred in honour of Mr Roihan Han, a Malaysian deep dive record holder (at a depth of 164 m), who also led the Turtle Tomb exploration activity. Consequently, the name is a noun in the genitive singular.

Differential diagnosis and remarks. The new taxon belonged to the superfamily Pseudocyclopoidea Giesbrecht, 1893, indicated by the following diagnostic characteristics mentioned in Bradford-Grieve et al. (2014):

1. fully developed the arthrodial membrane between body somites and limb segments,
2. identical configuration of mouthparts in both sexes,
3. segments I–VIII of Exp of the antenna with one seta each,
4. segment V of Endp of maxilliped with outer seta,
5. right antennule of the male geniculate,
6. P1–P5 with both three-segmented rami,
7. Exp-3 of P1–P5 with two, two, three, three, and three outer spines, respectively.

Epacteriscidae Fosshagen, 1973 and Pseudocyclopidae Giesbrecht, 1893 (Bradford-Grieve et al. 2014) are two families of primitive calanoid fauna that have been recently accepted within it. Among these two taxa, Epacteriscidae is the basal calanoid fauna from a phylogenetic perspective (Bradford-Grieve et al. 2010).

Following the recent morphological examination, the new species demonstrated a close affinity to the family Pseudocyclopidae through the presence of the following shared characteristics:

1. rostrum single plate with a rounded tip and without rostral filaments,
2. furcal ramus symmetrical and without modification of the left furcal seta VI,
3. mandibles with well-developed Endp forming the main axis of the mandibular palp,
4. maxillulae with marginal setae IX on coxal epipodite,
5. maxillipeds with normally developed endopod segments II–VI longer than coxa,
6. distolateral corner of Exp-2 the female P5 extended,
7. Exp-2 of the female P5 offset in oblique angle to the main axis of the rami.
8. Exp-2 of the left leg of the male P5 with the inner process.

It was noted that the new species exhibited an affinity to the family Epacteriscidae, characterised by the presence of aesthetasc on the ancestral segment IV of the antennule and the absence of inner process on Exp-2 of the right leg of the male P5. Furthermore, a combination of the presence of aesthetasc on the ancestral segment XIX of antennule in both sexes and the presence of aesthetasc on the ancestral segment XX of the female antennule, as identified in the new species, had been observed exclusively in *Caiconectes* Fosshagen & Iliffe, 2007. Nevertheless, the new species could not be classified as a member of this family due to its lack of a bilobed rostrum, rostral filament, and raptorial-adaptive features of mouthparts. An example of the last characteristic was the enlargement of the ventral teeth (e.g., Fosshagen et al. 2001; Fosshagen and Iliffe 2007). In light of this, the presence of the aesthetasc on the ancestral segment XX of the female antennule was probably convergent among the new species and *Caiconectes*. The taxonomic placement of the latter genus remained uncertain, having been more recently classified as incerta sedis. The assumption that *Caiconectes* belonged to the Epacteriscidae phylogenetic lineage, whereas the new species belonged to the Pseudocyclopidae lineage, was supported by the differences observed in the following characteristics between the new species and *Caiconectes*: configuration of the rostrum, feeding mode adaptive feature of mouthparts, ornamentation of the distolateral corner of the P1 Exp-2.

Consequently, the placement of the new species within the superfamily Pseudocyclopoidea and the family Pseudocyclopidae was deemed justified. It was suggested that the presence of aesthetasc on ancestral segment IV of the female antennule and the absence of inner process on Exp-2 of the right leg of the male P5 constituted merely an occasional occurrence of the characteristic within the representatives of the justified family. Following the synonymisation of the families Boholinidae and Ridgewayiidae with the family Pseudocyclopidae, 14 calanoid genera were included. The genera *Boholina*, *Exumella*, *Placocalanus*, *Pseudocyclops* and *Ridgewayia* are polytypic; whereas the remaining genera are monotypic, represented by one species. Among these genera, the monotypic genus *Pinkertonius* is considered the basal taxon. The phylogenetic study indicated four characteristics that distinguished *Pinkertonius* from other genera: (1) the separation of ancestral segments II and III of the female antennule, (2) the presence of aesthetasc on the ancestral segment IV of the male antennule, (3) the presence of medial seta 4 on the female P5 Exp-3, and (4) the separation of Exp-2 and Exp-3 of both rami of the male P5. Based on the aforementioned characteristics, the new species represented one of the phylogenetic transitional stages between the genus *Pinkertonius* and other genera, as the same conditions of characteristics (2), (3), and (4) were present in the new species with separated ancestral segments II and III of the female antennule. Other characteristics shared by the new species and *Pinkertonius ambiguus* Bradford-Grieve, Boxshall & Branco-Bercial, 2014 included (1) the shape and the armament of Exp-3 and Endp of the right leg of the male P5, (2) the absence of armature element of maxillular basal exite, and (3) the relative length of ancestral segment XXVII of antennule.

Nevertheless, the new species was unable to be classified as a member of the genus *Pinkertonius* and all genera of the family Pseudocyclopidae based on the combination of the following characteristics:

1. furcal rami lacking seta III,
2. furcal seta VII inserted beside seta VI rather than in front of the seta V or seta VI,
3. antennule with aesthetasc on ancestral segment IV in both sexes,
4. ancestral segments XIX–XXIII of the male antennule without modified setae
5. maxillulae with six setae on coxal endite,
6. seta 4 of the endopodal segment II of maxilliped transformed,
7. basis of P1–P5 without lateral seta,
8. the male P5 Endp-1 lacking inner seta,
9. the right leg of the male P5 lacks process on the inner margin of Exp-2.

Consequently, the new generic rank *Sipadantonius* gen. nov. was established within the family Pseudocyclopidae, intended to accommodate the new calanoid species from the Turtle Tomb of Sipadan Island, Sabah, Malaysia. Furthermore, the female exhibited the most plesiomorphic characteristics of the family Pseudocyclopidae by having aesthetascs on the ancestral segments IV and XX of antennule and six setae on the maxillular coxal endite. The number of setae on the maxillular coxal endite in Calanoida exhibited variability; however, it was noted that there had never been more than five setae (Boxshall and Halsey 2004). To date, the presence of six elements on the coxal endite was recorded in the order Misophrioida Gurney, 1933, as well as the families Canuellidae Lang, 1944 and Longipediidae Boeck, 1865 (Boxshall and Halsey 2004).

Discussion

The order Calanoida had been divided into nine superfamilies by Andronov (1974). Subsequently, after Fosshagen and Iliffe (1985) raised the family Platycopiidae Sars, 1911 to full order rank, namely Platycopioida Fosshagen, 1985 and following the introduction of two new superfamilies by Park (1986), ten superfamilies were recognised. They included Augaptiloidea Sars, 1905, Bathypontioidea Brodsky, 1950, Centropagoidea Giesbrecht, 1893, Clausocalanoidea Giesbrecht, 1893, Epacteriscoidea Fosshagen, 1973, Eucalanoidea Giesbrecht, 1893, Megacalanoidea Sewell, 1947, Pseudocyclopoidea Giesbrecht, 1893, Ryocalanoidea Andronov, 1974, and Spinocalanoidea Vervoort, 1951, in which

Andronov (2007) suggested the merger of Epacteriscoidea within Pseudocyclopoidea. According to a morphology-based phylogenetic study, the monophyly of numerous recognised superfamilies was established (Bradford-Grieve et al. 2010); the finding was subsequently corroborated by the multiple gene-based phylogenetic analysis (Blanco-Bercial et al. 2011). Bradford-Grieve et al. (2014) indicated that the families Boholinidae, Pseudocyclopidae, Ridgewayiidae, and Epacteriscidae were included in the re-definition of the superfamily Pseudocyclopoidea, based on the recovery of the monophyletic relatedness among the superfamilies Epacteriscoidea and Pseudocyclopoidea. Although the clade was formed with low jackknife support due to a considerable number of homoplastic characters, evidence indicated that each superfamily possessed a distinct set of morphological characteristics that reflected the unique genetic basis of the superfamily. This may have been the reason that the previous gene-based phylogenetic analysis of the Calanoida aligned with the earlier morphology-based phylogenetic inference (Park 1986; Bradford-Grieve et al. 2010, 2014). In the case under consideration, it was observed that most of the ancestral characteristics of Pseudocyclopoidea were retained in the new species. They included a triangular rostral plate without a rostral filament, a complete separation of ancestral segment IV, which resulted in antennules with 27 segments, a maxilliped with six-segmented Endp, P5 with both rami three-segmented, separated genital apertures each hidden under its operculum, and presence of inner seta on Exp-1 of the female P5 (Andronov 2014). Furthermore, the weak expression of the sexual dimorphism of P5 and the configuration of swimming legs, which were regarded as indicative of the origin from a single species of the Pseudocyclopoidea (Andronov 2014), is relevant for the new species. The characteristic of P2 Exp-3 with two outer spines was observed in other families, including Calanidae Dana, 1846, Paracalanidae Giesbrecht, 1893, Pseudodiaptomidae Sars, 1902, Sulcanidae Nicholls, 1945, and Tortanidae Sars, 1902. The representatives of these families have P5 bearing Exp-3 with two outer spines at most. Furthermore, the considerable reduction of Enp of the female P5 and the strong expression of sexual dimorphism of P5 were evident in most of the aforementioned families (Boxshall and Halsey 2004; Andronov 2014).

Bradford-Grieve et al. (2014) noted certain modifications of the mandible, maxilla, and maxilliped that were associated with the families Epacteriscidae and Pseudocyclopidae, thereby indicating their feeding habits (e.g., Fosshagen 1968; Fosshagen et al. 2001; Jaume and Humphreys 2001; Fosshagen and Iliffe 2003, 2004a, 2004b, 2007; Suárez-Morales and Iliffe 2007; Boonyanusith et al. 2020). Recently, the family Epacteriscidae is comprised of *Balinella* Fosshagen, Boxshall & Iliffe, 2001, *Bofuriella* Fosshagen, Boxshall & Iliffe, 2001, *Bomburiella* Fosshagen, Boxshall & Iliffe, 2001, *Cryptonectes* Fosshagen & Iliffe, 2004, *Iboyella* Boxshall & Jaume, 2003, *Oinella* Fosshagen, Boxshall & Iliffe, 2001, *Bunderia* Jaume & Humphreys, 2001, *Edaxiella* Fosshagen, Boxshall & Iliffe, 2001, *Epacteriscus* Fosshagen, 1973, *Enantronoides* Fosshagen, Boxshall & Iliffe, 2001, *Enantiosis* Barr, 1984, *Enantronia* Fosshagen, Boxshall & Iliffe, 2001, *Gloinella* Fosshagen, Boxshall & Iliffe, 2001, *Minnonectes* Fosshagen & Iliffe, 2004, *Erebonectes* Fosshagen, in Fosshagen & Iliffe, 1985, and *Miheptneria* Fosshagen & Iliffe, 2004) had been considered as raptorial feeders, based on the characteristics such as the gnathobase of the mandible with enlarged ventral teeth, the mandibular palp with reduced Endp and the well-developed

Exp forming the main axis of the palp, the transformation of setae on the distal part of the maxilla and maxilliped to stout, elongate, spinous setae or the reduction of setae on both appendages, and the maxilliped bearing a shortened Endp. On the other hand, the feeding habits of the family Pseudocyclopidae were observed to be more variable. Genera such as *Boholina*, *Hondurella*, *Ridgewayia* and *Stygoridgewayia* were presumably particle feeders (Fosshagen and Iliffe 2003; Suárez-Morales and Iliffe 2007; Tang et al. 2008; Boonyanusith et al. 2020), *Exumella* were considered to be a benthic scavenger, based on the reduction of the seta of the Endp of the mandible (Jaume and Boxshall 1995), in addition to *Exumellina* and *Stargatia* are believed raptorial feeders, deduced from the paddle-like adaptive feature of the mandible and the Endp of maxillule (Fosshagen and Iliffe 1998). The new species was presumed to be a particle feeder, demonstrating a close affinity with the family Pseudocyclopidae from a taxonomic perspective based on the four following morphological characteristics, which include: (1) the mandible armed with numerous small teeth on the cutting-edge of the gnathobase; (2) the well-developed Endp of the mandible with four and more than nine setae on the proximal and the distal segments, respectively, and representing the main axis of the mandibular palp; (3) the maxilla with elongate endite on the basis and armed with normal plumose setae; (4) the Endp of the maxilliped elongate. The new species exhibited a modification of a seta on the Endp of maxilliped, also observed in *Brattstromia* (Fosshagen and Iliffe 1991); however, the shape of the transformed seta differed between the new species and the genus mentioned above. In *Brattstromia*, the tip of the seta was serrated and sharpened, which related to its cutting function (Fosshagen and Iliffe 1991). In the new species, the tip of the seta was ornamented with long spinules, which bore a resemblance to the feather-like spine that has frequently been observed in the cave-dwelling harpacticoid genus *Elaphoidella* (Brancelj et al. 2010). It was hypothesised that the transformed seta on the maxilliped of the new taxon could be utilised as a collecting apparatus, in accordance with the assumption posited by Brancelj et al. (2010), who postulated that the modified seta plays a role in collecting food particles, such as fine detritus or bacteria.

The existence (= the presence/absence) of aesthetascs on certain segments of the antennule was employed in morphology-based phylogenetic analysis of the superfamily Pseudocyclopoidea (Bradford-Grieve et al. 2014). The presence of aesthetascs on all other ancestral segments was utilised for the analyses; I, II, III, VII, XVI, XXII, XXIII, XXIV, and XXVI–XXVIII of the ancestral segments were refrained. This was likely attributable to the low phylogenetic implication of the characteristic, which may have indicated the consistency in the existence of aesthetascs on the aforementioned ancestral structures in the superfamily Pseudocyclopoidea. *Pinkertonius* and *Sipadantonius* gen. nov., as well as the three basal taxa of the superfamily, namely *Caiconectes*, *Erebonectoides*, and *Azygonectes*, consistently exhibited a presence of aesthetascs on the ancestral segments I, III, VII, XVI, and XXVII–XXVIII and consistently lacking aesthetascs on the ancestral segments II, XXII, XXIII, XXIV, and XXVI (Fosshagen and Iliffe 1994, 2007; Bradford-Grieve et al. 2014). Thus, the presence or absence of aesthetascs in the segments mentioned above was presumably plesiomorphic in the superfamily. In contrast, the retention of aesthetascs on the ancestral segments IV, XIX and XX of the antennule in both sexes indicated that the new species also exhibited an affinity to the Epacteriscidae. Nevertheless, an inconsistency in the presence of an aesthetasc on a particular ancestral segment was frequently observed in the Epacteriscidae, a close relative of the Pseudocyclopidae, thereby suggesting that the characteristic was homoplastic. The initial instance of an inconsistent appearance in the retention of aesthetascs in the Epacteriscidae was observed in the genus *Oinella*; only the taxon lacked an aesthetasc on the ancestral segment IV of the female antennule (Fosshagen et al. 2001), whereas this characteristic was evident in females of all other genera. The retention of aesthetascs on ancestral segments XIX and XX was sporadically observed within the superfamily Pseudocyclopoidea, predominantly among the Epacteriscidae. In *Caiconectes*, an aesthetasc was present on the ancestral segments XIX and XX of the female antennules and on the segment XIX of the males (Fosshagen and Iliffe 2007). In the female of *Erebonectoides* and *Oinella*, as well as the male of *Enantiosis*, *Bomburiella* and *Exumella* (Fosshagen and Iliffe 1994; Jaume and Boxshall 1995; Fosshagen et al. 2001), an aesthetasc was documented to be present in the ancestral segment XIX of the antennule, and the retention of an aesthetasc on ancestral segment XX has been reported in the females of *Gloinella* (Fosshagen et al. 2001). The examples supported the assumption that the retention of aesthetascs in these three segments could occur independently within the superfamily Pseudocyclopoidea. Furthermore, the presence of a distolateral process on the P1 Exp-2 and the absence of the rostral filament supported the placement of the new species within the family Pseudocyclopidae. Although the process was identified in several other genera, including *Badijella*, *Boholina*, *Stygoridgewayia*, *Pseudocyclops* and *Ridgewayia* (Ohtsuka et al. 1999, 2000; Kršinic 2005; Tang et al. 2008; Boonyanusith et al. 2020), it had not been reported in Epacteriscidae. In contrast, the rostral filament, which was consistently present in the representatives of Epacteriscidae, was absent in the new species. Moreover, the rostral filament has been reported from numerous genera of Pseudocyclopidae, such as *Badijella*, *Robpalmeria*, *Normancavia*, *Exumella* and *Pinkertonius*. The characteristics of their buccal appendages exhibited an adaptive feature of particle feeders or scavengers. Furthermore, the maxillular coxal epipodite which bore seta 9, as observed in the new species, differed from most of Epacteriscidae, in which seta 9 was absent (Jaume and Boxshall 1995; Fosshagen and Iliffe 2003; Kršinic 2005; Bradford-Grieve et al. 2014).

Five plesiomorphic characteristics of *Pinkertonius* were noted: (1) the female antennule segmentation between the ancestral segments II and III; (2) the male antennule with aesthetasc on the ancestral segment IV; (3) Endp-1 of the male right P5 with medial seta; (4) Exp-3 of the female P5 with medial seta 4; (5) the P5 with three-segmented Endp in both sexes. The new species exhibited a close phylogenetic relatedness with *Pinkertonius*, characterised by the presence of the combination of characteristics (2), (4), and (5), which served to distinguish the new species and *Pinkertonius* from all other Pseudocyclopidae. The characteristic (2) demonstrated a high phylogenetic signal in morphology-based phylogenetic analyses of the superfamily (Bradford-Grieve et al. 2014), having been shared by nearly all of the Epacteriscidae and three additional genera, namely *Azygonectes*, *Erebonectoides* and *Caiconectes*. The assumption regarding the close relationship between *Sipadantonius* gen. nov. and *Pinkertonius* was supported by the observation that the characteristic of the P5 with a three-segmented Endp in both sexes was shared by a few numbers of calanoid genera of Pseudocyclopidae which includes *Sipadantonius* gen. nov., *Pinkertonius* and *Exumella*. Nevertheless, the reduction of the Exp was deemed relevant in *Exumella* (Jaume and Boxshall 1995; Suárez-Morales and Iliffe 2005). Furthermore, the Endp of the male P5 was derived in various patterns of segmentation reduction in other Pseudocyclopidae. For instance, it was observed that the Endp of the male P5 exhibited a two-segmented ramus on one side and a three-segmented on the other one in *Brattstromia*, *Exumellina*, and *Stargatia* (Fosshagen and Iliffe 1985, 1998, 2003). In contrast, it bore a two-segmented ramus on both sides in *Badijella* and one-segmented rami on both sides in *Boholina*, *Hondurella*, *Stygoridgewayia* or *Robpalmeria* (Fosshagen and Iliffe 1989, 2003; Kršinic 2005; Suárez-Morales and Iliffe 2007; Tang et al. 2008). The sole significant distinction observed in the male P5 Endp between the new species and *Pinkertonius* was the reduction of the inner seta on the Endp-1.

Certain characteristics link *Pinkertonius* to the family Pseudocyclopidae, including: (1) the existence of an aesthetasc on a certain segment of the female antennule; (2) segmentation and armament of the Endp of the mandible; (3) the armament of epipodite of the maxillule; (4) ornamentation of the basis of the P1, and (5) segmentation and ornamentation of the male P5 (Bradford-Grieve et al. 2014). Based on the aforementioned characters, the new species and *Pinkertonius* were differentiated from one another by the characters (1), (2), and (5). Nevertheless, this study posited that the new species and *Pinkertonius* were close relatives due to their shared characteristics of having aesthetascs on the ancestral segment IV of the male antennule. Furthermore, the variation in the number of armature elements of Endp-2 of the mandible and ornamentation of Exp-2 of the male right P5 had commonly been observed in Pseudocyclopidae, even among the representatives of a monophyletic clade. This study, thus, posited that the differences in these two characters between the new species and *Pinkertonius* were merely the result of the reduction/transformation of the structure within the closely related phylogenetic lineage. The two examples that supported the argument were the differences in the number of the armature element of Endp-2 among the genera *Hondurella* and *Stygoridgewayia*, as well as the differences in the ornamentation with the medial process of Exp-2 of the male right P5 among the genera *Placocalanus* and *Pseudocyclops*. *Hondurella* and *Stygoridgewayia* were identified as the sister taxon, constituting a monophyletic clade in morphology-based phylogenetic analyses (Bradford-Grieve et al. 2014). However, *Hondurella* bore nine setae on Endp-2 of the mandible instead of 11 setae presented in *Stygoridgewayia* (Suárez-Morales and Iliffe 2007; Tang et al. 2008). Likewise, *Placocalanus* and *Pseudocyclops* constitute a monophyletic clade; however, the ornamentation with a medial process on Exp-2 of the male right P5 was present in *Pseudocyclops* but not in *Placocalanus* (Bradford-Grieve et al. 2014). The number of setae on Endp-2 of the mandible varied between six and eleven setae among the representatives of Pseudocyclopidae (Bradford-Grieve et al. 2014). Furthermore, the ornamentation with the medial process of Exp-2 of the male right P5 was absent in numerous genera, including *Boholina*, *Hondurella*, *Stygoridgewayia*, and *Placocalanus* (Ohtsuka et al. 1996; Suárez-Morales and Iliffe 2007; Tang et al. 2008; Boonyanusith et al. 2020).

It was noted that the new species bore six elements on the maxillular coxal endite and furcal rami, lacking furcal seta I and seta III. The presence of six elements on the maxillular coxal endite constituted the most plesiomorphic characteristic among the representatives of Calanoida, in which the maximum number of setae on the endite was five (Boxshall and Halsey 2004). On the other hand, the reduction of furcal seta I and sata III could be considered an apomorphic characteristic of the new species. These characteristics supported the placement of the new species outside either the family Pseudocyclopidae or the superfamily Pseudocyclopoidea. Nevertheless, the setation of the armament of the maxillular coxal endite and furcal rami exhibited variability, even within the same genus. The occurrence of six elements on the maxillular coxal endite was reported from the order Misophrioida, as well as the families Canuellidae Lang, 1944 and Longipediidae Boeck, 1865 (Boxshall and Halsey 2004). Examples of the difference in the setation of the maxillular coxal endite among representatives of a genus were *Misophriella* Boxshall, 1983 and *Longipedia* Claus, 1863. Six elements were present on the endite of both *M. schminkei* Martínez Arbizu & Jaume, 1999 and *L. ulleungensis* Bang, Moon & Back, 2021 (Martínez Arbizu and Jaume 1999; Bang et al. 2021). Furthermore, five elements were present in *M. tetraspina* Boxshall, 1983 and *L. koreana* Bang, Moon & Back, 2021 (Boxshall 1983; Bang et al. 2021).

A distinctive characteristic of the new species was the reduction of furcal setae I and III. In Pseudocyclopoidea, the complete reduction of furcal setae was reported for the furcal setae I and II, with the latter being specific to *Miheptneria* (Bradford-Grieve et al. 2014). In other families, the reduction of furcal setae was reported in *Temorites* Sars, 1900 of the Bathypontiidae Brodsky, 1950, and *Fosshagenia* Suárez-Morales & Iliffe, 1996, of the Fosshageniidae Suárez-Morales & Iliffe, 1996 (Sars 1900; Suárez-Morales and Iliffe 1996; Fosshagen and Iliffe 2004b). However, the retained setae were interpreted as seta III to seta VI (Bradford-Grieve et al. 2014). Thus, the reduction of furcal seta III was identified as a distinctive characteristic of the new species, thereby facilitating the classification of this new species within a newly established genus. An inconsistency in the setation of the furcal rami was found in certain other copepod taxa, even within the same genus, suggesting an influence of the ecological differentiation or the niche partitioning on the setation of furcal rami. An example was the genus *Pseudograeteriella* Brancelj, Boonyanusith & Sanoamuang, 2019 in which the variation of the armament of the furcal rami was found, even the two most closely related representatives were encountered within the same cave (Sanoamuang et al. 2019). Based on the evidence mentioned earlier, this study assumed that the presence of six elements on the maxillular coxal endite represented merely the retention of the plesiomorphic characteristic in the new species, while the reduction of the armament of furcal rami was influenced by the ecological differentiation, as had been observed in other Copepoda. Therefore, the new species could be classified in the family Pseudocyclopidae.

The superfamily Pseudocyclopoidea had frequently been reported from cave habitats, and it appeared likely that no relevant adaptive feature was specific to copepods inhabiting this type of environment. It was possible that such a morphological adaptation/modification was related to the zones of the water column in which the copepods lived (Boonyanusith et al. 2020). In general, the relatively long antennules (i.e., surpassing the prosome) were frequently observed in pelagic representatives collected from the water column of the cave, such as *Caiconectes*, *Azygonectes*, *Exumellina* and *Stargatia* (Fosshagen and Iliffe 1998, 2003, 2007). Conversely, the relatively short antennule, as found in some epacteriscids and pseudocyclopids like *Stygoridgewayia*, *Boholina*, and *Ridgewayia*, was deduced as a hyperbenthic adaptive feature (Fosshagen and Iliffe 1998; Tang et al. 2008; Boonyanusith et al. 2020). Other characteristics observed consistently in benthic copepods (Fosshagen 1973) included the compact body and strong spines on the exopods of the swimming legs (Bradford-Grieve 2002). Following the aforementioned assumption, the new taxon would be the pelagic adaptive Calanoida, characterised by long antennules surpassing the posterior margin of the second urosomite and conspicuous oar-shaped outer spines on the exopods of all swimming legs. In addition, it was posited that the hypothetical calanoid ancestor, as well as most of its relatives, are epi- or hyperbenthic colonisers (Huys and Boxshall 1991; Bradford-Grieve 2002). Thus, the colonisation of the pelagic realm was probably secondary, occurring subsequent to the divergence of the new species from the epibenthic ancestor.

The two assumptions regarding the pelagic adaptation and the secondary colonisation of the pelagic realm of the new species were likely interconnected with the geological history of the sampling area and the ecological characteristics of the cave. From a geological perspective, the Turtle Tomb is located beneath Sipadan Island, which is the top of a volcanic cone located within the complex zone formed by the convergence of three tectonic plates, namely the Philippines Sea, Indian and Pacific Plates (Bellon and Rangin 1991). Historically, the volcanic cone primarily originated from the vertical rising of the magma, followed by the extinction of the volcano and the subsequent growth of the corals on the extinct volcano. This indicated the richness of volcanic activities at the seabed in this area, attributable to the convergence of the Eurasian, Pacific and India-Australian Plates since the Miocene (Yang et al. 2024). The environmental catastrophes and toxic gases likely prompted an adaptation of the epibenthic ancestor of the new species for colonisation of the pelagic environment prior to the colonisation in the cave. Based on the richness of organic particles and the stability of the environmental conditions, the cave functions as a refugee for the new species.

The second possibility was hypothesised based on the ecological characteristics of the cave. The new species was collected in the Turtle Tomb, recognised as one of the largest marine caves of Southeast Asia, located at Sipadan Island, from ~ 20 meters below the sea surface within the cave. The cave has a large entrance measuring ~ 20 meters wide and a horizontal gallery with depths varying from ~ 18–21 meters. Crystal-clear water with settled sediment at the sampling site indicates a slow movement of water currents. The broad space of the cave, coupled with the slow movement of water currents, likely facilitates an adaptation towards the planktonic lifestyle, enabling organisms to navigate through the free water masses within the cave. *Exumellina* is another example of a copepod exhibiting a planktonic lifestyle, having been collected in the pelagic zone of a marine cave (i.e., Norman's Pond Cave). *Exumellina* is characterised by a slender body and relatively small and equal outer spines of Exp of P1–P4 (Fosshagen and Iliffe 1998).The disjunct biogeographic distribution of cave-dwelling calanoids in the two extremities of the Tethys

Sea has suggested the colonisation of the habitats where they inhibited prior to the closure of the Tethys Sea (Bradford-Grieve 2002; Belmonte 2022). In the family Pseudocyclopidae, five genera constitute a monophyletic clade, in which the genus *Ridgewayia* is regarded as the sister taxon of the other five genera, including *Boholina*, *Hondurella*, *Placocalanus*, *Pseudocyclops*, and *Stygoridgewayia* (Bradford-Grieve et al. 2014). Although *Ridgewayia* and *Pseudocyclops* are cosmopolites, the regional distribution of the other genera is relatively restricted, having been recorded from merely one or two geographical regions. In one extremity of the Tethys Sea, which corresponds to the western coast of the Pacific Ocean, the new species and the two genera of the aforementioned clade have been reported from Southeast Asia, including *Boholina* and *Pseudocyclops* (e.g., Fosshagen and Iliffe 1989; Ohtsuka et al. 1999; Boxshall and Jaume 2012; Moon and Soh 2014; Tran and Chang 2020). Additionally, *Stygoridgewayia*, *Placocalanus*, and *Ridgewayia* (two out of six species of the *typica* species-group, including *R. boxshalli* Barthélémy, Ohtsuka & Cuoc, 1998 and *R. flemingeri* Othman & Greenwood, 1988) have been reported along the western coast of the Pacific Ocean, (Ohtsuka et al. 1996, 2000; Tang et al. 2008), forming the Indo-West Pacific community. In the other extremity of the Sea, which corresponds to the coast of the Atlantic Ocean and the Mediterranean, *Placocalanus* and *Hondurella* have been found from the Honduran coast of the Caribbean Sea of the North Atlantic Ocean (Fosshagen 1970; Suárez-Morales and Iliffe 2007). *Placocalanus* is the only genus that has been found in the localities beyond the Caribbean Sea and the Mediterranean; moreover, the six other genera, namely *Exumella*, *Exumellina*, *Stargatia*, *Brattstromia*, *Normancavia*, and *Robpalmeria*, have been found only from these two regions (e.g., Fosshagen 1970; Grahame 1979; Fosshagen and Iliffe 1991, 1998, 2003; Jaume and Boxshall 1995; Suárez-Morales and Iliffe 2005). The disjunct pattern of the regional distribution previously described appeared to resemble that of the genus *Ridgewayia*, as most species of the *typica* species-group had been documented from localities beyond the Caribbean Seas and the Mediterranean. In contrast, nearly all the *gracilis* species and the *marki* species-groups had been found in the North Atlantic/Mediterranean (Ohtsuka et al. 2000). Ohtsuka et al. (2000) posited that the existence of a certain morphological species-group (= *marki* species-group) in both the Indo-West Pacific region and the North Atlantic/Mediterranean served to confirm the faunistic link between these two regions. Furthermore, the presence of *Hondurella* and *Placocalanus* constituted another example of the phenomenon mentioned above. Thus, the regional distribution of the family Pseudocyclopidae exhibited the Tethyan track.

Acknowledgements

Gratitude was extended to Roihan Han, Boy Jay Alexius Petrus, Ag Ahmad Zaki Abu Bakar, Rex Andoh, Jackson Tang, Maxime Cheminade, Por Parasu Komaradat and Fitria Mock for their assistance with the Turtle Tomb cave studies. Gratitude was expressed towards Dr. Nasrulhakim Maidin, Mr. Jufri Hj. Nasri, and Mr Johny Buis from the Sipadan Island Park (Sabah Parks) and Sabah Biodiversity Council (SaBC) for granting permission to conduct these investigations. The authors thank the reviewers for their constructive comments and helpful suggestions, which significantly enhanced the manuscript.

Additional information

Conflict of interest

The authors have declared that no competing interests exist.

Ethical statement

No ethical statement was reported.

Funding

The biological collections from Turtle Tomb received support from the Nagao Natural Environment Foundation-Japan for A.-R. Azman.

Author contributions

A.R.A. conceived the data collection and data validation; C.B., K.W. and A.R.A. collated the information. All authors analysed the results. C.B. wrote the first draft of the manuscript, and all authors contributed to the writing of the manuscript.

Author ORCIDs

Chaichat Boonyanusith https://orcid.org/0000-0003-1487-2160
Koraon Wongkamhaeng https://orcid.org/0000-0001-7671-8869
Abdul-Rahim Azman https://orcid.org/0000-0002-8964-6638

Data availability

All of the data that support the findings of this study are available in the main text.

References

Andronov VN (1974) Phylogenetic relations of large taxa within the suborder Calanoida (Crustacea, Copepoda) Zoologichesky Zhurnal 53: 1002–1012. [in Russian]

Andronov VN (2007) New genus and species of copepods (Crustacea, Calanoida) from the central-eastern Atlantic and problems of classification of the Superfamilies Pseudocyclopoidea and Epacteriscoidea. Zoologicheskij Zhurnal 86: 671–683. [In Russian]

Andronov VN (2014) Revision of systematics and phylogeny of copepod order Calanoida. Kalingrad: R.A.S. Institute of Oceanology P.P. Shirshov, Atlantic Section, 204 pp. [In Russian]

Balqiah BB, Rahim AA (2021) An updated checklist of marine Copepoda from Peninsular Malaysia with notes on their functional traits and distributional records. Borneo Journal of Marine Science and Aquaculture 5(1): 8–24. https://doi.org/10.51200/bjomsa.v5i1.2709

Bang HW, Moon H, Back J (2021) Two new species of the genus *Longipedia* Claus, 1863 (Copepoda: Harpacticoida: Longipediidae) from Korea, with an update and a key to species. Diversity 13(11): 590. https://doi.org/10.3390/d13110590

Bellon H, Rangin C (1991) Geochemistry and isotopic dating of Cenozoic volcanic arc sequences around the Celebes and Sulu Seas. In: Silver EA, Rangin C, von Breymann MT, et al. (Eds) Proceedings of the Ocean Drilling Program, Scientific Results; Ocean Drilling Program Volume 124. Texas A&M University: College Station, Texas, 321–338. https://doi.org/10.2973/odp.proc.sr.124.163.1991

Belmonte G (2022) A new species of Pseudocyclopiidae (Crustacea, Copepoda, Calanoida) from an anchialine environment of south-eastern Italy. Frontiers in Ecology and Evolution 10: 857–161. https://doi.org/10.3389/fevo.2022.857161

Blanco-Bercial L, Bradford-Grieve JM, Bucklin A (2011) Molecular phylogeny of the Calanoida (Crustacea: Copepoda). Molecular Phylogenetics and Evolution 59: 103–113. https://doi.org/10.1016/j.ympev.2011.01.008

Boonyanusith C, Wongkamhaeng K, Athibai S (2020) A new species of *Boholina* (Crustacea, Copepoda, Calanoida) and a first record for stygobiotic calanoid fauna from a cave in Thailand. ZooKeys 904: 1–22. https://doi.org/10.3897/zookeys.904.37609

Boxshall GA (1983) Three new genera of misophrioid copepods from the near-bottom plankton community in the North Atlantic Ocean. Bulletin of the British Museum (Natural History). Zoology 44(2): 103–124.

Boxshall GA, Halsey SH (2004) An Introduction to Copepod Diversity. The Ray Society, London, 966 pp.

Boxshall GA, Jaume D (2012) Three new species of copepods (Copepoda: Calanoida and Cyclopoida) from anchialine habitats in Indonesia. Zootaxa 3150: 36–58. https://doi.org/10.11646/zootaxa.3150.1.2

Bradford-Grieve JM (2002) Colonization of the pelagic realm by calanoid copepods. Hydrobiologia 485: 223–244. https://doi.org/10.1023/A:1021373412738

Bradford-Grieve JM, Boxshall GA, Ahyong ST, Ohtsuka S (2010) Cladistic analysis of the calanoid Copepoda. Invertebrate Systematics 24(3): 291–321. https://doi.org/10.1071/IS10007

Bradford-Grieve JM, Boxshall GA, Blanco-Bercial L (2014) Revision of basal calanoid copepod families, with a description of a new species and genus of Pseudocyclopidae. Zoological Journal of the Linnean Society 171: 507–533. https://doi.org/10.1111/zoj.12141

Brancelj A, Watiroyram S, Sanoamuang L (2010) The first record of cave-dwelling Copepoda from Thailand and description of a new species: *Elaphoidella namnaoensis* n. sp. (Copepoda, Harpacticoida). Crustaceana 83: 779–793. https://doi.org/10.1163/001121610X502894

Figueroa DF (2011) Phylogenetic analysis of *Ridgewayia* (Copepoda: Calanoida) from the Galapagos and of a new species from the Florida: keys with a reevaluation of the phylogeny of Calanoida. Journal of Crustacean Biology 31: 153–165. https://doi.org/10.1651/10-3341.1

Fosshagen A (1968) Marine biological investigations in the Bahamas. 4. Pseudocyclopidae (Copepoda, Calanoida) from the Bahamas. Sarsia 32: 39–62. https://doi.org/10.1080/00364827.1968.10411121

Fosshagen A (1970) Marine biological investigations in the Bahamas. 15. *Ridgewayia* (Copepoda, Calanoida) and two new genera of calanoids from the Bahamas. Sarsia 44: 25–58. https://doi.org/10.1080/00364827.1970.10411178

Fosshagen A (1973) A new genus and species of bottom living calanoid (Copepoda) from Florida and Columbia. Sarsia 52: 145–154. https://doi.org/10.1080/00364827.1973.10411237

Fosshagen A, Iliffe TM (1985) Two new genera of Calanoida and a new order of Copepoda, Platycopioida, from marine caves on Bermuda. Sarsia 70: 345–358. https://doi.org/10.1080/00364827.1985.10419688

Fosshagen A, Iliffe TM (1989) *Boholina*, a new genus (Copepoda: Calanoida) with two new species from an anchialine cave in the Philippines. Sarsia 74: 201–208. https://doi.org/10.1080/00364827.1989.10413429

Fosshagen A, Iliffe TM (1991) A new genus of calanoid copepod from an anchialine cave in Belize. Bulletin of Plankton Society of Japan Special Volume (1991): 339–346.

Fosshagen A, Iliffe TM (1994) A new species of *Erebonectes* (Copepoda, Calanoida) from marine caves on Caicos Islands, West Indies. In: Ferrari FD, Bradley BP (Eds) Developments in Hydrobiology 102: Ecology and Morphology of Copepods, Hydrobiologia. 292/293: 17–22. https://doi.org/10.1007/978-94-017-1347-4_3

Fosshagen A, Iliffe TM (1998) A new genus of the Ridgewayiidae (Copepoda, Calanoida) from an anchialine cave in the Bahamas. Journal of Marine Systems 15: 373–380. https://doi.org/10.1016/S0924-7963(97)00071-7

Fosshagen A, Iliffe TM (2003) Three new genera of Ridgewayiidae (Copepoda, Calanoida) from anchialine caves in the Bahamas. Sarsia 88: 16–35. https://doi.org/10.1080/00364820308465

Fosshagen A, Iliffe TM (2004a) New epacteriscids (Copepoda, Calanoida) from anchialine caves in the Bahamas. Sarsia 89: 117–136. https://doi.org/10.1080/00364820410004981

Fosshagen A, Iliffe TM (2004b) A new species of cave-living calanoid copepod from Grand Bahama. Sarsia 89: 346–354. https://doi.org/10.1080/00364820410002613

Fosshagen A, Iliffe TM (2007) New species of epacteriscids (Copepoda, Calanoida) from anchialine caves in the Caicos Islands and the Bahamas. Marine Biology Research 3: 37–92. https://doi.org/10.1080/17451000701274571

Fosshagen A, Boxshall BG, Iliffe TM (2001) The Epacteriscidae, a cave-living family of calanoid copepods. Sarsia 86: 245–318. https://doi.org/10.1080/00364827.2001.10425520

Grahame J (1979) A new species of *Exumella* Fosshagen (Copepoda, Calanoida), from Kingston Harbour, Jamaica. Crustaceana 36(1): 15–22. https://doi.org/10.1163/156854079X00168

Huys R, Boxshall GA (1991) Copepod Evolution. The Ray Society, London, 468 pp.

Jaume D, Boxshall GA (1995) A new species of *Exumella* (Copepoda: Calanoida: Ridgewayiidae) from anchihaline caves in the Mediterranean. Sarsia 80: 93–105. https://doi.org/10.1080/00364827.1995.10413584

Jaume D, Humphreys WF (2001) A new genus of epacteriscid calanoid copepod from an anchialine sinkhole on northwestern Australia. Journal of Crustacean Biology 21: 157–169. https://doi.org/10.1163/20021975-99990114

Kršinic F (2005) *Badijella jalzici* – a new genus and species of calanoid copepod (Calanoida, Ridgewayiidae) from an anchialine cave on the Croatian Adriatic coast Published in collaboration with the University of Bergen and the Institute of Marine Research, Norway, and the Marine Biological Laboratory, University of Copenhagen, Denmark. Marine Biology Research 1(4): 281–289. https://doi.org/10.1080/17451000500262025

Martínez Arbizu P, Jaume D (1999) New hyperbenthic species of *Misophriopsis* and *Misophriella*, first record of misophrioid copepods (Crustacea) from Antarctic waters. Helgoland Marine Research 53(2): 102–117. https://doi.org/10.1007/PL00012142

Moon SY, Soh HY (2014) A new species of *Boholina* (Copepoda, Calanoida, Boholinidae) from Ganghwa Island in western Korea. Journal of the Marine Biological Association of the United Kingdom 94: 537–545. https://doi.org/10.1017/S002531541300177X

Nakajima R, Yoshida T, Othman BHR, Toda T (2013) First record of a blue pigmented Acartiid copepod in the tropical coral reef waters of Malaysia. Galaxea Journal of Coral Reef Studies 15: 27–28. https://doi.org/10.3755/galaxea.15.27

Ohtsuka S, Fosshagen A, Soh HY (1996) Three new species of the demersal calanoid copepod *Placocalanus* (Ridgewayiidae) from Okinawa, southern Japan. Sarsia 81: 247–263. https://doi.org/10.1080/00364827.1996.10413623

Ohtsuka S, Fosshagen A, Putchakarn S (1999) Three new species of the demersal calanoid copepod *Pseudocyclops* from Phuket, Thailand. Plankton Biology and Ecology 46(2): 132–147.

Ohtsuka S, Kase T, Boxshall GA (2000) A new species of *Ridgewayia* (Copepoda: Calanoida) from a submarine cave in Palau, western Pacific. Species Diversity 5(3): 201–213. https://doi.org/10.12782/specdiv.5.201

Park T (1986) Phylogeny of calanoid copepods. In: Schriever G, Schminke HK, Shih C-t (Eds) Proceedings of the Second International Conference on Copepoda, Ottawa (Canada), August 1984. Syllogeus 58: 191–196.

Rezai H, Yusoff FM, Arshad A, Othman BHR (2009) Abundance and composition of zooplankton in the Straits of Malacca. Aquatic Ecosystem Health & Management 12(3): 264–270. https://doi.org/10.1080/14634980903149977

Sanoamuang L, Boonyanusith C, Brancelj A (2019) A new genus and new species of stygobiotic copepod (Crustacea: Copepoda: Cyclopoida) from Thien Duong Cave in Central Vietnam, with a redescription of *Bryocyclops anninae* (Menzel, 1926). Raffles Bulletin of Zoology 67: 189–205. https://doi.org/10.26107/RBZ-2019-0016

Sars GO (1900) Crustacea. In: Nansen F (Ed.) The Norwegian North Polar Expedition 1893–1896: Scientific Results Vol. 1. Longmans, Green, and Co. London, 11–41.

Suárez-Morales E, Iliffe TM (1996) New superfamily of Calanoida (Copepoda) from an anchialine cave in the Bahamas. Journal of Crustacean Biology 16(4): 754–762. https://doi.org/10.2307/1549194

Suárez-Morales E, Iliffe TM (2005) A new *Exumella* (Crustacea: Copepoda: Ridgewayiidae) from anchialine waters of the western Caribbean, with comments on regional biogeography. Bulletin of Marine Science 77(3): 409–424.

Suárez-Morales E, Iliffe TM (2007) A new genus of Ridgewayiidae (Copepoda: Calanoida) from a karstic cave of the western Caribbean. Journal of Crustacean Biology 27: 339–350. https://doi.org/10.1651/S-2720.1

Tang D, Barron H, Goater S (2008) A new genus and species of Ridgewayiidae (Copepoda: Calanoida) from subterranean waters of northwestern Australia. Journal of Crustacean Biology 28: 551–563. https://doi.org/10.1651/07-2869R.1

Tran DL, Chang CY (2020) First record of the genus *Boholina* (Copepoda, Calanoida, Pseudocyclopidae) in Vietnam, with description of a new species from an anchialine cave in Tra Ban Island. ZooKeys 977: 1–23. https://doi.org/10.3897/zookeys.977.55040

Yang Y, Xie X, He Y, Chen H (2024) Opening and Closure of the Sulu Sea: Revealed by Its Peripheral Subduction and Collision Processes. Journal of Marine Science and Engineering 12: 1456. https://doi.org/10.3390/jmse12081456

Yoshida T, Matias-Peralta H, Yusoff FMD, Toda T, Othman BHR (2012) Zooplankton research in Malaysia: Current status and future prospects. Coastal Marine Science 35(1): 208–213.

ZooKeys 1219: 331–346 (2024)
DOI: 10.3897/zookeys.1219.138793

Research Article

Four new species of the genus *Trilacuna* Tong & Li, 2007 (Araneae, Oonopidae) from China

Jimeng Ma[1*], Qiang Chen[2*], Yanfeng Tong[1]

1 *Life Science College, Shenyang Normal University, Shenyang 110034, China*
2 *Experimental Teaching Center, Shenyang Normal University, Shenyang 110034, China*
Corresponding author: Yanfeng Tong (tyf68@hotmail.com)

Abstract

Four new species of the genus *Trilacuna* Tong & Li, 2007, *Trilacuna guangwu* Ma & Tong, **sp. nov.** (♂), *Trilacuna qingliangfeng* Ma & Tong, **sp. nov.** (♂♀), *Trilacuna taoyuanyu* Ma & Tong, **sp. nov.** (♂) and *Trilacuna yunmeng* Ma & Tong, **sp. nov.** (♂), are described from China. Descriptions, diagnoses, and photographs are provided.

Key words: Distribution, goblin spiders, morphology, taxonomy

Introduction

Trilacuna Tong & Li, 2007 is a small genus in Oonopidae Simon, 1890 and currently comprises 44 species (WSC 2024). Known species are from East Asia (22 species in China and one in South Korea), Southeast Asia (15 species), South Asia (five species) and West Asia (one species) (Eichenberger and Kranz-Baltensperger 2011; Grismado et al. 2014; Malek-Hosseini et al. 2015; Seo 2017; Tong et al. 2024). In China, all the known species are recorded in southwestern China, of which seven from Chongqing, two are from Guizhou, and 13 are from Yunnan Province (Tong et al. 2019; Huang et al. 2020, 2021; Wang et al. 2021; Ma et al. 2023). Examination of oonopid specimens preserved in Hebei University (Baoding, China) found four new species of the genus *Trilacuna*, of which one species was collected from Anhui and Zhejiang Provinces, and three species were collected from Hebei, Fujian, and Sichuan Provinces, respectively. Until now, the record from Hebei is the northernmost record of this genus in the world. This work describes four new *Trilacuna* species from outside of southwestern China.

Materials and methods

Specimens were examined using a Leica M205 C stereomicroscope. Fine details were studied under an Olympus BX51 compound microscope. Endogynes were cleared in lactic acid. Photomicroscope images were taken with a Canon EOS 750D zoom digital camera (24.2 megapixels) mounted on an Olympus

OPEN ACCESS

Academic editor: Alireza Zamani
Received: 8 October 2024
Accepted: 12 November 2024
Published: 6 December 2024

ZooBank: https://zoobank.org/28598A15-2CD6-4D21-AB49-C667F85A57AB

Citation: Ma J, Chen Q, Tong Y (2024) Four new species of the genus *Trilacuna* Tong & Li, 2007 (Araneae, Oonopidae) from China. ZooKeys 1219: 331–346. https://doi.org/10.3897/zookeys.1219.138793

---

* These authors contributed equally to this work.

BX51 compound microscope. Raw photos were first stacked with Helicon Focus v. 8.2.0 to get the composite images, which were then processed in Adobe Photoshop CC 2020. Scanning electron microscope images (SEM) were taken under high vacuum with a Hitachi S-4800 after critical point drying and gold-palladium coating. All measurements were taken using an Olympus BX51 compound microscope and are in millimeters. Taxonomic descriptions follow Tong et al. (2020). Type material is deposited in Shenyang Normal University (SYNU) in Shenyang, Liaoning Province, China (curator: Yanfeng Tong).

The following abbreviations are used in the text and figures: **ALE** = anterior lateral eyes; **ap** = apodemes; **as** = anterior sclerite; **bep** = basal ear-shaped projection; **bls** = brush-like structure; **glo** = globular structure; **lcb** = lateral curved branch; **mb** = medial branch; **mr** = membranous region; **PLE** = posterior lateral eyes; **PME** = posterior media eyes; **psp** = posterior spiracle; **sar** = sclerotized, recurved arches; **sdb** = slightly curved distal branch; **tls** = thorn-like structure; **tsc** = transverse bars.

Taxonomy

Family Oonopidae Simon, 1890

Genus *Trilacuna* Tong & Li, 2007

Type species. *Trilacuna rastrum* Tong & Li, 2007 from Yunnan, China.

Diagnosis. See Tong et al. (2020).

Composition. 48 species, including four described here.

Distribution. Iran to the Korean Peninsula and south to Sumatra.

Trilacuna guangwu Ma & Tong, sp. nov.

https://zoobank.org/C85D9470-36D7-4DCF-9CD7-3DAF675BBB05
Figs 1, 2, 6C

Material examined. ***Holotype***: China • ♂ (SYNU-1179); Sichuan Province, Bazhong City, Nanjiang County, Guangwu Mountain, Taoyuan Scenic Area; 32°40'48"N, 106°48'12"E; 5.VIII.2014; F. Zhang leg.

Etymology. The specific name is a noun in apposition taken from the type locality.

Diagnosis. The new species is similar to *Trilacuna angularis* Tong & Li, 2007, but can be distinguished by the large, thorn-like structure (tls) and brush-like structure (bls) of embolus system (Fig. 2D, E, J, K) vs lacking, but with several strongly sclerotized sclerites (Tong and Li 2007: fig. 15–18), and slightly elevated epigastric region (Fig. 1H) vs flat (Tong and Li 2007: fig. 14).

Description. Male (Holotype). ***Body*:** reddish brown, chelicerae and sternum lighter, legs yellow; habitus as in Fig. 1A–C; body length 2.05. ***Carapace*:** 1.06 long, 0.81 wide; sides granulate, lateral margin rebordered (Fig. 1D). ***Eyes*:** nearly equal sized; posterior eye row straight from above, procurved from front; ALE separated from edge of carapace by 1.4 diameters (Fig. 1D, F). ***Mouthparts*:** chelicerae straight; labium rectangular, anterior margin deeply incised; endites slender, distally not branched, with a membranous region (Figs 1E, 6C).

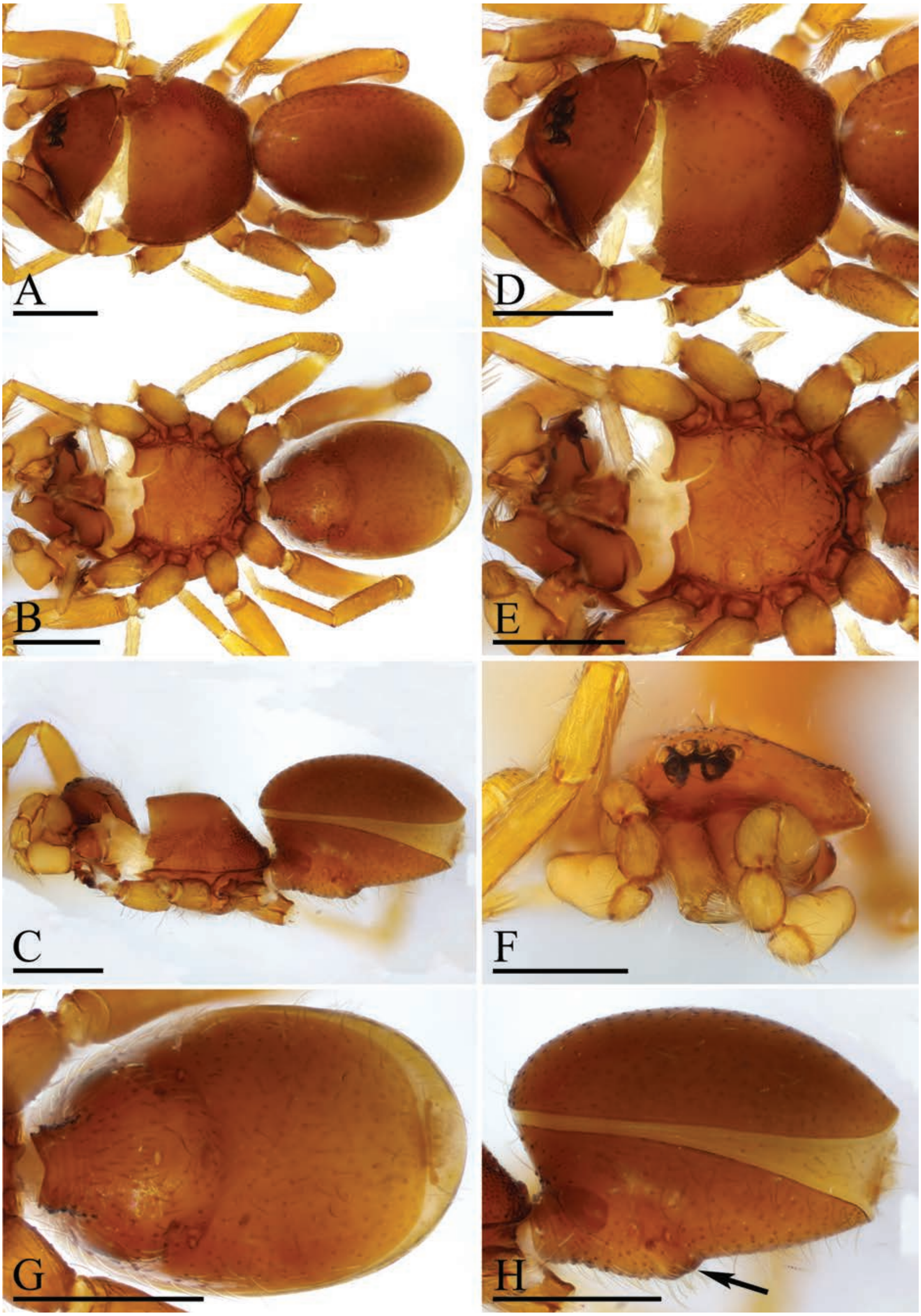

Figure 1. *Trilacuna guangwu* sp. nov., male holotype **A–C** habitus in dorsal, ventral and lateral views **D–F** prosoma in dorsal, ventral and anterior views **G–H** abdomen, ventral and lateral views, arrow shows the elevated epigastric region. Scale bars: 0.4 mm (**A–H**).

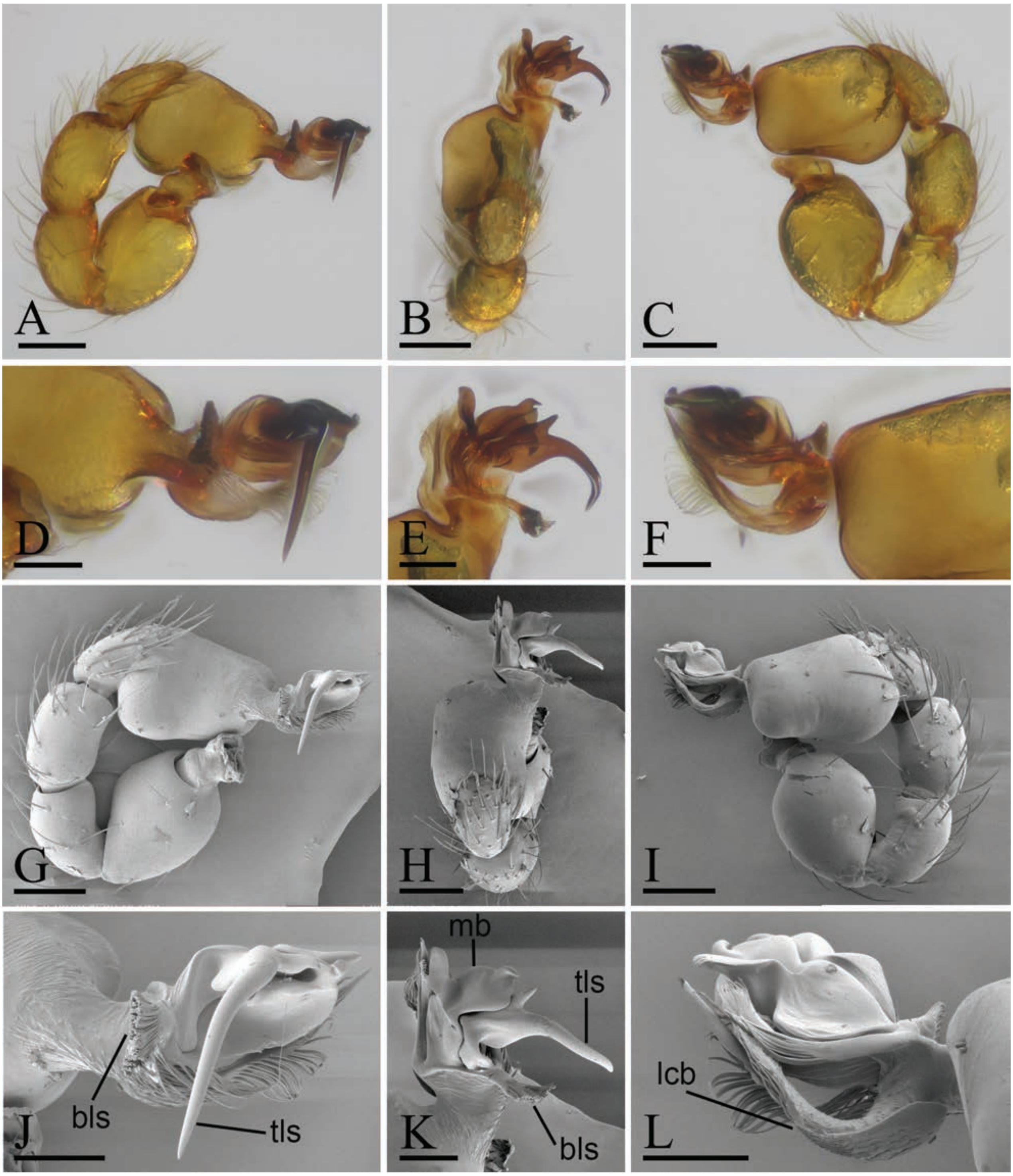

Figure 2. *Trilacuna guangwu* sp. nov., left male palp, **A–F** (light) and **G–L** (SEM) **A, G** prolateral view **B, H** dorsal view **C, I** retrolateral view **D, J** distal part of palpal bulb, prolateral view **E, K** distal part of palpal bulb, dorsal view **F, L** distal part of palpal bulb, retrolateral view. Abbreviations: bls = brush-like structure; lcb = lateral curved branch; mb = medial branch; tls = thorn-like structure. Scale bars: 0.1 mm (**A–C, G–I**); 0.05 mm (**D–F, J–L**).

***Sternum*:** surface rugose (Fig. 1E). ***Abdomen*:** 1.01 long, 0.65 wide; booklung covers ovoid, surface smooth; sperm pore situated at level of anterior spiracles; apodemes present, posterior spiracles connected by groove; epigastric region slightly elevated (Fig. 1G, H). ***Leg spination*:** legs I-II: tibia: v2-2-2-2-0, metatarsus: v2-2-0. ***Palp*:** orange; 0.66 long (0.21, 0.15, 0.15, 0.15); femur greatly enlarged (width/length = 0.74); bulb quadrangular; embolus system with a large, thorn-like structure (tls), a cluster of brush-like structure (bls), a broad median branch (mb) and a narrow lateral curved branch (lcb) (Fig. 2A–L).

Female. Unknown.

Distribution. Known only from the type locality (Fig. 11).

Trilacuna qingliangfeng Ma & Tong, sp. nov.

https://zoobank.org/9A23C7E9-4EB7-431B-8588-3A3DAFBB640B
Figs 3–5, 6A, B, D

Material examined. ***Holotype*:** China • ♂ (SYNU-1181); Anhui Province, Xuancheng City, Jixi County, Qingliangfeng National Nature Reserve, Zhanlingwan; 30°5'53"N, 118°51'59"E; 8.VI.2014; F. Zhang leg.

***Paratypes*:** China • 2 ♂ 8 ♀ (SYNU-1182–1191); same data as holotype • 4 ♂ 6 ♀ (SYNU-1207–1216); same data as holotype; 28.VIII.2014 • 1 ♂ 8 ♀ (SYNU-1217–1225); Qingliangfeng National Nature Reserve, Lantianao; 30°8'2"N, 118°49'42"E; 29.V.2014; F. Zhang leg. • 1 ♀ (SYNU-1227); Qingliangfeng National Nature Reserve, Yezhutan; 30°7'10"N, 118°51'10"E; 30.V.2014; F. Zhang leg. • 1 ♂ 9 ♀ (SYNU-1228–1237); Qingliangfeng National Nature Reserve, Fuling Town, Yonglai Village; 30°9'8"N, 118°51'3"E; 5.VI.2013; Cha and Zhang leg. • 1 ♂ 4 ♀ (SYNU-1202–1206); Qingliangfeng National Nature Reserve, Fuling Town, Yonglai Village; 30°9'8"N, 118°51'3"E; 3.VI.2013; Cha and Zhang leg. • 2 ♂ 1 ♀ (SYNU-1240–1242); Qingliangfeng National Nature Reserve, Fuling Town, Yonglai Village, Qingliangfeng Protection Station; 30°2'32"N, 118°50'27"E; 4.VI.2013; Cha and Zhang leg. • 2 ♀ (SYNU-1238–1239); Qingliangfeng National Nature Reserve, Fuling Town, Yonglai Village, Huihanggudao; 30°7'57"N, 118°48'17"E; 2.VII.2013; Cha and Zhang leg. • 3 ♀ (SYNU-1199–1201); Qingliangfeng National Nature Reserve, Shexian County, Zhupu; 29°50'51"N, 118°25'49"E; 6.VI.2013; Cha and Zhang leg.

Other materials. China • 1 ♂ 3 ♀ (SYNU-536); Anhui Province, Huangshan City, Xiuning County, Qiyun Mountain; 29°48'23"N, 118°2'24"E; 19.IV.2011; Zongxu Li and Luyu Wang leg. • 1 ♂ 1 ♀ (SYNU-537); same data as above • 2 ♀ (SYNU-538); same data as above • 1 ♀ (SYNU-1226); Anhui Province, Xiuning County, Lingnan Town, Dawu; 29°25'22"N, 118°8'12"E; 4.VI.2014; F. Zhang leg. • 7 ♀ (SYNU-1192–1198); Zhejiang Province, Tianmushan Mountain, Chanyuan Temple; 30°13'50"N, 119°26'55"E; 10.VI.2014; F. Zhang leg. • 1 ♂ (SYNU-1243); Zhejiang, Tianmushan Mountain, Qianmutian; 30°23'30"N, 119°26'54"E; 10.VI.2014; F. Zhang leg.

Etymology. The specific name is a noun in apposition taken from the type locality.

Diagnosis. The new species is similar to *Trilacuna wenfeng* Tong & Li, 2021, but can be distinguished by the slightly elevated epigastric region and a group of strong setae behind the level between posterior spiracles (Fig. 3C, H) vs strongly elevated, with a cluster of densely short setae in front of the level between posterior spiracles (Wang et al. 2021: fig. 6E, G, H), by the ridges on central area of sternum (Fig. 3E) vs lacking (Wang et al. 2021: fig. 6D), and by the small globular structure of endogyne (Fig. 6B) vs spiral-shaped (Wang et al. 2021: fig. 5D).

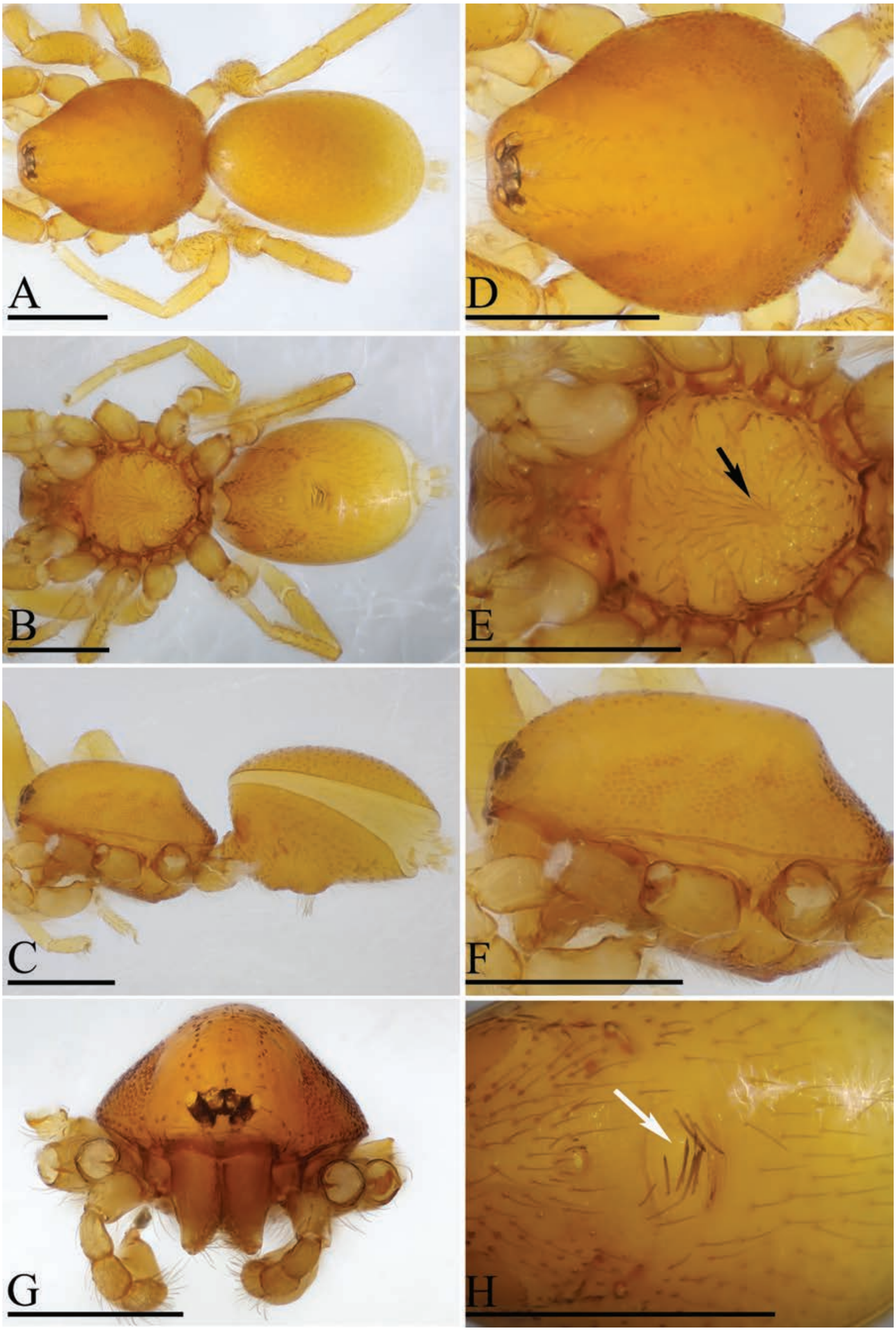

Figure 3. *Trilacuna qingliangfeng* sp. nov., male holotype **A–C** habitus in dorsal, ventral and lateral views **D–G** prosoma in dorsal, ventral, lateral and anterior views, arrow shows the small ridges **H** abdomen, ventral view, arrow shows the clustered setae. Scale bars: 0.4 mm (**A–H**).

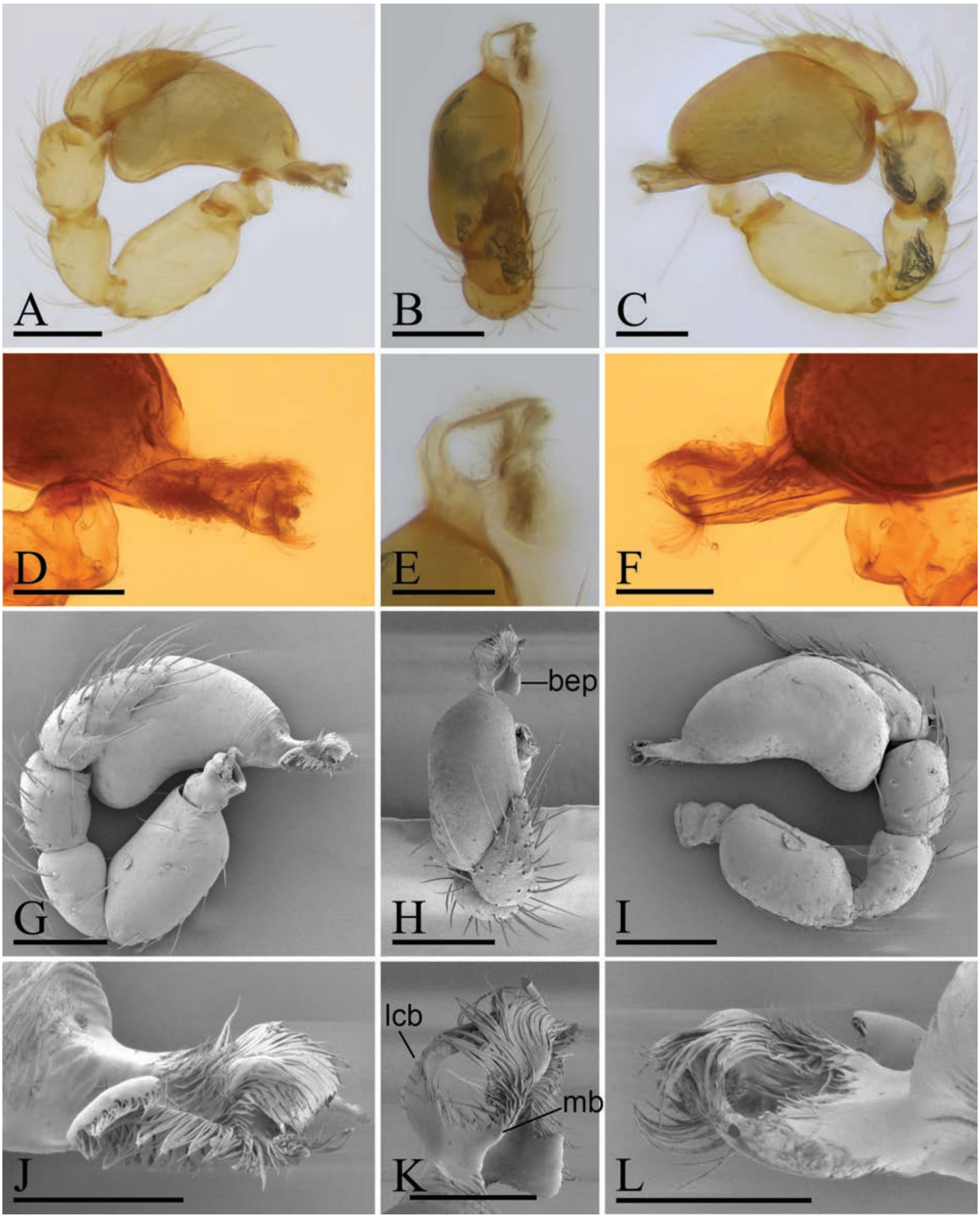

Figure 4. *Trilacuna qingliangfeng* sp. nov., left male palp, **A–F** (light) and **G–L** (SEM) **A, G** prolateral view **B, H** dorsal view **C, I** retrolateral view **D, J** distal part of palpal bulb, prolateral view **E, K** distal part of palpal bulb, dorsal view **F, L** distal part of palpal bulb, retrolateral view. Abbreviations: bep = basal ear-shaped projection; mb = medial branch; lcb = lateral curved branch. Scale bars: 0.1 mm (**A–C, G–I**); 0.05 mm (**D–F, J–L**).

Description. Male (Holotype). ***Body*:** yellow, legs lighter; habitus as in Fig. 3A–C; body length 1.63. ***Carapace*:** 0.78 long, 0.63 wide; sides granulate, lateral margin rebordered (Fig. 3D). ***Eyes*:** nearly equal sized; posterior eye row

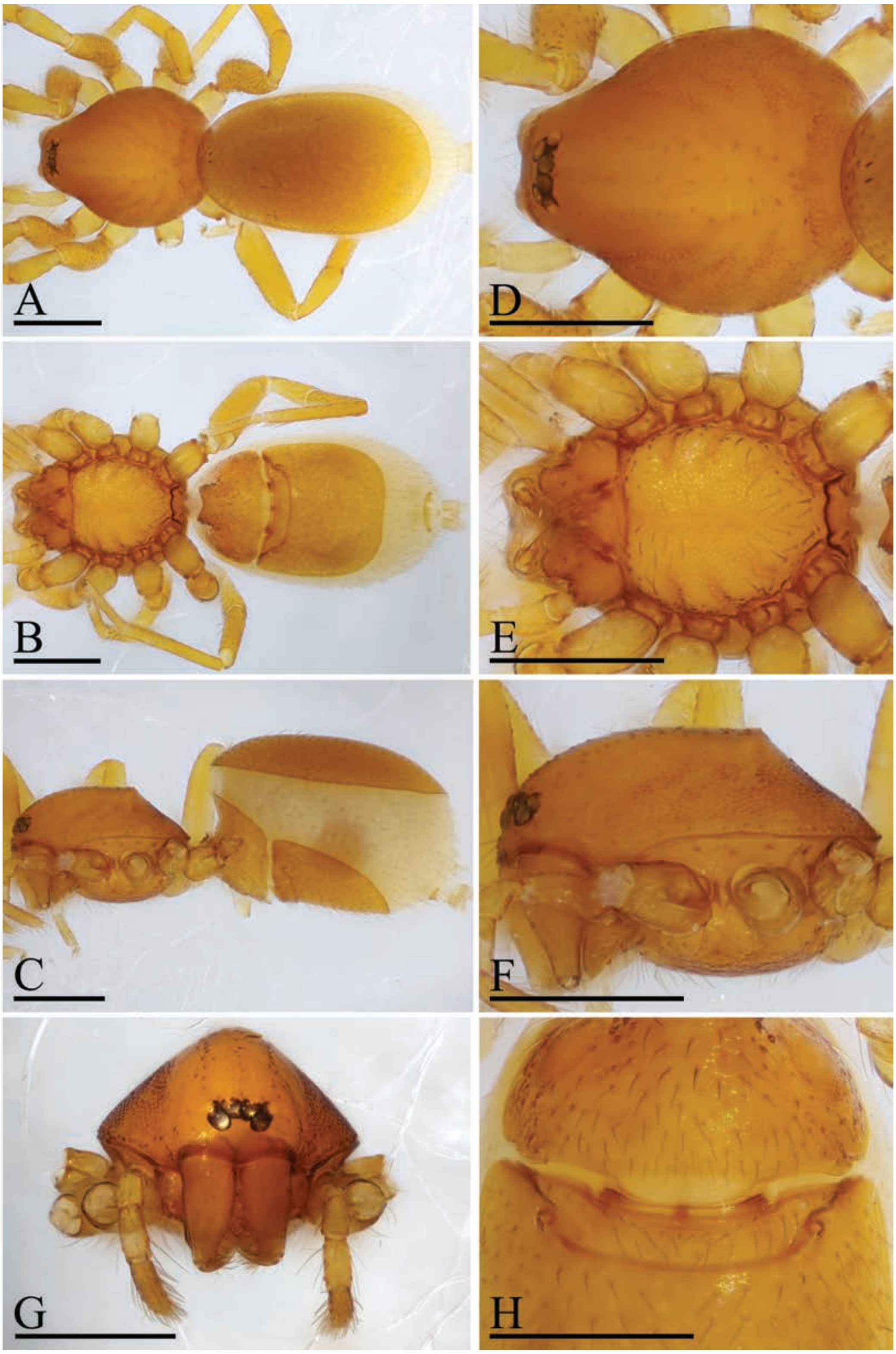

Figure 5. *Trilacuna qingliangfeng* sp. nov., female paratype **A–C** habitus in dorsal, ventral, and lateral views **D–G** prosoma in dorsal, ventral, lateral and anterior views **H** abdomen in ventral view. Scale bars: 0.4 mm (**A–H**).

recurved from above, procurved from front; ALE separated from edge of carapace by 1.3 diameters (Fig. 3D, G). ***Mouthparts:*** chelicerae straight; labium rectangular, anterior margin deeply incised; endites slender, distally branched (Figs 3E, 6D). ***Sternum:*** surface finely smooth, with several ridges on central

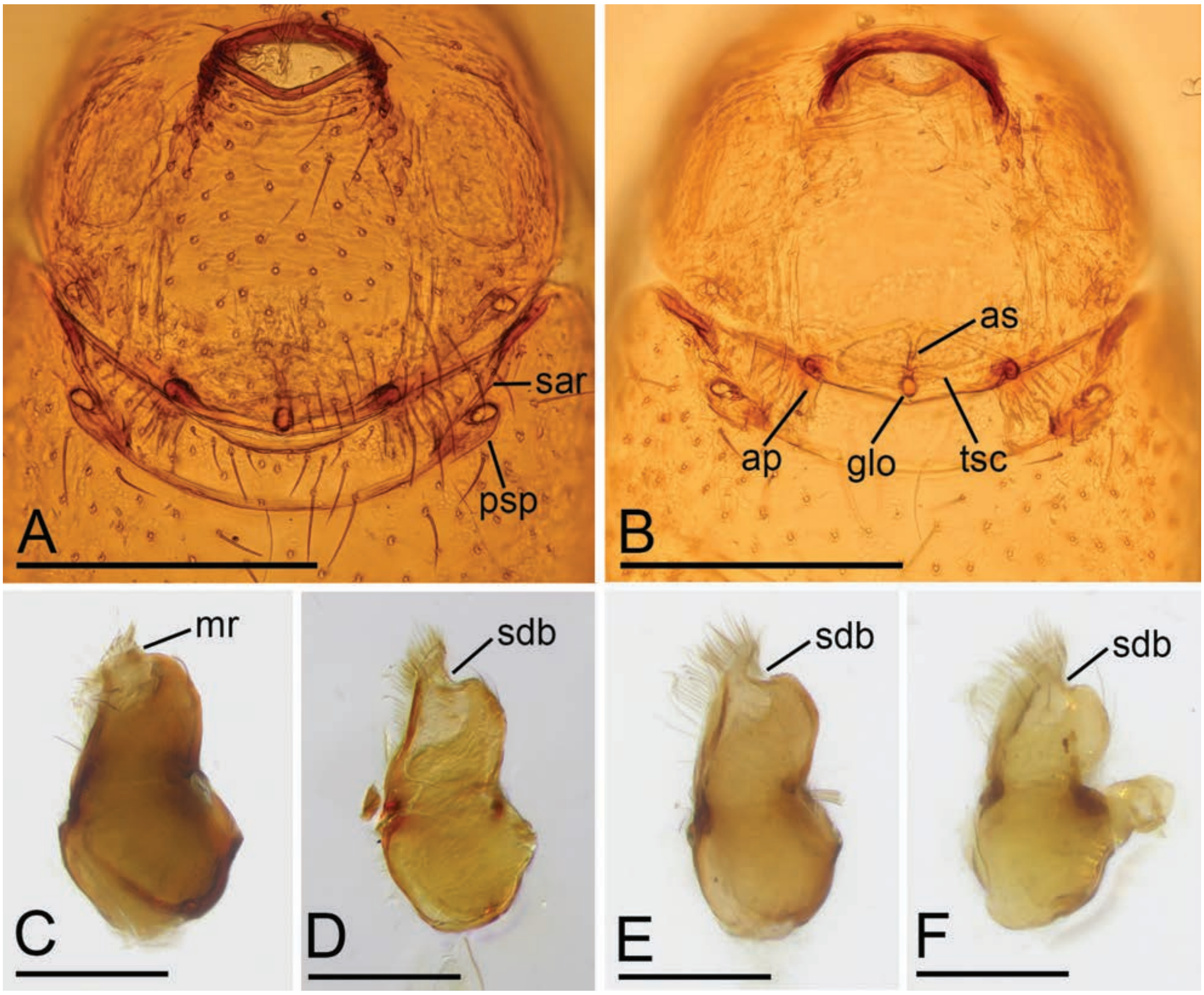

Figure 6. *Trilacuna qingliangfeng* sp. nov., female paratype (**A, B**), *Trilacuna guangwu* sp. nov., male holotype (**C**), *Trilacuna qingliangfeng* sp. nov., male holotype **(D),** *Trilacuna taoyuanyu* sp. nov., male holotype (**E**), *Trilacuna yunmeng* sp. nov., male holotype (**F**) **A, B** copulatory organ in ventral and dorsal views **C–F** endites in ventral view. Abbreviations: ap = apodemes; as = anterior sclerite; glo = globular structure; mr = membranous region; psp = posterior spiracle; sar = sclerotized, recurved arches; sdb = slightly curved distal branch; tsc = transverse bars. Scale bars: 0.4 mm (**A, B**); 0.2 mm (**C–F**).

area (Fig. 3E). ***Abdomen*:** 0.91 long, 0.57 wide; booklung covers ovoid, surface smooth; sperm pore situated at level of anterior spiracles; apodemes present, posterior spiracles not connected by groove; epigastric region slightly elevated, with a group of strong setae (Fig. 3C, H). ***Leg spination*:** legs I-II: tibia: v2-2-2-2-0, metatarsus: v2-2-0. ***Palp*:** orange; 0.55 long (0.18, 0.11, 0.10, 0.16); femur elongated (width/length = 0.57); bulb kidney-shaped, basally strongly bulged; embolus system with ear-shaped projection (bep) at base, with a lateral curved branch (lcb) and narrow medial branch (mb) (Fig. 4A–L).

Female (paratype, SYNU-1184). As in male except as noted. ***Body*:** habitus as in Fig. 5A–C; body length 1.98. ***Carapace*:** 0.82 long, 0.66 wide. ***Mouthparts*:** endites unmodified. ***Sternum*:** without ridges on central area (Fig. 5E). ***Abdomen*:** 1.24 long, 0.71 wide. ***Epigastric area*:** with recurved, strongly sclerotized arches (sar) (Figs 5H, 6A). ***Endogyne*:** with narrow, transversally elongated sclerite (tsc); with an anterior T-shaped sclerite (as) and a posterior small globular structure (glo) (Fig. 6B).

Distribution. Known only from the type locality (Fig. 11).

Trilacuna taoyuanyu Ma & Tong, sp. nov.

https://zoobank.org/1264BFD5-911F-4D6F-8871-4246597B9858

Figs 6E, 7, 8

Material examined. ***Holotype*:** China • ♂ (SYNU-1178); Fujian Province, Wuyishan City, Wuyi Mountain Scenic Area, Taoyuanyu; 27°39'15"N, 117°56'54"E; 9.VI.2013; C. Jin leg.

Etymology. The specific name is a noun in apposition taken from the type locality.

Diagnosis. The new species is similar to *Trilacuna bawan* Tong, Zhang & Li, 2019, but can be distinguished by the strongly elevated epigastric region and two strong setae on it (Fig. 7H, I), vs slightly elevated, without strong setae (Tong et al. 2019: fig. 1H, I), and the kidney-shaped palpal bulb (Fig. 8A, C) vs oval, with deeply constriction on distal region (Tong et al. 2019: figs 2A, B, 22A, B).

Description. Male (Holotype). ***Body*:** reddish brown, chelicerae and sternum lighter, legs yellow; habitus as in Fig. 7A–C; body length 1.71. ***Carapace*:** 0.79 long, 0.63 wide; sides granulate, lateral margin rebordered (Fig. 7D). ***Eyes*:** ALE largest, PLE and PME nearly equal sized; posterior eye row recurved from above, procurved from front; ALE separated from edge of carapace by 1.4 diameters (Fig. 7D, G). ***Mouthparts*:** chelicerae straight; labium rectangular, anterior margin deeply incised; endites slender, distally branched (Figs 6E, 7E). ***Sternum*:** surface rugose, with several ridges on posterior area (Fig. 7E). ***Abdomen*:** 0.92 long, 0.56 wide; booklung covers ovoid, surface smooth; sperm pore situated at level of anterior spiracles; apodemes present, posterior spiracles connected by groove; epigastric region strongly elevated, with 2 very long, strong setae (Fig. 7H, I). ***Leg spination*:** legs I-II: tibia: v2-2-2-2-0, metatarsus: v2-2-0. ***Palp*:** orange; 0.54 long (0.19, 0.11, 0.09, 0.15); femur elongated (width/length = 0.59); bulb kidney-shaped, basally slightly bulged; embolus system with ear-shaped projection (bep) at base, with a lateral curved branch (lcb) and narrow medial branch (mb) (Fig. 8A–L).

Female. Unknown.

Distribution. Known only from the type locality (Fig. 11).

Trilacuna yunmeng Ma & Tong, sp. nov.

https://zoobank.org/B6941EF8-9CE0-486F-A338-2053D7607BD7

Figs 6F, 9, 10

Material examined. ***Holotype*:** China • ♂ (SYNU-1180); Hebei Province, Baoding City, Yi County, Yunmeng Mountain; 39°23'52"N, 115°16'17"E; 11.VI.2012; F. Zhang leg.

Etymology. The specific name is a noun in apposition taken from the type locality.

Diagnosis. The new species is similar to *Trilacuna hansanensis* Seo, 2017, but can be distinguished by the many ridges on posterior area of sternum (Fig. 9E), vs a pair of ridges (Seo 2017: fig. 1B), and the steeply elevated epigastric region (Fig. 9H) vs flat (Seo 2017: fig. 1B).

Description. Male (Holotype). ***Body*:** yellow, legs lighter; habitus as in Fig. 9A–C; body length 1.57. ***Carapace*:** 0.67 long, 0.57 wide; sides granulate, lateral margin rebordered (Fig. 9D). ***Eyes*:** nearly equal sized; posterior eye row recurved

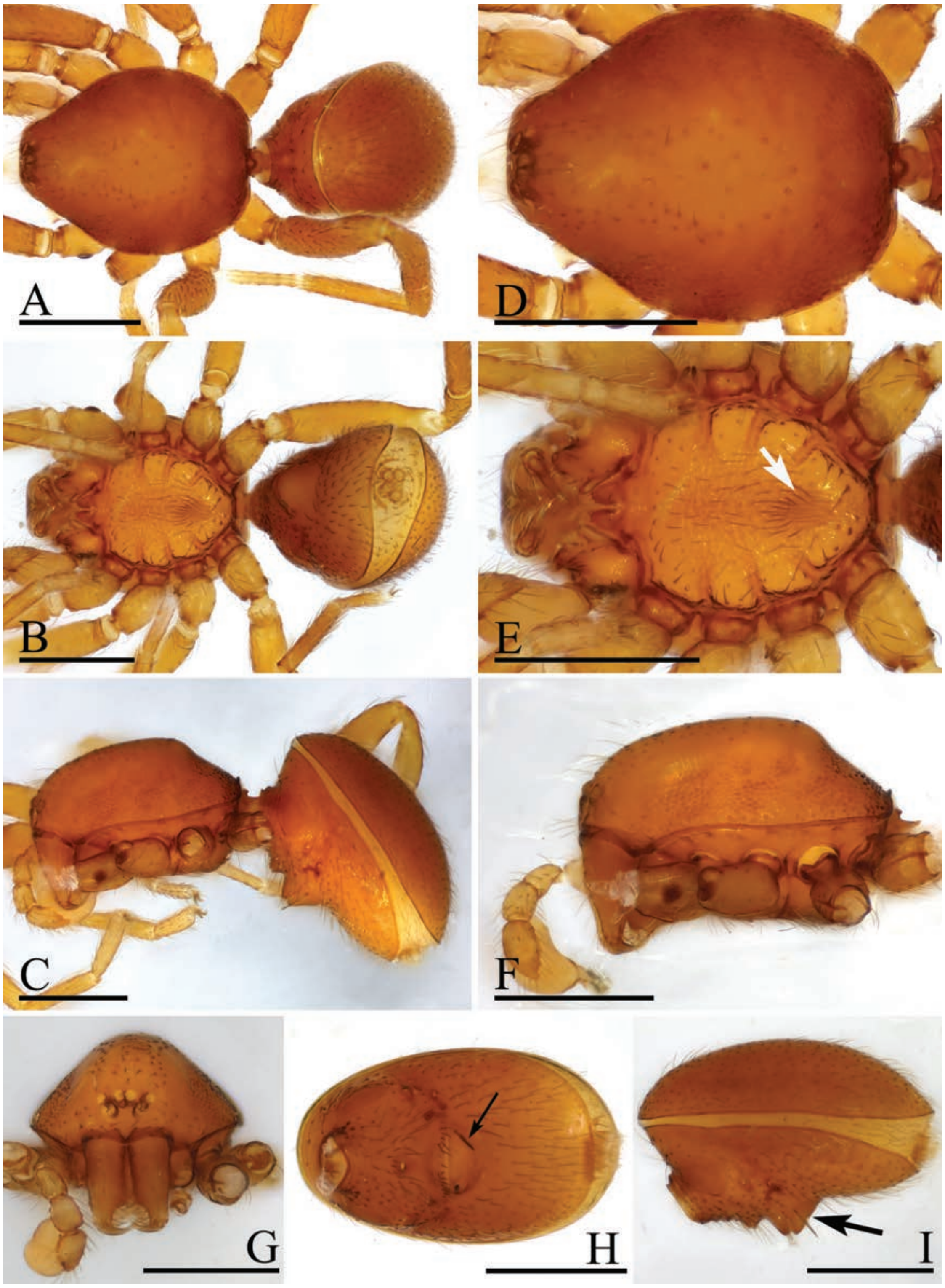

Figure 7. *Trilacuna taoyuanyu* sp. nov., male holotype **A–C** habitus in dorsal, ventral, and lateral views **D–G** prosoma in dorsal, ventral, lateral and anterior views, white arrow shows the small ridges **H–I** abdomen, ventral and lateral views, arrow in **H** shows the strong setae, and arrow in **I** shows the strong elevated epigastric region. Scale bars: 0.4 mm (**A–I**).

from above, procurved from front; ALE separated from edge of carapace by 1.3 diameters (Fig. 9D, G). ***Mouthparts*:** chelicerae straight; labium rectangular, anterior margin deeply incised; endites slender, distally branched (Figs 6F, 9G). ***Sternum*:** surface finely smooth, with many ridges on posterior area (Fig. 9E).

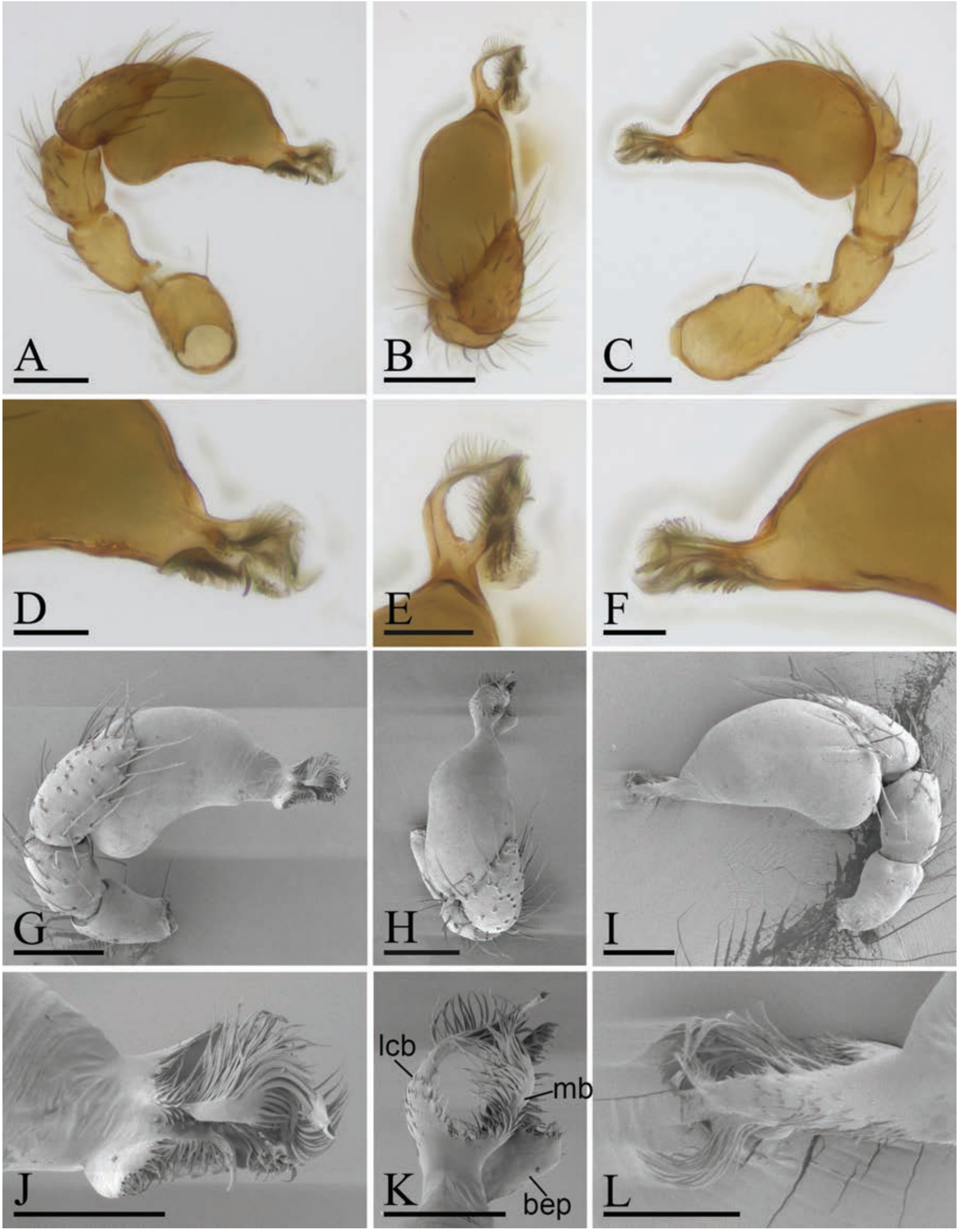

Figure 8. *Trilacuna taoyuanyu* sp. nov., left male palp, **A–F** (light) and **G–L** (SEM) **A, G** prolateral view **B, H** dorsal view **C, I** retrolateral view **D, J** distal part of palpal bulb, prolateral view **E, K** distal part of palpal bulb, dorsal view **F, L** distal part of palpal bulb, retrolateral view. Abbreviations: bep = basal ear-shaped projection; lcb = lateral curved branch; mb = medial branch. Scale bars: 0.1 mm (**A–C, G–I**); 0.05 mm (**D–F, J–L**).

***Abdomen*:** 0.84 long, 0.57 wide; booklung covers ovoid, surface smooth; sperm pore situated at level of anterior spiracles; apodemes present, posterior spiracles not connected by groove; epigastric region steeply elevated (Fig. 9C). ***Leg spination*:** legs I–II: tibia: v2-2-2-2-0, metatarsus: v2-2-0. ***Palp*:** orange; 0.50 long (0.14,

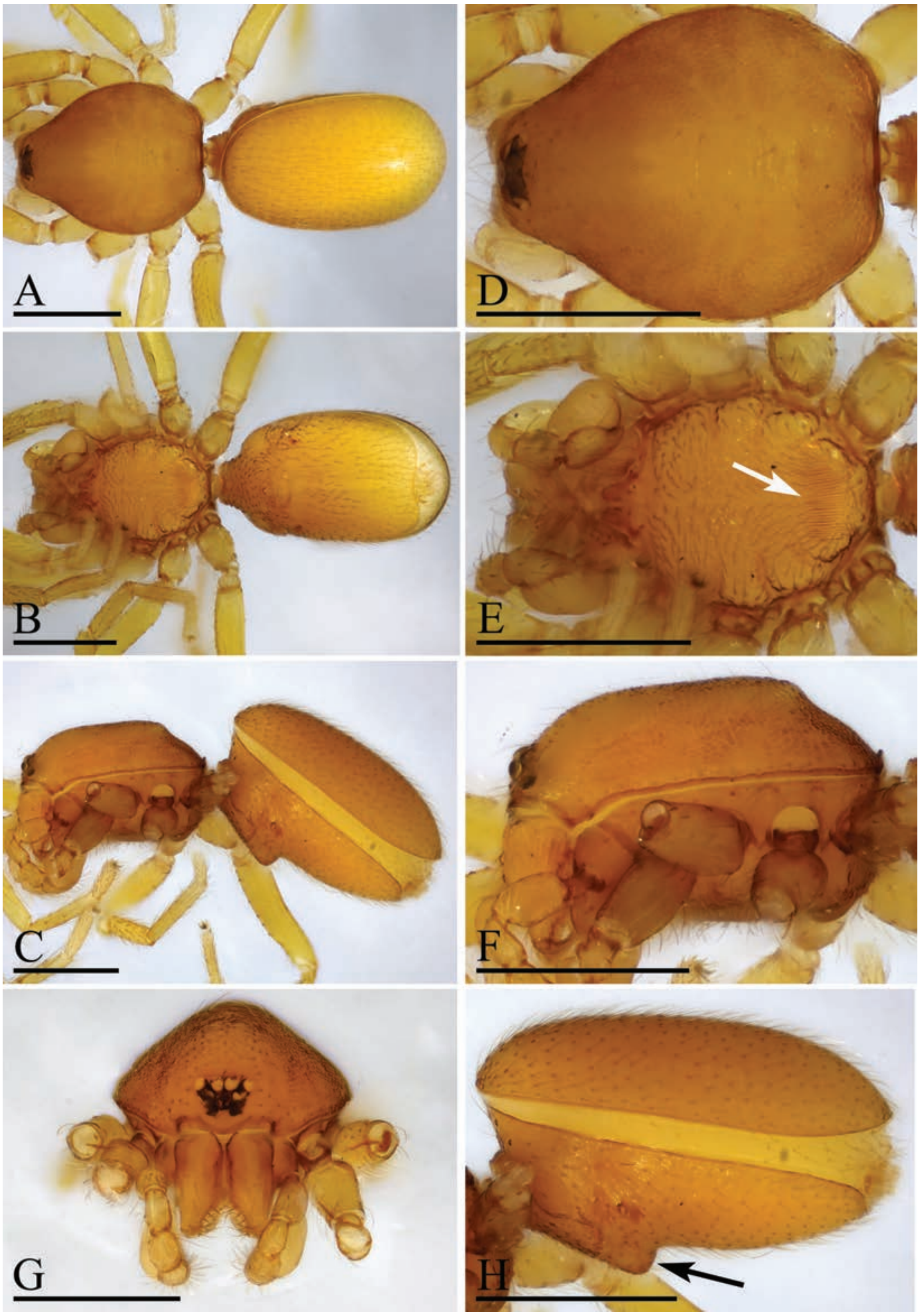

Figure 9. *Trilacuna yunmeng* sp. nov., male holotype **A–C** habitus in dorsal, ventral and views **D–G** prosoma in dorsal, ventral, lateral and anterior views, arrow shows the small ridges **H** abdomen, lateral view, arrow shows the steeply elevated epigastric region. Scale bars: 0.4 mm (**A–H**).

0.11, 0.11, 0.14); femur elongated (width/length = 0.62); bulb triangular, basally strongly bulged; embolus system with ear-shaped projection (bep) at base, with a lateral curved branch (lcb) and narrow medial branch (mb) (Fig. 10A–L).

Female. Unknown.

Distribution. Known only from the type locality (Fig. 11).

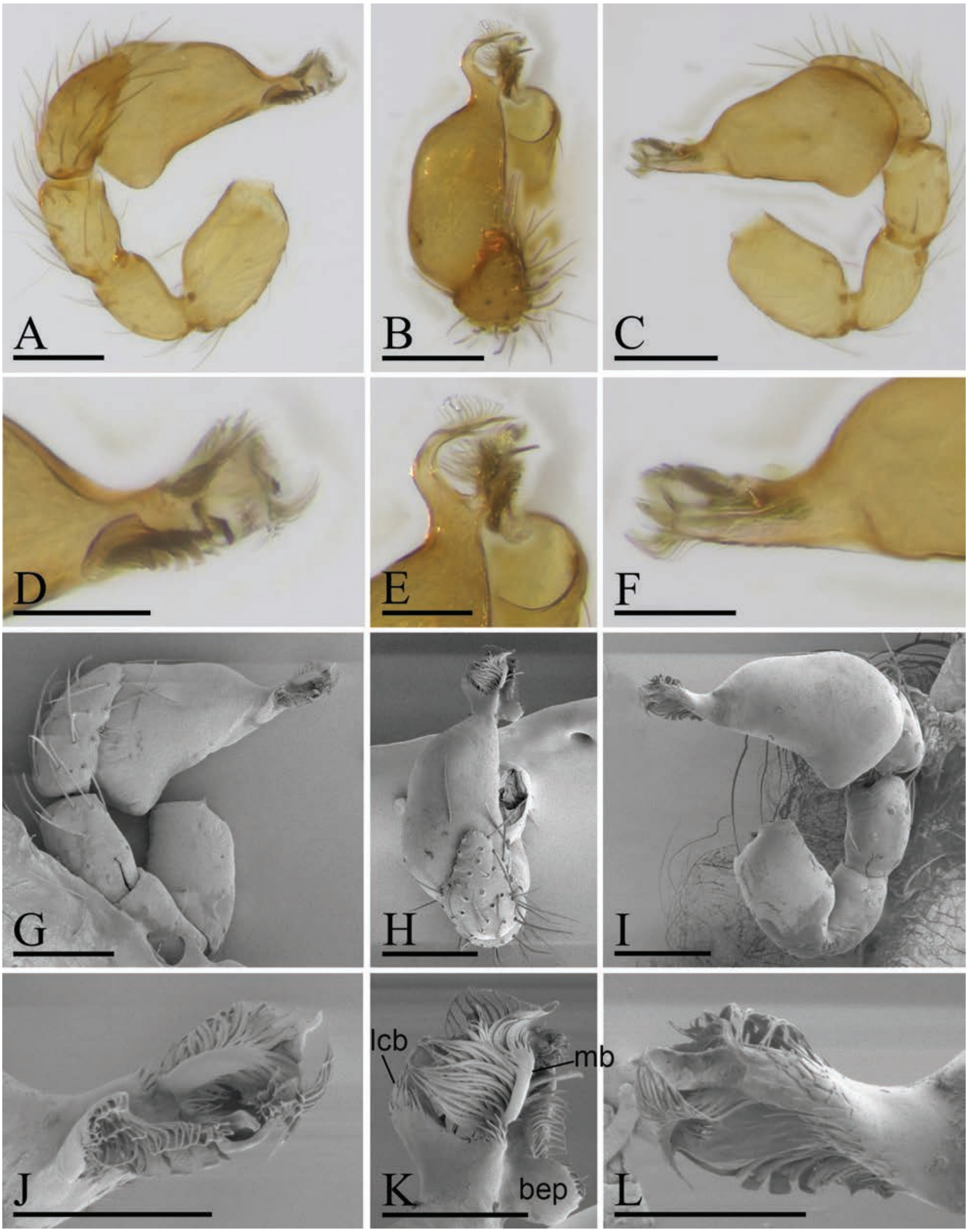

Figure 10. *Trilacuna yunmeng* sp. nov., left male palp, **A–F** (light) and **G–L** (SEM) **A, G** prolateral view **B, H** dorsal view **C, I** retrolateral view **D, J** distal part of palpal bulb, prolateral view **E, K** distal part of palpal bulb, dorsal view **F, L** distal part of palpal bulb, retrolateral view. Abbreviations: bep = basal ear-shaped projection; lcb = lateral curved branch; mb = medial branch. Scale bars: 0.1 mm (**A–C, G–I**); 0.05 mm (**D–F, J–L**).

Figure 11. Distribution records of four new species from China. 1 = *Trilacuna guangwu* sp. nov.; 2 = *Trilacuna qingliangfeng* sp. nov.; 3 = *Trilacuna taoyuanyu* sp. nov.; 4 = *Trilacuna yunmeng* sp. nov.

Acknowledgements

The manuscript benefitted greatly from comments by Alireza Zamani (Turku, Finland), Yucheng Lin (Chengdu, China), and one anonymous referee. We are grateful to Feng Zhang (Hebei University, Baoding, China) for providing the specimens. Abid Ali (University of Agriculture Faisalabad, Pakistan) kindly checked the English in the final draft.

Additional information

Conflict of interest

The authors have declared that no competing interests exist.

Ethical statement

No ethical statement was reported.

Funding

This study was supported by the National Natural Science Foundation of China (NSFC-32370479, 31972867).

Author contributions

YT designed the study. JM and QC finished the descriptions and took the photos. YT drafted and revised the manuscript.

Author ORCIDs

Jimeng Ma https://orcid.org/0009-0008-4579-3506
Qiang Chen https://orcid.org/0009-0007-9722-1561
Yanfeng Tong https://orcid.org/0000-0002-4348-7029

Data availability

All of the data that support the findings of this study are available in the main text.

References

Eichenberger B, Kranz-Baltensperger Y (2011) New *Trilacuna* species from Thailand, Malaysia and Sumatra (Araneae, Oonopidae). Zootaxa 2823: 1–31. https://doi.org/10.11646/zootaxa.2823.1.1

Grismado CJ, Deeleman-Reinhold CL, Piacentini LN, Izquierdo MA, Ramírez MJ (2014) Taxonomic review of the goblin spiders of the genus *Dysderoides* Fage and their Himalayan relatives of the genera *Trilacuna* Tong and Li and *Himalayana*, new genus (Araneae, Oonopidae). Bulletin of the American Museum of Natural History 387: 1–108. https://doi.org/10.1206/843.1

Huang Y, Zhang W, Tong Y, Li S (2020) A new species of the genus *Trilacuna* (Araneae, Oonopidae) from Guizhou Province, China. Acta Arachnologica Sinica 29(2): 94–98. https://doi.org/10.3969/j.issn.1005-9628.2020.02.003

Huang Y, Bian D, Tong Y, Zhang Z, Li S (2021) Two new species of the genus *Trilacuna* (Araneae: Oonopidae) from Jinyun Mountain of Chongqing, China. European Journal of Taxonomy 748: 1–14. https://doi.org/10.5852/ejt.2021.748.1337

Ma J, Bian D, Tong Y, Yang Z, Zhang Z (2023) Three new species of the genus *Trilacuna* Tong & Li, 2007 (Araneae, Oonopidae) from Yunnan Province, China. ZooKeys 1174: 289–300. https://doi.org/10.3897/zookeys.1174.106130

Malek-Hosseini MJ, Grismado CJ, Sadeghi S, Bakhshi Y (2015) Description of the first cave dwelling species of the spider genus *Trilacuna* Tong & Li from Iran (Araneae: Oonopidae). Zootaxa 3972(4): 549–561. https://doi.org/10.11646/zootaxa.3972.4.6

Seo BK (2017) Four new species of the genera *Trilacuna*, *Orchestina* and *Hahnia* of the families Oonopidae and Hahniidae (Araneae) from Korea. Korean Journal of Environmental Biology 35(2): 184–190. https://doi.org/10.11626/KJEB.2017.35.2.184

Tong Y, Li S (2007) One new genus and four new species of oonopid spiders from southwest China (Araneae: Oonopidae). Annales Zoologici, Warszawa 57: 331–340.

Tong Y, Chen H, Bai S, Zhang Z, Li S (2019) Seven new species of the genus *Trilacuna* Tong & Li, 2007 from Yunnan, China (Araneae, Oonopidae). ZooKeys 821: 11–44. https://doi.org/10.3897/zookeys.821.29599

Tong Y, Li S, Bian D (2020) Taxonomic studies on the genus *Trilacuna* (Araneae, Oonopidae) from Myanmar. ZooKeys 960: 39–62. https://doi.org/10.3897/zookeys.960.54053

Tong Y, Shao Y, Bian D, Li S (2024) Two new oonopid spiders (Arachnida, Araneae) from Xishuangbanna tropical rainforest, Yunnan, China. ZooKeys 1205: 333–348. https://doi.org/10.3897/zookeys.1205.124183

Wang Y, Tong Y, Bian D, Li S (2021) Two new species of the genus *Trilacuna* from Chongqing Municipality, China (Araneae, Oonopidae). Zootaxa 4927(3): 431–443. https://doi.org/10.11646/zootaxa.4927.3.6

World Spider Catalog (2024) World Spider Catalog. Version 25.5 Natural History Museum Bern. http://wsc.nmbe.ch [accessed on 29 Sept. 2024]